OHIO STATE UNIVERSITY
FEB 13 1962
LIBRARY

BULLETIN OF THE CHEMICAL SOCIETY OF JAPAN

Vol. 34 No. 10 October 1961

CONTENTS

General and Physical

Thermodynamical Studies on Binary Systems Consisting of Polar and Non-polar Liquids. III. Calculation of the Electrostatic Part of the Thermodynamic Excess Functions due only to the Dipole of the Polar Molecule for the Binary System Composed of Polar and Non-polar Liquids according to Onsager's Model. . . . . K. AMAYA 1349

The Crystal Structure of Orthorhombic Aniline Hydrobromide, $C_6H_5NH_3Br$. . . . . I. NITTA, T. WATANABE and I. TAGUCHI 1405

Molecular Rotations of Terpenes in Relation to their Structures. I. The Internal Conformation of Isopropyl Group in Menthol-like Substance. . . . . S. YAMANA 1414

Infrared Absorption Spectra of Water of Crystallization in Cobaltous Chloride Hexa- and Dihydrate Crystals. . . . . I. GAMO 1430

Infrared Absorption Spectra of Water of Crystallization in Ferrous Chloride Tetrahydrate Crystal . . . . . I. GAMO 1433

Photochemical Processes due to n-π and π-π Transitions of 2-Picoline *N*-Oxide in the Vapor Phase . . . . . N. HATA 1440

Photochemical Processes due to n-π and π-π Transitions of 3-Picoline *N*-Oxide in the Vapor Phase . . . . . N. HATA 1444

Infrared Spectra of Acyclic Imides. IV. Effects of Alkali Halides on the Infrared Spectra of Diacetamide. . . . . T. UNO, K. MACHIDA and I. HAMANAKA 1448

Some Observations on the Process of Dehydration and Rehydration of Gypsum by Means of Proton Magnetic Resonance. . . . . T. SAITO 1454

Studies on the Surface Structure of Porous Materials. . . . . A. TSURUIZUMI 1457

Non-empirical Study of the π-Electronic Structure of Vinyl Chloride Molecule by Valence Bond Method. . . . . S. TAKEKIYO 1466

Molecular Structure Investigation of Chlorotrifluoroethylene by Electron Diffraction. . . . . T. KAWAI, H. SEKINE and M. IGARASHI 1472

Energy Distribution of Secondary Electrons from Copper-Beryllium Alloy by Positive Ions of Inert Gases. I. Electro-polished Surface. . . . . T. SUGIURA 1475

On the Structures of *p-tert*-Butyl Phenol Resin and α-Naphthol Resin. II. Infrared Absorption Spectra of *p-tert*-Butyl Phenol and α-Naphthol. . . . . R. SODA 1482

Infrared Absorption Spectra of Quartz and Some other Silica Modification. . . . . R. SODA 1491

Silanes. Vibrational Assignments and Frequency Correlations. . . G. J. JANZ and Y. MIKAWA 1495

Syntheses and Infrared Absorption Spectra of Deuterated Polyvinyl Alcohols $-(-CD_2-\underset{\underset{OH(D)}{|}}{CD}-)_n-$. . . . . H. TADOKORO, H. NAGAI, S. SEKI and I. NITTA 1504

The Study of Adsorption of Detergents at a Solution-Air Interface by Radiotracer Method. IV. The Valency and Concentration Effects of Added Electrolytes on the Adsorption of Alkyl Sulfate Ion. . . . . R. MATUURA, H. KIMIZUKA and A. MATSUBARA 1512

Analytical and Inorganic

Absorptiometric Determination of Micro-amounts of Iron in Nuclear Grade Graphite and Urania-Graphite Fuel; Nitroso R Salt Method after Coprecipitation of Iron with Manganese Dioxide. . . . . M. MIYAMOTO 1435

(Continued on inside cover)

Published by the Chemical Society of Japan

THE CHEMICAL SOCIETY OF JAPAN
(NIPPON KAGAKUKAI)

BULLETIN OF THE CHEMICAL SOCIETY OF JAPAN

Editor: Tadao SHIBA, Tokyo Institute of Technology, Tokyo
Assistant Editor: Tadashi SUEHIRO, Gakushuin University, Tokyo
Editorial Board:

Yoshié BANSHO	Hidehiro GOTÔ	Keniti HIGASI
Yoshimasa HIRATA	Hiroo INOKUCHI	Tatsujiro ISHIMORI
Tadashi KAMIKUBO	Michio KOBAYASHI	Ichiro MIYAGAWA
Masazumi NAKAGAWA	Shigeru OAE	Shigeru OHASHI
Kazuo SATAKE	Syûzô SEKI	Osamu SIMAMURA
Yoshitada TOMODA	Iwao YASUMORI	Koshiro YOSHIOKA

(Continued from outside cover)

Determination of Ortho-, Pyro- and Tripolyphosphate by the Use of a Small Column of Ion-exchange Resin . . . . . S. OHASHI and T. TAKADA 1516

Organic and Biological

Studies on the Mechanism of Rearrangement Reaction of 2-Phenyl-4-bromotropone to 2-Phenyl-benzoic Acid. . . . . Y. KITAHARA, I. MURATA and T. MUROI 1359
Condensation Reaction of Troponoids and Ethyl α-Cyano-β-aminoglutaconate. I . . . . . S. MATSUMURA 1361
Studies on Micro-paraffin. III. Properties and Spectra of Each Fraction of Micro-paraffin Separated by Urea Method and Chromatography. . . . . K. NEGORO 1366
Studies on Micro-paraffin. IV. On the Transformation of Paraffin Crystal by Addition of Pure Substances. . . . . K. NEGORO 1374
On 2-Aminotropothione Derivatives. . . . . T. NOZOE and K. MATSUI 1382
Synthesis of Some 8,8-Disubstituted Heptafulvene Derivatives. . . . . T. NOZOE, T. MUKAI, K. OSAKA and N. SHISHIDO 1384
Intramolecular Interaction between Hydroxyl Group and π-Electrons. XIII. ν_{O-H} Absorption of 2,6-Diphenylphenol and the Related Compounds. . M. ŌKI, H. HOSOYA and H. IWAMURA 1391
Intramolecular Interaction between Hydroxyl Group and π-Electrons. XIV. Electronic Effect of the Substituents on the Interaction in 2-Hydroxybiphenyls. . . . M. ŌKI and H. IWAMURA 1395
Studies on Meso-ionic Compounds. XIV. Synthesis of Meso-ionic Compounds from Pyridazine Derivatives Having a Carboxymethylmercapto Group . . . . . M. OHTA and K. KISHIMOTO 1402
Some Electrophilic Substitution Reactions of 4-Aminotropolone. . . . . K. DOI 1410
Structure of Enteromycin. I. Derivatives and Products in Various Reactions of Enteromycin. . . . . K. MIZUNO 1419
Structure of Enteromycin. II. Derivatives and Products in Various Reactions of Dimethoxy-enteromycin. . . . . K. MIZUNO 1425
Preparation of Perfluorocarboxylic Acids from Esters by Electrochemical Fluorination. . . . . S. NAGASE and R. KOJIMA 1468
Forschung über die katalytische Entwässerung des Isoamylalkohols. I. . . . . A. MITSUTOMI 1518
Forschung über die katalytische Entwässerung des Isoamylalkohols. II. Prüfung der Bedingungen für kontinuierliche Dehydratisierung bei Zinksulfat-Katalysator. . . . . A. MITSUTOMI 1525

Short Communications

On the Influence of Sodium Oxide upon the Crytical Structure of Tricalcium Silicate. . . . . G. YAMAGUCHI and H. UCHIKAWA 1536
Zur einfachen Bestimmung im Wasser Milliardestelmenge vorhandenen Kupfers(II) durch Anreicherung mit Mikroschicht der Chelatbildungsharze. . . . . M. FUJIMOTO 1537
Experimental Evidence for the Theoretical Condensation Isotherm on Spheres Arranged in the Closest Packing . . . . . I. HIGUCHI, Y. USHIKI and R. SUZUKI 1539
Synthesis of 4,6-Di-(D-glucopyranosyl)deoxystreptamine. . . . . S. UMEZAWA and Y. ITO 1540
Effect of Impurities on the ^{81}Br Quadrupole Resonance in *p*-Dibromobenzene . . . . . J. MARUHA, J. KOIZUMI, M. SUHARA and T. TONOMURA 1541
Syntheses of α-Keto Amides and Acids from Ethyl Alkylidenecyanoacetate. . . . . M. IGARASHI and H. MIDORIKAWA 1543
Rhodium-Platinum Oxide as a Catalyst for the Hydrogenation of Organic Compounds. II. Catalyst Preparation and Effects of Platinum in Rhodium-Platinum Oxide. . S. NISHIMURA 1544
Naphthalene as an Isolatable Reaction Intermediate in the Catalytic Vapor-phase Oxidation of Methylnaphthalenes to Phthalic Anhydride. . . . . C. J. NORTON 1545
Sudachitin, a New Flavone Pigment of Sudachi. . . . . T. HORIE, M. MASUMURA and F. S. OKUMURA 1547

Thermodynamical Studies on Binary Systems Consisting of Polar and Non-polar Liquids. III. Calculation of the Electrostatic Part of the Thermodynamic Excess Functions due only to the Dipole of the Polar Molecule for the Binary System Composed of Polar and Non-polar Liquids according to Onsager's Model

By Kazuo AMAYA

(Received March 4, 1961)

In the previous paper it has been shown that in the systems containing non-aromatic non-polar components, the increase of van Laar coefficient with the decrease of the concentration of the polar component may be due to its dipole moment and that a kind of stabilizing effect exists in the systems containing aromatic non-polar components. In order to confirm the fact that such a variation of the van Laar coefficient with concentration in the former group of the systems is due to the dipoles of the polar components and to elucidate the cause of the stabilization effect in the latter group of the systems, theoretical formulas based on Onsager's model of polar liquids are derived to explain the electrostatic part of the excess thermodynamic quantities due only to the dipole of the polar component, by neglecting the effect of higher multipoles for a binary system of polar and non-polar liquids, and are applied to the actual systems for which the heats of mixing were measured.

Derivation of Theoretical Expressions

In deriving the expressions of the electrostatic part of the thermodynamic excess functions due only to the dipole of the polar component for a binary system of polar and non-polar liquids, the following assumptions are made according to Onsager[1]:

1) The polar molecules is spherical.

2) The dipole is a point dipole and is located at the center of the molecule.

3) The medium surrounding the polar molecule is a continuous one having macroscopic isotropic dielectric constant.

4) The polarizability of the polar molecule is isotropic.

Then further the following assumption is imposed:

5) There is no volume change on mixing.

If a molecule of dipole moment μ and of polarizability α is placed at a cavity of radius a in a medium of dielectric constant ε, the reaction field R due to the dielectric is

$$R = \mu \cdot g \tag{1}$$

where g is given by

$$g = \frac{2(\varepsilon - 1)}{2\varepsilon + 1 - (2\alpha/a^3)(\varepsilon - 1)} \cdot \frac{1}{a^3} \tag{2}$$

The electrostatic work w required for the formation of a dipole μ in the medium is given by

$$w = -1/2 \cdot g \cdot \mu^2 \tag{3}$$

Then according to Barker[2], the electrostatic part of the free energy of mixing F^{Eel}, which is equal to G^{Eel} for a condensed system, for 1 mol. of a binary mixture in which the two components have the same molecular size and polarizability but different dipole moments μ_1 and μ_2, is given by

$$F^{\mathrm{Eel}} = G^{\mathrm{Eel}} = \frac{1}{2} N_{\mathrm{A}} (\mu^2{}_1 - \mu^2{}_2) \times \left(x_1 \int_{x_1}^{1} g \mathrm{d}x_1 - x_2 \int_{0}^{x_1} g \mathrm{d}x_1 \right) \tag{4}$$

where N_{A} is the Avogadro Number, x_1 and x_2 denote the mole fraction of the components 1 and 2 respectively. For a binary solution in which one component is polar and the other is non-polar, the electrostatic part of the free energy of mixing is given by

$$G^{\mathrm{Eel}} = \frac{1}{2} N_{\mathrm{A}} \mu^2 \left\{ x_2 \int_{x_2}^{1} g \mathrm{d}x_1 - (1 - x_2) \int_{0}^{x_2} g \mathrm{d}x_2 \right\} \tag{5}$$

where μ denotes the dipole moment of the polar molecule, and x_2 the mole fraction of the polar component in the solution.

Then other thermodynamic functions may be derived from the well-known thermodynamic relations:

$$H^{\mathrm{Eel}} = G^{\mathrm{Eel}} - T \cdot \frac{\partial G^{\mathrm{Eel}}}{\partial T}$$

1) L. Onsager, *J. Am. Chem. Soc.*, **58**, 1486 (1936).

2) J. A. Barker, *Proc. Roy. Soc.*, **A219**, 367 (1953).

$$S^{\mathrm{Eel}} = -\frac{\partial G^{\mathrm{Eel}}}{\partial T}$$

and the following expressions are obtained.

$$H^{\mathrm{Eel}} = \frac{1}{2} N_{\mathrm{A}} \mu^2 \left\{ x_2 \int_{x_2}^{1} h \mathrm{d}x_2 - (1-x_2) \int_{0}^{x_2} h \mathrm{d}x_2 \right\} \tag{6}$$

$$S^{\mathrm{Eel}} = \frac{1}{2} N_{\mathrm{A}} \mu^2 \left\{ x_2 \int_{x_2}^{1} s \mathrm{d}x_2 (1-x_2) \int_{0}^{x_2} s \mathrm{d}x_2 \right\} \tag{7}$$

where

$$h = g - T \cdot \partial g / \partial T \tag{8}$$

and

$$s = -\partial g / \partial T \tag{9}$$

If the polarizability α of the polar molecule is expressed by

$$\frac{n_2^2 - 1}{n_2^2 + 2} = \frac{4}{3} \pi N \alpha \tag{10}$$

where N is the number of polar molecules in a unit volume of the pure liquid and n_2 is the refractive index of the polar liquid, and the molar volume of the polar molecule, V_{M} is taken as $4/3 \cdot \pi N_{\mathrm{A}} a^3$. Then g is expressed as

$$g = \frac{8}{3} \pi \frac{1}{V_{\mathrm{M}}} \cdot N_{\mathrm{A}} \cdot \frac{\varepsilon(x_2) - 1}{2\varepsilon(x_2) + n_2^2} \cdot \frac{n_2^2 + 2}{3} \tag{11}$$

For 1 mol. of solution the above quantities are given as follows.

$$G^{\mathrm{Eel}} = \frac{4}{3} \pi \frac{N_{\mathrm{A}}^2}{V_{\mathrm{M}}} \cdot \frac{n_2^2 + 2}{3} \mu^2 \times \left\{ x_2 \int_{x_2}^{1} \frac{\varepsilon(x_2) - 1}{2\varepsilon(x_2) + n_2^2} \mathrm{d}x_2 - (1-x_2) \int_{0}^{x_2} \frac{\varepsilon(x_2) - 1}{2\varepsilon(x_2) + n_2^2} \mathrm{d}x_2 \right\} \tag{12}$$

$$H^{\mathrm{Eel}} = \frac{4}{3} \pi \frac{N_{\mathrm{A}}^2}{V_{\mathrm{M}}} \cdot \frac{n_2^2 + 2}{3} \mu^2 \times \left\{ x_2 \int_{x_2}^{1} \frac{\varepsilon(x_2 - 1)}{2\varepsilon(x_2) + n_2^2} (1 - A(x_2) \cdot T) \mathrm{d}x_2 - (1-x_2) \int_{0}^{x_2} \frac{\varepsilon(x_2) - 1}{2\varepsilon(x_2) + n_2^2} \times (1 - A(x_2) \cdot T) \mathrm{d}x_2 \right\} \tag{13}$$

$$S^{\mathrm{Eel}} = \frac{4}{3} \pi \frac{N_{\mathrm{A}}^2}{V_{\mathrm{M}}} \cdot \frac{n_2^2 + 2}{3} \mu^2 \times \left\{ x_2 \int_{x_2}^{1} \frac{\varepsilon(x_2) - 1}{2\varepsilon(x_2) + n_2^2} A(x_2) \mathrm{d}x_2 - (1-x_2) \int_{0}^{x_2} \frac{\varepsilon(x_2) - 1}{2\varepsilon(x_2) + n_2^2} A(x_2) \mathrm{d}x_2 \right\} \tag{14}$$

where $A(x_2)$ is given by

$$A(x_2) = \frac{1}{V_{\mathrm{M}}} \frac{\mathrm{d}V_{\mathrm{M}}}{\mathrm{d}T} + \left(\frac{1}{\varepsilon(x_2) - 1} - \frac{2}{2\varepsilon(x_2) + n_2^2} \right) \frac{\mathrm{d}\varepsilon(x_2)}{\mathrm{d}T} + \left(\frac{1}{n_2^2 + 2} - \frac{1}{2\varepsilon(x_2) + n_2^2} \right) 2n_2 \frac{\mathrm{d}n_2}{\mathrm{d}T} \tag{15}$$

which is easily derived by taking the logarithm of g and differentiating it with temperature. In the above expressions the following notations are used:

$\varepsilon(x_2)$: the dielectric constant of the solution in which the mole fraction of the polar component is x_2,

n_2: the refractive index of the polar liquid,

N_{A}: Avogadro's number,

V_{M}: the molar volume of the polar liquid, and

T: absolute temperature.

The Application of the Theory to the Actual Systems

The Necessary Data for the Calculation.—In applying the theory to the actual systems, it is necessary to have the numerical values of the following quantities:

1) the thermal expansion coefficient of the polar liquid,

2) the dielectric constant of the pure polar liquid, ε_2,

3) the temperature dependence of ε_2, $\mathrm{d}\varepsilon_2/\mathrm{d}T$,

4) the refractive index of the pure polar liquid, n_2,

5) the temperature dependence of n_2, $\mathrm{d}n_2/\mathrm{d}T$,

6) the density of the pure polar liquid, d,

7) the dipole moments of the polar component in vacuum, μ,

8) the dielectric constant of the solution, ε_{12}, and

9) the temperature dependence of ε_{12}, $\mathrm{d}\varepsilon_{12}/\mathrm{d}T$.

It is preferable to use the values of these constants which are determined experimentally, but unfortunately they are not available for all the systems considered in this experiment. In fact, for 1, 2, 4, 6 and 7 the values are available for all the components, but for 3 and 5 the values are only partly available and for 8 and 9 none of the values are available for all the systems. For those which are not available in the literature, they are derived from the relevant values on reasonable assumptions or the experimental rules as described in the following.

The Derivation of the Values of the Quantities which are not Available in the Literature.—(1) The temperature dependence of the dielectric constant of the polar liquid. According to Onsager, the dielectric constant of a

TABLE I. PHYSICAL CONSTANTS OF THE COMPONENTS USED FOR THE CALCULATION

Substance	Therm.exp. coeff., $\times 10^3$ per °C	Dielectric const., ε	Refractive index for Na D line n_D	Temp. dependence of $\varepsilon \times 10^2$ per °C	Temp. dependence of $n_D \times 10^4$ per °C	Molecular volume cc.	Dipole moment Debye unit
Chlorobenzene	0.981	5.612	1.52211	−1.6	−5.4	101.74	1.70
Bromobenzene	0.887	5.40	1.55762	−1.76*	−4.9	105.51	1.74
Benzonitrile	0.88	25.2	1.5265	−8.7	−3.4	103.50	4.39
Nitrobenzene	0.824	34.89	1.55057	−18.6	−4.0	103.16	4.21
Diethyl ketone	1.203	17.00	1.39003	−8.43*	−4.7	106.40	2.71
Methyl propyl ketone	1.203	17.00	1.39003	−8.43*	−4.7	106.40	2.71
n-Butylchloride	1.25	7.39	1.39954	−3.24*	−5.0	105.73	2.07
n-Butylcyanide	1.15	20.3	1.38170	−8.87*	−4.3	105.15	4.09
Cyclohexanone	0.947	18.3	1.44941	−8.58*	−4.9	104.67	2.75
Chlorocyclohexane	0.949	7.906**	1.46555	−3.28*	−5.1	119.37	2.07
Bromocyclohexane	0.891	7.945**	1.5020	−3.23*	−5.2	124.43	2.15
Pyridine	1.029	12.3	1.5067	−5.59	−5.0	81.31	2.22
cis-Dichloroethylene	1.288	9.0	1.44903	−4.45*	−6.5	76.17	1.80
trans-Dichloroethylene	1.67	2.14	1.4405	−0.263*	−10.1	77.28	0
Methylcyclohexane	1.13	2.020	1.42058	−0.16	−5.1	128.38	0
Cyclohexane	1.197	2.0199	1.42353	−0.16	−5.4	108.09	0
Toluene	1.109	2.3661	1.49413	−0.24	−5.6	106.85	0(0.37)
Benzene	1.197	2.284	1.49790	−0.20	−6.4	89.40	0
1,4-Dioxane	1.34	2.209	1.42025	−0.226*	−4.3	85.80	0

* Calculated according to the formula 16.
** Kindly measured by Mrs. K. Sasaki of this Institute.

TABLE II. THE CALCULATED VALUES OF THE ELECTROSTATIC PART OF THERMODYNAMIC EXCESS FUNCTIONS FOR BINARY SYSTEMS CONTAINING POLAR AND NON-AROMATIC NON-POLAR COMPONENTS

System	x_2	G^{Eel}_{calcd}	H^{Eel}_{calcd}	TS^{Eel}_{calcd}
	1.000	0	0	0
	0.916	36.8	58.4	21.6
	0.829	70.2	112.6	42.4
	0.743	97.3	158.4	61.6
Chlorobenzene	0.653	119.0	196.7	77.7
—Cyclohexane	0.559	133.6	224.7	91.1
	0.462	139.2	239.2	100.0
	0.360	133.5	234.9	101.4
	0.251	113.2	203.0	89.9
	0.132	72.1	131.8	59.7
	0	0	0	0
	1.000	0	0	0
	0.914	38.7	62.5	23.8
	0.827	72.7	118.9	46.2
	0.738	101.7	168.2	66.5
Bromobenzene	0.647	123.9	208.5	84.6
—Cyclohexane	0.553	138.5	237.3	98.8
	0.456	144.0	251.3	107.3
	0.354	137.9	245.2	107.3
	0.246	111.5	211.8	100.3
	0.130	70.3	137.5	67.2
	0	0	0	0

System	x_2	G^{Eel}_{calcd}	H^{Eel}_{calcd}	TS^{Eel}_{calcd}
	1.000	0	0	0
	0.908	234.3	216.6	−17.7
	0.816	452.4	426.4	−26.0
	0.722	652.8	626.2	−26.6
	0.628	829.2	812.2	−17.0
Benzonitrile	0.532	974.0	978.6	4.6
—Cyclohexane	0.435	1073.4	1113.9	40.5
	0.337	1107.3	1199.0	91.7
	0.231	1032.7	1189.0	156.9
	0.129	823.5	1015.8	192.3
	0.070	541.3	713.5	172.2
	0	0	0	0
	1.000	0	0	0
	0.908	199.9	130.3	−69.6
	0.814	389.8	262.0	−127.8
	0.720	566.0	394.4	−171.6
	0.625	725.0	527.6	−197.4
Nitrobenzene	0.529	859.2	658.9	−200.3
—Cyclohexane	0.431	959.4	788.7	−170.7
	0.333	1007.6	902.4	−105.2
	0.232	970.2	977.3	7.1
	0.127	777.1	913.5	136.4
	0.069	519.6	719.6	200.0
	0	0	0	0

TABLE II. (Continued)

System	x_2	G^{E}_{calcd}	H^{E}_{calcd}	TS^{E}_{calcd}
	1.000	0	0	0
	0.910	59.9	89.2	29.3
	0.819	113.2	178.6	65.4
	0.727	158.6	259.8	101.2
n-Butylchloride	0.633	194.7	326.6	131.9
—Cyclohexane	0.538	219.9	378.9	159.0
	0.440	230.8	411.3	180.5
	0.340	223.4	414.3	190.9
	0.236	191.5	371.9	180.4
	0.124	124.0	254.3	130.3
	0	0	0	0
	1.000	0	0	0
	0.906	85.9	87.2	1.3
	0.811	165.3	171.9	6.6
	0.716	236.3	252.6	16.3
Diethyl ketone	0.620	296.9	327.6	30.7
(Methyl	0.524	344.1	384.2	40.1
propyl ketone)	0.427	373.4	448.1	74.7
—Cyclohexane	0.328	377.7	489.9	112.2
	0.227	343.9	470.9	127.0
	0.121	244.6	369.7	125.1
	0.064	152.1	246.9	94.8
	0	0	0	0
	1.000	0	0	0
	0.902	104.0	99.2	−4.8
	0.809	194.7	190.0	−4.7
	0.715	276.4	277.1	0.7
	0.620	346.6	358.8	12.2
Cyclohexanone	0.525	401.9	432.1	30.2
—Cyclohexane	0.428	436.8	491.7	54.9
	0.329	442.7	527.8	85.1
	0.227	403.7	518.4	114.7
	0.119	283.5	403.2	119.7
	0.060	169.1	258.8	89.7
	0	0	0	0
	1.000	0	0	0
	0.906	185.4	170.2	−15.2
	0.812	358.1	336.9	−21.2
	0.717	514.2	497.3	−16.9
	0.621	649.8	648.9	−0.9
n-Butylcyanide	0.524	757.5	786.0	28.5
—Cyclohexane	0.427	828.3	901.6	73.3
	0.328	845.8	977.5	131.7
	0.227	780.3	976.1	195.8
	0.121	565.4	789.0	223.6
	0.062	347.0	529.0	182.0
	0	0	0	0

System	x_2	G^{E}_{calcd}	H^{E}_{calcd}	TS^{E}_{calcd}
	1.000	0	0	0
	0.915	49.5	69.9	20.4
	0.828	94.2	135.7	41.5
	0.740	133.2	196.4	63.2
Chlorocyclohexane	0.649	165.1	249.8	84.7
—Methylcyclohexane	0.555	188.0	292.9	104.9
	0.459	199.3	320.9	121.6
	0.358	195.3	326.6	131.3
	0.251	169.9	297.4	127.5
	0.134	112.2	208.1	95.9
	0	0	0	0
	1.000	0	0	0
	0.912	53.9	75.5	21.6
	0.824	102.3	146.0	43.7
	0.734	144.0	210.1	66.1
Bromocyclohexane	0.642	177.7	266.0	88.3
—Methylcyclohexane	0.548	201.5	310.6	109.1
	0.452	212.8	338.9	126.1
	0.352	207.8	343.5	135.7
	0.246	180.2	301.5	131.3
	0.131	118.8	216.8	98.0
	0	0	0	0
	1.000	0	0	0
	0.908	64.1	103.5	39.4
	0.815	121.3	199.6	78.3
cis-Dichloro-	0.727	166.9	280.6	113.7
ethylene	0.626	208.7	360.7	152.0
—*trans*-Dichloro-	0.529	240.5	419.4	178.9
ethylene	0.430	256.8	454.9	198.1
	0.328	247.5	456.6	209.1
	0.222	209.3	405.2	195.9
	0.107	126.5	260.2	133.7
	0	0	0	0
	1.000	0	0	0
	0.913	91.5	107.0	15.5
	0.824	175.3	209.7	34.4
	0.734	249.9	306.3	56.4
Pyridine	0.643	312.6	394.2	81.6
—1,4-Dioxane	0.550	360.9	470.2	109.3
	0.454	388.9	527.0	138.1
	0.356	389.9	554.2	164.3
	0.253	351.6	530.2	178.6
	0.141	251.0	408.6	157.6
	0	0	0	0

TABLE III. THE CALCULATED VALUES OF THE ELECTROSTATIC PART OF THERMODYNAMIC EXCESS FUNCTIONS FOR BINARY SYSTEMS CONTAINING POLAR AND AROMATIC NON-POLAR COMPONENTS

System	x_2	G^{Eel}_{calcd}	H^{Eel}_{calcd}	TS^{Eel}_{calcd}
Chlorobenzene —Toluene	1.000	0	0	0
	0.905	34.5	55·3	20.8
	0.806	64.6	105.1	40.5
	0.707	87.8	145.3	57.5
	0.613	103.4	173.5	70.1
	0.498	112.4	192.1	79.7
	0.386	110.2	192.0	81.8
	0.269	94.5	168.9	74.4
	0.143	61.2	111.9	50.7
	0.005	2.8	5.2	2.4
	0	0	0	0
Bromobenzene —Toluene	1.000	0	0	0
	0.902	36.4	64.2	27.8
	0.802	67.3	120.3	53.0
	0.700	92.2	166.5	74.3
	0.595	109.2	200.5	91.3
	0.488	117.3	218.9	101.6
	0.376	114.5	216.5	102.0
	0.248	98.0	185.9	87.9
	0.133	57.3	115.8	58.5
	0	0	0	0
Benzonitrile —Toluene	1.000	0	0	0
	0.906	224.9	204.8	−20.1
	0.810	434.4	401.4	−33.0
	0.714	624.8	587.8	−37.0
	0.618	789.7	759.2	−30.5
	0.519	922.1	910.0	−12.1
	0.421	1007.4	1026.9	19.5
	0.321	1025.7	1091.1	65.4
	0.214	932.6	1053.3	120.7
	0.109	648.6	794.4	145.8
	0.049	349.9	457.6	107.7
	0	0	0	0
Nitrobenzene —Toluene	1.000	0	0	0
	0.905	189.3	121.0	−68.3
	0.810	367.9	242.9	−125.0
	0.714	532.1	364.2	−167.9
	0.617	677.7	483.8	−193.9
	0.519	798.5	599.7	−198.8
	0.420	884.2	707.3	−176.9
	0.320	916.8	795.4	−121.4
	0.218	861.7	835.2	−26.5
	0.112	631.2	719.7	88.5
	0.054	377.9	491.0	113.1
	0	0	0	0
n-Butylchloride —Toluene	1.000	0	0	0
	0.901	56.1	86.4	30.3
	0.802	104.6	168.3	63.7
	0.701	144.5	240.2	95.7
	0.600	174.0	298.9	124.9
	0.496	191.4	339.5	148.1
	0.390	193.1	355.2	161.2
	0.281	174.6	334.7	160.1
	0.168	128.9	259.7	130.8
	0.046	43.8	92.8	49.0
	0	0	0	0
Cyclohexanone —Toluene	1.000	0	0	0
	0.908	89.0	84.8	−4.2
	0.802	181.9	178.1	−3.8
	0.705	257.1	258.8	1.7
	0.607	320.1	333.2	13.1
	0.508	367.5	397.9	30.4
	0.409	393.8	447.3	53.5
	0.307	390.0	470.5	80.5
	0.203	339.8	443.3	103.5
	0.092	205.9	298.0	92.1
	0.031	81.7	126.9	45.2
	0	0	0	0
n-Butylcyanide —Toluene	1.000	0	0	0
	0.903	181.0	167.6	−13.4
	0.805	348.0	330.3	−17.7
	0.707	497.9	486.4	−11.5
	0.609	625.9	632.1	6.2
	0.510	725.5	762.2	36.7
	0.410	786.6	866.9	80.3
	0.309	792.9	928.0	135.1
	0.205	714.1	903.4	189.1
	0.098	482.8	674.5	191.7
	0.040	206.1	318.9	112.8
	0	0	0	0
Pyridine —Benzene	1.000	0	0	0
	0.914	88.7	107.0	18.3
	0.827	170.2	210.0	39.8
	0.738	243.3	308.4	65.1
	0.647	304.9	398.3	93.4
	0.553	352.3	475.5	123.2
	0.456	379.6	533.4	153.8
	0.356	379.5	559.6	180.1
	0.249	339.0	530.9	191.9
	0.134	233.5	394.9	161.4
	0	0	0	0

polar liquid ε_2 is related to temperature as

$$\varepsilon_2 - n_2^2 = \frac{3\varepsilon_2}{2\varepsilon_2 + n_2^2} \cdot \frac{(n_2^2+2)^2}{3} \cdot \frac{4\pi N}{3kT} \mu^2 \quad (16)$$

By assuming that the dipole moment μ of the polar molecule is independent of temperature, we obtain the following expression, by taking the logarithm of both sides of the formula 16 and differentiating it with the temperature:

$$\left(\frac{1}{\varepsilon_2 - n_2^2} + \frac{2}{2\varepsilon_2 + n_2^2} - \frac{1}{\varepsilon_2}\right)\frac{d\varepsilon_2}{dT} + \left(\frac{1}{2\varepsilon_2 + n_2^2} - \frac{1}{\varepsilon_2 - n_2^2} - \frac{2}{n_2^2+2}\right)2n_2\frac{dn_2}{dT} = \frac{1}{N}\cdot\frac{dN}{dT} - \frac{1}{T} \quad (17)$$

where $1/N \cdot dN/dT$ is the thermal expansion coefficient of the polar liquid reversed in sign. All the values in the above expression are available except $d\varepsilon_2/dT$. Then the values of $d\varepsilon_2/dT$ can be derived by the relevant values such as ε_2, n_2, dn_2/dT, T and the thermal expansion coefficient.

(2) The temperature dependence of the refractive index of the liquid. The refractive index n of a liquid can approximately be expressed as $(n^2-1)/(n^2+2)\cdot 1/\rho = \text{const.}$ where ρ is the density of the liquid. Differentiating it with temperature, we obtain

$$\frac{dn}{dT} = \frac{(n^2-1)(n^2+2)}{6n}\cdot\frac{1}{\rho}\cdot\frac{d\rho}{dT} \quad (18)$$

$1/\rho \cdot d\rho/dT$ is the thermal expansion coefficient of the liquid reversed in sign. Then we can derive the values of dn/dT from the refractive index and the thermal expansion coefficient of the liquid.

(3) The dielectric constant of the solution, ε_{12}. According to Onsager, the dielectric constant of a binary solution of polar and non-polar liquid is expressed as

$$3(1-v_2)(\varepsilon_{12}-n_1^2)\frac{\varepsilon_{12}}{2\varepsilon_{12}+n_1^2} + 3v_2(\varepsilon_{12}-n_2^2)\frac{\varepsilon_{12}}{2\varepsilon_{12}+n_2^2} = \frac{4\pi N v_2 \mu^2}{3kT}\left\{\frac{\varepsilon_{12}(n_2^2+2)}{2\varepsilon_{12}+n_2^2}\right\}^2 \quad (19)$$

where v_2 is the volume fraction of the polar components.

By replacing μ^2 in the above expression with

$$\frac{9(\varepsilon_2-n_2^2)(2\varepsilon_2+n_2^2)kT}{\varepsilon_2(n_2^2+2)^2\cdot 4\pi N}\mu^2 \quad (20)$$

which is obtained from Onsager's expression of the dielectric constant for a pure polar liquid, we obtain[3]

3) T. Hanai, N. Koizumi and R. Gotō, *J. Chem. Soc. Japan, Pure Chem. Sec.* (*Nippon Kagaku Zasshi*), **80**, 17 (1959).

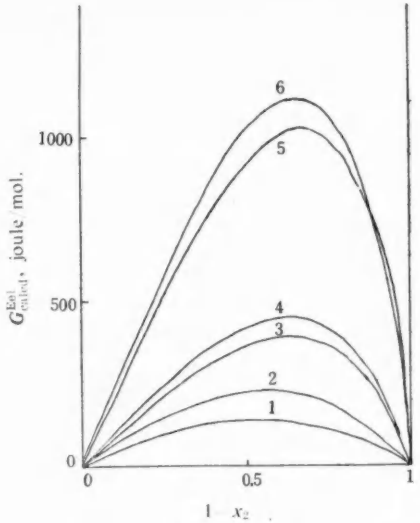

Fig. 1. G^{Eel}_{calcd} vs. mol. fraction.
1. Chlorobenzene—Cyclohexane
2. *n*-Butylchloride—Cyclohexane
3. Diethyl ketone—Cyclohexane
4. Cyclohexanone—Cyclohexane
5. Nitrobenzene—Cyclohexane
6. Benzonitrile—Cyclohexane

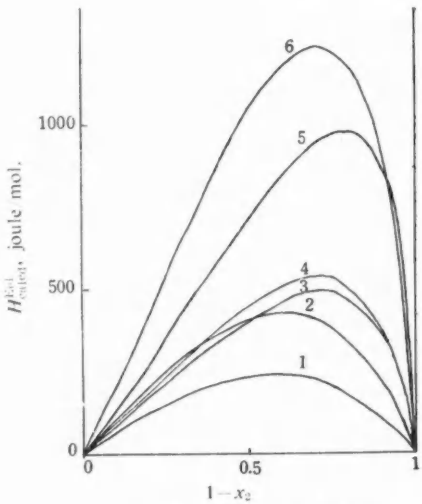

Fig. 2. H^{Eel}_{calcd} vs. mol. fraction.
1. Chlorobenzene—Cyclohexane
2. *n*-Butylchloride—Cyclohexane
3. Diethyl ketone—Cyclohexane
4. Cyclohexanone—Cyclohexane
5. Nitrobenzene—Cyclohexane
6. Benzonitrile—Cyclohexane

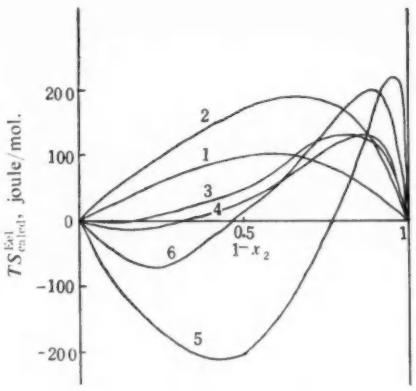

Fig. 3. TS^{Ecl}_{calcd} vs. mol. fraction.

1. Chlorobenzene—Cyclohexane
2. *n*-Butylchloride—Cyclohexane
3. Diethyl ketone—Cyclohexane
4. Cyclohexanone—Cyclohexane
5. Nitrobenzene—Cyclohexane
6. Benzonitrile—Cyclohexane

$$\frac{\varepsilon_{12}-\varepsilon_1}{2\varepsilon_{12}-n_1^2}\cdot(1-v_2)+\frac{(\varepsilon_{12}-\varepsilon_2)(2\varepsilon_{12}\varepsilon_2+n_2^4)}{\varepsilon_2(2\varepsilon_{12}+n_2^2)^2}v_2=0 \tag{21}$$

where ε_1 and n_1 are the dielectric constant and refractive index of the non-polar liquid respectively, other notation being the same as those already described. All the values in the above expression 21 are known except ε_{12} and v_1. The dielectric constant of the solution ε_{12} can be calculated from the expression 21 for any given values of concentration v_2.

(4) The temperature dependence of ε_{12}, $d\varepsilon_{12}/dT$. It is approximated by a weighted mean such as

$$\frac{d\varepsilon_{12}}{dT}=\frac{\varepsilon_2-\varepsilon_{12}}{\varepsilon_2-\varepsilon_1}\cdot\frac{d\varepsilon_1}{dT}+\frac{\varepsilon_{12}-\varepsilon_1}{\varepsilon_2-\varepsilon_1}\cdot\frac{d\varepsilon_2}{dT} \tag{22}$$

$d\varepsilon_1/dT$ is the temperature dependence of the dielectric constant of the non-polar liquid. If $d\varepsilon_1/dT$ is not available, it is derived by using the following expression

$$\frac{\varepsilon_1-1}{\varepsilon_1+2}\cdot\frac{1}{\rho}=\text{constant} \tag{23}$$

Table IV. The electrostatic part of van Laar coefficients, a^{el}_{calcd} calculated according to Onsager's model for binary systems consisting of polar and non-aromatic non-polar molecules

System	v_2	a^{el}_{calcd} joule/cc.	System	v_2	a^{el}_{calcd} joule/cc.
	1.000	7.18		1.000	23.21
	0.9115	7.07		0.9045	24.13
	0.8203	7.43		0.8089	26.44
	0.7312	7.80		0.7132	29.22
Chlorobenzene	0.6387	8.20		0.6173	32.68
—Cyclohexane	0.5441	8.67	Benzonitrile	0.5208	37.12
	0.4468	9.20	—Cyclohexane	0.4244	42.98
	0.3460	9.81		0.3269	51.15
	0.2395	10.47		0.2236	64.03
	0.1256	11.19		0.1239	87.05
	0	12.03		0.0672	105.58
				0	131.96
	1.000	7.28		1.000	13.67
	0.9123	7.39		0.9036	14.45
	0.8235	7.72		0.8071	16.17
	0.7332	8.10		0.7106	18.31
Bromobenzene	0.6412	8.52		0.6139	21.09
—Cyclohexane	0.5470	8.98	Nitrobenzene	0.5171	24.78
	0.4498	9.50	—Cyclohexane	0.4199	30.17
	0.3485	10.09		0.3223	37.98
	0.2417	10.75		0.2235	50.93
	0.1267	11.52		0.1214	75.65
	0	12.35		0.0664	101.21
				0	141.11

TABLE IV. (Continued)

System	v_2	α^{el}_{calcd} joule/cc.	System	v_2	α^{el}_{calcd} joule/cc.
	1.000	9.34		1.000	7.10
	0.9080	10.08		0.9091	7.04
	0.8154	11.18		0.8176	7.53
	0.7227	12.17		0.7253	8.10
n-Butylchloride	0.6278	13.11	Chlorocyclohexane	0.6320	8.77
—Cyclohexane	0.5323	14.25	—Methylcyclohexane	0.5373	9.55
	0.4350	15.63		0.4407	10.48
	0.3352	17.33		0.3411	11.61
	0.2315	19.44		0.2371	13.04
	0.1214	22.12		0.1256	14.90
	0	25.22		0	17.15
	1.000	17.50		1.000	7.14
	0.9038	18.57		0.9098	7.37
	0.8074	20.50		0.8190	7.87
	0.7109	22.83		0.7273	8.44
	0.6143	25.79	Bromocyclohexane	0.6345	9.12
n-Butylcyanide	0.5173	29.54	—Methylcyclohexane	0.5403	9.91
—Cyclohexane	0.4199	34.65		0.4439	10.84
	0.3216	41.83		0.3444	11.98
	0.2218	52.64		0.2401	13.41
	0.1181	70.32		0.1277	15.23
	0.0625	87.26		0	17.37
	0	109.10			
	1.000	8.83		1.000	15.23
	0.9045	9.48		0.9062	15.97
	0.8088	10.42		0.8120	17.12
	0.7129	11.55		0.7236	18.34
Diethyl ketone	0.6167	12.95	*cis*-Dichloroethylene	0.6213	20.00
(Methyl propyl ketone)	0.5202	14.36	—*trans*-Dichloroethylene	0.5244	21.91
—Cyclohexane	0.4230	17.10		0.4257	24.19
	0.3248	20.77		0.3244	27.04
	0.2245	25.54		0.2188	30.71
	0.1196	32.54		0.1056	35.62
	0.0632	38.65		0	40.74
	0	46.69			
	1.000	9.81		1.000	15.44
	0.8991	10.41		0.9083	15.73
	0.8039	11.45		0.8163	17.04
	0.7084	12.70		0.7237	18.57
	0.6127	14.27	Pyridine	0.6306	20.41
Cyclohexanone	0.5165	16.28	—1,4-Dioxane	0.5365	22.69
—Cyclohexane	0.4197	18.16		0.4411	25.52
	0.3217	22.62		0.3436	29.18
	0.2216	28.01		0.2425	34.09
	0.1157	36.60		0.1346	41.19
	0.0583	43.69		0	51.24
	0	52.08			

TABLE V. THE ELECTROSTATIC PART OF VAN LAAR COEFFICIENTS, a^{el}_{calcd} CALCULATED ACCORDING TO ONSAGER'S MODEL FOR BINARY SYSTEMS CONSISTING OF POLAR AND AROMATIC NON-POLAR MOLECULES

System	v_2	a^{el}_{calcd} joule/cc.	System	v_2	a^{el}_{calcd} joule/cc.
	1.000	6.06		1.000	8.31
	0.9005	6.04		0.9004	9.10
	0.7978	6.34		0.8002	9.94
	0.6972	6.67		0.6992	10.77
Chlorobenzene	0.6011	6.98	*n*-Butylchloride	0.5970	11.70
—Toluene	0.4855	7.37	—Toluene	0.4934	12.78
	0.3747	7.81		0.3878	14.06
	0.2595	8.33		0.2792	15.62
	0.1371	8.92		0.1661	17.58
	0.0051	9.59		0.0456	20.21
	0	9.67		0	21.03
	1.000	6.61		1.000	16.65
	0.9007	6.79		0.9014	17.91
	0.7998	7.29		0.8028	19.78
	0.6972	7.45		0.7039	22.09
Bromobenzene	0.5923	7.83		0.6049	24.99
—Toluene	0.4844	8.25	*n*-Butylcyanide	0.5055	28.77
	0.3727	8.71	—Toluene	0.4057	33.87
	0.2557	9.17		0.3050	41.16
	0.1315	9.51		0.2026	52.51
	0	9.64		0.0961	72.80
				0.0388	79.91
				0	91.86
	1.000	21.37		1.000	8.93
	0.9027	22.46		0.8963	8.61
	0.8053	24.58		0.7985	10.53
	0.7077	27.20		0.7004	11.71
	0.6099	30.45		0.6021	13.18
Benzonitrile	0.5114	34.65	Cyclohexanone	0.5032	15.36
—Toluene	0.4131	40.18	—Toluene	0.4036	17.54
	0.3136	47.92		0.3028	20.99
	0.2082	60.20		0.1994	26.10
	0.1056	79.09		0.0901	34.09
	0.0470	95.65		0.0303	40.48
	0	112.10		0	44.22
	1.000	12.41		1.000	15.74
	0.9023	13.26		0.9068	15.44
	0.8045	14.87		0.8133	16.72
	0.7066	16.86		0.7194	18.32
	0.6086	19.42	Pyridine	0.6249	20.19
Nitrobenzene	0.5104	22.87	—Benzene	0.5294	22.47
—Toluene	0.4119	27.75		0.4328	25.35
	0.3128	35.02		0.3341	29.07
	0.2124	47.09		0.2321	34.08
	0.1085	69.87		0.1235	41.32
	0.0521	93.30		0	50.97
	0	122.20			

By differentiation with temperature, we obtain

$$\frac{d\varepsilon_1}{dT} = \frac{1}{\rho}\frac{d\rho}{dT}\frac{(\varepsilon_1-1)(\varepsilon_1+2)}{3} \quad (24)$$

which can be calculated from the values of ε_1 and the thermal expansion coefficient of the non-polar liquid.

The values used for the calculations are shown in Table I.

The Results and Discussions

The calculation is carried out for the systems for which the heats of mixing were measured. For the systems where toluene is the non-polar component, it is assumed that the dipole-moment of toluene is zero. No serious difference occurs even if the finite value of its dipole moment is taken into account (the difference being only 4% at most). The results obtained are shown in Tables II and III and some of them are shown in Figs. 1—3.

As is seen from the above tables, the electrostatic part of the excess free energy and the excess enthalpy of mixing for the above systems derived on the Onsager model, are all positive over all the concentrations and the quantities for 1 mol. of mixture deviate from the parabola expressed by $Kx_2(1-x_2)$, where K is a constant and x_2 is the mole fraction of the polar components. The larger the dipole moments of the polar components are, the larger are the deviations and the larger the shift of x_{max}, x_{max} designating the concentration where these quantities are maximum.

The electrostatic part of the excess entropy of mixing for 1 mol. of the mixture shows a specific behavior. For the systems containing polar components of small dipole moments, they are positive over the whole concentration, but for those of large dipole moments, the values are negative over the range of larger values of x_2, and rapidly increase and take very large positive values as x_2 decreases.

It is naturally expected that these values do not differ so much if the non-polar component, cyclohexane, is replaced by toluene, because of the similar dielectric constant, since according to the assumption of the theory the values are the function of dielectric constant only.

The calculated values of the electrostatic part of van Laar coefficients α^{el}_{calcd} were also calculated by the relation: $\alpha^{el}_{calcd} = H^{Eel}_{calcd}/v_2(1-v_2)\cdot V$, where V is the molar volume of the mixture. They are shown in Tables IV and V.

It is seen from the results that the values of α^{el}_{calcd} are positive and increase with the decrease of concentration x_2 of polar component, and the larger the dipole moments, the larger the values of α^{el}_{calcd} as well as their variations with concentration.

Summary

The electrostatic part of the excess functions for 21 binary systems consisting of polar and non-polar liquids were calculated according to Onsager's model. The electrostatic part of the excess free energy and excess enthalpy are positive over all the concentrations for all of these systems and these quantities are unsymmetric with regard to the mole fractions x against the value at the point $x=0.5$.

The concentrations x_{max} where these quantities have maximum values, shift to a lower concentration of polar component. The larger the dipole moment of the polar components, the larger the maximum values and the shifts are. The electrostatic part of excess entropies have positive values over the whole concentration for systems consisting of a polar component of small dipole moment, but for those consisting of one with a larger dipole moment, these quantities take negative values for a high concentration of polar component, but take positive values for a low concentration range. The electrostatic part of van Laar coefficients is also calculated and these values increase with the decrease of concentration of polar component.

The author wishes to express his thanks to Professor R. Fujishiro of Osaka City University and to Professor Yonezo Morino of the University of Tokyo for their constant encouragement and discussions.

Government Chemical Industrial Research Institute
Shibuya-ku, Tokyo

Studies on the Mechanism of Rearrangement Reaction of 2-Phenyl-4-bromotropone to 2-Phenylbenzoic Acid[1]

By Yoshio KITAHARA, Ichiro MURATA and Tadashi MUROI*

(Received January 26, 1961)

It had been found in the early period of studies on troponoid chemistry that the tropone derivatives having the halogen or methoxyl group in the 2-position undergo rearrangement to benzoic acid derivatives when treated with bases[2]. This rearrangement reaction has often been utilized for deriving unknown troponoid to known benzene derivatives to determine the position of various substituents in the seven-membered ring by the organic chemical method[2].

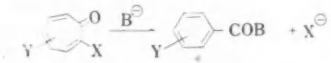

X = halogen, methoxyl

Two kinds of mechanism may be considered for this rearrangement reaction. One, route-A, involves the attack of the base on the carbonyl carbon (C-1), followed by ring contraction concerted with liberation of the substituent in C-2 as an anion[3]. The other, route-B, is the attack of the base on C-2 and subsequent rearrangement[4]. If the rearrangement proceeds through route-A, the carbon atom in the carboxyl group of the benzoic acid produced corresponds to the carbonyl carbon of tropone, and if the reaction goes through route-B, it will be the carbon atom at C-2 of the tropone. An investigation of the rearrangement with carbonyl-labeled 2,7-dibromo- and 2,4,7-tribromotropone proved that the modified mechanism of route-A is the correct one[5].

One of the authors (T. M.) found that the product obtained by treatment of 2-phenyl-4-bromotropone (I) with alkali was unexpectedly 2-phenylbenzoic acid (III), the same as the rearrangement product of 2-phenyl-7-bromotropone (II)[6].

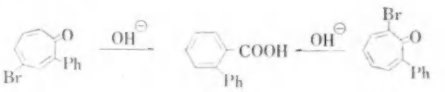

I III II

Differing from II, I does not possess any group easily liberated as an anion at the carbon adjacent to the carbonyl group and the rearrangement product, III, no longer possesses bromine atom. Consequently, the mechanism proposed by Doering and Denney[5] cannot be applied to this rearrangement reaction.

The following mechanism was considered for this abnormal rearrangement reaction and tracer technique using heavy water was utilized to prove this assumption.

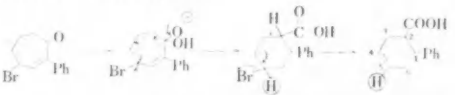

If the rearrangement proceeds through this route, the reaction carried out in a system containing deuterium as an origin of hydrogen should give a product with the carbon-bound deuterium only in the 5-position of the biphenyl formed.

A solution of I dissolved in a solution of deuterium oxide[7], sodium hydroxide-*d*, and methanol-*d*[8] was refluxed for 30 min. and 2-phenylbenzoic acid was isolated from the acid portion. To remove deuterium from the carboxyl group, the acid was converted into its methyl ester with diazomethane and the ester was hydrolyzed to deuterated 2-phenylbenzoic acid (III) of m. p. 108~110°C[9]. The

1) Paper read at the Tohoku Local Meeting of the Chemical Society of Japan, Akita, October, 1959.

* Present address: Hitachi Research Laboratory, Hitachi Ltd., Sukekawa-machi, Hitachi, Ibaraki.

2) T. Nozoe, *Sci. Repts. Tohoku Univ., I*, **34**, 199 (1950); T. Nozoe, *Nature*, **167**, 1055 (1951); J. W. Cook and J. D. London, *Quart. Revs. (London)*, **5**, 99 (1951); P. L. Pauson, *Chem. Revs.*, **55**, 9 (1950).

3) W. von E. Doering and L. H. Knox, *J. Am. Chem. Soc.*, **73**, 828 (1951); T. Nozoe, Y. Kitahara and S. Masamune, *Proc. Japan Acad.*, **27**, 649 (1951); Y. Kitahara, *Sci. Repts. Tohoku Univ., I*, **39**, 250 (1956).

4) W. von E. Doering and L. H. Knox, *J. Am. Chem. Soc.*, **74**, 5683 (1952).

5) W. von E. Doering and D. B. Denney, ibid., **77**, 4619 (1955).

6) T. Muroi, *J. Chem. Soc. Japan, Pure Chem. Sec. (Nippon Kagaku Zasshi)*, **80**, 303 (1959).

7) Norsk Hydro-electrisk; purity, 99.78%. d_4^{20} 1.10514.

8) D. H. Hill, B. Stewart, S. W. Kantor, W. A. Judge and C. R. Hauser, *J. Am. Chem. Soc.*, **76**, 5129 (1954).

9) Under this rearrangement condition, 2-phenylbenzoic acid was proved to be free from secondary deuteration on aromatic nucleus, since the infrared absorption spectrum of the product obtained by treatment of 2-phenylbenzoic acid under the same conditions as for rearrangement of I was identical with that of the original substance. D. J. G. Ives (*J. Chem. Soc.*, **1938**, 81) also reported that deuteration did not take place on the benzene ring when benzoic acid was treated in a deuterium oxide-sodium hydroxide-*d* system.

TABLE I. COMPARISON OF INFRARED ABSORPTION BANDS OF DEUTERATED COMPOUNDS AND CORRESPONDING NON-DEUTERATED COMPOUNDS*

III'	III	IV'	IV	V'	V
3070	3065	3370	3370	3275	3270
3030		3175	3175	3230	3215
2890	2920	3055		3020	3010
2655	2670				
2520	2525				
	2280				
1949	1955				
1692	1695	1692	1692	1658	1658
1601	1597	1640	1640		1598
	1502	1619	1618	1587	1583
1483	1481	1602	1594	1533	1530
1456	1450	1582	1578	1497	
1445			1498	1477	1473
1408	1412	1482	1477	1453	1444
	1400	1455		1437	
1290	1282	1442	1447		1403
1260	1252		1418	1372	1370
1180	1182	1400		1303	1303
1164			1383		1287
1139	1143	1150	1150	1254	1248
	1110	1112	1111	1157	1154
1094		1075	1074		1125
1073	1073	1010	1005	1112	
1047	1049	957		1073	1073
1007	1003		905	1047	1051
929			860	1010	1004
910	908	841		975	975
	884	800	800	941	
	856	778	774	922	916
694	694	743	751		904
673	673		725		832
654	651	696	696	776	772
			670	756	
				742	740
				705	701
				662	655

* IR spectra are measured using a Perkin-Elmer Model 21 double beam spectrophotometer in KBr pellet.

infrared absorption spectrum of III (Table I.) was different from that of III'[10], and this fact indicated that it contained the deuterium atom.

In order to determine the position of the deuterium atom in III, the following reaction was carried out. III was allowed to react with thionyl chloride at room temperature and the resulting acid chloride, treated with ammonia water, gave the amide (IV), m. p. 172.5~173°C. The Hofmann reaction of IV by the method of

III: X=COOH, Y=D
IV: X=$CONH_2$, Y=D
V: X=$NHCOCH_3$, Y=D
VI: X=$NHCOCH_3$, Y=Br
III': X=COOH, Y=H
IV': X=$CONH_2$, Y=H
V': X=$NHCOCH_3$, Y=H

Graebe[11] yielded the corresponding amine and the product was acetylated to give deuterated 2-acetamidobiphenyl (V), m. p. 113~114°C. The infrared absorption spectra of IV and V so obtained (Table I) and determination of deuterium by mass analysis (cf. Experimental) indicated that the deuterium atom has remained during the series of these reaction steps.

Bromination of V and V' with 1 mol. of bromine in glacial acetic acid gives the known 2-acetamido-5-bromobiphenyl (VI)[12] of m. p. 127.5~128.5°C in a quantitative yield from both. The infrared absorption spectra of VI derived from both V and V' were entirely identical, indicating that the deuterium atom in V had been substituted with a bromine atom in this bromination procedure. VI is a known substance and the position of its bromine atom has already been determined. These facts have proved that the deuterium atom in II, IV and V is in 5-position in the biphenyl ring and, consequently, the reaction mechanism assumed for this abnormal rearrangement might be proved to be correct.

Experimental[13]

Rearrangement Reaction of 2-Phenyl-4-bromotropone (I) in Heavy Water System.—To a solution of sodium (1.38 g.) dissolved in methanol-*d* (35 ml.), deuterium oxide (25 ml.) and I (4.9 g.) were added and the mixture, provided with a calcium chloride tube, was refluxed for 30 min. on a water bath. Methanol was evaporated in a reduced pressure, the residue was diluted with 10 ml. of water, and extracted with chloroform to remove the neutral portion. The aqueous layer was acidified with hydrochloric acid to Congo red, the precipitated acid portion was extracted with chloroform, and the extract was washed with water. After drying over magnesium sulfate, chloroform was evaporated from the extract and the residue was sublimed in reduced pressure, from which 2.3 g. of crude crystals, m. p. 99~104°C, was obtained.

Without further purification, this product was dissolved in ether and ether solution of diazomethane was added to effect esterification. The residue obtained on evaporation of ether was dissolved in ethanol (30 ml.), 2 N sodium hydroxide (10 ml.) was added, and the mixture was refluxed

10) The same reaction was carried out in parallel, using 2-phenylbenzoic acid synthesized from fluorene[11]. The compounds not containing deuterium are represented by the same compound number as the corresponding deuterated compounds but with a prime.

11) C. Graebe and A. S. Rateanu, *Ann.*, **279**, 257 (1894).

12) H. A. Scarborough and W. A. Waters, *J. Chem. Soc.*, **1927**, 89.

13) All melting points are uncorrected.

for 2.5 hr. to effect hydrolysis. Ethanol was evaporated, the residue was acidified with diluted hydrochloric acid extracted with chloroform. The crystals obtained from this extract were sublimed in reduced pressure and afforded 2.15 g. (61.6%) of crystals melting at 95~103°C. Recrystallization from cyclohexane gave III m. p. 108~110°C.

Found: D, 8.93. Calcd. for $C_{13}H_9DO_2$: D, 10.00 atom%.

2-Carbamoylbiphenyl-5-*d* **(IV).**—The addition of thionyl chloride (2 ml.) to III (1.9 g.) resulted in vigorous reaction with evolution of hydrogen chloride. The mixture was allowed to stand at room temperature for 1.5 hr., excess thionyl chloride was distilled off in reduced pressure, and the oily residue was added to 28% ammonia water under ice-cooling, by which white precipitates formed at once. The precipitates were collected and the crude amide (1.8 g) of m. p. 145~158°C so obtained was recrystallized from hydrous ethanol to IV, m. p. 172.5~173°C.

Found: D, 8.37. Calcd. for $C_{13}H_{10}DNO$: D, 9.08 atom%.

2-Acetamidobiphenyl-5-*d* **(V).**—IV (1.75 g.) was triturated with water (10 ml.) in a mortar and transferred to a beaker. A solution of sodium hypobromide, prepared from bromine (1.75 g.), sodium hydroxide (3.5 g.), and water (22 ml.) at 0°C, was added into the beaker with ice-cooling and the mixture was stirred for 1 hr. A trace of insoluble matter was removed by filtration, the filtate was heated at 50~55°C for 1 hr., and submitted to steam distillation. The distillate was extracted with chloroform, the extract was washed with water, dried, and chloroform was evaporated. The residue (1 g.) was dissolved in dehydrated pyridine (3 ml.) and acetyl chloride (0.7 g.) was added dropwise under ice-cooling. The mixture was allowed to stand for 30 min. and poured into 2 N hydrochloric acid containing cracked ice. The crystals that separated out were collected by filtration (1.1 g.), m. p. 104~108°C. Recrystallization from hydrous ethanol gave V, m. p. 113~114°C.

Found: D, 6.60. Calcd. for $C_{14}H_{12}DNO$: D, 7.70 atom%.

2-Acetamido-5-bromobiphenyl (VI).—A solution of bromine (390 mg.) in glacial acetic acid (2 ml.) was added to a solution of V (500 mg.) dissolved in glacial acetic acid (3 ml.), with stirring, and the mixture was allowed to stand overnight. The mixture was then poured into ice-water, and crude crystals (750 mg.) of m. p. 115~118°C were sublimed in reduced pressure. Recrystallization of the sublimate from hydrous ethanol gave V as colorless needles m. p. 127.5~128.5°C.

Found: C, 57.64; H, 4.40; N, 4.37. Calcd. for $C_{14}H_{12}ONBr$: C, 57.93; H, 4.17; N, 4.83%.

The determination of deuterium by mass analysis was carried out by Dr. Sumio Horibe, Faculty of Science, Tokyo Metropolitan University, and the infrared spectral measurement was made by Mr. Hideji Aono of this Institute, to both of whom the authors express their sincere gratitude.

The Chemical Research Institute of Non-Aqueous Solutions
Tohoku University
Katahira-cho, Sendai

Condensation Reaction of Troponoids and Ethyl α-Cyano-β-aminoglutaconate. I

By Shingo MATSUMURA

(Received February 2, 1961)

Nozoe and others have studied the reaction mechanism whereby azulene derivatives are formed by condensation of troponoids and cyanoacetic ester, and have considered the formation of an intermediate A during the course of this reaction[1]. There is also a possibility, in addition to the above mechanism,

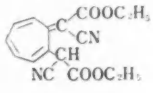

(A)

of formation of a dimer of cyanoacetic ester followed by its condensation with troponoids in the formation of 2-aminoazulene derivatives.

This paper describes some results obtained on examination of this point.

Reaction of 2-chlorotropone (I) and a dimer[2] of ethyl cyanoacetate, i.e. ethyl α-cyano-β-aminoglutaconate (II) in absolute ethanol, in the presence of sodium ethoxide, affords red needles (III), m. p. 165°C, orange scales (IV), m. p. above 260°C, and colorless scales (V), m. p. 197°C. The use of a tertiary amine as the condensation agent results in the formation of III and IV but not of V.

1) T. Nozoe, S. Seto, S. Matsumura and T. Asano, *Proc. Japan Acad.*, **32**, 339 (1956).

2) S. Matsumura, This Bulletin, in press.

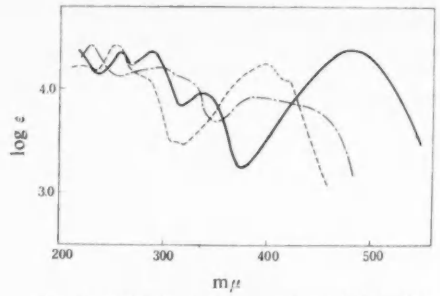

Fig. 1. UV absorption spectra of III, IV and V in methanol.
—— III, ---- IV, -·-· V

Examinations were made on the structure of these products. The ultraviolet absorption spectra[3] of III, IV and V are given in Fig. 1.

These absorption spectra indicate that these products are not 2-aminoazulene derivatives. The analytical values of III correspond to molecular formula of $C_{17}H_{16}O_4N_2$ and structures like IIIa and IIIb may be assumed from this molecular formula.

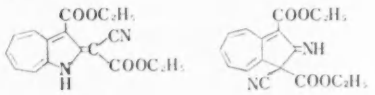

The infrared absorption spectrum[4] of III, as indicated in Fig. 2a, exhibits absorption bands at 3220 cm^{-1} for the imino or hydroxyl group, at 2200 cm^{-1} for the cyano group conjugated with unsaturated bond, at 1688 cm^{-1} for ester carbonyl conjugated with unsaturated bond, and at 1650 cm^{-1} for stretching vibration of ester carbonyl conjugated with unsaturated bond or that due to NH deformation vibration.

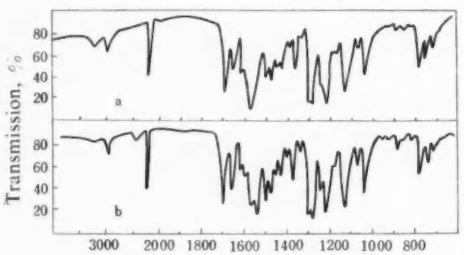

Fig. 2. IR absorption spectra of III (a) and III_D (b) in KBr.

3) Measured by a Beckman Model DU spectrophotometer.

4) IR spectra are measured using a Perkin-Elmer Model 21 double beam spectrophotometer by Mr. S. Aono of this Institute, to whom the author is deeply indebted.

The structure of III which satisfies these infrared spectral results is the formula IIIa.

III undergoes reaction with sodium alkoxide to form a red substance (VI) which is decomposed by water or dilute acid to revert to III. This shows that VI is a sodium salt of III.

III does not form a picrate on addition of an ethanolic solution of picric acid but a prolonged heating of such a solution produces a picrate of m. p. 156°C (decomp.), sparingly soluble in ethanol. III easily reacts with dilute hydrochloric acid to form a labile product of red needles (VII), m. p. 155°C.

Other structurally unknown substances of various colors are obtained but they are all unstable and cannot be isolated in pure form. VII forms a picrate of m. p. 156°C.

The passage of dry hydrogen chloride gas through dehydrated benzene solution of III gives yellow needles (VIII) assumed to be the hydrochloride of III. VIII is extremely labile and decomposes when left in the air. The neutralization of VIII with sodium hydrogen carbonate solution liberates VII, whose ultraviolet absorption spectrum, as indicated in Fig. 3, is similar to that of 1-azaazulene derivatives.

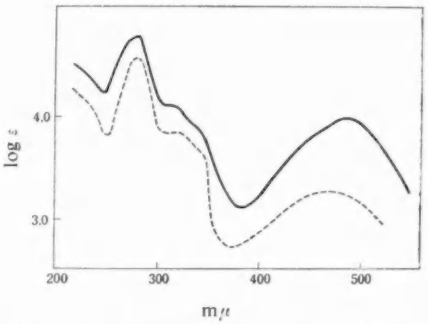

Fig. 3. UV absorption spectra of VII (——) and 3-ethoxycarbonyl-2-(diethoxycarbonylmethyl)-1-azaazulene (----) in methanol.

III is insoluble in water but dissolves in an aqueous solution of potassium hydroxide, from which it is extracted with an organic solvent. These foregoing facts show that III is an amphoteric substance and its behavior resembles that of pyrrole or indole to acids and alkalis.

These experimental results support the structure of IIIa for III.

Recently, Seto and others[5] prepared 2-chloro-3-ethoxycarbonyl-1-azaazulene (X) from 3-ethoxycarbonyl-1-azaazulan-2-one (IX) and

5) S. Seto et al., to be published.

obtained corresponding condensates by condensation of X with diethyl malonate and ethyl cyanoacetate.

Comparative examination of III with the condensate, m. p. 165°C, of X with ethyl cyanoacetate showed that they are the same substances. Consequently, III was proved to have IIIa structure, i. e. 2-(cyano-ethoxycarbonylmethylene)-3-ethoxycarbonyl-1-azaazulane.

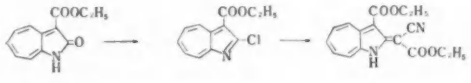

IX X III

Further examination was made on the absorption band at 1650 cm^{-1} in the infrared spectrum of III to see whether it is due to the ester carbonyl conjugated with unsaturated bond, stretching vibration of C=C, or to deformation vibration of N–H group. In order to confirm this point, a deuterated compound (III_D) of III was prepared.

III_D was easily obtained on decomposition of VI with deuterium oxide. Admixture of III_D with III showed no depression in the melting point and the ultraviolet absoption spectrum of III_D in anhydrous cyclohexane agreed with tnat of III. The infrared spectrum of III_D, indicated in Fig. 2b, shows that the absorption bands at 3220, 1225 and 710 cm^{-1} in III have disappeared and new bands have appeared at 2420, 1533 and 1186 cm^{-1} in the spectrum of III_D, with decreased intensity of the absorption band at 1563 cm^{-1}.

The wave number ratio of 3220 cm^{-1} in III and 2420 cm^{-1} in III_D is 1.330, which approximately agrees with the usual value of $\nu(N-H)/\nu(N-D)$[6]. Since the absorption band at 710 cm^{-1} in III is active to deuteration, this absorption can be assigned to the out-of-plane deformation vibration of the N–H group. The absorption band at 1650 cm^{-1} in III is still present in III_D so that it is not due to any deformation vibration of the N–H group but should be the stretching vibration of ester carbonyl or the exo-methylene group. If it were due to the carbonyl, the absorption has a very much lower frequency for that of unsaturated ester carbonyl. This fact indicates that there is a large contribution of ionic structures such as those shown in Scheme 1 in III.

In oder to determine the assignment of absorption bands at 1688 and 1650 cm^{-1}, 2-(dicyanomethylene)-3-ethoxycarbonyl-1-azaazulane (XI) and 2-(cyano-ethoxycarbonylmethylene)-3-cyano-1-azaazulane (XII) were prepared and their infrared spectra were measured. Condensation of X and sodiomalononitrile in dry dioxane afforded lustrous red crystals XI, m. p. above 260°C.

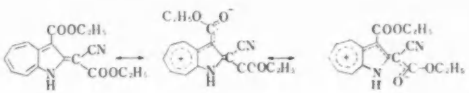

Scheme 1.

Condensation of 2-chloro-3-cyano-1-azaazulene (XIII) and ethyl sodiocyanoacetate in dehydrated dioxane produced dark red crystals (XII), m. p. 230°C. The ultraviolet absorption spectra of XI and XII are indicated in Fig. 4 and the infrared spectra of XI and XII are shown respectively in Fig. 5a and b. These infrared spectra exhibit an absorption band due to ester carbonyl at 1690 cm^{-1} in XI and at 1645 cm^{-1} in XII.

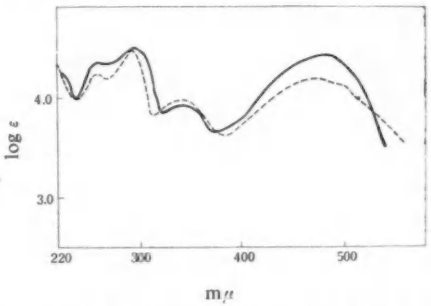

Fig. 4. UV absorption spectra of XI and XII in methanol.
—— XI, ---- XII

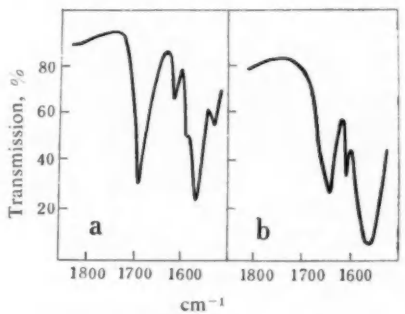

Fig. 5. IR absorption spectra of XI (a) and XII (b) in KBr disk.

These facts prove that the absorption band at 1688 cm^{-1} in III is due to the carbonyl group in the ester at 3-position and that at 1650 cm^{-1} is the absorption of the ester carbonyl group bonded to the methylene group

6) L. J. Bellamy, "The Infrared Spectra of Complex Molecules", Methuen (1958), p. 257.

and that it is not due to the stretching vibration of exo-methylene.

Analytical values of IV correspond to the molecular formula of $C_{15}H_{12}O_4N_2$ and its ultraviolet spectrum is similar to the absorption curve of 1-oxaazulan-2-one or 1-azaazulan-2-one derivatives. The infrared spectrum of IV, as indicated in Fig. 6a, exhibits the absorptions at 3380 and 3278 cm^{-1} for primary amino group, at 2205 cm^{-1} for cyano group conjugated with unsaturated bond, at 1740 cm^{-1} for carbonyl in unsaturated γ-lactone, and at 1675 cm^{-1} for ester carbonyl conjugated with unsaturated bond. From these results, IV is assumed to be a 1- oxaazulan-2-one derivative.

Seto obtained 1-oxaazulan-2-one (XIV), by decomposition of 3-ethoxycarbonyl-1-oxaazulan-2-one or 3-acetyl-1-oxaazulan-2-one with concentrated sulfuric acid.[7]

The same decomposition of IV with concentrated sulfuric acid afforded XIV, m. p. 69°C, and this has proved that IV is α-amino-α-(1-oxaazulan-2-on-3-yl)-β-cyano-β-ethoxycarbonyl-ethylene.

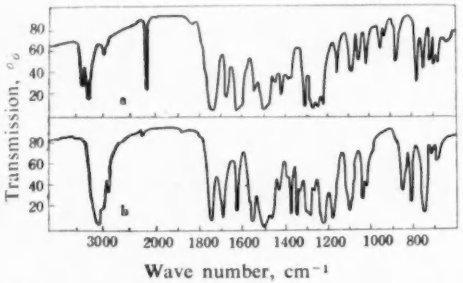

Fig. 6. IR absorption spectra of IV(a) and V(b) in KBr disk.

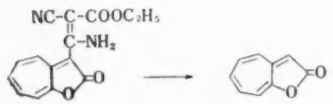

IV XIV

Analytical values of V correspond to the molecular formula of $C_{17}H_{18}O_5N_2$ and the infrared spectrum of V, indicated in Fig. 6b, exhibits a strong and broad absorption band at around 3100 cm^{-1}, absorption of cyano group at 2260 cm^{-1}, that of ester carbonyl at 1740 cm^{-1}, and that due to ester carbonyl conjugated with unsaturated bond at 1688 cm^{-1}.

Sometimes V is not obtained by condensation of I and II and the yield of V is generally poor. Further examination of this product was not made.

7) S. Seto, *Sci. Repts. Tohoku Univ.* (*I*), 37, 367 (1953).

Reaction of 2-methoxytropone (XV) and II in the presence of an alkoxide results in almost complete recovery of XV and III, IV and V are not obtained.

From the foregoing results, it was shown that 2-aminoazulene derivative was not formed in the condensation of troponoids with II.

Experimental

Reaction of 2-Chlorotropone (I) and Ethyl α-Cyano-β-aminoglutaconate (II).—a) To a solution of sodium ethoxide, prepared from 250 mg. of metallic sodium and 10 ml. of absolute ethanol, 2.45 g. of II was added and a solution of 1.5 g. of I dissolved in 30 ml. of absolute ethanol was added to it with stirring under ice-cooling. The solution colored red immediately. The mixture was allowed to stand at room temperature for 3 hr. and the red crystals that separated out were collected by filtration. The collected crystals were dissolved in benzene to separate them from colorless inorganic salt and evaporation of benzene left red crystals of m. p. 155~159°C. Repeated recrystallization from ethanol afforded 800 mg. of red needles (III), m. p. 163~165°C.

The reaction mixture left after the removal of the above crystals was evaporated to dryness under reduced pressure and the residue separated into crystalline and oily substances. This residual mixture was dissolved in benzene to be separated into benzene-soluble and insoluble portions.

The benzene-soluble portion afforded 350 mg. of III.

Found: C, 65.52; H, 5.38; N, 8.56. Calcd. for $C_{17}H_{16}O_4N_2$: C, 65.37; H. 5.16; N, 8.97%.

UV λ_{max}^{MeOH} mμ (log ε): 260 (4.32), 289.5 (4.37), 340 (3.98), 490 (4.37).

Addition of water to the benzene-insoluble portion precipitated 200 mg. of orange crystals insoluble in water. This substance is extremely sparingly soluble in various organic solvents. Its recrystallization from a large quantity of chloroform afforded orange-yellow scales (IV), m. p. above 260°C.

Found: C, 63.58; H, 4.01; N, 9.85. Calcd. for $C_{15}H_{12}O_4N_2$: C, 63.38; H, 4.26; N, 9.86%.

UV λ_{max}^{MeOH} mμ (log ε): 254 (4.43), 282 (4.14), 399 (4.27).

The water-soluble portion of this mixture produced, upon neutralization with dilute nitric acid, 750 mg. of brown precipitate and five recrystallizations from ethanol afforded 150 mg. of colorless scales V, m. p. 195~197°C.

Found: C, 61.85; H, 5.71; N, 8.83. Calcd. for $C_{17}H_{18}O_5N_2$: C, 61.81; H, 5.49; N, 8.48%.

UV λ_{max}^{MeOH} mμ (log ε): 230 (4.43), 300 (4.21), 388 (3.92).

b) To a solution of 1 g. of I and 1.7 g. of II dissolved in 30 ml. of absolute ethanol, 1.4 g. of tributylamine was added under ice-cooling and the solution changed from orange to red. After allowing the mixture to stand for 5 hr. at room

8) All melting points are uncorrected. The microanalyses were carried out by Mr. S. Ohyama and Miss. Y. Ende of this Institute, to whom the author is deeply indebted.

temperature, the red leaflet crystals that separated out were collected by filtration and treated with chloroform to be separated into chloroform-soluble and insoluble portions.

Red needle crystals separated from the chloroform-soluble portion and recrystallization from ethyl acetate gave 550 mg. of III. The solid sparingly soluble in chloroform was recrystallized from a large quantity of chloroform to 420 mg. of orange-yellow crystals IV.

The reaction mixture after separation of the above products was evaporated, the residue was dissolved in chloroform, and the solvent was evaporated to dryness from the chloroform extract. The red crystalline residue thereby obtained was recrystallized from ethanol to 140 mg. of III.

Sodium Compound (VI) of III.—A solution of sodium ethoxide, prepared from 10 mg. of metallic sodium and 1 ml. of absolute ethanol, was added to the solution of 100 mg. of III dissolved in 1 ml. of dehydrated benzene by which 100 mg. of amorphous orange-red solid (VI), m. p. above 260°C, formed immediately. The solid was collected, washed with benzene, and dried.

VI was dissolved in water and extracted with benzene. The benzene extract was dried over anhydrous sodium sulfate and evaporation of benzene left 70 mg. of III. The residual aqueous solution was adjusted to pH 7 and extracted with benzene. The benzene extract was dried over anhydrous sodium sulfate and evaporated, leaving 20 mg. of III.

Found: N, 8.46. Calcd. for $C_{17}H_{15}O_4N_2Na$: N, 8.35%.

Reaction of III and Picric Acid.—a) A mixture of 50 mg. of III and saturated solution of picric acid in ethanol was warmed on a water bath to effect solution and the solution was allowed to stand at room temperature. The red needle crystals that separated out were recrystallized from ethyl acetate and 40 mg. of III was recovered.

b) A mixture of 50 mg. of III and 100 mg. of picric acid was placed in a test tube and the tube was heated in a water bath at 90°C to effect solution. Addition of ethanol to this solution separated 120 mg. of orange-yellow crystals, m. p. 156~158°C (decomp.), sparingly soluble in ethanol.

Found: N, 12.81. Calcd. for $C_{23}H_{19}O_{11}N_5$: N, 12.79%.

Action of Aqueous Alkali Solution on III.—A solution of 20 mg. of III dissolved in 1 ml. of 10% potassium hydroxide aqueous solution was heated on a water bath for 1 hr., cooled, and adjusted to pH 7. The red crystals thereby produced were recrystallized from ethanol and ca. 15 mg. of III was recovered.

Action of Acetic Anhydride on III.—A solution of 50 mg. of III dissolved in 1 ml. of acetic anhydride to which was added 1 drop of pyridine was heated at 120°C for 3 hr. Acetic anhydride was evaporated and the residue was recrystallized from ethanol, by which 30 mg. of III was recovered.

Action of Diazomethane of III.—The excess of ether solution of diazomethane was added to the solution of 20 mg. of III dissolved in 30 ml. of ether and the mixture was allowed to stand at room temperature for 4 hr. Evaporation of ether left crystals which were recrystallized from ethyl acetate and III was recovered.

Action of Acid on III.—a) Dropwise addition of 0.2 ml. of 2 N hydrochloric acid to a solution of 50 mg. of III dissolved in 1 ml. of ethanol by application of heat resulted in yellowing of the solution. Ethanol was evaporated from this mixture, the residue was neutralized with sodium hydrogencarbonate solution, and the dark red precipitate that formed was extracted with benzene. The benzene extract was dried over anhydrous sodium sulfate and passed through a column of alumina, by which the product separated into red, blue and green bands.

Elution of the red band with benzene afforded ca. 5 mg. of red leaflets VII, m. p. 153~155°C.

Elution of the green band with ethyl acetate failed to give any crystalline product.

VII formed a picrate of m. p. 156~158°C on addition of saturated ethanol solution of picric acid.

Found: N, 13.02. Calcd. for $C_{23}H_{19}O_{11}N_5$: N, 12.79%.

b) Dry hydrogen chloride gas was passed through a solution of 50 mg. of III dissolved in dehydrated benzene and the yellow needle crystals (VIII) that separated out were collected by filtration. This product underwent a change by atmospheric moisture. The product was dissolved in water, neutralized with sodium hydrogencarbonate, and the precipitate was extracted with benzene from which 10 mg. of a substance agreeing with VII, m. p. 153~155°C, was obtained.

Deuterated Compound (III_D).—A solution of 100 mg. of VI dissolved in 1 ml. of deuterium oxide to which was added 1 drop of acetic anhydride was allowed to stand at room temperature for 1 hr. The red needle crystals that separated out were recrystallized from dehydrated benzene-cyclohexane mixture and 60 mg. of III_D, m. p. 163~164°C, undepressed on admixture with III, was obtained.

Synthesis of 2-(Dicyanomethylene)-3-ethoxycarbonyl-1-azaazulane (XI).—To a sodium ethoxide solution prepared from 50 mg. of metallic sodium and 2 ml. of absolute ethanol, 250 mg. of malononitrile was added to form its sodio compound and ethanol was evaporated completely. The residue was suspended in 2 ml. of dehydrated dioxane, 250 mg. of 2-chloro-3-ethoxycarbonyl-1-azaazulene (X) was added to it, and the mixture was heated at 90°C for 1 hr. The reaction mixture colored dark red and orange precipitate separated gradually. Dioxane was evaporated from this mixture, the residue was dissolved in water, and the solution was acidified with acetic acid by which a lustrous crystalline precipitate was produced. Recrystallization from acetone gave 120 mg. of lustrous red crystals XI, m. p. above 260°C.

Found: C, 67.74; H, 4.08; N, 15.98. Calcd. for $C_{15}H_{11}O_2N_3$: C, 67.91; H, 4.18; N, 15.84%.

UV λ_{max}^{MeOH} mμ (log ε): 259 (4.23), 295 (4.47), 340 (3.92), 483 (4.43).

Synthesis of 2-(Cyano-ethoxycarbonylmethylene)-3-cyano-1-azaazulane (XII).—To a suspension of 50 mg. of sodium in 2 ml. of dehydrated dioxane,

400 mg. of ethyl cyanoacetate was added and the mixture was warmed to form the sodio compound. A mixture of this sodio compound and 200 mg. of 2-chloro-3-cyano-1-azaazulene (**XIII**) was heated at 90°C for 1 hr., by which the solution became dark red and a reddish orange precipitate began to separate out. Dioxane was evaporated, the residue was dissolved in water, and the aqueous solution was acidified with acetic acid. The dark red precipitate thereby formed was recrystallized from acetone and 280 mg. of dark red needles XII, m. p. 230°C (decomp.), was obtained.

Found: C, 67.83; H, 4.26; N, 15.67. Calcd. for $C_{15}H_{11}O_2N_3$: C, 67.91; H, 4.18; N, 15.84%.

UV λ_{max}^{MeOH} $m\mu$ (log ε): 256 (4.21), 293 (4.46), 340 (3.80), 490 (4.18).

Formation of 1-Oxaazulan-2-one (XIV). — A solution of 100 mg. of IV dissolved in 0.2 ml. of concentrated sulfuric acid was heated on a water bath for 1 hr. and the brownish orange solution that formed was diluted with water. This was extracted with benzene, the extract was washed thoroughly with water, and dried over anhydrous sodium sulfate. Evaporation of benzene left an oily substance with aroma.

This residue was digested with hot cyclohexane, the orange crystals thereby obtained were sublimed in reduced pressure, and the sublimate was recrystallized from cyclohexane, affording XIV, m. p. 69~71°C.

The author takes this opportunity to express his sincere gratitude to Professor Tetsuo Nozoe and Professor Shuichi Seto for their kind guidance throughout the course of this work, and to Mr. Fumio Sato for his cooperation in carrying out the experiments.

The Chemical Research Institute of Non-Aqueous Solutions
Tohoku University
Katahira-cho, Sendai

Studies on Micro-paraffin. III. Properties and Spectra of Each Fraction of Micro-paraffin Separated by Urea Method and Chromatography

By Kazuo NEGORO

(Received December 20, 1960)

Since Bengen's discovery in 1940[1,2], it has been observed with interest that crystalline molecular compounds, that is to say, urea adductible components, were formed by urea and organic compounds of straight-chain structure and numerous studies on this reaction have been reported. The application of this reaction has been remarkably developed as one of the excellent separation methods of organic compounds[3]. Phillips[4] explained that 20~90% of urea adductible compenents were contained in microcrystalline waxes.

Molecular compounds, formed by urea and ordinary paraffin waxes, were previously reported[5,6], and the studies on micro-paraffins will be explained in this report. The micro-paraffin was separated into two groups of compounds; one was of the straight-chain structure forming adducts with urea and the other was of the non-straight-chain structure forming no adducts. Then, each group was separated into three fractions soluble in pentane, benzene, and alcohol, successively, by chromatography with silica gel. The crystal properties of each soluble fraction were studied and its ultraviolet and infrared absorption spectra were measured.

As a result of these experiments, it was confirmed that it was reasonable to consider that the cause of the micro-crystallization of the so-called micro-paraffin should be not essential, but derived by secondary factor. It was also confirmed that about 60% of the micro-paraffins obtained from the tank residue of Arabian crude oil (Aramo oil in Saudi-Arabia)[7] consisted of urea adductible paraffins which had higher melting points and lower refractive indices than those of non-adductible ones. However, it was found when the ultraviolet spectra of each soluble fraction was separated by chromatography that small quantities of various aromatics were mixed with the fractions and an absorption band due to the double band was observed on the infrared

1) F. Bengen, German Pat. O. Z 12438 (1940).
2) F. Bengen, *Angew. Chem.*, **63**, 207 (1951).
3) "The Chemistry of Petroleum Hydrocarbons" (Sekiyu Tankasuiso Kagaku) I, Kyoritsu Shuppan Co., Tokyo (1956), p. 26.
4) J. Phillips, *Petroleum Refiner*, **38**, No. 9, 193 (1959).
5) E. Kuraku, S. Yagi and K. Negoro, *Science* (*Kagaku*), **22**, 216 (1952).
6) E. Kuraku, S. Yagi and K. Negoro, ibid., **22**, 363 (1952).
7) K. Negoro, *J. Chem. Soc. Japan, Ind. Chem. Sec.* (*Kogyo Kagaku Zasshi*), **64**, 295 (1961).

spectrum of the benzene soluble fraction. After recrystallization of each fraction with ethyl alcohol, it was observed by the microscope that the adductible paraffin formed plate crystals, and the fractions soluble in pentane and benzene separated from micro-paraffin by chromatography also formed plate crystals. These phenomena were proved by the infrared spectra indicating that each fraction showed the characteristic crystal band[8] in the wavelength of 13.7~13.9 μ (wave number of 730~710 cm^{-1}).

On the contrary, the non-adductible paraffin showed a micro-crystalline state; the only exception was the pentane soluble fraction separated from non-adductible micro-paraffins by chromatography, which formed plate crystals.

Experimental

Formation of Urea Adducts.—Micro-paraffin was dissolved in benzene and treated with solid urea. The activators for the reaction were water and methyl alcohol. The formed molecular compounds of urea and straight chain paraffins (urea adducts) were separated from the non-adductible paraffin with urea by a suction filter with a vacuum pump.

The adducts were dried to constant weight watching the temperature to avoid decomposition, and finally, were decomposed with hot water. The adductible paraffins were separated from urea by dissolving them in hot water.

They were separated by filtration as they solidified with the drop of temperature. They were completely dried in a desiccator and weighed. The so-called urea reject or adductible paraffin, was weighed after benzene, methyl alcohol and water were expelled by solvent recovery apparatus. The conditions of the experiments are shown in Table I.

TABLE I. UREA ADDUCTS REACTION

Micro-paraffin	112.5 g.
Benzene	1700 cc.
Urea	450.0 g.
Methyl alcohol for activator	45 cc.
Water	4.5 cc.
Reaction temp.	33°C
Reaction time	50 min.
Drying temp. of adducts	35~45°C
Drying time of adducts	60 hr.
Hot water	6000 cc.
Temp. of hot water	70~80°C

The materials used in the experiment were as follows:

Methyl alcohol: b. p. 65°C, refined from commercial first grade product by distillation.

Benzene: b. p. 80°C, refined from commercial product by ordinary method[9].

Urea: m. p. 132.6°C, refined by recrystallization method.

Chromatography. — Each of the adductible and non-adductible paraffins was dissolved in a large quantity of pentane.

Twenty grams of the adductible paraffin was weighed out and dissolved in 16 l. of pentane; and 20 g. of the non-adductible paraffin was weighed out as above and dissolved in 12 l. of pentane.

Each of the two was charged into the column for chromatography, and treated with pentane, benzene, and ethyl alcohol to be separated into their soluble fractions.

The column used was a glass tube of 160 cm. in length and 6 cm. in diameter, and packed with 3 kg. of 80 mesh silica gel that had been dried for 8 hr. at 120°C.

Measurement of Physical Properties. — *Mean Molecular Weight.*—Measured by the depression of freezing point[10] in refined benzene.

Melting Point.—Measured by the method of dropping point[11].

Refractive Index.—Measured by an Abbe refractometer at 70°C (higher than melting point of paraffins).

Observation of Crystals[12].—The adductible and non-adductible paraffins and their pentane, benzene and ethyl alcohol soluble fractions separated by chromatography were recrystallized with solvent (ethyl alcohol; b. p. 78°C). The crystals were observed with ordinary or phase-contrast microscopes. One gram of each paraffin sample was dissolved in 300 cc. of ethyl alcohol and the solution was warmed to 70°C in a thermostat. Then, it was gradually cooled to room temperature and recrystallized.

Measurement of Ultraviolet Absorption Spectrum. — A photo-electric spectrophotometer of Type EPU-2 manufactured by Hitachi Mfg., Co. was used for the measurement of ultraviolet absorption spectrum. About 0.5 g. of the sample was taken and weighed accurately, and then dissolved in 5 g. of refined *n*-hexadecane to make up the solution of concentration of 10 wt. %. The solution was diluted to a tenth its former strength by the weighing method, successively, to make concentrations of 1, 0.1 and 0.01%. The ultravioled spectra of these solutions were measured at room temperature. *n*-Hexadecane, refined from commercial special grade product by the same process as the previous report[13], was confirmed to be fit for a diluent by measuring the degree of transparency in the range of wavelength of 220~420 mμ.

8) K. Negoro, *J. Chem. Soc. Japan, Pure Chem. Sec.* (*Nippon Kagaku Zasshi*), **82**, 229 (1951)..

9) "Text-book of Chemical Experiment" (Jikken Kagaku Koza) 2 (Fundamental Technique II), Maruzen, Tokyo (1956), p. 73.

10) J. Sameshima, "Experimental Methods of Physical Chemistry" (Butsuri Kagaku Jikkenho), Shokabo, Tokyo (1941), p. 227.

11) Nippon Oil Co., "Test-methods of Petroleum" (Sekiyu Shikenho), Sekiyu-keizai-kenkyukai, Tokyo (1954), p. 218.

12) S. Yagi and K. Negoro, *Chem. Ind. Japan* (*Kagaku Kogyo*), **8**, 1112 (1957).

13) K. Negoro, *Report of Central Research Laboratory, Nippon Mining Co.* (*Nikko Chuo Shikenjo Shoho*), **11**, No. 3, 1139 (1960).

Measurement of Infrared Absorption Spectrum. — A infrared spectrophotometer of Perkin Elmer Model-21 was used for the measurement of infrared spectrum. The sample of the adductible or non-adductible paraffins and each fraction separated by chromatography were applied on the spectrophotometer and measured.

Results and Discussions

Results of Urea Adducts Formation. — The micro-paraffins which were obtained from the tank residues of Arabian crude oil were treated with urea, and the results are shown in Table II.

TABLE II. UREA TREATMENT OF MICRO-PARAFFIN

Material	Weight, g.	Yield, %
Micro-paraffin	112.5	100.0
Urea adductible paraffin	69.5	61.8
Urea non-adductible paraffin	33.1	28.9
Loss	9.9	9.3

According to Philips[4], it was reported that micro-crystalline waxes contained 20~90% of urea adductible components. Turner et al.[14] reported that ordinary crystalline waxes contained 80~90% of *n*-paraffin by the results of the examination by mass-spectra on 16 sorts of paraffins. As results of the above reports, it is considered that the so-called micro-paraffins have higher molecular weight than that of the ordinary crystalline waxes and that the former contain side chain substances in a larger amount than the latter. It seems to be reasonable to consider that isoparaffins which have some side chains and the paraffins which have one or two aromatic or naphthene rings form adducts with urea as reported by Zimmerschied[15].

It will not be stated that all the components of such urea adductible paraffins consist of *n*-paraffin alone (small quantities of side-chain paraffins may be contained). The above consideration will also be confirmed by the results of chromatography, ultraviolet spectroscopy, and infrared spectroscopy as mentioned below.

Results of Chromatography and Properties of Each Fraction. — The adductible and non-adductible paraffins were separated by chromatography with silica gel.

The yields of each fraction are shown in Table III.

Great differences of the yields of each fraction were not seen between the two paraffins. However, there were great differences between the results of the physical properties of each fraction as shown in Table IV.

The non-adductible paraffins have higher mean molecular weights, lower melting points, and very much higher refractive indices than the adductible paraffins. Then, it was shown that in micro-paraffins, straight-chain hydrocarbons were separated effectively from substances having side-chains and aromatics.

TABLE III. RESULTS OF CHROMATOGRAPHY

	Micro-paraffin	Urea adductible paraffin	Urea non-adductible paraffin
Pentane soluble fraction	75.4 (76.8)*	79.0 (86.8)	76.5 (84.5)
Benzene soluble fraction	17.0 (17.3)	9.5 (10.4)	9.5 (10.5)
Ethyl alcohol soluble fraction	5.8 (5.9)	2.5 (2.8)	4.5 (5.0)
Loss	1.8 (—)	9.0 (—)	9.5 (—)
Total	100.0 (100.0)	100.0 (100.0)	100.0 (100.0)

* The values in ( ) show the yield (%) of each fraction, from which loss is subtracted.

TABLE IV. PHYSICAL PROPERTIES OF EACH FRACTION

	Mean molecular weight		M. p., °C		Refractive index, n_D^{70}	
	A Urea adductible paraffin	B Urea non-adductible paraffin	A	B	A	B
Base micro-paraffin	613	620	67.0	54.4	1.4400	1.4460
Pentane soluble fraction	607	636	65.0	54.0	1.4390	1.4410
Benzene soluble fraction	591	602	20	20	1.5050	1.5200
Alcohol soluble fraction	636	627	67.0*	46.5*	—**	—**

* Though each fraction was dropped at 57.0 or 46.5°C in measuring, some parts of the residues were solid. It was difficult to determine the melting point.

** Measurements were impossible.

14) W. R. Turner et al., *Ind. Eng. Chem.*, **47**, 1219 (1955).

15) W. J. Zimmerschied et al., ibid., **42**, 1300 (1950).

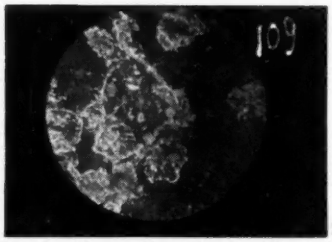

×100

Fig. 1. Urea adductible paraffin (A).

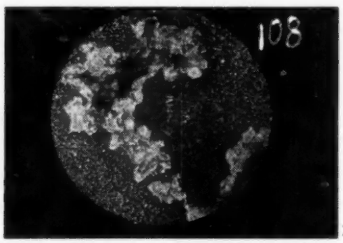

×100

Fig. 2. Urea non-adductible paraffin (B).

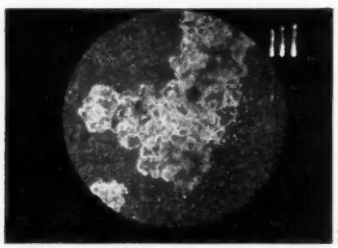

×100

Fig. 3. Pentane franction of A.

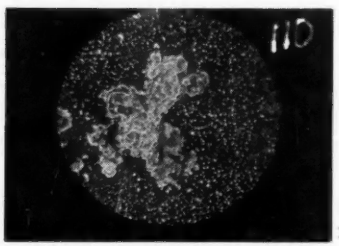

×100

Fig. 4. Pentane fraction of B.

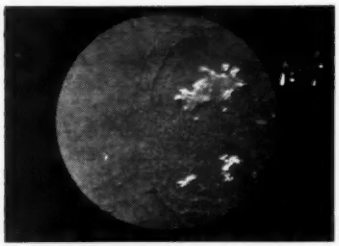

×100

Fig. 5. Benzene fraction of A.

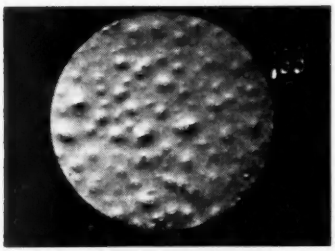

×100

Fig. 6. Benzene fraction of B.

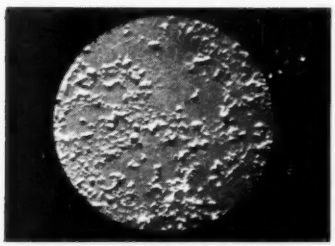

×100

Fig. 7. Alcohol fraction of A.

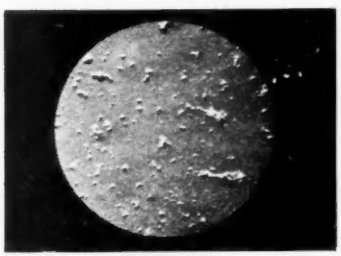

×100

Fig. 8. Alcohol fraction of B.

In particular, by the fact that the non-adductible paraffins have very high refractive indices, it should be suggested that they consist of complicated compounds[16].

It has already been known that hydrocarbons with side-chains and aromatic or naphtheric substances have lower melting points and higher refractive indices[17,18].

16) P. T. Edwards, *Petroleum Refiner*, **36**, 180 (1957).
17) A. N. Sachanen, "The Chemical Constituents of Petroleum", Reinhold Publ. Corp., New York (1945), pp. 289—296.
18) K. Negoro, *Chemistry (Kagaku)*, **15**, No. 5, 16 (1960).

Results of the Observation of Crystals.—Each fraction obtained by chromatography from the non-adductible paraffins was recrystallized with ethyl alcohol and observed through a microscope.

The results of the observation are shown in Figs. 1—8. Figure 1 shows the adductible paraffin which forms plate crystals smaller than those of the ordinary crystalline paraffin wax.

On the other hand, the non-adductible paraffin is in a very micro-crystalline state as shown in Fig. 2.

The growth of plate crystals of the pentane soluble fraction of urea adductible paraffin (Fig. 3) has progressed further than those of base paraffin, and the pentane soluble fraction of urea non-adductible paraffin (Fig. 4) also develops to plate crystals. The benzene soluble fraction of urea adductible paraffin from plate crystals as shown in Fig. 5, but that of urea non-adductible paraffin is microcrystalline as shown in Fig. 6. The ethyl alcohol soluble fractions of the two (adductible and non-adductible) were very fine and amorphous as shown in Figs. 7 and 8. These were very different from the other fractions.

The results of such observations through the microscope conformed to the results of measurement of infrared spectra of each paraffin, and these facts are interesting for the investigation on microcrystallization of micro-paraffin.

Results of Measurement of Ultraviolet Spectrum. — Each fraction of urea adductible or non-adductible paraffins was diluted with *n*-hexadecane, and its degree of transparency

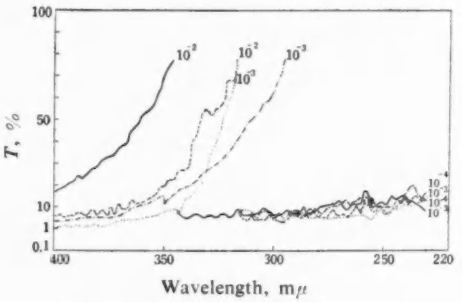

Fig. 9. Urea adductible paraffins.
——— Urea adductible paraffin (A)
– – – – Pentane fraction of A
—·—· Benzene fraction of A
····· Alcohol fraction of A

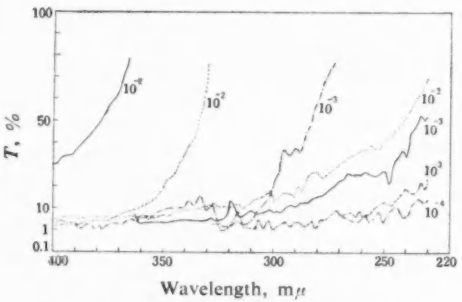

Fig. 10. Urea non-adductible paraffins.
——— Urea non-adductible paraffin (B)
– – – – Pentane fraction of B
—·—· Benzene fraction of B
····· Alcohol fraction of B

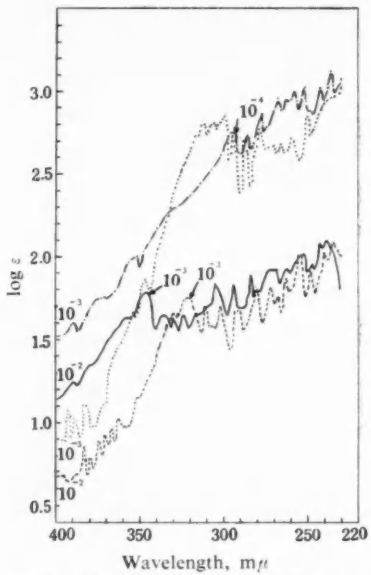

Fig. 11. Ultraviolet spectra of urea adductible paraffins.
——— Urea adductible paraffin (A)
– – – – Pentane fraction of A
—·—· Benzene fraction of A
····· Alcohol fraction of A

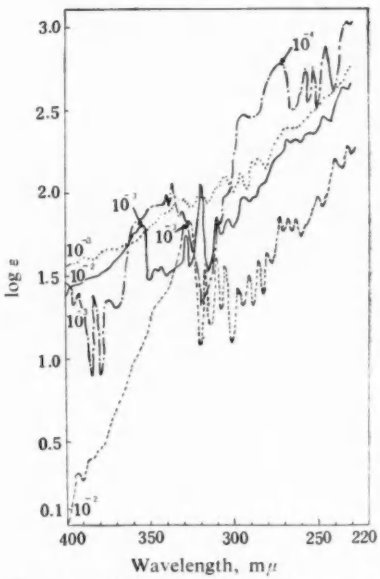

Fig. 12, Ultraviolet spectra of urea non-adductible paraffins.
——— Urea non-adductible paraffin (B)
– – – – Pentane fraction of B
—·—· Benzene fraction of B
····· Alcohol fraction of B

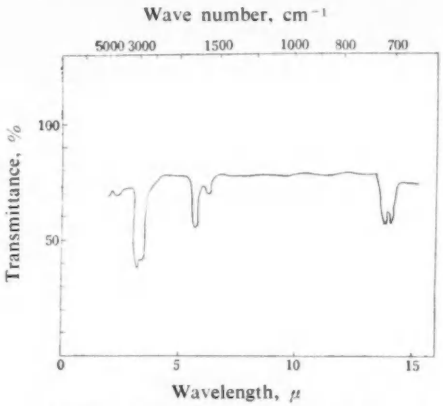

Fig. 13. Infrared spectrum of the urea adductible paraffins.

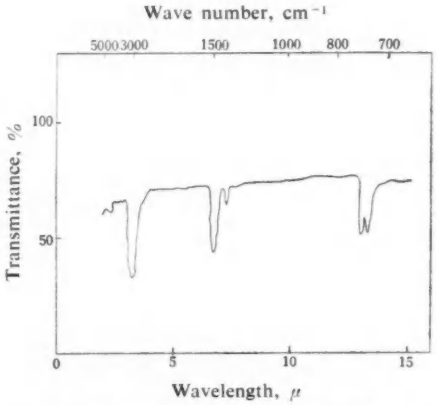

Fig. 14. Infrared spectrum of the pentane fraction of urea adductible paraffins.

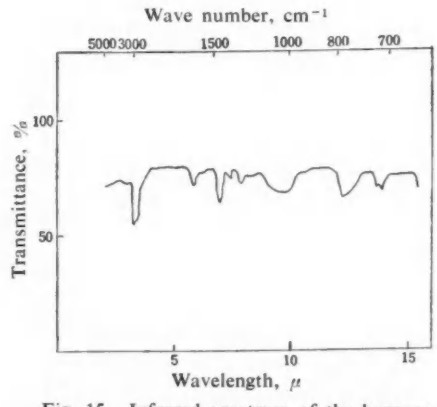

Fig. 15. Infrared spectrum of the benzene fraction of urea non-adductible paraffins.

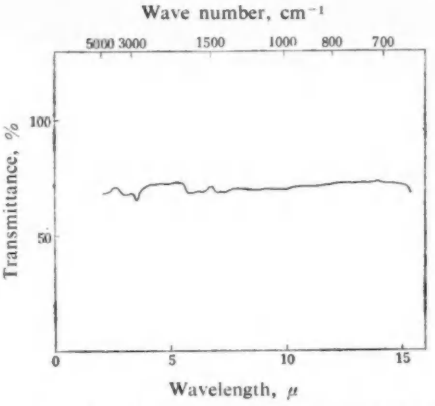

Fig. 16. Infrared spectrum of the alcohol fraction of urea adductible paraffins.

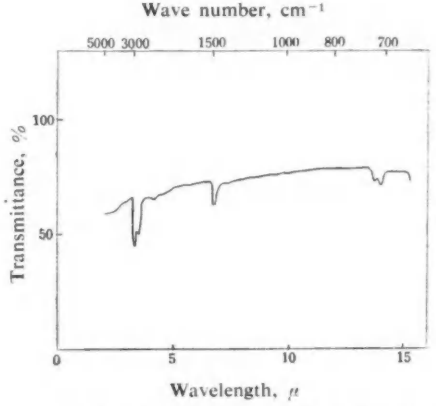

Fig. 17. Infrared spectrum of the urea non-adductible paraffins.

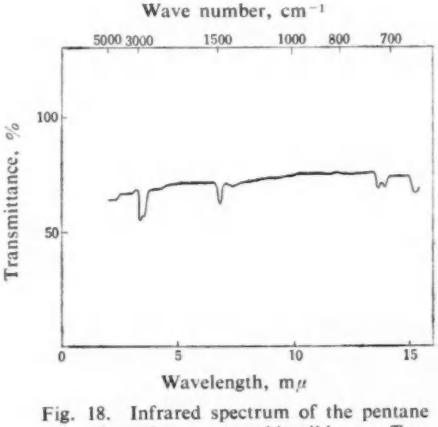

Fig. 18. Infrared spectrum of the pentane fraction of urea non-adductible paraffins.

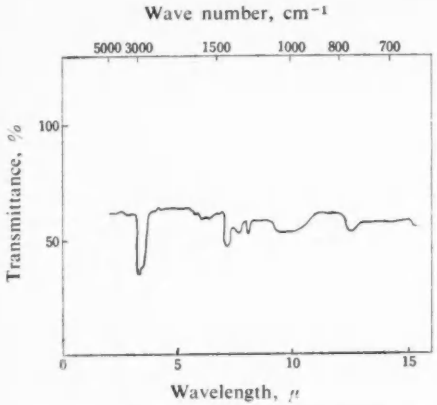

Fig. 19. Infrared spectrum of the benzene fraction of urea non-adductible paraffins.

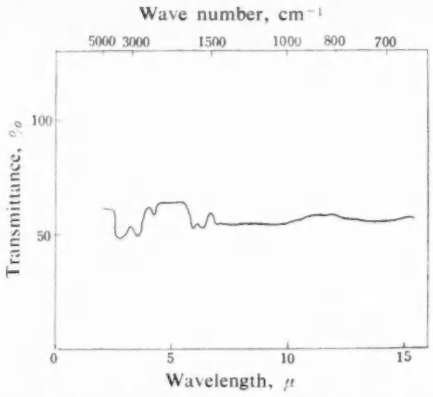

Fig. 20. Infrared spectrum of the alcohol fraction of urea non-adductible paraffins.

Tabble V. Infared spectrum of the urea adductible paraffin

Wavelength, μ	Wave number, cm⁻¹	Assignment of vibrations
3.35	2990	C-H (aliphatic) stretching vibration
3.43	2850	C-H (aliphatic) stretching vibration
6.85	1458	Deg-C-H bending vibration
7.29	1369	Syn-C-H bending vibration
13.83	723	Crystal band
14.04	712	Crystal band

Table VI. Infared spectrum of the pentane fraction of the urea adductible paraffin

Wavelength, μ	Wave number, cm⁻¹	Assignment of vibrations
3.37	2950	C-H (aliphatic) stretching vibration
3.44	2820	C-H (aliphatic) stretching vibration
6.84	1460	Deg-C-H bending vibration
7.27	1372	Syn-C-H bending vibration
13.82	723	Crystal band
14.02	713	Crystal band

Table VII. Infrared spectrum of the benzene fraction of the urea adductible paraffin

Wavelength, μ	Wave number, cm⁻¹	Assignment of vibrations
2.90	3450	O-H stretching vibration
3.37	2950	C-H (aliphatic) stretching vibration
3.40	2850	C-H (aliphatic) stretching vibration
5.85	1708	C=O stretching vibration
6.25	1597	Conjugated double bond stretching vibration ?
6.84	1460	Deg-C-H bending vibration
7.27	1373	Syn-C-H bending vibration
7.96	1254	Aromatic derivative vibration ?
12.62	792	
13.83	724	Crystal band
14.02	713	Crystal band

Table VIII. Infrared spectrum of the alcohol fraction of the urea adductible paraffin

Wavelength, μ	Wave number, cm⁻¹	Assignment of vibrations
2.95	3390	O-H stretching vibration
3.40	2880	C-H (aliphatic) stretching vibration
5.83	1710	C=O stretching vibration

Table IX. Infrared spectrum of the urea non-adductible paraffin

Wavelength, μ	Wave number, cm^{-1}	Assignment of vibrations
3.36	2950	C-H (aliphatic) stretching vibration
3.44	2820	C-H (aliphatic) stretching vibration
4.00	2380	
6.83	1461	Deg-C-H bending vibration
13.84	723	Crystal band
14.03	713	Crystal band

Table X. Infrared spectrum of the pentane fraction of the urea non-adductible paraffin

Wavelength, μ	Wave number, cm^{-1}	Assignment of vibrations
3.36	2950	C-H (aliphatic) stretching vibration
3.44	2820	C-H (aliphatic) stretching vibration
6.85	1580	Deg-C-H bending vibration
7.31	1365	Syn-C-H bending vibration
13.85	722	Crystal band
14.04	712	Crystal band

Table XI. Infrared spectrum of the benzene fraction of the urea non-adductible paraffin

Wavelength, μ	Wave number, cm^{-1}	Assignment of vibrations
2.55	3930	
3.37	2950	C-H (aliphatic) stretching vibration
3.44	2820	C-H (aliphatic) stretching vibration
5.88	1700	C=O stretching vibration
5.99	1695	
6.27	1590	Conjugated double bond stretching vibration ?
6.87	1455	Deg-C-H bending vibration
7.29	1360	Syn=C-H bending vibration
7.97	1254	Aromatic derivatives vibration ?
12.55	797	
14.07	712	$-(CH_2)-$ rocking vibration

Table XII. Infrared spectrum of the alcohol fraction of the urea non-adductible paraffin

Wavelength, μ	Wave number, cm^{-1}	Assignment of vibrations
2.50	4000	
2.58	3880	
2.86	3500	O-H stretching vibration
3.37	2950	C-H (aliphatic) stretching vibration
3.44	2820	C-H (aliphatic) stretching vibration
4.20	2760	
5.82	1715	C=O stretching vibration
5.87	1700	
6.05	1650	
6.21	1610	Conjugated double bond stretching vibration ?
6.49	1540	
6.85	1458	
7.32	1358	

($T\%$) was measured; the results are shown in Figs. 9 and 10.

The ultraviolet spectra of the two paraffins are shown in Figs. 11 and 12, in which ordinate means $\log \varepsilon$ and abscissa wavelength ($m\mu$) calculated from the above results.

As [the results of such ultraviolet spectra, it is considered that both of the urea adductible and non-adductible paraffins contain various aromatics though their quantities are small.

Results of Measurement on Infrared Spectrum. —The results of the infrared spectra measured on each fraction of urea adductible and non-adductible paraffins are shown in Figs. 13—20. Though it is difficult to analyze any spectra on each fraction, the assignment of the main

vibrations has been considered as shown in Tables V—XII in reference to the results of Randall and others[19].

It was reported in our previous paper[7,8] that the results of the observation by microscope was noteworthy, showing that any substances in plate crystals had a crystal band in the range of wave number of 710～730 cm^{-1} (or wavelength of 13.7～13.9 μ).

Conclusion

Comparing the urea adductible with non-adductible paraffin, there have been considerable differences in each fraction. In particular, it is very interesting that the alcohol fraction has the spectrum assigned to O-H streching vibration, which has been suggested to be the cause of micro-crystallization. It is considered that the substances which are the cause of micro-crystallization shall be contained in the alcohol fraction of urea non-adductible paraffins.

The author expresses his sincere appreciation to Professor Ryozo Goto and Professor Saburo Yagi, Kyoto University, for their cordial guidance in these studies, and is also grateful to the personnel in Osaka Ind. Tech. Lab., who co-operated with the author on the experiments of infrared spectrum.

Central Research Laboratory
Nippon Mining Co.
Kitaadachi-gun, Saitama

19) H. N. Randall et al., "Infra-red Determination of Organic Structure", O. van Nostrand Co., New York (1949).

Studies on Micro-paraffin. IV. On the Transformation of Paraffin Crystal by Addition of Pure Substances

By Kazuo NEGORO

(Received January 23, 1961)

Numerous phenomena, concerning the micro-crystallization of microparaffin derived by secondary cause, were previously reported[1]. Many investigations were made for the crystal growth of paraffin wax in the field of lubricating oils, because it was supposed to have great effects on the pour points of oils[2]. The pour points of lubricating oils are not the melting points of oils, but it seems to be reasonable to consider that the pouring phenomenon happens when the whole fluidity of lubricating oils is lost by the crystallization of wax components contained in the oils. Therefore, additional agents are used for pour point depressants to keep the fluidity of lubricating oils in low temperature inhibiting the crystal growth of paraffin waxes. They are supposed to inhibit the crystal growth of paraffin waxes, because they are adsorbed by paraffin waxes rather than oils.

The addition of any inorganic and organic substances to ordinary crystalline paraffin waxes were examined and their structure which should inhibit the crystal growth of paraffin waxes. In particular, as seen in the report[3], the cause of micro-crystallization of microparaffins was considered to be affected by substance with hydroxyl groups derived by the results of studies on ultraviolet and infrared spectra, etc. of the components separated from the micro-paraffin by a propane deasphalting method, urea adducts method, and chromatography: hence, the behavior of various organic compounds having OH groups should be noticed. Then, many pour point depressants for lubricating oils, additional agents to paraffin waxes[4], and direct dyes[5] were examined at the same time. Furthermore, pure organic substances considered to be effective for the crystal growth of paraffin waxes were studied at the base of pure *n*-dotriacontane (forming plate crystals), and their effects on crystal growth of *n*-hydrocarbon (simple substance, but not mixture) were investigated.

As the above results, such as Santopour or pour point depressants for lubricating oils, picric acid, *p*-hydroxydiphenyl, and some direct

1) K. Negoro, *J. Chem. Soc. Japan, Ind. Chem. Sec.* (*Kogyo Kagaku Zasshi*), **64**, 295 (1961).
2) K. Horiguchi, "Junkatsuyu Kagaku" (The Chemistry of Lubricating Oils), Sankyo, Tokyo (1958), p. 295.
3) K. Negoro, *J. Chem. Soc. Japan, Pure Chem. Sec.* (*Nippn Kagaku Zasshi*), **82**, 229 (1961).
4) K. Negoro, *Oil Chemistry* (*Yukagaku*), **7**, 23 (1958).
5) S. Inokawa, *J. Chem. Soc. Japan, Pure Chem. Sec.* (*Nippon Kagaku Zasshi*), **76**, 726 (1955).

dyes were found to be the substances affected on the transformation of crystal growth of paraffins.

These behaviors shall be cleared by future studies, they are now being investigated by X-ray diffraction, and infrared spectra of microparaffins. However, it is very interesting that the existence of the above organic substances with hydroxyl groups and similar molecular structure, affects the transformation of the crystal of paraffin waxes. It was found, also, that there was a difference between the paraffin waxes (mixture of various hydrocarbons) and *n*-dotriacontane for such effects of addition. Therefore, the composition of paraffin was considered to be effective for the micro-crystallization of microparaffins.

Experimental

Materials.—*Crystalline Paraffin.*—The sample of wax was made in the Funakawa Refinery, Nippon Mining Co., m. p. 53.5°C, and refractive index $1.4308^{70.0}$.

n-Dotriacontane.—The product of Fischer Scientific Co., and purchased from Pacific Gulf Oil Co.,[6] m. p. 69.2°C, sp. gr. $0.7831^{70.0}$, and refractive index $1.4308^{70.1}$.

n-Dotriacontane was of a high purity, but a content of some impurities was recognized by the result of the ultraviolet spectrum (wavelength 220～400 mμ) measurement with purified *n*-hexadecane as diluent. Accordingly, purification was conducted with 10% of activated clay at 75°C (yield of 78%). Such purified *n*-dotriacontane was confirmed to contain no impurities by a measurement of the ultraviolet spectrum as above, m. p. 69.5°C and refractive index $1.4315^{73.0}$.

The above values were confirmed to be almost equal to those in the literature[7].

Chemicals.—Many inorganic and organic chemicals, added to the crystalline paraffin or *n*-dotriacontane, were of special or 1st grade made by Kanto Kagaku Co.

Solvents.—Ethyl alcohol was purified by a general method[8], and its boiling point was 78.0°C.

Crystallization.—Crystalline paraffin or *n*-dotriacontane was weighed accurately on a chemical balance; and 10, 1 and 0.1 wt.% of each inorganic or organic chemicals (as additive) were also weighed accurately. Both the paraffin and the additive were placed in an Erlenmeyer's flask and melted at 80°C in a thermostat. Even when there were some chemicals not melted at 80°C, the next operation was started; 1 g. of purified ethyl alcohol was added to 300 cc. of each sample with a pipette, and was warmed at 75±1°C in the thermostat to make the sample soluble in ethyl alcohol with intermittent stirring. Then, it was gradually cooled to room temperature for the growth of the crystal of the paraffin.

Observation of Crystals by Microscope[9].—The crystal of each sample was placed on a slide glass with a syringe, and was observed with an ordinary or phase-contrast microscope; and then, photographs of the state of each crystal were taken.

Results and Discussion

Effects of Various Substances on Crystallization of Crystalline Paraffin.—*Effects of Inorganic Substances.*—The effects of the existence of various inorganic substances on the crystallization of crystalline paraffin were investigated. The crystalline paraffin at the base forms thin and large plate crystals as shown in Fig. 1, which mainly consists of *n*-paraffin (containing 88～90% of the straight chain adductible paraffin), and it is supposed that the average number of carbon chains of hydrocarbons contained to be 27*1.

×225

Fig. 1. Crystals of crystalline paraffin.

In the case of each 10% of various metals, oxides, acids, alkalis, salts, etc., such as sulfur, zinc powder, manganese dioxide, silica, zinc oxide, aluminum chloride, sodium bicarbonate, potassium chlorate, alum, silver nitrate, ammonium vanadate, sulfuric acid, hydrochloric acid, sodium hydroxide, etc., existed with crystalline paraffin, no transformation were observed in the crystallization of the crystalline paraffins.

Effects of Organic Substances.—Next, the effects of 0.1～10% of various pure organic substances on crystalline paraffin were also examined. Experiments were conducted on various organic compounds; and at the same time, as explained above by the investigation of the crystal properties[1,3], ultraviolet spectra and infrared spectra on each fraction of microparaffin separated by the application of propane deasphalting method, urea adducts method, chromatography etc., the compound with hydoroxyl or carbonyl groups was considered

6) Personal communication from H. I. Goodman (Pacific Gulf Oil Co.).

7) F. Francis, O. M. Watkins and R. W. Wallington, *J. Chem. Soc.*, **121**, 1529 (1922).

8) "Text-book on Chemical Experiments" (Jikken Kagaku Koza), 2 (Fundamental Technique II), Maruzen, Tokyo (1956), p. 78.

9) S. Yagi and K. Negoro, *Chem. Ind., Japan* (*Kagaku Kogyo*), **8**, No. 12, 32 (1957).

*1 It is presumed by X-ray diffraction method (X-ray diffraction of various paraffins will be mentioned in the later report of this series to be continued).

Table I. Effects of organic substances on the crystallization of paraffin

Sample	Molecular formula	M. p.*1	Solubility in alcohol*2	Effects on crystallization of paraffin
p-Hydroxydiphenyl	$C_6H_5C_6H_4OH$	161.5	Sol.	Transformation (micro-crystallization)
Picric acid	$HOC_6H_2(NO_2)_3$	118	Sol.	Transformation (micro-crystallization)
Glucose	$C_6H_{12}O_6$	134	Sol.	Transformation
Quinizarine	$C_6H_4{<}^{CO}_{CO}{>}C_6H_2(OH)_2$	177.5	Sol.	Transformation (micro-crystallization)
Calcium stearate	$(C_{17}H_{35}COO)_2Ca$	110～115	Insol.	Transformation
Barium stearate	$(C_{17}H_{35}COO)_2Ba$	195～200	Insol.	Transformation
Aluminum stearate	$(C_{17}H_{35}COO)_3Al$	118～120	Insol.	Transformation
Zinc naphthate	$(C_6H_{11}COO)_2Zn$		Sol.	Transformation
Lead naphthate	$(C_6H_{11}COO)_2Pb$		Sol.	Transformation

*1 Melting point measured by the capillary tube method.
*2 Sol, soluble Insol, insoluble

to give effects on the micro-crystallization of microparaffin. Under the above circumstances, in particular, the various types of organic compounds with functional groups such as hydroxyl or carbonyl group were examined in a wide scope. In the case of each 10% of various aromatics, alcohols, aldehydes, ketones, acids, esters, salts, phenols, amines, nitrogen compounds, sulfur compounds, etc., such as naphthalene, *tert*-butyl alcohol, cetyl alcohol, cholesterol, phenol, α- and β-naphthol, resorcinol, glycerine, pyrogallol, *p*-hydroxydiphenyl, picric acid, *m*- and *p*-nitrophenol, *o*-, *m*- and *p*-dinitrobenzene, aniline, lauril amine, triethanolamine, phenylhydrazine, azobenzene, methyl orange, hydroxyazobenzene, dinitrophenyl hydrazine, benzaldehyde, glucose, methylisobutyl ketone, acetophenone, α- and β-naphthoquinone, quinizarine, benzoic acid, acetic acid, naphthenic acid, oleic acid, stearic acid, oxalic acid, adipic acid, 2.3- and 2.5-dihydroxybenzoic acid, salicylic acid, calcium acetate, calcium, barium and aluminum stearate, lead oleate, zinc and lead naphthate, amyl acetate benzyl acetate, ethyl chloride, trichloroethylene, methylchlorostearate, *n*-heptyl mercaptane, dibenzyl disulfide, etc. exist with crystalline paraffin, were observed in the crystallization of the crystalline paraffin, were observed in the crystallization of the crystalline paraffins. Each of the various organic compounds which transformed the crystalline properties of paraffin when being added to it, are shown in Table I.

The substances having hydroxyl groups combined with an alkyl group or a benzene ring, were hardly affected on crystallization of paraffins. Glycerine, ethylene glycol, pyrogallol, etc.[2] which were said to drop the pour points of lubricating oils when being added, were not much affected on the crystal growth of paraffins. However, in the case of *p*-hydroxydiphenyl and picric acid, the crystal growth of crystalline paraffins was evidently inhibited as shown in Figs. 2 and 3, respectively, and it is very interesting that they show a microcrystalline state.

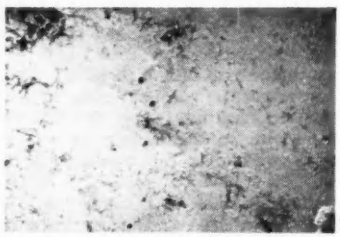

×225

Fig. 2. Transformation of crystals of crystalline paraffin caused by the addition of *p*-hydroxydiphenyl.

×225

Fig. 3. Transformation of crystals of crystalline paraffin caused by the addition of picric acid.

In the next stage, nitrogen compounds such as compounds having nitro, amino or azo groups, etc. were examined. But almost no effects were observed on such compounds as shown above. As the results of investigations on the compounds having aldehyde or ketone groups, quinizarine (having two hydroxyl groups in addition to ketone groups and

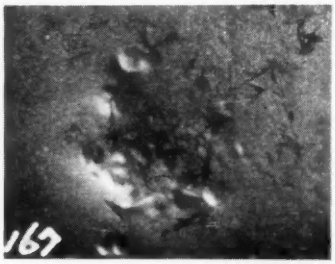

×225

Fig. 4. Transformation of crystals of crystalline paraffin caused by the addition of quinizarine.

benzene nucleus) formed the microcrystallization of crystalline wax as shown in Fig. 4. Almost no effects were given by various types of organic acids having hydroxyl groups. However, in the presence of metallic salts of stearic or naphthenic acid, microcrystalline crystals were found accompanied by plate crystals of crystalline paraffin. The metallic soaps of fatty acids are used for the pour point depressant of lubricating oils[10], and they are said to have larger effects when their molecular weights are larger. For instance, the effects of the existence of metallic salts of stearic and naphthenic acids on the crystals of a crystalline paraffin are shown in Figs. 5 and 6, respectively.

×225

Fig. 5. Transformation of crystals of crystalline paraffin caused by the addition of calcium stearate.

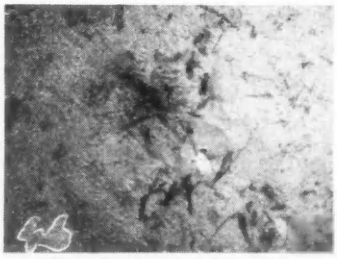

×225

Fig. 6. Transformation of crystals of crystalline paraffin caused by the addition of zinc naphthate.

Though effects of the addition of a few compounds of sulfur were investigated, so far, substances inhibiting the crystal growth of crystalline paraffins have not been found.

The substances giving effects on the transformation of crystallization are shown in Table I.

Effects of Addition Agents.—The results of the investigations on addition agents of paraffin waxes had been already reported[11]. The effects of the existence of such agents on the crystals of paraffin waxes were examined. Also the pour point depressants, recently being in practical use in the field of lubricating oils, are considered to have effects on keeping the fluidity of lubricating oil in lower temperature[2] by inhibiting the growth of paraffin crystals mixed in oils. Then, the effects of depressants on sale upon the crystallization of crystalline paraffins when mixed in the paraffins were also examined as above, and the results are shown in Table II.

It was found that the substance, having the most remarkable effect on the change of the crystals of paraffin wax, was Santopour. In

Table II. Effects of addition agents on the crystallization of paraffin

Sample	Effects on crystallization of paraffins	Summary
Polyethylene	no	Improver of m. p. which micronizes the structure of paraffin
Acra wax c	no	Synthetic paraffin. Improver of m. p.
Carbo wax	no	Poly (ethylene glycol) (mol. wt. 4000)
Vistac	no	Polybutene (mol. wt. 1100 and 3400)
Ar wax	no	Paraffin added by polyethylene
Stroba wax	no	Paraffin mixed with a small quantity of resin
Adva wax	Somewhat transformation	Microparaffin added by polyethylene
Chloro-naphthalene	Transformation	Chlorinated naphthalene
Santopoid 23RI	no	Addition agents of lubricating oils
Ionol	no	Addition agents of lubricating oils
Santopour	Transformation (micro-crystallization)	Addition agents of lubricating oils
Santolube 70	no	Addition agents of lubricating oils

10) Y. Tanaka, R. Kobayashi and T. Tsukuda, *J. Soc. Chem. Ind. Japan* (*Kōgyō Kwagaku Zassi*) **38**, 10, 28, 1033 (1935).

11) K. Negoro, *Oil Chemistry* (*Yukagaku*), **7**, 97 (1958).

Table III. Effect of direct dyes

Sample	Structural formula	Effects on crystallization of paraffin
p-Aminodiphenyl	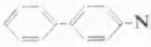	no
Congo red		no
Benzopurprine	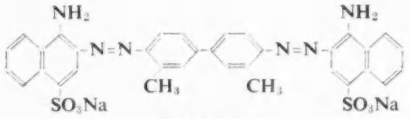	no
Nippon green B conc.	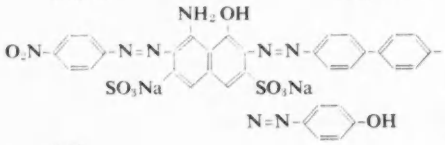	Transformation (micro-crystallization)
Nippon orange R	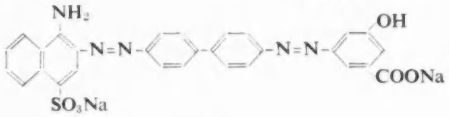	Transformation
Nippon brown 3G	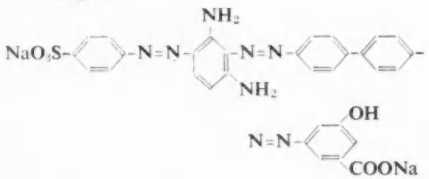	Transformation
Nippon dark green B conc.	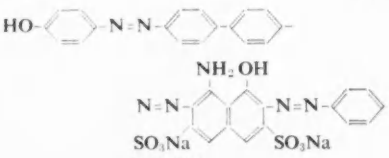	Transformation
Nippon deep black ex. conc.	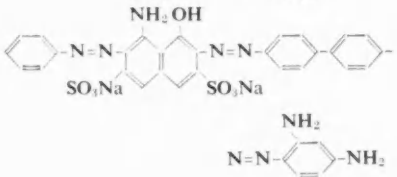	Transformation

this case, the phenomenon of micro-crystallization as picric acid, *p*-hydroxydiphenyl, etc. was confirmed by microscopy as shown in Fig. 7.

Santopour is the product made from phenol and paraffin wax[12], and it is said to form the following structure. It is attractive that the structure is similar to that of picric acid which caused the crystals of the crystalline paraffins to micro-crystallize.

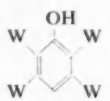

(W: paraffinic chain)

Chloronaphthalene*, which was made by blowing chlorine into naphthalene, was added to the crystalline paraffin. Then, the crystal growth of paraffin was inhibited, and almost no crystal of paraffin appeared by cooling under the same condition; it was attractive

12) N. Iimure, "Guide-book of Petroleum Products", Sangyo Tosho, Tokyo (1956), p. 162.

* The trial product by K. Hashizume (Fukushima Paraffin Paper Co.), was used and its composition is obscure.

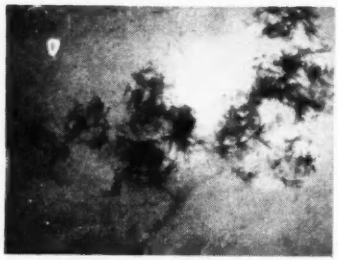
×225

Fig. 7. Transformation of crystals of crystalline paraffin caused by the addition of Santopour.

×225

Fig. 8. Transformation of crystals of crystalline paraffin caused by the addition of chloronaphthalene.

that only a small amount of amorphous crystals was observed as shown in Fig. 8.

Effects of Direct Dyes.—It has been reported[5] that the direct dyes having functional groups such as hydroxyl group, amino group, etc. made the gelatin of methyl cellulose by bridge-making through each molecule. Then, the effects of such dyes on crystal growth of the paraffin were examined. The results of experiments on 9 sorts of dyes are shown in Table III.

It is very interesting that in the case of direct dyes also, only the compounds having hydroxyl groups gave effects on crystal growth of the crystalline paraffin.

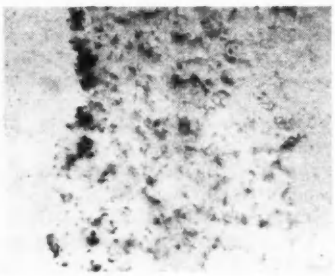
×225

Fig. 9. Transformation of crystals of crystalline paraffin caused by the addition of Nippon green B conc.

Effects of Asphalt Components.—Similarly, the asphalt component separated from heavy oil containing microparaffin[1] by propane deasphalting method was added to the crystalline paraffin. Then, the crystals of the paraffin were microcrystallized as shown in Fig. 10, and it was interesting that the micro-crystalline state was very closely similar to that caused by the addition of Santopour, picric acid, *p*-hydroxydiphenyl, etc.

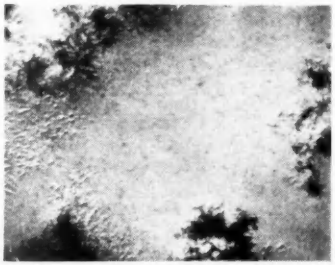
×225

Fig. 10. Transformation of crystals of crystalline paraffin caused by the addition of asphalt component.

Effects of Various Substances on Crystallization of *n*-Dotriacontane.—Each of the various organic compounds which transformed the crystalline properties of paraffin when being added to it, were added to a purified *n*-dotriacontane (formed thin plate crystals as shown in Fig. 11) as the above examination. Then, its effects on the crystallization of *n*-dotriacontane were investigated. These results are shown in Table IV.

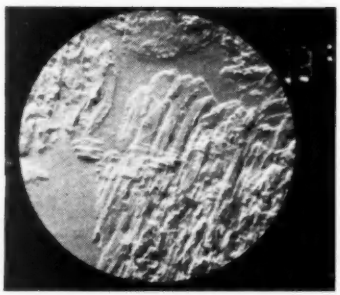
×225

Fig. 11. The crystals of *n*-dotriacontane.

The phenomena of micro-crystallization which gave effects on the crystal when *p*-hydroxydiphenyl or picric acid was added to *n*-dotriacontane are in Figs. 12 and 13, respectively. Figure 14 shows the photograph of crystal transformations of *n*-dotriacontane when Santopour, addition agent of lubricating oils, was added to it, and it is easy to find out crystals of needles.

Table IV. Effects of various organic substances on the crystallization of *n*-dotriacontane

Sample	Effects on crystallization of *n*-dotriacontane	Sample	Effects on crystallization of *n*-dotriacontane
p-Hydroxydiphenyl	Transformation (micro-crystallization)	Adva wax	Almost no transformation
Picric acid	Transformation (micro-crystallization)	Santopour	Transformation (micro-crystallization)
Glucose	Almost no transformation	Nippon green B conc.	Transformation
Quinizarine	Almost no transformation	Nippon orange R	Almost no transformation
Calcium stearate	Almost no transformation	Nippon brown 3G	Almost no transformation
Barium stearate	Almost no transformation	Nippon dark green B conc.	Almost no transformation
Aluminum stearate	Almost no transformation	Nippon deep black ex. conc.	Almost no transformation
Zinc naphthate	Almost no transformation	Chloronaphthalene	Almost no transformation
Lead naphthate	Almost no transformation	Asphalt component	Transformation

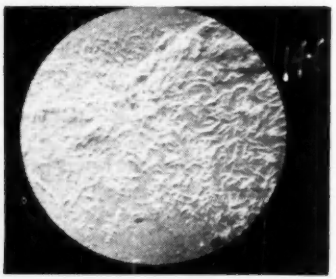

×150

Fig. 12. Transformation of crystals of *n*-dotriacontane caused by the addition of *p*-hydroxydiphenyl (micro-crystallized).

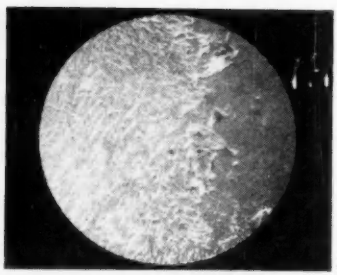

×150

Fig. 13. Transformation of crystals of *n*-dotriacontane caused by the addition of picric acid (micro-crystallized).

Though the dyes in general gave no remarkable effects, only in the case of "Nippon green B conc." formed micro-crystallization in some parts as shown in Fig. 15.

The examples of almost no effects were the results of photomicrographs of the addition of chloronaphthalene or barium stearate to *n*-dotriacontane, which are shown in Figs. 16 and 17, respectively.

×225

Fig. 14. Transformation of crystals of *n*-dotriacontane caused by the addition of Santopour (micro-crystallized).

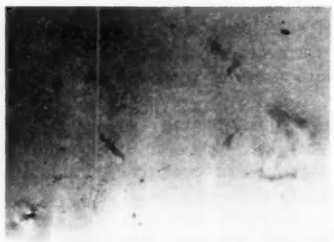

×225

Fig. 15. Transformation of crystals of *n*-dotriacontane caused by the addition of "Nippon green B conc." (hardly micro-crystallized).

In the case of the asphalt component obtained by propane deasphalting method, its effect was not so remarkable though a little transformation of the crystals of *n*-dotriacontane was seen (Fig. 18).

As mentioned above, two cases were considered; one was of crystalline paraffin, a mixture of various hydrocarbons, in which the

×225

Fig. 16. Transformation of crystals of *n*-dotriacontane caused by the addition of chloronaphthalene (almost no change).

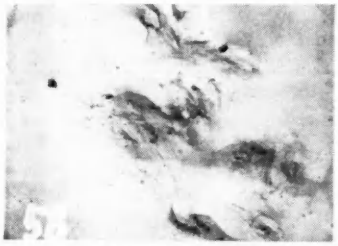

×225

Fig. 17. Transformation of crystals of *n*-dotriacontane caused by the addition of barium stearate (almost no change).

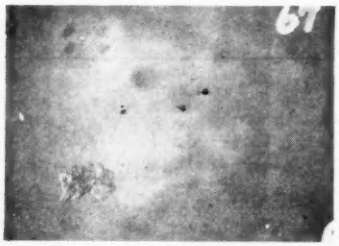

×225

Fig. 18. Transformation of crystals of *n*-dotriacontane caused by the addition of asphalt component (hardly micro-crystallizad).

content of straight paraffins was nearly 90% and containing paraffin side chains, naphthene rings, and aromatic rings; and other was of *n*-dotriacontane, *n*-paraffin series hydrocarbon of carbon number 32. Then, the effects of addition of various organic compounds were different between both, and the composition of the paraffin gave effects on the facility of micro-crystallization of the paraffin. It had already been found[3] that the content of the adductible compounds of the straight chain in the microparaffin was nearly 60%. Accordingly, the easiness of micro-crystallization of microparaffin should be considered to be caused by the existence of more side chains of paraffin in microparaffin than in the crystalline paraffin wax. By observation with the microscope, the phenomenon of micro-crystallization is seemd to be that very fine crystals of plate are rolled up to make minute crystals of needle.

It was found that Santopour, picric acid, *p*-hydroxydiphenyl, and a few direct dyes formed a considerable micro-crystallization of pure hydrocarbons of a straight chain too. It is interesting that all these compounds contain hydroxyl groups and being in somewhat similar structures. Essential investigation will be made by X-ray diffraction, infrared spectrum, observation by electron microscope etc. with regard to the reason why these substances form micro-crystallization of the crystals of paraffin. It should be caused by the fact that the properties of paraffin molecules arranging regularly and growing up to the fundamental crystal of plate are inhibited or obstructed. However, it will be cleared in detail by future studies.

The author expresses his sincere appreciation to Professor Ryozo Goto and Professor Saburo Yagi, Kyoto University, for their cordial guidance and discussion throughout this research.

Central Research Laboratory
Nippon Mining Co.
Kitaadachi-gun, Saitama

On 2-Aminotropothione Derivatives

By Tetsuo Nozoe and Kazuo Matsui

(Received March 22, 1961)

2-Mercaptotropone (I) with two possible tautomeric structures, A and B, was synthesized in 1953 in our laboratory[1,2]. Although the structure of 2-mercaptotropone (B) was assigned at that time from its chemical behaviors, further examinations on its physicochemical properties as well as those of its homologs suggested that I should take the structure A of 2-hydroxytropothione rather than B, in a static state[3].

(A) (B)

As another type of tropothione derivatives, 2-aminotropothiones (1-amino-7-thioxo-1, 3, 5-cycloheptatrienes) were recently synthesized by Brasen et al.[4] from 2-aminotroponeimines (1-amino-7-imino-1, 3, 5-cycloheptatrienes) by the action of hydrogen sulfide. This report deals with another synthesis of 2-aminotropothiones, probably identical with Brasen's compounds and reactions thereof.

Heating 2-aminotropone (II) with excess of phosphorus pentasulfide in pyridine for 2 hr. on a water bath yields 2-aminotropothione (III) as orange red prisms, m. p. 135~136°C, in 60% yield. III is neutral substance and stable in air, and gives benzoate, m. p. 136~137°C. Hydrolysis of III with excess of potassium hydroxide in ethanol affords I.

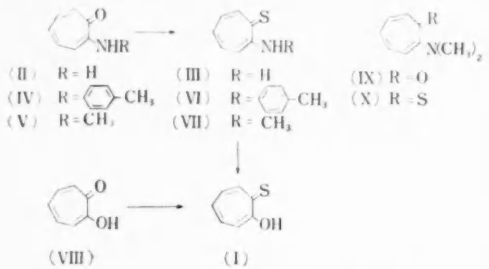

(II) R=H (III) R=H (IX) R=O
(IV) R=p-CH$_3$C$_6$H$_4$ (VI) R=p-CH$_3$C$_6$H$_4$ (X) R=S
(V) R=CH$_3$ (VII) R=CH$_3$

(VIII) (I)

Similarly, 2-*p*-toluidinotropothione (VI), orange red plates of m. p. 98~99°C, and 2-methylaminotropothione (VII), orange needles of m. p. 67~68°C, are obtained respectively from 2-*p*-toluidinotropone (IV) and 2-methylaminotropone (V). Both VI and VII are stable substances and benzene layer colors dark red with cupric acetate by the formation of chelate compound.

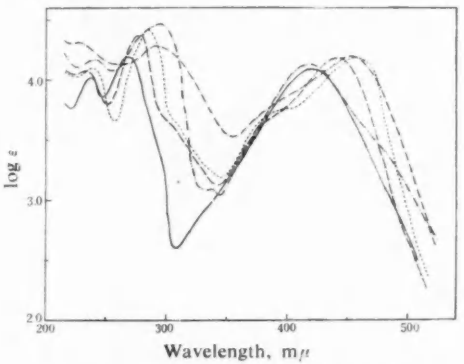

Fig. 1. Ultraviolet absorption spectra of I (——), III (——), VI (-·-·), VII (----) and benzoate of III (-···-) in methanol.

Reaction of tropolone (VIII) with phosphorus pentasulfide gives I even in a lower yield. But 2-dimethylaminotropone (IX) failed to give any objective 2-dimethylaminotropothione (X) except resinous materials by the same method.

These facts imply that hydrogen bond formation between C=S and NH or OH group considerably affects the stability of tropothione derivatives.

As electrophilic substitution, bromination of III in acetic acid was carried out, but only a yellow complex was obtained and heating of it with water ended in decomposition with the recovery of the original substance (III).

There can be two tautomeric structures, C and D, for each III, VI and VII. But their ultraviolet spectra fairly resemble that of 2-hydroxytropothione (I) (structure A) (Fig. 1). This fact suggests, that all these should exist as 2-aminotropothiones (structure C).

(C) (D)

1) T. Nozoe, M. Sato and K. Matsui, *Proc. Japan Acad.*, **29**, 22 (1953).
2) Idem., *Sci. Repts. Tohoku Univ., Ser. I*, **37**, 211 (1953).
3) T. Nozoe and K. Matsui, This Bulletin, **34**, 616 (1961).
4) W. R. Brasen, H. E. Holquist and R. E. Benson, *J. Am. Chem. Soc.*, **82**, 995 (1960).

Infrared spectrum of III is shown in Fig. 2. Absorption assignable to SH group usually seen at 2600~2550 cm^{-1} is absent, and according to Mecke's law,[5] strong absorption at 1045 cm^{-1} must correspond to $\nu_{C=S}$. Thus, the infrared spectrum also supports the structure C for III. This result is in agreement with that obtained by Brasen from nuclear magnetic resonance studies[4].

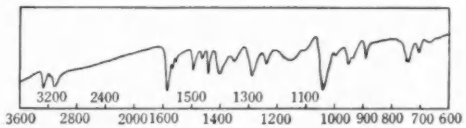

Fig. 2. Infrared absorption spectum of III (KBr disk).

It is known that although I takes structure A in the static state, it behaves like 2-mercaptotropone (structure B) during various reactions, affording only *S*-substituted derivatives[1,2]. However, the possibility of the structure of 2-mercaptotroponeimine (D) for III is excluded even during chemical reactions from its inertness toward diazomethane and the formation of *N*-benzoate as described below.

Two possible structures are assumed for benzoate of III, i.e. *N*- and *S*-benzoate. Its ultraviolet spectrum, however, considerably resembles that of III itself (Fig. 1), and $\nu_{C=S}$ appears at 1065 cm^{-1} in its infrared spectrum. It has therefore been clarified, that this must be *N*-benzoate.

These experiments thus show an essential difference in the chemical properties between I and III.

Experimental[6]

2-Aminotropothione (III).—A mixture of 0.5 g. of 2-aminotropone (II), 1.5 g. of phosphorus pentasulfide and 5 ml. of pyridine was stirred on a water bath for 2 hr. After removal of pyridine under a reduced pressure, water was added to the residue and separated crystals were collected by filtration and dried. This was extracted with methanol for 1 hr. and left cooling. Precipitated crystals were filtered off and methanol was evaporated. The residue was extracted with hot benzene and the crystals obtained was recrystallized from benzene to give 0.3 g. of III as orange red prisms, m. p. 136~137°C.

Found: C, 61.42; H, 4.83; N, 10.00. Calcd. for C_7H_7NS: C, 61.27, H, 5.15, N, 10.21%.

Benzoate: Prepared from III and benzoyl chloride in pyridine, and recrystallized from ethanol to red leaflets, m. p. 136~137°C.

Found: C, 69.66; H, 4.45; N, 5.40. Calcd. for $C_{14}H_{11}ONS$: C, 69.68; H, 4.59; N, 5.81%.

Hydrolysis of III; Formation of 2-Mercaptotropone (I).—A mixture of 30 mg. of III, 1 ml. of 20% potassium hydroxide and 4 ml. of ethanol was refluxed for 6 hr., ethanol was evaporated under a reduced pressure, water was added to the residue and the solution was treated with activated carbon. The filtrate thereby obtained was acidified with 6 N sulfuric acid and the crystals that separated out were collected by filtration. Sublimation of this product under 3 mmHg pressure afforded I as orange red crystals m. p. 54~55°C. Yield, 15 mg. This was identified by mixed fusion with authentic sample.

2-*p*-Toluidinotropothione (VI).—A mixture of 0.3 g. of 2-*p*-toluidinotropone (IV), 1 g. of phosphorus pentasulfide and 5 ml. of pyridine was stirred on a water bath for 2 hr. Pyridine was removed under a reduced pressure, water was added to the residue and extracted with chloroform. Extract was washed with 2 N hydrochloric acid and the solvent was evaporated in vacuo. The residue was extracted with hot ethanol, and the substance so obtained was recrystallized first from cyclohexane then from ethanol to give VI as orange red plates, m. p. 98~99°C. Yield, 50 mg.

Found: C, 74.31; H, 5.49; N, 5.85. Calcd. for $C_{14}H_{13}NS$: C, 73.99; H, 5.76; N, 6.17%.

2-Methylaminotropothione (VII).—A mixture of 0.3 g. of 2-methylaminotropone (V), 1.5 g. of phosphorus pentasulfide and 5 ml. of pyridine was stirred on a water bath for 1.5 hr. Pyridine was removed under a reduced pressure, water was added to the residue and extracted with chloroform. After evaporation of chloroform, the residue was triturated with 5 ml. of methanol and insoluble materials were filtered off. Methanol was evaporated in vacuo and the residue was extracted with hot cyclohexane. Extracted material was recrystallized two times from cyclohexane to give 50 mg. of VII as orange needles, m. p. 67~68°C.

Found: C, 63.92; H, 5.68; N, 9.27. Calcd. for C_8H_9NS: C, 63.53; H, 6.00; N, 9.27%.

Reaction of Tropolone (VIII) and Phosphorus Pentasulfide; Formation of I.—A mixture of 0.2 g. of VIII, 0.5 g. of phosphorus pentasulfide and 5 ml. of pyridine was stirred on a water bath for 30 min. Pyridine was evaporated under a reduced pressure, 10 ml. of 2 N potassium hydroxide was added to the residue, and the solution was treated with activated carbon. The filtrate thereby obtained was acidified with 6 N sulfuric acid and the crystals that separated were collected by filtration. Sublimation of this product under 3 mmHg pressure and recrystallization of the sublimate from petroleum ether afforded I as orange red prisms, m. p. 53~55°C. Yield, 20 mg. This was identified by admixture.

Reaction of Dimethylaminotropone (IX) and Phosphorus Pentasulfide.—To a solution of 1 g. of IX dissolved in 5 ml. of pyridine, 1.5 g. of phosphorus pentasulfide was added under stirring. The solution colored red immediately and darkened after a short time. After stirring for 1.5 hr. at room temperature, pyridine was evaporated under a reduced pressure, water was added to the residue and separated dark

5) R. Mecke, R. Mecke and A. Lüttringhaus, *Chem. Ber.*, **90**, 975 (1957).

6) All m. p. are uncorrected. The microanalyses were carried out by Miss A. Iwanaga and Miss M. Suzuki to whom the authors express their deep gratitude.

crystals were collected by filtration. This was extracted with methanol for 1 hr., but only small amounts of resinous materials were obtained.

Bromination of III.—A solution of 40 mg. of bromine in 0.5 ml. of acetic acid was added to 30 mg. of III dissolved in 3 ml. of acetic acid under stirring. Yellow crystals that separated were collected by filtration. This substance, m. p. over 280°C, is insoluble in benzene or ethanol. By heating it with water, followed by extraction with chloroform and sublimation of the extract under 3 mmHg pressure, 15 mg. of III, m. p. 130~135°C, was recovered, identified by mixed fusion.

Department of Chemistry
Faculty of Science
Tohoku University
Katahira-cho, Sendai

Synthesis of Some 8,8-Disubstituted Heptafulvene Derivatives[1]

By Tetsuo NOZOE, Toshio MUKAI, Kazutoshi OSAKA* and Nobuyuki SHISHIDO**

(Received March 23, 1961)

Heptafulvene (methylenecycloheptatriene) (A) can be regarded as a methylene analog of tropone and is also one of the typical non-alternant hydrocarbones with a cyclic conjugated double bond system. Its structure suggests more or less the contribution of a 6-π

(A)

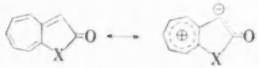

(B)

electron system as tropylium ion. Consequently, it seems of interest to examine the aromaticity and reactivity of this type of compounds comparing with those of azulenes and azulane-2-one type of compounds (B: X=O or NH)[2]. Theoretical interests on the unique ring system attracted also much attention of physical chemists as well as organic chemists and calculation by molecular orbital method has been carried out by Berthier and Pullman[3], Bergman et al.[4] and Julg and Pullman[5,6].

Attempts have already been made for synthesis of heptafulvene derivatives. In 1953, Grundmann, Ottman and Gollner[7], and van Aardt[8] in 1954, attempted the elimination of water from tropyl carbinols (C) but a facile formation of a polymer or styrenes as a rearrangement product was observed and the desired compound could not be obtained. In 1954, Doering and Wiley[9] succeeded in obtaining heptafulvene by the Hofmann elimination of

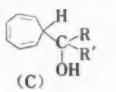

(C)

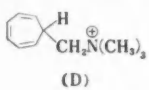

(D)

the quaternary ammonium salt (D), obtained from norcaradienecarboxamide, under special conditions. Recently details of this work have been published[10]. According to Doering and Wiley, heptafulvene is a very unstable compound and easily undergoes polymerization but its structure has been proved from the formation of methylcycloheptane by hydrogenation and of dimethyl azulene 1,2-dicarboxylate by addition with dimethyl acetylene dicarboxylate followed by oxidation. Matteson, Drysdale and Sharkey[11] also obtained heptafulvene, though in a minute amount, by pyrolytic decomposition of methylenecycloheptadienes.

The reason for the larger lability of heptafulvene compared with tropone is considered to be due to the difference in the electron-withdrawing power of the carbonyl and methylene

1) A part of this work was presented at the Local Meeting of Tohoku District of the Chemical Society of Japan, Yamagata, June, 1959.

* Present address: Research Institute of Asahi Chemical Industries, Ltd., Itabashi-ku, Tokyo.

** Present address: Mitsubishi Chemical Industries, Ltd., Yawata, Fukuoka Japan.

2) T. Nozoe, S. Seto, S. Matsumura and T. Terasawa, *Chem. & Ind.*, **1954**, 1356.

3) G. Berthier and B. Pullman, *Trans. Faraday Soc.*, **45**, 484 (1949).

4) E. D. Bergman, E. Fischer, D. Ginsburg, Y. Hirshberg, D. Lavie, M. Mayot, A. Pullman and B. Pullman, *Bull. soc. chim. France*, **V18**, 684 (1951).

5) A. Julg, *J. Chem. Phys.*, **52**, 50 (1955).

6) A. Julg and B. Pullman, ibid., **52**, 481 (1955).

7) C. Grundmann, G. Ottman and G. Gollner, *Ann.*, **582**, 178 (1953).

8) Van Aardt, *J. Chem. Soc.*, **1954**, 2965.

9) Abstract of papers presented at The 126th Meeting of the American Chemical Society, New York, N. Y., September, 1954, p. 10.

10) W. von E. Doering and D. W. Wiley, *Tetrahedron*, **11**, 183 (1960).

11) D. S. Matteson, J. J. Drysdale and W. H. Sharkey, *J. Am. Chem. Soc.*, **82**, 2853 (1960).

group, that is, the difference in the contribution of the tropylium-type structure. If this is the case, it may be anticipated that a more stable heptafulvene derivative would be obtained by the introduction of an electron-withdrawing group, such as cyano or ethoxycarbonyl, into the 8-position of heptafulvene. The present series of work was undertaken on such assumption.

Condensation of tropylium ion and active methylene compound has been reported by Vol'pin, Ahrem and Kursanov[12], and by Conrow[13]. Similar to their method, reaction of tropylium ion and malononitrile gave tropylmalononitrile (I) and ditropylmalononitrile (II). Further reaction of I with tropylium ion also afforded II. Such a fact and the ultraviolet and infrared spectra in Table I supported the structures of I and II to be correct.

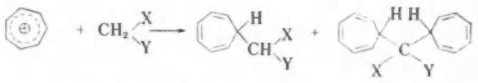

X=Y=CN or CO_2Et (I) X=Y=CN (II) X=Y=CN

(III) X=CN, Y=CO_2Et (IV) X=CN, Y=CO_2Et

(V) X=Y=CO_2Et

Condensation of tropylium ion and ethyl cyanoacetate proceeded in the same way by which ethyl tropylcyanoacetate[12] (III) and ethyl ditropylcyanoacetate (IV) were obtained. IV was also obtained by the reaction of III with tropylium ion. The structures of III and IV were supported by their ultraviolet and infrared spectroscopic data given in the Table.

It is already known that diethyl tropylmalonate (V) is obtained by the reaction of tropylium ion and diethylmalonate[12,13], but the reaction of V with tropylium ion failed to afford diethyl ditropylmalonate. This is probably rather attributed to the smaller electron-withdrawing power of the ethoxycarbonyl group than that of the cyano group or to the steric hindrance of the bulky ethoxycarbonyl group.

As was expected, application of a dehydrogenation agent to the tropilidene derivatives, I, III and V, successfully afforded the desired 8,8-disubstituted heptafulvenes. Application of one mole of bromine to I in chloroform, and subsequent heating of the bromide thereby obtained, resulted in the formation of reddish crystals (VI), $C_{10}H_6N_2$, m.p. 200°C, in 50% yield, with liberation of hydrogen bromide. Oxidation of I with *N*-bromosuccinimide in *tert*-butanol containing pyridine and water also gave VI, in 70% yield, accompanying a small amount of rearrangement product, benzalmalononitrile (VII)[14]. VI could be obtained by refluxing I with chloranil in xylene. The infrared absorption of the cyano group in VI shifted to a smaller wave number by 55 cm^{-1} than in I (cf. Table) and shows there is a fair degree of conjugation of the cyano group with the unsaturated system. The ultraviolet spectrum of VI is similar to that of 1-oxa-azulan-2-one derivatives (Fig. 1). These facts

TABLE I. ULTRAVIOLET AND INFRARED SPECTRUM

Compd.	UV in MeOH mμ (log ε)	IR, cm^{-1}
I	260(3.71)	2900, 2260(CN), 1406, 1340, 1330, 1289, 1184, 1064, 930, 900, 813, 764, 695 (a)
II	255(3.81)	3010, 2870, 2260(CN), 1615, 1530, 1445, 1440, 1275, 1210, 1196, 772, 735, 695 (a)
III	256(3.46)	2980, 2260(CN), 1740(CO), 1468, 1448, 1404, 1370, 1332, 1285, 1250, 1207, 1095, 1028, 850, 735, 700 (b)
IV	256(3.76)	2990, 2250(CN), 1732(CO), 1610, 1445, 1396, 1270, 1257, 1211, 1197, 1107, 1015, 1005, 747, 740, 702, 687 (a)
V	257.5 (3.49)(c)	2967, 1730(CO), 1443, 1440, 1365, 1305, 1265, 1230, 1170, 1112, 1095, 1030, 860, 744, 703 (b)
VI	225(4.01) 255(4.08) 384(4.36)	2205(CN), 1633*, 1585, 1520*, 1490*, 1406, 1269*, 885*, 830*, 763* (a)
VIII	254(3.96) 386(4,22)	2200(CN), 1693(CO), 1630*, 1530*, 1500*, 1483, 1420, 1412, 1390, 1255*, 1215, 1135, 1105, 1033, 830*, 820*, 780* (a)
X	246 355 (d)	1718(CO), 1685(CO), 1635*, 1545*, 1515*, 1430, 1369, 1260*, 1205, 1070, 1031, 877, 806*, 782*, 740, 704 (b) (d)

(a) KBr disk
(b) Liquid state
(c) Conrow's datum. See Ref. 12.
(d) X is comtaminated with V.

12) M. E. Vol'pin, I. S. Ahrem, D. N. Kursanov, *Isvest. Akad. Nauk U. S. S. R., Otdel Khim. Nauk*, **1957**, 1501; *Zhur. Obschchei Khim.*, **30**, 1187 (1960).

13) K. Conrow, *J. Am. Chem. Soc.*, **81**, 5461 (1959).

14) B. B. Corson and R. W. Stroughton, ibid., **50**, 2830 (1928).

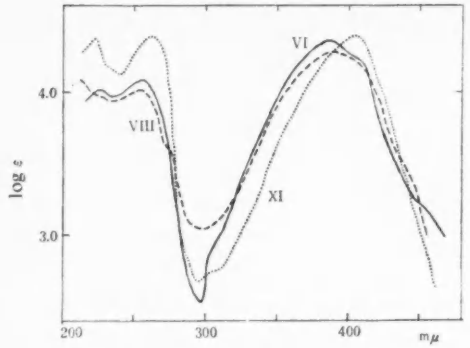

Fig. 1. Ultraviolet absorption spectra of VI (——), VIII (----) and XI (……) in methanol.

support that VI possesses the structure of 8, 8-dicyanoheptafulvene (heptafulvene-8, 8-dicarbonitrile). Heating of ditropylmalononitrile (II) at 140~150°C for 30 min. resulted in formation of VI and tropilidene in an almost quantitative yield. This reaction is considered to proceed through the intermediate depicted below (four-centered type reaction)[15].

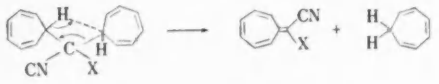

(II) X = CN (VI) X = CN
(IV) X = CO_2Et (VIII) X = CO_2Et

8-Cyano-8-ethoxycarbonylheptafulvene (VIII) as red crystals, m. p. 63.5°C was successfully synthesized in about a 40% yield by dehydrogenation of ethyl tropylcyanoacetate (III) with chloranil in boiling xylene. Pyrolysis of ethyl ditropylcyanoacetate (IV) gave also VIII in about a 25% yield. The reason why IV gave a poorer yield of VIII than in the case of pyrolysis of II can be attributed to the smaller electron-withdrawing power of ethoxycarbonyl than in the cyano group to split the bond between the tropyl group and the carbon atom to which it is attached. It was found that the reaction of III with *N*-bromosuccinimide under the condition described previously for I gave ethyl α-cyanocinnamate[16] (IX) rather than the expected VIII in a good yield. The absorption maxima of the infrared spectrum of VIII are given in the Table I. The shift of absorption bands of the carbonyl and cyano groups to a smaller wave number than those of III indicates the conjugation of these functional groups with the unsaturated system. On comparison of the infrared spectra of the two kinds of heptafulvenes, VI and VIII, it is learned that there are some absorption maxima characteristic to them. (indicated by an asterisk in the Table).

8, 8-Diethoxycarbonylheptafulvene (X) was obtained as a red oil by dehydrogenation of diethyl tropylmalonate (V) with chloranil. X was somewhat more labile than VI or VIII and tended to undergo polymerization on being left in the air. The structure of X is evident from the similarity of its ultraviolet spectrum with those of VI and VIII, and from the presence of absorption bands in its infrared spectrum characteristic to heptafulvenes (see Table 1). The absorption of carbonyl in X shifted to a small wave number from that of V. Bromination-dehydrobromination of diethyltropylmalonate (V) gave 3-ethoxycarbonyl-1-oxaazulan-2-one (XI)[17] whose formation may have passed through X as an intermediate, but this point requires further examination.

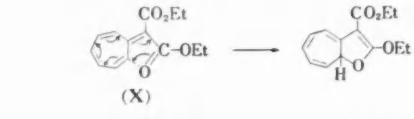

(X)

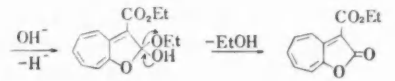

(XI)

In parallel with this work, Doi synthesized 3, 4-dihydroxy-8, 8-dicyanoheptafulvene by the reaction of 3-iodotropolone and malononitrile in the presence of sodium amide in liquid ammonia[18]. A few months later, Kitahara and Doi et al. successfully synthesized VI by condensation of tropone and malononitrile[19], and recently they obtained VI, VIII and X from tropylium ion and bromo compounds of malononitrile, ethyl cyanoacetate and diethyl malonate[20]. Their examination of the properties of heptafulvenes revealed some interesting facts as mentioned in Refs. 21 and 24.

15) A similar reaction mechanism involving an intermediate of a five membered ring can be possible. The examples of this type of reaction mechanism can be found in the explanation of the Cope Rearrangement. A. C. Cope, K. E. Hoyle and D. Heyl, *J. Am. Chem. Soc.*, **63**, 1843 (1941); E. G. Foster, A. C. Cope and F. Daniels, ibid., **69**, 1893 (1947).

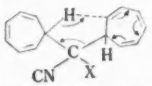

16) J. T. Carrik, *J. Prakt. Chem.*, **45**, 500 (1892).

17) S. Seto, *Science Repts. Tohoku Univ., Ser. I*, **37**, 367 (1954).

18) Paper presented at the Local Meeting of Tohoku District of the Chemical Society of Japan, Yamagata, June, 1959.

19) Paper presenteted at the General Meeting of Tohoku District of the Chemical Society of Japan, Akita, October, 1959.

20) Paper presented at the General Meeting of Hokkaido District of the Chemical Society of Japan, Sapporo, July, 1960.

8,8-Dicyanoheptafulvene (VI) is sparingly soluble in organic solvent and has a fairly high melting point, but 8-cyano-8-ethoxycarbonyl- (VIII) and 8,8-diethoxycarbonylheptafulvene (X) are more soluble than VI. VI and VIII do not form perchlorate, picrate, styphnate, or trinitrobenzene complex. VI and VIII are fairly stable to acids and do not change on being refluxed for 2 hr. with 6 N hydrochloric acid, while VI changes into a yellow solid on being heated with 75% sulfuric acid. On the other hand, VI and VIII are labile towards alkali[21]. Such behavior of 8,8-substituted heptafulvenes is different from that of heptafulvene (A)[10]. This is reminiscent of the fact that cyano and ethoxycarbonyl groups situated at 1- or 3-position of azulene are also difficult to hydrolyse with acids[22]. VI is stable to bromination and neither substitution nor addition reaction occurs on application of excess bromine in chloroform. These facts can be explained by the great contribution of the 6-π electron structures E and F due to electron-attracting groups at 8-position. In fact, as has been published[23], measurement of the dipole moment has shown that the value are 7.49 D (dioxane, 25°C) for VI and 4.40 D (benzene, 25°C) for VIII.

(E) (F)

In order to examine the aromaticity and double bond character of heptafulvenes, Diels-Alder reaction and hydrogenation were carried out. 8,8-Diethoxycarbonylheptafulvene (X) tends to undergo polymerization, while 8,8-dicyanoheptafulvene (VI) does not form an adduct even on being refluxed with maleic anhydride in xylene. 8-Cyano-8-ethoxycarbonylheptafulvene (VIII) shows an intermediate reactivity and partially undergoes addition reaction with maleic anhydride to form the adduct (XII), which has an absorption at 247 mμ. VI resists catalytic hydrogenation over palladium carbon but easily absorbs three moles of hydrogen by the use of platinum oxide as catalyst and forms a pale yellow oil[24], which still retains the absorption at 239 mμ in its ultraviolet spectrum. On the other hand, X easily absorbs 4 mol. of hydrogen and forms an octahydro compound XIII, which was converted to cycloheptylmalonic acid[25] on hydrolysis.

These experimental results have shown that the stability of 8,8-disubstituted heptafulvenes depends on the nature of the substituent present and the high stability of the compound with a strongly negative group like the cyano group which agrees with the presumption.

Experimental[26,27]

The Condensation Reaction of Tropylium Bromide and Malononitrile.—To a solution of 2.41 g. (0.037 mol.) of malononitrile in 30 ml. of pyridine was gradually added 6 g. (0.035 mol.) of crude tropylium bromide[28] with stirring for 30 min. After stirring for 2 hr. at room temperature, the mixture was poured into 110 ml. of 6 N hydrochloric acid and extracted with benzene. The benzene extract was washed with water, diluted sodium hydrogen carbonate and water, dried over sodium sulfate and evaporated. The brown oily residue crystallized partly on standing. Addition of ethanol and cooling affored 1.6 g. of crystals, m.p. 58~60°C, as first crop, 1.4 g. of crystals, m.p. 89~99°C, as second crop, and 2 g. of crystals, m.p. 38~48°C containing oil as third crop. Recrystallization of the first crop from benzene gave 1.24 g. (yield 22.7 %) of tropylmalononitrile (I) as colorless crystals, m.p. 61~62°C, which showed m.p. 62.8~63.5°C on recrystallization from benzene once more.

Found: C, 77.38; H, 5.26; N, 17.73. Calcd. for $C_{10}H_8N_2$: C, 76.90; H, 5.16; N, 17.94%.

The solution of the third crop in petroleum ether-benzene (1 : 2) was chromatographed through a column containing 40 g. of alumina. An elution with the same solvent gave 0.64 g. of crystals, m. p. 94~105°C. This substance and the second crop were combined and recrystallized from ethanol to give ditropylmalononitrile (II) as colorless prisms, m. p. 107~108°C.

Found: C, 82.78; H, 5.57; N, 11.15. Calcd. for $C_{17}H_{14}N_2$: C, 82.90; H, 5.73; N, 11.37%.

The Condensation Reaction of Tropylium Bromide and Tropylmalononitrile (I).—To a solution of 0.31 g. (2 mmol.) of I in 6.3 ml. of pyridine 0.35 g. (2 mmol.) of crude tropyl bromide was added and the solution resulted was heated on a water bath for 1.5 hr. After addition of 21.7 ml. of 6 N hydrochloric acid under ice-cooling, the mixture was extracted with benzene. The benzene extract was washed with diluted sodium hydrogen carbonate and water, dried over sodium sulfate and distilled to give 0.39 g. (yield 80%) of crystals, m.p. 102~104°C. Recrystallization from ethanol gave colorless crystals, m.p. 104~105.5°C, which showed no depression on admixture with II.

21) Y. Kitahara et al. reported that VI and VIII rearranged to the corresponding styrene derivatives on treating with dilute alkali.

22) Unpublished work by T. Asano and M. Tada in this Laboratory.

23) M. Yamakawa, H. Watanabe, T. Mukai, T. Nozoe and M. Kubo, *J. Am. Chem. Soc.*, **82**, 5665 (1960).

24) Y. Kitahara et al. found that VI absorbed 4 mol. of hydrogen to give an octahydro compound which on hydrolysis gave cycloheptylmalonic acid.

25) I. Vogel, *J. Chem. Soc.*, **1928**, 2025.

26) All melting points and boiling points were uocorrected.

27) The microanalyses were performed by Mr. S. Azumi and Miss A. Iwanaga to whom the authors expressed their gratitude.

28) Tropylium bromide was synthesized from tropilidene by the method of Doering and Knox. *J. Am. Chem. Soc.*, **79**, 352 (1957).

The Condensation Reaction of Tropylium Bromide and Ethyl Cyanoacetate.—To a solution of 16.4 g. (0.145 mol.) of ethyl cyanoacetate in 150 ml. of pyridine, 20.4 g. (0.12 mol.) of crude tropyllium bromide was gradually added with stirring under ice-cooling. The reaction mixture was allowed to stand overnight at room temperature to which 260 ml. of concentrated hydrochloric acid was added dropwise under ice-cooling. The acidic solution was extracted with ether and the ether extract was filtered off, washed with diluted sodium hydrogen carbonate and water, and dried over sodium sulfate. Evaporation of ether gave 22.30 g. of a brown oil which crystallized partially on standing. Filtration afforded 6.3 g. of crystals, m.p. 115~117°C, which were recrystallized from ethanol to give 5.3 g. (yield 15%) of ethyl ditropylcyanoacetate (IV) as colorless prisms, m.p. 124~125°C.

Found: C, 78.12; H, 6.35; N, 4.84. Calcd. for $C_{19}H_{19}O_2N$, C, 77.79; H, 6.53; N, 4.77%.

Distillation of the filtrate in reduced pressure gave 10.97 g. (yield 45.0%) of ethyl tropylcyanoacetate (III) as orange viscous oil, b.p. 130~135°C /4 mmHg. After one more distillation, the oil of b.p. 125~130°C/2 mmHg was submitted for microanalysis and spectrum determination.

Found: C, 70.22; H, 6.45; N, 7.06. Calcd. for $C_{12}H_{13}O_2N$. C, 70.91; H, 6.45; N, 6.89%.

The Condensation Reaction of Tropylium Bromide and Ethyl Tropylcyanoacetate (III).—A solution of 0.43 g. (2.5 mmol.) of crude tropyl bromide and 0.5 g. (2.5 mmol.) of III in 10 ml. of pyridine was warmed at 40~50°C in a water bath for 30 min. Under ice-cooling, the reaction mixture was neutralized by adding 36 ml. of 6 N hydrochloric acid and extracted with benzene. The benzene extract was washed with water, dried over sodium sulfate and evaporated. Recrystallization of residual crystals from ethanol gave 0.57 g. (yield 78%) of colorless crystals, m. p. 122~123°C, which were proved to be identical with IV by mixed melting point determination.

Bromination and Dehydrobromination of Tropylmalononitrile (I).—A solution of 0.32 g. (2 mmol.) of bromine in 0.3 ml. of chloroform was added dropwise to a solution of 0.31 g. (2 mmol.) of I in 3 ml. of chloroform at room temperature. During stirring for 40 min., the color of bromine disappeared and evaporating chloroform in reduced pressure at room temperature gave a pale orange oil. Heating the oil in a boiling water bath for 10 min., it changed to orange red crystals with the evolution of hydrogen bromide gas. Addition of ethanol and filtration affored 150 mg. (yield 50%) of reddish crystals, m.p. 180~185°C, which on recrystallization from ethanol gave 8, 8-dicyanoheptafulvene (VI) as red needles, m.p. 198~199°C.

Found: C, 78.09; H, 4.20; N, 17.77. Calcd. for $C_{10}H_6N_2$: C, 77.90; H, 3.92; N, 18.17%.

Dehydrogenation of Tropylmalononitrile (I) with *N*-Bromosuccinimide.—Five hundred milligrams (3.2 m mol.) of I and 550 mg. (3.0 m mol.) of *N*-bromosuccinimide were added to a solution of 11 ml. of *tert*-butanol, 2 ml. of pyridine and 1 ml. of water and the mixture was allowed to stand at room temperature for 90 hr. During this period, reddish needles separated. The filtration gave 250 mg. of red needles, m.p. 194~199°C. After adding 60 ml. of water, the filtrate was extracted with ether. The ether extract was washed with water, dried over magnesium sulfate and evaporated to 160 mg. red needles, m. p. 195~198°C and the filtrate was dissolved in benzene and chromatographed using 3 g. of alumina. After evaporation, the first elutes with benzene gave 65 mg. of colorless needles, m. p. 81~82°C, (VII) which showed no depression on admixture with benzalmalononitrile, m. p. 83°C[14]. The second elutes with benzene gave 60 mg. of red needles, m. p. 194~198°C. Three hundred and fifty milligrams (yield 70%) of total red needles were combined and recrystallized from ethanol to give red needles, m. p. 198~199°C, which is identical with VI.

Dehydrogenation of Tropylmalononitrile (I) with Chloranil.—Three hundred milligrams (1.9 mmol.) of I and 510 mg. (2.1 mmol.) of chloranil were added to 5 ml. of xylene and the mixture was refluxed for 2 hr. The dark brown precipitate separated on cooling was filtered and dissolved in benzene. The benzene solution was washed with 1 N sodium hydroxide solution and water and dried over sodium sulfate. Epaporation of benzene gave 60 mg. of orange red crystals, m. p. 179~188°C. Recrystallization from ethanol gave 50 mg. (yield 17%) of red needles, m. p. 189~199°C, which showed no depression on admixture with the authentic sample VI.

Thermal Decomposition of Ditropylmalononitrile (II).—One gram (6.4 mmol.) of II was placed in the sublimation apparatus with a cold-finger condenser and heated at 140~150°C in an oil bath for 30 min. Sublimation in 2 mmHg at the same temperature gave 540 mg. (yield 86%) of red needles, m.p. 188~193°C. Recrystallization from ethanol afforded red crystals, m.p. 199~200°C, which showed to be identical with VI on admixture with the authentic sample. During thermal decomposition and sublimation, about 200 mg. of a yellowish oil was caught in a trap cooled with dry ice-acetone. One hundred and twenty five milligrams of this oil and 147 mg. (1.5 mmol.) of maleic anhydride were added to 1.5 ml. of xylene and the mixture was refluxed for 4.5 hr. An addition of 5 ml. of petroleum ether to the solution gave 110 mg. (yield 41%) of pale yellow crystals, m. p. 98~99°C, on cooling. Recrystallization from carbon tetrachloride afforded crystals, m. p. 99~100°C, which showed no depression on admixture with adduct, m. p. 99~100°C. of tropilidene and maleic anhydride[29].

Dehydrogenation of Ethyl Tropylcyanoacetate (III) with Chloranil.—To 100 ml. of xylene, 19.6 g. (0.08 mol.) of chloranil and 10 g. (0.051 mol.) of III were added and the mixture was refluxed for 1.5 hr., while a lot of dark brown crystals separated. The crystals (A) obtained by filtration were digested several times with methanol (B) and then benzene (C). Thus 7.1 g. of chloranil was recovered as an insoluble part. The residue obtained from ethanol washings (B) by evaporation was digested with benzene (D) to give 2.1 g. of dihydrochloranil. The washings C and D were

29) K. Alder and G. Jacobs, *Ber.*, **86**, 1528 (1953).

combined and chromatographed through a column containing 60 g. of alumina. Elution of a dark red band with benzene and evaporation of benzene gave 2.84 g. of dark red oil (E) which crystalized partially. The xylene filtrate from A was evaporated in reduced pressure and the residue obtained was washed with methanol (F) to give 2.1 g. of chloranil. Methanol washings were evaporated and the residue was dissolved in benzene and chromatographed using 60 g. of alumina. Evaporation of red benzene eluates affored 1.66 g. of red crystals (G), m.p. 46~54°C. Four and a half grams (yield 45%) of the combined red crystals, E and G were dissolved in benzene and chromatographed again using alumina to give 8-cyano, 8-ethoxycarbonylheptafulvene (VIII) as red crystals, m. p. 61~63°C. Recrystallization from petroleum ether gave red prisms, m. p. 63.5°C.

Found: C, 72.06; H, 5.50; N, 6.78. Calcd. for $C_{12}H_{11}O_2N$: C, 71.62; H, 5.51; N, 6.9%.

Thermal Decomposition of Ethyl Ditropylcyanoacetate (IV).—One gram (3.4 mmol.) of IV in a small Claisen flask was heated at 170~195°C in an oil bath and distilled in 2 mmHg at the same temperature to give a red viscous oil. Addition of a little amount of ethanol afforded yellow crystals, m.p. 118~120°C, which proved to be starting IV, by mixed m.p. determination. The red filtrate, after evaporating ethanol, was dissolved in benzene and chromatographed using alumina. An elution of a red absorption band with benzene and evaporation of benzene gave 150 mg. (yield 22%) of a red oil which crystallized on standing and showed m.p. 55~60°C. Repeated recrystallization from petroleum ether gave red prisms, m.p. 63°C, which showed no depression on admixture with VIII.

The Reaction of Ethyl Tropylcyanoacetate (III) and *N*-Bromosuccinimide. — Four hundred milligrams (2 mmol.) of III and 420 mg. (2.4 mmol.) of *N*-bromosuccinimide were dissolved in a mixture of 10 ml. of *tert*-butanol, 2 ml. of pyridine and 1 ml. of water. The reaction mixture was allowed to stand at room temperature for about 1 week, then poured to 30 ml. of water and extracted with ether. The ether extracts were washed with diluted hydrochloric acid and water, dried over magnesium sulfate and evaporated to 340 mg. of brown oil. On adding a small amount of ethanol. it crystallized to give 300 mg. of crystals, m.p. 45~47°C. Recrystallization from petroleum ether afforded colorless plates (IX), m. p. 49~50°C, which showed no depression on admixture with authentic ethyl α-cyanocinnamate, m. p. 50°C[16].

Dehydrogenation of Diethyl Tropylmalonate (V) with Chloranil.—To boiling xylene were added 7.5 g. (0.03 mol.) of V and 8.8 g. (0.036 mol.) of chloranil and the reaction mixture was refluxed for 1.5 hr. After cooling, dark red crystals separated, and this was filtered to give 2.8 g. of dihydrochloranil as crystals, m.p. 228°C. Distillation of xylene from the filtrate under reduced pressure afforded precipitates from which 2.0 g. of chloranil, m.p. 285°C, were obtained by washing with methanol (A). The washings A were evaporated and the residue was dissolved in benzene and chromatographed through a column containing 50 g. of alumina. An elution of a red band with benzene and evaporation of solvent gave 4.1 g. of red oil (B). It seemed to contain a little amount of starting material, because of the presence of infrared absorption at 705 and 740 cm^{-1} due to tropilidene nucleus. The distillation of the oil (B) in reduced pressure gave the following fractions. 1) 0.32 g. of oil, b.p. 122~130°C/3 mmHg. 2) 1.00 g. of red oil, b.p. 130~140°C/3 mmHg. 3) 0.63 g. of red oil, b.p. 140~150°C/3 mmHg and a considerable amount of residue.

Found: C, 67.77; H, 6.54 (for fr. 3); C, 67.42; H, 6.91 (for fr. 2). Calcd. for $C_{14}H_{16}O_4$: C, 67.73; H, 6.50%.

Fraction 2 (0.68 g.) was allowed to stand at room temperature for about 2 weeks, thereby red gelatinous material was] obtained. On being dissolved in hot ethanol and cooled, it gave 0.35 g. of pale yellow amorphous product which softens at about 120°C. This is sparingly soluble in ether and ethanol, but soluble in acetone, benzene and ethyl acetate. It has a weak absorption maximum at 255 mμ.

Found: C, 67.46; H, 6.24. Calcd. for $C_{14}H_{16}O_4$: C, 67.73; H, 6.50%. mol. wt.: 1000 (by Rast method using camphor).

Bromination and Dehydrobromination of Diethyl Tropylmalonate (V).—To a solution of 0.96 g. (4 mmol.) of V in 5 ml. of chloroform was added a solution of 0.64 g. of bromine (4 mmol.) in 2 ml. of chloroform. After stirring for 30 min., the solvent was evaporated from the mixture to give 1.5 g. of a pale yellow oil. Heating the oil in a boiling water bath for 60 min. resulted in evolution of hydrogen bromide gas to give 1.1 g. of a brownish oil. It was dissolved in benzene and the benzene layer was washed with diluted sodium hydrogen carbonate and water, dried over sodium sulfate and chromatographed through a column containing 20 g. of alumina. The evaporation of benzene elutes gave 350 mg. of red oil which has an ultraviolet absorption maxima at 274 and 355 mμ. An elution with ethyl acetate afforded 300 mg. of brown oil which crystallized. Recrystallization from ethanol gave 50 mg. of yellow crystals (XI), m.p. 130°C, which proved to be identical with 3-ethoxycarbonyl 1-oxaazulan-2-one, m.p. 130°C, by mixed melting point determination[17].

Behavior of 8,8-Disubstituted Heptafulvene, VI and VIII against Acid and Alkali. — a) 6 N Hydrochloric acid and ethanol: 60 mg. of VI was dissolved in a mixture of 3 ml. of concentrated hydrochloric acid and 3 ml. of ethanol and the solution was refluxed for 2 hr. On cooling, red needles were crystallized and 40 mg. of starting material, m.p. 198°C, was collected by filtration.

One hundred miligrams of VIII was treated in the same way as above and the reaction mixture was poured into 50 ml. of water and extracted with benzene. The benzene extracts were washed with water, dried over sodium sulfate and evaporated to 85 mg. of red oil which crystallized and showed m.p. 59~61°C. Recrystallization from petroleum ether gave red prisms, m.p. 62~63°C, which was proved to be identical with starting VIII.

b) 75% sulfuric acid: 100 mg. of VI was added to 2.5 ml. of 75% sulfuric acid and the mixture was heated in a boilding water bath. After 6 hr.,

all crystals were dissolved and no carbon dioxide evolved. Dilution with 5 ml. of water and addition of sodium hydrogen carbonate to pH 2.5 separated an yellow amorphous material which is sparingly soluble in water or ether, but soluble in sodium hydrogen carbonate.

c) 2 N potassium hydroxide and ethanol solution: 50 mg. of VI was dissolved in 1 ml. of 6 N potassium hydroxide and 2 ml. of ethanol and the resulted mixture was refluxed for 1 hr. 20 mg. of solid resinous material separated. Extraction of the filtrate with benzene gave no starting VI.

Bromination of 8, 8-Dicyanoheptafulvene (VI).—To a solution of 80 mg. (0.55 mmol.) of VI in 3 ml. of chloroform was added a solution of 160 mg. of bromine (1 mmol.) in 0.6 ml. of chloroform and the reaction mixture was stirred at room temperature for 4 hr. Bromine still remained. Evaporation of chloroform at room temperature gave 70 mg. of red needles, m.p. 192~194°C, which were recrystallized from ethanol to give a starting material (VI) as crystals, m.p. 199~200°C.

Reaction of 8-Cyano, 8-Ethoxycarbonylheptafulvene (VIII) and Maleic Anhydride.—A solution of 300 mg. (1.5 mmol.) of VIII and 176 mg. (1.8 mmol.) of maleic anhydride in 6 ml. of xylene was refluxed for 34 hr. After xylene was distilled under reduced pressure and a small amount of methanol was added, a red viscous oil crystallized. Sixty milligrams (yield 13.4%) of light yellow crystals, m.p. 170~174°C, were obtained by filtration and recrystallized from methanol to give an adduct (XII) as crystals, m.p. 177°C.

Found: C, 63.67; H, 4.08; N, 4.62. Calcd. for $C_{16}H_{12}O_5N$: C, 64.21; H, 4.38; N, 4.68%. λ_{max}^{MeOH} 297 mμ (log ε 4.23).

Evaporation of methanol from the filtrate gave 250 mg. of a red oil which was dissolved in benzene and chromatographed through column containing 6 g. of alumina. An elution with benzene afforded 100 mg. (yield 33%) of VIII as red crystals, m.p. 50~55°C.

Reaction of 8, 8-Dicyanoheptafulvene (VI) and Maleic Anhydride.—Two hundred and fifty milligrams (1.7 mmol.) of VI and 190 mg. (1.9 mmol.) of maleic anhydride was added to 6 ml. of xylene and the resulted mixture was refluxed for 13 hr. On cooling, red needles crystallized. Evaporation of xylene and addition of ethanol to residue gave 200 mg. of starting VI as red needles, m.p. 195°C.

Catalytic Reduction of 8, 8-Dicyanoheptafulvene (VI).—a) One hundred milligrams (0.65 mmol.) of VI was dissolved in 40 ml. of ethanol and hydrogenated in the presence of 30 mg. of Pd-carbon (5%) at ordinary temperature and pressure. Only 20 ml. (0.9 mmol.) of hydrogen was absorbed for 6 hr. Treated in the usual way, 90 mg. of red needles, m.p. 184~188°C were obtained which was identical with VI.

b) With Pt-oxide. A solution of 120 mg. (0.82 mmol.) of VI in 55 ml. of ethanol was hydrogenated in the presence of 15 mg. of Pt-oxide at ordinary temperature and pressure. After 42 ml. (2.3 mmol.) of hydrogen had been absorbed, the color of the solution changed and at 57 ml. (3.1 mmol.) of hydrogen the velocity became slow and at 61 ml. (3.3 mmol.) hydrogenation was stopped. Catalysts were filtered and the filtrate was evaporated to give 120 mg. of yellow oil which showed infrared absorption at 3345, 3445 cm^{-1} due to NH_2 group. It was dissolved in benzene and passed through a column containing 9 g. of alumina. Evaporation of the benzene eluate gave 30 mg. of a colorless oil which has no infrared absorption maximum due to NH_2 or NH group, but showed an absorption maximum at 239 mμ in methanol. Evaporation of the ether eluates gave 45 mg. of a brown oil which has infrared absorption at 3345 and 3445 cm^{-1}.

Catalytic Reduction of 8, 8-Diethoxycarbonylheptafulvene (X).—A solution of 500 mg. (2 mmol.) of X in 40 ml. of ethanol was hydrogenated in the presence of 10 mg. of Pt-oxide as catalyst at ordinary temperature and pressure. After 107 ml. (4.9 mmol.) of hydrogen had been absorbed, the red color of the solution disappeared and the absorption of hydrogen almost ceased at 175 ml. (7.8 mmol.). The filtrate obtained by removal of the catalyst was evaporated to 400 mg. of an yellow oil (XIII). It has no absorption maximum in the ultraviolet spectrum.

Two hundred and fifty milligrams of XIII was added to a mixture of 2.5 ml. of 6 N potassium hydroxide and 2.5 ml. of ethanol and the solution was refluxed for 2 hr. After evaporating ethanol and diluting with water, the reaction mixture was acidified with diluted hydrochloric acid and extracted with ether. The ether extracts were washed with water, dried over sodium sulfate and evaporated to 200 mg. of colorless crystals, m.p. 145~149°C (decomp.). Repeated recrystallization from a mixture of carbon tetrachloride and acetone gave colorless crystals, m.p. 160~161°C (decomp.).

Found: 60.49; H, 7.72. Calcd. for $C_{10}H_{16}O_4$: C, 59.98; H, 8.05%.

Reported melting point for cycloheptylmalonic acid is 164.5°C[25].

The authors express their gratitude to Shell Petroleum Company for the kind donation of tropilidene used as the starting material, and to Sankyo Co., Ltd. for donation of a research fund which covered a part of the expenses for this work. The authors also thank Mr. H. Tsuruta for repeating some experiments.

Department of Chemistry
Faculty of Science
Tohoku University
Katahira-cho, Sendai

Intramolecular Interaction between Hydroxyl Group and π-Electrons. XIII[1]. *ν_{O-H} Absorption of 2,6-Diphenylphenol and the Related Compounds*

By Michinori Ōki, Haruo Hosoya and Hiizu Iwamura

(Received March 27, 1961)

It has been clarified, by a series of reports[2] from this laboratory, that, if a hydroxyl group and the π-electrons are located at suitable positions, the intramolecular interaction takes place to the extent which is determined by the structure of the molecule, the strength of the proton-donor, and the strength of the proton-acceptor. Thus, in a usual case, two O-H stretching (ν_{O-H}) absorption bands corresponding to the free and the interacting hydroxyl groups appear in the 3μ region. The above consideration leads to the deduction that, if the steric factors force the hydroxyl group to approach the π-electrons, there would be no free hydroxyl group. Tribenzylcarbinol[3] will be one of the examples in this category.

Pauling suggested[4] that the hydrogen atom of the phenolic hydroxyl group is located in the plane of the aromatic nucleus because of the resonance stabilization. Later, the suggestion was found to be true when 2,6-dichlorophenol was found[5] to possess only an O-H···Cl bonded hydroxyl group from the O-H stretching absorption in the infrared region and the microwave data also[6] led to the same conclusion as Pauling's suggestion. Therefore, if a phenol carries two groups at both ortho-positions of the hydroxyl group, which contain π-electrons, the compound can be another example which has no free hydroxyl group. In this paper, 2,6-diphenylphenol and the related compounds are taken as examples and absence or presence of the free hydroxyl group will be discussed in terms of the steric factor.

Experimental

Measurement and Calculation.—The measurement of the absorption in the 3μ region was carried out with a Perkin Elmer 112G grating spectrometer and quartz cells of 2 and 5 cm. lengths as required. Carbon tetrachloride was used as a solvent. The concentration was $1\sim2\times10^{-3}$ mol./l. and the spectral slit width 1 cm^{-1} in this region. The calculation of the band intensities was performed as reported previously[7], the integrated intensities being the authors' choice. However, on some occasions, the assumption that the appearance of the two peaks or the asymmetric curve indicates the overlap of the two symmetric curves, each of which is expressed by the Lorentz function, is proved to be false, suggesting the presence of the third band. In such cases, the molecular extinction coefficients were taken instead of the integrated intensities for the convenience of the calculation.

Materials.—The compounds used for this work are known unless otherwise mentioned and their physical constants agreed with those reported in the literature.

4-Nitro-2,6-diphenylphenol.—This compound was prepared by condensation of nitromalonaldehyde and dibenzyl ketone according to the method described by Hill[8]. The melting point of the compound was 115°C after four recrystallizations from ethanol. However, the melting point was suddenly raised up to 135°C when a large crystal was scratched, and the compound melting at 115°C has never been obtained thereafter. This phenomenon must be a type of polymorphism but the physical measurement was not carried out with the unstable form because of the lack of the sample. The melting point of the stable form was 135~136°C (lit.[8], 135~136°C).

3,5-Dimethyl-2,6-dipropenylphenol.—A mixture of 20 g. (0.123 mol.) of 2-allyl-3,5-dimethylphenol, 15.7 g. (0.13 mol.) of allyl bromide, 18.0 g. (0.13 mol.) of potassium carbonate and 50 ml. of acetone was refluxed for ten hours. The filtrate from the reaction mixture was fractionated and gave 22 g. (87%) of allyl 2-allyl-3,5-dimethylphenyl ether, b. p., 148~150°C/15 mmHg. The ether was refluxed with an equal amount of *N,N*-diethylaniline for three hours and, after cooling, the mixture was diluted with petroleum ether. The solution was shaken with dilute hydrochloric acid to remove *N,N*-diethylaniline and then extracted with Claisen's alkali. When the alkaline solution was diluted with water, an oil separated, which was distilled to give 83% 2,6-diallyl-3,5-dimethylphenol, b. p., 105~106°C/2 mmHg, n_D^{19} 1.5410.

Found: C, 82.94; H, 9.05. Calcd. for $C_{14}H_{18}O$: C, 83.12; H, 8.97%.

The phenol (10 g.) was dissolved in 30 ml. of

1) Part XII: M. Ōki and H. Iwamura, *Tetrahedron*, in press.
2) See Part XII of this series and the preceding papers cited therein.
3) M. Ōki and H. Iwamura, This Bulletin, 33, 1632 (1960).
4) L. Pauling, *J. Am. Chem. Soc.*, 58, 94 (1936).
5) O. R. Wulf, U. Liddel and S. B. Hendricks, ibid., 58, 2287 (1936).
6) Presented by T. Kojima before the 13th Annual Meeting of the Physical Society of Japan at Kyoto, October 1958. Also private communication from Prof. K. Shimoda, The University of Tokyo.
7) M. Ōki and H. Iwamura, This Bulletin, 32, 567 (1959).
8) H. B. Hill, *Am. Chem. J.*, 24, 1 (1900).

methanol containing 10 g. of potassium hydroxide and the solvent was evaporated until the temperature of the solution rose to 130°C. The mixture was refluxed for twenty hours at that temperature, cooled, diluted with water and extracted with ether. The ethereal extract was dried over potassium carbonate and fractionated to give 7.3 g. of 3,5-dimethyl-2,6-dipropenylphenol, b. p., 155°C/18 mmHg. The compound solidified and was recrystallized from petroleum ether. The melting point was 59~60°C.

Found: C, 83.04; H, 9.12. Calcd. for $C_{14}H_{18}O$: C, 83.12; H, 8.97%.

Results and Discussion

The ν_{O-H} absorptions of substituted 2,6-diphenylphenols and of 2-chloro-6-phenylphenol are summarized in Table I. As expected, these phenols did not possess absorption at the position (ca. 3600 cm^{-1}) where ordinary phenols do, but at the position which is too low a wave number to be assigned to the free hydroxyl group. Absorptions of 4-substituted 2,6-diphenylphenols are symmetric and appear at lower wave numbers as the substituent at 4 position is more electronegative, the phenomenon being common for the ordinary phenols[9] and 4-substituted 2,6-di-*tert*-butylphenols[10].

Table I. ν_{O-H} absorptions of phenols
[2,4,6-XY(C_6H_2)C_6H_2OH]

Substituent X	Substituent Y	ν_{max} cm^{-1}	ε_{max}	$A \times 10^{-4}$ mol^{-1} l. cm^{-2}
C_6H_5	NO_2	3531.2	366	2.54
C_6H_5	H	3553.3	305	1.93
C_6H_5	NH_2	3567.9	305	1.85
Cl	H	3550.2 3535.6	41 184	0.30 1.22

Since the hydroxyl group of the 4-substituted 2,6-diphenylphenols is considered to be all interacting with the π-electrons of the adjacent phenyl groups, it may be interesting to compare the absorptions of these compounds with those of the corresponding phenols in benzene. Thus the ν_{O-H} absorption of *p*-nitrophenol was measured in benzene solution, the absorption maximum being at 3527.4 cm^{-1}. The difference (3.8 cm^{-1}) from 4-nitro-2,6-diphenylphenol is rather small and supports the above mentioned idea. However, it must be considered that this difference is the combination of the solvent effect and the electronic effect of the substituent. 4-Nitro-2,6-diphenylphenol in benzene showed the ν_{O-H} absorption at 3523.3 cm^{-1}. Therefore, the difference between 3527.4 cm^{-1} and 3523.3 cm^{-1} may be attributed to the effect of two phenyl groups at *o*-positions. Phenol in benzene is known to show its ν_{O-H} maximum at 3562 cm^{-1} [11]. The deviation from 3553.3 cm^{-1} may be interpreted similarly.

2-Chloro-6-phenylphenol has its ν_{O-H} absorption maximum at 3535.6 cm^{-1} but the curve shows a shoulder at the higher wave number side. Therefore, the curve was divided into two, assuming that it was an overlap of two symmetric curves which could be expressed by the Lorentz function (Fig. 1). The authors

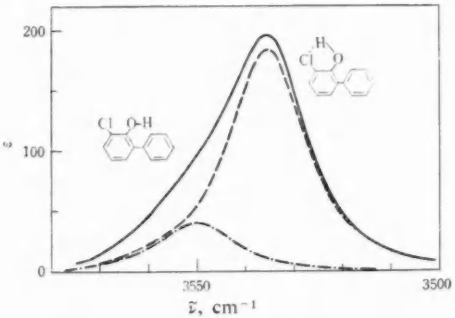

Fig. 1. ν_{O-H} absorption of 3-chloro-2-hydroxybiphenyl.
——— the observed curve
– – – O-H···Cl
—·—·— O-H···π

have data, concerning the interacting form of 2-hydroxybiphenyl and the hydrogen-bonded form of *o*-chlorophenol, which reveal the fact that the former is located at 3565.0 cm^{-1} and the latter at 3547.0 cm^{-1}. Then it will be most probable to assign the band maximum at 3535.6 cm^{-1} to the hydrogen-bonded form of the hydroxyl group with ortho chlorine atom and that at 3550.2 cm^{-1} to the interacting form with π-electrons. The lowering of the wave number must be derived from the effect of the electron-drawing substituents. As to the integrated intensities of each component, the O-H···Cl bonded form is apparently large, but it may not necessarily mean that the molecule having the hydrogen bond between the hydroxyl group and the chlorine atom is greatly in the majority, since it is a well-known fact that the absorption intensity per molecule becomes stronger on O-H···Cl hydrogen bond formation.

As the source of the π-electrons, the propenyl group might be considered equally effective with the aromatic nucleus. Thus, various phenols containing propenyl groups are prepared and their ν_{O-H} absorptions examined. The results are summarized in Table II. As is clear from Table II, replacement of a phenyl

9) P. J. Stone and H. W. Thompson, *Spectrochim. Acta*, **10**, 17 (1957).
10) K. U. Ingold, *Can. J. Chem.*, **38**, 1092 (1960).
11) M. L. Josien, P. Dizabo and P. Saumagne, *Bull. soc. chim. France*, **1957**, 423.

Table II. ν_{O-H} absorption of phenols containing propenyl group
[2,6-X(CH_3CH=CH)C_6H_3OH]

X	O-H	ν_{max} cm^{-1}	$\varepsilon^a{}_{max}$	$\Delta\nu_{max}$ cm^{-1}
H	f*	3611.1	159.0	58.8
	i*	3552.2	34.0	
CH_3CH=CH-	f	3603.5	78.0	57.5
	i	3546.0	72.0	
C_6H_5	f	3607.4	21.3	44.2
	i	3563.2	241.6	

* f and i denote the free and the interacting forms, respectively.

group by a propenyl group gives rise to the appearance of an absorption due to the free form of the hydroxyl group and this phenomenon is enhanced when two propenyl groups are introduced in place of the phenyl groups of 2, 6-diphenylphenol. One of the possibilities which reasonably explains the phenomenon is the concept of the rotational isomerism. *o*-Propenylphenol is taken as an example for the explanation, because of its simplicity. In this case, the consideration of the cis form[4] will suffice to cover the possibilities, since 2, 6-dipropenylphenol contains only this form whichever direction the O-H points.

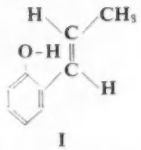

I

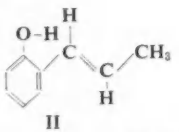

II

The authors are assured that *o*-propenylphenol assumes the trans form with respect of the ethylenic linkage[12]. Then there will be two rotational isomers about the $C_{Ph}-C_{\alpha}$ axis, being represented by I and II. Structure II will possess a free hydroxyl group, if a pair of π-electrons are necessary for the interaction and/or if the hydrogen atom of the hydroxyl group must approach from the upper side to the π-electron cloud in order to establish the interaction. Thus, structure I may be the only form which possesses the interaction in *o*-propenylphenol. The availability of the π-electrons of 2, 6-diphenylphenol, on the other hand, will not be altered no matter what rotational position is taken, because the structure corresponding to I is always involved in this compound. If the above assumption is correct, a compound which is forced to take structure I will have no free hydroxyl group. The enforcement may be given by the steric hindrance. 3, 5-Dimethyl-2-propenylphenol and 3, 5-dimethyl-2, 6-dipropenylphenol were chosen as examples. The results are shown in Table III.

12) It is supported by the fact that *o*-propenylphenol possesses an absorption at 968.6 cm^{-1} due to C-H out-of-plane deformation.

Table III. ν_{O-H} absorptions of 6-substituted 3, 5-dimethyl-2-propenylphenols
[6,3,5,2-X(CH_3)$_2$(CH_3CH=CH)C_6H-OH]

X	O-H	ν_{max} cm^{-1}	$\varepsilon^a{}_{max}$	$\Delta\nu_{max}$ cm^{-1}
H	f	3607.7	19.4	68.5
	i	3539.2	101.9	
CH_3CH=CH-	f	—	—	—
	i	3526.5	120.2	

The steric effect of the methyl group may be too great to assume structure III and the structure IV becomes favorable. Therefore, the structure of 3, 5-dimethyl-2-propenylphenol may be represented by IV. The structure IV is, at the same time, favorable for the internal interaction and these considerations predict that 3, 5-dimethyl-2-propenylphenol contains more interacting molecules than 2-propenylphenol in spite of the fact that the methyl group is the electron-donating group which weakens the proton donating power of the phenols. Comparison of the data in Tables II and III indicates that this is really the case. Since 2, 6-dipropenyl-3, 5-dimethylphenol has two propenyl groups which are sterically enforced to take the structure as IV, it is naturally expected that this compound will possess single ν_{O-H} absorption at a rather low frequency. Actually a perfectly symmetrical band is found at 3526.5 cm^{-1}. Hence, it is proved that the propenyl group can also be the source of the π-electrons which give th ν_{O-H} absorption at extraordinarily low frequency.

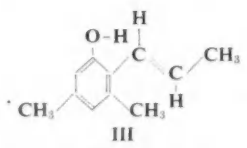

III

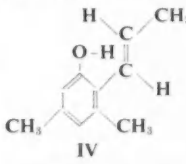

IV

As to the steric effect on the interaction, it may also be interesting to examine the ν_{O-H} absorption of 2-methyl-6-propenylphenol. Since the hydroxylic hydrogen atom is located on the plane of the benzene nucleus, it is reasonably expected that, in *o*-cresol, the molecule will be more stable when the hydroxylic hydrogen is located on the opposite side of the methyl group. Therefore, in 2-methyl-6-propenylphenol, the contribution of structure V may be more than that of structure VI. This consideration suggests that there will be more molecules, which have the intramolecular interaction between the hydroxyl group and π-electrons, in 2-methyl-6-propenylphenol than in 2-propenylphenol. The former compound has one absorption maximum at 3617.0 cm^{-1}

($\varepsilon^a_{max}=83.8$) and another at 3548.3 cm^{-1} ($\varepsilon^a_{max}=39.3$). Comparison of the results with these compounds indicates that the above consideration is correct, since both $J\nu_{max}$ and $\varepsilon_i/\varepsilon_f$ are greater in 2-methyl-6-propenylphenol.

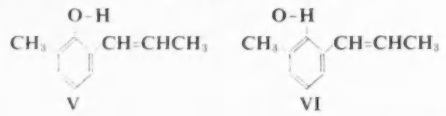

V VI

The ν_{O-H} absorptions of the precursors of the propenyl compounds, the phenols carrying allyl groups, are also examined in connection with the freedom of rotation and the basicity of the ethylenic linkage. The results are shown in Table IV. The diagrams of the ν_{O-H} absorptions of 2-allyl-3, 5-dimethylphenol and 2, 6-diallyl-3, 5-dimethylphenol are also given in Fig. 2, because of the difficulty of understanding the matter from the mere numericals. The $\varepsilon_i/\varepsilon_f$ of the phenols carrying allyl groups are always greater than those of the propenylphenol derivatives unless they carry methyl groups at 3 and 5 positions. This will mean that the effect of the basicity of the ethylenic

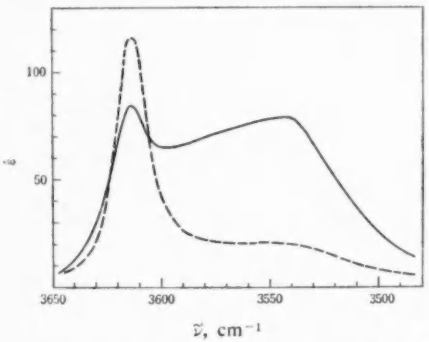

Fig. 2. The apparent ν_{O-H} absorption of 2, 6-diallyl-3, 5-dimethylphenol (——) and 2-allyl-3, 5-dimethylphenol (– – –).

TABLE IV. ν_{O-H} ABSORPTIONS OF PHENOLS CARRYING ALLYL GROUPS

Phenol	O-H	ν_{max} cm^{-1}	ε^a_{max}	$J\nu_{max}$ cm^{-1}
3-Allyl-2-hydroxybiphenyl	f	3609.2	13.9	46.0
	i	3563.2	259.5	
2, 6-Diallylphenol	f	3616.0	45.5	71.7
	i	3544.3	88.3	
2-Allyl-3, 5-dimethylphenol	f	3614.0	116.0	66.8
	i	3547.2	20.6	
2, 6-Diallyl-3, 5-dimethylphenol	f	3614.0	84.5	72
	i	3542*	79	
2-Allyl-6-methylphenol	f	3619.0	77.8	71.0
	i	3548.0	52.3	

* Four place number is given because of the uncertainty due to the broadness of the band (see Fig. 2).

bond plays the major role and the rotation about $C_{Ph}-C_\alpha$ axis the minor role, for the interaction. This is because the basicity of the ethylenic linkage in the propenylphenols is rather low due to the conjugation with the benzene nucleus. In contrast with the above situation, when methyl groups are present at 3 and 5 positions, the allylphenols show smaller $\varepsilon_i/\varepsilon_f$ value than those of the corresponding propenylphenols. This is without doubt caused by the freedom of rotation. That is, it is possible for "cis" 2-allyl-3, 5-dimethylphenol to take the conformations illustrated, for example, by VII and VIII, which are unfavorable for the intramolecular interaction. The possibilities of taking these unfavorable structures are owing to the rotation about $C_{Ph}-C_\alpha$ and $C_\alpha-C_\beta$ axes, while, in 3, 5-dimethyl-2-propenylphenol, the rotation about the $C_{Ph}-C_\alpha$ is at least partially restricted due to the resonance stabilization and the steric interference of the methyl group, possibly causing all the cis forms to be the interacting. Baker and Shulgin[13] have mentioned that the steric effect of the methyl group in 2-allyl-3, 5-dimethylphenol is favorable for the interaction, when compared with 2-allylphenol, probably because the contribution of structures such as VIII is less. Nevertheless, the conclusion is not contradictory, since it may be possible for

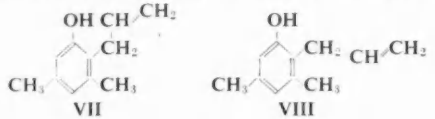

VII VIII

structure VIII to be present to a small extent and it is out of the question at the present time which structure is the main contribution for the free cis form.

When an asymmetrical band is assumed to be an overlap of the symmetrical bands, the compounds which contain one or two propenyl groups at ortho positions of the hydroxyl group usually possess three ν_{O-H} bands unless the absorption corresponding to the interacting form is very strong. In the case of 2-phenyl-6-propenylphenol, the three bands may be reasonably assigned to the free, the interacting with the phenyl group, and the interacting with the propenyl group. However, the situation must be further studied with other compounds before obtaining a general conclusion.

The authors are indebted to Professors Yoshiyuki Urushibara and Saburo Nagakura for their valuable advice and encouragement throughout this work. A part of the cost

13) A. W. Baker and A. T. Shulgin, *J. Am. Chem. Soc.*, **80**, 5358 (1958).

was defrayed from the Grant in Aid for Fundamental Scientific Research of the Ministry of Education, for which the authors' thanks are due.

Department of Chemistry
Faculty of Science
The University of Tokyo
Hongo, Tokyo

Intramolecular Interaction between Hydroxyl Group and π-Electrons. XIV[1]*. Electronic Effect of the Substituents on the Interaction in 2-Hydroxybiphenyls*

By Michinori Ōki and Hiizu Iwamura

(Received March 27, 1961)

Since the observation by Wulf and his co-workers[2], it has been occasionally reported that 2-hydroxybiphenyl shows doublet O-H stretching band in the infrared absorption spectrum. The phenomenon was explained on the assumption that 2-hydroxybiphenyl would be composed of cis and trans isomers. Such an explanation had been adopted by Pauling[3] for the like phenomenon observed in the infrared spectrum of *o*-chlorophenol. As the cis isomer seems to be less stable because of

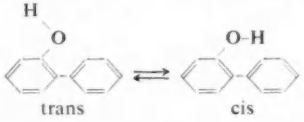

the steric interference, there must exist a cause which makes the appearance of this form possible. Wulf and his co-workers attributed stabilizing force to the approach of the hydroxyl group to the first carbon atom of the benzene ring which is ortho to the hydroxyl group and to the consequent attraction between them, but failed to show the true nature. Later, Mecke[4] explained the phenomenon from the polarizable nature of the π-electrons in the benzene nucleus and assumed that a so-called π-complex was formed intramolecularly, without giving further details. Recently Musso and von Grunelius[5] reported some ν_{O-H} absorptions of 2, 2'-dihydroxybiphenyl and their derivatives and discussed the competitive intramolecular hydrogen bond formation between O-H···O and O-H···π systems, with special reference to the geometrical consideration. The examples are, however, too complicated to help us to understand the nature of the latter interaction separately.

The present authors have preliminarily reported[6] that the energies of the intramolecular interaction between the hydroxyl group and the π-electrons in 2-hydroxy-4- and -4'-nitrobiphenyls are 2.5 and 0.9 kcal./mol., respectively. The present study was initiated on the expectation that the electronic effect of the substituents on the interaction will provide additional informatin in regard to the true nature of the interaction.

Experimental

Measurement and treatment of the infrared spectra were carried out as described previously[7]. The known samples were prepared according to the literature, and the new as described below. Their physical constants and analytical data are listed in Table I.

Materials. — *2-Hydroxyl-4-methoxybiphenyl.* — 2-Amino-4-methoxybiphenyl[8] (0.02 mol., 4.0 g.) was dissolved in aqueous sulfuric acid (4.5 ml. of concentrated sulfuric acid and 6 ml. of water) and diazotized with 1.5 g. of sodium nitrite in 3 ml. of water. The excess of nitrite was decomposed by a lump of urea and the solution was poured into 20 ml. of boilng 30% aqueous sulfuric acid. The separated dark oil was taken up in ether and the ether layer was extracted thrice with 20% aqueous sodium hydroxide solution. The alkaline extract was acidified and extracted with ether. The ether extract was treated with active charcoal, filtered and evaporated. The tarry residue was extracted with hot petroleum ether and the extract deposited prisms after cooling. The pure sample was obtained by recrystallization from petroleum ether.

1) Part XIII: M. Ōki, H. Hosoya and H. Iwamura, This Bulletin, **34**, 1391 (1961).
2) O. R. Wulf, U. Liddel and S. B. Hendricks, *J. Am. Chem. Soc.*, **58**, 2290 (1936).
3) L. Pauling, ibid., **58**, 94 (1936).
4) W. Lüttke and R. Mecke, *Z. Elektrochem.*, **53**, 241 (1949).
5) H. Musso and S. von Grunelius, *Ber.*, **92**, 3101 (1959).
6) M. Ōki, H. Iwamura and Y. Urushibara, This Bulletin, **31**, 770 (1958).
7) M. Ōki and H. Iwamura, ibid., **32**, 567 (1959).

TABLE I. PHYSICAL CONSTANTS AND ANALYTICAL DATA OF THE SUBSTITUTED 2-HYDROXYBIPHENYLS

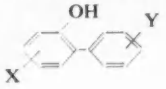

Substituent X	Substituent Y	M. p. or b. p. observed (lit.)	Analytical Data Found C	Found H	Found N	Calcd. C	Calcd. H	Calcd. N
H	H	59°C (59°C[8])						
4-MeO	H	66~67°C	78.08	6.25		77.98	6.04	
4-Cl	H	38.5~39°C	70.46	4.43	(Cl=17.39)	70.42	4.43	(Cl=17.33)
4-NO_2	H	103~105°C (102°C[9])						
5-Et	H	122°C/2 mmHg (171~172°C/18 mmHg[10])	84.92	7.09		84.81	7.12	
5-PhN_2	H	95~96°C (94~95°C[11])						
5-CO_2Me	H	128~129.5°C	73.81	5.52		73.67	5.30	
5-NO_2	H	128°C (128°C[11])						
H	3'-MeO	90~91°C	78.13	6.09		77.98	6.04	
H	3'-CO_2Me	88~89°C	73.77	5.48		73.67	5.30	
H	3'-NO_2	99.5~100°C	66.78	4.22	6.44	66.97	4.22	6.51
H	4'-MeO	65~65.5°C	78.13	6.15		77.98	6.04	
H	4'-Cl	51~52°C (53°C[12])						
H	4'-Br	60°C (60~61°C[12])						
H	4'-I	74°C	48.79	3.15		48.67	3.06	
H	4'-CO_2Me	133~133.5°C	73.85	5.43		73.67	5.30	
H	4'-NO_2	123~124°C (122°C[12])						

4-Chloro-2-hydroxybiphenyl.—A half moles (86.3 g.) of 4-chloro-2-nitroaniline[14] was diazotized in 150 ml. of concentrated hydrochloric acid with 35 g. of sodium nitrite in 50 ml. of water, and decomposed in the presence of 2 l. of thiophene free benzene by adding an excess of sodium acetate. Stirring was continued over-night. The benzene layer was washed with aqueous sodium hydroxide and the solvent evaporated. 4-Chloro-2-nitrobiphenyl distilled at 160~166°C/2 mmHg, and solidified in the receiver. It was recrystallized from petroleum ether-benzene to give prisms melting at 53°C (lit.[15], 52~53°C). The nitro-compound (23 g., 0.1 mol.) was catalytically hydrogenated over platinized Raney nickel[16] in ethanol, 6.5 l. of hydrogen being absorbed in 2 hr. 2-Amino-4-chlorobiphenyl was, without further purification, diazotized in aqueous sulfuric acid with sodium nitrite and decomposed by pouring into 30% aqueous sulfuric acid. 4-Chloro-2-hydroxybiphenyl was recrystallized from carbon tetrachloride to form prisms.

5-Ethyl-2-hydroxybiphenyl.—To a solution of 5 g. of 5-acetyl-2-hydroxybiphenyl[10] in 100 ml. of acetic acid was added a few drops of 3 N hydrochloric acid and 100 mg. of platinum oxide. On shaking under hydrogen atmosphere, 1.1 l. of hydrogen was absorbed under the atmospheric pressure and at the room temperature. The solvent was evaporated under reduced pressure and the residue was distilled at 122°C/2 mmHg, giving the desired phenol, n_D^{15} 1.5893.

2-Hydroxy-5-methoxycarbonylbiphenyl.—5-Acetyl-2-hydroxybiphenyl[10] in pyridine was oxidized with iodine to the corresponding β-ketoalkylpyridinium iodide, which was cleft by aqueous alcoholic sodium hydroxide to 2-hydroxybiphenyl-5-carboxylic acid, as is specified by King[17]. The carboxylic acid was recrystallized from benzene to give plates melting at 148°C (lit.[18], 148~149°C). A suspension of 8 g. of the hydroxycarboxylic acid in 100 ml. of methanol was saturated with hydrogen chloride, refluxed on a water bath for two hours and then poured into 500 ml. of ice-water. The crystals were collected and recrystallized from benzene to give plates.

2-Hydroxy-3'-methoxybiphenyl.—To a mixture of 30 g. of *m*-bromoanisole and 50 g. of *o*-nitrochlorobenzene was added in five portions 50 g. of copper bronze at 200°C. The temperature was kept at 200~240°C for five hours longer. After cooling, the solid mass was extracted with acetone and the extract was fractionally distilled under diminished pressure, the fraction boiling at 150~175°C/1~2 mmHg being collected. On fractional recrystalliza-

8) W. Hückel, O. Neunhoeffer, A. Gercke and E. Frank, *Ann.*, **477**, 123 (1930).
9) C. Finzi and A. Mangini, *Gazz. chim. ital.*, **62**, 664 (1932).
10) K. von Auwers and G. Wittig, *J. prakt. Chem.*, **108**, 99 (1924).
11) W. Borsche and B. G. B. Scholten, *Ber.*, **50**, 600 (1917).
12) J. C. Colbert and R. M. Lacy, *J. Am. Chem. Soc.*, **68**, 271 (1946).
13) F. C. Coppa and L. P. Walls, *J. Chem. Soc.*, **1950**, 314.
14) M. A. F. Holleman, *Rec. trav. chim. Pay-Bas*, **34**, 207 (1915).
15) K. Hoegerle and P. L'Écuyer, *Can. J. Chem.*, **37**, 2074 (1959).
16) S. Nishimura, This Bulletin, **32**, 61 (1959).
17) L. C. King, *J. Am. Chem. Soc.*, **66**, 894 (1944).
18) K. H. Stotta and A. E. Nold, *Ber.*, **68**, 2230 (1935).

tion of the distillate from methanol, 10 g. of 3'-methoxy-2-nitrobiphenyl, melting at 83~84°C was obtained. Found: N, 6.28. Calcd. for $C_{13}H_{11}O_3N$: N, 6.11%. Catalytic reduction of the nitrocompound gave 2-amino-3'-methoxybiphenyl which was characterized as the acetyl derivative (m. p., 114°C) and analyzed. Found: C, 74.88; H, 6.48; N, 5.81. Calcd. for $C_{15}H_{15}O_2N$: C, 74.66; H, 6.27; N, 5.81%. Diazotization of the amine and the subsequent hydrolysis gave 2-hydroxy-3'-methoxybiphenyl.

2-Hydroxy-3'-methoxycarbonylbiphenyl.—2-Amino-3'-methoxycarbonylbiphenyl[19] was diazotized in aqueous sulfuric acid and decomposed at 80°C. The oily layer was extracted with ether and washed with aqueous sodium carbonate solution. The solvent was evaporated and the residue was recrystallized from carbon tetrachloride, to give prisms.

2-Hydroxy-3'-nitrobiphenyl.—To a solution of 3 g. of 2-methoxy-3'-nitrobiphenyl (m. p., 68.5~69°C)[20] in 50 ml. of acetic acid was added 20 ml. of 48% aqueous hydrobromic acid. The mixture was warmed on a water bath for five hours, when the oily layer disappeared. The solution was concentrated under reduced pressure and the residue was diluted with 50 ml. of water. Brown oil was extracted with benzene and the benzene layer was extracted with 20% aqueous sodium hydroxide. The aqueous layer was acidified and the product recrystallized from methanol to form needles.

2-Hydroxy-4'-methoxybiphenyl.—4'-Methoxy-2-nitrobiphenyl[21] (2.3 g., 0.01 mol.) was reduced with 13 g. of stannous chloride dihydrate and 15 ml. of concentrated hydrochloric acid in 20 ml. of alcohol by refluxing for two hours. The amine[22] in 30 ml. of water and 2 ml. of sulfuric acid was diazotized with 0.7 g. of sodium nitrite in 2 ml. of water and hydrolyzed as usual to the desired phenol. The phenol was recrystallized from a mixture of carbon tetrachloride and petroleum ether (1 : 1).

2-Hydroxy-4'-iodobiphenyl.—4'-Amino-2-hydroxybiphenyl[23] (3.7 g., 0.02 mol.) was diazotized in aqueous sulfuric acid (2.4 g. of concentrated sulfuric acid and 20 ml. of ice-water) with 1.5 g. of sodium nitrite in 3 ml. of water. The diazonium solution was added dropwise to the boiling aqueous potassium iodide solution (4 g. of potassium iodide in 5 ml. of water) and the separated brown oil was extracted with ether. On evaporation the ether extract gave heavy oil which was heated with hot petroleum ether and decanted. Repetition of the process gave thick prisms.

2-Hydroxy-4'-methoxycarbonylbiphenyl.—To a mixture of 50 g. (0.32 mol.) of *o*-nitrochlorobenzene and 26 g. (0.1 mol.) of methyl *p*-iodobenzoate, heated at 230~240°C, was added 80 g. of copper bronze for three hours. After cooling, the mass was extracted with acetone using a Soxlet extractor. The acetone extract deposited a large amount of 2,2'-dinitrobiphenyl, which was filtered off. The mother liquor was evaporated and the residue was refluxed with 500 ml. of ethanol and 160 ml. of 10% aqueous sodium hydroxide for three hours. The mixture was diluted with water to make up 1 l. and boiled for several minutes with active charcoal and then filtered. The filtrate was acidifed and the precipitate was collected. Recrystallization from acetic acid gave 6 g. of 2-nitrobiphenyl-4'-carboxylic acid, melting at 247°C (lit.[24], 250°C). It was catalytically hydrogenated over platinum oxide, as described in the literature[24]. The aminocarboxylic acid was diazotized and hydrolyzed as usual. The crude hydroxycarboxylic acid was used, without further purification, for the preparation of the corresponding ester. Esterification was carried out by saturating the methanolic suspension with hydrogen chloride nd refluxing the mixture for two hours. Recrystallization from carbon tetrachloride gave prisms.

Results and Discussion

It must be confirmed in the first place that two bands which appear in the 3 μ region in the infrared are not derived from the intermoleculer hydrogen bonding but from the intramolecular origin. With 2-hydroxybiphenyl, the infrared spectra were measured over the concentration range from 0.5 to 0.001 mol./l. in carbon tetrachloride. At concentration of over 0.1 mol./l., a third band appears at 3460 cm^{-1}, which is assigned to the ν_{O-H} of the associated hydroxyl group, but, below 0.01 mol./l., this band disappears and the ratio of intensities of the remaining ones scarcely depend upon concentraion. All the following data were obtained in these conditions, usually 0.001 mol./l. solution being employed.

The absorption at the higher wave number of 2-hydroxybiphenyl is located at 3607 cm^{-1} and, referring to the free ν_{O-H} of phenol, 3610 cm^{-1} [25], is assigned to the trans form of the molecule having the free hydroxyl group (f). The other absorption at the lower wave number is tentatively assigned to the cis form having the intramolecular interaction with π-electrons of another benzene ring and having a less force constant of the O-H stretch (i). The intensities and the maxima of these two bands vary considerably with different substituents on each benzene ring. The apparent effect of the substituents on the infrared absorption spectra is shown in Figs. 1 and 2, and the numerical data are in Tables II and III. If the varied band properties can be explained reasonably in terms of the intramolecular interaction with π-electrons, the above assignment will be justified.

Substitution has been confined to the positions at 4, 5, 3' or 4' of the hydroxyl group

19) R. Adams and T. L. Cairns, *J. Am. Chem. Soc.*, **61**, 2179 (1939).
20) W. J. Dunstan and G. K. Hughes, *J. Proc. Roy. Soc. N. S. Wales*, **80**, 77 (1947); *Chem. Abstr.*, **42**, 4161a (1948).
21) B. Jones and F. Chapman, *J. Chem. Soc.*, **1952**, 1832.
22) I. G. M. Campbell and D. J. Morrill, ibid., **1955**, 1666.
23) W. G. Christiansen and S. E. Harris, *J. Am. Pharm. Assoc.*, **22**, 723 (1933); *Chem. Abstr.*, **29**, 4382 (1935).
24) I. G. M. Campbell, *J. Chem. Soc.*, **1950**, 3113.
25) P. J. Stone and H. W. Thompson, *Spectrochim. Acta*, **10**, 17 (1957).

Table II. ν_{O-H} absorptions of 2-hydroxybiphenyls substituted in A-ring

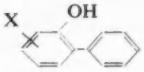

X	OH	ν_{max} cm^{-1}	$\Delta\nu^{a}_{1/2}$ cm^{-1}	$A\times10^{-4}$ mol^{-1} l. cm^{-2}	$\Delta\nu_{max}$ cm^{-1}	A_i/A_f
H	f	3607.0	18.2	0.20	42.0	6.4
	i	3565.0	15.0	1.28		
4-MeO	f	3606.0	22.8	0.20	43.2	7.2
	i	3562.8	15.8	1.44		
4-Cl	f	3601.5	20.8	0.20	43.3	7.3
	i	3558.2	15.6	1.45		
4-NO_2	f	3597.8	19.6	0.23	44.0	7.4
	i	3553.8	19.4	1.70		
5-Et	f	3610.2	20.3	0.23	41.5	5.6
	i	3568.7	16.0	1.27		
5-PhN_2	f	3599.0	24.0	0.21	45.8	8.3
	i	3553.2	16.8	1.74		
5-CO_2Me	f	3596.7	18.6	0.18	46.1	8.8
	i	3550.6	15.8	1.59		
5-NO_2	f	3590.0	24.6	0.22	47.4	8.6
	i	3542.6	16.6	1.90		

Table III. ν_{O-H} absorptions of 2-hydroxybiphenyls subsituted in B-ring

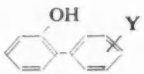

Y	O-H	ν_{max} cm^{-1}	$\Delta\nu^{a}_{1/2}$ cm^{-1}	$A\times10^{-4}$ mol^{-1} l. cm^{-2}	$\Delta\nu_{max}$ cm^{-1}	A_i/A_f
H	f	3607.0	18.2	0.20	42.0	6.4
	i	3565.0	15.0	1.28		
3'-MeO	f	3607.1	17.4	0.15	47.9	9.3
	i	3559.2	17.0	1.40		
3'-CO_2Me	f	3605.0	18.8	0.44	30.7	2.4
	i	3574.3	17.0	1.06		
3'-NO_2	f	3602.6	19.0	0.99	20.4	0.66
	i	3582.2	16.6	0.65		
4'-MeO	f	2607.1	18.0	0.15	47.6	9.7
	i	3559.5	17.6	1.45		
4'-Cl	f	3605.0	17.8	0.37	35.0	3.1
	i	3570.0	15.6	1.14		
4'-Br	f	3606.0	14.8	0.36	34.9	3.3
	i	3576.1	16.0	1.19		
4'-I	f	3605.3	13.4	0.32	35.1	4.1
	i	3570.2	16.0	1.32		
4'-CO_2Me	f	3304.4	17.2	0.34	33.0	3.6
	i	3571.4	16.2	1.21		
4'-NO_2	f	3602.1	17.2	0.79	22.5	0.97
	i	3579.6	17.6	0.77		

Added in proof: After this paper had been received, W. Beckering (*J. Phys. Chem.*, **65**, 206 (1961)) reported O-H$\cdots\pi$ interaction in some of the examples included in the present study.

at 2-position in biphenyl skeleton in order to avoid either another intramolecular hydrogen bond[1] and/or steric influence[26], which make the consideration more complex. For the sake of convenience, the substituted 2-hydroxybiphenyls are calssified into two groups; one is those with the substituent on the benzene ring (A) which bears the hydroxyl group and the other those on the other ring (B).

The varied $\Delta\nu_{max}$ and A_i/A_f in Tables II and III may be considered to correspond to the strength of the interaction, since the former is known to be approximately proportional to the enthalpy (Eq. 1)[27] and the latter to the equilibrium constant (Eq. 2)[28] of the interaction. Therefore, neither value should be independent of the other and the relation between $\Delta\nu_{max}$ and $\log(A_i/A_f)$ must be linear (Eq. 3) if ΔS of the interaction, and the constants a and b are independent of the

26) Unpublished work. See also Ref. 5.

27) R. M. Badger and S. H. Bauer, *J. Chem. Phys.*, **5**, 839 (1937).

28) M. Ōki and H. Iwamura, This Bulletin, **33**, 1600 (1960).

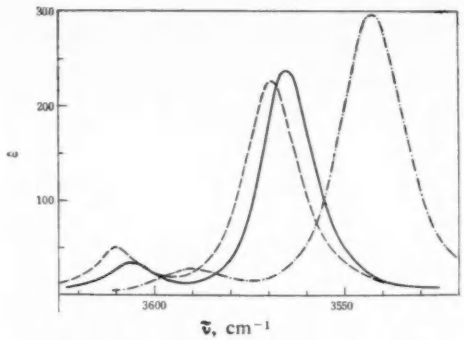

Fig. 1. The apparent ν_{O-H} absorptions of 2-hydroxybiphenyls (A).

——— 2-hydroxybiphenyl
– – – 5-ethyl-2-hydroxybiphenyl
—·—·— 2-hydroxy-5-nitrobiphenyl

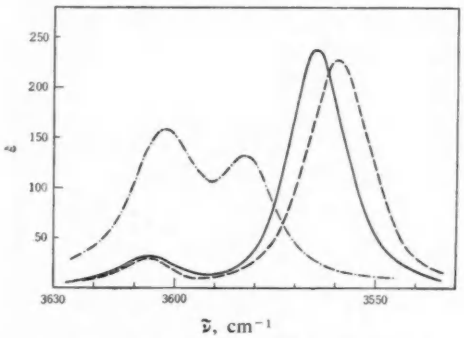

Fig. 2. The apparent ν_{O-H} absorptions of 2-hydroxybiphenyls (B).

——— 2-hydroxybiphenyl
– – – 2-hydroxy-3′-methoxybiphenyl
—·—·— 2-hydroxy-3′-nitrobiphenyl

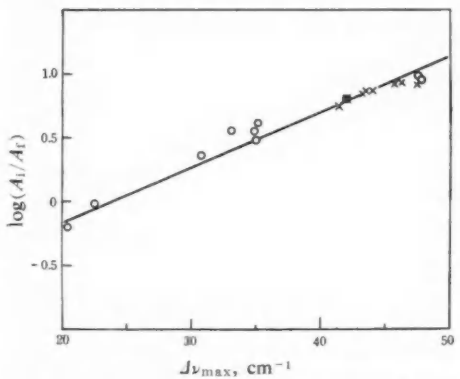

Fig. 3. Relation between $\log(A_i/A_f)$ and $\Delta\nu_{max}$, the cross and circle representing 2-hydroxybiphenyls substituted in the A and B ring, respectively.

substituents. The case is realized from Fig. 3. Strictly speaking, however, the line has a little convex curvature upwards, which may be attributed to the second order term neglected in

$$-\Delta H = a\Delta\nu_{max} \quad (1)$$

$$K = bA_i/A_f \quad (2)$$

$$RT\cdot\ln(A_i/A_f) = a\Delta\nu_{max} + (T\Delta S - RT\cdot\ln b) \quad (3)$$

the approximation, assuming the constancy of a, b and ΔS. From the gradient of the line, a constant a in the equation can be estimated to be 0.057 kcal.cm^{-1} at the measured temperature. It may be expressed otherwise by saying that the wave number shift of 18 cm^{-1} corresponds to the energy of the interaction of one kcal./mol. Compared with the ordinary hydrogen bonding, in which displacement of ν_{O-H} by 40 cm^{-1} corresponds to one kcal./mol. of the enthalpy change[27], these interactions seem to have the characteristic that a smaller $\Delta\nu_{max}$ corresponds to an appreciable enthalpy change. This is, however, overestimated, since the term $T\Delta S$ in Eq. 3 is some what dependent on $\Delta\nu_{max}$ and the greater $\Delta\nu_{max}$ makes the absolute value of ΔS, which is inherently negative, greater. It will tend to make its value less.

It is further shown in Fig. 3, that the points representing 2-hydroxybiphenyls substituted on the B-ring spread wider by about five times than those having the substituent on the A-ring; that is, the effect of the substituents on the phenomenon is more fully developed in the B-ring. As the first approximation, the strength of the intramolecular interaction between the hydroxyl group and π-elctrons is expected to be influenced by the substituent on the B-ring by directly affecting the π-electron density and the proton accepting character of the B-ring, while the substituent on the A-ring will not touch the π-electron density of the B-ring but affect the proton donating character of the hydroxyl group. The above observation means that the former effect is predominant.

As to the latter effect, it is well known that acid dissociation constant (pK_a) of phenols[29] and spectroscopically free ν_{O-H} of phenols in carbon tetrachloride solution[30], are in linear relationship with Hammett's sigma constants of the substituents. The free ν_{O-H} of 2-hydroxybiphenyls substituted in the A-ring have been examined in this connection and the results are presented in a Hammett sigma-rho plot in Fig. 4. A line with rho value of −13.8 is

29) H. C. Brown, D. H. McDaniel and O. Häfliger, "Determination of Organic Structures by Physical Methods", Ed. by E. A. Braude and F. C. Nachod, Academic Press Inc., New York (1955), p. 589.
30) L. L. Ingraham, J. Corse, G. F. Bailey and F. Stitt, *J. Am. Chem. Soc.*, **74**, 2297 (1952).

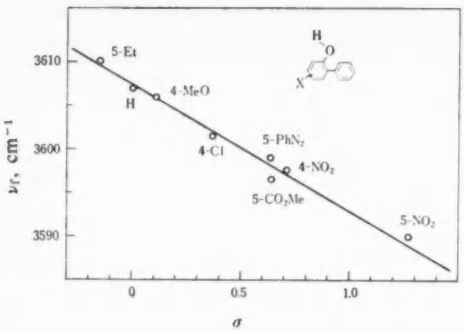

Fig. 4. ν_{O-H} frequencies of the free hydroxyl group in 2-hydroxybiphenyls substituted in the A ring versus the Hammett sigma constants.

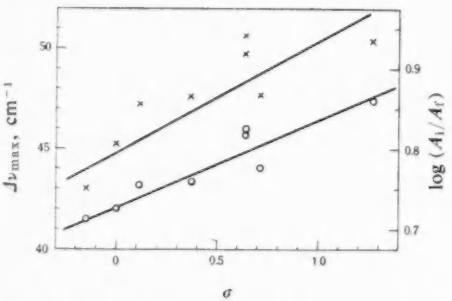

Fig. 5. Dependence of the two band properties, $J\nu_{max}$ (the circles to the left ordinate) and $\log (A_i/A_f)$ (the crosses to the right ordinate) on the substituents in A-ring.

obtained, comparable to $\rho = -12.6$ in the substituted phenols[30]. This suggests that the substituents in the A-ring are really pertaining to the proton donating character of the hydroxyl group just as in phenols and thus must be affecting the strength of the intramolecular interaction. In Fig. 5, it is illustrated to what extent the strength of the interaction, i.e., $J\nu_{max}$ and $\log (A_i/A_f)$ depends on the sigma constants of the substituents. It can be concluded from Figs. 4 and 5, that the intramolecular interaction between the hydroxyl group and π-electrons strengthens as the electron drawing power of the substituents or the acidity of the hydroxyl group enhances, and weakens with the electron-donating substituents.

As the substituents on the ring B govern the density and polarizability of π-electrons acting as the hydrogen accepter, it is natural that the variation in the B-ring substituent causes a salient change in the degree of the interaction in such a direction that the electron donating substituents (e.g., methoxyl) enhance the interaction, while the electron-attracting substituents (e.g., nitro) disfavor the interaction. Two kinds of band properties, $J\nu_{max}$ and $\log (A_i/A_f)$ have again been tested for Hammett's sigma-rho relation, in the expectation that π-electron density and/or polarizability at the site of the interaction will be expressed in terms of sigma values, just as in the case of the electrophilic nuclear substitution reaction[31]. Although Wulf et al.[2] suggested that the hydroxyl group would approach the first carbon atom (1′-carbon), there is no a priori reason which of the 3′- or 4′- substituents may be regarded as *m*- or of *p*-position in respect of the site of the interaction. In the previous papers[32,33] the authors have succeeded in assigning the position of the hydroxylic proton in the interaction in benzyl and phenethyl alcohols by plotting $\log (A_i/A_f)$ against Hammett's sigma values considering the various possibilities, and by choosing the assignment of better linearity. The trial has again been applied to the present system but failed to obtain the precise linearity in either case. In Fig. 6 is shown the relation between $\log (A_i/A_f)$s' relative to that for 2-hydroxybiphenyl and the Hammett sigma constants, *m*- and *p*-values of which are allotted to 4′- and 3′-substituents, respectively. These are

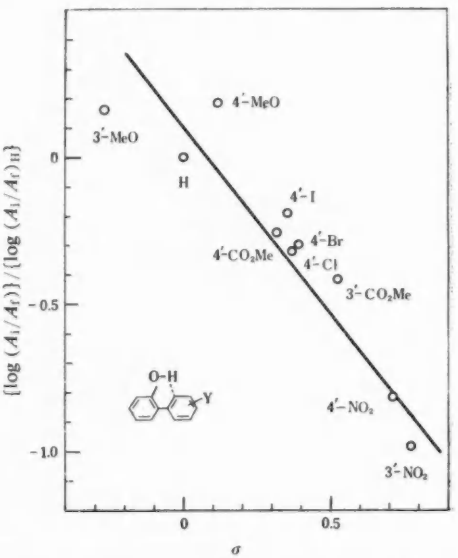

Fig. 6. Relation between $\{\log (A_i/A_f)\}/\{\log (A_i/A_f)_H\}$ and the Hammett sigma constants in 2-hydroxybiphenyl substituted in B-ring.

31) C. W. McGary, Jr., Y. Okamoto and H. C. Brown, ibid., 77, 3037 (1955).
32) M. Ōki and H. Iwamura, This Bulletin, 32, 955 (1959).
33) M. Ōki and H. Iwamura, ibid., 32, 1135 (1959).

in better linearity than the reverse assignment in so far as 3′-electrophilic substituents (e. g., nitro) disfavor the interaction more than the 4′-ones. Here it may be said that the hydroxylic proton is more concerned with π-electrons at 2′-carbon than at the 1′. Methoxyl group at 3′- and 4′-positions, however, favors the interaction equally, in spite of the fact that their sigma constants are of opposite sign and differ by 0.38. If the interaction is solely concerned with π-electrons at 2′-carbon, the methoxyl group at 4-position would not have favored the interaction. Putting the emphasis upon the last observation and regarding the difference in the electrophilic substituents minor, it may tentatively be concluded that the hydroxylic proton is concerned with π-electron density between 1′ and 2′ carbon atoms, like the structure of the complex formed between silver ion and benzene[34].

It has been assumed that the electronic effect of the substituents might be confined to the ring to which it is attached. Biphenyls are, however, characteristic of its conjugation between two phenyl rings, and a considerable conjugation has been demonstrated by the kinetic study[35] and the ultraviolet spectroscopy[36], even when it is substituted at one ortho-position by a rather small group[37]. Although there is no datum available for the 2-hydroxybiphenyl system, if the conjugation exists between two rings in this system, the free ν_{O-H} must also be dependent on the substituents on the B-ring. In Fig. 7 the wave number where the free ν_{O-H} appears is plotted to Hammett's sigma constants, *m*- and *p*-sigma values being alloted to the substituents at 3′- and 4′-positions, respectively. A line having an inclination of −3.9 is obtained and, compared with that of Fig. 4, −13.8, it can be

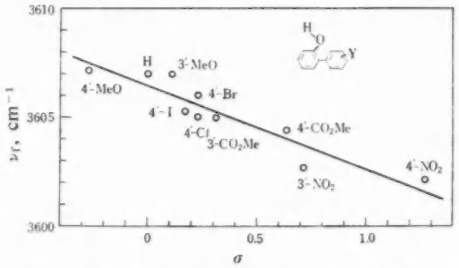

Fig. 7. ν_{O-H} frequencies of the free hydroxyl group in 2-hydroxybiphenyls substituted in the B-ring, versus the Hammett sigma constants.

34) R. E. Rundle and J. H. Goring, *J. Am. Chem. Soc.*, **72**, 5337 (1950).
35) E. Berliner and L. H. Liu, ibid., **75**, 2417 (1953).
36) V. P. Kreiter, W. A. Bonner and R. H. Eastmann, ibid., **76**, 5770 (1954).
37) G. H. Beaven, D. M. Hall, M. S. Lesslie and E. E. Turner, *J. Chem. Soc.*, **1952**, 854.

stated that in 2-hydroxybiphenyls 28% of the electronic effect of the substituents can be transmitted across the pivot bond through mesomerism and/or induction. The degree of conjugation is rather great in spite of the ortho substitution when compared with biphenyls free from the substituent[35,36], because Berliner obtained, for example, $\rho=0.37$ from the dissociation constants of the substituted biphenyl-4-carboxylic acids, deducing 37% propagation of the substituent effect[38]. This may be reasonable, however, because the data obtained for 2-hydroxybiphenyls are for free ν_{O-H} of trans configration, which, unlike cis form, has only a little excessive steric hindrance compared with a hydrogen atom.

With these new informations of conjugative effect, the effect of the substituents at the A and the B-rings on the electron donating power of the B-ring and on the proton donating character of the hydroxyl group, respectively, must be reevaluated. Since the effect of the substituents is more strongly exerted by affecting the proton accepting power than the proton donating one, as shown in Fig. 3, the effect of the B-ring substituents on the apparent interaction by affecting the proton donating character of the hydroxyl group of the A-ring may be neglected. On the other hand, the effect of the A-ring substituents on the proton accepting character of the B-ring must be taken into account, since it amounts to 28% of that caused by the B-ring substituents and has as much influence on the interaction as the effect on the proton donatining power of the hydroxyl group. The electron attracting substituents (e. g., nitro), for example, influence the interaction as a result of two opposing effects. That is, they favor the interaction by strengthening the proton donating character of the hydroxyl group and disfavor it by lessening the proton accepting charactor of the B-ring. Although it is as yet impossible to separate the two competing effects quantitatively, it is clear that the pure effect of A-ring substituents on the proton donating character of the hydroxyl group is more pronounced than is estimated from Fig. 3.

The authors are indebted to Professor Yoshiyuki Urushibara for his encouragement and discussuion throughout this work. The authors' thanks are also due to the Ministry of Education for the Grant in Aid for Fundamental Scientific Research.

Department of Chemistry
Faculty of Science
The University of Tokyo
Hongo, Tokyo

38) E. Berliner and E. A. Blommers, *J. Am. Chem. Soc.*, **73**, 2479 (1951).

Studies on Meso-ionic Compounds. XIV[1]*. Synthesis of Meso-ionic Compounds from Pyridazine Derivatives Having a Carboxymethylmercapto Group*

By Masaki OHTA and Kimio KISHIMOTO

(Received April 3, 1961)

In the previous paper of this series, the reaction of several kinds of azoles (5-phenyl-1, 3, 4-triazole, 5-phenyl-1, 3, 4-oxadiazole, 1, 5-diphenyl-1, 3, 4-triazole, benzothiazole, benzoxazole, cyclohexeno- and cyclopentenothiazoles) having a carboxymethylmercapto group with acetic anhydride was reported[2]. Although no formation of pigments had been reported by Duffin et al.[3], it was demonstrated that not only the corresponding meso-ionic compounds but also pigments are formed in the reaction.

In this paper, the present authors further extended this reaction to pyridazine derivatives and studied whether the meso-ionic compounds are obtained or not from the pyridazine derivatives possessing a carboxymethylmercapto group by the loss of one mole of water. The structure of the resulting meso-ionic compounds from pyridazine derivatives was confirmed by infrared absorption, hydrolysis, and the reaction of the compounds with phenylhydrazine or mercuric chloride.

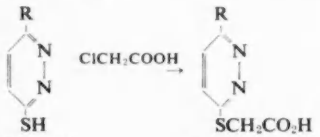

I (a—f) II (a—f)

a: R=CH_3 d: R=Cl
b: R=SCH_3 e: R=Ph
c: R=SCH_2Ph f: R=SH

Pyridazine derivatives possessing a carboxymethylmercapto group[4] were prepared from the corresponding mercapto pyridazine derivatives by the reaction with monochloroacetic acid. By the action of acetic anhydride or acetic anhydride-pyridine on 3-methyl-6-(carboxymethylmercapto)-pyridazine (IIa), violet pigment, which was not prosecuted for detailed investigation because of its difficult purification, was formed, and no corresponding meso-ionic compound was formed. But the present authors have found that IIa reacts readily with acetic anhydride-pyridine-triethyl amine to give a red meso-ionic compound IIIa by the loss of one mole of water, and in the same manner as in the case of IIa the other meso-ionic compounds IIIa—IIIe are obtained from those corresponding parent acids IIa—IIe, respectively. Unlike those reported previously[2], however, the present compounds are not formed in the absence of triethylamine as a more basic tertiary base, and by moisture in the air or in the solvent of recrystallization the new red compounds IIIa—IIIe immediately are turned into pale yellow compounds of which analytical values show their structures to be meso-ionic compounds IIIa—IIIe having a water of crystallization and which reversibly return to the red compounds of IIIa—IIIe on drying. These

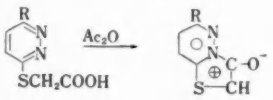

II (a—e) III (a—e)

meso-ionic compounds are heat-unstable solids which are readily soluble in polar and non-polar solvents. For example, meso-ionic compounds give yellow aqueous solutions with the exception of IIIe and red solution in absolute ethanol or dry benzene. The influence of the substituent in 3-position of pyridazine on the ring closure of II by acetic anhydride was scarecely observed. Only 3-mercapto-6-(carboxymethylmercapto)-pyridazine (IIf) gave no mese-ionic compound. On storage, IIIa deteriorated and became black after about two weeks at room temperature. Though the other compounds IIIb—IIIe are stable, IIIa—IIIe turn black in pyridine or 10% aqueous sodium hydroxide. The infrared spectra of IIIa—IIIe respectively, in comparison with those of the parent acids, have a new strong absorption at 1630~1650 cm^{-1} with the disappearance of a band near 1700 cm^{-1} due to carbonyl vibration of the carboxy group. This similar remarkable change of the spectra of meso-ionic compounds from these pyridazine derivatives has been observed also in infrared spectra of meso-ionic

1) Part XIII, This Bulletin, **34**, 668 (1961).
2) M. Hashimoto and M. Ohta, ibid., **33**, 1394 (1960).
3) G. F. Duffin and J. D. Kendall, *J. Chem. Soc.*, **1951**, 734; ibid., **1956**, 361.
4) M. Kumagai, *J. Chem. Soc. Japan, Pure Chem. Sec.* (*Nippon Kagaku Zasshi*), **81**, 1604, 1886 (1960).

compounds derived from 2-(carboxymethylmercapto)-pyridine, whose structure had been confirmed synthetically[3], and from azoles having a carboxymethylmercapto group[2]. By 50% aqueous sulfuric acid IIIa—IIIe were easily hydrolyzed to the corresponding parent acids IIa—IIe respectively. The meso-ionic compounds IIIa, IIIb and IIIe reacted with

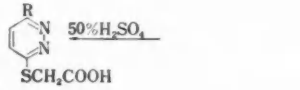

II (a—e)

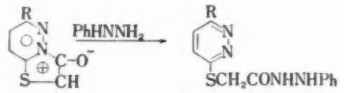

III IV(a, b and e)

mercuric chloride in methanol respectively to give pale yellow precipitates, whose analytical values suggest the structures to be IIIa+2$HgCl_2$, IIIb+HgCl and IIIe+HgCl respectively[5,6], but in the case of the parent acids IIa—IIe no such precipitates were formed. When meso-ionic compounds IIIa, IIIb and IIIe were heated with phenyl hydrazine in ethanol, the corresponding phenylhydrazides (IVa, IVb and IVe) were obtained. The fact that the corresponding phenylhydrazones were not formed, suggests that the C–O bond of the meso-ionic compounds has no ketonic character.

Experimental

3-Benzylmercapto-6-mercaptopyridazine.—A solution of benzylchloride (0.8 g.) in methanol (2 ml.) was poured into a solution of 3,6-dimercaptopyridazine[4] (0.8 g.) and sodium hydroxide (0.2 g.) in methanol (14 ml.). The solution was heated at 70°C on a water bath for 5 min., and 10% aqueous sodium hydroxide was added. The insoluble substance was filtered off. The filtrate was neutralized with aqueous hydrochloric acid to precipitate 3-benzylmercapto-6-mercaptopyridazine. Recrystallization from glacial acetic acid gave pale yellow needles (0.9 g.), m. p. 178~179°C. Yield 68.7%.

Found: N, 11.90. Calcd. for $C_{11}H_{10}N_2S_2$: N, 11.96%.

The alkali insoluble substance described above was recrystallized from ethanol to give white needles of 3,6-bis(benzylmercapto)-pyridazine, m. p. 121~122°C.

Found: N, 8.74. Calcd. for $C_{18}H_{16}N_2S_2$: N, 8.64%.

3-Methyl-6-(carboxymethylmercapto)-pyridazine (Ia).—A solution of chloroacetic acid (3.75 g.) and sodium hydroxide (1.6 g.) in water (16 ml.) was

Table I. 3-Substituted pyridazine derivatives having a carboxymethylmercapto group in the 6-position

	R	Appearance	M. p., °C	Yield, %	Formula	Anal. N% Found	(Calcd.)
IIb	SCH_3	White plates	183~184	78.3	$C_7H_8O_2N_2S_2$	13.04	(12.96)
IIc	SCH_2Ph	White plates	108~109	72.5	$C_{13}H_{13}O_2N_2S_2$	9.67	(9.59)
IId	Cl	7)					
IIe	Ph	White plates	149~150	theor.	$C_{12}H_{10}O_2S$	11.60	(11.38)
IIf	SH	Yellow prisms	180 (decomp.)	71.4	$C_6H_6O_2N_2S_2$	13.56	(13.86)

Table II. Meso-ionic compounds from acids IIb—IIe

	M. p., °C	Yield, %	Formula	Anal. C% Found (Calcd.)	H% Found (Calcd.)	N% Found (Calcd.)
IIIb	>300	theor.	$C_7H_6ON_2S_2$	42.20 (42.43)	3.14 (3.05)	14.20 (14.14)
IIIc	167~168	81.8	$C_{13}H_{10}ON_2S_2$	57.07 (56.93)	3.89 (3.68)	10.19 (10.22)
IIId	>250	80.0	$C_6H_3ON_2SCl$	38.30 (38.57)	1.96 (1.61)	14.87 (11.38)
IIIe	110 (decomp.)	(60.0)	$C_{12}H_{10}O_2N_2S$ (having H_2O)	60.43 (58.53)	4.38 (4.09)	11.38 (11.38)
	122 (decomp.)	60.0	$C_{12}H_8ON_2S$	62.78 (63.16)	3.55 (3.53)	12.13 (12.28)

5) G. F. Duffin and J. D. Kendall, *J. Chem. Soc.*, **1956**, 3189.
6) H. Kato et al., *J. Chem. Soc. Japan, Pure Chem. Sec.* (*Nippan Kagaku Zasshi*), **78**, 707 (1957).
7) J. Kinugawa et al., *J. Pharm. Soc. Japan* (*Yakugaku Zasshi*), **80**, 1559 (1960).

added to a solution of 3-methyl-6-mercapto-pyridazine (5.0 g.)[4] and sodium hydroxide (1.6 g.) in water (16 ml.). The solution was warmed on a water bath at 60~65°C for an hour. After cooling, the reaction mixture was neutralized with 10% aqueous hydrochloric acid and the resulting precipitate was filtered off. Recrystallization from ethanol gave white plates (4.3 g.) m. p. 138~139°C. Yield 58.9%.

Found: C, 45.50; H, 4.52; N, 14.90. Calcd. for $C_7H_8O_2N_2S$: C, 45.65; H, 4.34; N, 15.22%.

IIb, IIc, IId, IIe and IIf[4]. — These acids were prepared by the same procedure as used for Ia. The following Table I set forth these results.

Meso-ionic Compound IIIa from IIa.—The acid IIa (4.0 g.) was dissolved at room temperature in a mixture of acetic anhydride, pyridine and triethylamine (volume ratio of 1 : 1 : 1) (5 ml.). The solution immediately turned red and after a few minutes orange crystals were separated, which were filtered off, and completely washed with ether. Recrystallization from ethanol-ligroin gave pale yellow needles, m. p. 106°C (decomp.), which have a water of crystallization.

Found: C, 45.60; H, 4.45; N, 15.14. Calcd. for $C_7H_6ON_2S \cdot H_2O$: C, 45.65; H, 4.38; N, 15.21%.

When this compound was heated at about 65°C under reduced pressure, the water of crystallization was removed, affording red crystals of IIa, m. p. 135°C (decomp.). Yield 2.0 g. (50.0%).

Found: C, 50.30; H, 3.72; N, 16.54. Calcd. for $C_7H_6ON_2S$: C, 50.60; H, 3.64; N, 16.87%.

Meso-ionic Compound IIIb, IIIc, IIId and IIIe Derived from Acids IIb, IIc, IId and IIe Respectively.—In exactly the same manner as in the case of IIa, these meso-ionic compounds were obtained from the corresponding parent acids IIb, IIc, IId and IIe respectively, and are listed in Table II.

Action of Aqueous Sulfuric Acid on IIIa.—A suspension of IIIa (0.3 g.) in 50% aqueous sulfuric acid (1 ml.) was refluxed gently for 5 min. The solution slowly turned red to yellow. After cooling, the solution was neutralized with 10% aqueous sodium hydroxide and was concentrated under diminished pressure. Absolute ethanol (50 ml.) was added to the concentrated solution and the resulting precipitate was filtered off. Crude crystals obtained by concentration of the filtrate were recrystallized twice from ethanol, to afford white plates (0.15 g.), m. p. 139°C, which were undepressed by admixture with an authentic sample of IIa.

Action of Aqueous Sulfuric Acid on IIIb and IIIe.—The reaction product, from IIIb or IIIe by a method similar to that for IIa, was undepressed by the admixture with authentic sample of IIb or IIe. Yield of IIb, 81.7% and that of IIe 40%.

Action of Aqueous Sulfuric Acid on IIIc. — A suspension of IIIc (0.1 g.) with 50% aqueous sulfuric acid (2 ml.) was gently boiled for 10 min., and after cooling, the solution was neutralized with 10% aqueous sodium hydroxide and was extracted with ether. The extract was dried over anhydrous sodium sulfate and was evaporated to dryness. The residue was recrystallized from glacial acetic acid affording 0.07 g. of white plates m. p. 108~109°C, which showed no depression on admixture with an authentic specimen of IIc.

Action of Aqueous Sulfuric Acid on IIId. — In the same manner as in the case of IIIc, the parent acid IIc was obtained.

Reaction of IIIa, IIIb and IIIe Respectively, with Mercuric Chloride[5,6]. — The solution of IIIa (0.7 g.) and sodium acetate (0.7 g.) in 50% aqueous methanol (20 ml.) was added to a solution of mercuric chloride (1.1 g.) in 50% aqueous methanol (5 ml.). The solution immediately turned yellow to separate a yellow precipitate (1.3 g.). Recrystallization from ethanol gave pale yellow crystals, m. p. > 230°C.

Found: N, 4.22. Calcd. for $C_7H_6ON_2SHg_2Cl_4$: N, 3.94%.

Yellow precipitate from IIIb or IIIe was prepared by the same method as used for IIIa and yellow precipitate from IIIb has m. p. > 300°C.

Found: N, 6.71. Calcd. for $C_7H_5ON_2S_2HgCl$: N, 6.47%. M. p. 250°C (decomp.) from IIIe, Found: N, 5.73, 5.71. Calcd. for $C_{12}H_7ON_2SHgCl$: N, 6.05%.

Action of Phenylhydrazine on IIIa.—A solution of phenylhydrazine (0.1 g.) in absolute ethanol (1 ml.) was added to a solution of IIIa (0.1 g.) in absolute ethanol (2 ml.) and the solution was refluxed on a water bath for 15 min. and decolorized with charcoal. The residual oil obtained by evaporation of alcohol solidified giving crude crystals (0.1 g.), m. p. 125~126°C, on cooling in an ice bath for 1 hr. Twice recrystallization from ethanol-ligroin yielded a pure sample of the corresponding phenylhydrazide (IVa) as orange needles, m. p. 138~139°C.

Found: C, 56.43; H, 5.21; N, 20.32, 20.24. Calcd. for $C_{13}H_{14}ON_4S$: C, 56.92; H, 5.15; N, 20.43%.

Action of Phenylhydrazine on IIIb and IIIe.—In exactly the same manner as described above, phenylhydrazides (IVb and IV) were prepared, IVe was plates (33.9%), m. p. 181~181.5°C.

Found: C, 64.14; H, 4.93; N, 16.42. Calcd. for $C_{13}H_{16}ON_4S$: C, 64.27; H, 4.80; N, 16.66%. IV, m. p. 152~153°C. Found: N, 18.75. Calcd. for $C_{13}H_{14}ON_4S_2$: N, 18.29%.

The authors are indebted to Dr. Asaji Kondo for microanalyses.

Laboratory of Organic Chemistry
Tokyo Institute of Technology
Meguro-ku, Tokyo

The Crystal Structure of Orthorhombic Aniline Hydrobromide, $C_6H_5NH_3Br$

By Isamu NITTA*, Tokunosuké WATANABÉ and Inao TAGUCHI†

(Received March 13, 1961)

It has been reported in the previous paper[1], that aniline hydrobromide, $C_6H_5NH_3Br$, shows a phase transition of λ-type in the neighborhood of room temperature. It is monoclinic below 27.5°C, and is orthorhombic above this temperature. In the present paper, the crystal structure of the high temperature modification will be given.

Experimental

Crystals of aniline hydrobromide were obtained by slow evaporation from methanol solutions. They were made into small cylindrical rods parallel to the b- and c-axis, less then 0.1 mm. in diameter, by partial dissolution with filter paper moistened with methanol. The hot air stream method[2] was applied to take oscillation and Weissenberg photographs. The temperature of the crystals was maintained at 70 ± 1°C during exposure.

The unit cell containing four formula units was found to have the following dimensions:

$$a=16.77\pm0.06\,\text{Å}$$

$$b=6.05\pm0.03\,\text{Å}$$

and

$$c=6.86\pm0.03\,\text{Å}$$

The space group was uniquely determined, from missing reflections, to be D_{2h}^{16}-Pnaa.

In order to collect intensity data, unfiltered Cu-K radiations were used for taking Weissenberg photographs. This allowed us to make use of K_β in addition to K_α[3]. The multiple-film technique was applied, and the relative intensities of reflections were visually estimated by comparison with standard intensity scales for each series due to K_α and K_β. Corrections for Lorentz and polarization factors were made in the usual way. Corrections for absorption were made using Bradley's method for cylindrical specimens[4]. The linear absorption coefficients for Cu-K_β were calculated using Walter's rule[5] from the values for Cu-K_α. The extinction effect was more or less minimized by putting larger weights on the relative intensity values obtained from smaller specimens.

Structure Determination

Since there are four formula units in the unit cell, four bromine atoms must lie on one of the four-fold equivalent positions, a, b, c and d, given by D_{2h}^{16}-Pnaa[6]. Two of these, a and b, have the eigen symmetry C_i-$\bar{1}$, and the other two, c and d, have C_2-2. Inspection of the observed intensities of reflections (h 0 0) ruled out the possibility of placing these four bromine atoms either on a or b, hence they must lie either on c or d. There are four aniline molecules in the unit cell and their longest molecular axis on which lie the atoms, N, C_1 and C_4 must occupy either c or d. Now neither the bromine atoms nor aniline molecules can occupy simultaneously the same equivalent positions, neither c nor d, since the axial length a is too short to be accommodated with these. This case is definitely eliminated also by a qualitative disagreement between observed and calculated structure factors (0 k l) even for lower order reflections. Therefore, if the bromine atoms are placed on c, the atoms N, C_1 and C_4 must be placed on d, or vice versa. The choice of these two alternatives is immaterial, since it depends only on the choice of origin. Thus, the atomic coordinates for each atom are those given in Table I.

TABLE I. ATOMIC COORDINATES ASSIGNED TO EACH ATOM

4Br	$x\,\frac{1}{4}\,\frac{1}{4}$, $\bar{x}\,\frac{3}{4}\,\frac{3}{4}$, $\frac{1}{2}+x\,\frac{1}{4}\,\frac{1}{4}$, $\frac{1}{2}-x\,\frac{3}{4}\,\frac{3}{4}$;
4N, 4C_1 and 4C_4:	$x\,\frac{3}{4}\,\frac{1}{4}$, $\bar{x}\,\frac{1}{4}\,\frac{3}{4}$, $\frac{1}{2}+x\,\frac{3}{4}\,\frac{1}{4}$, $\frac{1}{2}-x\,\frac{1}{4}\,\frac{3}{4}$;
8C_2 and 8C_3:	$x\,y\,z$, $x\,\frac{1}{2}-y\,\frac{1}{2}-z$, $\frac{1}{2}-x\,\frac{1}{2}+y\,\bar{z}$, $\frac{1}{2}-x\,\bar{y}\,\frac{1}{2}+z$, $\bar{x}\,\bar{y}\,\bar{z}$, $\bar{x}\,\frac{1}{2}+y\,\frac{1}{2}+z$, $\frac{1}{2}+x\,\frac{1}{2}-y\,z$, $\frac{1}{2}+x\,y\,\frac{1}{2}-z$

The number of positional parameters to be determined is ten in all. However, if we assume the usual bond distances and bond angles for the aniline molecule, they can be reduced to only three. They are x_{Br}, x_N and α, the last one representing the angle between the benzene ring and the plane (010). An approximate value 0.025 for x_{Br} was easily obtained from the Patterson synthese, $P(xz)$ and $P(xy)$. Using this value, trial and error methods gave

* Present address: Department of Chemistry, Kwansei Gakuin University, Uegahara, Nishinomiya.

† Deceased, 26 May, 1959.

1) I. Taguchi, This Bulleten, **34**, 392 (1961).

2) I. Taguchi, *Annual Report Inst. Fibre Research, Osaka Univ.*, **8**, 45 (1945).

3) T. Watanabé and I. Taguchi, *Acta Cryst.*, **14**, 67 (1961).

4) A. J. Bradley, *Proc. Roy. Soc.*, **A47**, 879 (1935).

5) "Internationale Tabellen zur Bestimmung von Kristallstrukturen", II., Gebrüder Borntträger, Berlin (1935), p. 576.

6) "International Tables for X-Ray Crystallography", I, The Kynoch Press, Birmingham (1952), p. 144.

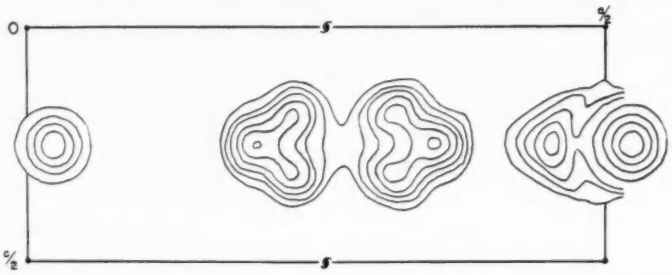

Fig. 1. Electron density projection along the b-axis. Contours for the carbon and nitrogen atoms are drawn at intervals of 1 $Å^{-2}$, starting at the 3 e $Å^{-2}$ level. Contours for the bromine atom are drawn at intervals of 10 e $Å^{-2}$, starting at the 10 e $Å^{-2}$ level.

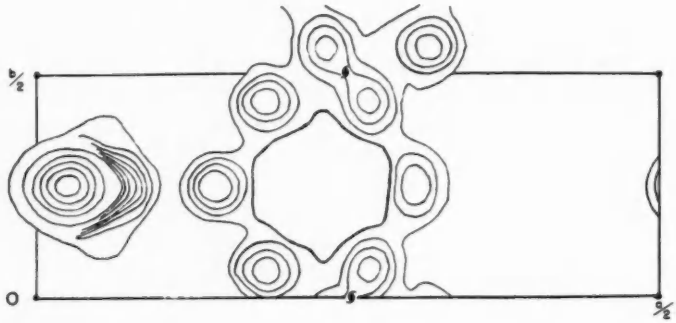

Fig. 2. Electron density projection along the c-axis. Contours intervals are the same as in Fig. 1.

approximate values, $x_N=0.43$ and $\alpha=25°$, from $(0kl)$ reflections.

The electron density projections along the b- and c-axis were then calculated, based on this trial structure, a few terms of doubtful sign being ommitted. They showed all the atoms except nitrogen. Afer three cycles of refinement, there were no terms whose signs were to be changed. The final electron density projections, $\rho(xz)$ and $\rho(xy)$, are shown in Figs. 1 and 2. From the $\rho(xz)$ projection, a more accurate value for x_{Br} was obtained assuming the Gaussian curvature near the peak. Those of the carbon atoms were also obtained graphically from these two projections. As the nitrogen atom in these projections is partially masked by the bromine atom, the location of the nitrogen atom was evaluated by subtracting the observed electron density distribution of the bromine atom from $\rho(xz)_{z=(1/4)}$, assuming that the former has the same distribution along $+X$ and $-X$ from x_{Br}. Using the atomic coordinates thus obtained, the discrepancy factors were found to be 11.5% for $(h0l)$ and 11.2% for $(hk0)$ reflections, the overall temperature factor being assumed to be isotropic, with a value 4.0 $Å^2$.

Refinement of the Structure

Two difference syntheses, $D(xz)$ and $D(xy)$, prepared at this stage indicated an appreciable anisotropy of thermal vibration of the bromine atom, in addition to a slight shift of the atomic coordinates for each atom. The bromine parameter was refined, using mainly $(h0l)$ reflections, and those of the other atoms were made, using both $(h0l)$ and $(hk0)$ reflections. Since the direction of the maximum vibration of the bromine atom is along the c-axis, its atomic scattering factor can be given by[7]

$$f_{Br}=f_{Br}\text{ (free atom) }\exp(-\gamma)$$

$$\gamma=(A+B\sin^2\varphi)\sin^2\theta/\lambda^2$$

where φ is the angle between $\boldsymbol{a}$ and $\boldsymbol{h}$, and A and B are unknown quantities to be determined. In order to allow for the anisotropic vibration of the bromine atom, the variation of the temperature parameter with φ was first determined

7) E. W. Hughes, *J. Am. Chem. Soc.*, **63**, 1717 (1941).

in the following way. The contributions of the carbon and nitrogen atoms were subtracted from the observed structure factors to give a set of F'_O values. These F'_O values were divided into groups with $\varphi=0\sim15°$, $15\sim30°$,……, $75\sim90°$, and for each group γ was obtained from a plot, $\log F_{Br}/F'_O$ against $(\sin\theta/\lambda)$, where F_{Br} stands for the calculated bromine contribution without temperature factor. Further refinement followed, assuming that the temperature factors for the carbon and nitrogen atoms were the same and isotropic.

At this stage, the secondary extinction effect was corrected using the equation[8], $I_o=I_c \exp(-gI_c)$.

Finally the contributions of the hydrogen atoms were allowed for. It was assumed that the hydrogen atoms attached to the carbon atoms were located in the outward directions bisecting the angle between consecutive C–C bonds, at a distance 1.05 Å, and that the hydrogen atoms attached to the nitrogen atom were distributed tetrahedrally with respect to the C–N bond, at a distance 1.01 Å. It was further assumed that these hydrogen atoms were rotating freely around the C–N bond as in the case of methylammonium chloride[9]. Now the contribution from the rotating hydrogen atoms to the structure factor can be written by

$$\pm 12 f_H \exp-(\sin\theta/\lambda)^2 B_H \times J_o(K\sin\theta/\lambda)\begin{matrix}\cos 2\pi h x_H \\ \sin 2\pi h x_H\end{matrix}$$

where J_o is the zeroth order Bessel function and the argument K is $4\pi r_o \sin\theta_o$. In this expression, r_o and θ_o are the radius of the orbit and the angle between $\boldsymbol{a}$ and $\boldsymbol{h}$ respectively, and x_H is the common x parameter for hydrogen atoms. The temperature factor for hydrogen, B_H, was assumed to be isotropic with a value 6.5 Å^2. The agreement between observed and calculated strucrure factors was found definitely improved especially for lower order reflections. The discrepancy factors were decreased to 7.9% and 6.5% for $(h0l)$ and $(hk0)$ reflections, including all the non-observed terms up to $\sin\theta/\lambda=0.67$. The final positional parameters and temperature factors for each atom are listed in Table II. The interatomic distances and bond angles calculated from these positional parameters are given in Tables III and IV. In Tables V and VI, the observed and calculated structure factors for $(h0l)$ and $(hk0)$ reflections are given.

Discussion

The crystal structure of aniline hydrobromide can be said to belong to a distorted CsCl-type, consisting of bromine and anilinium ions. The C_2–C_3 distance in the benzene ring is slightly shorter than the other C–C distances. The C_1–N distance is 1.47 Å, suggesting a single bond nature.

The structue can also be described as built up with alternating layers, parallel to the (100) plane, one layer containing anilinium ions and the other bromine ions. The structure may further be taken as a superstructure along the a-axis, since every other layer contains anilinium ions in different orientations, as can be seen in Fig. 4. The inclination of the benzene ring to the plane (010) is $\pm22.5°$, so that the angle between the neighboring benzene rings is 45°. The bromine ions lie nearly on the same plane, the deviation from the plane being 0.386 Å.

The shortest intermolecular atomic distances are found between carbon atoms. These distances (see Table IV) are somewhat shorter than the usually accepted van der Waals' contact, 3.70 Å.

Between the consecutive layers, the strongest interactions will be those between the bromine ion and the nitrogen atom of the anilinium ion. Each bromine ion is surrounded by four nitrogen atoms, and each nitrogen atom by four bromine ions, which from a rhomb parallel to

Table II. Positional parameters and temperature factors

	Positional parameter			Temperature factor, Å^2		
	x	y	z	Bx	By	Bz
Br	0.0230	0.25	0.25	4.3	3.7	5.3
N	0.4441	0.75	0.25			
C_1	0.3564	0.75	0.25			
C_2	0.3152	0.5650	0.1833		6.0	
C_3	0.2323	0.5650	0.1833			
C_4	0.1914	0.75	0.25			

Table III. Bond distances and bond angles

Bond distance, Å		Bond angle	
C_1–C_2	1.42	$\angle$N–C_1–C_2	121°34′
C_2–C_3	1.39	$\angle C_2$–C_1–C_2'	116°52′
C_3–C_4	1.42	$\angle C_1$–C_2–C_3	121°34′
N–C_1	1.47		

Table IV. Intermolecular atomic distances, Å

C_4(I)……C_5(II)	3.76
C_2(I)……C_5(II)	3.61
C_3(I)……C_5(II)	3.57
C_4(I)……C_6(II)	3.54
Br(A)……N(II)	3.30
Br(A)……N(III)	
Br(C)……N(II)	3.48
Br(E)……N(II)	

8) J. Houstry and J. Clastre, *Acta Cryst.*, **10**, 696 (1957).
9) E. W. Hughes and W. N. Lipscomb, *J. Am. Chem. Soc.*, **63**, 1737 (1941).

the (100) plane. Of the interatomic distances between the nitrogen and bromine atoms, two are shorter, 3.3 Å, and the other two are longer, 3.48 Å. The angles subtended at the nitrogen atom by the four bromine atoms are 99° and 114°. The direction of the maximum thermal vibration of the bromine atom within the layer is nearly parallel to the longer distance of Br

TABLE V. OBSERVED AND CALCULATED STRUCTURE FACTORS FOR ($h0l$) REFLECTIONS

$h\,0\,l$	F_O	F_C	$h\,0\,l$	F_O	F_C
0 0 0		344.0	0 0 4	66.0	71.2
2 0 0	58.8*	61.2	2 0 4	50.8	56.4
4 0 0	115.6*	114.4	4 0 4	36.0	40.0
6 0 0	75.2*	73.2	6 0 4	30.4	31.6
8 0 0	8.8	12.0	8 0 4	12.4	11.6
10 0 0	—	0.8	10 0 4	—	0.8
12 0 0	10.4	− 9.6	12 0 4	10.4	− 6.4
14 0 0	17.2	−17.6	14 0 4	8.0	− 7.2
16 0 0	11.6	−12.0	16 0 4	10.0	− 8.8
18 0 0	17.2	−16.8	18 0 4	11.6	− 9.6
20 0 0	11.6	−12.4			
			2 0 5	11.6	− 9.6
2 0 1	11.6	3.6	4 0 5	13.5	−15.6
4 0 1	42.0	−41.6	6 0 5	28.4	−25.6
6 0 1	70.8*	−70.8	8 0 5	24.8	−25.2
8 0 1	33.2	−41.6	10 0 5	19.6	−19.2
10 0 1	67.2*	−70.4	12 0 5	27.2	−26.0
12 0 1	39.2	−42.4	14 0 5	11.6	−11.6
14 0 1	32.8	−37.6	16 0 5	8.8	− 8.4
16 0 1	16.8	−17.2			
18 0 1	10.4	−10.4	0 0 6	24.0	−25.6
20 0 1	—	2.4	2 0 6	26.4	−30.8
			4 0 6	15.6	−16.4
0 0 2	189.6*	−190.4	6 0 6	15.6	−15.2
2 0 2	58.8*	−72.8	8 0 6	7.2	− 6.4
4 0 2	78.8*	−82.0	10 0 6	—	− 0.4
6 0 2	57.2*	−55.6	12 0 6	7.2	3.6
8 0 2	12.4	−14.0	14 0 6	—	2.8
10 0 2	—	− 1.2	16 0 6	4.4	5.2
12 0 2	10.8	8.8			
14 0 2	13.6	14.0	2 0 7	5.6	4.8
16 0 2	12.0	11.2	4 0 7	5.6	4.8
18 0 2	16.0	14.4	6 0 7	14.0	11.6
20 0 2	10.0	10.8	8 0 7	13.2	11.6
			10 0 7	7.2	7.6
2 0 3	10.8	11.6	12 0 7	15.6	12.0
4 0 3	25.6	28.8			
6 0 3	46.4	48.0	0 0 8	9.2	8.8
8 0 3	35.2	39.6	2 0 8	12.0	12.0
10 0 3	42.4	44.0	4 0 8	5.6	6.0
12 0 3	35.2	36.8	6 0 8	6.8	5.6
14 0 3	23.6	24.8	8 0 8	3.6	2.4
16 0 3	12.8	13.6			
18 0 3	8.4	8.0			
20 0 3	—	2.0			

* Corrected for extinction

TABLE VI. OBSERVED AND CALCULATED STRUCTURE FACTORS FOR ($hk0$) REFLECTIONS

$h\,k\,0$	F_O	F_C	$h\,k\,0$	F_O	F_C
2 1 0	62.8*	−60.0	0 4 0	68.8	68.8
4 1 0	80.4*	−81.6	2 4 0	54.8	53.6
6 1 0	68.4*	−73.3	4 4 0	38.0	39.2
8 1 0	82.4*	−84.0	6 4 0	32.4	30.4
10 1 0	47.6	−53.2	8 4 0	14.0	12.0
12 1 0	35.2	−39.6	10 4 0	5.6	1.6
14 0 1	26.8	−26.8	12 4 0	6.4	− 6.0
16 1 0	18.4	−19.6	14 4 0	8.4	− 7.6
18 1 0	8.4	− 8.0	16 4 0	8.0	− 9.2
20 1 0	4.0	− 3.6	18 4 0	8.8	−12.4
22 1 0	—	0.0			
			2 5 0	21.6	−16.4
0 2 0	104.4*	−110.0	4 5 0	21.6	−21.2
2 2 0	116.8*	−123.2	6 5 0	26.0	−25.2
4 2 0	57.2*	−60.4	8 5 0	32.0	−31.2
6 2 0	54.0	−53.2	10 5 0	20.4	−20.0
8 2 0	18.8	−20.8	12 5 0	19.2	−19.6
10 2 0	—	− 0.4	14 5 0	10.4	−11.2
12 2 0	15.2	11.6	16 5 0	7.6	−10.4
14 2 0	6.4	9.2			
16 2 0	15.2	14.8	0 6 0	40.0	36.8
18 2 0	14.8	14.8	2 6 0	22.8	−21.6
20 2 0	6.4	8.8	4 6 0	22.0	−22.4
22 2 0	6.8	8.0	6 6 0	16.4	−15.6
			8 6 0	5.6	− 6.0
2 3 0	28.8	25.2	10 6 0	—	− 1.2
4 3 0	58.4	56.4	12 6 0	—	2.8
6 3 0	41.2	42.8	14 6 0	6.4	5.2
8 3 0	45.6	46.8			
10 3 0	15.2	11.6	2 7 0	7.6	5.2
12 3 0	13.6	16.8	4 7 0	11.2	10.8
14 3 0	28.8	27.6	6 7 0	11.2	10.8
16 3 0	12.4	11.6	8 7 0	11.6	12.4
18 3 0	6.0	6.4	10 7 0	10.0	11.6
20 3 0	—	2.8			
			0 8 0	8.0	10.4
			2 8 0	11.2	11.6
			4 8 0	6.4	8.0

* Corrected for extinction

TABLE VII. MELTING POINTS AND TEMPERATUER FACTORS OF SEVERAL AMINE HYDROHALIDES

Substance	M. p. °C	Mean temp. factor, Å²
Aniline hydrochloride[a)]	198	4.0
Aniline hydrobromide[b)]	283	5.8
Aniline hydroiodide[c)]	365	6.0
Cyclohexylamine hydrochloride[d)]	206	5.0

a) C. J. Brown, *Acta Cryst.*, **2**, 228 (1949).
b) Present investigation
c) I. Nitta, I. Taguchi and H. Hiyama, to be published.
d) A. Shimada, Y. Okaya and M. Nakamura, *Acta Cryst.*, **8**, 819 (1955).

···Br. The cleavage plane, (001), is also perpendicular to this longer distance.

Since the anilinium ion in this structure should have the two-fold rotational symmetry demanded by the space group, the three hydrogen atoms bound to the nitrogen atom must occupy statistical positions by some means.

Two plausible models of arrangement of these three hydrogen atoms are shown in Fig. 5. Case A, in Fig. 5, includes two strong and one weak hydrogen bonds. On the other hand, in case B there are one strong and two weak hydrogen bonds. These are the two extremes. A model of free rotation around the C–N axis is another extreme. This model of free rotation was incorporated into the structure factor calculations as described in the section of refinement.

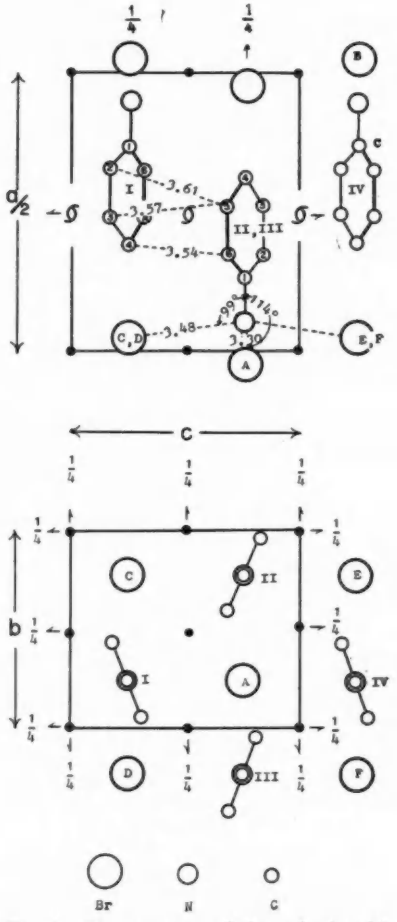

Fig. 3. The structure of the orthorhombic aniline hydrobromide projected on to the (010) and (100) planes.

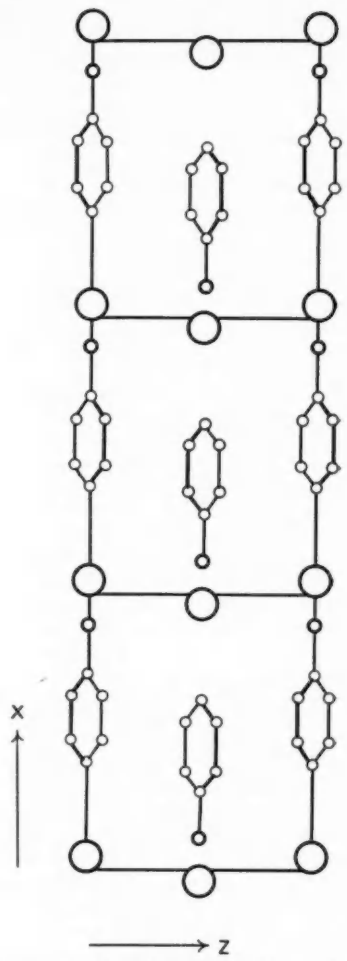

Fig. 4. A schematic representation of the superstructure along the b-axis.

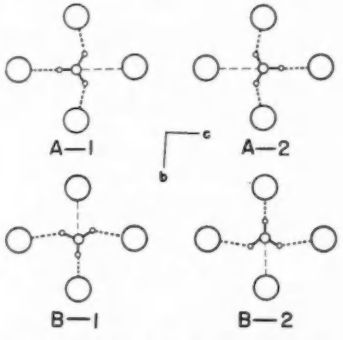

Fig. 5. Statistical arrangements of the three hydrogen atoms bound to the nitrogen atom.

Now, the actual structuer may be represented by an average of all the possible states arising from these extremes stated above, with an appropriate weight on each. Such a statistical arrangement of the hydrogen atoms will vanish when the phase transition takes place.

The mean temperature factor is 5.8Å^2. This value is considerably large for a crystal whose melting poing is as high as 283°C. The temperature factors and melting points of several related compounds are listed in Table VI. That these amine hydrohalides have large thermal vibration and relatively high melting points will probably be due to the partially ionic and partially molecular character of these compounds. The large thermal motion will arise from their molecular character, whereas the ionic character will be responsible for their high melting points. It is interesting to note that these amine hydrohalides have these common characteristics notwithstanding their different crystal structures.

Let us now compare the crystal structure of aniline hydrobromide with those of alkylamine hydrohalides. Both methyl- and propyl-ammonium chlorides crystallize in the tetragonal system, and the alkylammonium ions are characterized by the four-fold axial symmetry. In methylammonium chloride, the three hydrogen atoms attached to nitrogen occupy statistical positions, or they are in rotation. In propylammonium chloride, not only these hydrogen atoms but also the nitrogen and carbon atoms, too, are rotating. The difference between the four-fold axial symmetry of the alkylammonium ions and the two-fold axial symmetry of the anilinium ions may be due to the difference in their molecular shape. All these crystals are apolar, so that their structures can be described as an alternating disposition or antiparallel arrangement of dipoles along their principal axes. The nitrogen atoms in these alkylammonium chlorides have four halogen atoms as their immediate neighbors, so also the nitrogen atoms in aniline hydrobromide, though these four distances in the latter are not exactly the same.

There are some indications of a possible hindered oscillation of the anilinium ion around its longest axis. The final difference projection, $D(xz)$, shows that the temperature factors of C_2 and C_3 are larger than those of C_1 and C_4. Some reflections such as (112) whose structure factors have contributions from C_2 and C_3 alone are associated with diffuse spots, presumably due to the thermal motion stated above.

Faculty of Science
Osaka University
Nakanoshima, Osaka

---

*Some Electrophilic Substitution Reactions of 4-Aminotropolone**

By Kozo Doi

(Received March 29, 1961)

In the course of investigations of 4-aminotropolone (I) and its derivatives, the author has established general methods of their syntheses, which include amination of 3-iodotropolones with potassium amide in liquid ammonia[1], applications of the Schmidt reaction to acetyl-, formyl- and isopropenyltropolones[2] and of the Curtius reaction to 4-carboxytropolones[1], and amination of 4-bromotropolone with aqueous ammonia[3].

On the other hand, there have been little informations on reactivities of 4-aminotropolones except on a diazotization of 4-amino-6-methyltropolone (II)[4], whereas the reactions of the isomeric 3- and 5-amino derivatives have been much investigated[5]. Recently the author has reported in brief the synthetic applications of I, involving preparations of some pyridotropolones[6] and of 4-aminotropone[7]. In this communication the author wishes to take up some electrophilic substitution reactions of the aminotropolone (I).

* This work was presented at the 12th Annual Meeting of the Chemical Society of Japan, Kyoto, April, 1959.

1) K. Doi, This Bulletin, **34**, 497 (1961).
2) K. Doi, ibid., **34**, 501 (1961).
3) K. Doi, ibid., **34**, 504 (1961).
4) W. D. Crow, R. D. Haworth and P. R. Jefferies, *J. Chem. Soc.*, **1952**, 3705.
5) Cf. P. L. Pauson, *Chem. Revs.*, **55**, 9 (1955).
6) K. Doi, *Bull. Chem. Res. Inst. Non-Aqueous Solutions, Tohoku Univ.*, **9**, 19 (1959).
7) K. Doi, This Bulletin, **33**, 887 (1960).

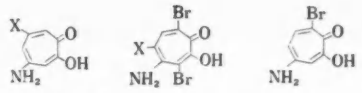

I: X=H III: X=Br IV
II: X=Me V: X=H

On bromination the aminotropolone (I) has been found to give nuclear substitution products in the same manner as many other tropolones. For example, in the presence of sodium acetate as a hydrogen bromide acceptor, I consumes three molar equivalents of bromine to afford in a good yield the tribromotropolone (III). On the other hand, in the absence of any hydrogen bromide acceptor, I reacts with one molar equivalent of bromine to give not only a monobromo derivative, IV, which was identified with that obtained from an application of the Schmidt reaction to the known 6-acetyl-3-bromotropolone[2], but also a dibromo compound, V, whose respective yield is better in the latter than the former. Such a preferential formation of dibromo compound by one molar equivalent of bromine has also been observed in the case of tropolone itself[5].

In Fig. 1 are indicated the ultraviolet absorption spectra of the above two substitution products, III and V, comparing with that of the monobromo compound IV. Tsuboi[8] observed that an introduction of one bromine atom into the 3 (or 7)- and 5-position of tropolone caused a red shift of the maximum in the longest wavelength by 10 and 15 mμ, respectively. Now, the above three bromotropolones (III, IV and V) have the maximum in the longest wavelength at 410, 380 and 390 mμ, respectively. The difference of the maxima of V and IV is 10 mμ, and that of III and V is 20 mμ, the fact of which suggests that the dibromotropolone (V) may be a 3, 7-dibromo derivative rather than a 3, 5-dibromo one.

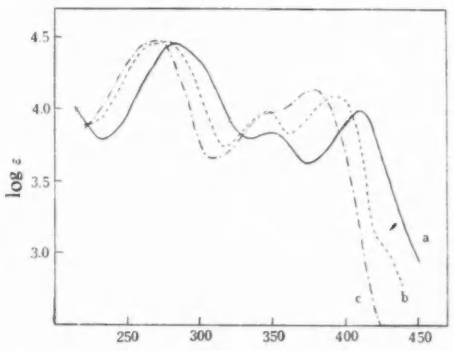

Fig. 1. The ultraviolet absorption spectra.
(a): 4-Amino-3, 5, 7-tribromotropolone (III)
(b): 4-Amino-3, 7-dibromotropolone (V)
(c): 6-Amino-3-bromotropolone (IV)

8) M. Tsuboi, This Bulletin, 25, 369 (1952).

The position of the two bromine atoms of the dibromo compound V is also understood from a comparison of the characteristic bands due to the CH out-of-plane vibration (864 cm^{-1}) with those of some other 3, 4, 7-trisubstituted tropolones, which possess bands in the 820~875 cm^{-1} region[9], in the infrared absorption spectra. Table I indicates frequencies of the CH out-of-plane vibration of V, comparing with those of some other 3, 4, 7-trisubstituted tropolones.

Table I. Frequencies of the CH out-of-plane vibration of some 3, 4, 7-trisubstituted tropolones

Compound	ν_{CH} cm^{-1}	Ref.
4-Amino-3, 7-dibromotropolone (V)	864	
4-Isopropyl-3, 7-dibromotropolone	835	10
7-Bromo-3-iodo-4-methyltropolone	847	11
7-Bromotropolone-3, 4-dicarboxylic anhydride	872	12
7-Hydroxytropolone-3, 4-dicarboxylic anhydride	882	12

4-Aminotropolone (I), differing from its isomeric 3- and 5-amino derivatives, has been found to be fairly stable in pace of the action of nitric acid. Thus an attempt to obtain a nitro compound from I in an usual reaction condition for nitration of tropolones causes to yield not any substitution product but merely a nitrate, possessing a composition of $C_7H_7O_2N \cdot HNO_3 \cdot H_2O$. With fuming nitric acid, however, I reacts vigorously to form in a poor yield 4-amino-5-nitrotropolone (VI), whose structure was confirmed by the fact that the ultraviolet absorption is practically identical with that of the product obtained by an application of the Schmidt reaction to 4-acetyl-5-nitrotropolone[2].

In order to obtain further informations with respect to orientation of electrophilic substitution, nitration has also been carried out on 4-acetylaminotropolone (VII), which is readily prepared from the reaction of I and acetyl chloride in pyridine. Nitration of VII with fuming nitric acid in an acetic acid solution gives also a 5-nitro derivative, VIII, whose structure is confirmed by the formation of VI on its alkaline hydrolysis.

9) Y. Ikegami, *J. Japanese Chem.* (*Kagaku-no-Ryoiki*), Extra No. 38, 33 (1959).
10) T. Nozoe, E. Sebe, S. Mayama and S. Iwamoto, *Sci. Repts. Tohoku Univ. Ser. I*, 36, 184 (1952).
11) T. Nozoe, K. Doi, K. Kitahara and K. Omura, to be published.
12) T. Nozoe, K. Doi and T. Hashimoto, This Bulletin, 33, 1071 (1960).

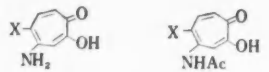

VI: X=NO_2 VII: X=H
IX: X=NH_2 VIII: X=NO_2
X: X=*p*-Tolylazo

The absorption maximum at 400 mμ (log ε 3.90) of VIII indicates more decreased values both in wavelength and absorption intensity than that at 435 mμ (log ε 4.41) of 5-nitrotropolone itself[13]. This is not consistent with the bathochromic effect of the acetylamino group, having been attributed recently to the steric inhibition of resonance between the nitro group and the tropolone nucleus by the adjacent acetylamino group[14].

From a catalytic hydrogenation of the 5-nitro derivative VIII over palladized charcoal, 4,5-diaminotropolone (IX) is readily obtained. In the previous paper[2], the author found that an application of the Schmidt reaction to 4-acetyltropolone resulted in the formation of 4-aminotropolone sulfate instead of the expected acetylamino derivative VII, attributing this mechanism to the hydrolyzable nature of VII in the condition employed. Actually it has now been found that the acetylamino compound VII affords easily 4-aminotropolone sulfate on being merely dissolved in concentrated sulfuric acid even at room temperature. This fact justifies the previous mechanism in the Schmidt reaction of the acetyltropolones.

Bromination and nitration of 5-aminotropolones have already been reported, but in no cases has isolation of the substitution products been described[15]. With 3-aminotropolone, some electrophilic substitutions involving bromination, nitration, and azo coupling have been attempted with no isolation of any reaction products[16]. On the contrary, 4-aminotropolone (I) gives easily nuclear substitution products in some electrophilic reactions. This fact is probably considered to be connected with that the amino and hydroxyl groups in the aminotropolone (I) are situated at the positions where they cooperate with each other to increase the reactivity of the tropolone ring, whereas the two groups in the 3- and 5-isomers are not in such positions.

The aminotropolone (I), similarly to the other tropolones, undergoes azo coupling to give a nuclear substitution product of red dyestuff, not a diazoamino derivative. Thus on being treated with diazotized *p*-toluidine in an alkaline solution, I affords in a good yield 4-amino-5-*p*-tolylazotropolone (X), whose hydrogenolysis leads to the diaminotropolone (IX).

In a similar manner to *o*-phenylenediamine, the diamino compound IX gives an imidazole, XI, on being heated with formic acid, and a

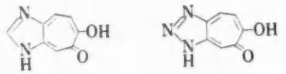

XI XII

triazole, XII, on being diazotized. Informations on tautomerism between these reaction products and their possible isomers of the aza-azulene type have not been obtained in detail, but it is probably concluded that they may not be their possible dihydroxy-azaazulene derivatives, since their respective ultraviolet absorption is resembling that of imidazolo[d]tropone[17] and of triazolo[d]tropone[18] (Fig. 2).

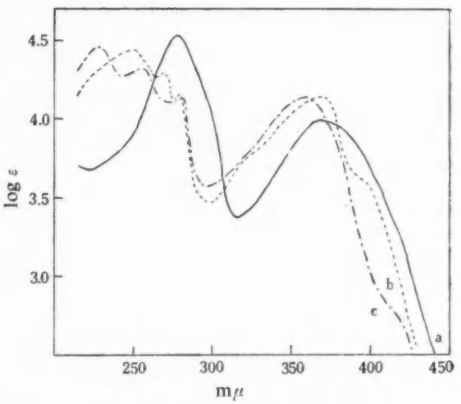

Fig. 2. The ultraviolet absorption spectra.
(a): 4,5-Diaminotropolone (IX)
(b): Imidazolo[d]tropolone (XI)
(c): Triazolo[d]tropolone (XII)

Experimental

All of the ultraviolet absorption spectra were measured in methanol solution with a Beckman model DU quartz spectrophtometer. The infrared spectra were measured on potassium bromide disks with a Perkin-Elmer model 21 infrared spectrometer, using a rock salt prism.

Tribromination of 4-Aminotropolone (I).—To a stirred mixture of I (70 mg.), sodium acetate trihydrate (200 mg.) and methanol (2 ml.) was added dropwise a cold solution of bromine (240 mg.) in methanol (2 ml.). The reaction mixture was

13) T. Nozoe, Y. Kitahara, K. Doi and T. Arai, *Bull. Chem. Res. Inst. Non-Aqueous Solutions, Tohoku Univ.*, **7**, 13 (1957).
14) Y. Kitahara, K. Doi and T. Hashimoto, ibid., **9**, 91 (1960).
15) T. Nozoe, S. Ebine, S. Ito and A. Konishi, *Proc. Japan Acad.*, **27**, 10 (1951); T. Nozoe, S. Seto, S. Ito and M. Sato, ibid., **27**, 426 (1951).
16) K. Doi, unpublished work.
17) T. Nozoe, M. Sato, S. Ito, K. Matsui and T. Matsuda, *Proc. Japan Acad.*, **29**, 565 (1953).
18) T. Nozoe, S. Ito and K. Matsui, ibid., **30**, 313 (1954).

diluted with water, and the precipitated solid, after collection by filtration, sublimation in vacuo, and subsequent recrystallization from acetic acid, gave 4-amino-3, 5, 7-tribromotropolone (III, 160 mg.) as yellow needles, m. p. 203°C.

Found: N, 3.80. Calcd. for $C_7H_4O_2NBr_3$: N, 3.75%.

λ_{max} mμ (log ε): 282 (4.47), 350 (3.84), 410 (4.00).

Monobromination of I.—To a stirred cold solution of I (0.41 g.) in methanol (10 ml.) was added dropwise a solution of bromine (0.48 g.) in methanol (2 ml.). After 30 min., the solution was evaporated in vacuo, the residue was diluted with water (5 ml.), and the deposited solid, after collection by filtration, was crystallized fractionally from methanol to give less soluble 4-amino-3,7-dibromotropolone (V, 016 g.) as yellow prisms, m. p. 224~225°C.

Found: N, 5.01. Calcd. for $C_7H_5O_2NBr_2$: N, 4.75%.

λ_{max} mμ (log ε): 276 (4.46), 345 (3.99), 390 (4.10).

From the more soluble portion, 6-amino-3-bromotropolone (IV) as yellow needles, m. p. and mixed[2] m. p. 214°C, was obtained. Further bromination of the preceding products, IV and V, afforded respectively the tribromotropolone (III).

Nitration of 4-Aminotropolone (I).—a) To a stirred solution of I (0.41 g.) and acetic acid (3 ml.) was added dropwise at room temperature a solution of fuming nitric acid (0.2 g., *d* 1.84) and acetic acid (1 ml.). After evaporation of the solvent, the residual solid was recrystallized from a mixed solvent of acetic acid and methanol to give 4-aminotropolone nitrate (0.26 g.) in the form of colorless needles, m. p. 163~164°C (decomp.).

Found: C, 41.96; H, 4.06; N, 13.80. Calcd. for $C_7H_7O_2N \cdot HNO_3 \cdot H_2O$: C, 42.00; H, 4.03; N, 14.00%. This substance is soluble in water and its aqueous solution decomposes sodium hydrogen carbonate.

b) Addition of fuming nitric acid (0.2 g.) to the aminotropolone (I, 0.41 g.) resulted in a vigorous reaction to form a deep red solution, which was immediately chilled in ice and allowed to stand for 30 min. Then this solution was diluted with water (2 ml.), the residual solid was collected by filtration, and crystallized from acetic acid to yield 4-amino-5-nitrotropolone (VI) as yellow needles, m. p. above 300°C, which was identified with an authentic specimen[2] through ultraviolet absorption.

4-Acetylaminotropolone (VII).—After acetyl chloride (3.1 g.) was added dropwise during 10 min. to a stirred cold solution of I (2.8 g.) in pyridine (10 ml.), the reaction mixture was allowed to stand for 4 hr. The mixture was diluted with water, allowed to stand overnight, and then acidified to Congo red with dilute hydrochloric acid. The solid which separated on chilling this mixture was collected and recrystallized from methanol to afford 4-acetylaminotropolone (VII, 2.2 g.) as colorless needles, m. p. 166~167°C.

Found: C, 55.43; H, 5.33; N, 7.14. Calcd. for $C_9H_9O_3N \cdot H_2O$: C, 54.82; H, 5.62; N, 7.10%.

λ_{max} mμ (log ε): 267 (4.54), 365 (3.84).

4-Acetylamino-5-nitrotropolone (VIII).—To a stirred mixture of VII (1.3 g.) and acetic acid (4 ml.) was added dropwise at room temperature a solution of fuming nitric acid (0.5 g.) and acetic acid (1 ml.), the deep red solution so formed was allowed to be stirred for further 1 hr., diluted with water (40 ml.), and extracted with four 25-ml. portions of ether. The ether extract, after evaporation of the solvent followed by recrystallization from a mixed solvent of acetic acid and methanol, gave VIII (0.46 g.) as yellow needles, m. p. 230°C (decomp.).

Found: C, 48.53; H, 3.88; N, 12.31. Calcd. for $C_9H_8O_5N_2$: C, 48.53; H, 3.60; N, 12.50%.

λ_{max} mμ (log ε): 274 (4.53), 400 (3.90).

Hydrolysis of VIII.—A mixture of VIII (0.2 g.), potassium hydroxide (0.2 g.), and water (8 ml.) was heated at 60°C on a water bath for 30 min., and then the resulting red solution was acidified with dilute hydrochloric acid to separate the aminotropolone (VI, 0.15 g.), whose structure was confirmed by the comparison of the ultraviolet absorption with that of an authentic sample[2].

4, 5-Diaminotropolone (IX).—A mixture of the nitroamine (VI, 0.18 g.), 5% palladium-on-carbon (50 mg.) and methanol (100 ml.) was shaken in an hydrogen atmosphere until the uptake of hydrogen had ceased. Then the catalyst was removed by filtration, the filtrate evaporated in vacuo, and the residue crystallized twice from ethyl acetate to give 4,5-diaminotroplone (IX, 60 mg.) as yellow prisms, m. p. 215°C (decomp.).

Found: C, 54.98; H, 5.21; N, 18.57. Calcd. for $C_7H_9O_2N_2$: C, 55.25; H, 5.30; N, 18.41%.

λ_{max} mμ (log ε): 278 (4.54), 371 (3.99).

4-Amino-5-*p*-tolylazotropolone (X).—A diazonium chloride solution prepared from *p*-toluidine (2 g.) was added dropwise during 10 min. to a stirred cold solution of I (2.8 g.), potassium hydroxide (6 g.) and water (100 ml.). After 30 min., the reaction mixture was acidified with acetic acid, the solid which separated was collected, and recrystallized from ethyl acetate to afford X (4.5 g.) of red needles, m. p. 230°C (decomp.).

Found: N, 16.22. Calcd. for $C_{14}H_{13}O_2N_3$: N, 16.46%.

λ_{max} mμ (log ε): 260 (4.37), 300 (4.38), 375 (4.11), 470 (4.41).

Hydrogenation of X in methanol over 5% palladized carbon afforded easily a diamino derivative IX.

Imidazolo[d]tropolone (XI).—A mixture of IX (0.15 g.) and 80% formic acid (10 ml.) was heated under reflux for 2 hr., the solvent was evaporated to dryness, and the residue, after sublimation in vacuo, was recrystallized from acetic acid to give XI (60 mg.) of colorless prisms, m. p. above 275°C

Found: C, 59.08; H, 3.55; N, 17.60. Calcd. for $C_8H_6O_2N_2$: C, 59.26; H, 3.73; N, 17.28%.

λ_{max} mμ (log ε): 250 (4.44), 268 (4.28), 280 (4.14), 372 (4.14).

Triazolo[d]tropolone (XII).—A solution of sodium nitrite (60 mg.) in water (1 ml.) was added dropwise during 5 min. to a stirred cold solution of IX (0.15 g.), acetic acid (0.2 ml.), concentrated hydrochloric acid (0.4 ml.) and water (6 ml.). After 2 hr., the mixture was diluted with water (40 ml.), neutralized with sodium hydrogen carbonate, and extracted continuously with ether for 5 hr. The ether extract, after evaporation of the solvent, sublimation of the residue in vacuo followed by

crystallization from acetic acid, gave XII (50 mg.) of colorless prisms, m. p. 265°C (decomp.).

Found: C, 51.20; H, 2.98; N, 25.78. Calcd. for $C_7H_5O_2N_3$: C, 51.54; H, 3.09; N, 25.76%.

λ_{max} mμ (log ε): 228 (4.48), 256 (4.34), 282 (4.14), 360 (4.17).

The author wishes to express his sincere gratitude to Professor Yoshio Kitahara for his kind guidance throughout the course of the present experiment, to Mr. Hideji Aono for the infrared spectral measurements, and to Messrs. Shin-ichi Ohyama, Kuni Kato and Ayako Iwanaga for microanalyses.

The Chemical Research Institute of Non-Aqueous Solutions
Tohoku University
Katahira-cho, Sendai

Molecular Rotations of Terpenes in Relation to their Structures. I. The Internal Conformation of Isopropyl Group in Menthol-like Substance[1]

By Shukichi YAMANA

(Received December 27, 1960)

In liquid or dissolved state, C^9H_3 and $C^{10}H_3$ in the isopropyl group of menthol-like substance are considered to be free to rotate about the axis of C^4–C^8 bond and the position which has minimal potential and makes these methyl groups rest, may be decided by steric repulsions and intramolecular van der Waals' forces etc. between the atoms in the molecule (Fig. 1).

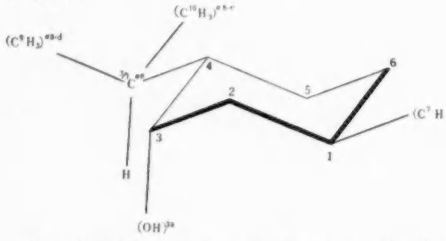

Fig. 1[2]. Perspective drawing of the molecular model of (+)neomenthol.

On the other hand, by uing the PM-method, the author recently tried to explain the molecular rotations of polyhydroxycyclohexanes[3,4]. From the standpoint of the fact that a menthol-like substance is a kind of polyhydroxy (or monohydroxy)-cyclohexane, the type of the internal conformation of its isopropyl group at an equilibrium state, above mentioned, is discussed in this article.

1) Presented at the Symposium on the Structural Chemistry of the Chemical Society of Japan, Sapporo, August, 1960.

2) $C^{\alpha 5}$-Atom is C^8-atom which is situated in α-orientation (i. e. under the cyclohexane-ring in Fig. 1). $(CH_3)^{\alpha 5}$ means the CH_3 group which combines with $C^{\alpha 5}$-atom. Concerning the symbols, d- and e-, refer to "Method Proposed" in this article.

3) S. Yamana, This Bulletin, 33, 1741 (1960).

Molecular Model and Data Used

According to Jefferies' investigation of menthol-like substances by infrared spectrum[5], it was concluded that in their molecules, isopropyl group usually takes equatorial orientation and that two methyl groups repulse each other. Referring to Jefferies' work, only the compounds which have a six-membered ring of C 1 conformation are treated in this article.

The unit groups in their molecules and their corresponding molecular rotations are given in Table I.

The molecular model and the optical properties of the hydroxyl group (except the value of ζ-coefficient), used in the preceding article[3] were adopted here without any correction. Values of mean polarizability α and of anisotropy ratio β of methyl group are 2.27×10^{-24} (cc.) and 0.35 respectively[1,7]. The optical

4) In the previous paper[3], by using $[M]_D^{20}$(W) of (−) 1, 3/2, 4 cyclohexanetetrol, the value of $(\zeta_{OH})^2$ was calculated as 3.6402 $\{3/(n^2+2)\}$. But strictly speaking, it was apparent there that if 3.6402 $\{3/(n^2+2)\}$ is used, $\sum[\mu]_{Dobs}^{20}$ of (−)1/2 cyclohexanediol becomes somewhat smaller than its corresponding $[M]_D^{20}$(W) and $\sum[\mu]_{Dobs}^{20}$ of (+) 3, 5, 6/1, 2, 4 cyclohexanehexitol becomes somewhat larger than its corresponding $[M]_D^{20}$(W). That fact can be explained superficially by the assumption of the changeability of $(\zeta_{OH})^2$ according to the number of hydroxyl groups in a molecule. When $[M]_D^{20}$(W) of (−) 1/2 cyclohexanediol is used, the value of $\zeta_{OH}{}^2$ is calculated as follows;

$$\sum[\mu]_{Dobs}^{20} \text{ of } (-)\ 1/2 \text{ cyclohexanediol} = (OH)\cdot {}^{1\beta}\chi(OH)^{2\alpha} + (OH)^{1\beta}\chi\text{ch.R} + (OH)^{2\alpha}\chi\text{ch.R}$$

$$= -11.73\{(n^2+2)/3\}\zeta_{OH}{}^2 + 0 + 0 \equiv -48.2$$

$$\therefore\ \zeta_{OH}{}^2 = 4.1091\{3/(n^2+2)\} \qquad (4)^*$$

(Ref. Tables I and II of the previous paper[3]).

5) A. R. H. Cole and P. R. Jefferies, *J. Chem. Soc.*, 1956, 4391.

TABLE I.

Name	Unit groups	$[M]_D^{20}$ [6]
(−)1/2 Cyclohexanediol	$[(OH)^{1\beta}, (OH)^{2\alpha},$ ch. R[7]$]$	-48.2_w[9]
(−)*trans*-2-Methylcyclohexanol	$[(OH)^{1\beta}, (CH_3)^{2\alpha},$ ch. R $]$	-42.4[9]
(+)Neomenthol	$[(CH_3)^{1\beta},$ $(OH)^{3\alpha}, (iso\text{-}C_3H_7)^{4\alpha},$ ch. R $]$	30.6[10]
(−)*cis*-2-Hydroxyneomenthol	$[(CH_3)^{1\beta}, (OH)^{2\alpha}, (OH)^{3\alpha}, (iso\text{-}C_3H_7)^{4\alpha},$ ch. R $]$	-50.6_{ch}[11]
(+)*trans*-2-Hydroxyneomenthol	$[(CH_3)^{1\beta}, (OH)^{2\beta}, (OH)^{3\alpha}, (iso\text{-}C_3H_7)^{4\alpha},$ ch. R $]$	70.3_{ch}[11]
(−)*trans*-2-Hydroxymenthol	$[(CH_3)^{1\beta}, (OH)^{2\alpha}, (OH)^{3\beta}, (iso\text{-}C_3H_7)^{4\alpha},$ ch. R $]$	-16.0_{ch}[11]
(−)*cis*-2-Hydroxymenthol	$[(CH_3)^{1\beta}, (OH)^{2\beta}, (OH)^{3\beta}, (iso\text{-}C_3H_7)^{4\alpha},$ ch. R $]$	-56.7_{ch}[11]
(−)Isomenthol	$[(CH_3)^{1\alpha},$ $(OH)^{3\beta}, (iso\text{-}C_3H_7)^{4\alpha},$ ch. R $]$	-39.4_{ch}[12]
(−)Menthol	$[(CH_3)^{1\beta},$ $(OH)^{3\beta}, (iso\text{-}C_3H_7)^{4\alpha},$ ch. R $]$	-77.5_{et}[13]
(−)Carvomenthol	$[(CH_3)^{1\beta}, (OH)^{2\alpha},$ $(iso\text{-}C_3H_7)^{4\alpha},$ ch. R $]$	-41.2[14]
(+)*cis*-1,2-Menthanediol	$[(CH_3)^{1\beta}, (OH)^{1\alpha}, (OH)^{2\alpha}, (iso\text{-}C_3H_7)^{4\alpha},$ ch. R $]$	24.1_{ac}[15]
(+)Neocarvomenthol	$[(CH_3)^{1\beta}, (OH)^{2\beta},$ $(iso\text{-}C_3H_7)^{4\alpha},$ ch. R $]$	65.2[14]
(+)*trans*-1-Hydroxyneo-carvomenthol	$[(CH_3)^{1\beta}, (OH)^{1\alpha}, (OH)^{2\beta}, (iso\text{-}C_3H_7)^{4\alpha},$ ch. R $]$	79.2_{ac}[16]

w: water solution, ch: chloroform solution, et: ethyl alcohol solution, ac; acetone solution.

center of a unit group is located at the center of the mass of its corresponding bond. In order to simplify the calculations, the refractive indices of the homogeneous substances and of the solutions under discussion are all assumed to be about 1.46[18].

Method Proposed

Strictly speaking, as isopropyl group has no optical axis of cylindrical symmetry, the calculations of $[\mu]^{20}_{D\,\text{calcd}}$ which are concerned with isopropyl group are impossible. In order to avoid this difficulty, the following two simplifications are introduced.

Simp. I

$$(iso\text{-}C_3H_7)^{4\alpha} = (C^8H)^{4\alpha} + (C^9H_3)^{\alpha 8} + (C^{10}H_3)^{\alpha 8} \simeq [2] (C^8H_3)^{4\alpha} + (C^9H_3)^{\alpha 8} + (C^{10}H_3)^{\alpha 8}$$

Simp. II

$$(iso\text{-}C_3H_7)^{4\alpha}\bar{\chi}A = \{(C^8H)^{4\alpha} + (C^9H_3)^{\alpha 8} + (C^{10}H_3)^{\alpha 8}\}\bar{\chi}A \simeq (C^8H)^{4\alpha}\bar{\chi}A + (C^9H_3)^{\alpha 8}\bar{\chi}A + (C^{10}H_3)^{\alpha 8}\bar{\chi}A$$

From Simps. I and II,

$$(iso\text{-}C_3H_7)^{4\alpha}\bar{\chi}A \simeq (C^8H_3)^{4\alpha}\bar{\chi}A + (C^9H_3)^{\alpha 8}\bar{\chi}A + (C^{10}H_3)^{\alpha 8}\bar{\chi}A \quad (1)$$

Next, the positions of minimal potential for $(C^9H_3)^{\alpha 8}$ or $(C^{10}H_3)^{\alpha 8}$ will be mentioned. Referring to the steric repulsion between one of these methyl groups and the C-atom in the cyclohexane-ring (C^3- and C^5-atoms), it can be easily understood that there should be three positions of minimal potential for methyl groups. The author names these three positions d-, e- and f-positions, respectively (Fig. 2).

But, d-position is trans to C^4–C^5 bond and e-position is trans to C^4–C^3 bond and f-position is gauche to both C^4–C^5 and C^4–C^3 bonds. As

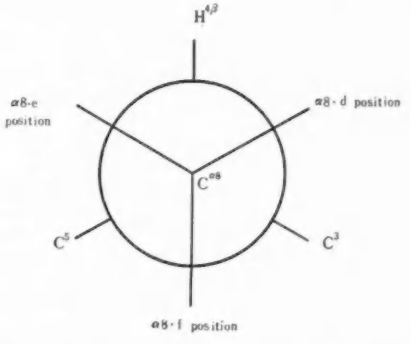

Fig. 2. Positions of minimal potential of CH_3 in $iso\text{-}C_3H_7$, viewed along $C^{\alpha 8}$–C^4 axis.

6) $[M]^{20}_D$ of pure materials in liquid state or of chloroform solutions are adopted, preferentially. Some values were presumed from $[M]_D$ which had been observed in the neighborhood of 20°C. (Ref. 3).
7) ch. R is an abbreviated symbol of a cyclohexane-ring.
8) Th. Posternak, D. Reymond and H. Friedli, *Helv. Chim. Acta*, **38**, 205 (1955).
9) G. A. C. Gough, H. Hunter and J. Kenyon, *J. Chem. Soc.*, **1926**, 2052.
10) O. Zeitshel and H. Schmidt, *Ber.*, **59**, 2298 (1926).
11) P. R. Jefferies and B. Milligan, *J. Chem. Soc.*, **1956**, 2363.
12) W. Hückel and H. Miggemeyer, *Ber.*, **72**, 1354 (1939).
13) J. Read and W. J. Grubb, *J. Chem. Soc.*, **1934**, 313.
14) R. G. Johnston and J. Read, ibid., **1935**, 1138.
15) H. Schmidt, *Suomen Kemistilehti B.*, **31**, 61 (1958); *Chem. Abstr.*, **52**, 20226 (1958).
16) P. Ham, G. Dupont, J. Wiemann and R. Dulou, *Compt. rend.*, **249**, 700 (1959).
17) S. Yamana, This Bulletin, **31**, 564 (1958).
18) The refractive index, n, is as follows; homogeneous state (1.46), chloroform solution (1.45), acetone solution (1.36), ethyl alcohol solution (1.36). If n changes from 1.46 to 1.36, $\{(n^2+2)/3\}$ changes by $\partial/\partial n\{(n^2+2)/3\}\delta n \simeq 0.0973$. The magnitude of this value of $\{(n^2+2)/3\}$-change is about 7% of the value of $\{(n^2+2)/3\} \simeq 1.3772$.

movable groups in isopropyl group are $(C^9H_3)^{\alpha 8}$, $(C^{10}H_3)^{\alpha 8}$ and one H atom, it is obvious that any two of these three positions (d-, e- and f-positions) must be occupied by two methyl groups and the remaining one position should be occupied by one H atom. Then, the following three types of the internal conformation of $(iso\text{-}C_3H_7)^{4\alpha}$ are possible (Table II).

TABLE II. THE TYPE OF THE INTERNAL CONFORMATION OF $(iso\text{-}C_3H_7)^{4\alpha}$

Name of type	$\alpha 8$-d-Position	$\alpha 8$-e-Position	$\alpha 8$-f-Position
Symmetrical	CH_3	CH_3	H
Unsymmetrical I	H	CH_3	CH_3
Unsymmetrical II	CH_3	H	CH_3

Substances which Have $(OH)^{3\alpha}$.—It is apparent in Table III that the distance between O-atom in $(OH)^{3\alpha}$ and f-position is 2.52 Å and is shorter than the sum of van der Waals' radius of methyl group and that of $(OH)^{3\alpha}$.

TABLE III. THE DISTANCES BETWEEN O-ATOM IN $(OH)^3$ AND THREE POSITIONS OF MINIMAL POTENTIAL OF METHYL GROUP IN $(iso\text{-}C_3H_7)^{4\alpha}$

	$\alpha 8$-d-Position	$\alpha 8$-e-Position	$\alpha 8$-f-Position
$(OH)^{3\alpha}$	3.49 Å	4.30 Å	2.52 Å
$(OH)^{3\beta}$	2.52 Å	4.30 Å	3.49 Å

Then, owing to the steric repulsion, $(OH)^{3\alpha}$ may refute the idea that any movable methyl group in isopropyl group stays at f-position. In this case, the symmetrical type is only one possible type of the internal conformation of isopropyl group. For these reasons, it is concluded that in $(iso\text{-}C_3H_7)^{4\alpha}$ of (+)neomenthol in the liquid or dissolved state, two $(CH_3)^{\alpha 8}$'s are forced to stay at d- and e-positions (Fig. 1).

$$\therefore\quad (iso\text{-}C_3H_7)^{4\alpha} = (C^8H)^{4\alpha} + (C^9H_3)^{\alpha 8\text{-d}}\ ^{20)} + (C^{10}H_3)^{\alpha 8\text{-e}} \simeq (C^8H_3)^{4\alpha} + (C^9H_3)^{\alpha 8\text{-d}} + (C^{10}H_3)^{\alpha 8\text{-e}}\ ^{21)} \qquad (2)$$

Referring to Table I and Eq. 2, $\sum[\mu]^{20}_{D\ obs}$ of (+)neomenthol can be calculated by the following equation.

$$\begin{aligned}\sum[\mu]^{20}_{D\ obs}\ \text{of (+)neomenthol} &= (CH_3)^{1\beta}\text{Ⲗ}(OH)^{3\alpha} + (CH_3)^{1\beta}\text{Ⲗ}(CH_3)^{4\alpha} + (CH_3)^{1\beta}\text{Ⲗ}(CH_3)^{\alpha 8\text{-d}} + (CH_3)^{1\beta}\text{Ⲗ}(CH_3)^{\alpha 8\text{-e}} + (CH_3)^{1\beta}\text{Ⲗch. R} + (OH)^{3\alpha}\text{Ⲗ}(CH_3)^{4\alpha} \\ &+ (OH)^{3\alpha}\text{Ⲗ}(CH_3)^{\alpha 8\text{-d}} + (OH)^{3\alpha}\text{Ⲗ}(CH_3)^{\alpha 8\text{-e}} + (OH)^{3\alpha}\text{Ⲗch. R} + (CH_3)^{4\alpha}\text{Ⲗ}(CH_3)^{\alpha 8\text{-d}} \\ &+ (CH_3)^{4\alpha}\text{Ⲗ}(CH_3)^{\alpha 8\text{-e}} + (CH_3)^{4\alpha}\text{Ⲗch. R} + (CH_3)^{\alpha 8\text{-d}}\text{Ⲗ}(CH_3)^{\alpha 8\text{-e}} + (CH_3)^{\alpha 8\text{-d}}\text{Ⲗch. R} \\ &+ (CH_3)^{\alpha 8\text{-e}}\text{Ⲗch. R} \qquad (3)\end{aligned}$$

On the other hand, $[\mu]^{20}_{D\ calcd}\{3/(n^2+2)\}$, caused by the dynamical coupling effect between any two members of unit groups in menthol-like substance, can be calculated by using the theoretical formulae[19]. The results of calculation are shown in Table IV.

By using Table IV, Eq. 3 is rewritten as follows;

$$\begin{aligned}\sum[\mu]^{20}_{D\ obs}\ \text{of (+)neomenthol} &= (-4.04\zeta'_{CH_3}\zeta'_{OH}{}^{22)} + 0 - 4.41\zeta'_{CH_3}{}^2 + 4.41\zeta'_{CH_3}{}^2 + 0 + 25.30\zeta'_{CH_3}\zeta'_{OH} + 3.09\zeta'_{CH_3}\zeta'_{OH} - 4.04\zeta'_{CH_3}\zeta'_{OH} + 0 + 0 + 0 + 0 + 0)\{(n^2+2)/3\} + D - D \\ &= 20.31\zeta'_{CH_3}\zeta'_{OH}\{(n^2+2)/3\}\end{aligned}$$

The corresponding observed value is 30.6[23].

$$\therefore\quad 20.31\zeta'_{CH_3}\zeta'_{OH}\{(n^2+2)/3\} \equiv 30.6$$

or

$$\zeta'_{CH_3}\zeta'_{OH} = 1.5066\{3/(n^2+2)\} \qquad (4)$$

On the other hand, the value of $\zeta_{CH_3}\zeta_{OH}$ in the case of hydroxycyclohexane can be calculated by using (−)*trans*-2-methylcyclohexanol as below;

$$\begin{aligned}\sum[\mu]^{20}_{D\ obs}\ \text{of (−)}trans\text{-2-methylcyclohexanol} &= (OH)^{1\beta}\text{Ⲗ}(CH_3)^{2\alpha} + (OH)^{1\beta}\text{Ⲗch. R} + (CH_3)^{2\alpha}\text{Ⲗch. R}^{23)} \\ &= -25.30\{(n^2+2)/3\}\zeta_{CH_3}\zeta_{OH} + 0 + 0^{24)} \\ &\equiv -42.4\end{aligned}$$

$$\therefore\quad \zeta_{CH_3}\zeta_{OH} = 1.6759\{3/(n^2+2)\} \qquad (5)$$

The value of $\zeta'_{CH_3}\zeta'_{OH}$ of menthol-like substance, shown in Eq. 4 is almost equal to that of $\zeta_{CH}\zeta_{OH}$ of methylcyclohexanol given in Eq. 5. This fact indicates that the value of $\zeta'_{CH_3}\zeta'_{OH}$ in Eq. 4 is trustworthy. Moreover, by using Eq. 4, $\sum[\mu]^{20}_{D\ obs}$ of (+)*trans*-2-hydroxyneomenthol which has $(OH)^{3\alpha}$ in its molecule is calculated to be 69.5. This calculated value is almost equal to the corresponding observed value, 70.3. This fact may mean that the value of $\zeta'_{CH_3}\zeta'_{OH}$ in Eq. 4 is a suitable one for the calculation of $\sum[\mu]^{20}_{D\ obs}$ of menthol-like substances.

Next, by using a method similar to that described above, an equation can be obtained as follows;

19) S. Yamana, This Bulletin, 30, 203 (1957).
20) $(CH_3)^{\alpha 8\text{-d}}$ means $(CH_3)^{\alpha 8}$ which stays at d-position, and so on (Ref. 2).
21) Simp. I is used here.
22) ζ' is ζ-coefficient of a unit group in the case of menthol-like substance.
23) Ref. Table I.
24) Table IV is used, here.

TABLE IV. $[\mu]^{20}_{D\,\text{calcd}}\{3/(n^2+2)\}$, CAUSED BY THE DYNAMICAL COUPLING EFFECT BETWEEN ANY TWO MEMBERS OF UNIT GROUPS IN MENTHOL-LIKE SUBSTANCE OF C 1 CONFORMATION

	$(CH_3)^{\alpha 8\cdot f}$	$(CH_3)^{\alpha 8\cdot e}$	$(CH_3)^{\alpha 8\cdot d}$	$(CH_3)^{4\alpha}$	$(OH)^{3\beta}$	$(OH)^{3\alpha}$	$(OH)^{2\beta}$	$(OH)^{2\alpha}$
ch. R	0	$-D$	D	0	0	0	0	0
$(OH)^{1\alpha}$	0	−0.74	0.74	0	1.88	0	0	11.73
$(CH_3)^{1\alpha}$	0	−1.75	1.75	0	4.20	0	0	25.30
$(CH_3)^{1\beta}$	0	4.41	−4.41	0	0	−4.04	25.30	−25.30
$(OH)^{2\alpha}$	−4.74	0	4.74	0	11.73	−11.73		
$(OH)^{2\beta}$	0	4.64	−0.11	−4.04	−11.73	0		
$(OH)^{3\alpha}$	0	−4.04	3.09	25.30				
$(OH)^{3\beta}$	−3.07	4.04	0	−25.30				
$(CH_3)^{4\alpha}$	0	0	0					
$(CH_3)^{\alpha 8\cdot d}$	0	0	0					
$(CH_3)^{\alpha 8\cdot e}$	0	0	0					
$(CH_3)^{\alpha 8\cdot f}$	0	0	0					

Note: D cannot be calculated, theoretically.

TABLE V. $\sum[\mu]^{20}_{D\,\text{obs}}$ OF MENTHOL-LIKE SUBSTANCE

Name	Type		
	S	I	II
(−)*trans*-2-Hydroxymenthol	−12.8	$-29.4-D$	$-33.0+D$
(−)*cis*-2-Hydroxymenthol	−43.4	$-45.5-D$	$-63.4+D$
(−)Isomenthol	−25.7	$-31.3-D$	$-35.5+D$
(−)Menthol	−32.0	$-34.3-D$	$-45.1+D$
(−)Carvomenthol	−31.0	$-42.9-D$	$-40.5+D$
(+)*cis*-1,2-Menthanediol	19.2	$6.2-D$	$10.8+D$
(+)Neocarvomenthol	38.9	$41.4-D$	$29.5+D$
(+)*trans*-1-Hydroxyneocarvomenthol	38.9	$40.3-D$	$30.6+D$

S: Symmetrical type, I: Unsymmetrical I type, II: Unsymmetrical II type.

$$\sum[\mu]^{20}_{D\,\text{obs}} \text{ of } (-)cis\text{-2-hydroxyneomenthol} \equiv(-11.73\zeta'^{2}_{OH}-0.25\zeta'_{CH_3}\zeta'_{OH})\times\{(n^2+2)/3\}\equiv-50.6 \quad (6)$$

Combining Eq. 4 with Eq. 6,

$$\zeta'^{2}_{OH}=4.2796\{3/(n^2+2)\} \quad (7)$$

or

$$\zeta'_{OH}=2.0687\{3/(n^2+2)\}^{1/2} \quad (7')$$

The value of ζ'^{2}_{OH} in Eq. 7 is nearly equal to that of ζ^{2}_{OH}, $4.1091\{3/(n^2+2)\}$ which was obtained for the case of (−)1/2 cyclohexanediol[25]. This fact can easily be understood by considering that both (−)*cis*-2-hydroxyneomenthol and (−) 1/2 cyclohexanediol have only two hydroxyl groups ,which are adjacent to each other in their molecules. Thus, the value of ζ'^{2}_{OH} Eq. 7 seems to be reliable. From Eqs. 4 and 7′,

$$\zeta'_{CH_3}=0.7283\{3/(n^2+2)\}^{1/2}$$

and

$$\zeta'^{2}_{CH_3}=0.5304\{3/(n^2+2)\} \quad (8)$$

Substances which Have $(OH)^{3\beta}$. — Referring to Table III, the nearest position from O-atom in $(OH)^{3\beta}$ is $\alpha 8$·d-position. Then, owing to the steric repulsion, $(OH)^{3\beta}$ may refute the idea that any movable $(CH_3)^{\alpha 8}$ in $(iso\text{-}C_3H_7)^{4\alpha}$ stays at $\alpha 8$·d-position. In this case, the internal conformation of $(iso\text{-}C_3H_7)^{4\alpha}$ may be forced to take the unsymmetrical I type. But if an atom or group which combines whith C^2-atom attracts $(OH)^{3\beta}$ off $\alpha 8$·d-position, the influence of $(OH)^{3\beta}$ on the type of the internal conformation of $(iso\text{-}C_3H_7)^{4\alpha}$ may be greatly weakened. Now, by using Eqs. 4 and 7, $\sum[\mu]^{20}_{D\,\text{obs}}$ of the menthol-like substances which have $(OH)^{3\beta}$ are calculated in each type of the internal conformation of $(iso\text{-}C_3H_7)^{4\alpha}$. The results of calculation are shown in the upper part of Table V.

For lack of experimental data in relation to the cyclohexane-ring, D cannot be calculated theoretically. Then, the author resorted to a quasi-empirical evaluation of it. (−)Menthol has $(OH)^{3\beta}$ but it has no atom or group which combines with the C^2-atom and attracts $(OH)^{3\beta}$. And moreover, as the orientation of its $(CH_3)^{1\beta}$ is equatorial, the influence of $(CH_3)^{1\beta}$ on the type of the internal conformation of its $(iso\text{-}C_3H_7)^{4\alpha}$ will be very small. Then, the internal conformation of its $(iso\text{-}C_3H_7)^{4\alpha}$ is expected

25) Ref. Eq. 4* in the foot-note 4.

TABLE VI. COMPARISON OF $[M]_D^{20}$ WITH $\sum[\mu]_{D\,obs}^{20}$

Name	at C^3	$[M]_D^{20}$ [23]	$\sum[\mu]_{D\,obs}^{20}$ S	I	II	%
(+)Neomenthol	$(OH)^{3\alpha}$	30.6	30.6			100% S
(−)*cis*-2-Hydroxyneomenthol	$(OH)^{3\alpha}$	−50.6	−50.6			100% S
(+)*trans*-2-Hydroxyneomenthol	$(OH)^{3\alpha}$	70.3	69.5			100% S
(−)*trans*-2-Hydroxymenthol	$(OH)^{3\beta}$	−16.0	−12.8	−72.6	10.2	95% S + 5% I
(−)*cis*-2-Hydroxymenthol	$(OH)^{3\beta}$	−56.7	−43.4	−88.7	−20.2	71% S +29% I
(−)Isomenthol	$(OH)^{3\beta}$	−39.4	−25.7	−74.5	7.7	72% S +28% I
(−)Menthol	$(OH)^{3\beta}$	−77.5	−32.0	−77.5	−1.9	100% I
(−)Carvomenthol	none	−41.2	−31.0	−86.1	2.7	82% S +18% I
(+)*cis*-1,2-Menthanediol	none	24.1	19.2	−37.0	54.0	86% S +14% II
(+)Neocarvomenthol	none	65.2	38.9	−1.8	72.7	22% S +78% II
(+)*trans*-1-Hydroxyneocarvomenthol	none	79.2	38.9	−2.9	73.8	100% II

S: Symmetrical type, I: Unsymmetrical I type, II: Unsymmetrical II type.

to be of the unsymmetrical I type. Accordingly, by referring to Table V, $\sum[\mu]_{D\,obs}^{20}$ of (−) menthol should be $(-34.3-D)$. The corresponding observed value is −77.5[23].

$$\therefore \quad -34.3-D\equiv -77.5$$

or

$$D=43.2 \qquad (9)$$

By using Eq. 9, Table V can be rewritten into Table VI.

The seventh column of Table VI indicates the percentage of two types in order to explain the corresponding observed value. But, as the observed value, $[M]_D^{20}$, has some probable errors and the calculated value, $\sum[\mu]_{D\,obs}^{20}$, was obtained by using some assumptions, the absolute values of the percentage in the seventh column should not be considered to be conclusive. Thus, it becomes apparent that even in this series, the symmetrical type can be prevalent when there are some groups which attract $(OH)^{3\beta}$ or to not allow any $(CH_3)^{\alpha 8}$ to say at the $\alpha 8$-f-position. But the ratio of these two types is affected greatly by the orientations of the other atoms or groups in the molecules.

Substances which Have no $(OH)^3$.—By using a method similar to those mentioned above, $\sum[\mu]_{D\,obs}^{20}$ of the substances which have not $(OH)^3$ are calculated and the results are shown in the lower parts of Tables V and VI. In this case also, the symmetrical type is prevalent. But it is strange that in (+)neocarvomenthol and (+)*trans*-1-hydroxyneocarvomenthol, the unsymmetrical II type is prevalent among the three types. This may mean that there is a kind of intramolecular (or intermolecular) van der Waals' attractive force between $(CH_3)^{\alpha 8}$ and the hydroxyl group which combines with the C^2- or C^1-atom, but this point is left for future study.

Summary

From the standpoint of the fact that a menthol-like substance is a kind of hydroxycyclohexane, the molecular rotations of menthol-like substances are calculated by using the PM-method. A comparison of the calculated values with the corresponding observed values seems to make it possibe to presume the type of the internal conformation of $(iso\text{-}C_3H_7)^{4\alpha}$.

Department of Chemistry
Kyoto Gakugei University
Fushimi-ku, Kyoto

Structure of Enteromycin. I. Derivatives and Products in Various Reactions of Enteromycin*

By Kōmei MIZUNO

(Received April 4, 1961)

Streptomyces albireticuli isolated by Nakazawa[1] in 1951 produces several biologically active antibiotics including eurocidine[2], enteromycin[3], carbomycin[4] (magnamycin)[5,6] and tertiomycin[7], which are different from each other in properties and they all show low toxicity. Nakazawa et al. isolated eurocidin[2] from a methanolic extract of the mycelium of the microorganism and carbomycin[4] from an ethyl acetate extract of the filtered broth which had been made alkaline beforehand, and Miyake et al. obtained tertiomycin[8] from the mother liquor of carbomycin. Nakazawa et al. also isolated enteromycin, an antibiotic active against Gram-negative bacteria, from the ethyl acetate extract of the above filtered broth which had been made acid, and assigned to it an empirical formula of $C_6H_8O_5N_2$, but its structure has so far remained unclarified. The present author, however, from the results of experiments to be published in four reports hence, has made clear that the antibiotic is *N*-(*O*-methyl-*aci*-nitroacetyl)-3-aminoacrylic acid. It is a peptide-type[9] compound and seems to be the first so far isolated from natural products as a substance having a *O*-methyl-*aci*-nitro group.

Enteromycin (I) is sparingly soluble in water and other solvents, but can be recrystallized from plenty of hot methanol and gives two kinds of interchangeable crystals Ia and Ib according to the extent of cooling. The p*K*a of this compound is 4.3, and from its molecular weight calculated from the amount of the alkali consumed and from its analytical values the molecular formula of $C_6H_8O_5N_2$ was assigned to it. Enteromycin has a methoxy group, and is optically non-active and negative to the phenolic OH reaction (referred to as Barton[10] reaction hereafter) by the ferric chloride-potassium ferricyanide reagent, but reduces the Fehling's reagent. A methanolic solution of this compound exhibits three absorption maxima at λ 230 mμ (ε 9000), 275 mμ (ε 13000) and 298 mμ (ε 16000) (Fig. 1), and the infrared spectra of Ia and Ib show absorptions at the following wavelengths (ν_{max}^{Nujol} cm^{-1}): 3300~3330 (NH), 2560~2670 (COOH), 1680~1690 (CO), 1620~1640 (conj. C=N), 1600 (conj. C=C), 1560 (-CO-NH-), 992 (Ia), 988 (Ib) (trans C=C). When methylated with diazomethane Ia and Ib gave the same product II [m. p. 141°C (decomp.), $C_7H_{10}O_5H_2$] and the infrared spectrum (Fig. 4) of the product clearly exhibited the absorption (1720 cm^{-1}) of COOR. II, having two methoxy groups, is obviously the methyl ester of I and so I seems sure to have a methoxy group detectable by the Zeisel method and a free carboxyl group, and therefore the formula A was assigned to it.

$$C_6H_8O_5N_2 \quad (C_4H_4O_2N_2) \rightarrow \begin{matrix} -COOH \\ -OCH_3 \end{matrix}$$

A

Since further reaction of II with diazomethane yielded a product (III) [m. p. 121°C (decomp.), $C_8H_{12}O_8N_4$] suspected to be a molecular compound from its molecular formula, the skeleton of I was assumed to have one or more double bonds.

I is unstable to heat, acid and alkali, and when heated with water it gave off formaldehyde (IV), acetaldehyde (V), carbon dioxide (VI), and others. In addition to V and VI, I also produced ammonia (VII), glyoxylic acid (VIII), oxalic acid (IX), etc. by heating with diluted hydrochloric acid, and acetaldehyde when reacted with hydroiodic acid, but no formaldehyde was yielded in these acid decompositions. Heating of I with sodium hydrogen carbonate solution afforded oxamic acid (XI). When subjected as such to thermal decomposition, I changed, under evolution of formaldehyde, into a substance which was positive to

* This constitutes Part XXXV of a series entitled "Studies on Antibiotics" by S. Tatsuoka, and was reported at the Forum on Natural Organic Compounds held on October 16, 1960.

1) K. Nakazawa, *J. Agr. Chem. Soc. Japan*, (*Nippon Nōgei-kagaku Kaishi*), **29**, 647 (1955).
2) K. Nakazawa, ibid., **29**, 650 (1955).
3) K. Nakazawa, ibid., **29**, 659 (1955).
4) K. Nakazawa et al., ibid., **29**, 661 (1955).
5) F. W. Tanner et al., *Antibiotics & Chemotherapy*, **2**, 441 (1952).
6) R. B. Woodward, *Angew. Chem.*, **69**, 50 (1957).
7) R. Utahara et al., *J. Antibiotics*, **A**, **7**, 120 (1954).
8) A. Miyake et al., ibid., **12**, 59 (1959).
9) A. J. Birch and H. Smith, Ciba Foundation Symposium. Amino Acids and Peptides with Antimetabolic Activity, Spottitwoode, Ballantyne & Co., Ltd., London and Colchester (1958), p. 247.
10) G. M. Barton et al., *Nature*, **170**, 249 (1952).

the Barton reaction and easily soluble in water and methanol. The substance was recrystallized from water in plates (XII) [m. p. 175°C (decomp.), $C_5H_6O_4N_2$] and needle-like crystals XIII [m. p. 169°C (decomp.), $C_{11}H_{14}O_8N_4$], and XII further afforded two kinds of interchangeable products XIIa and XIIb when recrystallized from water. XII (p*K*a 4.3 and 8.3) is an acid substance consuming two moles of alkali, and it is positive to the Barton reaction and reduces the Fehling's reagent but has no methoxyl group detectable by the Zeisel method. A methanolic solution of this substance exhibited two absorption maxima at λ 225 mμ (ε 16500) and 280 mμ (ε 18000), and from infrared spectra of XIIa and XIIb (Figs. 6, 7) the presence of OH (3450 cm^{-1}), NH (3330), COOH (2560~2670), CO (1680), conj. C=N (1630), conj. C=C (1610) and trans C=C (975, 990) was presumed.

XIII has a methoxy group and from its ultraviolet spectrum (Fig. 8) and antibiotic activity,

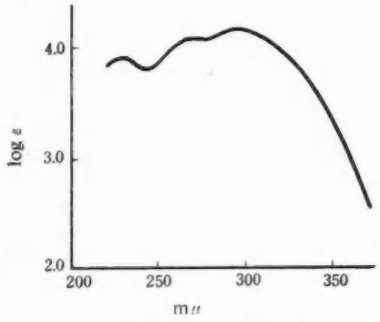

Fig. 1. Ultraviolet absorption spectrum of enteromycin (Ia, Ib) in methanol.

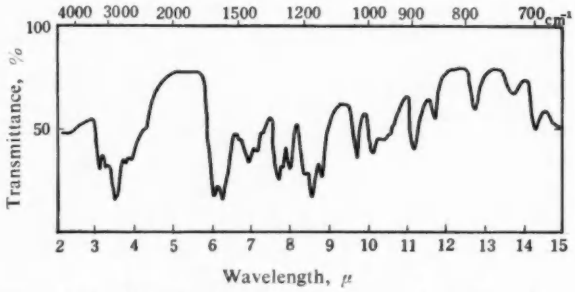

Fig. 2. Infrared absorption spectrum of enteromycin (Ia).

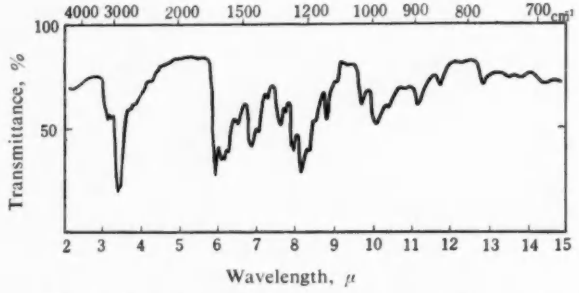

Fig. 3. Infrared absorption spectrum of enteromycin (Ib).

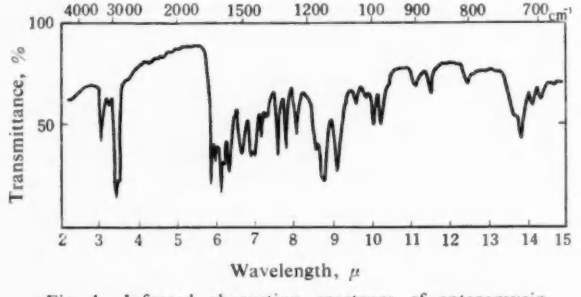

Fig. 4. Infrared absorption spectrum of enteromycin methylester (II).

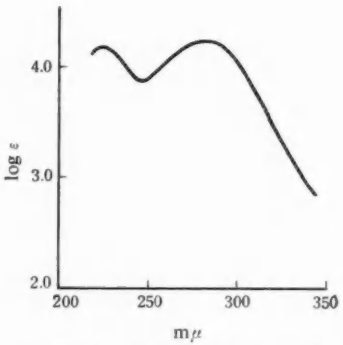

Fig. 5. Ultraviolet absorption spectrum of demethoxyenteromycin (XII) in methanol.

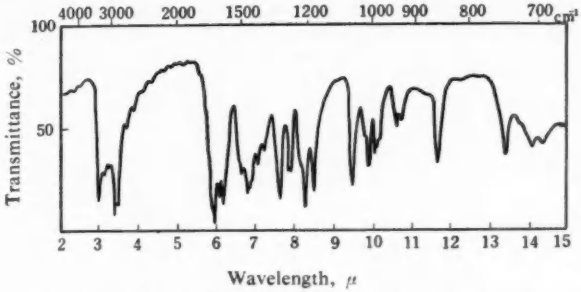

Fig. 6. Infrared absorption spectrum of demethoxy-enteromycin (XIIa).

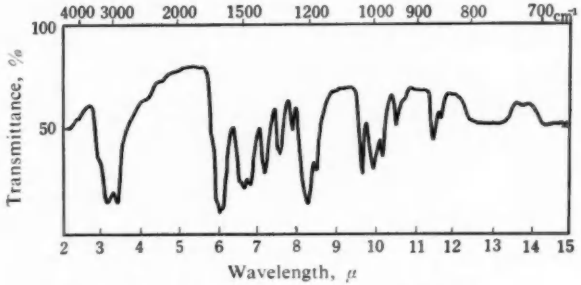

Fig. 7. Infrared absorption spectrum of demethoxy-enteromycin (XIIb).

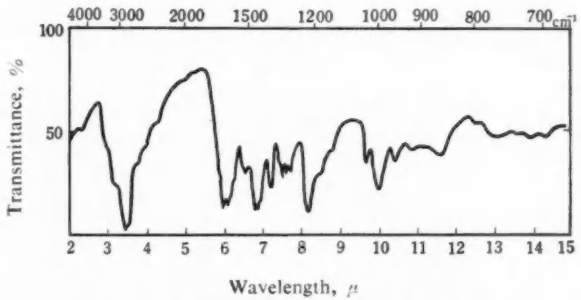

Fig. 9. Infrared absorption spectrum of XIII.

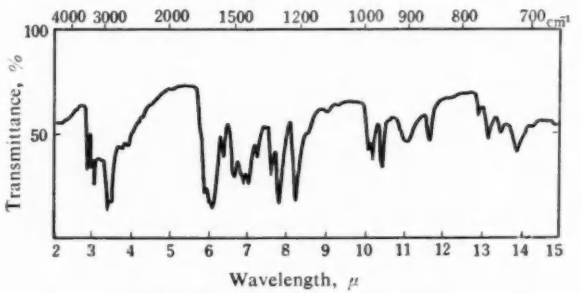

Fig. 10. Infrared absorption spectrum of enteromycin amide (XIV).

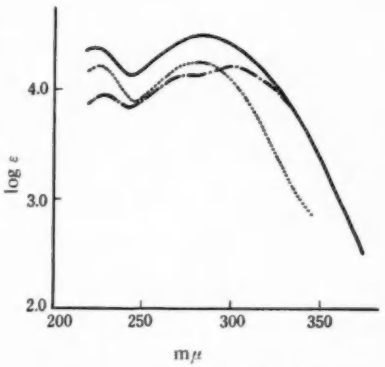

Fig. 8. Ultraviolet absorption spectra of I (—·—·—), XII (----), and molecular complex XIII (——) in methanol.

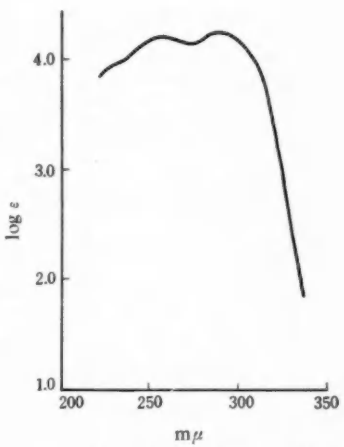

Fig. 11. Ultraviolet absorption spectrum of XIV in methanol.

it is assumed to be a molecular compound consisting of I and XII, and this assumption was confirmed by the infrared spectrum (Fig. 9) of the product prepared from equimolecular amounts of the two components. Demethoxylation** of I by heating afforded XII or XIII as mentioned above depending on the temperature and time of heating, and from the kind and amount of the product the progress of the demethoxylation could be checked. The thermal decomposition proceed to a considerable extent when I was left standing at 30°C for some ten days. However, since neither formaldehyde nor a substance positive to the Barton reaction was produced when I was allowed to stand in a methanolic solution of trimethylamine at 0°C for a long time, I seems to have no such a group as $-CH_2OH$ which produces formaldehyde by general dehydroxymethylation. Considered together with the results of decompositions of I with acid and water, the methoxy group detectable by the Zeisel method appears to be split off as formaldehyde, and therefore I is assumed to have a specific functional group including a methoxy group. So XII may be called demethoxyenteromycin. Amidation of I produced light yellow crystals, m. p. 163°C (decomp.) (neither urotropine nor IV was found in the mother liquor), which were converted into stable prisms (XIV) [m. p. 208°C (decomp.), $C_5H_7O_4N_3$], when treated with diluted acetic acid. As this product was positive to the Barton reaction and its infrared spectrum (Fig. 10) exhibited various absorptions characteristic of amides, it may be called enteromycin amide. The ultraviolet spectrum (Fig. 11) of the product showed two maxima at λ 255 mμ (ε 15000) and 290 mμ (ε 18000), but as the spectrum did not resemble that of I, the product is likely to have a structure considerably different from that of I.

As mentioned before, I seems to have one or more double bonds, so it was subjected to catalytic reduction to make its skeleton clear, whereupon XII was produced first but the final product was XV [m. p. 225°C (decomp.), $C_5H_{10}O_3N_2$]. This product has no methoxy group and is positive to the ninhydrin reaction, and it may be called dehydroxytetrahydrodemethoxyenteromycin from its molecular formula.

From the above results the methoxyl group of I appears to be split off by catalytic reduction, and though I seems apparently to be amidated, it has no $COOCH_3$ group, so the amidation must be due to a specific functional group mentioned before. The carbon dioxide produced in the acid decomposition of I seems to have derived from the COOH group, and since acetaldehyde was produced in the same decomposition, the molecule of I ought to have $-CH=CH-$ or $-CH_2-CH=$ combination. Further the fact that ammonia, oxalic acid, and glyoxylic acid were produced in the decomposition and that oxamic acid was obtained in the alkali decomposition seems to suggest that I has $-NH-CO-\overset{|}{C}H-$ or $=N-CO-\overset{|}{C}H-$ combination.

Chart 1.

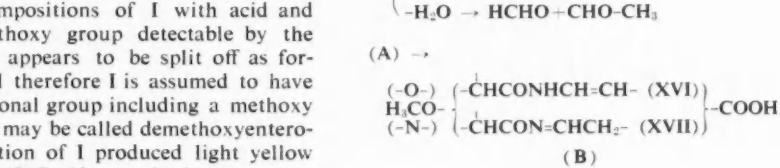

Chart 2.

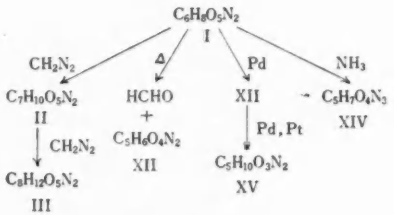

Experimental

Enteromycin (I). — A hot solution of 1 g. of enteromycin in 500 cc. of methanol was filtered with 100 g. of decolorizing charcoal and the filtrate was left standing, separating 500 mg. of long needle-like crystals Ib. Concentration of the mother liquor gave an additional crop of 300 mg. A solution of 200 mg. of Ib in 150 cc. of hot methanol was concentrated to about 50 cc. under reduced pressure and cooled to yield fine prisms Ia. Working up of the mother liquor afforded another crop, making the total yield 180 mg. Ia and Ib were clearly distinguishable in infrared spectrum. They dissolved in aqueous sodium hydrogen carbonate solution with evolution of carbon dioxide and colored yellow at 142°C, brown at 158°C and melted at 172°C with decomposition.

Found: C, 38.21; H, 4.41; N, 15.14; O-CH_3, 16.14. Calcd. for $C_6H_8O_5N_2$: C, 38.30; H, 4.29; N, 14.89; O-CH_3, 16.54% (one O-CH_3).

The pK_a of this compound is 4.3 and its molecular weight is 180±10 when calculated from the amount of the alkali consumed.

** Whether this phenomenon is to be called demethoxylation or deformaldehyde reaction was unknown at first, but preference was given to the former as experiments proceeded.

Enteromycin Methylester (II).—To a suspension of 600 mg. of pure I in 60 cc. of ethanol was added an ether solution of diazomethane produced from 5 g. of nitrosomethylurea in several portions at 10~15°C. When evolution of nitrogen subsided, the almost colorless reaction mixture was concentrated under reduced pressure, giving 630 mg. of white crystals, which melted at 141°C (decomp.) after recrystallization from ethanol. This product gives off no carbon dioxide in sodium hydrogen carbonate solution and is negative to the ferric chloride-potassium ferricyanide reaction.

Found: C, 41.86; H, 4.75; N, 13.48; O-CH_3, 30.01. Calcd. for $C_7H_{10}O_5N_2$: C, 41.58; H, 4.99; N, 13.86; O-CH_3, 30.70% (two O-CH_3).

Diazomethane Addition Product of Enteromycin Methylester (III).—To a solution of 200 mg. of II in 20 cc. of ethanol was added a solution of diazomethane in 50 cc. of ether which was produced from 2 g. of nitrosomethylurea, and the reaction mixture was left standing at room temperature for 10 hr. and then concentrated at low temperature under diminished pressure to precipitate crystals. The crystals, after washing with ethanol, were dissolved in hot methanol, the solution was filtered, and the crystals obtained from the filtrate were recrystallized from ethanol, giving 100 mg. of needles, m. p. 121°C (decomp.). This compound is positive to the ferric chloride-potassium ferricyanide reaction and gives orange-red color with the Dragendorff[11] reagent.

Found: C, 39.40; H, 5.02; N, 22.50; O-CH_3, 25.02. Calcd. for $C_8H_{12}O_5N_4$: C, 39.24; H, 4.95; N, 22.94; O-CH_3, 25.42% (two O-CH_3).

Decomposition of Enteromycin with Hot Water.—A suspension of 100 mg. of I in 6 cc. of water was heated at 100°C for 1 hr. in vessel A under introduction of nitrogen. The aldehydes and carbon dioxide evolved were collected in receivers B and C containing pure water and baryta water, respectively. After the reaction, about 25 mg. of barium carbonate was obtained. A solution of 20 mg. of 2,4-dinitrophenylhydrazine in 5 cc. of concentrated hydrochloric acid was added to the receiver B, the mixture was allowed to stand for 3 hr. and the resulting hydrazones were extracted with ethyl acetate. The extract was washed with water, dried over anhydrous sodium sulfate and concentrated at low temperature under reduced pressure, separating 25 mg. of yellowish orange 2,4-dinitrophenylhydrazones (referred to as 2,4-DNPH hereafter). Paper chromatography of a solution of the products in chloroform-acetone (1 : 1) by the method of Gasparic[12] gave the two yellow spots at R_f 0.25 and 0.38, which were identified as of 2,4-DNPH of formaldehyde (IV) and that of acetaldehyde (V).

Decomposition of Enteromycin with Hydrochloric Acid.—A suspension of 200 mg. of I in 2 cc. of 1 N hydrochloric acid was treated as above at 95°C for 1 hr. In addition to 140 mg. of barium carbonate, the following substances were obtained.

Acetaldehyde (V).—The aldehyde produced was converted to 2,4-DNPH with a solution of 2,4-dinitrophenylhydrazine in hydrochloric acid and the resulting crude product, m. p. 141°C (ca. 40 mg.) was purified by recrystallization from ethanol, when m. p. rose to 160°C. The R_f value in paper chromatography and infrared spectrum of the product where in complete accord with those of 2,4-DNPH of synthetic acetaldehyde, and a mixed melting point determination of both substances showed no depression.

Found: C, 43.37; H, 3.73; N, 24.83. Calcd. for $C_9H_9O_4N_4$: C, 42.86; H, 3.60; N, 24.99%.

Oxalic Acid (IX).—The reaction mixture was extracted with 20 cc. of ether and the extract was concentrated to give 20 mg. of white crystals, m. p. 96°C, which was subjected to paper chromatography by the method of Stark[13] et al. (solvent: 75% phenol containing 1% of formic acid), affording a spot at R_f 0.20, suspected to be of oxalic acid. The sodium salt of the product was converted to *S*-benzylthiuronium salt and purified by recrystallization from ethanol, m. p. 193°C.

Found: N, 13.17. Calcd. for $C_{18}H_{22}O_4N_4S_2$: N, 13.27%.

Glyoxylic Acid (VIII).—A solution of 2,4-dinitrophenylhydrazine in hydrochloric acid was added to the reaction mixture which had been extracted with ether, and after 3 hr. the resulting hydrazone was extracted with ethyl acetate. Concentration of the extract yielded a small amount of yellow crystals, which when paper-chromatographed in parallel with 2,4-DNPH of synthetic glyoxylic acid, gave a spot of 2,4-DNPH of glyoxylic acid at R_f 0.40.

Ammonia (VII).—The reaction mixture from which 2,4-DNPH of glyoxylic acid had been separated was made alkaline and steam-distilled. The evolving basic gas was collected in diluted hydrochloric acid and the solution was evaporated to dryness to yield some plates. The product was identified as ammonium chloride because it gave, on paper chromatography (solvent: the upper layer of a mixture of *n*-butanol, acetic acid and water (4 : 1 : 5)), a spot at R_f 0.14 which was positive to the ninhydrin reaction and took on a grayish brown color with the ammonical silver nitrate solution.

2,4-DNPH of Glyoxylic Acid.—One and three tenths grams of ethyl diethoxyacetate, $(EtO)_2CH$-COOEt, synthesized by Moffett's method[14] was hydrolyzed by heating in 5 cc. of 5 N sodium hydroxide at 65°C for one hour and the reaction mixture, after neutralizing with hydrochloric acid, was shaken with ether to remove the unreacted material. One gram of 2,4-dinitrophenylhydrazine was dissolved in the aqueous layer, 25 cc. of concentrated hydrochloric acid was added, the mixture was stirred for 30 min. at 80°C, yielding 1.5 g. of yellow crystals. The crystals were dissolved in a solution of 1.5 g. of sodium bicarbonate in 30 cc. of water, the solution was acidified with hydrochloric acid and extracted with ethyl acetate, and the extract, after being washed with water and dried, was evaporated under reduced pressure, leaving 1.1 g. of a residue, which crystallized from hot methanol into yellow needlelike crystals, m. p. 193°C (decomp.).

11) A. Zaffaroni et al., *J. Biol. Chem.*, **177**, 109 (1949).

12) J. Gasparic and M. Vecera, *J. Chromatog.* **1**, xviii (1958).

13) J. B. Stark et al., *Anal. Chem.*, **23**, 413 (1951).

14) R. B. Moffett, *Org. Syntheses*, **35**, 59 (1955).

Found: C, 37.89; H, 2.66; N, 21.79. Calcd. for $C_5H_6O_6N_4$: C, 37.80; H, 2.38; N, 22.05%.

Paper Chromatography of 2,4-DNPH of Glyoxylic Acid. — Each of 2,4-DNPH of various aldehydes, dissolved in a 1 : 1 mixture of chloroform and acetone, was developed by the ascending method on a piece of Tōyō filter paper No. 7 (4×45 cm.) acetylated by Micheel's method[15], using a solvent of cyclohexane-benzene-chloroform-ethyl acetate-acetone (5 : 5 : 10 : 1 : 5). R_f values of various 2,4-DNPH at the time when the solvent front migrated about 20 cm. from the starting point were as shown below.

Substance	R_f value
2,4-Dinitrophenylhydrazine	1.00
2,4-DNPH of acetone	0.90~0.95
〃 of formaldehyde	0.84
〃 of acetaldehyde	0.73
〃 of glyoxylic acid	0.40

Under ultraviolet rays all the spots were observed as light absorbing spots and all of them exhibited a peculiar brownish purple color when immersed in 90% ethanol containing 2% of sodium hydroxide.

Decomposition of Enteromycin with Hydroiodic Acid. — Fifty milligrams of I was heated with 4 cc. of the hydroiodic acid mixture (hydroiodic acid-phenol-propionic anhydride) at 60~80°C for 40 min. and at 80~120°C for 2 hr. under introduction of nitrogen, and the aldehyde in the distillate was converted to 2,4-DNPH. On paper chromatography as before, the 2,4-DNPH gave a single yellow spot at R_f 0.35, which was identified as 2,4-DNPH of acetaldehyde.

Decomposition of Enteromycin with Alkali Carbonate. — *Oxamic Acid (XI).* — A mixture of 500 mg. of I and 5 cc. of 10% sodium carbonate solution was heated on the water bath and after being concentrated to 1.2 cc. cooled to yield ca. 100 mg. of crystals. The crystals were dissolved in 3 cc. of water, the solution was passed through a column of Amberlite IR-120 (H-form), and the effluent, after concentration under reduced pressure, was mixed with a little ethanol to separate 50 mg. of yellowish white crystals. The crystals were dissolved again in water and reprecipitated with ethanol, giving 30 mg. of white crystals, m. p. 203°C (decomp.). The product, melting at 210°C after drying at 120°C for 2 hr. in vacuo, was identified as oxamic acid having one mole of water of crystallization.

Thermal Decomposition of Enteromycin (1). — Three hundred milligrams of I was heated at 110~120°C for 40~50 min. in a 5 cc. flask connected through a Liebig condenser with a vessel containing 5 cc. of cold pure water, under gentle introduction of nitrogen which was washed with an alkaline pyrogallol solution and dried with calcium chloride. And the following substances were obtained.

Demethoxyenteromycin (XII). — The yellow contents of the flask were dissolved in 3 cc. of methanol and the solution, after being filtered to remove the unreacted material (70 mg.), was evaporated at low temperature under diminished pressure. The white residue was dissolved in 2 cc. of hot water and cooled to separate about 40 mg. of needles XIII. The mother liquor from the needles was concentrated, yielding 140 mg. of prisms XIIa, which, after several recrystallizations from water, gave about 40 mg. of plates XIIb. Both kinds of the crystals colored brown at 157°C and melted at 175°C with decomposition. They were positive to the ferric chloride-potassium ferricyanide reaction and could be distinguished from each other by their infrared spectra.

Found (XIIa): C, 37.82; H, 3.91; N, 17.85. Found (XIIb): C, 37.78; H, 3.97; N, 17.97; O-CH_3, undetected. Calcd. for $C_5H_6O_4N_2$: C, 37.98; H, 3.83; N, 17.72%.

Formaldehyde (IV). — The aldehyde collected in the water-containing vessel was converted to 2,4-DNPH (ca. 30 mg.), which afforded a single yellow spot at R_f 0.25 on paper chromatography[12]. The product melted at 168°C after recrystallization from methanol and it was identified as 2,4-DNPH of formaldehyde from its infrared spectrum and by mixed melting point determination.

Found: C, 40.38; H, 3.08; N, 27.00. Calcd. for $C_7H_6O_4N_4$: C, 40.00; H, 2.88; N, 26.66%.

Thermal Decomposition of Enteromycin (2). — *Enteromycin Demethoxyenteromycin Molecular Compound.* — When I was left standing at room temperature for more than several months, it gave off the smell of formaldehyde and colored yellow. The product was treated as in the case of XII to give needle-like crystals (XIII), m. p. 169°C (decomp.), which were positive to the ferric chloride-potassium ferricyanide reaction and had about one half antibiotic activity of that of I.

Found: C, 38.52; H, 3.88; N, 16.68. Calcd. for $C_{11}H_{14}O_9N_4(C_6H_8O_5N_2 \cdot C_5H_6O_4N_2)$: C, 38.10; H, 4.05; N, 16.20%.

Fifty milligrams of I and 50 mg. of XII were dissolved in 5 cc. of hot water and the solution was cooled to yield needle-like crystals having the same infrared spectrum as XIII.

Non-dehydroxymethylation. — A solution of 50 mg. of I in 5 cc. of 1% methanolic trimethylamine solution was left standing at 5°C for one week and concentrated at low temperature under reduced pressure. The residue (ca. 50 mg.) was dissolved in 3 cc. of water and the solution was acidified with several drops of acetic acid, giving about 45 mg. of crystals showing the same infrared spectrum as I.

Enteromycin Amide (XIV). — A solution of 500 mg. of I in 100 cc. of methanol saturated with ammonia was allowed to stand overnight at room temperature, and the solvent was distilled off, leaving 450 mg. of crude crystals. The crystals were dissolved in 7 cc. of water and the solution was filtered and made acid with acetic acid to separate 380 mg. of crystals, m. p. 196~203°C (decomp.). The product, after recrystallization from methanol, melted at 208°C (decomp.) and was positive to the ferric chloride-potassium ferricyanide reaction.

Found: C, 34.59; H, 4.02; N, 24.50; O-CH_3,

15) F. Micheel and H. Schweppe, *Microchim. Acta*, **1954**, 60.

undetected. Calcd. for $C_5H_7O_4N_3$: C, 34.68; H, 4.08; N, 24.24%.

A solution of 30 mg. of 2,4-dinitrophenylhydrazine in 10 cc. of concentrated hydrochloric acid was added to the above acid mother liquor and the mixture, after being heated at 100°C for 10 min. and left standing for one hour, was extracted with ethyl acetate. The 2,4-DNPH obtained from the extract showd the spot of 2,4-DNPH of acetaldehyde at R_f 0.35 on paper chromatography[12].

Catalytic Reduction of Enteromycin.—*Demethoxyenteromycin (XII).*—A solution of 300 mg. of I in 300 cc. of hot pure methanol was rapidly cooled and catalytically reduced on palladium-carbon, when one mole of hydrogen was absorbed in about 30 min. The catalyst was filtered off and the filtrate was concentrated at low temperature under reduced pressure, separating crystals. The mother liquor from the crystals was further concentrated and a solution of the residue (ca. 200 mg.) in 5 cc. of hot water was allowed to stand to deposite needle-like crystals. The crystals were filtered and the filtrate was concentrated to about 3 cc., yielding ca. 150 mg. of plates, m.p. 175°C (decomp.). The infrared spectrum of the product was in complete agreement with that of XIIa.

Found: C, 38.10; H, 4.00; N, 17.62. Clacd. for $C_5H_6O_4N_2$: C, 37.98; H, 3.83; N, 17.72%.

Dehydroxytetrahydrodemethoxyenteromycin (XV).—A solution of 300 mg. of I in 300 cc. of hot pure methanol was cooled and reduced in the presence of 100 mg. of Adams platinum oxide when 4 mol. of hydrogen was absorbed about 2 hr. The catalyst was filtered and washed well with water, and the combined filtrate and washing were concentrated at low temperature under reduced pressure. The resulting white crystals (200 mg.), after recrystallization from aqueous methanol, melted at 225°C and were positive to the ninhydrin reaction.

Found: C, 40.97; H, 7.11; N, 18.92; $-NH_2$, 11.55. Calcd. for $C_5H_{10}O_3N_2$: C, 41.09; H, 6.90; N, 19.17; $-NH_2$, 10.45% (one-NH_2).

On paper chromatography by the method of Consden[16] et al. (80 g. phenol, 19.3 cc. water and 0.7 cc. concentrated aqueous ammonia) the product afforded a spot at R_f 0.68, which with the ninhydrin reagent gave a color changing from yellow to blue.

16) R. Consden et al., *Biochem. J.*, **38**, 224 (1944).

Summary

In order to know its functional groups and the combining state of the groups, enteromycin was subjected to such reactions as methylation, amidation, degradation, and catalytic reduction, and the properties of the products were investigated.

Research Laboratories
Takeda Chemical Ind., Ltd.
Higashiyodogawa-ku, Osaka

Structure of Enteromycin. II. Derivatives and Products in Various Reactions of Dimethoxyenteromycin*

By Kōmei MIZUNO

(Received April 4, 1961)

Dehydroxytetrahydrodemethoxyenteromycin (XV)[1] obtained by the catalytic reduction of enteromycin (I) or demethoxyenteromycin (XII) seems to have the same skeleton as that of the latter two. And from the course of changes of I, XII appears to be in the closest relation with I. In the present work, the structure of XV was established, and the functional group of XII and its derivatives were investigated in detail.

The infrared spectrum (Fig. 1) of XV exhibited the absorptions of NH, COOH and $COO^- \cdot NH_3^+$ (2100, 1620, 1370 cm^{-1}), but its ultraviolet spectrum showed no specific absorption at the long wave region beyond λ 220 mμ. Also, an amino group was detected in this compound by azotometry. Since the compound was considered to be a saturated peptide in view of the above facts, it was hydrolyzed with hydrochloric acid and the product was subjected to paper chromatography, detecting glycine (XXIII) and β-alanine (XXV). The DNP derivatives[2] of both amino acids were also confirmed by paper chromatography. Hydrolysis of the DNP derivative of XV produced no DNP-amino acid, but since β-alanine was obtained as a free amino acid, XV was

* This constitutes part XXXVI of a series entitled "Studies on Antibiotics" by S. Tatsuoka, and was reported at the Forum on Natural Organic Compounds held on October 16, 1960.

1) K. Mizuno, This Bulletin, **34**, 1419 (1961).

2) W. W. Bromer, *J. Am. Chem. Soc.*, **79**, 2794 (1957).

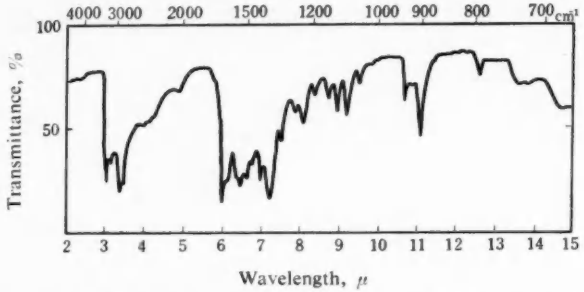

Fig. 1. Infrared absorption spectrum of dehydroxytetrahydrodemethoxyenteromycin (glycyl-β-alanine) (XV).

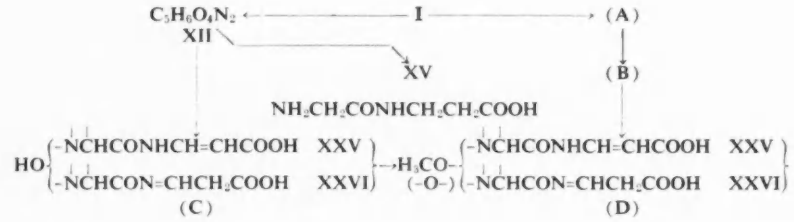

assumed to be glycyl-β-alanine. So *N*-formylglycine was condensed with β-alanine ethyl ester in the presence of dicyclohexylcarbodiimide and the resulting *N*-formylglycyl-β-alanine ethyl ester was hydrolyzed with sodium hydroxide to give *N*-formyl-β-alanine. The product was deformylated by the method of Miyamoto[3] et al., and the infrared spectrum, melting point (decomp.), and R_f value in paper chromatography of the resultant product were found to be in full accord with those of XV. From these results the formula C was presumed for XII and the formula D for I.

The two acidic groups[1] in XII were confirmed by acetylation and methylation of XII. The product was obtained as prisms (XVIII) [m. p. 181°C (decomp.), $C_7H_8O_5N_2$] negative to the Barton reaction, and since its infrared spectrum (Fig. 2) showed a clear absorption of >NO-COR[4] (1775 cm^{-1}), it was called *O*-acetyldemethoxyenteromycin.

Reaction of XII with diazomethane products, one of which (XIX) [m. p. 159°C, $C_7H_{10}O_5N_2$] was obtained as prisms and had a methoxy group and the other (XX) [m. p. 137°C, $C_7H_{10}O_4N_2$] was yielded as needles and had two methoxy groups. As the infrared spectra (Figs. 3 and 4) of both products showed the absorption of COOR (1710 cm^{-1}), they were called *N*-methyldemethoxyenteromycin methyl ester and *O*-methyldemethoxyenteromycin methyl ester, respectively.

From the formation of these compounds, it is obvious that XII representable by the formula C has a phenolic hydroxyl group in addition to a free carboxyl group. Decomposition of XII with hydrochloric acid produced acetaldehyde (V), carbon dioxide (VI), ammonia (VII), and glyoxylic acid (VIII), but not formaldehyde, and boiling of XII with water also afforded no formaldehyde, and therefore the structure of XII would be almost the same as that of I, except the special functional[1] group including a methoxy group. Amidation of XII gave a compound (XXI) m. p. 168°C (decomp.), $C_5H_9O_4N_3$] as needles, which positive to the ninhydrin reaction and reverted to the original compound by treatment with heat, water, or diluted acetic acid. And as the infrared spectrum (Fig. 5) of this product exhibited the absorption characteristic of amides, it was called demethoxyenteromycin amide. Also similarity of the ultraviolet spectrum of the product to that of XII suggested that it has a structure considerably different from that of entromycin amide (XIV).

Finally the course of the change of XII to XV by catalytic reduction was investigated in detail. Namely, catalytic reduction of XII on palladium-carbon first yielded prisms (XXII) [m. p. 203°C (decomp.), $C_5H_8O_3N_2$] which were sparingly soluble in cold water and gave a

3) M. Miyamoto et al., *J. Pharm. Soc. Japan* (*Yakugaku Zasshi*), in press.
4) H. Bredereck et al., *Chem. Ber.*, **89**, 1533 (1956).

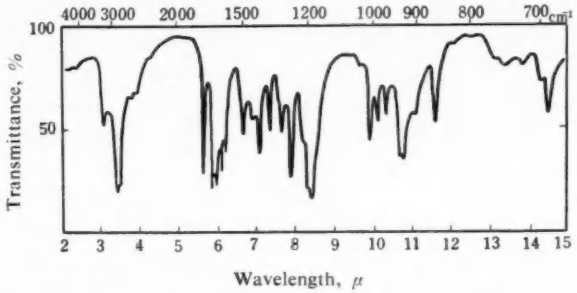

Fig. 2. Infrared absorption spectrum of *O*-acetyldemethoxyenteromycin (XVIII).

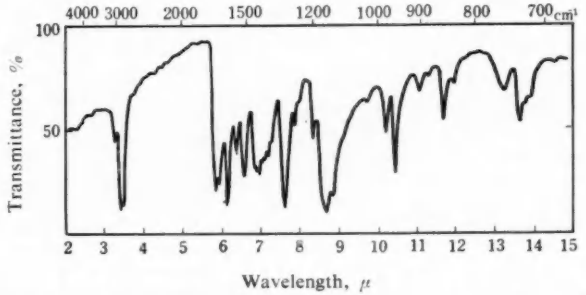

Fig. 3. Infrared absorption spectrum of *N*-methyldemethoxyenteromycin methyl ester (XIX).

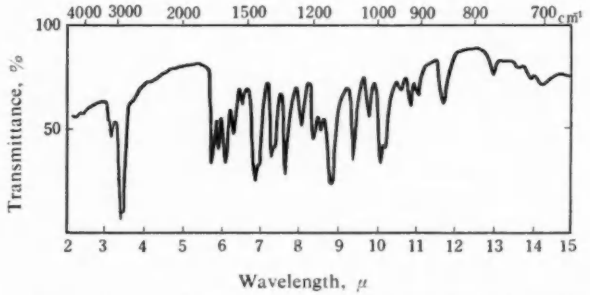

Fig. 4. Infrared absorption spectrum of *O*-methyldemethoxyenteromycin methyl ester (XX).

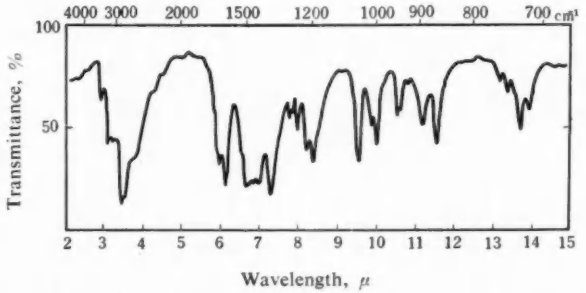

Fig. 5. Infrared absorption spectrum of demethoxyenteromycin amide (XXI).

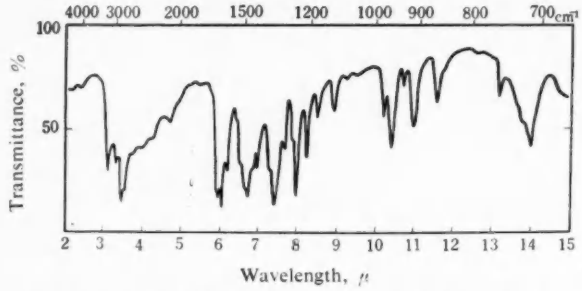

Fig. 6. Infrared absorption spectrum of dehydroxydihydrodemethoxyenteromycin (XXII).

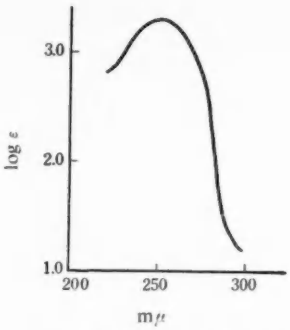

Fig. 7. Ultraviolet absorption spectrum of XXII in water.

yellow ninhydrin reaction, and further reduction resulted in the formation of glycyl-β-alanine (XV). From its molecular formula, XXII was called dehydroxydihydrodemethoxyenteromycin, and since its infrared spectrum (Fig. 6) exhibited the absorptions of NH, COOH and $COO^- \cdot NH_3^+$, it was considered to be a peptide. The ultraviolet spectrum (Fig. 7) of the compound showed a single absorption maximum (ε_{max} 2000) at λ_{max} 250 mμ.

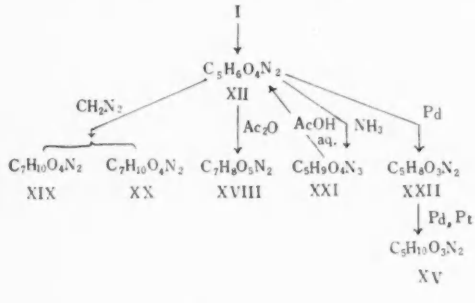

Experimental

Hydrolysis of Dehydroxytetrahydrodemethoxyenteromycin (XV).—A solution of 10 mg. of XV in 1 cc. of 6 N hydrochloric acid was heated at 110°C for 5 hr. in a sealed tube, the air in which was replaced with nitrogen. The reaction mixture was evaporated to dryness, the residue was dissolved in 1 cc. of water, and part of the solution was subjected to paper chromatography according to the method described in Report I, giving two spots at R_f 0.42 and 0.65. The former spot colored brownish pink with ninhydrin and the latter, blue, and they were identified as glycine and β-alanine, respectively. Five tenths cc. of the above aqueous solution was adjusted to pH 8 with 30 mg. of sodium hydrogen carbonate, the mixture was allowed to react with a solution of 8 mg. of 1-fluoro-2,4-dinitrobenzene in 0.5 cc. of ethanol, and the product was extracted by the method of Bromer[2]. The product was developed in the dark on filter paper, Whatman No. 1, with the upper layer of *n*-butanol-0.1% aqueous ammonia (1 : 1), giving two yellow spots at R_f 0.28~0.33 and 0.37~0.40. They were identified as DNP-glycine and DNP-β-alanine. Each of the two spots was extracted with 4 cc. of hot water, and the absorption of the extracts was measured, finding that the two products were contained in the material in equimolecular amounts.

Hydrolysis of DNP-Dehydroxytetrahydrodemethoxyenteromycin.—To a solution of 10 mg. XV in 2 cc. of water was added a solution of 7 mg. of 1-fluoro-2,4-dinitrobenzene in 2 cc. of ethanol, followed by 20 mg. each of sodium hydrogen carbonate and sodium carbonate, and the mixture was treated as in the preceding experiment. The reaction mixture was extracted first with ether at acid pH to remove 2,4-dinitrophenol and then with isobutanol to obtain the DNP-derivative of the peptide compound. Part of the product was subjected to two dimensional paper chromatography; namely it was, developed first with the same solvent system as in the preceding experiment to detect a yellow spot at R_f 0.26, which migrated to R_f 0.26 in the second development with a solution of sodium dihydrogen phosphate (1 M) and disodium hydrogen phosphate (0.5 M) in 1 l. of water. The above DNP-derivative was hydrolyzed by heating with 0.5 cc. of 10 N hydrochloric acid at 100°C for 3 hr. and the ether soluble portion of the product was chromatographed as above, detecting the spot of 2,4-dinitrophenol at R_f 0.44~0.49 (in the first development) and 0.26 (in the second development) and the spot of 2,4-dinitroanilin at 0.85~0.95 (in the first development) and 0.00 (in the second development), but no spot of DNP-glycine was observed. The acid solution from which the ether solube portion had been separated was evaporated to dryness and the residue was chromatographed as in the preceding experiment, whereupon a spot coloring blue with ninhydrin was detected at R_f 0.65, which was identified as β-alanine.

Synthesis of Glycyl-β-alanine.—To a solution of 2.1 g. of *N*-formylglycine in 20 cc. of ethanol was added 2.4 g. of β-alanine ethyl ester, followed by

4.2 g. of dicyclohexylcarbodiimide, and the mixture was allowed to stand overnight with cooling. The separated urea derivative was filtered off, the filtrate was evaporated under reduced pressure, and the residue was dissolved in 20 cc. of ethyl acetate. The solution was filtered and the needle-like crystals, m. p. 72°C (ca. 2.5 g.) obtained from the filtrate was purified by recrystallization from ethyl acetate. The product melted at 75°C.

Found: C, 47.81; H, 7.09; N, 14.13. Calcd. for $C_5H_{14}O_4N_2$ (*N*-formylglycyl-β-alanine ethyl ester): C, 47.52; H, 6.97; N, 13.85%.

One gram of the product dissolved in 20 cc. of dioxane was hydrolyzed by standing with 6~7 cc. of 1 N sodium hydroxide at room temperature, the reaction mixture was passed through a column of Amberlite IR-120 (H-form) to remove sodium ion, and the effluent was concentrated under diminished pressure to give white crystals, which were recrystallized from ethanol in prisms, m. p. 121°C (600 mg.).

Found: C, 41.68; H, 5.81; N, 15.84. Calcd. for $C_6H_6O_4N_2$ (*N*-formylglycyl-β-alanine): C, 41.38; H, 5.79; N, 16.09%.

To a solution of 450 mg. of the product in 2 cc. of methanol was added 0.25 cc. of hydrazine hydrate (80%), and the mixture was heated for 5 hr. on the water bath. The resulting crystals were washed with methanol and recrystallized from aqueous methanol, yielding 250 mg. of prisms, m. p. 225°C (decomp.). The infrared spectrum, R_f value in paper chromatography and coloration in the ninhydrin reaction of the product were in complete agreement with those of XV described in Report I.

Found: C, 40.75; H, 7.10; N, 18.84. Calcd. $C_5H_{10}O_3N_2$ (glycyl-β-alanine): C, 41.09; H, 6.90; N, 19.17%.

***O*-Acetyldemethoxyenteromycin (XVIII).**—To a solution of 300 mg. of demethoxyenteromycin (XII) in 15 cc. of hot water was added dropwise 2 cc. of acetic anhydride at 55~60°C over a period of about 15 min. with vigorous stirring. The mixture once became clear, but white crystals m. p. 180°C (decomp.) (ca. 320 mg.), gradually separated there from, which were recrystallized from methanol in prisms, m. p. 181°C (250 mg.). The product is negative to the ferric chloride-potassium ferricyanide reaction and resists ester exchange with methanol and decomposes when dried at a temperature over 70°C in vacuo.

Found: C, 42.33; H, 4.33; N, 13.97; $-COCH_3$, 20.50. Calcd. for $C_7H_8O_5N_2$: C, 42.00; H, 4.03; N, 14.00; $-COCH_3$, 21.50%.

***N*-Methyldemethoxyenteromycin Methyl Ester (XIX).**—To a solution of 600 mg. of XII in 30 cc. of ethanol was added a solution of diazomethane (produced from 7 g. of nitrosomethylurea) in 80 cc. of ether and the mixture was left standing at room temperature for 10 hr. The solvent was distilled off and the resulting white crystals, m. p. 120°C (150 mg.) were recrystallized from 1.5 cc. of methanol in needles (XIX), m. p. 159°C (ca. 60 mg.). This product is negative to the ferric chloride-potassium ferricyanide reaction.

Found: C, 45.16; H, 5.21; N, 15.22; O-CH_3, 16.38. Calcd. for $C_7H_{10}O_4N_2$: C, 45.16; H, 5.41; N, 15.05; O-CH_3, 16.67%.

***O*-Methyldemethoxyenteromycin Methyl Ester (XX).**—The mother liquor from XIX was concentrated to 0.7 cc. and left standing, separating 70 mg. of needles, which after crystallization from methanol melted at 137°C. Like XIX, the product is negative to the phenolic OH reaction, and its molecular weight is 180 ± 20 when measured by the Rast method, using camphor as solvent.

Found: C, 45.15; H, 5.45; N, 15.04; O-CH_3, 32.45. Calcd. for $C_7H_{10}O_4N_2$: C, 45.16; H, 5.41; N, 15.05; O-CH_3, 33.30%.

Decomposition of Demethoxyenteromycin with Hydrochloric Acid.—According to the method described in Report I, a mixture of 100 mg. of XII and 3 cc. of 1 N hydrochloric acid was heated in the atmosphere of nitrogen at 100°C for about one hour in flask A, which was connected with vessel B containing pure water and vessel C containing baryta water. The reaction mixture changed from brown to redish brown and plenty of barium carbonate deposited. After the reaction, the aldehyde in the vessel B was converted to the 2,4-DNPH derivative with a solution of 2,4-dinitrophenylhydrazine in hydrochloric acid, and the product was chromatographed as before, detecting a single spot of the 2,4-DNPH of acetaldehyde at R_f 0.38.

A solution of 2,4-dinitrophenylhydrazine in hydrochloric acid was added to one half of the contents of the flask A, the resulting 2,4-DNPH derivative was extracted with ethyl acetate, and the extract was shaken with sodium hydrogen carbonate solution. The aqueous layer was made acid and extracted again with ethyl acetate, and the extract, after washing with water and drying, was concentrated under reduced pressure to give yellow crystals, which on paper chromatography exhibited the spot of the 2,4-DNPH derivative of glyoxylic acid at R_f 0.42. The remaining half of the contents of the flask A was made alkaline and steam-distilled, and the distillate neutralized with hydrochloric acid was evaporated to dryness, affording white crystals, which, when paper chromatographed as described in Report I, gave the spot of ammonium chloride at R_f 0.14.

Demethoxyenteromycin Amide (XXI).—An amount of 500 mg. of XII was dissolved in 100 cc. of methanol saturated with ammonia and the solution, after standing overnight, was concentrated in the atmosphere of nitrogen at low temperature under reduced pressure, giving about 200 mg. of a residue which became light yellow prisms melting at 168°C (decomp.) after washing with a mixture of acetone and ethanol. The same treatment of the mother liquor yielded 250 mg. of unchanged XII. The product, m. p. 168°, colors blue with ninhydrin and is positive to the ferric chloride-potassium ferricyanide reaction. It produces XII quantitatively when treated with diluted acetic acid or hot water.

Found: C, 34.54; H, 5.49; N, 23.93. Calcd. for $C_5H_9O_4N_3$: C, 34.28; H, 5.18; N, 23.99%.

Dehydroxydihydrodemethoxyenteromycin (XXII).—A 200 mg. portion of XII dissolved in 20 cc. of pure methanol was reduced on 150 mg. of palladium

carbon (1 : 10) until about 2 mol. of hydrogen was absorbed. The catalyst was filtered and washed with hot water, the combined washing and filtrate were concentrated under reduced pressure, and methanol was added to the concentrate, giving about 150 mg. of crystals. The product was treated with a little cold water and the insoluble portion was recrystallized from water, yielding 70 mg. of prisms, m. p. 203°C (decomp.), which colored yellow with ninhydrin and gave a spot at R_f 0.63 on paper chromatography[2].

Found: C, 41.46; H, 5.79; N, 19.48; $-NH_2$, 11.06. Calcd. for $C_5H_9O_3N_2$: C, 41.66; H, 5.59; N, 19.44; $-NH_2$, 9.86%.

Catalytic reduction of a solution of 30 mg. of XXII in 10 cc. of a mixture of glacial acetic acid and methanol on about 30 mg. of Adams platinum oxide (or palladium-carbon) afforded about 20 mg. of glycyl-β-alanine.

Summary

The structure of dehydroxytetrahydrodemethoxyenteromycin was established to be glycyl-β-alanine. Demethoxyenteromycin yielded *O*-acetyldemethoxyenteromycin by acetylation, *N*-methyl- and *O*-methyldemethoxyenteromycins by methylation, and demethoxyenteromycin amide by amidation. Catalytic reduction of demethoxyenteromycin gave first dehydroxydihydrodemethoxyenteromycin and then glycyl-β-alanine. Acid decomposition products of demethoxyenteromycin were the same those of enteromycin, except methyliodide.

Research Laboratories
Takeda Chemical Ind., Ltd.
Higashiyodogawa-ku, Osaka

Infrared Absorption Spectra of Water of Crystallization in Cobaltous Chloride Hexa- and Dihydrate Crystals

By Itaru GAMO

(Received February 13, 1961)

The infrared absorption spectra of cobaltous chloride hexahydrate and dihydrate have been separately subject to two investigations[1,2]. However, there has been no comparative study of the two crystals in relation to their structural difference.

In the present paper, observed spectra were examined in relation to the difference of the binding states of the water molecules in them. The two crystals have an advantage over the hydrated salts of oxy-acids such as hydrated sulfates, because all the observed bands can be attributed to the vibrations of water molecules without ambiguity except for those due to the skeletal vibrations of the metal atom and ligands. Furthermore their structures are well determined by X-ray diffraction[3] and by electron diffraction[4] respectively.

Experimental

Preparation.—Commercial cobaltous chloride hexahydrate of guaranteed grade was recrystallized from water. Cobaltous chloride dihydrate was obtained by keeping the purified hexahydrate over calcium chloride at ordinary temperature for 24 hr.[5]

Measurement.—Spectra were recorded by means of a Kōken DS 301 infrared spectrophotometer using a sodium chloride or potassium bromide prism. The potassium bromide disk technique was employed.

Results

The spectra are given in Fig. 1. In the 3 μ region one peak is observed for the hexahydrate at 3430 cm^{-1}, and one shoulder and two peaks for the dihydrate at 3564, 3444 and 3226 cm^{-1}. These are comparable to the peaks of various inorganic hydrated salts[6] in this region, and can be assigned to the O–H stretching vibrations of water molecules affected by coördination on a cobalt atom and by the hydrogen bonding with a chlorine atom or an oxygen atom of an outer water molecule. Overlapping of several stretching bands is probably responsible for the broadness of the band for the hexahydrate. In the 6 μ region, two bands of medium intensity are observed at 1625 and 1599 cm^{-1} for the hexahydrate. The latter is fairly sharp. Both can be assigned to the bending mode of water molecules, the former being presumably due to a ligand water

1) J. Lecomte, *J. chim. phys.*, **50**, C 53 (1953).
2) O. Glemser and E. Hartert, *Naturwiss.*, **42**, 534 (1955).
3) J. Mizuno, K. Ukei and T. Sugawara, *J. Phys. Soc. Japan*, **14**, 383 (1959).
4) B. K. Vainstein, *Doklady Akad. Nauk. S. S. S. R.*, **68**, 301 (1949).
5) L. Gmelin, "Handbuch der anorganischen Chemie", Verlag Chemie, Berlin (1932), No. 58, p. 276.
6) I. Gamo, This Bulletin, **34**, 760 (1961).

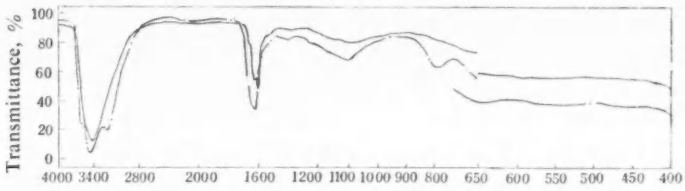

Fig. 1. Observed bands of $CoCl_2 \cdot 6H_2O$ and $CoCl_2 \cdot 2H_2O$.
$CoCl_2 \cdot 6H_2O$ —·—· $CoCl_2 \cdot 2H_2O$

molecule and the latter to a water molecule free from coördination. For the dihydrate, one band of medium intensity is observed at 1610 cm^{-1}. It can be assigned to the bending mode of a ligand water molecule. In the 9 μ region, the spectrum of the hexahydrate shows a very broad weak band at 1090 cm^{-1}, and that of the dihydrate shows a similar one at 1100 cm^{-1}. The origins of these bands cannot be decided at present. Probably they are the combinations or overtones of some restricted rotation modes of water molecules. The band observed at 790 cm^{-1} for the dihydrate can be attributed to the wagging vibration of a ligand water molecule affected by hydrogen bonding, because of its position, intensity and shape. The bands so far reported were observed in the sodium chloride region.

In the potassium bromide region, no band was observed for the hexahydrate. For the dihydrate only one very broad band was observed at 642 cm^{-1}. It is tentatively attributed to the rocking mode of the water molecule which is responsible for the wagging band at 790 cm^{-1}, because the twisting band of a water molecule is usually too weak to be observed. It cannot be assigned to any skeletal vibration of the metal atom and ligands since the skeletal vibration bands should appear in a lower frequency region.

Tables I and II summarize these results.

Table I. Observed frequencies of $CoCl_2 \cdot 6H_2O$

Wave number, cm^{-1}	Assignment
3430 s	O–H stretch.
1625 m	H–O–H bend.
1599 m, sh	H–O–H bend.
1090 w, v.b	

Table II. Observed frequencies of $CoCl_2 \cdot 2H_2O$

Wave number, cm^{-1}	Assignment
3564 s, shoulder	
3444 s	O–H stretch.
3226 s	O–H stretch.
1610 m	H–O–H bend.
1100 w, v.b	
790 w, b	H_2O wag.
642 m, v.b	H_2O rock.

Abbreviations: s, strong; m, medium; w, weak; v, very; b, broad; sh, sharp.

Discussion

According to X-ray analysis[3], four water molecules and two chlorine atoms in cobaltous chloride hexahydrate are coördinated on the cobalt atom, making an octahedron with the cobalt atom at the center. Two other water molecules are far distant from the cobalt atom, and each of their oxygen atoms forms a hydrogen bond with one of the two O–H bonds of a ligand water molecule. The other O–H bond of this water molecule forms another hydrogen bond with a chlorine atom of a neighboring octahedron (for details, see Fig. 2).

An electron diffraction study[4] shows that two water molecules and two chlorine atoms in

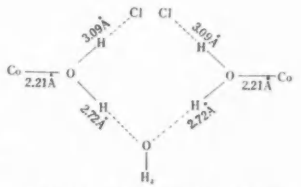

Fig. 2. Arrangement of atoms in $CoCl_2 \cdot 6H_2O$.

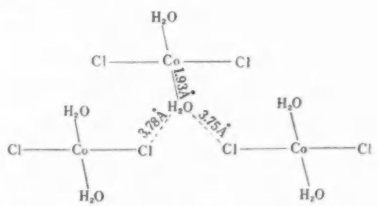

Fig. 3. Arrangement of atoms in $CoCl_2 \cdot 2H_2O$*.

* The three parallelograms are respectively in different planes. The values 3.75 and 3.78 Å were calculated from the data in Ref. 4.

cobaltous chloride dihydrate are coördinated on the cobalt atom, making a parallelogram with the cobalt atom at the center (Fig. 3).

As in the previous studies[6,7], it shall be assumed that the water frequencies are influenced by coördination and hydrogen bonding.

As is seen from Fig. 2, at least four O–H stretching frequencies are expected theoretically for the hexahydrate: one for the O–H bond of the ligand water molecule which forms the hydrogen bond O–H···Cl, one for the bond O–H···O, and two (symmetric and antisymmetic) for the almost free water molecule. The peak observed at 3430 cm^{-1} probably corresponds to either one of the first two, because the frequency shift from the value of the vapor state is of the same order as in many cases[6] where the water molecule is affected by coördination and hydrogen bonding. The last two frequencies should appear in a higher region since they correspond to an almost free water molecule. Probably they are weak and hidden in the above-mentioned band.

In the dihydrate, the nearest distance between a ligand water molecule and a chlorine atom of a neighboring parallelogram is 3.75 Å, and the next to the nearest distance is 3.78 Å. The two observed bands, at 3444 and 3226 cm^{-1} can be explained in relation to the crystal structure by the following assumption: one of the O–H bonds of the ligand water molecule forms a hydrogen bond with one of these two chlorine atoms, and the other is free from hydrogen bonding. We can correlate the 3226 cm^{-1} band with the fomer O–H bond and the 3444 cm^{-1} band with the latter since hydrogen bonding lowers the stretching frequency and the coördination effects are equal in the two cases. It is unlikely that one of the O–H bonds forms a hydrogen bond of distance 3.75 Å and the other forms a hydrogen bond of distance 3.78 Å respectively with each of the two chlorine atoms, because the frequency difference of 218 cm^{-1} is far too great to be explained by the difference of the hydrogen bond distances 0.03 Å since the stretching frequency is relativery insensitive to the hydrogen bonding effect. The shoulder at 3564 cm^{-1} cannot be interpreted for the present.

For the bending vibration in the hexahydrate two frequencies are observed. They can be explained readily from the crystal structure. The higher frequency (1625 cm^{-1}) can be attributed to the mode of the coördinated and hydrogen bonded water molecule, and the lower frequency (1599 cm^{-1}), the value of which is almost equal to that of the vapor state frequency (1595 cm^{-1}), can be assigned to the almost free water molecule since in general the two effects are likely to increase the bending frequency[8]. For the dihydrate there is observed only one bending frequency (1610 cm^{-1}), corresponding to the fact that there is only one kind of water molecule in the unit cell of the crystal. It is 15 cm^{-1} lower than that for the ligand water molecule in the hexahydrate. This indicates that the additive effect of coördination and hydrogen bonding is greater in the hexahydrate than in the dihydrate although the coördination distance between the cobalt atom and the water molecule is somewhat shorter, and so the coördination effect is greater in the dihydrate.

The position and the shape of the wagging band at 790 cm^{-1} for the dihydrate are reasonable as compared with those in the usual cases. For the hexahydrate no band was observed in this region. (These results suggest that the band at 781 cm^{-1} reported for the hexahydrate in a previous paper[6] may be in fact due to the dihydrate which may have happened to be produced by partial dehydration of part of the hexahydrate during the vacuum process in the preparation of the KBr disk.)

The position and the shape of the rocking band at 642 cm^{-1} for the dihydrate seem also to be reasonable. The frequencies of the wagging and the rocking band are somewhat lower than the corresponding frequencies for aluminum sulfate octodecahydrate[8] respectively.

Summary

The observed spectra of the water of crystallization were interpreted by the effects of coördination and hydrogen bonding. The total difference in the spectra of the two crystals was explained in relation to the difference in their atomic arrangements.

The author wishes to express his thanks to Professor Takehiko Shimanouchi of the University of Tokyo for his helpful guidance.

Institute for Science and Engineering Research
Waseda University
Shinjuku-ku, Tokyo

7) I. Gamo, ibid., **34**, 764 (1961).

8) I. Gamo, ibid., to be published.

Infrared Absorption Spectra of Water of Crystallization in Ferrous Chloride Tetrahydrate Crystal

By Itaru GAMO

(Received February 13, 1961)

The crystal structure of ferrous chloride tetrahydrate has been determined in detail by X-ray diffraction[1]. Therefore it is possible to correlate the infrared absorption spectra of the water of crystallization with the structure.

In the present study, the characteristic bands of the water of crystallization in the crystal were determined for this purpose. Like cobaltous chloride hexahydrate and dihydrate[2], the crystal has an advantage in that observed bands can be attributed to the vibrations of water molecules almost uniquely. The spectra have an interesting feature in the bending region that has not been observed in other cases in this series of studies[2-6].

Experimental

Preparation.—Commercial ferrous chloride tetrahydrate of guaranteed grade was recrystallized from water.

Measurement.—Spectra were recorded by a Kōken DS 301 infrared spectrophotometer equipped with a sodium chloride prism. The potassium bromide disk technique was employed.

Results

The spectra are given in Fig. 1. In the 3 μ region, one peak is observed at 3442 cm^{-1} and one shoulder at 3238 cm^{-1}. These are comparable to the peaks of various inorganic hydrated salts in this region, and can be assigned to the O–H stretching vibrations of water molecules affected by the interaction with an iron atom and by the hydrogen bonding with a chlorine atom. The overlapping of several stretching bands is probably responsible for the somewhat broad feature of the band. In the 5 μ region, a broad and very weak band is observed at 2301 cm^{-1}. It can be assigned to the combination of the bending and the wagging mode of a water molecule. It is somewhat overlapped by the carbon dioxide band at 2352 cm^{-1}. A similar band observed at 1740 cm^{-1} is probably due to an overtone of some restricted rotation mode or a combination of such modes. In the 6 μ region, two remarkably sharp peaks of medium intensity are observed at 1626 and 1603 cm^{-1}, the former being a little weaker than the latter. They are assigned to the bending vibrations of water molecules affected by the same effects as in the cases of streching modes. They are the sharpest bending bands that have been observed in this series of studies. Hitherto only one bending band was observed or in the case of two peaks at least one was not sharp[2,4]. This is not because the present instrument is better in resolving power than that used in most of the previous measurements. An infrared study of the crystal by the latter instrument gave two equally sharp bands in the same region. The shoulder at 1492 cm^{-1} is too low to be assigned to the bending mode and therefore should be attributed to the first overtone of the wagging mode (see below). Probably the weak band at 1229 cm^{-1} has its origin in a combination or an overtone. The 755 cm^{-1} band can be

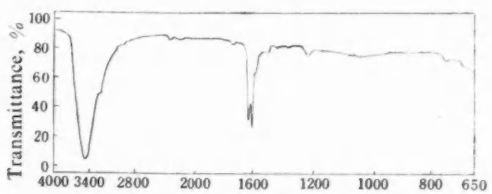

Fig. 1. Observed bands of $FeCl_2 \cdot 4H_2O$.

Table I. Observed frequencies of $FeCl_2 \cdot 4H_2O$

Wave number, cm^{-1}	Assignment
3442 v. s	$\nu(H_2O)$ stretch.
3238 m, shoulder	$\nu(H_2O)$ stretch.
2301 v. w, b	$\nu_2+\nu_R(H_2O)$ bend.+wag.
1740 v. w, b	
1626 m, v. sh	$\nu_2(H_2O)$ bend.
1603 m, v. sh	$\nu_2(H_2O)$ bend.
1492 w, shoulder	$2\nu_R(H_2O)$
1229 w, b	
755 w, b	$\nu_R(H_2O)$ wag.

Abbreviations: s, strong; m, medium; w, weak; v, very; b, broad; sh, sharp.

1) B. R. Penford and J. A. Grigor, *Acta Cryst.*, **12**, 850 (1959).
2) I. Gamo, This Bulletin, **34**, 1430 (1961).
3) I. Gamo, ibid., **34**, 760 (1961).
4) I. Gamo, ibid., **34**, 764 (1961).
5) I. Gamo, ibid., to be published.
6) I. Gamo, ibid., to be published.

assigned to the wagging mode of a water molecule because of its position and shape.

Table I summarizes these results.

Discussion

According to X-ray analysis[1], the crystal is monoclinic and belongs to space group $P2_1/c$ with a=5.91, b=7.17, c=8.44 Å and $\beta=112°10'$. The structure consists of discrete groups, two per unit cell. Each group contains one iron atom, four water molecules, and two chlorine atoms. It is a distorted octahedron. There are two iron-oxygen distances: 2.09 and 2.59 Å. Hereafter the corresponding oxygen atoms will be called oxygen I and II, and the corresponding water molecules will be called type I and type II, respectively. The distance 2.59 Å is considerably greater than the sum of the ionic radii of iron and oxygen (2.16 Å). Therefore oxygen II is very weakly held in the group. The analysis suggests that oxygen I forms a pair of hydrogen bonds with two chlorine atoms in the manner shown in Fig. 2, and in oxygen II two hydrogen atoms are used to form three hydrogen bonds (Fig. 3). Therefore they are likely to be more or less bifurcated.

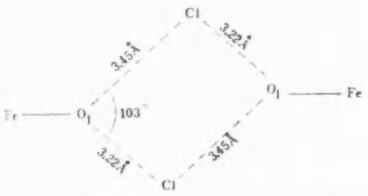

Fig. 2. Suggested hydrogen bonds for O_I. The error in each bond length is ±0.04 Å.

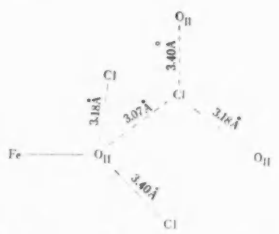

Fig. 3. Suggested hydrogen bonds for O_{II}. The error in each bond length is ±0.025 Å.

As in the previous studies[2-5], it will be assumed that the water frequencies are influenced by coördination and hydrogen bonding.

Figure 2 may suggest, at first sight, couplings between vibrations of two water molecules of type I due to hydrogen bonding. But it is unlikely because of the considerable difference between the distances of the two hydrogen bonds connected by the same chlorine atom. The situation is similar in the case of type II (Fig. 3). Therefore the observed two stretching frequencies are not due to splitting by hydrogen bonding. Further, there is a considerable difference between two O–H distances in each molecule because the corresponding hydrogen bonds are different in length. This suggests that the observed bands are not due to the symmetric and the antisymmetric vibration respectively.

The stretching frequency of water is in general likely to decrease by the effect of coördination, as suggested by comparison of the frequency of the ammonium ion with that of the ammonia molecule[7]. Hydrogen bonding of course lowers the frequency; therefore the two effects will be additive.

From this standpoint, it will first be assumed that the observed two bands at 3442 and 3238 cm^{-1} are both due to water of type II. Since the metal-to-oxygen bond is almost purely electrostatic in this case, we have only to take into account the hydrogen bonding effect. Then, from Glemser's relationship[8] between the stretching frequency and the hydrogen bond length, the corresponding O–H···Cl distances are estimated to be 3.32 and 3.11 Å, respectively. Both values seem to be compatible with the above-mentioned suggestion concerning hydrogen bonding for oxygen II, indicating the validity of the assumption. Bands due to water of type I should appear in a lower region because the coördination effect is fairly large (distance 2.09 Å). Probably they escape detection due to their weak intensity.

The two effects influence the bending frequency also. Hydrogen bonding increases the frequency as seen in the case of ice. The observed two frequencies 1626 and 1603 cm^{-1} are lower than the value 1644 cm^{-1} in ice, which is free from coördination. This suggests that coördination lowers the bending frequency. The situation may be similar to that in the case of the degenerate deformation frequency of the ammonia molecule in a metal ammine complex[9], which is somewhat lower than the corresponding value of the vapor state. Probably in the case of water in general the effect of coördination should cancel partly the effect of hydrogen bonding. This seems to be responsible for the relatively small change in the bending frequency by the two effects, as compared with that in the stretching frequency.

From the above-mentioned standpoint, the stronger coördination results in the lower

7) I. Gamo, *J. Chem. Soc. Japan, Pure Chem. Sec.* (*Nippon Kagaku Zasshi*), **73**, 594 (1952).
8) O. Glemser and E. Hartert, *Naturwiss.*, **42**, 534 (1955).
9) G. F. Svatos, D. M. Sweeny, S. Mizushima, C. Curran and J. V. Quagliano, *J. Am. Chem. Soc.*, **79**, 3313 (1957).

bending frequency. Thus the observed bands at 1626 and 1603 cm^{-1} can be reasonably attributed to water molecules of type II and of type I, respectively, since the coördination is considerably weaker in the former and the hydrogen bonding effects are approximately equal in the two cases. For the present, their remarkable sharpness cannot be correlated with the crystal structure.

Experimental results[3,5] show that either of the two effects increases the wagging frequency. The band at 755 cm^{-1} is reasonably attributed to the wagging mode of water of type I, the metal-oxygen distance being 2.09 Å. The wagging band due to type II should appear in a lower region, because in this case the coördination effect is very small (distance 2.59 Å) and the hydrogen bond strength is of the same order as in ice, which is free from coördination and has a wagging band near 600 cm^{-1}.

Summary

The observed spectra of the water of crystallization were correlated with the crystal structure determined by X-rays. They were interpreted as affected by coördination and hydrogen bonding. The coördination was concluded to lower the bending frequency of water in general. Two remarkably sharp bending bands were found.

The author wishes to express his thanks to Professor Takehiko Shimanouchi of the University of Tokyo for his helpful guidance.

Institute for Science and Engineering Research
Waseda University
Shinjuku-ku, Tokyo

---

*Absorptiometric Determination of Micro-amounts of Iron in Nuclear Grade Graphite and Urania-Graphite Fuel; Nitroso R Salt Method after Coprecipitation of Iron with Manganese Dioxide**

By Masatoshi MIYAMOTO

(Received January 24, 1961)

It has been necessary, in the author's laboratory, to determine micro-amounts of iron in nuclear grade graphite and urania-graphite fuel for a nuclear reactor. Spectrographic methods have been used to estimate the iron impurity in graphite. Recently[1], the impurity in graphite of high purity was determined after concentration by a chemical method. Little literature on absorptiometric determination of the impurity in nuclear grade graphite and urania-graphite fuel is seen at present. The author has applied a method with nitroso R salt, sodium 1-nitroso-2-naphthol-3, 6-disulfonate[2,3], to these samples because the reagent has the highest sensitivity to iron at present giving very stable green color[4]. In this paper, the effect of diverse ions, preliminary separation and contamination with foreign iron are discussed.

Experimental

Apparatus and Materials. — A Hitachi spectrophotometer, model EPU-2, was used for all measurements of absorbancy, matched 1 cm. cells being used. A Beckman pH-meter, model H-2, was used for acidity measurements. An electric furnace used for the ashing of samples was equipped with a protector assembled with fused silica plates to keep the sample out of possible contamination with dust from the wall of the furnace.

All the chemicals were of JIS special grade including starting materials in the following preparation of chemicals unless otherwise stated. Nitroso R salt was recrystallized from 50% aqueous ethanol. Hydrochloric acid and aqueous ammonia were purified by distillation. Cobalt sulfate was prepared by the pyrolysis of chloropentaminecobalt(III) chloride followed by furming with sulfuric acid and recrystallization. The cobalt complex was prepared according to the description by M. Biltz and W. Biltz[5]. Manganese chloride was prepared from iron-free potassium permanganate by reduction with

* Presented at the Tohoku Local Meeting of the Chemical Society of Japan, Sendai, September, 1960.

1) A. A. Demidov and L. B. Gorbunova, *Zavodskaya Lab.*, **25**, 956 (1959); *Chem. Abstr.*, **54**, 10634 (1960).

2) C. P. Sideris, *Ind. Eng. Chem., Anal. Ed.*, **14**, 756 (1942).

3) Y. Oka and M. Miyamoto, *Japan Analyst*, (*Bunseki Kagaku*), **1**, 23 (1952); *Bull. Res. Inst. Min. Dress. Met., Tohoku Univ.*, **9**, 25 (1953).

4) Y. Oka and M. Miyamoto, *J. Chem. Soc. Japan, Pure Chem. Sec.* (*Nippon Kagaku Zasshi*), **75**, 864 (1954); *Sci. Rep. RITU.*, **A7**, 84 (1955); *J. Chem. Soc. Japan, Pure Chem. Sec.* (*Nippon Kagaku Zasshi*), **76**, 672 (1955); *Sci. Rep. RITU.*, **A7**, 482 (1955).

5) M. Biltz and W. Biltz, "Ubungsbeispiele aus der unorganischen Experimentalchemie", (1920), p. 166.

ethanol and dissolution of resulting manganese dioxide followed by recrystallization. For the removal of iron impurity, the permanganate was dissolved in water containing a small amount of aluminum sulfate followed by the precipitation of aluminum hydroxide with aqueous ammonia.

Standard Iron Solution.—A solution containing 2 mg. of iron per milliliter was made by dissolving ammonium ferric sulfate in 0.1 N hydrochloric acid. The iron concentration was checked titrimetrically with a standard permanganate solution after the reduction of iron by stannous chloride. The iron solution was appropriately diluted in time for use.

Nitroso R Salt Solution.—0.500 g. of the reagent was dissolved in 100 ml. of water.

Buffer Solution.—A 4.00 M solution of recrystallized sodium acetate.

Hydroxylamine Sulfate Solution.—5.00 g. of the salt was dissolved in 100 ml. of water.

Manganese Solution.—A 0.2 M solution of manganese chloride.

Ammonium Carbonate Solution.—A 0.1 M solution was made by dissolving the salt in 0.3 N aqueous ammonia followed by standing over night and filteration.

Acidified Hydroxylamine Solution.—Three parts of the hydroxylamine sulfate solution were mixed with 1 part of 6 N hydrochloric acid.

Method.—The absorptiometric determination of iron was made as follows unless otherwise stated: a test solution was taken in a 25 ml. volumetric flask and neutralized with dilute aqueous ammonia either against a drop of a methyl orange indicator solution or till just before the precipitation of iron. Two milliliters of 0.1 N hydrochloric acid and 1.0 ml. of the hydroxylamine sulfate solution were added and the liquid was swirled well followed by dilution to about 20 ml. Two milliliters each of the reagent solution and the buffer solution were added in the order with stirring. The liquid was diluted to the mark. The flask was immersed in boiling water for about 10 min. followed by cooling to room temperature with running water. The intensity of the resulting color was measured at 715 and 650 mμ., the wavelength widths being 1.0 mμ.

The coprecipitation of iron with manganese dioxide was made as follows unless otherwise stated: to a test solution, 10 ml. of the manganese solution was added and the solution was diluted to about 100 ml. Ten milliliters of the ammonium carbonate solution was added. Five milliliters of about 3% hydrogen peroxide was added with stirring and the solution was heated on a boiling water bath for 30 to 40 min. The resulting precipitate was centrifuged at 3,000 r. p. m. for 10 min. followed by washing with about 15 ml. of water. It was dissolved in 5 ml. of the acidified hydroxylamine solution. The resulting solution was transferred into a quartz dish and evaporated on a water bath till dryness. The residue was taken with 2.0 ml. of hot 0.1 N hydrochloric acid and transferred into a 25 ml. volumetric flask for the determination of iron.

Results and Discussion

In the following discussions, a deviation within 2% was allowed.

Adjustment of Acidity and Effect of Diverse Ions.—An optimum pH-range for the full color development was reported by the present author[3] to be 5.3 to 6.5. The acidity of a test solution, which contains 0.5 to 4.0 ml. of 0.1 N hydrochloric acid can be satisfactorily adjusted within the optimum range by the addition of 2.0 ml. of the buffer solution.

Griffing and Mellon[6] reported the effect of many diverse ions. The present results obtained with several ions are shown in Table I. According to the previous workers, vanadium-(V) interferes strongly because of its color formation. The present result, however does not indicate any interference with the color intensity of iron complex by the presence of at least 10 p. p. m. of the ion. Manganese(II) gives an absorption band around 440 mμ. The strong effect of an increased amount of the reagent or the metal ion on the intensity of the band suggests that the manganese(II) complex formed is unstable. The instability of the complex permits the presence of a large amount of the metal ion without interference in the color development of iron. An intense red color of cobalt(III) complex, which has disappeared by the heating for completion of the color reaction of iron, gradually appears again when the solution is left to stand. Fortunately, the red complex does not give absorption at 715 mμ. Because of the high stability of the red complex, however, the use of increased amounts of the reagent is required for the full color development of iron. Uranium(VI) does not give any absorption in long wavelength region. The presence of a very large amount of the ion is thus permitted. This is parallel with Nageswara Rao and

TABLE I. EFFECT OF DIVERSE IONS ON THE DETERMINATION

Each test solution contains 2.00 p. p. m. of iron at the final concentration.

Diverse ions* added, p. p. m.		Errors, %		Amounts of the reagent soln. used, ml./25 ml.
		715 mμ	600 mμ	
Sodium	4,600	−0	1	2.00
Vanadium(V)	10	1	0	2.00
Manganese(II)	835	2	12	2.00
Cobalt(II)	10	2	45	4.00
Nickel	10	2	9	2.00
Uranium(VI)	4,760	1	5	2.00

* Added as sodium chloride, ammonium metavanadate, manganese chloride, nickel nitrate and uranyl nitrate, respectively.

6) M. Griffing and M. G. Mellon, *Anal. Chem.*, 19, 1014 (1947).

Raghava Rao's results[7] on the reaction of uranyl ion with the reagent.

Removal of Diverse Ions by Coprecipitation of Iron with Manganese Dioxide. — Dean and Lady[8] selectively decomposed colored complexes of diverse ions with hydrazine under a carefully controlled condition without affecting the color intensity of the iron complex. Very recently, Ishii[9] extracted iron with tributyl phosphate for absorptiometric determination of iron impurity in uranium metal with 1, 10-phenanthroline. The present author coprecipitated iron with manganese from an ammoniacal carbonate solution leaving the diverse ions as well as uranium in the solution. The manganese was precipitated as dioxide by the oxidation of manganese(II) ion. The method is simple and appropriate for the extraction of iron out of sample solutions which contain "concentrated" uranium. Coprecipitation of iron with aluminum hydroxide was found unsuitable for the present purpose because of the resistance of the precipitate to dissolution in a dilute acid and of possible precipitation of aluminum hydroxide at the stage of the color development of the iron.

Coprecipitation of Iron.—Figure 1 shows the completeness of the coprecipitation of iron with 1.2 mg. of manganese. Increases in the blank absorption at 715 and 600 mμ. may be attributed to iron impurity in the reagents used. Figure 2 shows the amounts of manganese required for complete precipitation of iron. It also indicates that 2 ml. of bromine water may be used as an oxidizing agent instead of hydrogen peroxide when the solution is boiled for 10 to 15 min. Hydrogen peroxide, however, is superior to bromine water because the former gives a well coagulated precipitate by warming on a water bath. Three milliliters of 3% hydrogen peroxide is sufficient for complete precipitation of manganese(II) ion. Precipitation of manganese by the reduction of permanganate[10] with formate, sulfite or ethanol[11] was found unsuitable for the present purpose because of difficulty in the collection of a very fine precipitate formed.

Filteration of the precipitate by a filter paper is unsuitable because of possible contamination with foreign iron from the filter. The amounts of iron impurity found in the Toyo, No. 5B

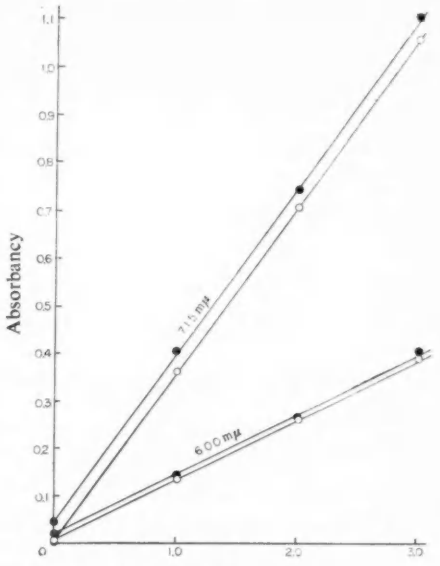

Fig. 1. Amounts of iron and color intensity.
The final volume was 25 ml. ○, coprecipitation was not made; ●, coprecipitation with 1.2 mg. of manganese was made.

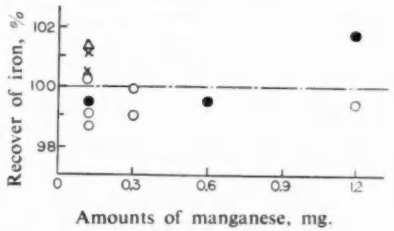

Fig. 2. Amounts manganese and recovery of iron by the coprecipitation.
Amounts of iron taken are: ●, 50 μg. (oxidation with bromine water); △, 25 μg.; ○, 50 μg. and ×, 75 μg.

(7 cm.) were 0.6 to 2.6 μg. per each filter. The precipitate is dissolved in the acidified hydroxylamine solution with ease. The minimum amount of the solvent required to dissolve the precipitate is 1.25 ml. A hot hydrogen peroxide solution containing hydrochloric or sulfuric acid, as the solvent, is inferior to the former.

Separation of Iron from Diverse Ions. — Results shown in Table II indicate that the separation by this method is effective to eliminate the diverse ions. One fourth milligram of platinum associated with uranium is satisfactorily removed from iron (cf. No. 5 in Table

7) M. Nageswara Rao and Bh. S. V. Raghava Rao, *Z. Anal. Chem.*, **142**, 161 (1954).
8) J. A. Dean and J. H. Lady, *Anal. Chem.*, **23**, 1096 (1951).
9) D. Ishii, *Japan Analyst (Bunseki Kagaku)*, **9**, 693 (1960).
10) H. N. Stokes and J. R. Cain, *J. Am. Chem. Soc.*, **29**, 409 (1907).
11) E. B. Sandell, "Colorimetric Determination of Traces of Metals", Interscience Publishers, New York (1950), p. 374.

TABLE II. ERRORS OF THE DETERMINATION AFTER THE PRELIMINARY SEPARATION

Each test solution contains 50.00 μg. of iron

No.	Divers ions added, mg.	Errors, %		Amounts of the reagent soln. used, ml./25 ml.
		715 mμ	600 mμ	
1	Cu(II), 0.25	−1	−1	2.00
		0	1	2.00
		−1	−1	2.00
2	Cr(VI), 0.25	−0	−2	2.00
		−0	−1	2.00
		2	1	2.00
3	Co(II), 5.0	−13	−5	4.00
4	Pt(VI), 2.0	12	19	2.00
		12	18	2.00
5	Pt(VI), 0.25; U(VI), 100	−0	−1	2.00
		−1	−1	2.00
		−1	−0	2.00
6	Cu(II), V(V), P (phosphate), Cr(VI), Co(II) and Ni; 0.25 of each. U(VI), 100	0	4	2.00
		0	21	2.00
		0	17	2.00
		−0	30	4.00
		−0	32	4.00
7	Cu(II), V(V), P(phosphate), Cr(VI), Co(II), Ni and Pt(IV); 0.25 of each. U(VI), 100	2	19	2.00
		3	31	2.00
		3	30	2.00

II) while the presence of the same amount of platinum associated with many diverse ions altogether tends to give a slight positive error (cf. No. 7). The removal of cobalt is not effective (cf. No. 3). Sixty five to seventy-one percent of the original cobalt was found in manganese dioxide precipitated from a solution containing 0.25 mg. of cobalt and 50 μg. of iron.

Determination of Iron Impurity in Nuclear Grade Graphite and Urania-Graphite Fuel.—Copper and Chromium, which may strongly interfere with the absorptiometry, are scarcely found in appreciable amounts in nuclear grade graphite. This enables us to apply the method to samples of the graphite without any preliminary separation. The method can be applied to samples of ordinary grade graphite in the same way because iron forms the greater part of the impurities in general. In this case, absorption at 600 mμ. may be used to check the degree of interference by diverse impurities comparing the intensity of the absorption with that obtained at 715 mμ. Preliminary separation is required in the case of urania-graphite fuel because of comparatively large amounts of impurities in the urania component.

Sampling.—Contamination with foreign iron should be avoided during the sampling of analytical specimens. The use of a drill tipped with a tungsten-cobalt alloy, G2[12], is suitable for the sampling from graphite blocks by drilling. In the author's experience, the weight loss of the drill was 1.2 mg. when 2 kg. of graphite was pulverized by the drilling while the loss of an alloyed steel drill was about 6 mg. (3 p. p. m. as to the graphite) under the same conditions. The average hardness of the graphite blocks used was 27.3 by Shore unit. Crashing with a press and pulverizing in an agate mortor may also be done.

Contamination with Foreign Iron from Platinum Crucibles.—It was said that[11] platinum wares contain iron impurity which may be dissolved out with hot acids, giving erroneous results in determinations of micro-amounts of iron. The present author evaporated 4 ml. each of 18 N sulfuric acid in platinum crucibles on a hot plate till dryness. The crucibles were cleaned by pyrosulfate fusion and immersion in 1 to 1 hydrochloric acid successively before use. Each residue was taken with 1 ml. of hot water followed by the determination of iron. Results are shown in Fig. 3. The amounts of iron extracted from the platinum crucibles do not depend on the fuming time. This was confirmed by a statistical treatment of the data. The average amount of the iron extracted is 1 μg. which is the same amount as that found in the sulfuric acid used. From the results, platinum crucibles cleaned carefully may be used for ashing of samples and fuming with sulfuric or perchloric acid. Porcelain crucibles, "SCP" Brand, may also be used. The above fuming test applied to the crucibles gave substantially

12) JIS, H 5501 (1953).

TABLE III. IRON IMPURITY IN GRAPHITE AND URANIA-GRAPHITE FUEL

	Iron found, p. p. m.					
	Without the preliminary septn.			With the preliminary septn.		
	715 mμ	600 mμ	Difference	715 mμ	600 mμ	Difference
Natural graphite	151×10	158×10	7×10	—	—	—
Nuclear grade graphite, A	40.4	40.5	0.1	—	—	—
B	24.4	26.2	1.8	—	—	—
C	5.4	7.0	1.6	5.3	5.4	0.1
Urania-graphite fuel, A	47.0	60.2	13.2	59.4	59.1	0.3
B	32.0	41.9	9.9	52.1	51.6	0.5

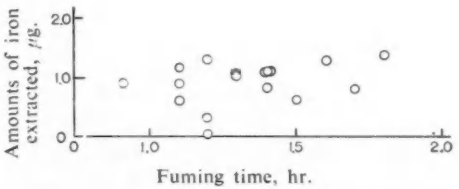

Fig. 3. Fuming time and amounts of iron extracted from platinum crucibles
Capacity of platinum curcibles, 30 ml.; 18 N sulfuric acid, 4.00 ml.; heated on a hot plate.

the same results as those obtained in the case of the platinum crucibles.

Recommended Procedure. — Five grams of a graphite sample is ashed in a platinum crucible at about 800°C. Washed oxygen gas may be introduced into the furnace, if necessary. The ash is treated with 2 ml. of 6 N hydrochloric acid on a water bath and evaporated to dryness. The ash dissolves during the evaporation. Colored insoluble matter, if any, should be completely dissolved with the aid of 1 ml. of hydrofluoric acid followed by fuming with 1 ml. of perchloric or sulfuric acid till dryness. The resulting residue is taken with 10 ml. of 0.1 N hydrochloric acid. The solution is diluted to 50.00 ml. Ten milliliter portions of the test solution are taken in a 25 ml. volumetric flask. One milliliter of the hydroxylamine sulfate solution is added and the determination is made as described in the section "Experimental", the color intensity being measured at 715 mμ. For the preparation of the working curve a set of standard iron solutions containing 0, 1, 2 and 3 p. p. m. at the final concentrations is used.

The amount of a sample to be taken may be reduced to less than 1 g. depending on the content of iron impurity in the sample when the whole of the test solution is used for the color development. The author, however, recommends the use of 5 g. of a sample, which contains a very small amount of iron impurity, to reduce errors due to contamination and segregation of the iron impurity. The lower limit of the determination may be expected to be 2 p. p. m.

In the case of samples of urania-graphite fuel, the coprecipitation of iron should be made as described in the section "Experimental." In this case, the fuming with perchloric acid is made prior to the coprecipitation to convert chromium impurity into chromate ion. Blank tests are required when either or both the fuming and the coprecipitation are carried out.

Iron impurities in several samples determined by the method are shown in Table III. Results obtained at 600 mμ. are also shown for comparison. In the case of samples of the urania-graphite fuel, low results were obtained when the removal of diverse ions was ommitted. They are thought to be due to the consumption of the reagent by large amounts of diverse ions present.

Summary

An absorptiometric determination of micro-amounts of iron with nitroso R salt was satisfactorily applied to the routine analysis of nuclear grade graphite. An ashed sample is brought into a solution and the color of iron is developed by the reagent with the aid of hydroxylamine sulfate. Adjustment of pH to the optimum range is easily made by the addition of a definite amount of an acetate buffer. The intensity of the color is measured at 715 mμ. The range of the determination covers 2 to 75 p. p. m. when 1 g. of a sample is taken, the final volume being 25 ml. In the case of a sample of urania-graphite fuel, the ash is fumed with perchloric acid and a preliminary separation is made by coprecipitation with manganese dioxide which is produced by the oxidation of manganese(II) ion with hydrogen peroxide in a hot ammoniacal carbonate solution. The recovery of

iron is quantitative and the removal of diverse ions is satisfactory. All of the uranium is also removed here. Contamination with foreign iron from a drill used for sampling and from the platinum or percelain crucibles used is negligible. The effect of diverse ions on the absorptiometry was also examined.

The author is indebted to Mr. H. Nihei and Miss Fukamachi for their experimental work. Acknowledgment is made to Drs. K. Ono and Y. Oka, Professors of Tohoku University, for their encouragement and also to Tokai Electrode Mfg. Co. Ltd. for their permission to publish the results.

Technical Research Laboratory
Tokai Electrode Mfg. Co. Ltd.
Fujisawa-shi, Kanagawa-ken

Photochemical Processes due to n-π and π-π* Transitions of 2-Picoline N-Oxide in the Vapor Phase*

By Norisuke HATA*1

(Received February 8, 1961)

As reported in the previous paper[1], the main photolytic product of pyridine *N*-oxide due to irradiation by 3261 or 2537 Å was pyridine in both cases. We observed a remarkable difference in the relation between the quantum yield of pyridine produced and the temperature.

In the case of 2-picoline *N*-oxide, however, it may be expected that the introduction of a methyl group in the 2-position of the pyridine ring might cause photochemical behavior different from that of pyridine *N*-oxide. In order to investigate the effect of 2-methyl substitution on the photolysis of pyridine *N*-oxide, the present author carried out the gaseous photolysis of 2-picoline *N*-oxide by irradiating with the 3261 Å (Cd $^3P_1$) or 2537 Å (Hg $^3P_1$) resonance line, which corresponds to absorption due to an n-π^* or a π-π^* transition of this substance, respectively. It was found from this experiment that 2-picoline *N*-oxide undergoes a photochemical rearrangement to isomerize to 2-pyridinemethanol at 3261 Å and a fission of N→O bond to produce 2-picoline at 2537 Å.

Experimental

The 2-picoline *N*-oxide used in this experiment was prepared by the method described by Ochiai and purified by vacuum distillation several times[2]. B. p., 105~106°C/4 mmHg.

A pyrex cadmium resonance lamp was used as a light source for the photolysis in the n-π^* absorption region, while a quartz mercury resonance lamp was used in the π-π^* absorption region, and these lamps were those used for the photolysis of pyridine *N*-oxide.

The gaseous photolysis of 2-picoline *N*-oxide was carried out by a procedure similar to that of pyridine *N*-oxide described in the previous paper[1]. Photolytic products were also divided into fractions A, B, C and D just as those of pyridine *N*-oxide, where

Fraction A: Gaseous product not condensed at −196°C (liquid nitrogen).

Fraction B: Gaseous product condensed at −196°C and not condensed at −95°C (liquid nitrogen in methanol).

Fraction C: Liquid product condensed at −95°C and not condensed at −75°C (dry ice in methanol).

Fraction D: Dark brown polymer.

The pressures of fractions A and B were each measured with a Toepler-gauge, and analyzed by using a mass-spectrometer and a low-pressure gas-chromatograph (column: benzyl ether). The analysis of fraction C was done with a Shimadzu quartz spectrophotometer QB-50 and also a Shimadzu gas-chromatograph GC-1A (column: cetyl alcohol). The analysis of fraction D was not carried out.

Results and Discussion

The ultraviolet absorption spectra of several methylpyridine *N*-oxides have been measured in polar solvents by Ikekawa et al.[3], where they discussed a relation between the maximum of π-π^* absorption and the position of the methyl group in the pyridine ring. The author has also observed a weak shoulder absorption

*1 Present address: Tokyo Electrical Engineering College, Kanda, Chiyoda-ku, Tokyo.

1) N. Hata *J. Chem. Phys.*, in press.

2) E. Ochiai, *J. Org. Chem.*, **18**, 534 (1953).

3) N. Ikekawa and Y. Sato, *Pharm. Bull.*, **2**, 400 (1954).

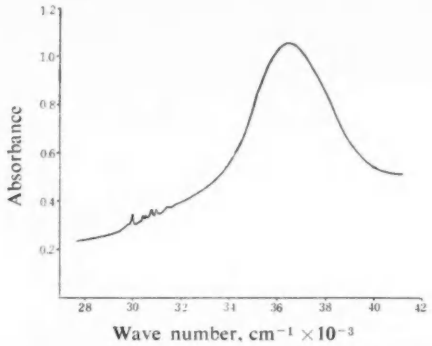

Fig. 1a. Vapor spectrum of 2-picoline *N*-oxide at room temperature. (Absorption region due to n-π^* and π-π^* transition.)

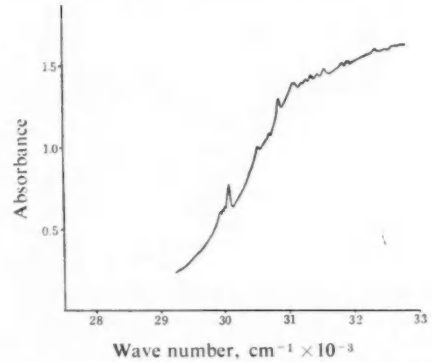

Fig. 1b. Vapor spectrum of 2-picoline *N*-oxide at 80°C. (Absorption region due to n-π^* transition.)

with three isomeric picoline *N*-oxides in a non-polar solvent and in the vapor[1]. The absorption was regarded as due to an n-π^* transition. Figure 1 shows the vapor spectrum of 2-picoline *N*-oxide which was measured with a Cary recording spectrophotometer 14 M*2.

As described in the experimental part, the photolytic products at 3261 or 2537 Å irradiation were divided into fractions A, B, C and D. Fraction A was mainly hydrogen but included a small amount of oxygen, and fraction B was identified as carbon dioxide. Fraction C obtained as a liquid product was 2-pyridinemethanol at 3261 Å irradiation, whereas it was 2-picoline in the case of 2537 Å irradiation. The experimental results were expressed as quantum yields of fractions A, B and C at different temperatures as shown in Figs. 2 and 3.

4) N. Hata, This Bulletin, to be published.
*2 The spectral measurement was performed by Dr. A. Kuboyama, to whom the author's thanks are due.

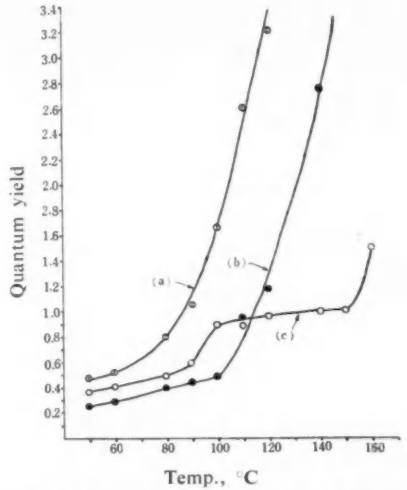

Fig. 2. Quantum yields of products versus temperature in the case of 2537 Å irradiation.
(a) —○—: Fraction A
(b) —●—: Fraction B
(c) —○—: Fraction C

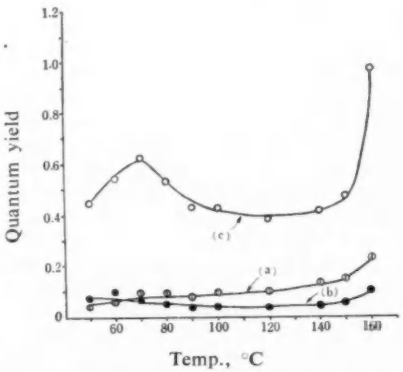

Fig. 3. Quantum yields of products versus temperature in the case of 3261 Å irradiation.
(a) —○—: Fraction A
(b) —●—: Fraction B
(c) —○—: Fraction C

The processes succeeding to a π-π^* transition of 2-picoline *N*-oxide may be expressed as follows, assuming that the excited molecule passes through a triplet state as in the case of pyridine *N*-oxide[1]. That is,

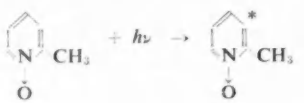

(1)

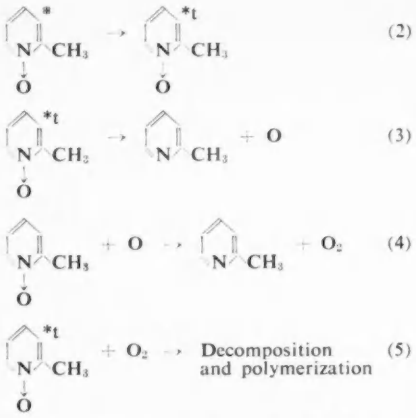

(2)

(3)

(4)

(5)

(* and *t denote the excited singlet and triplet states, respectively.)

Fig. 2 indicates how the quantum yield of each photolytic product at 2537 Å irradiation changes with temperature. Although the quantum yield of fraction C (2-picoline) is 0.4~0.5 at low temperatures, it increases steeply at about 90°C to a saturated value (0.9~1.0) at temperatures above 100°C. (Such a temperature dependence of the quantum yield has not been observed in the case of pyridine *N*-oxide at 2537 Å irradiation, in which case the quantum yield of pyridine produced did not change substantially with temperature.) This observation suggests that an activation energy would be required for the production of 2-picoline. This may be interpreted qualitatively as follows. Excited 2-picoline *N*-oxide, due to a π-π^* transition, presumably passes into a triplet state crossing with the excited singlet state to dissociate to 2-picoline and atomic oxygen in a predissociative manner as in the case of pyridine *N*-oxide (cf. Fig. 3 in Ref. 1). Since, for the pyridine *N*-oxide[1] or 3-picoline *N*-oxide[5] which does not possess a methyl group in the 2-position of the pyridine ring, the quantum yield of fraction C is independent on the temperature, the temperature dependence observed in the case of 2-picoline *N*-oxide must be associated with the interaction between the methyl group and the N→O group. The N→O bond energy of 2-picoline *N*-oxide is approximately the same as in pyridine *N*-oxide, i. e. ca. 110 kcal. mol^{-1}, although it may be smaller than 110 kcal. mol^{-1} owing to the decrease of N→O double bond character caused by the hyperconjugative effect of 2-methyl group. Therefore, the process 3, by which the excited triplet 2-picoline *N*-oxide dissociates to 2-picoline and atomic oxygen, possibly does not need an activation energy. Thus, process 4 which is the alternative reaction producing 2-picoline is probably influenced by the interaction between the 2-methyl group and the N→O group. Investigation of the ultraviolet absorption spectrum of 2-picoline *N*-oxide[3,4], suggests the formation of a weak hydrogen bond between the methyl group and N→O group as shown in A. Such a weak

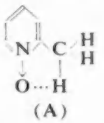

(A)

hydrogen bond formation may bring about a retarding effect for process 4 at low temperatures. Since the hydrogen bond is broken by the thermal perturbation caused by the increasing temperature, however, the abstraction reaction 4 would be facilitated by increasing temperature. Therefore, it is expected that the quantum yield of 2-picoline may rapidly increase to become about twice the value at low temperature. Figure 2 indicates distinctly the existence of such a tendency. The activation energy necessary for the production of 2-picoline estimated from the temperature-dependence of the quantum yield is about 1.1 kcal. mol^{-1}.

2-Picoline *N*-oxide gives rise also to substantial amounts of hydrogen upon irradiation with 2537 Å, where the quantum yield increases remarkably with rising temperature as shown in Fig. 2. This is probably due to a participation of the following processes in addition to the process 5.

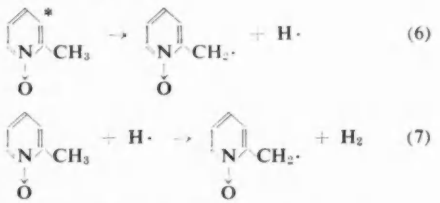

(6)

(7)

Although D(CH_2–H) in 2-picoline *N*-oxide is not known, it is reasonable to assume processes 6 and 7, since the gaseous photolysis of toluene produces hydrogen[6].

In addition to processes 6 and 7, the production of fractions A, B and D probably resulted from the process 5 between excited 2-picoline *N*-oxide and oxygen produced by process 4 as in the case of pyridine *N*-oxide. To confirm the correctness of this reaction the gaseous photolysis was attempted for the mixture of 2-picoline *N*-oxide and oxygen, expecting that the 2-picoline would decrease and other products

5) N. Hata, This Bulletin, 34, 1444 (1961).

6) R. R. Hentz and M. Burton, *J. Am. Chem. Soc.*, 73, 536 (1953); G. Porter, *Chem. Soc. (London), Spec. Publ.* p. 139, No. 9 (1957).

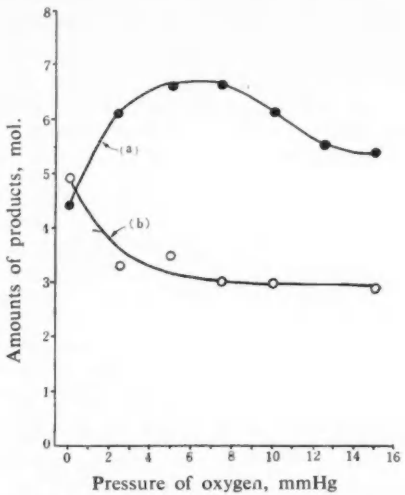

Fig. 4. Amounts of products versus oxygen pressure in the photolysis for the mixture of 2-picoline *N*-oxide and oxygen at 2537 Å (irradiation time: 10 min., temperature: 90°C).
(a) —●—: Fraction B
(b) —○—: Fraction C

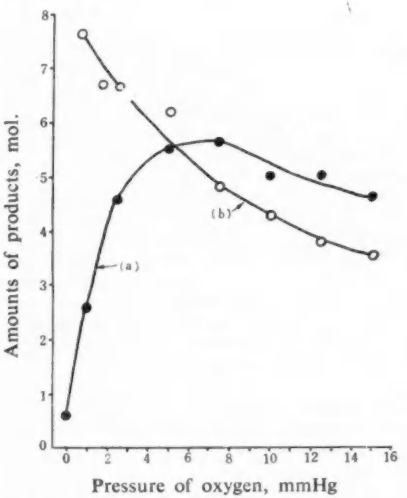

Fig. 5. Amounts of products versus oxygen pressure in the photolysis for the mixture of 2-picoline *N*-oxide and oxygen at 3261 Å (irradiation time: 2 hr., temperature: 70°C).
(a) —●—: Fraction B
(b) —○—: Fraction C

would increase with increasing oxygen pressure. The experimental results are expressed as amounts of fractions B (carbon dioxide) and C (2-picoline) in the decomposed products under the different pressures of oxygen. The results support clearly the occurence of process 5 described above.

In the case of 3261 Å irradiation (n-π^* transition), 2-picoline *N*-oxide isomerizes to 2-pyridinemethanol by a rearrangement of the oxygen atom of N→O group to the methyl group as shown in process 8 and the production of fractions A, B and D were very small.

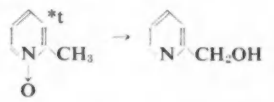

(8)

As seen from Fig. 3, the quantum yield of fraction C shows a maximum value at about 70°C and approximate temperature-independence at temperatures greater than 100°C. The fact that the quantum yield is affected by changes in temperature seems to indicate that process 8 requires some activation energy. Its activation energy estimated from the quantum yield and the temperatures[*3] is about 3.4 kcal. mol^{-1}. This production of 2-picoline from its *N*-oxide at 3261 Å irradiation requires, presumably, an activation energy of about 11～12 kcal. mol^{-1}, considering the fact that the activation energy for the production of pyridine[1] or 3-picoline[5] from its *N*-oxide is about 11～12 kcal. mol^{-1}. Since the activation energy necessary for the photoisomerization of 2-picoline *N*-oxide to 2-pyridinemethanol is estimated to be about 3.4 kcal. mol^{-1}, however, the excited triplet molecule resulting from 3261 Å irradiation may largely undergo process 8 involving a smaller potential barrier than that for the N→O bond split.

If the photochemical behavior due to n-π^* transition is only the rearrangement process described above, its products should be 2-pyridinemethanol alone. However, the fact that small amounts of decomposed and polymerized products are detected in the products as seen in Fig. 3 seems to indicate that processes 3—7 occur simultaneously with process 8. The experimental results of the photolysis for the mixture of constant amounts of 2-picoline *N*-oxide and different pressures of oxygen suggest that the above assumption is reasonable. That is, as seen from Figs. 4 and 5 the fact that fraction B increases rapidly and fraction C decreases with increasing pressures of oxygen

[*3] The quantum yield of 2-pyridinemethanol (fraction C) decreases at temperatures above 80°C, which may probably be ascribed to the increase of quenching of the excited molecule with increasing pressures of 2-picoline *N*-oxide. Therefore, the calculation of the activation energy necessary for the production of 2-pyridinemethanol was performed by using some of the quantum yields at temperatures below 80°C.

may be regarded as evidence for the reaction between excited 2-picoline *N*-oxide and oxygen.

Summary

The gaseous photolysis of 2-picoline *N*-oxide was carried out by irradiation with the 3261 Å (Cd $^3P_1$) or 2537 Å (Hg $^3P_1$) resonance lines corresponding to an n-π^* or a π-π^* absorption of this substance, respectively.

In the case of 3261 Å irradiation, the major product was 2-pyridinemethanol, whose quantum yield showed a marked temperature-dependence. The activation energy necessary for the production of 2-pyridinemethanol was estimated to be about 3.4 kcal. mol^{-1}.

On the other hand, the photolytic products at 2537 Å irradiation were 2-picoline and other decomposition products and polymers. The quantum yield of 2-picoline showed a marked temperature-dependence, which may be attributed to the interaction between the 2-methyl group and the N→O group. The activation energy necessary for the production of 2-picoline was estimated to be about 1.1 kcal. mol^{-1}.

In conclusion, the author wishes to express his hearty thanks to Professor Ikuzo Tanaka for his kind guidance and encouragement. Thanks are also due to Mr. Y. Mori and Dr. K. Naiki for their helpful discussions during the course of this work.

Laboratory of Physical Chemistry
Tokyo Institute of Technology
Meguro-ku, Tokyo

Photochemical Processes due to n-π and π-π* Transitions of 3-Picoline N-Oxide in the Vapor Phase*

By Norisuke HATA[*1]

(Received February 15, 1961)

The photochemical reactions caused by an n-π^* or a π-π^* transition of pyridine *N*-oxide and 2-picoline *N*-oxide were previously studied in the vapor phase[1,2], by irradiating with the 3261 Å (Cd $^3P_1$) or 2537 Å (Hg $^3P_1$) resonance line, respectively. As reported in the previous paper[2], the introduction of the 2-methyl group in pyridine *N*-oxide strongly influences the photochemical behavior of pyridine *N*-oxide both in n-π^* and π-π^* transitions. However, it is considered that the photochemical reactions of 3-picoline *N*-oxide are similar to those of pyridine *N*-oxide, because the hyperconjugative effect and also the interaction with the N→O group could be neglected with the 3-methyl group. Therefore, the present author has attempted the gaseous photolysis of 3-picoline *N*-oxide by irradiation with 3261 Å (Cd $^3P_1$) and 2537 Å (Hg $^3P_1$) resonance lines, each of which corresponds respectively to the absorption region due to an n-π^* or a π-π^* transition of 3-picoline *N*-oxide.

Experimental

The synthesis of the 3-picoline *N*-oxide used in this experiments was done by a method similar to that of pyridine *N*-oxide*[2]. The product was purified by vacuum distillation several times[3]. B. p., 123°C/5 mmHg.

The light sources employed for the photolysis in the n-π or π-π^* absorption region were a pyrex cadmium resonance lamp or a quartz mercury resonance lamp, respectively, which were used in the case of pyridine *N*-oxide[1] and 2-picoline *N*-oxide[2].

Since the experimental methods are similar to those of pyridine *N*-oxide and 2-picoline *N*-oxide as reported in a previous paper[1], the description of the experimental techniques are omitted in this paper. The photolytic products were divided into fractions A, B, C and D just as in the photolysis of pyridine *N*-oxide or 2-picoline *N*-oxide, where

Fraction A: Gaseous products not condensed at −196°C (liquid nitrogen).

Fraction B: Gaseous products condensed at −196°C and not condensed at −95°C (liquid nitrogen in methanol)

Fraction C: Liquid products condensed at −95°C and not condensed at −75°C (dry ice in methanol).

Fraction D: Dark brown polymers.

The pressures of fractions A and B were each measured with a Toepler-gauge, and analyzed by using a mass-spectrometer and a low pressure gas-chromatograph (column: benzyl ether). The analysis of fraction C was done with a Shimadzu

*1 Present address: Tokyo Electrical Engineering College, Kanda, Chiyoda-ku, Tokyo.

1) N. Hata and I. Tanaka, *J. Chem. Phys.*, in press.

2) N. Hata, This Bulletin, **34**, 1440 (1961).

3) E. Ochiai, *J. Org. Chem.*, **18**, 534 (1953).

*2 The 3-picoline used in the synthesis of 3-picoline *N*-oxide was supplied by Dr. T. Kubota, to whom the author's thanks are due.

quartz spectrophotometer QB-50 and also a Shimadzu gas-chromatograph (column: cetyl alcohol). The analysis of fraction D was not carried out.

Results and Discussion

3-Picoline *N*-oxide has two absorption systems in the region of the near ultraviolet both in the solution of a non-polar solvent and in the vapor[1]. Figure 1 shows the absorption curves of 3-picoline *N*-oxide in the vapor phase, which was measured with a Cary recording spectrophotometer 14 M*[3]. As seen from Fig. 1, there are two absorption regions between 28000 and 40000 cm^{-1}, one of which is the weak absorption at about 30000 cm^{-1} and the other a stronger absorption at about 35500 cm^{-1}. As will be described in a later paper[4], the weak absorption at the longest wavelength which consists of sharp vibrational structures having an O-O band at 29368 cm^{-1} corresponds to the n-π^* absorption due to an excitation of non-bonding electrons localized on the oxygen atom to the antibonding π-orbital. On the other hand, the strong absorption having its absorption maximum at about 35703 cm^{-1} is considered to be due to a π-π^* transition.

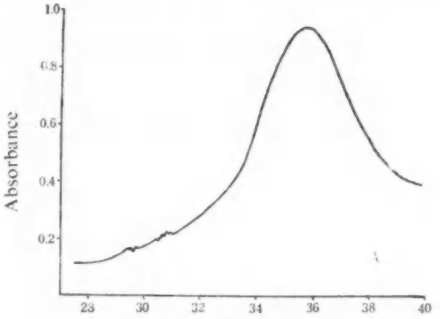

Fig. 1a. Vapor spectrum of 3-picoline *N*-oxide at 70°C. (Absorption region due to n-π^* and π-π^* transitions.)

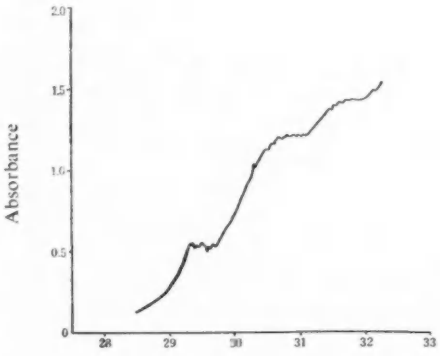

Fig. 1b. Vapor spectrum of 3-picoline *N*-oxide at 100°C. (Absorption region due to n-π^* transition.)

As described in the experimental part, the photolytic products due to irradiation with 3261 or 2537 Å were divided into fractions A, B, C and D. Fraction A was largely hydrogen, although small amounts of oxygen were detected in this fraction. Fraction B was identified as carbon dioxide. Fraction C, obtained as a liquid product, was 3-picoline. The experimental results were expressed as the quantum yield of fractions A, B and C at different temperatures as shown in Figs. 2 and 3. The quantum yields of the products at temperatures greater than 160°C were not shown in these figures, because the thermal decomposition of 3-picoline *N*-oxide occurs simultaneously with the photochemical decomposition at these higher temperatures.

The experimental results of the photolysis for 3-picoline *N*-oxide are summarized as follows.

a) A Relation between the Quantum Yield of Fraction C (3-Picoline) and the Temperature. — In the case of 3261 Å irradiation (n-π^* transition), the quantum yield increases markedly at about 80~100°C, although it has a comparatively low value at temperatures below 80°C. A further increase of the temperature causes a decrease in the quantum yield to some extent. On the other hand, the quantum yield at 2537 Å irradiation (π-π^* transition) is independent of the temperature, and has a value of about 0.55.

b) A Relation between the Quantum Yield of Fraction A (Mainly Hydrogen) or Fraction B (Carbon Dioxide) and the Temperature. — The quantum yields of fractions A and B increase continuously with rising temperature with both 3261 and 2537 Å irradiation.

c) In either case (i.e., 3261 and 2537 Å) comparatively greater amounts of fraction D (dark brown polymer) are obtained.

d) When the photolysis of a mixture of 3-picoline *N*-oxide and oxygen was carried out at different pressures of oxygen, the amount of fraction B markedly increased with increasing oxygen pressure, but that of fraction C decreased.

From the experimental results described above, it is concluded that the photochemical reaction of 3-picoline *N*-oxide is quite similar to that of pyridine *N*-oxide, but not to that

4) N. Hata, This Bulletin, to be published.

*3 The spectral measurement was performed by Dr. A. Kuboyama, to whom the author's thanks are due.

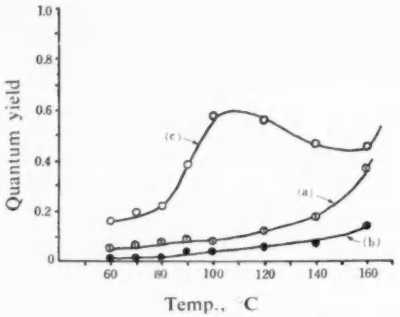

Fig. 2. Quantum yields of products versus temperature in the case of 3261 Å irradiation.
(a) —◫—: Fraction A
(b) —●—: Fraction B
(c) —○—: Fraction C

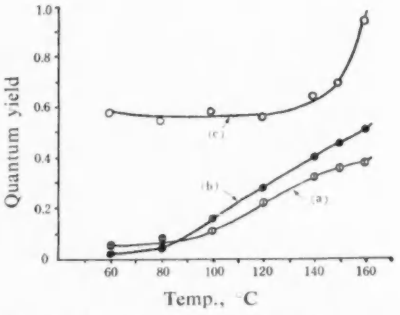

Fig. 3. Quantum yields of products versus temperature in the case of 2537 Å irradiation.
(a) —◫—: Fraction A
(b) —●—: Fraction B
(c) —○—: Fraction C

of 2-picoline *N*-oxide. This fact suggests that the hyperconjugative effect of methyl group or the interaction between N→O group and methyl group may be neglected in the photolysis of 3-picoline *N*-oxide. Therefore, it may be considered that the mechanism of the photochemical reaction of 3-picoline *N*-oxide would be similar to that of pyridine *N*-oxide. Thus, we assumed the following mechanism as the processes succeeding to an n-π^* and a π-π^* transitions of 3-picoline *N*-oxide.

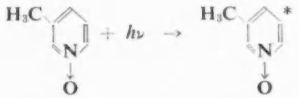

(1)

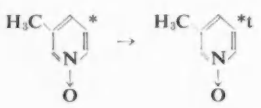

(2)

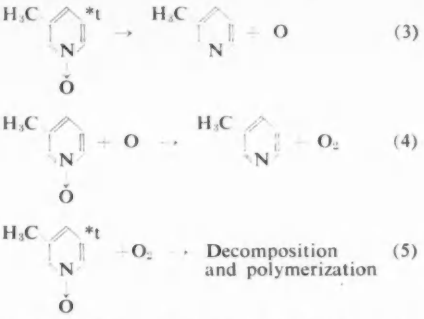

(* and *t denote the excited singlet and triplet states, respectively.)

First the 3-picoline *N*-oxide molecule is excited to the corresponding excited singlet state due to an n-π^* or a π-π^* transition caused by an absorption of 3261 or 2537 Å radiation. (Cf. the schematic potential curves for pyridine *N*-oxide as depicted in Fig. 4 of Ref. 1 for the succeeding description). Such an excited molecule probably decomposes to 3-picoline and atomic oxygen in a predissociative manner, in which a triplet state crossing with the first excited state exists presumably as a short lived intermediate. As seen from Figs. 2 and 3, the quantum yield of 3-picoline at 3261 Å irradiation shows a remarkable temperature dependence as pointed out in the experimental results a, while at 2537 Å irradiation it is independent of the temperature. This fact means that activation energy would be required for the production of 3-picoline at 3261 Å, but not at 2537 Å. The activation energy necessary for the production of 3-picoline in the case of 3261 Å irradiation is about 11.5 kcal. mol^{-1}, which was estimated from the relation between the quantum yield of produced 3-picoline and the temperature, and this value coincides nearly with that of pyridine *N*-oxide. Of the processes 3 and 4, which are possibly the essential reactions producing 3-picoline, the process 3 might be the only reaction requiring an activation energy. If an appreciable activation energy is required for process 4, the quantum yield of 3-picoline must also depend on the temperature even at 2537 Å irradiation. (However, the experimental results do not show any temperature-dependence of the quantum yield of 3-picoline at 2537 Å irradiation). As reported in a previous paper for the case of 2-picoline *N*-oxide[2], the temperature-dependence of the quantum yield of 2-picoline observed at 2537 Å irradiation was attributed to the interaction between the 2-methyl group and the N→O group as one of the main factors. Therefore, in the case of 3-picoline *N*-oxide the experimental result obtained at 2537 Å irradiation

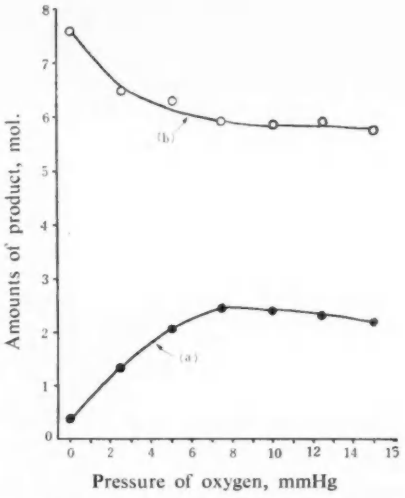

Fig. 4. Amounts of products versus oxygen pressure in the photolysis of mixtures of 3-picoline *N*-oxide and oxygen at 3261 Å (irradiation time: 2 hr., temperature: 100°C).
(a) —●—: Fraction B
(b) —○—: Fraction C

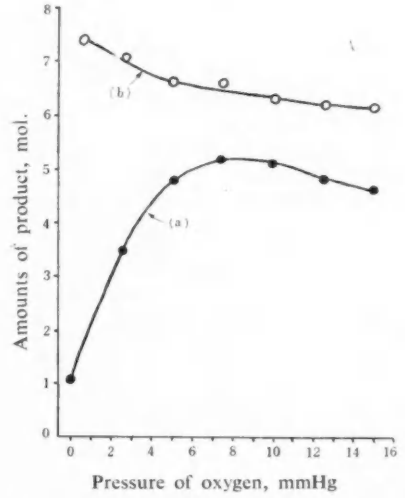

Fig. 5. Amounts of products versus temperature in the photolysis of mixtures of 3-picoline *N*-oxide and oxygen at 2537 Å (irradiation time: 10 min., temperature: 80°C).
(a) —●—: Fraction B
(b) —○—: Fraction C

(which is similar to that of pyridine *N*-oxide) supports the idea of the importance of the interaction between 2-methyl group and N→O group in the photolysis of 2-picoline *N*-oxide.

The results of the photolysis of mixtures of constant amounts of 3-picoline *N*-oxide and different pressures of oxygen are shown in Figs. 4 and 5 for the cases of 3261 and 2537 Å irradiations, respectively. These results indicate that the amounts of 3-picoline decrease and that of fraction B (carbon dioxide) increases with increasing oxygen pressure. This is regarded as evidence for the occurrence of the reaction 5 between the excited molecule and oxygen. In Figs. 4 and 5, the tendency for the amounts of products observed at oxygen pressures greater than about 7.5 mmHg to approach a saturated value may be ascribed to collisional deactivation of the excited molecule by oxygen with increasing pressures of oxygen.

Summary

Gaseous photolysis of 3-picoline *N*-oxide was attempted by irradiation with the 3261 Å (Cd $^3P_1$) or 2537 Å (Hg $^3P_1$) resonance line corresponding to an n-π^* or a π-π^* absorption region, respectively, of this substance. In either case, the photolytic products were mainly 3-picoline, and we observed a remarkable temperature-dependence for the quantum yield of 3-picoline in the case of 3261 Å irradiation but not in the case of 2537 Å irradiation. This observation suggests that an activation energy would be required for the production of 3-picoline at 3261 Å only. The activation energy estimated from the relation between the quantum yield of produced 3-picoline and the temperature at 3261 Å irradiation was about 11.5 kcal. mol^{-1}, which is almost about the same value as that of pyridine *N*-oxide. The reactions succeeding to an n-π^* or a π-π^* transition of 3-picoline *N*-oxide were considered to be similar to the case of pyridine *N*-oxide.

In conclusion, the author wishes to express his hearty thanks to Professor Ikuzo Tanaka for his kind guidance and encouragement. Thanks are also due to Mr. Y. Mori and to Dr. K. Naiki for their helpful discussion during the course of this work.

Laboratory of Physical Chemistry
Tokyo Institute of Technology
Meguro-ku, Tokyo

Infrared Spectra of Acyclic Imides. IV. Effects of Alkali Halides on the Infrared Spectra of Diacetamide

By Toyozo UNO, Katsunosuke MACHIDA and Ikuko HAMANAKA

(Received February 6, 1961)

Anomalies in the infrared spectra of some polar molecules in the alkali halide disk technique have often been reported[1]. In case of benzoic acid[2], potassium iodide disks have been recommended to obtain the same infrared spectra as those of pastes. On the other hand, molecules containing the –CONHCO– group such as succinimide[3], cyanuric acid[4] and barbituric acid[5], have been reported to undergo spectral changes depending on the method of preparation of samples. In the present paper, we will report that diacetamide (CH_3–CONHCO–CH_3), which has been revealed to exhibit dimorphism[6], also shows an analogous anomaly. An inversion of configuration of the –CONHCO– group is suggested to take place in the course of this spectral change. The ionic radii of the anions and the cations of alkali halides involved as well as the amount of water contained in the sample have been proved to influence the spectral change. The effect of compression in the disk technique has also been examined.

Results and Discussion

Alkali Halide Anomaly and Dimorphism of Diacetamide. — The crystal of diacetamide in form A undergoes marked changes in infrared spectra on the addition of various alkali halides. This phenomenon was observed at first for potassium iodide, in the course of measurements in the disk technique. As reported in the preceding paper[6], diacetamide in form A shows two C=O stretching bands at 1734 and 1700 cm^{-1}, the stronger one being the band at 1700 cm^{-1}. This was always the case for Nujol or hexachlorobutadiene pastes. For potassium bromide disks however, both of these bands sometimes underwent changes in relative intensities so that the band at 1734 cm^{-1} became the stronger one. In an attempt to prevent this spectral change, the use of potassium iodide as the matrix[2] was made to result in a marked spectral change of different type over the whole region measured.

On the other hand, another crystal form (form B) was found for diacetamide[6] and a close similarity in infrared spectra was observed between pastes of the form B and potassium iodide disks of form A. Furthermore, form A and form B were proved to involve the trans-cis and the trans-trans –CONHCO– group respectively, giving rise to infrared spectra markedly different from each other. Thus, the above fact concerning potassium iodide suggests that the configuration of the –CONHCO– group is changed from the trans-cis to the trans-trans configuration in the course of preparation of potassium iodide disks from form A. To confirm this, further investigations with the use of various alkali halides have been made and the following results have been obtained.

Effects of Various Alkali Halides. — *1) Potassium Iodide, Sodium Iodide and Sodium Bromide.*—The presence of these alkali halides gives rise to analogous changes in infrared spectra of the form A of diacetamide not only in the disk technique but also in the paste method. Here, the paste method means the technique in which the mixture of diacetamide in form A and one of potassium iodide, sodium iodide and sodium bromide (the molar ratio being approximately one to one) is mulled with Nujol or hexachlorobutadiene. It is seen from this fact that the primary factor for the spectral change is not in the disk technique itself but in the alkali halide used. By the application of the paste method, the effect of water adsorbed on alkali halides or other impurities can be made negligible since in this case the amounts of diacetamide and alkali halide are comparable to each other. Furthermore, the paste method is preferable to examine the corresponding spectral changes for diacetamide-*d* since the infrared spectra of highly pure diacetamide-*d* can be obtained only with a rapid technique such as the paste method. Considering these advantages of the paste method, we have carried out the measurements in the present study mainly on the

1) For example, see O. Amakasu and A. Ito. *J. Chem. Soc. Japan, Pure Chem. Sec.* (*Nippon Kagaku Zasshi*), **81**, 683 (1960). A number of literatures were cited in it.
2) V. C. Farmer, *Spectrochim. Acta*, **8**, 374 (1957).
3) A. W. Baker, *J. Phys. Chem.*, **61**, 453 (1957).
4) W. M. Padgett, II., J. M. Talbert and W. F. Hamner, *J. Chem. Phys.*, **26**, 959 (1957).
5) B. Cleverley and P. P. Williams, *Chem. & Ind.*, **1959**, 49.
6) T. Uno and K. Machida, This Bulletin, **34**, 545 (1961).

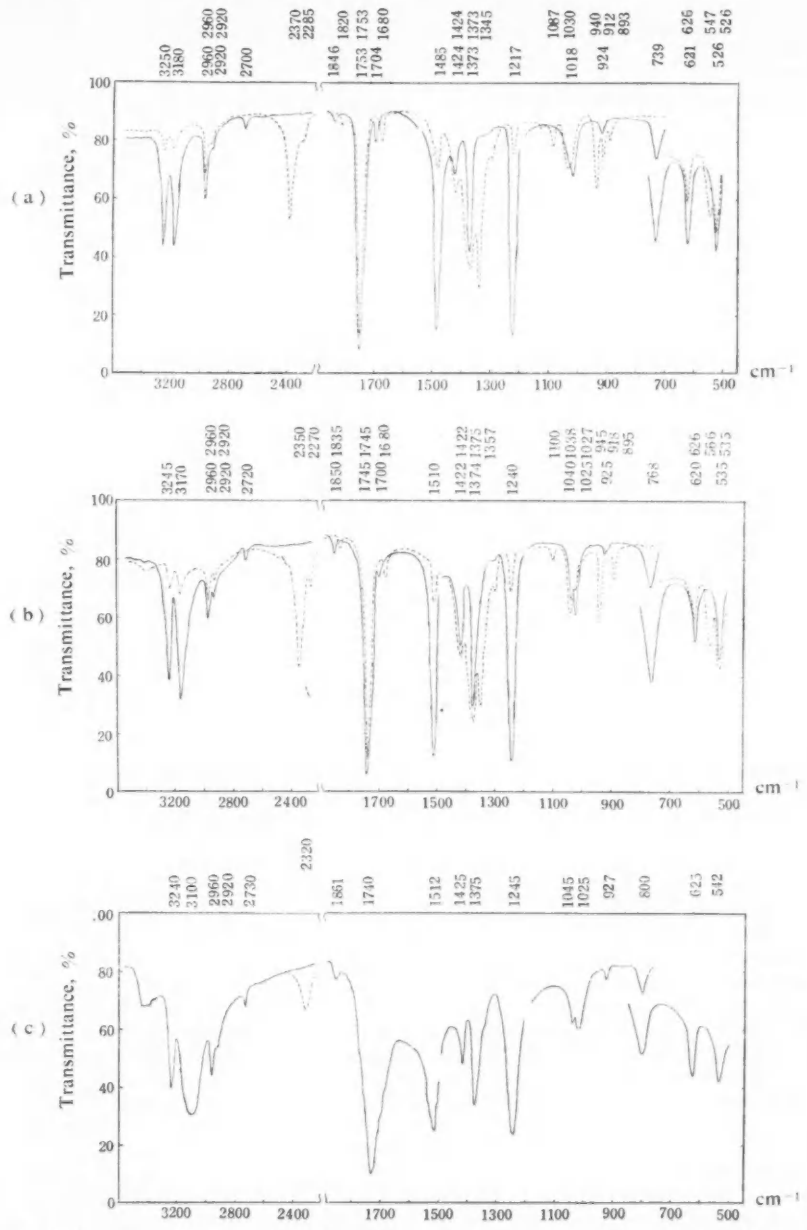

Fig. 1. Infrared spectra of diacetamide in the two-component systems containing alkali halides.

(a) Diacetamide-KI (3600~2200 cm^{-1} and 1550~1200 cm^{-1}, hexachlorobutadiene paste; 1900~1550 cm^{-1} and 1200~500 cm^{-1}, Nujol paste).

(b) Diacetamide-NaBr (3600~2200 cm^{-1} and 1490~1200 cm^{-1}, hexachlorobutadiene paste: 1900~1490 cm^{-1} and 1200~500 cm^{-1}, Nujol paste).

(c) Diacetamide-LiCl (3600~2200 cm^{-1} and 1490~1200 cm^{-1}, hexachlorobutadiene paste: 1900~1490 cm^{-1} and 1200~500 cm^{-1}, Nujol paste).

solid lines: undeuterated species.

broken lines: *N*-deuterated species.

pastes of the two-component systems of diacetamide and various alkali halides[7].

The infrared spectra of the two-component systems containing potassium iodide and sodium bromide are shown in Figs. 1, (a) and (b) respectively. It is obviously seen that these spectra resemble that of diacetamide in the form B[8]. These two-component systems show the sharp symmetric imide I band near 1750 cm^{-1} as well as the weak but well resolved antisymmetric imide I band near 1700 cm^{-1}. The latter band has been supposed to be overlapped by the broad symmetric imide I band in the spectrum of the undeuterated species in form B[8]. Furthermore, the low-frequency shift of the antisymmetric imide I band on deuteration is obviously observed for these two-component systems. There is only a little difference in the corresponding characteristic frequencies between the system containing sodium iodide and that containing potassium iodide. The system containing sodium bromide shows however, the infrared spectrum in which some characteristic frequencies related mainly to the N–H bond are appreciably different from those observed for the systems containing iodides. The similarity in the infrared spectra between form B and the two-component system containing one of these alkali halides is also observed in the case of diacetamide-*d*.

2) Potassium Bromide, Potassium Chloride and Sodium Chloride.—The infrared spectrum of the two-component system consist of form A and one of these alkali halides is identical with that of form A. In other words, these alkali halides bring about no spectral change. The comparison of alkali halides described in 1 and 2 suggests that both the cation and the anion of alkali halides participate in the spectral change under consideration.

3) Lithium Iodide, Lithium Bromide and Lithium Chloride.—These lithium salts bring about the spectral change. Infrared spectra analogous to Figs. 1, (a) and (b) are obtained for the systems containing lithium iodide and lithium bromide respectively. The infrared spectrum of the system containing lithium chloride is shown in Fig. 1, (c), which is appreciably different from either (a) or (b) in the regions 3600 to 2000 cm^{-1} and 1000 to 700 cm^{-1}. Since lithium halides adsorb an appreciable amount of water during the preparation of pastes, the examination of the spectral change for diacetamide-*d* on addition of lithium halides seriously suffers from the interference of the undeuterated species. Consequently, the characteristic bands of diacetamide-*d* in the two-component systems containing lithium halides could hardly be identified except for the N–D stretching band.

On the basis of the above fact, those infrared spectra obtained by the addition of these alkali halides may be conveniently classified into three types B_1, B_2 and B_3 according to the anion involved. Thus, we have three iodides, two bromides and one chloride giving rise to the spectral types B_1, B_2 and B_3 in that order. Differences among the types B_1, B_2 and B_3, as represented by Figs. 1, (a), (b) and (c) respectively, are mainly in the N–H (and N–D) stretching and the imide V (and V') frequencies[6,8,9]. Table I shows these frequencies for each spectral type. The other characteristic frequencies[5] of diacetamide in the two-component systems are shown in Table II. Discussions on these frequencies will be given later.

Table I. The characteristic frequencies (in cm^{-1}) of diacetamide depending on the anion

Anion	I^-	Br^-	Cl^-	Form B[8]
Spectral types*1	B_1	B_2	B_3	
N–H Stretch.*2	3250m*3	3245m	3240m	3280 s
	3180m	3170 s	3100 s	3205 s
Imide V	739m	768m	800m	739m
N–D Stretch.	2370m	2350m	2320m	2405 s
Imide V'	547m	566m	—	547m

*1 : See also Table III.
*2 : The origin of the splitting of this band was discussed in Ref. 9.
*3 : s, strong; m, medium.

Table II. The characteristic frequencies (in cm^{-1}) of diacetamide depending on both the anion the cation

		Li^+	Na^+	K^+
Cl^-	Sym. imide I	1740 s		
	Imide II	1512 s		
	Imide III	1245 s		
	Imide II'	?		
	Imide III'	?		
Br^-	Sym. imide I	1740 s	1745 s	
	Imide II	1510 s	1510 s	
	Imide III	1245 s	1240 s	
	Imide II'	?	1357m	
	Imide III'	?	945m	
I^-	Sym. imide I	1742 s	1748 s	1753 s
	Imide II	1500 s	1490 s	1485 s
	Imide III	1237 s	1220 s	1217 s
	Imide II'	?	1349m	1345m
	Imide III'	?	941m	940m

Effect of Water.—Since lithium halides are extremely hygroscopic and it is difficult to

7) For the method of preparation of samples, see Experimental Part 2.
8) T. Uno and K. Machida, This Bulletin, 34, 551 (1961).
9) T. Uno and K. Machida, ibid., 34, 821 (1961).

avoid the adsorption of water during the preparation of pastes, the effect of a small amount of water on this spectral change must be taken into account if lithium halides are involved. Instead of removing water from the systems containing lithium halides, the other alkali halides were re-examined in the presence of a small amount of water[10]. The result was such that sodium chloride and potassium bromide partly give rise to the spectral change in the presence of water while potassium chloride does not.

These results are summarized in Table III, from which it is seen that the presence of water favors this spectral change. This may

Table III. The spectral types* of diacetamide-alkali halide systems

		Li^+	Na^+	K^+
Cl^-	Without water	—	A	A
	With water	B_1	B_1 (partly)	A
Br^-	Without water	—	B_2	A
	With water	B_2	B_2	B_2 (partly)
I^-	Without water	—	B_1	B_1
	With water	B_1	B_1	B_1

* A is the identical spectrum with that of form A. B's are the spectra analogous to that of form B. Suffices differentiate the features of the N–H stretching and the imide V band (see text and Table I).

be understood in connection with the fact that the recrystallizing solvent for form B is water[6]. It is also seen however, that the ionic radii of the anion and the cation are concerned with this spectral change in both samples with and without water. In the alkali halide disk technique, the contamination of water is hardly avoidable since an excess of alkali halides which are usually hygroscopic must be used in comparison with the sample. As seen from Table III, the spectral change of diacetamide in the two-component system containing potassium bromide takes place only in the presence of water. Situations may be analogous for potassium bromide disks. The water adsorbed on the matrix partly gives rise to the spectral change related to the changes in intensities of the C–O stretching bands at 1734 and 1700 cm^{-1} previously mentioned.

Effect of Compression in the Disk Technique. — When the disk technique is applied to form B of diacetamide with potassium bromide or potassium chloride as the matrix, it is observed that the absorption bands due to form A appear partly[11]. This fact may be interpreted in terms of the degradation of crystal lattices under pressure as has been reported for substances with melting points below 90°C[3]. Since diacetamide (m. p. 81°C) is crystallized in form A from the molten liquid[6], it is not surprising that the degradation of form B is followed by the formation of form A. Thus, in the potassium bromide disk technique, the presence of water favors the change from form A to form B[12] while the compression favors the reverse change. The infrared spectra of diacetamide in potassium bromide disks may vary with changes in these two factors.

Interaction between Diacetamide and Various Alkali Halides. — Differences in the characteristic frequencies among the two-component systems under consideration may be interpreted in terms of interaction between the –CONHCO– group and the ions of alkali halides. As seen from Table I, the N–H (and N–D) stretching and the imide V (and V′) frequencies depend only on the anion. This fact suggests the occurrence of an ion-dipole interaction between the imide hydrogen atom and the anion. Such an interaction, if any, is expected to become weaker as the ionic radius of the anion increases. The tendency of frequency shifts shown in Table I is in accord with this expectation. As the anion is changed from Cl^- through Br^- up to I^-, the N–H (and N–D) stretching frequency increases while the imide V (and V′) frequency decreases. On the other hand, as seen from Table II, the frequencies of the bands due mainly to the vibrations of the C–O or C–N bonds depend on both the cation and the anion, suggesting that there occurs another ion-dipole interaction between the C–O oxygen atoms and the cation of alkali halides. If otherwise, the frequencies shown in Table II should depend also only on the anion. Thus, the frequency differences shown in Tables I and II suggest that the ion-dipole interaction between the anion and the N–H bond and that between the cation and the C–O bonds occur simultaneously. Table II shows that the imide I frequency increases with the ionic radii of both the anion and the cation, while the imide II, III and II′ frequencies show the reverse shifts. The frequency shifts of the characteristic bands of monosubstituted amides depending on the polarity of the molecule have been well investigated[13]. Since similar shifts on the change of polarity are expected for the corresponding characteristic frequencies of acyclic imides, the above fact may be taken as indicating that the polar

10) Estimation of the amount of water added was described in Experimental Part 3.

11) For the conditions of preparations of disks, see Experimental Part 4.

12) Strictly speaking, a certain form in which the -CONHCO- group takes a configuration similar to that in form B.

13) T. Miyazawa, *J. Chem. Soc. Japan, Pure Chem. Sec.* (*Nippon Kagaku Zasshi*), **77**, 321, 619 (1956).

character of the molecule of diacetamide becomes more predominant as the ionic radii of the anion and the cation of alkali halide decrease. Furthermore, the symmetric imide I frequencies shown in Table II are higher than that of form B of diacetamide (1734 cm^{-1}). This fact means that the bond order of the C=O bond involved in the ion-dipole interaction with the cations is greater than that of the C=O bond involved in hydrogen bond in form B. The ion-dipole interaction between the cations and the C=O bonds seems to be so weak that this does not affect the nature of the N-H bond appreciably, resulting in the independence of the frequencies shown in Table I on the cation.

All the molecules of diacetamide in the two-component system under consideration can be involved in the ion-dipole interactions supposed from the spectral change only if the crystal lattice of form A degrades completely. This was confirmed by the powder X-ray diffraction measurement. Figure 2, (a) shows the diffraction pattern of the intimate mixture of diacetamide and potassium iodide (the molar ratio being approximately one to one)[14]. The diffraction pattern of diacetamide in form A is shown in Fig. 2, (b). It is seen that no diffraction line in (a) appears in (b). Thus, the crystal lattice of form A of diacetamide does not remain in the two-component system with potassium iodide. Furthermore, the appearance of new diffraction lines in (b) obviously indicates the formation of different lattices. These results give support to the explanation of the spectral change in terms of the ion-dipole interactions suggested above.

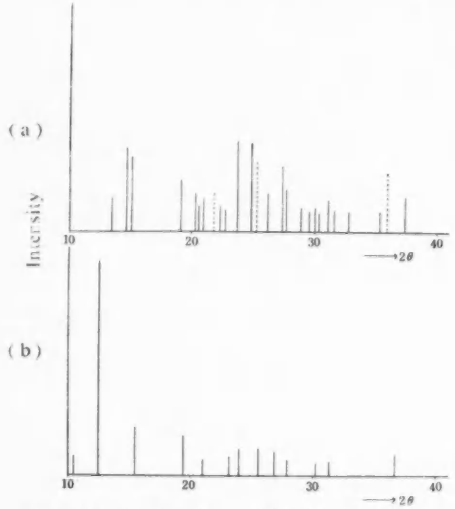

Fig. 2. Powder X-ray diffraction patterns.
(a) Diacetamide-KI system (Broken lines indicate the lines due to KI).
(b) Diacetamide in form A.

14) See Experimental Part 5.

Table III shows that larger anions and smaller cations are favorable to give rise to the spectral change. Discussions will now be conducted regarding this fact on the basis of the ion-dipole interactions. The spectral change under consideration seems to be the evidence for the change in the configuration of the -CONHCO- group. Owing to the repulsive force between two oxygen atoms of the -CONHCO- group in the trans-trans configuration, the molecule in this configuration is expected to be less stable than that in the trans-cis configuration. In fact, as reported in the preceding paper[2], this is true for diacetamide. However, if a large anion such as I^- approaches the hydrogen atom of a molecule in the trans-cis configuration, a strong repulsive force will be exerted between this anion and the oxygen atom at the cis position with respect to the hydrogen atom. This repulsive force may be expected to increase with the ionic radius of the anion. On the other hand, if a cation approaches the oxygen atoms of a molecule in the trans-trans configuration, the repulsive force between these two oxygen atoms will be partly compensated for by the attractive forces between this cation and the oxygen atoms. The smaller the cation is, the more closely it can approach these oxygen atoms, so that the repulsive force between these two oxygen atoms decreases with the ionic radius of the cation. Thus, the simultaneous effects of the cation and the anion will give rise to the inversion from the trans-cis configuration to the trans-trans one and, as the experiment shows, the larger the anion and the smaller the cation of alkali halide are, the more easily the inversion takes place.

The actual situation in the crystalline state may be somewhat different from the monomolecular model for the ion-dipole interaction supposed above. However, it is noticed here that such a simplified model is sufficient for the qualitative elucidation of the marked spectral change. From the above discussions, it is expected that the energy difference between the trans-cis and the trans-trans configuration is rather small for diacetamide. Besides the electrostatic and the steric contribution to the energy, the energy of the formation of hydrogen bond must be taken into account to estimate the energy difference between these two configurations. However, as the problem is related to the solid state, it is difficult to determine which of these two configurations has the greater advantage for the formation of

hydrogen bond, whose natures may be very different from each other for these two configurations.

Conclusion

It has been found that the alkali halide disk technique gives rise to marked changes in infrared spectra of diacetamide under some conditions. This phenomenon has been proved to be related to the contamination of water, to the compression in this technique and to the ionic radii of the anion and the cation of alkali halide used. Similar spectral changes of diacetamide on the addition of various alkali halides have been interpreted in terms of the inversion of the –CONHCO– group from the trans-cis to the trans-trans configuration. In a qualitative consideration on the basis of both the electrostatic interactions and the steric effect, it has been pointed out that the possibility of the inversion is closely related to the ionic radii of both the cation and the anion.

Experimental

1) Materials. — Commercially available G. P. grade sodium chloride and potassium chloride were purified according to Hales' method[15]. Commercially available E. P. grade lithium iodide and lithium bromide, G. P. grade potassium iodine, potassium bromide, sodium iodide, sodium bromide and lithium chloride were used without further purification. These alkali halides were ground to 200 mesh, dried over phosphorus pentoxide at 150~200°C, in 5~10 mmHg for 10~15 hr., and stocked over phosphorus pentoxide in a vacuum desiccator. The preparation of form A and form B of diacetamide and diacetamide-*d* has been described[6].

2) Preparation of Pastes. — Each of the alkali halides (2~3 mg.) described in 1 was added on a drop of Nujol or hexachlorobutadiene in an agate mill and ground by hand carefully. Then form A of diacetamide or diacetamide-*d* (2~3 mg.) was added and ground by hand rapidly for ca 30 sec. The pastes thus obtained were immediately subjected to measurement. The preceding paper will be referred to for the details of the measurement[6].

3) Effect of Water. — Water was added with a thin glass rod on the sample containing each of potassium iodide, potassium bromide, potassium chloride, sodium iodide, sodium bromide and sodium chloride, and pastes were prepared as described in 2. The amounts of both water and diacetamide were adjusted so that the relative intensities of the O–H and the N–H stretching bands were similar to those of the corresponding bands observed for the samples containing lithium halides. In most cases the transmittance for the band maxima near 3400 and 3200 cm^{-1} were 60~70% and 30~50% respectively.

4) Preparation of Disks. — Potassium chloride or potassium bromide (ca. 500 mg.) and diacetamide in form B (1~2 mg.) were ground by hand in an agate mill for 3~5 min., and pressed under 120 kg./cm^2 in 2~3 mmHg for ca. 5 min. to prepare a disk.

5) X-Ray Diffraction Measurement. — Form A of diacetamide (ca. 500 mg.) and potassium iodide (ca. 830 mg.) were ground by hand carefully for 20~30 min., allowed to stand in a vacuum desiccator containing phosphorus pentoxide for a day, and subjected to the diffraction measurement (Fig. 2, (a)). Form A of diacetamide was treated similarly except for the addition of potassium iodide (Fig. 2, (b)). A Rigaku Denki X-ray diffractometer with GM counter was used and the Cu-K_α line was adopted.

The authors express their thanks to Dr. Tatsuo Miyazawa of Osaka University for his kind advice. Thanks are also due to Dr. Kiyoshi Nakamura of Research Laboratory, Dainihon & Co. Ltd. for his kind advice and for X-ray diffraction measurements.

Faculty of Pharmacy
Kyoto Uuiversity
Sakyo-ku, Kyoto

15) J. L. Hales and W. Kynaston, *Analyst*, **79**, 702 (1954).

Some Observations on the Process of Dehydration and Rehydration of Gypsum by Means of Proton Magnetic Resonance

By Tatsuo SAITO

(Received February 15, 1961)

In the previous paper[1], the proton resonance spectra of thermally dehydrated products of alumina trihydrate in vacuo and their rehydrated specimens were measured and the relations between the phase transformation and the movements of bound water were investigated.

In the present paper, the process of thermal dehydration of natural gypsum in vacuo and their rehydration by saturated water vapor were investigated by the variation of line shapes of proton resonance spectra.

On the study of the process of dehydration and rehydration of gypsum extensive literatures have appeared. Several authors[2-8] deduced that the hemihydrate obtained from the partial dehydration of gypsum has a zeolitic type of structure such that water molecules can enter and leave it without destroying the lattice. Other authors[9] deduced that the calcium sulfate hemihydrate has a definite chemical composition and that the process of dehydration is not zeolitic in character. On the other hand, Mitsuki[10] and Razouk[8] explained that the dehydration of gypsum in vacuo leads directly to the formation of a soluble anhydrite.

The present author found by the observations of the proton resonance spectra that the soluble anhydrite produced by the thermal dehydration of gypsum occludes some quantity of movable water in the space of its crystal lattice and that the hemihydrate obtained by the rehydration of dehydrated gypsum has a definite crystal water and some quantity of movable water.

Experimental

Experimental Apparatus.—The NMR measurements were performed at room temperature using the modulation technique described by Bloembergen, Purcell and Pound[11]. The detecting apparatus[12] has the ordinary constitution, which is composed of an r−f oscillator, an r−f amplifier, a detector, an audio frequency amplifier, a lock-in amplifier and a recorder. The pole face diameter of the permanent magnet is 140 mm. and the air gap length is 40 mm. The magnet has the field intensity of 4140 gauss, with a uniformity of 2×10^{-5} over the whole sample volume. Continuous variation of the static magnetic field linear with time was achieved by an automatic current scanning apparatus[13].

Specimens.—The starting material used in this experiment was fibrous gypsum (Produces in Iwasawa, Iwate Prefecture) containing the stoichiometric amount of water according to the formula, $CaSO_4\cdot 2H_2O$. The X-ray diffraction diagram of this material is shown in Fig. 1.

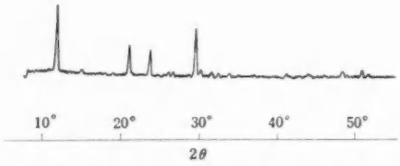

Fig. 1. X-ray diagram of the starting material, gypsum.

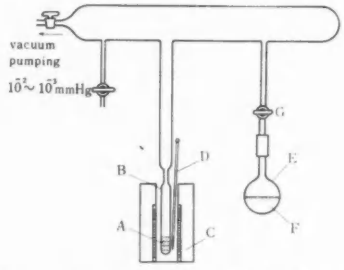

A: sample cake (dia. 8 mm.) B: resonance sample tube C: electric furnace D: thermometer E: flask (100 cc.) F: distilled water in evacuated flask G: cock.

Fig. 2. Apparatus used for the preparation of the specimens.

1) T. Saito, This Bulletin, **34**, 757 (1961).
2) G. Linck and H. Jung, *Z. anorg. allgem. Chem.*, **137**, 407 (1924).
3) C. S. Gibson and S. Holt, *J. Chem. Soc.*, **1933**, 638.
4) W. A. Caspari, *Proc. Roy. Soc.*, **A, 155**, 41 (1936).
5) C. W. Bunn, *J. Sci. Instru.*, **18**, 70 (1941).
6) S. J. Gregg and E. G. J. Willing, *J. Chem. Soc.*, **1951**, 2916.
7) R. Kiriyama and H. Ibamoto, This Bulletin, **26**, 109 (1953).
8) R. I. Razouk, A. S. Salem and R. S. Mikhail, *J. Phys. Chem.*, **64**, 1350 (1960).
9) H. B. Weiser, W. O. Milligan and W. C. Ekholm, *J. Am. Chem. Soc.*, **58**, 1261 (1936); H. B. Weiser and W. O. Milligan, ibid., **59**, 1456 (1937).
10) C. Mitsuki, *J. Ceram. Assoc. Japan*, **60**, 92 (1952).
11) N. Bloembergen, E. M. Purcell and R. V. Pound, *Phys. Rev.*, **73**, 679 (1948).
12) S. Yano, *J. Phys. Soc. Japan*, **14**, 952 (1959).
13) T. Sidei, S. Yano and S. Sasaki, *J. Appl. Phys. Japan*, **27**, 513 (1958).

Each dehydration-specimen or rehydration-specimen was prepared in the vacuum system illustrated in Fig. 2. To prepare each specimen by thermal dehydration in vacuo, about 2 g. of powdered gypsum was pressed in the form of small cakes A and put into the resonance sample tube B which was connected to the high vacuum system. This sample tube B was heated from outside by an electric furnace C for 3 hr. in a high vacuum and was then sealed off. The dehydration temperatures were 70, 80, 90, 95, 100, 105, 110, 115, 125, 150 and 200°C. For the preparation of rehydration-specimens, each sample after the treatment of the thermal dehydration in vacuo was immediately exposed for 15 hr. to saturated water vapor which was introduced through the cock G from the flask E at room temperature. Then, each sample tube containing this rehydrated specimen was pumped out to a high vacuum for 12 hrs. at room temperature and was then sealed off. In this experiment, the temperature of the dehydration in vacuo was 80, 95, 110, 125, 135, 150, 165, 180, 220, 250 and 300°C.

X-Ray powder diffraction was made with a "Geigerflex" recording X-ray spectrometer using filtered CuK_α radiation.

Results and Discussion

Thermal Dehydration in vacuo.—The experimental derivative curves of the proton resonance obtained from the dehydrated products are shown in Figs. 3 and 4. The photographs of a and b in Fig. 4 show the recorded spectra of the typical derivative curves.

As is seen in Fig. 3, the derivative curve of the starting material shows a typical line shape of two spin system[14] with broad width of about 14 gauss. While in the line shape of the specimen dehydrated at 70°C a single peak appeared overlapping the line of the starting material at its center, for the specimen dehydrated at 90°C only the center peak was observed. This characteristic single sharp peak was also observed for the specimen dehydrated at 150°C, while for the specimen dehydrated at 200°C no proton resonance signal was observed. It is known that this single sharp peak of proton resonance originates from the water molecules which are in the thermal motion.

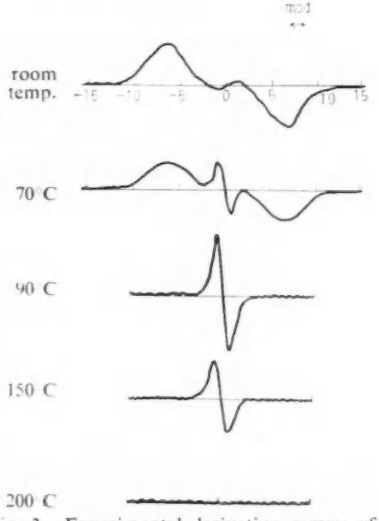

Fig. 3. Experimental derivative curves of proton resonance in the dehydration-specimens.

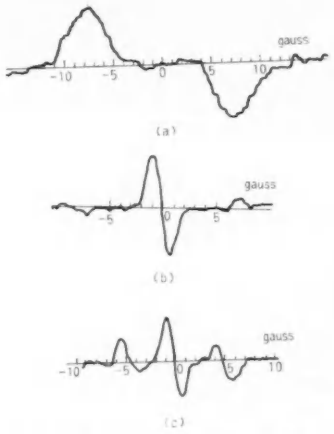

(a) starting material, gypsum.
(b) dehydrated gypsum at 95°C.
(c) rehydrated product of (b)

Fig. 4. Recorded derivatives of proton resonance in the dehydration or rehydration-specimens.

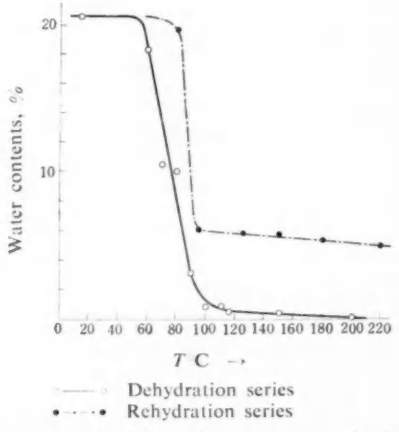

Fig. 5. Variation of water contents in the dehydration or rehydration-specimens the dehydration temperature.

14) G. E. Pake, *J. Chem. Phys.*, **16**, 327 (1948).

To compare the above results with the change of chemical composition, the water content of each dehydration-specimen was measured and the values of percentage of weight loss at 800°C were plotted in Fig. 5 as the function of the dehydration temperature.

As is seen in Fig. 5, the water content decreases suddenly at about 70°C from the value corresponding to dihydrate to the value of 1~2% corresponding to soluble anhydrite, while the remaining water can not be completely removed even at 150°C and in this process of dehydration the steps corresponding to the formation of hemihydrate were not observed. This is in agreement with the results obtained by other authors[6,10].

In the X-ray diffraction studies, the crystallographical phase transformation was observed for the dehydration at about 70°C as shown in Fig. 6.

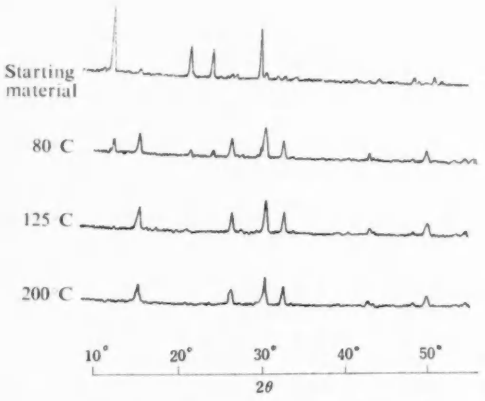

Fig. 6. X-ray diffraction diagrams of the dehydration-specimens.

From these experimental results, it is assumed that the decomposition of this gypsum occurs at 60~70°C, that some quantity of water released during the dehydration remains in the space of the crystal lattice which is introduced by the dehydration and that this movable water is gradually removed with rises of temperature, having no influence upon the crystal lattice.

On the other hand, the crystal structure of gypsum[15] may be described as a complex layer structure in which the layers are bound together by bonds from water molecules, each of which is joined to a Ca^{2+}, O atom of a SO_4^{2-} ion of one layer and an O atom of SO_4^{2-} ion of an adjacent layer.

It might be concluded from the experiments described above that these O-H-O bonds are so weak that the crystal structure of gypsum can be broken down even at low temperature and that the evolution of the binding water may occur at the same time, while some quantity of this water may remain in the space of the lattice which is introduced by the decomposition at low temperature.

Rehydration of the Dehydration-Specimens in vacuo. The NMR measurements were carried out on the specimens prepared by the rehydration of gypsum thermally dehydrated in vacuo. The typical experimental derivative curves obtained from these measurements are shown in Fig. 7.

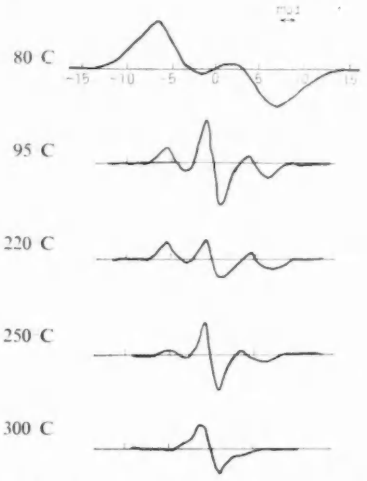

Fig. 7. Experimental derivative curves of proton resonance in the rehydration-specimens.

As is seen in Fig. 7, the rehydrated specimens of gypsum dehydrated at the temperature from 95 to 250°C show the same line shapes. The photograph of c in Fig. 4 shows the recorded spectrum of this typical derivative curve, while the rehydrated specimen of gypsum dehydrated at 80°C shows the same line shape as that of the starting material. From the measurements of the water content of these rehydrated specimens, it was found that the line shapes observed for the rehydrated specimens of gypsum dehydrated from 95 to 250°C correspond to the phase of hemihydrate, $CaSO_4 \cdot 1/2\,H_2O$. The values of the water content of these specimens were also plotted in Fig. 5 as the function of the dehydration temperature.

While these rehydration-specimens corresponding to hemihydrate were crystallographically quite similar to the dehydrated gypsum corresponding to soluble anhydrite from the result of the X-ray study, the line

15) A. F. Wells, "Structural Inorganic Chemistry", Oxford University Press, London (1950), p. 440.

shapes observed for these rehydration-specimens are different from that for the dehydrated gypsum and are presumably understood as the signal of three spin type with an intensive center peak. The line width of this line shape (the separation between peaks in side band) was about 11~12 gauss.

The product obtained from this hemihydrate by the thermal treatment at 100°C for 3 hr. in vacuo showed only the single center peak corresponding to the movable water. This movable water may also be explained as the zeolitic water existing in the space of the crystal lattice which was introduced by the dehydration of hemihydrate.

On the other hand, the rate of rehydration of gypsum dehydrated at 125°C by saturated water vapor was examined by NMR measurements and it was found that all the specimens obtained from the rehydration for one to 48 hr. showed the same line shapes as that corresponding to hemihydrate. This result means that hemihydrate is considerably stable against saturated water vapor and that the rate of hydration of soluble anhydrite is very high. This result is in agreement with the result obtained by other authors[8].

However, gypsum dehydrated at 80°C is easily rehydrated by saturated water vapor directly to dihydrate. This fact means that the product dehydrated at 80°C has the pseudolattice of gypsum and transforms easily to the phase of dihydrate by the addition of water molecules.

Summary

1) On the thermal dehydration in vacuo, the characteristic single sharp peak of proton resonance was observed for the specimens dehydrated at the temperature from 70 to 150°C.

It is assumed that this single sharp peak is attributed to the zeolitic water probably existing in the space of the crystal lattice of soluble anhydrite and that this zeolitic water can be interpreted as being a part of the water molecules which originate from dihydrate during the thermal decomposition.

2) Calcium sulfate hemihydrate was formed by the rehydration of gypsum dehydrated in vacuo. This hemihydrate showed the proton resonance spectrum corresponding to the signal of three spin type with an intensive center peak. This intensive center peak can be interpreted as an indication of the movable water existing in the space of the crystal lattice of hemihydrate.

3) This hemihydrate was considerably stable under the atmosphere of saturated water vapor. This was ascertained by the NMR measurements.

The author wishes to express his sincere thanks to Dr. Y. Kotera of this Institute for his kind advice.

The author also wishes to express his hearty thanks to Professor Tokutaro Hagiwara of Hiroshima University for his kind direction and also to Professor Tunahiko Sidei and Dr. Syukuro Yano of Kyoto University for their continual guidance and encouragement throughout this study.

Government Chemical Industrial Research Institute, Tokyo
Shibuya-ku, Tokyo

Studies on the Surface Structure of Porous Materials

By Akie Tsuruizumi

(Received December 29, 1960)

It has been generally accepted that the adsorption of gases on adsorbents such as active carbon and silica gel is both physical and chemical in nature, the latter being caused by the formation of complex surface compounds with residual active groups as well as by an ion exchange effect on the surface. The chemisorption plays a role in the earlier stage of the adsorption process, while the general behavior of the adsorption is characterized by the physical behavior.

Pore structure of the surface, which is important for both the theoretical and practical studies, could be visualized by combining

various methods such as porosimetries and adsorption measurements. A preferential physical adsorption of adsorbates with various molecular sizes could be used most effectively for classification of the pore-sizes.

In the present paper, the pore structures of various adsorbents such as active carbon and silica gel were studied. The results of adsorption measurements with water vapor and various organic vapors, the BET method using nitrogen, and mercury and water prosimetry were analyzed, and the size, shape and chemical nature of the pores were discussed in detail.

An emphasis was placed on the deviations from the prevailing theories, which are based on a simple pore model such as the cylindrical one. The analysis of the deviations enabled us to depict the shape of the pore, being of narrow-neck or ink-bottle shape. In addition, a new term, 'sieving coefficient' was proposed, which would be quite profitable for classification of the adsorbents.

Theoretical

The pores are classified into the following three groups: micro-pores, ca. 10 Å in radii; transitional pores, 100~500 Å; micro-pores, 10000 Å. The transitional and micro-pore distributions are determined empirically by a mercury porosimetry[1]. The micro-pore distribution is calculated by Thomson's formula,

$$r = -\frac{2v\sigma\cos\theta}{RT\ln P/P_0} \tag{1}$$

where v is the molecular volume, θ the contact angle, σ the surface tension, r the pore radius, P the vapor pressure of the meniscus, and P_0 that of the bulk phase.

A total volume of pores with a radius in a range between r and $r+dr$ is represented by

$$dv = D(r)dr \tag{2}$$

where v is the total volume of the pores, and $D(r)$ the distribution function of the pore radii. The function $D(r)$ is obtained by graphical differentiation of a curve drawn by plotting the total amount of adsorption against the radii of the pores. A plot of $dv/d\log r$ vs. $\log r$ was similar to the Gaussian probability curve.

Thomson's equation is implicitly based on the following assumptions: i) Adsorption of water is caused by the capillary condensation. ii) The pore is cylindrical in shape with a uniform diameter. iii) The water adsorbed in the pore has the same density as that in bulk phase.

1) H. L. Ritter and L. C. Drack, *Ind. Eng. Chem., Anal. Ed.*, **17**, 782 (1945).

Cohan[2], McBain[3] and Higuchi[4] have pointed out that the size distribution function of pores having diameters less than 10 Å can not be calculated by Thomson's equation. If the radii of pores are less than 10 Å, the condensation of water vapor inside the pore is impossible, because the diameter of the void space in the pore is reduced to 2~3 molecular sizes by preliminary formation of a monolyer on the inside wall in the earlier stage of the adsorption process.

In the range of higher radius, a minor correction for pore radius less than six per cent is necessary[5]. This is due to the reduction of the pore space by the formation of the adsorption film on the wall. This correction was, however, not applied in the present study. Actually, pore-size distribution curves obtained by using Thomson's equation are in good agreement with those obtained from the adsorption of nitrogen as has been shown by Joyer[6], with those obtained by the adsorption of benzene vapor and by the mercury porosimetry reported by the present author[7].

The radius of a cylindrical pore is given by the equation[8]

$$pr = 2\pi\sigma\cos\theta \tag{3}$$

where p is the applied pressure to press the mercury into the pore, σ the surface tension of mercury, r the redius of the pore and θ the contact angle.

Expressing p in kg./cm^2, r in cm., and putting $\sigma = 480$ dyn./cm. and $\theta = 140°$C[9,10], Eq. 3 is reduced to

$$pr = 7.5\times10^{-4} \tag{4}$$

If the pores are ink-bottle or bottle-neck shaped, the appearent radii obtained by the porosimetry are those of narrow-neck shape, being less than the true ones.

Experimental

Materials.—*Sugar Charcoals* (S_3, S_4, SZ_3, SZ_4).—S_3, S_4[11]: An aqueous solution of commercial white sugar decolored with an active carbon was passed through a column of ion exchange resins (Amberlite

2) L. H. Cohan, *J. Am. Chem. Soc.*, **60**, 433 (1938).
3) J. W. McBain, ibid., **57**, 691 (1935).
4) I. Higuchi, *Sci. Pap. Inst. Phys. Chem. Res.*, **20**, 130 (1941).
5) M. M. Dubinin, *Quart. Rev.*, **9**, 109 (1955).
6) L. G. Joyer, E. P. Barset and R. Skold, *J. Am. Chem. Soc.*, **73**, 3155 (1951).
7) A. Tsuruizumi, *J. Chem. Soc. Japan, Pure Chem. Sec.* (*Nippon Kagaku Zasshi*), **81**, 870 (1960).
8) E. W. Washburn, *Proc. Natl. Acad. Sci.*, **7**, 115 (1921).
9) H. L. Ritter and L. C. Drake, *Ind. Eng. Chem., Anal. Ed.*, **17**, 782, 787 (1945).
10) A. J. Juhola and E. O. Wiig, *J. Am. Chem. Soc.*, **71**, 2069, 2078 (1949).
11) A. Tsuruizumi, *J. Chem. Soc. Japan, Pure Chem. Sec.* (*Nipoon Kagaku Zasshi*), **79**, 266 (1957).

TABLE I. CLASSIFICATION OF PORE VOLUME

Sample	A v_1 Micro-P. vol. to 50 Å (r) cc./g.	B[a] v_2 Trans.-P. vol. 75~1000 Å cc./g.	C[b] v_3 Macro-P. vol. 1000~43000 Å cc./g.	D Pressed total mercury vol. B+C cc./g.	E V_t Total pore vol. A+D=A+B+C cc./g.
S_3	0.1205	0.0152	0.0590	0.0742	0.1947
S_4	0.1554	0.0162	0.0410	0.0572	0.2126
SZ_3	0.7950	0.0350	0.0680	0.1030	0.8980
SZ_4	0.8850	0.0370	0.2200	0.2570	1.1420
M. S.[c]	0.2140	0.0680	0.1330	0.2010	0.4150
Silica[d]	0.3750	0.0800	0.0410	0.1210	0.4960

a) B, b) C calculated from mercury porosimetry.
c) Molecular sieve 5 A.
d) Silica gel No. 28.

IRA 400 and IRC 120) repeatedly until its electrical conductivity was reduced to as low as 4~6 $\mu\mho$/cm. The crystals of the sugar purified by recrystallization from ethanol were dried at 40°C under 5~10 mmHg. The ashes in 10 g. of the purified sugar were undetectable with a chemical balance. The sugar placed on a quartz boat in a quartz combustion tube in an electric furnace was carbonized in a stream of nitrogen gas with a flow rate of 20~30 ml./min. The traces of oxygen in this were removed beforehand by passing through a layer of heated reduced copper. The temperature of the furnace was raised at a rate of 5°C/min., and then kept at a required temperature for 30 min. The rate of temperature rise was a factor to determine the pore structure. Carbonization temperatures and yields were as follows: S_3, 800°C and 23.44%; S_4, 1000°C and 21.30%. Granules of 70~100 meshes were collected with sieves. Spectroscopic analysis: Al (−), Si (+),·····.

SZ_3, SZ_4: A mixture of 10 g. of the purified sugar and 20 g. of zinc chloride (G. P. grade) with a few drops of hydrochloric acid was heated to 200°C on a evaporating dish. The charcoals obtained by the same carbonization process as that mentioned above from the residues were boiled with hydrochloric acid (1:1) to remove zinc chloride, washed with distilled water till pH values of the filtrates became 5~6, and dried for 4~6 hr. at 150~170°C. Granules of 70~100 meshes were collected. Ashes in 1 g. of the sample were undetectable with a chemical balance. No traces of zinc were detected by the dichizon method[12]. Spectroscopic analysis: Al (−), Mg(±), Si(+).

*Molecular Sieve 5A**. — Composition: $Me^{12}/n\{(AlO_2)_{12}-(SiO_2)_{12}\}27-30H_2O$, (Me: Ca, Na). Highly polar. Pore diameter noted by the manufacturer was 5 Å.

Silica Gel No. 28. — A gel precipitated from 3 N sodium silicate and 4 N sulfuric acid at a controlled pH of 5.5 was washed with water, electrodialized for 100 hr., dried at 20~30°C, and finally at 120~150°C. 70~100 meshes.

3SZ$_4$, 6SZ$_4$.—A sample of SZ_4 impregnated with 2 per cent nitrobenzene solution of polyvinyl chloride (Geon 103EP) was carbonized by the same method as that mentioned above at 1000°C. The process was repeated three times for $3SZ_4$ and six times for $6SZ_4$. The pore volumes and internal total wall areas were shown in Tables I and II.

TABLE II. TOTAL PORE VOLUME BY WATER OR MERCURY DISPLACEMENT METHODS

Sample	F Water displ. vol. cc./g.	G Mercury displ. vol. cc./g.	H Total pore vol. G−F cc./g.
SZ_3	0.540	1.541	1.001
SZ_4	0.528	1.580	1.051

TABLE III. EQUIVALENT INTERNAL WALL AREA OF EACH OF DISPERSE PORTIONS

Surface area by $S=2V_1/\bar{r}$

Sample	S_1 Surface area of micro-P. $m^2/g.$	S_2 Surface area of trans.-P. $m^2/g.$	S_3 Surface area of macro-P. $m^2/g.$	Surface area BET $m^2/g.$
S_3	241 [8.0][e] (10)[f]	2.4 (125.9)	0.11 (10.000)	400
S_4	380 [7.5] (8.2)	2.5 (125.9)	0.08 (10.000)	450
SZ_3	800 [15] (18.0)	2.0	0.14	1400
SZ_4	1180 [10] (15.0)	6.0	0.44	1600
M. S.[c]	660 [2.0] (6.5)	13.0	2.0	460
Silica[d]	681 [7.5] (11.0)	16.0	0.08	720

e) [Å] maximum distribution radius.
f) (Å) mean radius.

Formic Acid. — A guaranteed grade reagent was dehydrated with a boric acid of high melting point by being allowed to stand for a few days, and distilled under reduced pressure. The process was repeated. N_D^{20}: 1.3716.

n-Propionic Acid and n-Butyric Acid.—Guaranteed grade reagents supplied by Tokyo Oka Co., were

12) E. B. Sandell, "Colorimetric Determination of Metals", Interscience Publishers, Inc., New York (1950).
* The product of Linde Air Product Co., U. S. A.

used without further purification. N_D^{20}: 1.3873 and 1.3990.

n-Valeric Acid.—A guaranteed grade reagent supplied by Tokyo Oka Co., was used without further purification.

Benzene.—A guaranteed grade reagent supplied from Wako Junyaku Co., was dehydrated with metallic sodium and distilled under reduced pressure.

Measurements of Adsorption.—The adsorption of water vapor was measured at 30°C with a quartz spring balance of sensitivity of 2.4630 mg./mm. using a cathetometer graduated to 1/20 mm. The samples were out-gased at various temperatures for 6 hr. under 10^{-5} mmHg. The temperatures are: for sugar carbons, 300~350; for molecular sieve 5A, 250~300; for silica gel No. 28, 150~200°C. The poresize distribution was calculated from the desorption isotherm, the contact angle being assumed to be $\cos\theta = 0.49$[10]. Adsorptions of monocarboxylic acids and benzene were measured with a quartz spring balance at 38±0.1°C. The adsorbents were out-gased by heating at 300~350°C and 10^{-5} mmHg.

Measurement of Pore Volume.—The total pore volume was measured by a water and mercury

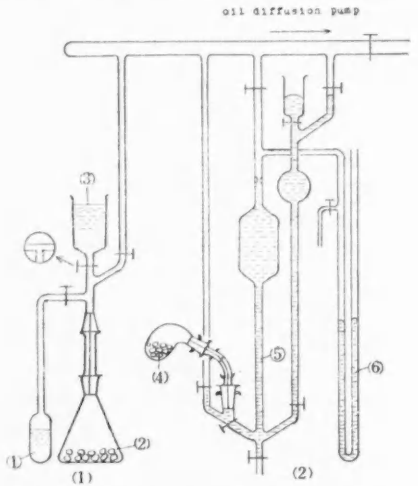

Fig. 1. Displacement volume measurement apparatus.
(1) Apparent density measurement by liquid displacement
(2) Apparent density measurement by mercury displacement
①③ Water ②④ Adsorbent
⑤ Mercury burette
⑥ Mercury manometer

displacement method using a modified Juhola and Wiig's apparatus[10] shown in Fig. 1. The liquid water was introduced into a flask from an upper reservoir after the samples in the flask adsorbed such an amount of water vapor from a side tube that the adsorption equilibrium was reached. The total pore volume was calculated from the difference of volum of water and mercury displaced.

Measurement of BET Area.—The BET surface area was obtained with a usual adsorption apparatus using nitrogen gas as an adsorbate.

Mercury Porosimetry.—A usual mercury porosimeter was used. In order to obtain high accuracy, the diameter of both platinum wire and dilatometer were made as small as possible. The applied pressure was measured with a gauge, and the maximum pressure reached was 1500 kg./cm^2. The temperature was kept at 0°C.

Experimental Results and Discussion

Pore Distribution.—*S_3 and S_4.*—Plots of $dv/d\log r$ vs. $\log r$ (Å) for the samples S_3 and S_4 are shown in Fig. 2, where a tri-disperse distribution is observed. The peaks are designated as micro-, transitional and macro-pore from left to right in the figure. The shape of the transitional distribution curve is changed by modification of the carbonization or activation condition as is shown later. The distribution curves for a range 3~4 in $\log r$ are not shown as they are less than 10^{-4}, being scaled out.

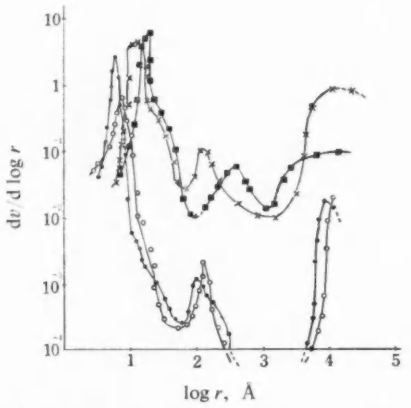

Fig. 2. Pore-size distribution in sugar carbons.
—●— S_4 —■— SZ_3
—○— S_3 —×— SZ_4

SZ_3 and SZ_4.—The pore-size distribution curves are also tri-disperse as a shown in Fig. 2. As is seen in Table IV, the total pore volume estimated from the results of mercury and water displacement method is in good agreement with that calculated as the total sum of the respective volumes of micro-, transitional, and macro-pores. The greater part of the surface areas of the sugar carbons (S_3, S_4, SZ_3 and SZ_4) being composed of the areas of the internal wall of the micro-pores, the number of transitional and macro-pores are too low to give any influence on the adsorption characteristics.

TABLE IV. CLASSIFICATION OF PORE VOLUME

Sample	A v_1 Micro-P. vol. to 50 Å (r) cc./g.	B[b] v_2 Trans.-P. vol. 75~1000 Å cc./g.	C[b] v_3 Macro-P. vol. 1000~43000 Å cc./g.	D Total mercury vol. pressed in B+C cc./g.	E V_t Total P. vol. A+D =A+B+C cc./g.	F[a] Water displ. vol. cc./g.	G[a] Mercury displ. vol. cc./g.	H Total pore vol. G−F cc./g.
SZ_4	0.885	0.037	0.220	0.257	1.142	0.528	1.580	1.051
$3SZ_4$	0.730	0.023	0.079	0.102	0.832	0.539	1.337	0.798
$6SZ_4$	0.620	0.018	0.065	0.083	0.703	0.535	1.207	0.672
S_4	0.155	0.016	0.041	0.057	0.212	—	—	—
Silica gel No. 28	0.375	0.080	0.041	0.121	0.496	—	—	—

a) Pore volume by water and mercury displacement methods.
b) Calculated from mercury porosimetry.

Molecular Sieve 5A. — The micro-pore distribution curves of molecular sieve 5A were obtained by assuming $\cos\theta=1$ in Thomson's equation because of its high polarity. A di-disperse distribution curve with sharp peaks is seen in Fig. 3.

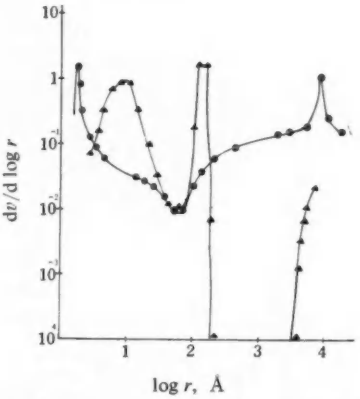

Fig. 3. Pore-size distribution in a silica gel and the molecular sievs 5A.
—▲— SiO_2 gel —⊗— M.S. (5A)

Silica Gel No. 28. — As is seen in Fig. 3, a tri-distribution curve is observed. The curve is, however, broken at a range $\log r=2\sim3$. The macro-pores are presumed to be produced by the secondary treatment, and the distribution curve is originally di-disperse. The total volumes of pores calculated from the respective peaks in the figures are shown in Table IV.

If it is assumed that the pore is a cylinder with a circular section, the total volume of the pores, V_t, and the inner surface area, S, in each peak can be calculated by the formula

$$V_t=\pi(\bar{r})^2L \qquad (5)$$

where $\bar{r}$ is an average radius of pores and L the length of the cylinder. The inner surface area is related to the pore radius by the equation

$$S=2\pi\bar{r}L \qquad (6)$$

In Tables III and V, the inner wall areas calculated by the equation

$$S=2V_t/\bar{r} \qquad (7)$$

and the BET area are compared, where the coincidence is noted only in the case of the silica gel. The discrepancy seen in the tables may be ascribed to both the complexity of the pore structure and a per-sorption[13]. Another minor factor to be taken into account is the difference of densities of nitrogen in the submicropore and in bulk phase. The BET area is usually greater than the true area.

TABLE V. INTERNAL WALL AREA OF DISPERSE

Sample	Surface area by $S=2V_t/\bar{r}$: Surface area of micro-P. $m^2/g.$	Surface area of trans.-P. $m^2/g.$	Surface area of macro-P. $m^2/g.$	Surface area by BET $m^2/g.$
SZ_4	1180 [10][a] (15.0)[b]	6.0	0.44	1600
$3SZ_4$	1000 [9.5] (14.5)	3.2	0.16	1460
$6SZ_4$	858 [9.0] (14.1)	2.8	0.13	1300
S_4	380 [7.5] (8.2)	2.5	0.08	450
Silica gel No. 28	681 [7.5] (11.0)	16.0	0.08	720

a) [Å] maximum distribution radius.
b) (Å) mean radius.

The total wall area of the silica gel No. 28, S (total sum of the areas of the micropores, transitional pores and macro-pores) is approximately 700 m./g. (Table V), and is in

13) A. Tsuruizumi, *J. Chem. Soc. Japan, Pure Chem. Sec. (Nippon Kagaku Zasshi)*, **79**, 142 (1957).

agreement with the nitrogen BET area of 720 m./g. The areas obtained by the various fatty acids are ranged between 680 and 750 m^2/g. as will be shown later. These facts prove that there are only a few pores of a narrow-neck or ink-bottle type, which complicate the nature of the adsorption. The radius of the maximum distribution in the molecular sieve 5A is ca. 2 Å.

Adsorption of Organic Vapors

The adsorption isotherms of both monocarboxylic acids and benzene vapor were S-shape for all the adsorbents studied, and fit the BET equation well. The adsorption isotherms of benzene vapor on the samples $3SZ_4$ and $6SZ_4$ are shown in Fig. 4. The samples

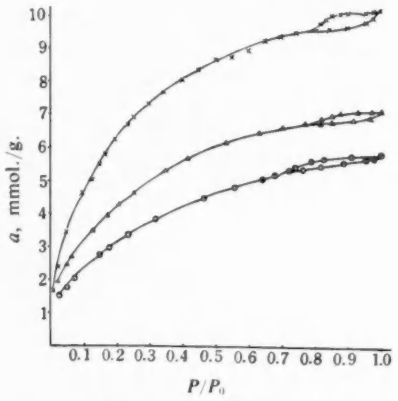

Fig. 4. Adsorption isotherm of benzene.
—×— SZ_4 —△— $3SZ_4$ —○— $6SZ_4$

$3SZ_4$ and $6SZ_4$ were prepared by carbonizing the sample SZ_4 impregnated with the nitrobenzene solution of polyvinyl chloride. The pores of the SZ_4 carbon were filled up to some extent, and the transitional pores were affected most sensitively. The transitional pore distribution curves for SZ_4, $3SZ_4$ and $6SZ_4$ obtained from the desorption isotherms of benzene vapor by using Thomson's equation are shown in Fig. 5, and the full distribution curves drawn by annexing the distribution curves estimated from the data of mercury porosimetry are shown in Fig. 6. The tri-disperse distribution is seen in the figure, and in each peak shift regularly according to the decrease in the pore volumes. The displacement of the transitional peaks are most conspicuous.

The distribution curve of the transitional pores estimated from the benzene adsorption shown in Fig. 4 was slightly higher than those obtained by the mercury porosimetry (Fig. 5).

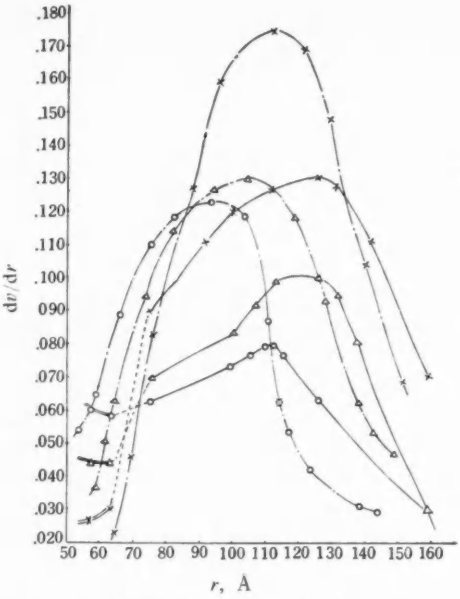

Fig. 5. Distribution of transitional-pores.
—·—· Calculated from benzene adsorption
——— Calculated from mercury porosimetry
═══ Calculated from water vapor adsorption (in the range of micro-pore distribution).
—×— SZ_4 —△— $3SZ_4$ —○— $6SZ_4$

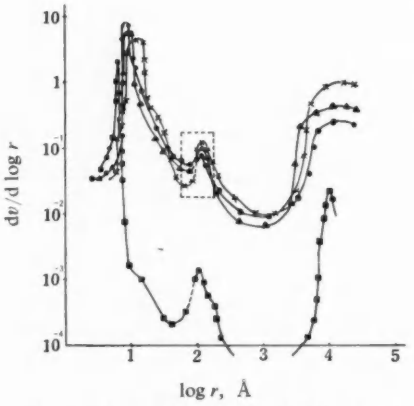

Fig. 6. Carbons pore-size distribution in sugar.
—×— SZ_4 —●— $6SZ_4$
—▲— $3SZ_4$ —■— S_4

The disagreement of the two curves may be ascribed to the errors arising from the application of Thomson's equation which is based on a number of assumptions inadequate in the

present case. Since in the mercury porosimetry no ambiguous assumptions are adduced other than the independency of the contact angle with respect to the applied pressure, the result of the porosimetry is most reliable.

A range of the distribution curve (shown by dotted lines in Figs. 5 and 6) between the micro-pore and transitional pore can not be determined precisely by the mercury porosimetry. Since the curves shown by broken lines with dots in Fig. 5 obtained by the adsorption method using benzene vapor were continuous in full range, it is quite resonable to bridge the gap between the solid line of the mercury porosimetry and the double line of the water adsorption with the dotted line as is shown in Fig. 5.

In the previous papers[11,13,14], the present author has suggested that the pore distribution of the active carbon is tri-disperse. The existence of the micro-pores of about molecular diameter size, the transitional pores (ca. 100 Å), and the macro-pores (ca. 100 μ) as cracks or cavities is hereby confirmed.

Effective areas of the adsorbents, calculated from the amounts of adsorbates in a monolayer coverage (Figs. 7, 8 and 9) by using the B-point method[15] are shown in Table VI. The

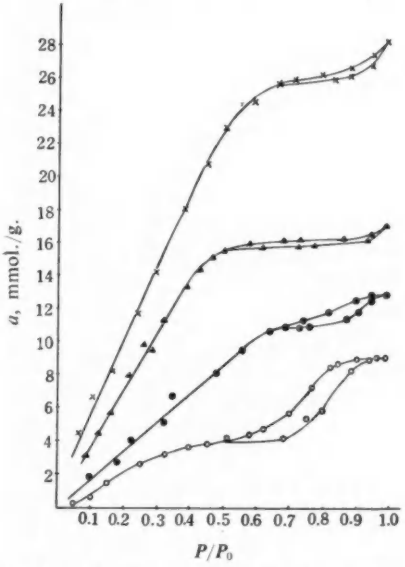

Fig. 7. Adsorption isotherms of *n*-carboxylic acid vapors (SZ_4, 38±0.1°C).
—○— *n*-Butyric acid —▲— Acetic acid
—○— *n*-Propionic acid —×— Formic acid

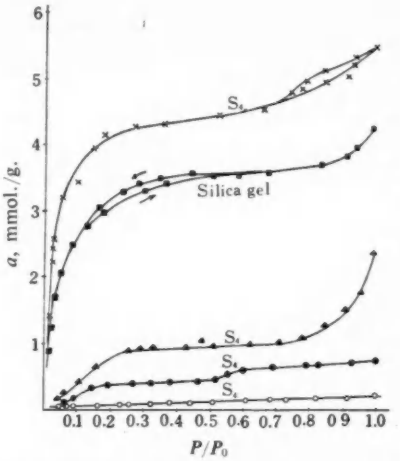

Fig. 8. Adsorption isotherms fo *n*-carboxylic acid vapors (38±0.1°C).
—○— *n*-Butyric acid —×— Formic acid
—●— *n*-Propionic acid —■— Benzene
—▲— Acetic acid

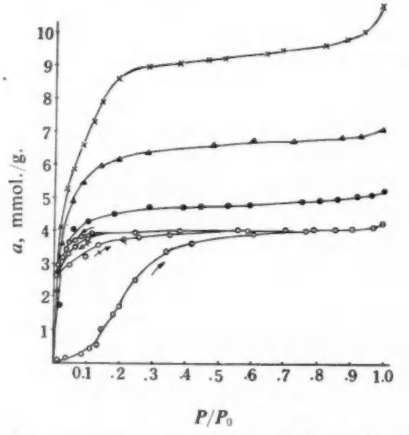

Fig. 9. Adsorption isotherms of *n*-carboxylic acid vapors (silica gel, 38±0.1°C).
⟶ —→ Adsorption ⟵ ⟶ First process
⟵ ←— Desorption ⟵ ⟶ Second process
—○— *n*-Butyric acid —▲— Acetic acid
—●— *n*-Propionic acid —×— Formic acid

sectional areas of the adsorbate molecules used for the calculation of the surface area are listed in Table VI. These were determined by the adsorption on SZ_4, S_4 and silica gel No. 28. The surface areas of sugar carbons obtained with formic and acetic acid are higher than the BET areas, while the higher acids gave lower

14) A. Tsuruizumi, ibid., **79**, 273 (1957).
15) A. Blackburn and J. J. Kipling, *J. Chem. Soc.*, **1955**, 1493.

TABLE VI. SURFACE AREA OBTAINED FROM ADSORPTION ISOTHERM

Adsorbates	Adsorptive sectional area, Å²	Surface area, m²/g. S_4 [450][a]	SZ_4 [1600]	Silica gel No. 28 [720]
Formic acid	13.38	342.0	2365.0	717.0
Acetic acid	19.58	106.0	1828.0	755.0
n-Propionic acid	25.01	55.0	1600.0	716.0
Benzene	29.13	26.5	1100.0	723.0
n-Heptane	(29.20)[b]	19.0	850.0	680.0
n-Butyric acid	31.35	0.9	717.0	730.0

a) [ ] Surface area from BET method.
b) If adsorptive section is circle from Fig. 10, its radius get 3.05Å as adsorptive sectional area is calculated 29.20Å².

values. This discrepancy can be explained as follows. The molecules of formic and acetic acid are small enough to diffuse into fine pores, and before the formation of a uniform monolayer, a capillary condensation takes place. This increases the apparent surface area. The critical temperatures of the formic and acetic acid are lower than those of the higher acids, but this is not the predominant factor for the earlier occurrence of the capillary condensation. The same situation was found in the adsorption of nitrogen gas as has been reported previously by the present author[13]. These effects of molecular size of the adsorbates on the adsorption characteristics suggest the existence of a number of pores of irregular shapes such as narrow-neck or ink-bottle on the sugar carbon surface.

BET type adsorption isotherms were observed for all the acids on S_4 as is shown in Fig. 8. A surface area of S_4 calculated by the B-point method is, however, remarkably smaller than the nitrogen BET area as is seen in Table VI, and this disagreement increased with the c-number of the acid molecule. This sieving effect of the carbon S_4 is presumed to be due to the special pore-distribution, a greater part of the surface being composed of the micropores of average radius less than 8.2Å. An adsorption isotherm of benzene (non-polar adsorbate) on silica gel No. 28 (polar adsorbent) obtained under the same conditions shows no hysteresis as is shown in Fig. 8, and a surface area calculated by the B-point method was identical with the nitrogen BET area as is shown in Table VI.

As is seen in the Fig. 8, the desorption curve of benzene vapor from the silica gel returns back to the original point, These facts indicate that no chemisorption takes place on the silica gel. BET type adsorption isotherms were observed for various carboxylic acids on silica gel No. 28 as is shown in Fig. 9. Values of the effective surface area of silica gel obtained by the B-point method for the series of carboxylic acids are equal to the nitrogen BET area as is seen in Table VI. These results lead us to conclude that there exist no pores of narrow-neck or ink-bottle shape on the surface of the silica gel, and the pore size is large enough to accommodate such large adsorbate molecules as the carboxylic acids.

In Fig. 9, the anomalous behavior of the adsorption of the carboxylic acids (*n*-butyric acid) on the silica gel is shown. According to a number of reports[16-23], the heat treatment in vacuo reduces the number of OH groups and changes the nature of S–O bonds. The OH groups on the silica gel were not exterminated by the usual calcination, and a greater part of the group are thought to remain in the samples of the present study. The unclosed hysteresis loop of the *n*-butyric acid is presumed to be due to the chemisorption with these residual OH groups. When the adsorption-desorption process is repeated once again from a point $P/P_0=0$, the loop returns back to the original point as is seen in Fig. 9. Clearly the second adsorption process was physical in nature, and no anomality appears in further repetitions of the process.

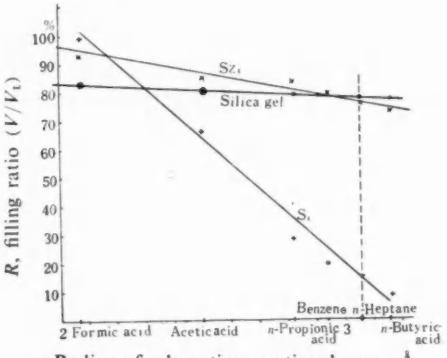

Fig. 10. Sieving coefficient.

16) J. J. Kipling and D. B. Peakall, ibid., **1957**, 834.
17) J. H. de Boer, M. E. A. Hermans and J. M. Vleeskens, *Konnikl. Ned. Akad. Wetenschap. Proc., Ser.* **B60**, 45 (1957).
18) J. H. D. de Boer and J. W. Vleeskens. ibid., **B60**, 234 (1957).
19) L. D. Belyakova and A. V. Kiselev, *Doklady Akad. Nauk S. S. S. R.*, **119**, 298 (1958).
20) A. V. Kiselev, V. V. Khopina and Yu. A. Elekov, *Izvest. Akad. Nauk S. S. S. R., Chem. Sci. Sec.*, 664 (1958).
21) K. G. Krasil'nikov, V. F. Kiselev and E. T. Sysoec., *Doklady Akad. Nauk S. S. S. R.*, **116**, 990 (1957).
22) S. P. Zhdanow and A. V. Kiselev., *Zhur. Fiz. Khim.*, **31**, 2213 (1957).
23) D. D. Belvakova, O. M. Dzhigit and A. V. Kiselev, ibid., **31**, 1577 (1958).

In Fig. 10, the filling ratio, $R=V/V_t$, is plotted against the radii of the adsorption sectional area of the adsorbate molecules, r, where V_t is the total volume of adsorbent (Tables IV and VII) and V, the total volume of the adsorbate adsorbed on the adsorbent (Table VII).

TABLE VII. ADSORBED VOLUME, A, OF ADSORBATES AT $P/P_0=1.0$

Adsorbate	Adsorbed volum, V		
	S_4	SZ_4	Silica gel
Formic acid	0.21	1.06	0.41
Acetic acid	0.14	0.97	0.40
n-Propionic acid	0.06	0.95	0.39
Benzene	0.04	0.90	0.387
n-Heptane	0.03	0.86	0.38
n-Butyric acid	0.018	0.83	0.38
Total pore vol., V_t	0.2126	1.142	0.4960

The adsorbed volume was calculated on the assumption that the density of the adsorbed liquid is the same as that in bulk. As for the *n*-heptane, the length and width of the molecule is reported to be 11.6 and 4.9 Å, respectively, but the radius of the cross section, r, is unknown. If the values of the filling ratio of *n*-heptane are marked on the lines in Fig. 10, the three points lie on a line which meets with the abscissa at right angles. The radius can be estimated from the cut on the abscissa as 3.05 Å which is proper in order of magnitude compared with the width.

The filling ratios change linearly with the radii of the adsorptive sectional area for respective adsorbents. The new term "sieving coefficient" is defined as the slope of these lines, which signifies an ability of the physical selective adsorption or the sieving effect. The sieving coefficient increases with the sharpness of the peak in the pore-size distribution curve. The coefficients for the adsorbents studied are as follows:

S_4 0.947_3, SZ_4 0.155_5, Silica gel No. 28 0.057.

The sieving coefficient would be quite a useful term to specify the adsorptive behavior of the adsorbents.

Summary

1. The adsorption characteristics of the sugar carbon prepared by carbonization or activation and silica gel were studied in detail by the adsorption of water, benzene and fatty acid vapors, and mercury porosimetry.

The pore distribution of the active carbon was tri-disperse. The effects of the partial filling of the pores were examined. The missing link in the distribution curve between the micro-pore and transitional pore in the previous reports was replenished.

2. The narrow-neck or ink-bottle structure of the pores of sugar carbon complicated the adsorption characteristics. The pores of the silica gel were cylindrical with a uniform section.

3. In order to specify the physical selective adsorption, the new term "sieving coefficient" was defined from the relation between the pore radii and cross sections of the adsorbates.

The author expresses his gratitude to Professor I. Sano of Nagoya University for his encouragement.

Department of Chemistry
Nagoya Municipal Industrial
Research Institute
Atsuta-ku, Nagoya

Non-empirical Study of the π-Electronic Structure of Vinyl Chloride Molecule by Valence Bond Method

By Shozaburo TAKEKIYO

(Received October 21, 1960)

In the year 1956, a semi-empirical consideration of conjugation in vinyl chloride molecule with molecular orbital method was performed by Goldstein[1] and recently the self-consistent field calculations of the π-electronic energy levels and the wave functions for the ground state have been carried out non-empirically by Simonetta and others[2].

On the other hand, it seems that no considerations by valence bond method have ever been made, except a semi-empirical calculation of the double bond character due to the resonance of the C–Cl bond in the molecule[3].

In this paper, the HLSP method[4] is applied to the non-empirical calculation of the π-electronic energy levels and other electronic properties of the molecule and the results are compared with those obtained by the method of LCAO self-consistent field.

Energy Levels and Wave Functions

The skeleton of the molecule is shown in Fig. 1.

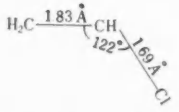

Fig. 1. Skeleton of vinyl chloride molecule.

For the carbon atoms and the chlorine atom, Slater $2p_\pi$- and $3p_\pi$-orbitals with $Z_C=3.18$, $Z_{Cl}=6.099$ have been assumed.

The approximate Hamiltonian operator H employed here is

$$H=\sum_i [T(i)+U_{\text{core}}(i)]+(1/2)\sum_{\substack{i,\ j\\ i\neq j}}(e^2/r_{ij})$$

where $T(i)$ is the kinetic energy operator for electron i and $U_{\text{core}}(i)$ is the potential energy operator for this electron in the field of the core.

Numerical values of integrals over atomic orbitals have been taken from Simonetta and others[2].

All the π-type resonance structures, whose corresponding bond eigenfunctions are linearly independent, and the energy values for these structures are shown in Fig. 2.

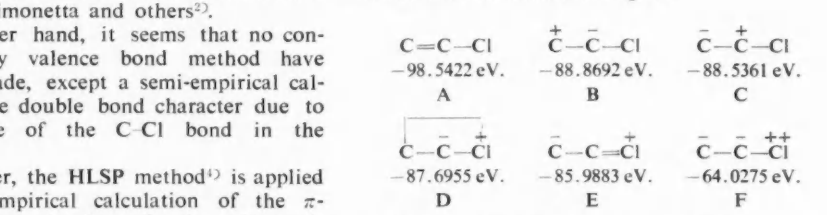

Fig. 2. Canonical structures and the energy values for the structures.

In the calculations all kinds of overlap and exchange integrals have been considered.

Wave functions for the molecule and the corresponding energy values are shown in Table I, where Φ_i is the wave function, corresponding to the energy E_i, and Ψ_K is the normalized bond eigenfunction for structure K.

TABLE I. WAVE FUNCTIONS FOR THE MOLECULE AND THE ENERGY VALUES

$$\Phi_1=0.73595\Psi_A+0.21845\Psi_B+0.22127\Psi_C+0.16156\Psi_D+0.11523\Psi_E+0.00667\Psi_F \qquad E_1=-100.91\text{ eV}.$$

$$\Phi_2=0.09265\Psi_A-0.01220\Psi_B-0.29470\Psi_C-0.31017\Psi_D+1.09225\Psi_E-0.30640\Psi_F \qquad E_2=-89.50\text{ eV}.$$

$$\Phi_3=0.09583\Psi_A-0.57177\Psi_B+0.71265\Psi_C-0.49640\Psi_D-0.04121\Psi_E+0.00000\Psi_F \qquad E_3=-85.50\text{ eV}.$$

$$\Phi_4=0.04141\Psi_A-0.05625\Psi_B-0.01469\Psi_C+0.02055\Psi_D-0.03334\Psi_E-0.00362\Psi_F \qquad E_4=-82.37\text{ eV}.$$

$$\Phi_5=0.61285\Psi_A-0.31888\Psi_B-0.78240\Psi_C-0.52176\Psi_D+0.70541\Psi_E+0.11148\Psi_F \qquad E_5=-76.41\text{ eV}.$$

$$\Phi_6=0.03309\Psi_A-0.00686\Psi_B-0.09569\Psi_C-0.07927\Psi_D+0.38669\Psi_E-1.02578\Psi_F \qquad E_6=-61.47\text{ eV}.$$

1) J. H. Goldstein, *J. Chem. Phys.*, **24**, 507 (1956).
2) M. Simonetta, G. Favini and S. Carra, *Mol. Phys.*, **1**, 181 (1958).
3) J. A. A. Ketelaar, *Rec. trav. chim.*, **58**, 266 (1939).
4) W. Heitler and F. London, *Z. Phys.*, **44**, 455 (1927); J. C. Slater, *Phys. Rev.*, **37**, 481 (1931); L. Pauling, *J. Am. Chem. Soc.*, **53**, 1367 (1931).

Probabilities of Resonance Structures, Charge Densities, and Bond Orders

Probability P_K for structure K has been calculated by the most popular expression

$$P_K = C_K \sum_L C_L \int \Psi_K \Psi_L d\tau$$

where C_K is the coefficient of bond eigenfunction Ψ_K in the wave function for the ground state of the molecule and $d\tau$ is the product of the volume elements for the four π-electrons. The results are as follows:

$$P_A = 0.6846 \qquad P_B = 0.1110 \qquad P_C = 0.1198$$
$$P_D = 0.0543 \qquad P_E = 0.0300 \qquad P_F = 0.0003$$

Then π-electron density D_i for atom i and bond order B_{ij} between atoms i and j have been evaluated by the following equations:

$$D_i = \sum_K P_K m_i^K$$

$$B_{ij} = \sum_K P_K (n_{ij}^K + 1)$$

where m_i^K is the number of π-electrons on atom i in structure K and n_{ij}^K is the number of the covalent π-bonds between atoms i and j in structure K. These results are shown in Fig. 3.

$$\underset{1.0391}{H_2C} \overset{1.6846}{\text{---}} \underset{1.0458}{CH} \overset{1.0300}{\text{---}} \underset{1.9151}{Cl}$$

Fig. 3. π-Electron densities and bond orders.

Discussion

The transition energy between the ground state and the first excited state is 11.41 eV. (Table I) The value, calculated by the method of LCAO self-consistent field, is

$$E_{V23} - E_N = 11.1842 \text{ eV}.^{4)}$$

The numerical difference between the two methods seems to be due to the neglect of the self-consistent procedure for the calculation of the excited state in the latter.

The formula of Pauling and others[5] has been used to evaluate the C–C and the neighboring C–Cl bond lengths from the semi-empirical values of bond radii[6], and the results are as follows:

$$R_{C-C} = 1.358 \text{ Å} \qquad R_{C-Cl} = 1.744 \text{ Å}$$

The values, obtained by Simonetta and others, are $R_{C-C} = 1.448$ Å and $R_{C-Cl} = 1.73$ Å[2], and the experimental values are 1.38 and 1.69 Å respectively[7].

The positive charge on the chlorine atom is evaluated as $2 - 1.9151 = 0.0849$ and the interpreted value from observation is 0.06[8].

The ionic character of the molecule, calculated from the values of the probabilities, is 31.54%.

Summary

π-electronic energy levels, probabilities of the resonance structures, π-electron densities, and the bond orders of the vinyl chloride molecule have been calculated non-empirically by the standard valence bond method, based on a complete set of the π-type resonance structures. Slater $2p_\pi$- and $3p_\pi$-orbitals have been assumed for the carbon and chlorine atoms and all the multiple exchange integrals have been considered. The calculated transition energy between the ground state and the first excited state is 11.41 eV., the ionic character is 31.54%, and the positive charge on the chlorine atom is 0.0849 (experimental value is 0.06.).

The author wishes to express his sincere thanks to Professor Kyosuke Omori, Kyushu University, for many helpful criticisms and suggestions. Thanks are also due to Professor Saburo Nagakura, the University of Tokyo, for his advice and valuable assistance.

Faculty of Liberal Arts
Nagasaki University
Ohashi, Nagasaki

5) L. Pauling, L. O. Brockway and J. Y. Beach, *J. Am. Chem. Soc.*, **57**, 2705 (1935); L. Pauling and L. O. Brockway, ibid., **59**, 1223 (1937).

6) L. Pauling, "The Nature of the Chemical Bond", Cornell University Press (1939), p. 154.

7) P. W. Allen and L. E. Sutton, *Acta Cryst.*, **3**, 46 (1950).

8) J. H. Goldstein and J. K. Bragg, *Phys. Rev.*, **78**, 347 (1950).

*Preparation of Perfluorocarboxylic Acids from Esters by Electrochemical Fluorination**

By Shunji NAGASE and Rimpei KOJIMA

(Received December 26, 1960)

Perfluorocarboxylic acids have been prepared from carboxylic acids, acid halides, acid anhydrides and acid amides, ketones, ethers etc. by electrochemical fluorination[1-4].

In a previous paper[5], it was shown that perfluorocarboxylic acids were prepared in a significant yield from alcohols which were known to give only fluorocarbons by electrochemical fluorination[1,6]. A possible mechanism of the fluorination of alcohols to perfluorocarboxylic acid fluorides was assumed to involve the first attack by fluorine on α-carbon atom of the alcohols, and dehydrofluorination followed by exhaustive fluorination of acid fluorides formed as intermediates to perfluoroacid fluorides.

The present paper deals with the work extended further to the fluorination of esters to obtain perfluorocarboxylic acids.

So far, there has been no detailed report on the electrochemical fluorination of simple esters. Simons[2] carried out the fluorination of butyl acetate and made decafluorobutane.

In the present series of work, ethyl, propyl and butyl acetates, ethyl, propyl and butyl propionates, and ethyl, propyl and butyl butyrates were fluorinated and trifluoroacetic, perfluoropropionic, and perfluorobutyric acids were obtained in good yields.

Again, the mechanism of dehydrofluorination at α-carbon atom of alcohols which takes place after hydrofluorolysis of esters into carboxylic acid fluorides and alcohols, could be applied to the formation of perfluorocarboxylic acid fluorides from esters.

The perfluorocarboxylic acid fluorides formed were converted into perfluorocarboxylic acids by treatment with water. No detectable amount of partially fluorinated esters and alcohols were found in the residue in the electrolytic cell but the presence of acid fluorides and unreacted esters, etc. was confirmed.

Experimental

Materials.—*Esters.*—Special or first grade commercial reagents were used after distillation through a fractionation column. Some of the esters were prepared in the usual manner in this laboratory.

Hydrogen Fluoride.—Hydrogen fluoride purity of 99.4% was supplied from a commercial cylinder.

Apparatus.—The apparatus used for this work essentially consisted of an electrolytic cell, a sodium fluoride tube, and an absorber, as described previously[5].

The electrolytic cell of 1 l. in capacity was a 10-cm. cylindrical nickel vessel provided with a copper condenser at the top to cool down vaporizing hydrogen fluoride and a drain at the bottom, and having 8 and 9 pieces of nickel plates (0.5 mm. in thickness) as anodes and cathodes, fastened together, suspended alternately from the top, and insulated from each other by Teflon pieces. The distance between the plates was 1.7 mm. and the effective surface area of the anodes and cathodes was 9.2 dm^2. A copper tubing was provided inside the cell to keep the optimum temperature by circulation of ice water during the reaction.

The sodium fluoride tube was an iron pipe containing sodium fluoride pellets to remove hydrogen fluoride.

The absorber used was a pair of polyethylene bottles containing 200 and 50 ml. of water.

Procedure.—One liter of hydrogen fluoride was introduced into the cell through the polyethylene container, and electrolysis was carried out without a sample to remove a trace of water in the hydrogen fluoride at an average of 5.2 V. for about 13 amp. hr. in nitrogen atmosphere. About 35 g. of the sample was then dissolved in this solution and electrolysis was carried out with the anodic current density of 2.5 to 3.5 amp./dm^2 at an average of 4.8 V., at 4~6°C for designated amp. hr. At the end, the voltage rose up to 5.2~5.3 V.

It was found that the amount of the electricity used up to this point corresponded to about 1.3 times that assumed to be required to form fluorine with discharging fluoride ion which would substitute with hydrogen in the sample and combine with it to form hydrogen fluoride.

The gaseous product generated from the cell, containing fluorocarbons, oxygen difluoride, perfluoro-acid fluorides, hydrogen, etc. was passed through

* Presented in part at the Tokai Local Meeting of the Chemical Society of Japan, Nagoya, November, 1960.

1) J. H. Simons et al., *J. Electrochemical Soc.*, **95**, 47 (1949).
2) J. H. Simons, U. S. Pat., 2519983 (1950).
3) A. R. Diesslin, E. A. Kauck and J. H. Simons, U. S. Pat., 2567011 (1951); U. S. Pat, 2593737 (1952).
4) E. A. Kauck and A. R. Diesslin, *Ind. Eng. Chem.*, **43**, 2332 (1951).
5) S. Nagase and R. Kojima, *J. Chem. Soc. Japan, Ind. Chem. Sec.* (*Kogyo Kagaku Zasshi*), in press.
6) J. Burdon and J. C. Tatlow, "Advances in Fluorine Chemistry", Vol. 1, Ed. by M. Stacey, J. C. Tatlow and A. G. Sharpe, Butterworths Scientific Publications Ltd., London (1959), p. 157.

the condenser and the sodium fluoride tube, and bubbled through water in the absorber where the perfluoro-acid fluorides reacted, and converted into perfluorocarboxylic acids. In this system, the gases which are inert to water should escape as gases.

When the reaction was over, the hydrogen fluoride in the cell was distilled into the polyethylene container which was used repeatedly by adding it into the new hydrogen fluoride for the next run, but for different kinds of esters, hydrogen fluoride freshly supplied from the cylinder was used. About 50 ml. of a residue consisting mainly of hydrogen fluoride remained at the bottom of the cell and its other components were investigated further by the method described earlier[5].

The aqueous solution of the perfluorocarboxylic acids in the absorber was neutralized with sodium carbonate, filtered and the filtrate was dried. The sodium perfluorocarboxylates formed were then extracted with absolute ethanol.

Quantitative analysis of the products was made by the base line method with potassium bromide pellet infrared absorption spectrum using 11.88 μ (for sodium trifluoroacetate), 9.68 μ (for sodium perfluoropropionate), and 10.65 μ (for sodium perfluorobutyrate) as key bands. The standard sodium carboxylates were prepared from trifluoroacetic acid secured from the Eastman Kodak Co., and perfluoropropionic and perfluorobutyric acids secured from the Minnesota Mining and Manufacturing Co. by treatment with sodium carbonate.

When several runs were repeated, the electrodes were stained with a grey substance, which was removed by electropolishing in 0.5% of potassium carbonate solution.

Results and Discussion

The effect of anodic current density on the yield was mainly examined in a similar manner as in the fluorination of alcohols. Trifluoroacetic acid was obtained from ethyl acetate and the results are shown in Table I. The yields shown were calculated on the basis that 1 mol. of ethyl acetate would give 2 mol. of sodium trifluoroacetate. The fluorination of ethanol also yielded trifluoroacetic acid, but the yield was usually less than that in the case of ester.

The calculation of current efficiencies shown was based on the amount of the electricity assumed to be required to form fluorine with a discharging fluoride ion which would substitute hydrogen in the ester and combine with it to form hydrogen fluoride. This means that the electricity to make 8 mol. of fluorine would be required for the fluorination of 1 mol. of ethyl acetate to form 2 mol. of sodium trifluoroacetate.

The results obtained from the fluorination of propyl acetate, from which trifluoroacetic and perfluoropropionic acids were obtained, are shown in Table II. The yields shown were also calculated on the basis that 1 mol. of propyl acetate would give 1 mol. of sodium trifluoroacetate and 1 mol. of sodium perfluoropropionate, which means that the acyl and the alkyl groups in the ester would give perfluorocarboxylic acids whose number of carbon atoms corresponds to those of the acyl and the alkyl group in the ester.

Table I. Fluorination of ethyl acetate

Electricity passed: 211 amp. hr.
Sample taken: 34.5 g.

D_A[a] amp./dm^2	Product obtained g.	Yield %	Current efficiency %
2.5	45.6	43.4	34.0
2.7	47.2	44.9	35.2
3.0	52.0	49.5	38.8
3.3	54.2	51.6	40.5
3.5	54.9	52.3	41.0

a) D_A: Anodic current density.

The current efficiency was also calculated by the same method as for ethyl acetate, i.e. the electricity assumed to make 10 mol. of fluorine would be required for the fluorination of 1 mol. of propyl acetate to form 1 mol. of sodium trifluoroacetate and 1 mol. of sodium perfluoropropionate.

The results obtained from the fluorination of butyl acetate, ethyl, propyl and butyl propionates, and ethyl, propyl and butyl butyrates are shown in the Tables. All of the yields and current efficiencies shown were calculated in the same way as was mentioned above.

It was found that the yield of the perfluorocarboxylic acid obtained from the fluorination of propyl propionate or butyl butyrate was much higher than that from propyl or butyl alcohol, but the degree of cleavage which would result in the formation of perfluorocarboxylic acids consisting of a smaller number of carbon atom than that of corresponding alcohol, or acyl or alkyl group in the ester was essentially the same in alcohols and esters.

It is of interest to know which side of the ester, acyl or alkyl group, would give perfluorocarboxylic acid more easily. Comparison between the results obtained from butyl acetate and ethyl butyrate or butyl propionate and propyl butyrate indicated that perfluorobutyric acid was obtained in better yield from ethyl and propyl butyrates than from butyl acetate and butyl propionate. This showed that perfluorocarboxylic acids are formed more easily from acyl than alkyl group in the ester.

When the number of carbon atoms increased in the ester, the degree of cleavage increased, as is usually observed in electrochemical fluorination. For example, propyl acetate gave sodium trifluoroacetate and sodium perfluoropropionate in molar ratio of about 1 to 0.9, but butyl acetate gave sodium trifluoroacetate

TABLE II. FLUORINATION OF PROPYL ACETATE
Electricity passed: 228 amp. hr.

Sample taken g.	D_A amp./dm²	Product obtained g.	Yield %	Current efficiency %	Composition[a] CF_3COONa	Composition[a] C_2F_5COONa
34.5	2.5	35.7	32.7	26.1	46	54
34.5	2.7	42.0	38.5	30.7	45	55
34.5	3.0	34.3	31.5	25.1	45	55
34.6	3.3	36.7	33.6	26.8	44	56
34.5	3.5	46.3	42.5	33.8	46	54

a) The composition of the products analyzed by infrared spectrophotometer is given in weight per cent.

TABLE III. FLUORINATION OF BUTYL ACETATE
Electricity passed: 240 amp. hr.

Sample taken g.	D_A amp./dm²	Product obtained g.	Yield %	Current efficiency %	Composition, wt. % CF_3COONa	C_2F_5COONa	C_3F_7COONa
34.6	2.5	32.7	29.5	23.5	60	2.4	38
34.5	2.7	27.1	24.5	19.4	63	1.9	33
34.5	3.0	32.7	29.6	23.5	56	4.7	40
34.5	3.3	30.8	27.9	22.2	64	1.9	34
34.6	3.5	39.7	35.8	28.6	54	2.7	43

TABLE IV. FLUORINATION OF ETHYL PROPIONATE
Electricity passed: 228 amp. hr.
Sample taken: 34.5 g.

D_A amp./dm²	Product obtained g.	Yield %	Current efficiency %	Composition, wt. % CF_3COONa	C_2F_5COONa
2.5	17.2	15.8	12.6	46	54
2.7	38.9	35.7	28.4	45	55
3.0	43.4	39.8	31.7	44	56
3.3	35.1	32.2	25.7	46	54
3.5	53.5	49.1	39.1	47	53

TABLE V. FLUORINATION OF PROPYL PROPIONATE
Electricity passed: 240 amp. hr.
Sample taken: 34.5 g.

D_A amp./dm²	Product obtained g.	Yield %	Current efficiency %	Composition, wt. % CF_3COONa	C_2F_5COONa
2.5	29.6	26.7	21.3	7.3	93
2.7	33.2	29.9	23.9	5.1	95
3.0	36.2	32.6	26.1	6.8	93
3.3	38.5	34.7	27.7	5.3	95
3.5	38.6	34.8	27.7	7.1	93

TABLE VI. FLUORINATION OF BUTYL PROPIONATE
Electricity passed: 250 amp. hr.
Sample taken: 34.5 g.

D_A amp./dm²	Product obtained g.	Yield %	Current efficiency %	Composition, wt. % CF_3COONa	C_2F_5COONa	C_3F_7COONa
2.5	30.3	27.1	21.5	6.5	65	28
2.7	30.7	27.5	21.7	6.9	67	26
3.0	33.6	30.0	23.8	7.7	62	31
3.3	29.7	26.6	21.1	7.8	64	29
3.5	43.1	38.6	30.6	6.3	64	30

Table VII. Fluorination of ethyl butyrate

Electricity passed: 240 amp. hr.
Sample taken: 34.5 g.

D_A amp./dm²	Product obtained g.	Yield %	Current efficiency %	Composition, wt. %		
				CF_3COONa	C_2F_5COONa	C_3F_7COONa
2.5	31.8	28.9	23.1	50	3.9	46
2.7	27.3	24.8	18.8	49	4.9	46
3.0	35.6	32.3	25.9	56	2.3	42
3.3	35.8	32.5	26.0	55	2.8	43
3.5	32.4	29.4	23.5	49	4.1	47

Table VIII. Fluorination of propyl butyrate

Electricity passed: 250 amp. hr.
Sample taken: 34.5 g.

D_A amp./dm²	Product obtained g.	Yield %	Current efficiency %	Composition, wt. %		
				CF_3COONa	C_2F_5COONa	C_3F_7COONa
2.5	24.2	21.7	17.2	6.3	60	34
2.7	31.3	28.0	22.2	6.2	59	35
3.0	31.5	28.2	22.3	6.4	55	38
3.3	28.0	25.1	19.9	6.2	56	38
3.5	30.1	26.9	21.3	6.3	58	36

Table IX. Fluorination of butyl butyrate

Electricity passed: 258 amp. hr.
Sample taken: 34.5 g.

D_A amp./$d_{F.I}$²	Product obtained g.	Yield %	Current efficiency %	Composition, wt. %		
				CF_3COONa	C_2F_5COONa	C_3F_7COONa
2.5	19.0	16.8	13.4	9.1	13	78
2.7	22.2	19.7	15.6	8.8	8.8	82
3.0	26.0	23.0	18.3	9.4	7.1	83
3.3	31.1	27.5	21.9	8.8	6.6	85
3.5	36.8	32.5	25.9	7.1	5.4	87

and sodium perfluorobutyrate in molar ratio of about 1 to 0.4, which indicates that butyl radical is degradated considerably as compared with propyl radical.

In the fluorination of alcohols, the maximum yield of perfluorocarboxylic acids was obtained with anodic current density of 3.3 amp./dm², and the yield decreased sharply with higher or lower current densities, irrespective of the kind of alcohols used, but there seemed to be no such simple relationship between the anodic current density and yield for the esters within the range of the current density applied. However, the yield generally increased with increasing current density.

The presence of a small amount of unreacted ester remaining in the residue in the cell along with the acetyl fluoride and partially fluorinated carboxylic acid fluorides was confirmed. The grey precipitate consisting mainly of nickel and copper fluorides was also found in the residue.

The mechanism of the fluorination of esters to form perfluorocarboxylic acid fluorides, although this reaction obviously could and probably did follow different routes simultaneously, might involve, in the first place, hydrofluorolysis of the esters in hydrogen fluoride to form acid fluorides and alcohols as shown below. Alcohols formed in this way would be converted into acid fluorides through the mechanism of dehydrofluorination at the α-carbon atom.

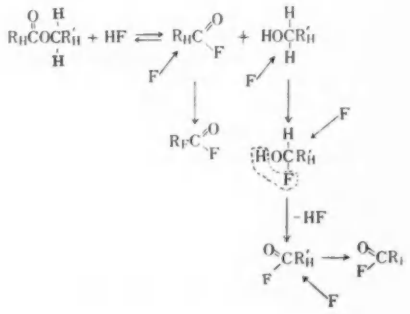

In these formulae, R_H and R_H' are hydrocarbon radicals, and R_F and R_F' are perfluorocarbon radicals. Acid fluorides R_H–COF and R_H'–COF thus formed would be fluorinated further to perfluorocarboxylic acid fluorides.

Conclusion

1) Perfluorocarboxylic acids were obtained from esters in a good yield by electrochemical fluorination and the relationship between anodic current density and yield was examined. Generally, the yield increased with increasing anodic current density.

2) The result of electrochemical fluorination of esters was compared with that of alcohols. A better yield was obtained from the esters.

3) The presence of a larger number of carbon atoms in the acyl or alkyl group in the ester caused more degradation than those of smaller numbers.

4) The mechanism of the formation of perfluorocarboxylic acid fluorides from esters was discussed.

The authors wish to express their sincere thanks to Osaka Metal Industries Co. for supplying hydrogen fluoride.

Government Industrial Research Institute, Nagoya
Kita-ku, Nagoya

Molecular Structure Investigation of Chlorotrifluoroethylene by Electron Diffraction

By Takeshi KAWAI, Hiroshi SEKINE and Masato IGARASHI

(Received January 30, 1961)

The molecular structures of chlorine and fluorine derivatives of ethylene such as tetrachloroethylene[1-3] and tetrafluoroethylene[4,5] have been studied by electron diffraction using a sector-microphotometer or visual methods (Table I).

In order to see the carbon-halogen bond distances and the valence angles of ethylene derivative including two kinds of halogens, we investigated chlorotrifluoroethylene (Kel F monomer) by electron diffraction using the visual method and compared it with those of the related compounds.

Experimental

The sample was prepared by Osaka Kinzoku Industrial Co.

The apparatus of electron diffraction was the same as that in the previous report[6]. In order to reduce the vapor pressure of the sample the liquid-sample reservoir was cooled by a mixture of dry ice and alcohol during the diffraction experiment. The diffraction photographs were measured by the visual method (Fig. 1).

Analysis and Results

The radial distribution and theoretical intensity curves have been calculated by the usual method. The thermal factors were omitted for convenience in all the theoretical intensity curves except curves D' and D'' in which the mean amplitudes listed in Table III were used. Some of the intensity curves are shown in Fig. 1 and the molecular parameters of the corresponding models are listed in Table II.

As can be seen from the first peak of the radial distribution curve (Fig. 2), it is difficult to distinguish the C=C and the three C–F bond distances separately. The mean value of them is 1.31 Å. The second peak shows that the C–Cl bond distance is 1.71 Å.

When the angles FCF and FCCl of the models are varied, the C=C and all the C–F bond distances being fixed at 1.31 Å and the C–Cl band distance at 1.71 Å, the features of the maxima or the shelves at about $q=28\sim41$ of the theoretical intensity curves change appreciably and the curves C and D, in which the two angles are equal to 115 and 114°, respectively, fit better with the observed curve

1) L. O. Brockway, J. Y. Beach and L. Pauling, *J. Am. Chem. Soc.*, **57**, 2693 (1935).
2) W. N. Lipscomb, Ph. D. Thesis, California Institute of Technology, 1946.
3) I. L. Karle and J. Karle, *J. Chem. Phys.*, **20**, 63 (1952).
4) I. L. Karle and J. Karle, ibid., **18**, 963 (1950).
5) T. T. Broun and R. L. Livingston, *J. Am. Chem. Soc.*, **74**, 6084 (1952).
6) T. Yuzawa and M. Yamaha, This Bulletin, **26**, 414 (1953).

TABLE I. MOLECULAR STRUCTURES OF TETRACHLOROETHYLENE AND TETRAFLUOROETHYLENE

Tetrachloroethylene

Reference	C-Cl, Å	C=C, Å	∠ClCCl	∠CCCl	Method
1	1.73±0.02	1.38		123.7±1°	visual
2	1.71±0.02	1.34±0.05	115.5±2°	122.1±1°	visual
3	1.72±0.01	1.30±0.03	113.5±1.5°		sector

Tetrafluoroethylene

Reference	C-F, Å	C=C, Å	∠FCF	Method
4	1.313±0.010	1.313±0.035	114±2°	sector
5	1.30 ±0.02	1.33 ±0.06	114±2°	visual

TABLE II. PARAMETERS OF MOLECULAR MODELS FOR THE THEORETICAL INTENSITY CURVES AND q_{calcd}/q_{obs} VALUES

Model	C=C Å	C-F Å	C-Cl Å	∠FCF	∠FCCl	∠CCCl	q_{calcd}/q_{obs}	Average deviation
A	1.31	1.31	1.71	120°	120°	120°		
B	1.31	1.31	1.71	117°	117°	121.5°		
C	1.31	1.31	1.71	115°	115°	122.5°	1.000	0.017
D	1.31	1.31	1.71	114°	114°	123°	1.004	0.015
E	1.31	1.31	1.71	112°	112°	124°		
F	1.31	1.31	1.71	114°	117°	121.5°		
G	1.31	1.31	1.71	114°	120°	117°		
H	1.31	1.31	1.71	114°	114°	120°		
I	1.31	1.31	1.71	114°	114°	126°	0.993	0.012
J	1.31	1.31	1.71	114°	114°	128°		
K	1.31	1.27	1.73	114°	114°	123°		
L	1.31	1.29	1.71	114°	114°	123°	1.003	0.016
M	1.31	1.33	1.71	114°	114°	123°	0.993	0.014
N	1.31	1.35	1.73	114°	114°	123°		
O	1.31	{1.31(2) {1.29(1)	1.73	114°	114°	123°	0.995	0.016
P	1.31	1.31	1.67	114°	114°	123°		
Q	1.31	1.31	1.69	114°	114°	123°	1.003	0.017
R	1.31	1.31	1.73	114°	114°	123°	0.996	0.015
S	1.31	1.31	1.75	114°	114°	123°	0.995	0.017
T	1.29	1.31	1.73	114°	114°	123°		
U	1.35	1.31	1.73	114°	114°	123°		
V	1.37	1.30	1.70	116°	116°	122°	0.990	0.018
W	1.39	1.29	1.69	117°	117°	121.5°	0.987	0.022
X	1.25	1.32	1.73	112°	112°	124°	1.003	0.014
Y	1.23	1.33	1.73	111°	111°	124.5°		
D'	1.31	1.31	1.71	114°	114°	123°	0.998	0.015
D''	1.31	1.31	1.71	114°	114°	123°	0.994	0.017

than any other curves of different bond angles.

By comparing the features and q_{calcd}/q_{obs} values of the intensity curves of the models which have bond angles different from those of models C and D, the acceptable regions of the two bond angles FCF and FCCl were determined as 114±2° and the bond angle CCCl as 123±2°.

And then by comparing the intensity curves of the models in which C-Cl bond distance was varied from 1.67 Å to 1.75 Å, the C-Cl bond distance was determined as 1.72±0.02 Å.

If either one of the C=C or the C-F bond distance is longer and the other is shorter than 1.31 Å, a considerably good intensity curve is obtained by altering both the bond angles and C-Cl distance in the acceptable regions which have been described previously. But as the contribution of the C-F atomic pairs to the total intensity curve is much greater than that of C=C atomic pair, the acceptable region of C=C distance is much larger than these of C-F distances. They were 1.31±0.06 Å for C=C and 1.31±0.02 Å for C-F, respectively.

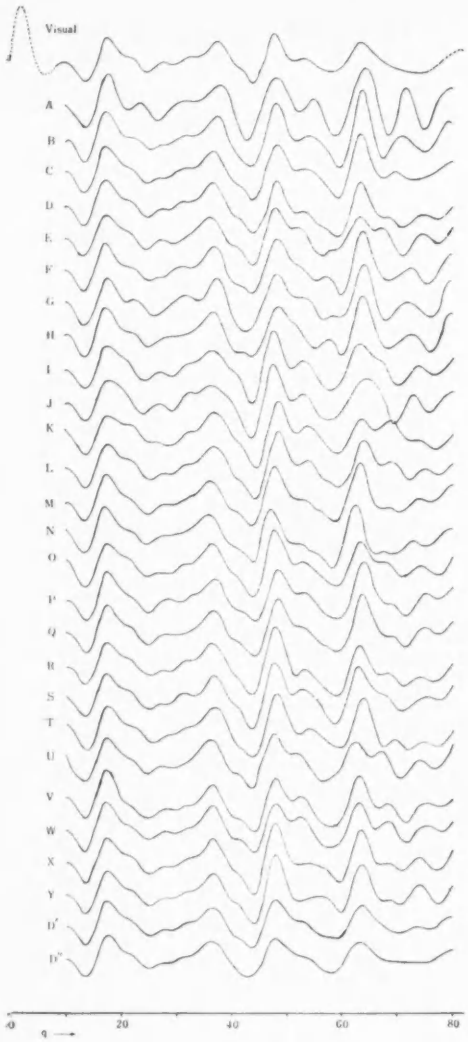

Fig. 1. Intensity curves.

Finally the theoretical intensity curves of model D including thermal factors listed in Table III are compared. They are not greatly different from that of the rigid model, but curve D' seems a little better than curve D''.

Vartical lines show the interatomic distances of model D.

Fig. 2. Radial distribution curve.

TABLE III. MEAN AMPLITUDES USED FOR THE CALCULATIONS OF INTENSITY CURVES D' AND D''

Atomic pair	Mean amplitude, Å	
	Model D'	Model D''
C=C	0.04	0.04
C-F	0.04	0.05
C-Cl	0.05	0.05
C···F	0.06	0.06
C···Cl	0.06	0.06
F···F	0.06	0.09
cis F···F	0.09	0.09
trans F···F	0.06	0.11
Cl···F	0.06	0.09
cis Cl···F	0.09	0.09
trans Cl···F	0.06	0.11

When the above results are compared with those in Table I, all the parameters of the molecule are practically identical with those of Refs. 3 and 4, although the present results by visual method have broader limits of uncertainty than those of the sector-microphotometer method.

The authors wish to express their sincere gratitude to Professor Akira Kotera for his kind guidance throughout this study. They also owe much to Dr. Nobuo Yamada, The Electrical Communication Laboratory, Nippon Telegraph and Telephone Public Corporation, to whom their thanks are due.

Department of Chemistry
Faculty of Science
Tokyo University of Education
Koishikawa, Tokyo

Energy Distribution of Secondary Electrons from Copper-Beryllium Alloy by Positive Ions of Inert Gases. I. Electro-polished Surface

By Toshio SUGIURA

(Received January 17, 1961)

A series of studies of electron ejection from copper-beryllium (4%) alloy by positive ions have been extended in this work. In a previous paper[1], the yields of the secondary electron emission from the variously treated copper-beryllium targets by inert gas ions and some hydrocarbons and their fragment ions were measured, and the surface composition of these alloy targets were also determined by electron diffraction analysis in order to discuss the correlation between the yields of the secondary electron emission and the surface composition of the ion targets.

The secondary electron emission by inert gas ions had been studied by Hagstrum[2-6] on the atomically clean surfaces of some transition metals. The energy distribution of the secondary electrons ejected by the Auger process obeying the assumed mechanism had been theoretically calculated by Hagstrum[7], and a good agreement had been obtained between the theory and his experimental results.

Generally, the ejection of secondary electrons from a metal surface by impact of a positive ion proceeds at the expense of the potential or kinetic energy of the incident ion. Potential ejection may take place only if the ionization potential of the incident ion exceeds twice the work function of the target metal. Kinetic ejection, on the other hand, is expected to increase with increasing ion energy, and is the dominant process for all ions with kinetic energy above a few thousand electron volts, and it also proceeds for positive ions whose ionization potential is less than twice that of the work function of the metal.

Recently, Waters[8] had intended to confirm this kinetic ejection, and had measured the kinetic energy distribution of the ejected electrons from the atomically clean surface of tungsten impacted by alkali ions.

Unfortunately, the theory of the kinetic ejection by the positive ion having low kinetic energy had not yet been clarified, but the mechanism of secondary electron emission by the impact of high speed ions had been made the analysis by Sternglass[9]. He had studied the process of secondary electron emission regarded as the component of two essentially important parts, namely the formation of secondaries inside the metal and their subsequent escape from the surface. Also he had postulated that the energy loss of the primary particle as a result of the excitation and ionization of the target materials results in the formation of internal secondary electrons, and that the secondaries formed might lose their energy by various collison processes so that only a fraction of them may be able to reach the surface of the metal with sufficient energy to escape from the surface. The assumption of Sternglass seems to be suggestive for the secondary electron emission from the practical (not atomically clean) surfaces by impact of the ions.

The main points of interest of the present work are the direct measurements of the kinetic energy distribution of the secondary electrons ejected from the practical surface usable as the first dynode of the secondary electron multiplier tube, and the confirmation of the correlation between the yield of the secondary electron emission and the energy distribution of the secondary electron emission and the energy distribution of the secondary electrons. The results reported in this paper are concerned with the energy distribution of the secondary electrons ejected from the electro-polished copper-beryllium surface by impact of the singly- and doubly-charged argon and neon ions and singly-charged herium ions, together with the influence of the kinetic energy of these incident ions.

Experimental

In the experimentals of the electron ejection, the beam of ions which is homogeneous in constitution and kinetic energy was allowed to impinge upon a target surface. In order to measure the yield of secondary electrons (γ_i, number of electrons per incident ion) and the distribution in kinetic energy

1) T. Hayakawa and T. Sugiura, This Bulletin, **34**, 58 (1961).
2) H. D. Hagstrum, *Rev. Sci. Instr.*, **24**, 1122 (1953).
3) H. D. Hagstrum, *Phys. Rev.*, **89**, 244 (1953).
4) H. D. Hagstrum, ibid., **91**, 543 (1953).
5) H. D. Hagstrum, ibid., **96**, 325 (1954).
6) H. D. Hagstrum, ibid., **104**, 317, 672, 1516 (1956).
7) H. D. Hagstrum, ibid., **96**, 336 (1954).
8) P. M. Waters, ibid., **109**, 1053 (1958); **111**, 1466 (1958).
9) E. J. Sternglass, ibid., **108**, 1 (1957).

of ejected electrons, both as functions of the ion and target and of the ion kinetic energy, the apparatus must incorporate an ion source, a mass analyzer, an arrangement of target and surrounding electron collector, and the means to vary the velocity of the ion beam while keeping it focused on the target.

Mass Spectrometer. — The present experiments were performed by a mass spectrometer constructed in our laboratory, and their details were already reported in the previous paper[1]. In this studies, in order to eliminate the influence of the fringing field of the analyzing magnet on the slow electrons, the magnetic shield composed of six sheets of soft iron plates of 1.0 mm. in thickness was attached to the middle part between the ion collector region and the analyzing magnet. By this shielding, the influence of the fringing field on the energy distribution of secondary electrons was considered negligible, as described below.

Ion Target and Electron Collector. — Since the measurements of the energy distribution of the ejected electrons were made by the retarding potential method, the target was made relatively small and placed at the center of the spherical electron collector.

The ion target and the electron collector designed for the study of energy distribution of secondary electrons are schematically shown in Figs. 1a and b. In Figs. 1a and b, T indicates the ion target box

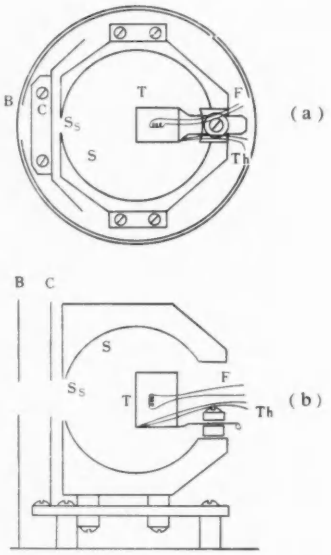

Fig. 1. Schematic top view (a) and side view (b) of the electron collector and ion target for the study of secondary electron emission by ion impact. T denotes the ion target, S the spherical electron collector, B, C and Ss the buffer, the collector and ion entrance slit, F the tungsten filament prepared for the heating of the ion target, Th the nickel-palladium thermocuple.

shaped from the copper-beryllium (4%) plate, and the front area of this box is 6×12 mm^2 and the target was mounted at the center of the spherical electron collector S by the steatite insulator. S was constructed by two pieces of the brass blocks fastened to each other and the inside of these brass blocks were spherically excavated, the diameter of this sphere is 27 mm., and the area of the ion entrance slit Ss is 10×3 mm^2. In order to minimize the tertiary electron emission by secondary electrons and the variation of the contact potential with contamination by adsorped gases, the inside surface of the electron collector was covered with evaporated gold films. C is the collector slit of 8×2 mm^2 in area and shaped from a molybudenum plate of 0.2 mm. in thickness, and B is the buffer slit of 10×5 mm^2 in area formed by a copper plate of 0.4 mm. in thickness. The tungsten filament F was prepared inside the ion target box for heating the ion target by electron bombardment, and the temperature of the ion target was measured by a nickel-palladium thermocouple Th.

By these assemblies, all ions strike only the front surface of the ion target inside the spherical electron collector, since the focusing of the mass analyzer is determined by ion beam width less than 0.3 mm. at the collector slit during the course of studies.

Measurements of Energy Distributions of Secondary Electrons.—Electron energy distributions were measured in this work by means of the retarding potential method. Currents I_s at the electron collector were measured as a function of the voltage V_{sT} supplied between the ion target and the electron collector. The net ion currents I_i were measured by the ion target to which -18 V. was supplied against the electron collector through a battery in order to eliminate secondary electrons, and the ratio of the currents I_s/I_i was obtained as a function of the retarding potential V_{sT}.

Typical retarding potential data for the singly-charged argon ions are shown in Fig. 2. The kinetic energy distributions of the ejected electrons ($N_0(E_k)=d(I_s/I_i)/dV_r$) have been obtained from the retarding potential data in the following way where V_r denotes the retarding potential corrected to the contact potential difference between copper-beryllium and gold against V_{sT}. The differences in I_s/I_i for each 0.25 V. retarding potential difference was plotted vs. V_r. Typical energy distribution curves obtained from the data shown in Fig. 2 are shown in Fig. 3 in which the unit of $N_0(E_k)$ is electrons per ion per electron volt. A UX-54 tube was used as the primary tube of the d. c. amplifier, and the output current was recorded by two galvanometers of different sensitivities. Since a high resistance of 1×10^{10} ohm was used and the measured current was less than 1×10^{-11} amp. in all measurements, the inaccuracy of the retarding potential caused by the incident electrons or the primary ions is less than 0.1 V. and this causes no effective error in this study.

Measurement of Contact Potential Difference.— The apparatus used for the measurements of the contact potential difference is shown in Fig. 4a. The vacuum line of apparatus was all constructed

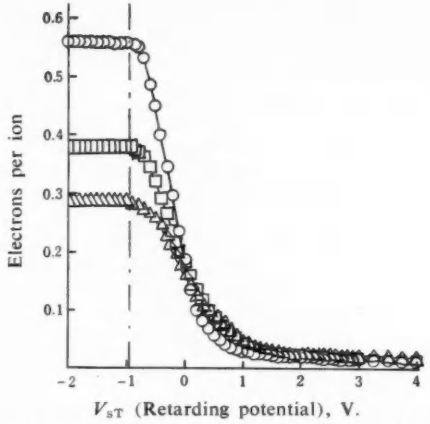

Fig. 2. Polt of ejected electron current I_s in electrons per ion as a function of the retarding potential V_{sT} for argon ions impinged on the electro-polished Cu-Be surface. Circule, square and triangle points denote impinged ion energy of 1240, 840 and 540 V., respectively.
The vertical line show on the electron energy scale indicates the contact potential difference between Au and electro-polished Cu-Be.

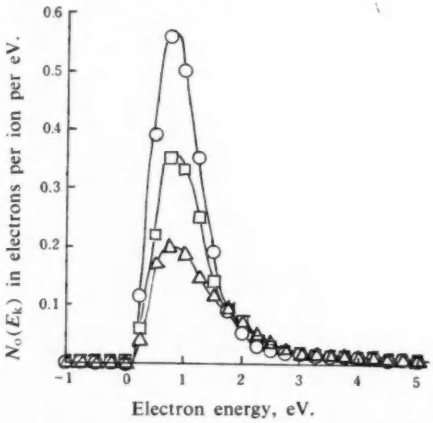

Fig. 3. Plot of the numbers of electrons per incident ion per eV. as a function of retarding potential V_r corrected for the contact potential difference. The curves plotted by circular, square and triangular points were obtained by differentiating the curves shown in Fig. 2.

by molybdenum glass and R in Fig. 4a is the measurement tube, and these were evacuated by the Hickman type oil diffusion pump through a liquid nitrogen trap, and the vacuum during the measurements was 1×10^{-6} mmHg. In Fig. 4b the electrode system is shown, the cylindrical electrode P was formed from a nickel plate of 0.2 mm. in thickness and the inside of this cylinder was covered

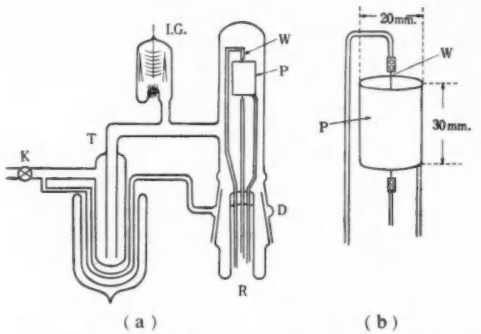

Fig. 4. Schematic diagram of the apparatus for the measurements of the contact potential difference (a). (b) show the electrode assembly. R denotes the measurement tube, P the retardation plate and the thermal electron collector, W the tungsten filament which supplying thermal electrons, I. G. the Bayard-Alpert ionization gauge, and T the liquid nitrogen trap.

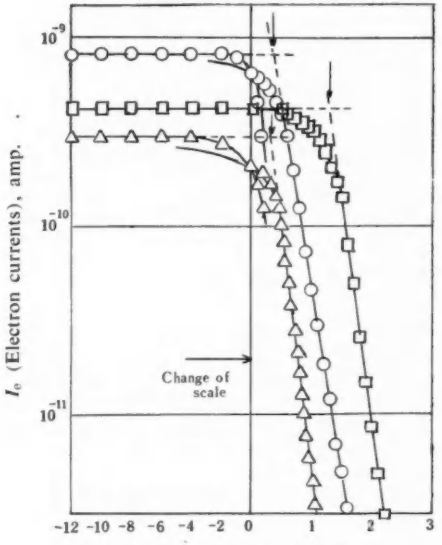

Fig. 5. Retarding potential data on thermoionic electron for the heated tungsten used to determine the contact potential difference between gold and electro-polished Cu-Be. The circle points show the Au—W system, the square points show the Cu-Be—W system, and the triangular points show the data of Hagstrum for Au—W system, in which the electron current scale is arbitrary for the Hagstrum's plot. The vertical arrow on each curve indicates the value for the zero field in each system.

with the evaporated gold film for the measurements of the contact potential difference between gold and tungsten, while for measurements of the contact potential difference between copper-beryllium and tungsten P was formed from a copper-beryllium plate of 0.15 mm. in thickness and was treated in the same manner as the ion target was. The tungsten filament F of 0.07 mm. in diameter was strung at the central axis of the electrode P. The electrode P and the tungsten filament F were mounted on a molybdenum rod in the measurement tube R. The geometry of the cylindrical electrode P was 20 mm. in inner diameter and 30 mm. in length. The stabilized 0.85 V. and 0.8 amp. were supplied to the filament in order to minimize the positive ion emission from the filament, the ionization of the residual gases and the photon radiation. Under these conditions, the thermal electron current of about 10^{-9} amp. was measured by a $\mu\mu$ ammeter. The retarding potential for the thermal electrons was applied on the center of the filament potential to the electrode P by dividing the battery potential. Typical results of the retarding potential curves for the thermal electrons emitted from the tungsten filament onto the gold plate or the copper-beryllium plate are shown in Fig. 5.

Materials.—The copper-beryllium ion target was shaped in a box-form after tempering and mechanical polishing with fine emery papers, and successively electro-polished in the solution which had been reported in the previous paper[1]. Spectroscopically pure argon and neon were used in the present experiments as well as in the previous sutdies, and also spectroscopically pure helium of the Teikoku Oxygen Co. was used without any further purifications. The mass spectrometric analyses of these gaseous samples revealed that the total impurities were less than 0.005% in volume.

Results

Contact Potential between Gold and Electro-polished Copper-Beryllium. — Typical retarding potential data obtained from the manner described above are shown in Fig. 5. In Fig. 5, the circle points indicate the retarding potential curve between the tungsten filament and the gold surface, while the square points show the retarding potential curve between tungsten filament and the electro-polished copper-beryllium surface. The triangle points in Fig. 5 indicate the results of the tungsten~gold system measured by Hagstrum[2] in which the electron current scale was shown in an arbitarary unit. As seen in Fig. 5, the retarding potential portion had been observed to be linear from 0.5 to 1.6 V. for the tungsten~gold system, and to be linear from 1.4 to 2.2 V. for the tungsten~copper-beryllium system, while in Hagstrum's data the linear portion is from 0.5 to 1.1 V. The point of zero field has been determined by the intersection of the extrapolated straight lines through the saturated current and retarding portions as shown by arrows in each curve in Fig. 5.

These treatments of semilog plot are strictly correct only for plane parallel geometry[10], although the present author measured by geometry of cylindrical symmetry and Hagstrum[2] had measured by spherical geometry. But the present results of the tungsten—gold system are in close agreement with Hagstrum's result, and the discrepancies between these observed values and the true values are expected to be smaller than 0.1 V. The observed value of the contact potential difference between gold and electro-polished copper-beryllium alloy is 0.95 eV., while the surface potential of the electro-polished copper-beryllium is 0.95 eV. more positive than that of gold.

Kinetic Energy Distribution of Secondary Electrons. — The distribution curves of the kinetic energy of the secondary electron by singly- and doubly-charged argon and neon ions and by singly-charged herium ions are shown in Figs. 3, 6, 7, 8 and 9, respectively. In these figures the results obtained for the incident ion energies of 1240, 840 and 540 V. are respectively indicated by circles, squares and triangles, and the correction of the contact potential difference between the ion target and

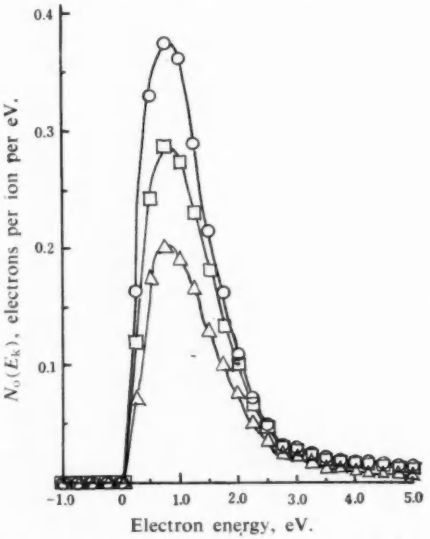

Fig. 6. Energy distributions of electron ejected from electro-polished Cu-Be by doubly-charged argon ions. Circular, square and triangular points denote the kinetic energy of incident ions of 1240, 840 and 540 V. respectively.

10) K. T. Compton and I. Langmuir, *Rev. Modern Phys.*, 3, 225 (1931).

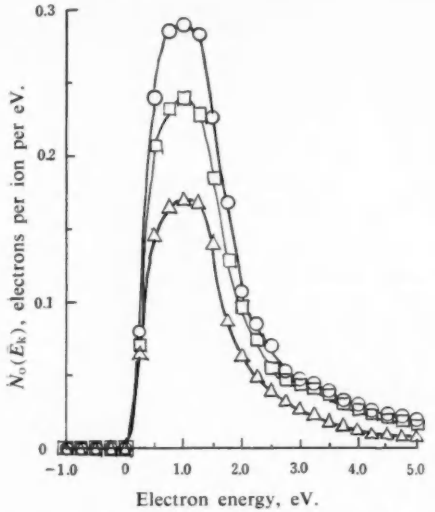

Fig. 7. Energy distributions of electron ejected from electro-polished Cu-Be by singly-charged neon ions. Circular, square and triangular points denote the kinetic energy of incident ions of 1240, 840 and 540 V. respectively.

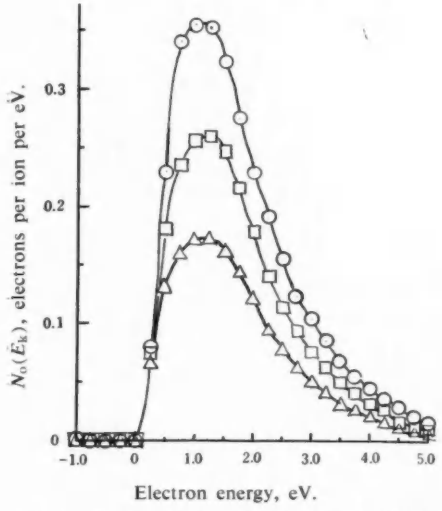

Fig. 8. Energy distributions of electron ejected from electro-polished Cu-Be by doubly-charged neon ions. Circular, square and triangular points denote the kinetic energy of incident ions of 1240, 840 and 540 V. respectively.

the electron collector was made for the retarding potential V_r.

These curves show that the fringing field of the analyzing magnet is negligible around the electron collector. If the fringing field is effective around the electron collector, then the electrons having low kinetic energy could not reach the electron collector and the distribution curves of the electron kinetic energy would have drifted to the low energy side. This effect has been studied by Hagstrum[3]. In the present studies, the magnetic field for the mass analyzer was varied for the focusing of ions having the various masses and kinetic energies, but every distribution curve obtained in this work practically showed that $N_0(E_k) = 0$ at the zero field in the retarding potential scale and no low energy tail has been observed.

The kinetic energy distribution shown by the half widths of each distribution curve and

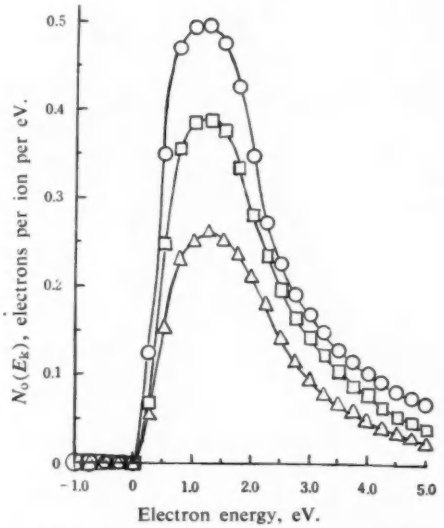

Fig. 9. Energy distributions of electron ejected from electro-polished Cu-Be by singly-charged herium ions. Circular, square and triangular points denote the kinetic energy of incident ions of 1240, 840 and 540 V. respectively.

TABLE I. VARIATION OF THE HALF WIDTHS OF THE ENERGY DISTRIBUTION CURVES AND YIELDS OF SECONDARY ELECTRONS FORM ELECTRO-POLISHED Cu-Be SURFACE WITH ION ENERGIES OF PRIMARY INERT GAS IONS

	Half widths of the energy distribution curves of secondary electrons in eV.			Yield of the secondary electrons γ_i in electrons per ion.		
Ion energy	1240	840	540	1240	840	540
Ion						
A^+	1.00	1.05	1.20	0.56	0.38	0.27
A^{2+}	1.30	1.35	1.40	0.58	0.43	0.36
Ne^+	1.40	1.45	1.50	0.57	0.43	0.31
Ne^{2+}	1.90	1.95	2.05	0.82	0.56	0.39
He^+	2.00	2.05	2.15	1.35	0.94	0.68

the yield γ_i of the secondary electrons are summarized in Table I.

Discussion

General Features of Energy Distribution Curves.—As seen in Figs. 3, 6, 7, 8 and 9, all distribution curves have their maximum at about 1 eV. But the sharpness of each distribution curve is more similar to that of the lithium ions and the tungsten surface by Waters[8] than that of the argon ions and the tungsten surface by Hagstrum[6], both shown in Fig. 10. Although the surface in this work

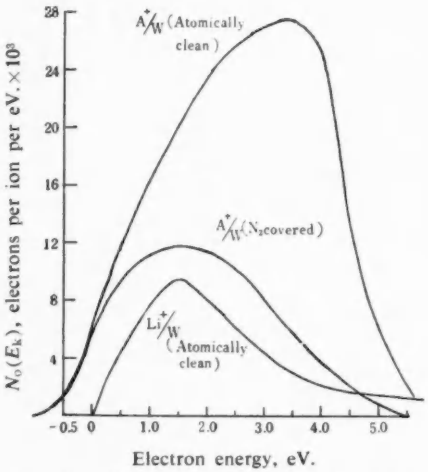

Fig. 10. Energy distributions of secondary electrons ejected by 10 eV. A^+ ions from atomically clean tungsten (W) and tungsten covered with the monolayer of nitrogen (N_2/W) given by Hagstrum[6], and the distribution curve of electron ejected by 1000 eV. Li^+ ions from atomically clean tungsten surface (Li^+) given by Waters[8].

was not atomically clean, the energy distribution curves observed in this work are not similar to that for the nitrogen covered surface of tungsten observed by Hagstrum shown in Fig. 10. The electron yields obtained in these studies are much greater than the results of Hagstrum and Waters. Since the present results were obtained from the alloy surface covered by residual gases and Hagstrum and Waters worked on the atomically clean surfaces of pure metals, the direct comparison of these data has no significant meaning, but the general features of the present distribution curves show much similarity of the kinetic ejection.

Effect of Ion Kinetic Energy.—As seen in Table I, the yield of the secondary electrons is clearly increased by increasing the kinetic energies of the incident ions, while the half width of the energy distribution curve of the secondary electrons is slightly decreased by increasing the ion kinetic energies. The difference between two distribution curves of different ion kinetic energies indicates the difference in the distribution of the different numbers of the secondary electrons emitted by different ion kinetic energies. In these different energy distributions, it is clearly shown that the increase in the electron yield as increasing the ion kinetic energies is mainly contributed to low energy electrons. This effect may be qualitatively explainable from the following idea similar to that of Sternglass[9]. Since the incident ions penetrate deeper as the ion kinetic energy increases, the number of secondary electrons formed in the alloy may be proportionally increased with the increase in the penetration depth. The formed secondary electrons may lose their energies in various types of collision processes, so that only a small fraction of them can reach the surface with sufficient energy to escape from the surface. But an increased number of electrons with the increase in the ion kinetic energy are formed in the deeper layer in the alloy, thus the detected secondary electrons might lose their initial energies during the passage through the layers in the alloy. The dependency of the distribution curves on the ion kinetic energy in these studies has previously been explained.

Influence of Ion Species.—As seen in Table I and Figs. 3, 7 and 9, the yield of the secondary electrons at any definite ion energy for the singly-charged inert gas ions is clearly increased in sequence from the argon, neon to helium ions, and this sequence has a correlation to their ionization potentials. Then, higher yield of the secondary electrons may be obtained by impact of the ion having the higher ionization potential.

As seen in Figs. 3, 7 and 9 and Table I, the energy distribution curves are broader for light ions than for heavier ions. These phenomena can not be explained by any similar explanation of the influence of the effect of the ion kinetic energy, since the ions of different masses are formed in the mass spectrometer with constant kinetic energy when the ions were accelerated by the acceleration voltage. If the penetration depth of the ions is assumed[9] to be simply dependent upon the ion kinetic energy, the penetration depth of the lighter ions is the same as that of the heavier ions. But the present results on the energy distribution clearly show the existence of the higher energy electrons in the case of lighter ions. They also indicate that the higher

energy electrons emitted by the ions have a higher ionization potential.

These phenomena indicate that the mechanism of the secondary electron ejection from the electro-polished copper-beryllium surface is not simple. The ionization potentials of argon, neon and helium are 15.76, 21.59 and 24.58 eV., respectively, and though the work function of the electro-polished copper-beryllium is not certain it may be presumed to be less than 6 eV. Then, it is considered from the present experimental conditions that the ionization potentials of the ions of the present consideration are larger then twice the work function of the alloy surface. Consequently, it remains open to discussion as to the mechanism of the potential ejection[7], but the general features of the distribution curves of the electron energies show considerable similarity to the kinetic ejection. For the reason mentioned above, it is difficult to deduce any simple conclusion on the mechanism of the electron emission by inert gas ions from the present work.

Effect of Ionic Charges.—From a comparison of Figs. 3 and 6 for argon ions and Figs. 7 and 8 for neon ions, the energy distribution curves by the doubly-charged ions are broader than those by the singly-charged ions, and the yield of the secondary electrons by the doubly-charged ions are greater than that by the singly-charged ions at any definite ion kinetic energy. Thus the energy distribution indicates that the doubly-charged ions ejected the higher energy electrons than the singly-charged ions do. This tendency is similar to the influence of the ion species on the yield and energy distribution of secondary electrons. The secondary ionization potential of the argon and neon ions are 43.52 and 62.57 eV., respectively, then the mechanism of the secondary electron emission from copper-beryllium may occur according to the complex mechanisms in which the secondary electron is ejected by contribution of both of the kinetic and the potential energies of the incident ions.

Summary

The distribution curves of the kinetic energies of the secondary electrons from the electro-polished copper-beryllium surface by inert gas ions were measured by the retarding potential method together with the yield of the secondary electron emission. The contact potential difference between the ion target (electro-polished copper-beryllium) and the electron collector (gold) was also measured by the retarding potential method for the thermal electrons from tungsten, and the correction of this contact potential difference was made for the kinetic energies of secondary electrons. The main results obtained are as follows.

(1) The contact potential difference between gold and electro-polished copper-beryllium (4%) is 0.95 eV. (gold, negative).

(2) The general features of the distribution curves of secondary electrons are similar to the distribution curves of the kinetic ejection measured by Waters.

(3) The present results of the energy distribution curves of secondary electrons by the inert gas ions indicate that the yield of secondary electrons is increased by increasing the kinetic energy of the primary ions, and that this increment in the yield is mainly contributed from the secondary electrons which have lower kinetic energies than that of the secondary electrons emitted by the incident ions of low kinetic energies. These phenomena are able to be postulated qualitatively by the idea of sternglass.

(4) The total number of emitted electrons is increased with the increase in the value of the ionization potential of incident ions, and the kinetic energies of emitted electrons become greater by increasing the potential energy of incident ions. These phenomena are difficult to explain by the mechanism of the kinetic ejection, therefore the electron emission from the electro-polished copper-beryllium surface by inert gas ions may occur according to the complicated mechanism in which the potential energies of incident ions contribute to the electron emission together with their kinetic energies.

(5) In contrast with the singly-charged ions, the doubly-charged ions give rise to the broadening of the energy distribution curves. This also suggests the occurrence of the complicated ejection mechanisms.

The author wishes to acknowledge his indebtedness to Professor Shoji Shida of the Tokyo Institute of Technology, Professor Teruo Hayakawa and Professor Osamu Toyama of University of Osaka Prefecture, under whose direction and guidance this work was carried out.

The expense has been defrayed in part from a grant given by the Ministry of Education, to which the author's thanks are due.

Department of Applied Chemistry
Faculty of Engineering
University of Osaka Prefecture
Sakai, Osaka

On the Structures of p-tert-Butyl Phenol Resin and α-Naphthol Resin. II. Infrared Absorption Spectra of p-tert-Butyl Phenol and α-Naphthol

By Reisuke SODA

(Received February 28, 1961)

It was previously reported[1] that a polymer, synthesized from *p-tert*-butyl phenol and formaldehyde, was a suitable material for coating the fiber of a dust respirator to obtain a high efficiency of filtration. This polymer showed anomalous phenomena in its benzene solution.

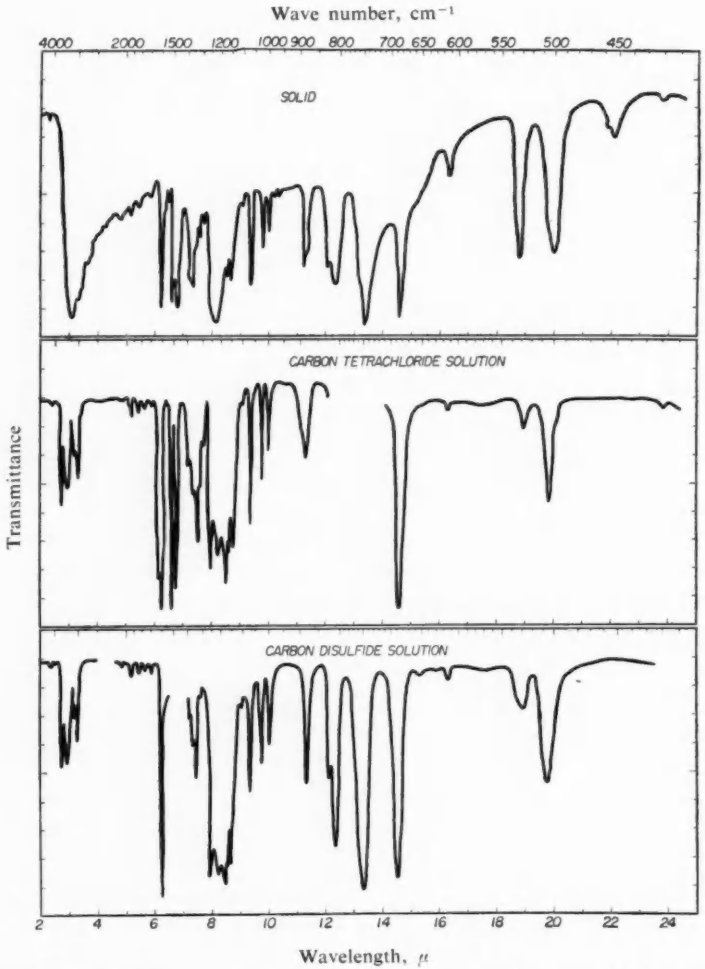
Wave number, cm⁻¹
4000 2000 1500 1200 1000 900 800 700 650 600 550 500 450
SOLID
CARBON TETRACHLORIDE SOLUTION
CARBON DISULFIDE SOLUTION
Transmittance
2 4 6 8 10 12 14 16 18 20 22 24
Wavelength, μ

Fig. 1. Spectra of phenol in solid and solutions. Spectrum is cut off in the region of interference due to solvents. Concentration of solution is about 0.1 M in carbon tetrachloride and 0.5 M in carbon disulfide.

1) R. Soda, *Bull. Natl. Inst. Ind. Health*, No. 3, 40 (1960).

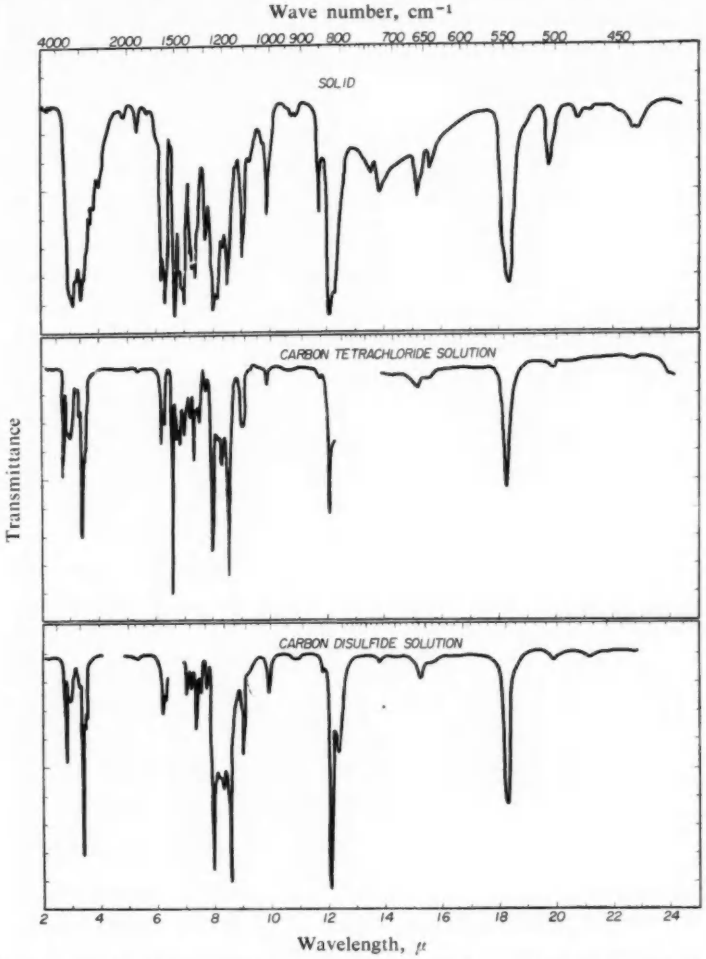
Wave number, cm⁻¹
4000 2000 1500 1200 1000 900 800 700 650 600 550 500 450
SOLID
CARBON TETRACHLORIDE SOLUTION
CARBON DISULFIDE SOLUTION
Transmittance
2 4 6 8 10 12 14 16 18 20 22 24
Wavelength, μ

Fig. 2. Spectra of *p-tert*-butyl phenol in solid and solutions. Spectrum is cut off in the region of interference due to solvents. Concentration of solution is about 0.3 M in carbon tetrachloride and 0.4 M in carbon disulfide.

The polymer had a relatively small molecular weight and both sides of the polymer chain were *p-tert*-butyl phenol. Also the OH bonds of the polymer were bound by a very strong intramolecular hydrogen bonding and this intramolecular hydrogen bonding was made partly loose only when the polymer was dissolved in benzene. Bands of the spectrum obtained in the region of sodium chloride prism were assigned, but some ambiguity remained in these assignments.

In the present work, to eliminate the above stated doubtfulness of the assignment, the infrared absorption spectra of *p-tert*-butylphenol and the other O–H compounds were precisely measured and the observed region was extended to about 33 μ in the region of cesium bromide optics, particularly the in-plane and the out-of-plane O–H deformation vibration were investigated in more detail.

Experimental

p-tert-Butyl phenol was purified by recrystallizing it from its saturated benzene solution and by vacuum distillation. α-Naphthol was recrystallized from ethyl alcohol. Phenol was purified by distillation. The solvents used were carbon tetrachloride and carbon disulfide, each being distilled once. The potassium bromide powder used for the measurement of the solid spectrum, was heated, ground to particle size of 200 to 300 mesh and dried by heating at 200°C. For the measurement of the spectrum of a solid some samples were resolidified

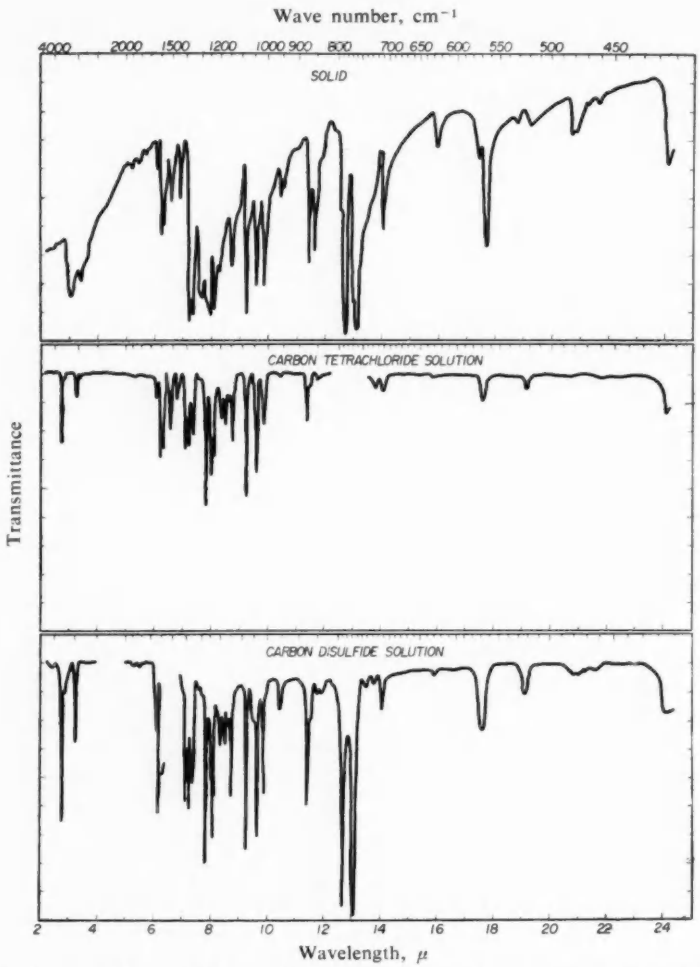
Wave number, cm⁻¹
4000 2000 1500 1200 1000 900 800 700 650 600 550 500 450
SOLID
CARBON TETRACHLORIDE SOLUTION
CARBON DISULFIDE SOLUTION
Transmittance
2 4 6 8 10 12 14 16 18 20 22 24
Wavelength, μ

Fig. 3. Spectra of α-naphthol in solid and solutions. Spectrum is cut off in the region of interference due to solvents. Concentration of solution is about 0.05 M in carbon tetrachloride and 0.1 M in carbon disulfide.

between two rock salt plates or potassium bromide plates which were polished at both surfaces to make flat. The sample powder was sandwiched between two heated window plates and cooled moderately to make a solid film. The other spectra were obtained with potassium bromide disks.

The cell used for the solution had the thickness of 1 mm. and its window was of potassium bromide or rock salt. The infrared spectrum was observed by a Perkin-Elmer Model 137 Infracord spectrophotometer, Perkin-Elmer Model 21 spectrophotometer and Perkin-Elmer Model 221 spectrophotometer.

Results and Discussion

The spectrum of solid of fused film between window plates was approximately the same as that of a potassium bromide pellet. It may be considered that the orientation effect does not exist in this case. Therefore the spectrum of solid obtained could be analyzed without caution of experimental condition. The spectra of phenol in the solid state, in solutions of carbon tetrachloride and of carbon disulfide are shown in Fig. 1. Those of *p-tert*-butyl phenol and of α-naphthol are illustrated in Figs. 2 and 3, respectively. The spectra of solids of these three compounds differ from those of solutions in several regions. The spectra of these compounds in solution change their features with the concentration of solution in some regions. Those changes of spectra are illustrated in Figs. 5 to 16. The spectra

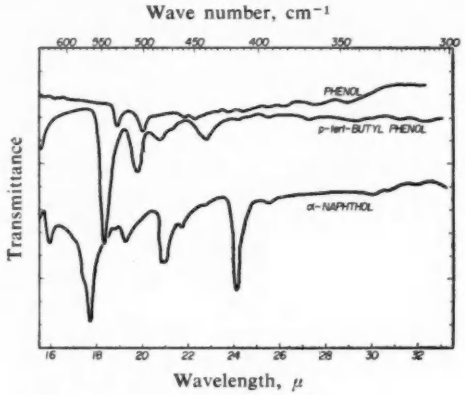

Fig. 4. Spectra of *p-tert*-butyl phenol and α-naphthol in CsBr region (KBr disk).

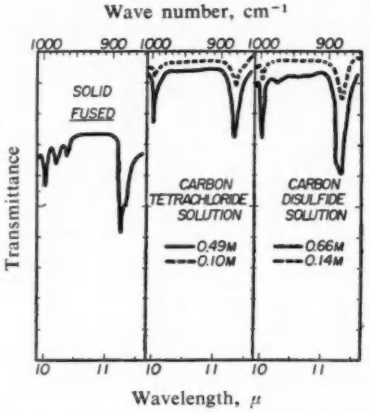

Fig. 7. Spectra of phenol in the region near 1000 cm⁻¹.

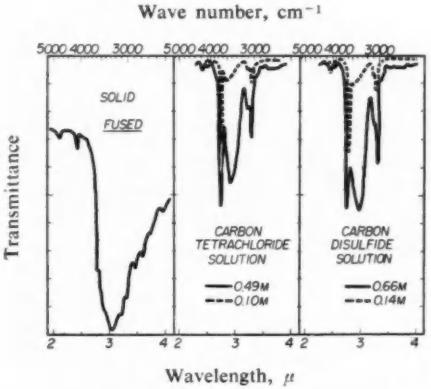

Fig. 5. Spectra of phenol in 3 μ region.

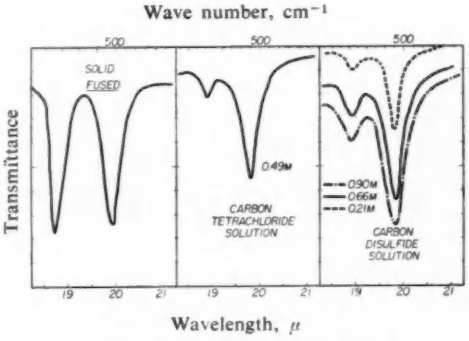

Fig. 8. Spectra of phenol in the region close to 500 cm⁻¹.

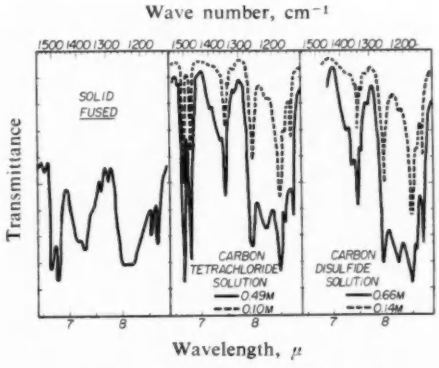

Fig. 6. Spectra of phenol in the region of 1500~1150 cm⁻¹. Spectrum is cut off in the region of interference due to solvents.

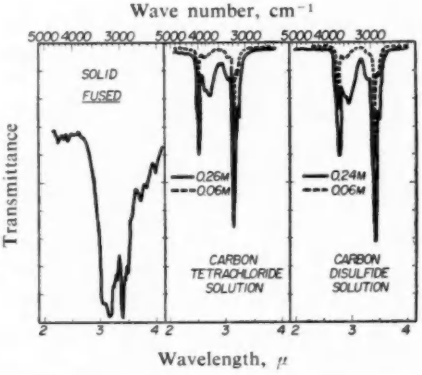

Fig. 9. Spectra of *p-tert*-butyl phenol in 3 μ region.

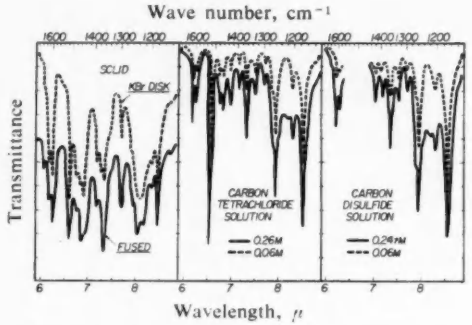

Fig. 10. Spectra of *p-tert*-butyl phenol in the region of 1600~1150 cm^{-1}. Spectrum is cut off in the region of interference due to solvents.

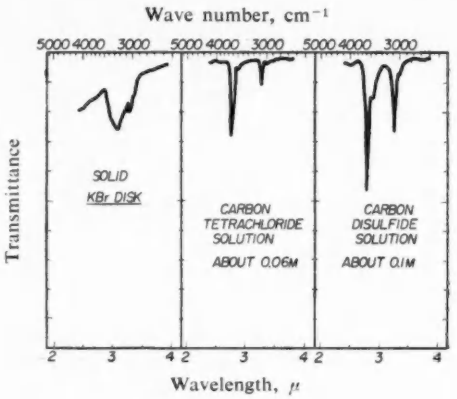

Fig. 13. Spectra of α-naphthol in 3 μ region.

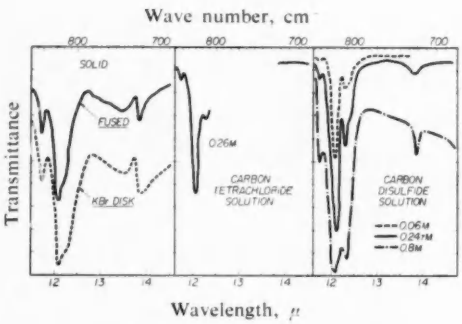

Fig. 11. Spectra of *p-tert*-butyl phenol in the region near 800 cm^{-1}. Spectrum is cut off in the region of interference due to solvents.

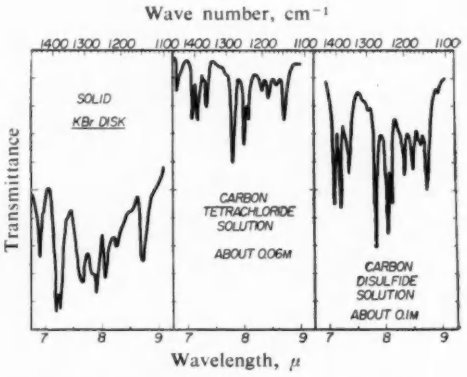

Fig. 14. Spectra of α-naphthol in 8 μ region. Spectrum is cut off in the region of interference due to solvents.

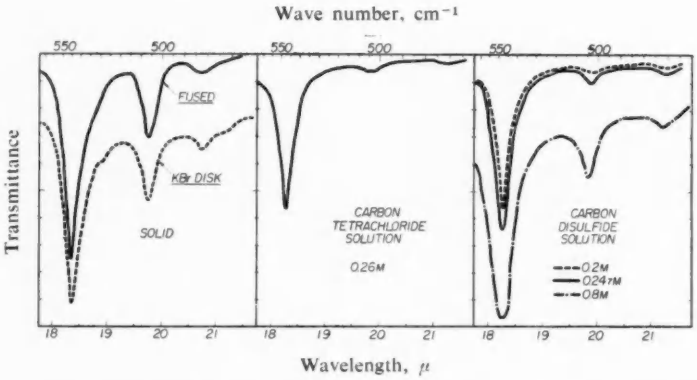

Fig. 12. Spectra of *p-tert*-butyl phenol in the region of 550~460 cm^{-1}.

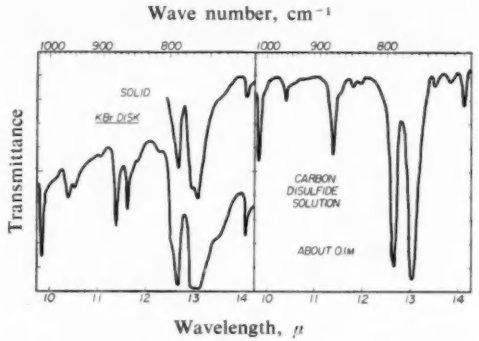

Fig. 15. Spectra of α-naphthol in the region of 1000~700 cm⁻¹.

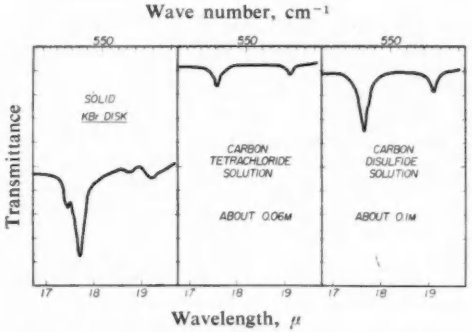

Fig. 16. Spectra of α-naphthol in the region near 550 cm⁻¹.

of these compounds in the region of cesium bromide optics are shown in Fig. 4. No strong band which is observable at ordinary concentration is found in the region of 25 to 34 μ. Considerable changes of spectra of these compounds are observed in three regions at 3, 7 to 8 and near 18 μ when the phase and the concentration alter. The other remarkable changes are found in the regions of 6, 11 and 14 μ, but these changes are much less than those in the former regions. The changes in the regions at 6, 11 and 14 μ are observed when the solids are brought into solution but are not observed when the concentrations of solutions alter. Changes of spectral region at 18 μ of *p-tert*-butyl phenol and α-naphthol are not clear compared with that of phenol.

Phenol. — The spectrum of phenol has been investigated by several authors. Kuratani[2] assigned OH deformation vibrations to it and concluded that this vibration coupled with C–O stretching vibration. He reported that these vibrations gave rise to the bands at 1280 and 1195 cm⁻¹ respectively. Mecke and Rossmy[3] reported that these bands which occurred at 1339 and 1174 cm⁻¹ shifted by complete deuteration to 1294 and 915 cm⁻¹, respectively, and that the band at 1174 cm⁻¹ had a larger part of O–H deformation vibration character than the band at 1339 cm⁻¹.

In the present experiment, as shown in Figs. 1 and 6, the appreciable change is found in region at 1200 cm⁻¹ with the change of phase and concentration of solution. The change at 1300 cm⁻¹ region is so complex that it is not easy to make a unique assignment. The band at 1220 cm⁻¹ of solid spectrum shifts to 1210 cm⁻¹ in solution spectrum and the intensity of this band decreases when the concentration of solution is lower. In the solution, a new band appears near 1180 cm⁻¹ and its relative intensity to that of 1210 cm⁻¹ band increases at the lower concentration. The 1390 cm⁻¹ band of solid decreases its intensity and a strong band appears near 1340 cm⁻¹ in the solution. The relative intensity of the latter band to the former increases in a lower concentration of solution. Then it may be concluded that the bands 1390 and 1220 cm⁻¹ in solid state and the bands 1380 and 1210 cm⁻¹ in solution are assigned to coupled modes of C–O stretching vibration and hydrogen-bonded O–H deformation vibration. The bands at 1340 and 1180 cm⁻¹ may be assigned to the coupled modes of C–O stretching vibration and free O–H deformation vibration. These conclusions do not contradict the results of other papers[2-5]. These conclusions agree with what is observed in 3 μ region. In this region the stretching vibration of the O–H bond gives rise to a broad at its center at 3300 cm⁻¹ in solid but in solution sharp band at 3600 to 3620 cm⁻¹ and broad band at 3370 cm⁻¹ or higher. The phenol molecule will associate to a large aggregate through the hydrogen bonding in the solid state. In the solution these molecules are dispersed into monomer with free O–H bond and partly associate to build up a small polymer through O–H···O linkage. Therefore the O–H vibration of solid shows the strong hydrogen bonding character due to a larger associated molecule and that of solution shows the characters of free hydroxyl bond and partly of the weakly hydrogen-bonded bond. Other changes are observed

2) K. Kuratani, *J. Chem. Soc. Japan, Pure Chem. Sec.* (*Nippon Kagaku Zasshi*), **73**, 758 (1952).

3) R. Mecke, and C. Rossmy, *Z. Elektrochem.*, **59**, 866 (1955).

4) L. J. Bellamy, "The Infrared Spectra of Complex Molecules", Metheu & Co., Ltd., London, J. Wiley & Sons Inc., New York (1954), pp. 64~69 and 96.

5) "Chemical Application of Spectrocopy", Ed. by W. West, Interscience Pub., Ltd., London (1956), pp. 388~434.

TABLE I. BAND POSITIONS AND ASSIGNMENT OF SPECTRUM OF PHENOL

Band, cm^{-1}		Assignment
Solid	Solution	
	3610	ν(O-H), free
	3480	ν(O-H), bonded
3360	3380	ν(O-H), bonded
3090	3070	ν(C-H), aromatic
3010	3030	ν(C-H), aromatic
1605	1605	Ring vibration
1597	1597	Ring vibration
1502	1501	Ring vibration
1473	1470	Ring vibration
1389	1387 to 1380	δ(O-H), bonded and ν(C-O)?
1370	1355	δ(O-H), bonded and ν(C-O)?
	1341	δ(O-H), free and ν(C-O)
1337	1330	Skeletal vibration
1318	1310	Skeletal vibration
1245	1256	Skeletal vibration
1222	1211	δ(O-H), bonded and ν(C-O)
	1177	δ(O-H), free and ν(C-O)
1168	1166	δ(C-H) or skeletal vibration
1153	1150	δ(C-H) or skeletal vibration
1071	1067	δ(C-H) or skeletal vibration
1024	1023	δ(C-H) or skeletal vibration
998	998	Skeletal vibration
883	882	Skeletal vibration
822	824	
810	809	
752	750	δ(C-H), out-of-plane
689	687	δ(C-H), out-of-plane
663	656	
615	616	Skeletal vibration
533	527	δ(O-H), out-of-plane?
503	505	δ(O-H), out-of-plane?

near 890 and 980 cm^{-1}. But these changes do not clearly show its origin and are smaller than those in the above-mentioned regions. Furthermore the changes in this region are not observed with variation of concentration of solution. These changes may be explained as influence of crystal field[6]. Each band is tentatively assigned as shown in Table I. Out-of-plane O-H deformation vibration is considered to give rise to the band in lower frequency region. As shown in Fig. 4, the main intense bands arise at 530 and 500 cm^{-1}. These bands change their relative intensities when this substance is dissolved from a solid. The frequency shifts are slight as shown in Fig. 8. In carbon disulfide solution and in a solid form this relative absorbance ratio (E_{530}/E_{500}) varies as follows:

State	Relative intensity Ratio
Solid	1.10
CS_2 soln.	
0.9 M	0.22
0.66 M	0.21
0.21 M	0.19
CCl_4 soln.	
0.49 M	0.19

Then the band at 530 cm^{-1} is tentatively assigned to OH out-of-plane deformation vibration of a solid and the 500 cm^{-1} band to that of free O-H bond and some other vibrations. No benzene gives rise to absorption bands in these regions but with toluene a weak band arises at 521 cm^{-1}. Chlorobenzene, bromobenzene and iodobenzene give rise to a strong band near 450 to 460 cm^{-1} and ethylbenzene at 486 cm^{-1}. Therefore the bands at 530 and 500 cm^{-1} may be connected with the O-H out-of-plane deformation vibration and the other skeletal vibration[5].

***p-tert*-Butyl Phenol.** — The spectra of this compound as illustrated in Figs. 2, 4, 9, 10, 11 and 12, are similar to those of phenol, particulary the bands which concern the O-H vibrations. Phenol is a monosubstituted benzene derivative and *p-tert*-butyl phenol is a 1,4 disubstituted derivative. These spectra differ from each other at the bands due to some benzene ring vibrations and ring C-H vibrations. As the latter substance has further a tertiary butyl group, there appear also the bands due to the methyl group and the $C\cdot(CH_3)_3$ group vibrations.

The change of phase and concentration causes changes of its association degree and state of molecule. This resembles that of phenol and hence O-H stretching vibration and O-H in-plane deformation vibration change their frequencies and intensities. These facts are illustrated in Figs. 9, 10 and 12. In Fig. 11, the bands at 820 and 760 cm^{-1} change slightly their features with phase. The reason is still unexplained exactly but may be attributed to the crystal field effect[6]. The assignments of bands are summarized in Table II.

The spectrum of phenol in the region at 18 to 22 μ is different from that of *p-tert*-butyl phenol. It is generally accepted that in this region the band is highly sensitive to the substituent[5]. 1, 4-Dimethyl benzene gives rise to a weak band at 645 cm^{-1} and a very strong band at 480 cm^{-1}. This strong band shifts to 432 cm^{-1} in 1, 3-dimethyl benzene and to 436 cm^{-1} in 1, 2-dimethyl benzene. Therefore it may be reasonable to conclude[5] that disubstituted

6) R. J. Grisemthwaite, and R. F. Hunter, *J. Appl. Chem.*, **6**, 324 (1956).

Table II. Band positions and assignment of spectrum of *p-tert*-butyl phenol

Band, cm^{-1}		Assignment
Solid	Solution	
	3610	ν(O-H), free
	3480	ν(O-H), bonded
3230	3380	ν(O-H), bonded
3060		ν(C-H), aromatic
3020	3030	ν(C-H), aromatic
2950	2960	ν(C-H), $-CH_3$
2900	2910	ν(C-H), $-CH_3$
2860	2880	ν(C-H), $-CH_3$
1613	1612	Ring vibration
1597	1595	Ring vibration
1520	1521	Ring vibration
1477	1477	δ(C-H), $-CH_3$
1460	1463	δ(C-H), $-CH_3$
1442	1425	δ(O-H), bonded and ν(C-O)
1391	1391	δ(C-H), $-CH_3$
1361	1363	δ(C-H), $-CH_3$
	1328	δ(O-H), free and ν(C-O)
1298	1294	Skeletal vibration
1263	1256	C-CH_3 rocking
1230	1217	δ(O-H), bonded and ν(C-O)
1200	1203	δ(C-H), aromatic and C-CH_3 rocking
	1173	δ(O-H), free and ν(C-O)
1112	1110	δ(C-H), aromatic
1084	1083	δ(C-H), aromatic
931	931	ν(C-C), C-CH_3
851	849	ν(C-C), C-CH_3
827	828	δ(C-H), out-of-plane
818	812	δ(C-H), aromatic or ν(C-C), C-CH_3
723	724	
660	659	Skeletal vibration or substituent characteristic
641	641	Substituent characteristic or skeletal vibration
545	546	δ(O-H), out-of-plane ?
507	503	δ(O-H), out-of-plane and others
472	473	
	469	δ(O-H), out-of-plane : free O-H
442	442	
416		C-C bending, C-CH_3

benzene gives rise to the band at 500 to 400 cm^{-1}. Solid of *p-tert*-butyl phenol absorbs at 545 cm^{-1} (strong), 506 cm^{-1} (medium), 482 cm^{-1} (weak) and 472 cm^{-1} (very weak). The band at 545 cm^{-1} remains unchanged when the compound is dissolved. The band at 482 cm^{-1} disappears and a new band appears at 470 cm^{-1}. No regularity is found among the relative intensities of bands at 545, 506, 482 and 470 cm^{-1}. The effect of the condition of measurement on these values is so remarkable that a quantitative argument has little meaning. Qualitatively, the bands at 506 and 480 cm^{-1} of solid and those at 503 and 472 cm^{-1} of solution are perhaps concerned with O-H out-of-plane deformation vibration, considering that of phenol. The other vibration may couple with this vibration. Further discussion can not be carried out now.

Other assignments are nearly the same as in the previous report[1] in the region of sodium chloride optics. These assignments are obtained with consideration of those of phenol, 1,4-disubstituted benzene and *tert*-butyl compounds.

α-Naphthol.—α-Naphthol is an aromatic O-H compound which has one group of three adjacent free hydrogen atoms and one group of four adjacent free hydrogen atoms. α-Naphthylamine in solid gives rise to a broad band near 3200 cm^{-1} but in solution gives rise to a sharp band at 3620 cm^{-1} and a weak band at 3500 cm^{-1}. This aspect of OH stretching vibration band is the same as those of phenol and *p-tert*-butyl phenol stated already. Regions 1400 to 1350 cm^{-1}, 1330 to 1250 cm^{-1} and 1210 to 1160 cm^{-1} vary with the change of phase. From those results it may be considered that the band due to OH deformation vibration appears near 1170 and 1330 to 1340 cm^{-1} for free α-naphthol molecule. There is also some possibility of considering the coupling of OH deformation vibration with the other mode of vibration rather than with the C-O stretching vibration. Then the above-mentioned regions which show the different features with the change of phase and concentration of solution, may be concerned with the OH deformation vibration. Tentatively for free α-naphthol, the bands near 1180 and 1359 cm^{-1} are assigned to those vibrations.

Out-of-plane deformation vibration of aromatic C-H bonds may give rise[4,5,7] to the bands at 760 to 740 cm^{-1} and 780 to 760 cm^{-1} (more generally 800 to 760 cm^{-1}) or 770 to 735 cm^{-1} and 810 to 750 cm^{-1} for α-naphthol. The other characteristic bands to the substitution may be considered to appear near 725 to 680 cm^{-1}, or more precisely at 740 to 710 cm^{-1}, (720 to 710 cm^{-1}), 710 to 690 and 650 cm^{-1}. Then the bands at 789 and 765 cm^{-1} may be assigned to that mode of vibration and other characteristic bands may be attributed to those at 730, 710 and 629 cm^{-1}. According to the literature[5,7] the three bands at 730, 710 and 629 cm^{-1} can be assigned to the in-plane deformation vibration of aromatic C-H bond.

The change of spectra in the region below 1000 cm^{-1} with phase change is yet to be explained clearly. The doublet of 959 cm^{-1},

7) H. Luther and H. Gunzler, *Z. Naturforsch* **10b**, 445 (1955).

the band at 867 cm^{-1} and bands at 769 and 765 cm^{-1} in solid are different from these in solution. The doublet bands disappear and the single band appears at 959 and 767 cm^{-1}, and the band 867 cm^{-1} disappears completely when the solid sample is dissolved. It is not suitable to consider that these bands are attributable to the vibration mode concerned with O–H vibration because O–H vibration does not give rise to bands in these regions in general. These changes may be caused from crystal field effect[6].

TABLE III. BAND POSITIONS AND ASSIGNMENT OF SPECTRUM OF α-NAPHTHOL

Band, cm^{-1}		Assignment
Solid	Solution	
	3620	ν(O–H), free
	3500	ν(O–H), bonded
3240		ν(O–H), bonded
3110		ν(O–H), bonded
3050	3060	ν(C–H), aromatic
1634	1634	Ring vibration
1600	1600	Ring vibration
1582	1582	Ring vibration
1560	1546	Ring vibration
1515	1517	Ring vibration
1453	1453	Ring vibration
1439	1404	
1387 or 1377	1388	δ(O–H), bonded and ν(C–O)
	1358	δ(O–H), free and ν(C–O)
1315	1312	δ(O–H), bonded and ν(C–O)?
1300	1297	δ(O–H), bonded and ν(C–O)?
1264	1276	Skeletal vibration
1253	1245	Skeletal vibration
1239	1235	Skeletal vibration
	1199	δ(O–H), free and ν(C–O)?
	1181	δ(O–H), free and ν(C–O)?
1172	1175	Skeletal vibration
1148	1145	δ(C–H)
1083	1082	δ(C–H) or skeletal vibration
1044	1040	Skeletal vibration
1015	1015	δ(C–H)
959	958	Skeletal vibration
875	877	Skeletal vibration
856	850	δ(C–H), out-of-plane ?
843	837	δ(C–H), out-of-plane
789	790	δ(C–H), out-of-plane
768	768	δ(C–H), out-of-plane
740	742	Skeletal vibration or δ(C–H), out-of-plane
731	725	δ(C–H), out-of-plane
712	710	δ(C–H), out-of-plane
628	629	Skeletal vibration
573 or 564	568	δ(O–H), out-of-plane ?
521	524	δ(O–H), out-of-plane ?
482	480	Substituent characteristic skeletal vibration
478	476	Substituent characteristic skeletal vibration
461	461	Substituent characteristic skeletal vibration
416	416	Substituent characteristic skeletal vibration

The tentative assignments are summarized in Table III. In the present experiment the concentration of solution is not altered. Therefore the assignment of the band concerned with OH vibration can not be carried out decidedly. Out-of-plane OH deformation vibration is expected to give rise to the bands in the region near 500 cm^{-1} with consideration of these bands of phenol and *p-tert*-butyl phenol: But α-naphthol shows such a complex aspect in this region that a simple assignment can not be carried out at present. Perhaps bands at 530, 520 and 460 cm^{-1} may be concerned with this vibration mode.

It may be accepted as true that the above three compounds give rise to the bands near 3600 cm^{-1} due to OH stretching vibration, those near 1170 cm^{-1} and near 1330 cm^{-1} due to free OH in plane deformation vibration and those near 500 cm^{-1} concerned in OH out-of-plane deformation vibration. These bands are attributed to free OH bond, but in a case of solid state or associated state, the bands at 3300 cm^{-1}, those at 1200 to 1230 cm^{-1} and 1380 to 1430 cm^{-1}, and those near 500 cm^{-1} may be assigned to the above mentioned vibration modes respectively. The bands in the region of 500 cm^{-1} can not be decidedly assigned now but may be determined by deuteration of OH bond, considering the argument given above.

In the next paper the assignment will be made of the absorption bands of *p-tert*-butyl phenol resin and α-naphthol resin according to the result of this work.

Summary

In connection with the work on a resin for dust respirator, the spectra of phenol, *p-tert*-butyl phenol and α-naphthol were observed in solid and in solution. Infrared absorption spectra can be explained by considering that these compounds associate by hydrogen bonding in solid form and that they hold the equilibrium between monomer and associated molecule in solution. Reasonable assignments were made to some of the bands observed. The deformation vibration of O–H (free) and stretching vibration of C–O seem to couple with each other and give rise to bands near 1340 and 1180 cm^{-1} in any of these three compounds. Bands due to the out-of-plane O–H deformation vibration could not be determined but it was found that the bands in the

550～500 cm^{-1} region were concerned with this vibrational mode.

The author wishes to express his hearty thanks to Assistant Professor T. Miyazawa and his collaborators at the Institute for Protein Research, Osaka University, for their kindness in permitting the use of a Perkin-Elmer Model 221 spectrophotometer. He wishes to express his thanks to Mr. M. Kawano at the Railway Technical Research Institute for the measurement of the spectrum in cesium bromide region. He also expresses his thanks to Dr. S. Koshi of this Institute for his kind supply of samples.

National Institute of Industrial Health
Kawasaki-shi, Kanagawa-ken

Infrared Absorption Spectra of Quartz and Some other Silica Modification

By Reisuke SODA

(Received February 28, 1961)

Recently it was reported that the surface of a quartz particle was forced to change its structure by grinding[3-5]. Infrared absorption spectra of the quartz perticle showed that the band near 950 cm^{-1} appeared as the result of grinding and disappeared when the particle was leached[1,2]. The origin of the band near 3400 cm^{-1} was assumed to be the stretching vibration of O–H bond and its intensity changed depending upon the treatment of the particle. The parallel relation was observed between the intensity of 3400 cm^{-1} band and that of 950 cm^{-1}. The intensities of the two bands increased with the degree of grinding. Another silica modification such as carplex gave rise to the 950 cm^{-1} band and the intensities of both the 950 cm^{-1} band and the 3400 cm^{-1} band of this compound were stronger than those bands of other silica modifications. Previously the author assigned it tentatively to the deformation vibration of O–H link of silanol group at the surface layer of the particle[1]. In the present paper more evidence will be given to confirm the assignment of this band.

Experimental

A quartz sample was prepared by grinding and in some cases by leaching the ground particle. The ground particle was fractionated by the particle size suspending it in water and separating it with centrifugal force. This procedure was reported in the other paper[1]. Ten per cent aqueous solution of sodium hydroxide was used to leach the particle. A quartz sample used was that was produced at Ishikawayama. The carplex was supplied by the Shionogi Co., Ltd. It was fine powder of particle size less than 0.5 μ. The sample powder was mixed with potassium bromide in an agate mortar. The potassium bromide used was c. p. grade and pulverized in agate mortar into particle size of 200 to 300 mesh by sieving with a stainless steel sieve and dried by heating above 200°C for about one day. The mixed powder was dried by heating at about 150°C for 3 hr. and poured into the die to be pressed under 10 tons per square centimeter after evacuation for about 10 min. A shaped disk was inserted into the cell for the potassium bromide disk method.

Infrared absorption spectra were measured with Perkin-Elmer model 137 infracord spectrophotometer and Perkin-Elmer model 221 spectrophotometer.

Notations showing kinds of sample particles are as follows[1]:

Q-I-2M is the sample Ishikawayama quartz ground for 2 min., Q-I-6H that ground for 6 hr., Q-I-24H for 24 hr., O-I-100H for 100 hr. and Q-I-2M-L is the sample Ishikawayama quartz ground for 2 min. and leached with aqueous sodium hydroxide.

Results

The spectrum of Q-I-2M gives rise to the bands at 1180, 1150 and 1070 cm^{-1}. These are very strong, but those at 800, 780 and 695 cm^{-1} are sharp and have medium intensities. Sometimes a band near 3400 cm^{-1} is observed with only a very weak intensity. The spectrum of Q-I-6H gives rise to the very weak band at 950 cm^{-1} and to a weak but clear band at 3300 to 3400 cm other than those of Q-I-2M. In

1) H. Sakabe et al., *Bull. Natl. Inst. Ind. Health*, No. 4 (1961), in press.
2) R. Soda, ibid., (1961), in press.
3) J. Brown, W. J. Jaap and P. D. Ritchie, *J. Appl. Chem.*, **9**, 153 (1959).
4) K. Wheatley, ibid., **9**, 159 (1959).
5) J. A. Van Lier, P. J. De Bruyn and J. Th. G. Overbeek, *J. Phys. Chem.*, **64**, 1675 (1960).

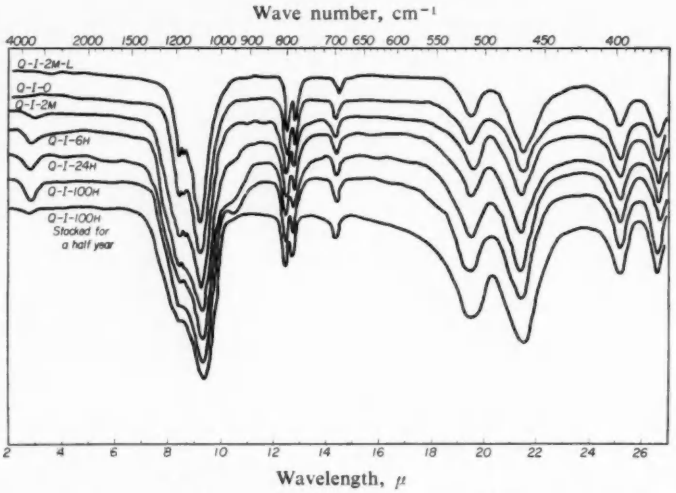

Fig. 1. Spectra of quartz particles prepared by various procedures. The range of particle size is 0.5~2 μ and mean size is about 1 μ. Samples are Ishikawayama quartz ground by hand (Q-I-0), ground mechanically for 2 min. (Q-I-2M), for 6 hr. (Q-I-6H), for 24 hr. (Q-I-24H) and for 100 hr. (Q-I-100H). Q-I-2M-L designates Ishikawayama quartz ground for 2 min. and leached by NaOH aq.

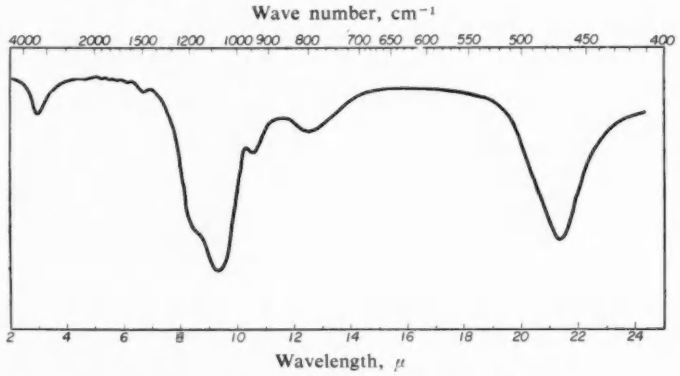

Fig. 2. Spectrum of amorphous silica "Carplex".

spectra of Q-I-24H and Q-I-100H the bands at 3300 to 3400 cm^{-1} and at 950 cm^{-1} are more intense than those of Q-I-6H. The intensities of those bands increase with grinding times. In the spectrum of Q-I-100H which has been kept in a desiccator for a half year, the intensities of the bands at 3400 and 950 cm^{-1} decrease and sometimes the band at 950 cm^{-1} is scarcely observed. The spectrum of carplex gives rise to the strongest bands at 1160 and 1090 cm^{-1} and to a very weak broad band near 800 cm^{-1}. Besides those bands, it gives rise to a band of medium intensity at 3300 cm^{-1} and to a well defined band near 950 cm^{-1} as shown in Fig. 2.

The spectrum of Q-I-2M-L gives rise to no bands at 3400 and 950 cm^{-1}. The three bands near 1100 cm^{-1} changed their aspects with their grinding times and with leaching. These band groups are sharply separated with leached quartz and lose their defined aspects with the grinding process. The band at 1070 cm^{-1} is broader and first the band at 1150 cm^{-1} becomes like the shoulder of 1070 cm^{-1} band and finally is masked by the latter band with the increment of grinding time. The band at 1180 cm^{-1} is like the shoulder of 1070 cm^{-1} band also when the grinding time is longer than about 20 hr. These changes are illustrated in Fig. 1. In the region of the cesium bromide

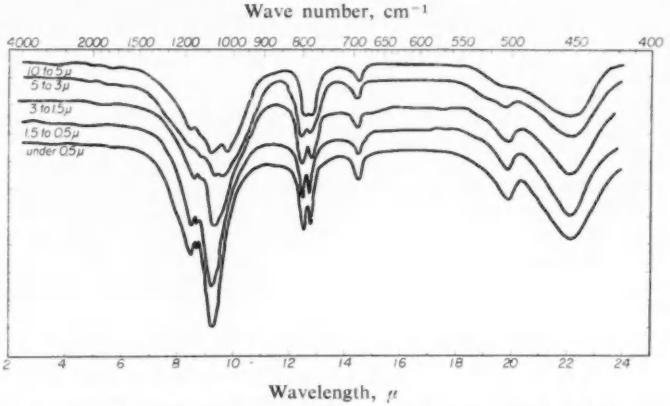

Fig. 3. Spectra of quartz in several range of particle size. Sample is Ishikawayama quartz ground for 2 min. and leached by NaOH aq.

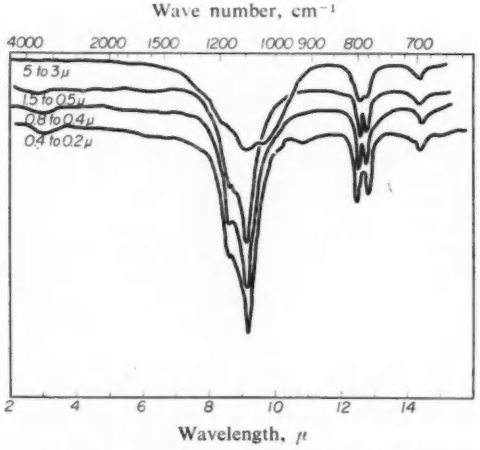

Fig. 4. Spectra of quartz in several range of particle size. Sample is Ishikawayama quartz ground for 100 hr.

optics, the spectrum of quartz powder is not influenced by the grinding times.

The spectrum of quartz powder changes its aspect with particle size in several regions. These changes are shown in Figs. 3 and 4. Figure 3 illustrates the spectra of Q-I-2M-L samples which have the particle size of the order of ten to zero microns. Figure 4 illustrates the spectra of Q-I-100H samples stocked for a half year, the particle sizes of which are from the order of 10 to that of 0.2 μ. The particle size has a remarkable influence on the spectrum in the region of 8 to 9 μ, and less remarkably on those in the regions of 12 and 20 μ. Particularly this effect is markedly seen when the particle size is larger than 3 μ. These results are summarized in Table I.

Discussion

In general, silica modifications give rise to strong bands in the region of 1200 to 1050 cm^{-1}. These bands may be assigned to stretching vibration of Si-O[6,7]. The bands at 800, 780 and 694 cm^{-1} of quartz are also attributed to the silica structure and are very sensitive to skeletal structure of silica. In the longer wavelength region of cesium bromide optics, the bands at 519, 470, 398 and 376 cm^{-1} are attributed to the vibrations concerned with skeletal structure. Beyond those bands, the bands at 3400 and 950 cm^{-1} which appear in the spectrum of carplex, Q-I-6H, Q-I-24H and Q-I-100H are not attributable to the above-mentioned structure sensitive vibrations but may be assigned mainly to hydroxyl group vibration of the silanol group[8-10]. Particle size has a very appreciable influence on the spectrum in the region of 8.5 to 9 μ and less but an effect which cannot be neglected on that in the region of 12 and 20~24 μ particularly when the particle size is larger than 3 μ. These phenomena have been observed by several investigators and explained in a few ways[11]. At present the author has little interest in these explanations of the phenomena,

6) E. R. Lippincott, A. Van Valkenburg, C. E. Weir and E. N. Bunting, *J. Res. Nat. Bur. Stds.*, **61**, 61 (1958).
7) J. M. Hunt, M. P. Wisherd and L. C. Bonham, *Anal. Chem.*, **22**, 1478 (1950).
8) R. McDonald, *J. Phys. Chem.*, **62**, 1168 (1958).
9) H. A. Benesi and A. J. Jones, ibid., **63**, 179 (1959).
10) H. Scholze, *Naturwiss.*, **47**, 226 (1960).
11) W. M. Tuddenham and R. J. P. Lyon, *Anal. Chem.*, **32**, 1630 (1960).

TABLE I. INFRARED ABSORPTION BANDS AND THEIR CHARACTERISTICS OF SILICA

Band positions cm^{-1}	Remarks
3400 to 3300	Band intensity: strong to weak; carplex, Q-I-100H, Q-I-24H, Q-I-6H, Q-I-2M and Q-I-2M-L. Generally assigned to O-H stretching.
1180, 1150 and 1070	Very strong band region of quartz. The sharp feature with Q-I-2M and Q-I-2M-L is lost and the broadth of 1070 cm^{-1} band develops with grinding; 1150 cm^{-1} band appears as shoulder of 1070 cm^{-1} band with Q-I-6H and Q-I-24H, the former being covered by the latter with Q-I-100H. 1180 cm^{-1} band also appears as the shoulder of 1070 cm^{-1} band. Particle size influences features of these bands, and a new band occurs at 1040 cm^{-1} and this shifts towards lower wave number side as the particle size is larger than 3 μ. In that case, this band group is diffuse and seems to be less intense.
1160 and 1090	Very strong band with carplex.
Close to 950	Intensity: medium to weak; carplex, Q-I-100H, Q-I-24H, and probably Q-I-6H. This band cannot be found out with Q-I-2M and Q-I-2M-L.
800	Broad weak band with carplex.
800, 780 and 694	Characteristic bands of quartz with medium intensity. No appreciable change in the feature is observed by grinding. Particle sizes larger than 3 μ have an influence on the aspects of bands at 800 and 780 cm^{-1} but no influence on 694 cm^{-1} band.
520, 470, 400 and 380	Characteristic bands of quartz. No appreciable change occurs with grinding. Particle size influences their aspects as it is larger than 3 μ.

but would like to remark on the fact that as the particle size of ground quartz is smaller the band at 950 cm^{-1} is more intense and the band group in the region of 8 to 9 μ is more diffuse. This will be concerned in the considerably irregular structure different from the original quartz structure. These aspects are illustrated in Figs. 3 and 4.

From spectral change with grinding and leaching as illustrated in Fig. 1, it may be recognized that the bands at 3400 and 950 cm^{-1} also change their aspects in parallel. These two characteristic bands increase their intensities with the grinding times, decrease during the stock of sample in desiccator under the reduced pressure and disappear when the particle is leached. The relative intensity of these two bands scarcely differs with the samples treated in various ways.

It is generally accepted[3-5] that quartz particle ground mechanically has a disturbed and easily soluble layer around the surface, the structure of which is different from quartz itself but not completely amorphous like silica gel. In this case it was observed by means of the BET method with argon or krypton that the surface area of particles increases with the grinding. The interior parent structure does not change its original structure during the grinding but the surface layer is gradually disturbed and the amount of disturbed layer or the thickness of this layer increases with grinding times. The leached sample decreases its surface area and it is considered that the spectrum of this sample is essentially the same as those of the original sample. The change of spectrum in the region of 8 to 9 μ is responsible for this disturbed structure on the particle surface. The more disturbed the layer is, the more diffuse bands appear in this spectral region. This will be caused by the superposition of the spectrum of the disturbed layer on the original spectrum[1]. According to the above consideration, it is concluded that the intensities of the bands at 3400 and 950 cm^{-1} increase with the increment of the amount of the disturbed layer surrounding the surface of the particle. The more the surface area increases, the more the number of SiOH bonds appears. Therefore the SiOH bonds exist mainly on the particle surface, particularly in the disturbed structure. The band at 3400 cm^{-1} which is assigned to the stretching vibration of OH bond will increase its intensities not only with the SiOH group but also with the absorbed water molecule. But the absorbed water molecule gives rise to the bands near 1600 cm^{-1} and does not at 900 to 1000 cm^{-1} generally[10]. From this consideration, the band at 950 cm^{-1} may be assigned to O-H deformation vibration of silanol group.

In the lower frequency region on new band was observed by the grinding. Therefore it is inadequate to consider that the band at 950 cm^{-1} be assigned to the overtone or combination tone. This argument supports indirectly above assignment of the band at 950 cm^{-1} to O-H deformation vibration. From the result of spectra obtained in this work, the band at 950 cm^{-1} may be reasonably assigned to the

O–H deformation vibration of silanol group on the surface of ground quartz particle.

Summary

Some silica modification such as carplex and ground quartz particle, gives rise to the bands near 950 cm^{-1}. This band has no relation with the skeletal structure of Si–O bond and can not be explained as overtone or combination tone. It is reasonable to assign this band to O–H deformation vibration of silanol group. The effect of particle size and grinding time on the spectrum of quartz was examined and it was concluded that the ground quartz particle was covered by some irregular structure on its surface, which was different from quartz structure. In this surface structure, the silanol group seems to be constructed.

The author wishes to express his thanks to Mr. A. Masuda at the University of Tokyo for the use of an infracord spectrophotometer. He wishes to express his thanks to Mr. M. Kawano at the Railway Technical Research Institute for their measurement of the spectrum in cesium bromide region. He also desires to express his hearty gratitude to Assistant Professor T. Miyazawa at the Institute for Protein Research, Osaka University for the use of a Perkin-Elmer model 221 spectrophotometer and also for valuable advice. Finally he wishes to thanks Mr. A. Hamada of this Institute for his kind supply of the dust sample to him.

National Institute of Industrial Health
Kawasaki-shi, Kanagawa-ken

Silanes. Vibrational Assignments and Frequency Correlations

By George J. Janz and Yukio Mikawa*

(Received February 17, 1961)

Silanes have received widespread attention during the last decade and are of continuing current interest[1-4]. As part of a program in this laboratory on the vibrational spectra, molecular structure, and thermodynamic properties of this class of compounds, a review of the widely scattered results was undertaken to assess the status of our information. It became apparent in the course of this review that a need existed for a critical evaluation of the vibrational assignments, and for the interpretation of the normal frequencies on a series of simplified vibrational modes. This communication reports the results thus obtained, together with a useful table of generalized characteristic frequencies and bond distances based on this work.

Status

Information for about one hundred silanes, widely scattered in the published literature, was reviewed relative to the subjects: frequency assignment (FA), infrared spectra (IR), Raman spectra (R) molecular structure (M), thermodynamic properties (T), normal coordinate vibrational analyses (NC) and force constants (FC). For reference and guidance, the status of knowledge is presented in summary form in Table I.

Vibrational Spectra

Relative to the vibrations associated with the silicon atom and the surrounding four atoms attached with tetrahedral angles, all of the silanes considered can be classified into three groups based on the symmetry of molecule; SiX_4, $SiXY_3$ and SiX_2Y_2. The designation of normal vibrations, symmetry class and selection rules for each type of molecules are shown in Table II, where the symbols ν, δ and τ denote stretching, deformation and twisting vibrations, respectively, and the suffixes a, e, f and b denote the class of symmetry group to which the vibration belongs. The simplified vibrational modes for each type of molecule are illustrated in Figs. 1—3. It is recognized that the exact feature of the normal mode differs from molecule to molecule depending on the masses of atoms and the force constants of the bonds, and can be calculated by the normal

* Present address: Research Laboratory, Mitsubishi Chemical Industries, Ltd. Kawasaki-shi.

1) H. Kriegsmann, *Z. anorg. Chem.*, **299**, 138 (1959).
2) A. L. Smith and N. C. Angelotti, *Spectrochim. Acta*, **1959**, 412.
3) R. N. Kniseley, V. A. Fassel and E. E. Conrad, *ibid.*, **1959**, 651.
4) H. W. Thompson, ibid., **16**, 238 (1960).

Table I. Status of knowledge for silanes

Silane	FA	IR	R	M	T	NC	FC	Ref.
SiH_4	×	×	×	×	×	×	×	7—17
H_2SiD_2	×	×			×			17, 18
$HSiD_3$	×	×		×	×			17—20
SiD_4	×	×			×			17—19
$H_3Si(CH_3)$	×	×		×		×	×	3, 21—23
$H_2Si(CH_3)_2$	×	×	×			×	×	21—25
$HSi(CH_3)_3$	×	×	×	×		×	×	21—23
$Si(CH_3)_4$	×	×	×	×	×	×	×	16, 17, 26—40
$H_3SiCH{=}CH_2$	×	×						21
$H_3SiC_2H_5$		×						21
$H_2Si(C_2H_5)_2$		×						21, 41
$HSi(C_2H_5)_3$		×						21
$Si(C_2H_5)_4$	×	×	×					21, 42, 43
$H_nSi(C_3H_7)_{4-n}$*		×						41, 44, 45
$Si(CH_2CH{=}CH_2)_4$		×						46
$H_3Si(C_4H_9)$		×						21, 45
$H_2Si(C_4H_9)_2$		×						41
$H_2Si(C_5H_{11})_2$		×						45
$H_3Si(C_6H_5)$		×						3, 73
$H_2Si(C_6H_5)_2$	×	×	×					41, 73
$HSi(C_6H_5)_3$		×						44, 73
$Si(C_6H_5)_4$				×				47
$D_3Si(C_6H_5)$		×						3
$DSi(C_6H_5)_3$		×						44
$H_3SiC_6H_{11}$		×						45
$H_2Si(C_6H_{11})_2$		×						41
$H_3SiC_{10}H_9$		×						45
$(CH_3)_nSi(C_2H_5)_{4-n}$*			×					35
$(CH_3)_2Si(C_3H_7)_2$		×						21
$(CH_3)_3Si(C_6H_5)$		×	×					48
$Si(OCH_3)_4$	×	×	×				×	49—53
$Si(OC_2H_5)_4$	×	×	×					49, 51, 54
$Si(OC_3H_7)_4$		×	×					49
$R_3Si(OR')$**	×	×	×					55
$R_2Si(OR')_2$**	×	×	×					55, 56, 115
$RSi(OR')_3$**	×	×	×			×		55, 56, 109
SiF_4	×	×	×	×	×	×	×	16, 17, 57—62
H_3SiF	×	×		×	×		×	17, 63—65
H_2SiF_2	×	×			×			17, 66, 67
$HSiF_3$	×	×		×	×			17, 65—68
D_3SiF	×	×		×	×			17, 64, 65, 67, 69
D_2SiF_2	×	×			×			17, 66
$DSiF_3$	×	×			×			17, 66, 67
$(CH_3)_3SiF$	×	×	×	×				70, 71
$(CH_3)_2SiF_2$	×	×	×					25
$(CH_3)SiF_3$	×	×	×	×	×		×	17, 65, 72
CH_3SiH_2F	×	×						24
$(C_6H_5)_nSiF_{4-n}$*	×	×	×					73
$SiCl_4$	×	×	×	×	×	×	×	5, 6, 14, 16, 17, 26—28, 52, 61, 62, 74, 79
H_3SiCl	×	×		×	×			14, 17, 75—78, 111
H_2SiCl_2	×	×	×	×	×			3, 17, 24, 42, 80, 81, 85
$HSiCl_3$	×	×	×	×	×	×	×	17, 19, 82—87
D_3SiCl	×	×		×				67, 69

TABLE I. (Countinued)

Silane	FA	IR	R	M	T	NC	FC	Ref.
$(CH_3)_3SiCl$	×	×	×	×	×	×	×	5, 17, 26—28, 43, 71, 83, 91, 93—95
$(CH_3)_2SiCl_2$	×	×	×	×	×	×	×	5, 17, 25—28, 43, 89, 92
$(CH_3)SiCl_3$	×	×	×	×	×	×	×	5, 17, 26—28, 43, 83, 88—91
$CH_2{=}CHSiCl_3$	×	×						97
$(C_2H_5)_3SiCl$	×		×					42, 43
$(C_2H_5)_2SiCl_2$	×		×					42, 43
$(C_2H_5)SiCl_3$	×	×	×					42, 43, 51
$(CH_2{=}CH{-}CH_2)_nSiCl_{n-4}$*		×						46
$(C_3H_7)SiCl_3$		×						51
$(C_4H_9)SiCl_3$		×						51
$(C_{10}H_7)SiCl_3$		×						96
$(C_6H_5)_nSiCl_{4-n}$*	×	×	×					73
CH_3SiCl_2H	×		×					43
$C_2H_5SiCl_2H$	×		×					43
$(CH_3O)_nSiCl_{4-n}$*	×	×	×					50, 52, 55, 113
$(C_2H_5O)_nSiCl_{4-n}$*	×		×					54, 114
$SiBr_4$	×		×	×	×	×	×	5, 12, 16, 17, 29, 74, 98
H_3SiBr	×		×	×	×	×	×	12, 13, 17, 63, 100, 101
H_2SiBr_2	×	×	×		×	×	×	13, 17, 80, 100, 102
$HSiBr_3$	×		×	×	×	×	×	12, 13, 17, 98, 102, 103
$(CH_3)_3SiBr$	×		×	×				29, 95, 104
$(CH_3)_2SiBr_2$	×	×	×	×				25, 29, 104
$(CH_3)SiBr_3$	×		×	×				29, 104
SiI_4	×		×	×	×	×	×	6, 17, 74, 105
H_3SiI	×	×		×			×	106—108
H_2SiI_2		×						24, 106
D_3SiI	×	×					×	108
$(CH_3)_3SiI$	×		×	×				95, 110
F_3SiCl				×				26, 65
F_3SiBr				×				65
F_2SiBr_2				×				65, 98
Cl_nSiBr_{n-4}*	×	×	×	×	×	×	×	6, 17, 74, 99, 111
Cl_3SiI	×		×		×	×	×	6, 17, 74
Cl_2SiI_2	×		×			×	×	6, 74
$ClSiI_3$	×		×		×	×	×	6, 17, 74
$(CH_3)_3SiOH$	×	×	×					71, 112
$(C_6H_5)_nSi(OH)_{4-n}$*	×	×	×					73
$(CH_3)_3SiSH$	×	×	×					71

* n=1, 2, 3 ** R, R′=CH_3 or C_2H_5

5) T. Shimanouchi, I. Tsuchiya and Y. Mikawa, *J. Chem. Phys.*, **18**, 1306 (1950).
6) M. Dewaulle, *J. Phys. Chem.*, **56**, 355 (1952); *J. Am. Chem. Soc.*, **74**, 5768 (1952).
7) K. Venkateswarlu and S. Sundaran, *J. Chem. Phys.*, **23**, 2365 (1955).
8) C. H. Tindal, J. W. Straley and H. H. Nielson, *Phys. Rev.*, **62**, 151 (1942).
9) W. D. Steward and H. H. Nielson, ibid., **47**, 828 (1935).
10) C. H. Tindal, J. W. Straley and H. H. Nielson, ibid., **58**, 1002 (1940).
11) F. B. Stett and D. M. Yost, *J. Chem. Phys.*, **4**, 82 (1936).
12) H. Murata and K. Kawai, ibid., **23**, 2451 (1955).
13) T. Shimanouchi, ibid., **17**, 245 (1949).
14) C. Cerny and E. Erdos, *Collection Czechoslov. Chem. Commun.*, **19**, 646 (1954).
15) A. P. Atlshuler, *J. Chem. Phys.*, **23**, 761 (1955).
16) T. Shimanouchi, ibid., **17**, 848 (1949).
17) Y. Mikawa, *J. Chem. Soc. Japan, Pure Chem. Sec.* (*Nippon Kagaku Zasshi*), **81**, 1521 (1960). "Selected Values of Properties of Chemical Compounds", Ed. by F. D. Rossini, MCA Research Project, Carnegie Institute of Technology, Pittsburgh, Pa., to be published.
18) J. H. Meal and M. Kent Wilson, *J. Chem. Phys.*, **24**, 385 (1956).

19) S. R. Pola and M. K. Wilson, Harvard University, Project No. R-351-30-13 (1954).
20) D. R. J. Boyd, *J. Chem. Phys.*, **23**, 922 (1955).
21) S. Kaye and S. Tannenbaum, *J. Org. Chem.*, **18**, 1750 (1953).
22) A. C. Bond and L. O. Brockway, *J. Am. Chem. Soc.*, **76**, 3312 (1954).
23) I. F. Kovalev, *Optics and Spectroscopy*, **8**, 166 (1960).
24) E. A. V. Ebsworth, M. Onyszchuk and N. Sheppard, *J. Chem. Soc.*, **1958**, 1453.
25) H. Kriegsmann, *Z. Elektrochem.*, **62**, 1033 (1958).
26) R. L. Livingston and L. O. Brockway, *J. Am. Chem. Soc.*, **66**, 94 (1944).
27) A. L. Smith, *J. Chem. Phys.*, **21**, 1997 (1953).
28) J. Goubeau, H. Siebert and M. Winterwerb, *Z. anorg. u. allgem. Chem.*, **259**, 240 (1949).
29) H. Murata and S. Hayashi, *J. Chem. Phys.*, **19**, 1217 (1951).
30) D. H. Rank, B. D. Saksean and E. R. Shull, *Discussions Faraday Soc.*, **9**, 187 (1950).
31) C. W. Young, J. S. Kohler and D. S. Mckinney, *J. Am. Chem. Soc.*, **66**, 1410 (1947).
32) F. Wall and C. R. Eddy, *J. Chem. Phys.*, **6**, 107 (1938).
33) D. H. Rank and E. R. Bordner, ibid., **3**, 248 (1935).
34) S. Silver, ibid., **8**, 919 (1940).
35) V. A. Kolesova, E. V. Kukharskaya and D. N. Andrew, *Izvest. Akad. Nauk. S. S. S. R., Otdel. Khim. Nauk*, 294 (1953).
36) I. Simon and H. O. McMahon, *J. Chem. Phys.*, **20**, 905 (1952).
37) J. G. Aston and R. M. Kennedy, *J. Am. Chem. Soc.*, **62**, 2567 (1940).
38) I. F. Kovalev, *Optics and Spectroscopy*, **5**, 387 (1957).
39) K. Shimizu and H. Murata, *J. Mol. Spectroscopy*, **5**, 44 (1960).
40) H. Siebert, *Z. anorg. u. allgem. Chem.*, **268**, 177 (1952).
41) R. West and E. G. Rochow, *J. Org. Chem.*, **18**, 303 (1953).
42) H. Murata, *J. Chem. Phys.*, **18**, 1308 (1950).
43) H. Murata, *J. Chem. Soc. Japan, Pure Chem. Sec. (Nippon Kagaku Zasshi)*, **73**, 465 (1952).
44) L. Kaplan, *J. Am. Chem. Soc.*, **76**, 5880 (1954).
45) H. E. Opitz, J. S. Peake and W. H. Nebergall, ibid., **78**, 292 (1956).
46) R. E. Scott and K. C. Firsch, ibid., **73**, 2599 (1951).
47) M. Yokoi, *J. Chem. Soc. Japan, Pure Chem. Sec. (Nippon Kagaku Zasshi)*, **73**, 822 (1952).
48) C. C. Cerato, J. L. Lauer and H. C. Beachell, *J. Chem. Phys.*, **22**, 1 (1954).
49) H. Kriegsmann and K. Licht, *Z. Elektrochem.*, **62**, 1163 (1958).
50) H. Murata, *J. Chem. Phys.*, **20**, 347 (1952).
51) A. L. Smith, *Spectrochim. Acta*, **16**, 87 (1960).
52) J. Goubeau and H. Behr, *Z. anorg. u. allgem. Chem.*, **272**, 2 (1953).
53) K. Iguchi, *J. Chem. Phys.*, **22**, 1937 (1954).
54) H. Murata, ibid., **20**, 1184 (1952).
55) R. Forneris and E. Funck, *Z. Elektrochem.*, **62**, 1130 (1958).
56) R. E. Richards and H. W. Thompson, *J. Chem. Soc.* **1949**, 124.
57) D. M. Yost, E. M. Lassettre and S. T. Gross, *J. Chem. Phys.*, **4**, 325 (1936).
58) H. Urey and C. Bradley, *Phys. Rev.*, **28**, 1970 (1932).
59) F. L. Voelz, A. G. Meister and F. F. Cleveland, *J. Chem. Phys.*, **19**, 1084 (1951); **20**, 1498 (1952).
60) E. A. Jones, Kirby-Smith, Woltz and Nielsen, ibid., **19**, 242 (1951).
61) L. Pauling and L. O. Brockway, *J. Am. Chem. Soc.*, **57**, 2684 (1935).
62) H. Siebert, *Z. anorg. u. allgem. Chem.*, **274**, 34 (1953).
63) C. Newman, J. K. O'Loane, S. R. Polo and M. K. Wilson, *J. Chem. Phys.*, **25**, 855 (1956).
64) F. A. Andersen and B. Bak, *Acta Chem. Scand.*, **8**, 738 (1954).
65) J. Sheridan and W. Gordy, *Phys. Rev.*, **77**, 719 (1950).
66) M. K. Wilson, ASTIA-AD-120452 (Harvard 1957).
67) C. Newman, S. R. Polo and M. K. Wilson, *Spectrochim. Acta*, **15**, 793 (1959).
68) G. A. Heath, L. F. Thomas and J. Sheridan, *Trans. Faraday Soc.*, **50**, 779 (1954).
69) B. Bak, J. Bruhn and J. Rastrup-Andersen, *J. Chem. Phys.*, **21**, 753 (1953).
70) R. G. Gunton, J. F. Ollom and H. N. Rexroad, ibid., **22**, 1942 (1954).
71) H. Kriegsmann, *Z. anorg. u. allgem. Chem.*, **294**, 113 (1958).
72) R. L. Collins and J. R. Nielsen, *J. Chem. Phys.*, **23**, 351 (1954).
73) H. Kriegsmann and K. H. Schowtka, *Z. Phys. Chem. (Leipzig)*, **209**, 261 (1958).
74) Y. Kakiuchi, This Bulletin, **26**, 260 (1953).
75) A. Monfils, *J. Chem. Phys.*, **19**, 138 (1951).
76) A. Monfils, *Compt. rend.*, **236**, 795 (1953).
77) H. Sharabaugh, *Phys. Rev.*, **74**, 1870 (1948).
78) B. P. Dailey, J. M. Mays and C. H. Townes, ibid., **76**, 136 (1949).
79) L. O. Brockway and J. Y. Beach, *J. Am. Chem. Soc.*, **60**, 1836 (1938).
80) J. Hawkins, S. Polo and M. K. Wilson, *J. Chem. Phys.*, **21**, 1122 (1953).
81) J. A. Hawkins and M. K. Wilson, ibid., **21**, 360 (1953).
82) T. G. Gibian and D. S. McKinney, *J. Am. Chem. Soc.*, **73**, 1431 (1951).
83) R. C. Mockler, J. H. Bailey and W. Gordy, *J. Chem. Phys.*, **21**, 1710 (1953).
84) M. H. Pirene, *Compt. rend.*, **206**, 516 (1938).
85) L. O. Brockway and I. E. Coop, *Trans. Faraday Soc.*, **34**, 1429 (1938).
86) K. Yamasaki, A. Kotera, M. Iwasaki and N. Tatematsu, *J. Chem. Soc. Japan, Pure Chem. Sec. (Nippon Kagaku Zasshi)*, **69**, 104 (1953).
87) T. G. Gibian and D. S. Mckinney, *J. Am. Chem. Soc.*, **73**, 1431 (1951).
88) L. Burnelle and J. Duchesne, *J. Chem. Phys.*, **20**, 1324 (1952).
89) M. C. Tobin, *J. Am. Chem. Soc.*, **75**, 1788 (1953).
90) K. Shimizu and H. Murata, This Bulletin, **32**, 46 (1959).
91) K. Shimizu and H. Murata, *J. Mol. Spectroscopy*, **4**, 201 (1960).
92) K. Shimizu and H. Murata, ibid., **4**, 214 (1960).
93) J. Duchesne, *J. Chem. Phys.*, **16**, 1006 (1948).
94) R. L. Livingston and L. O. Brockway, *J. Am. Chem. Soc.*, **68**, 719 (1946).
95) J. Goubeau and H. Sommer, *Z. anorg. u. allgem. Chem.*, **289**, 1 (1957).
96) J. W. Gilkey and L. J. Tyler, *J. Am. Chem. Soc.*, **73**, 4982 (1951).
97) E. R. Shull, R. A. Thursoch and C. M. Birdsall, *J. Chem. Phys.*, **24**, 147 (1956).
98) R. Spitzer, W. J. Howell, Jr., and V. Schomaker, *J. Am. Chem. Soc.*, **64**, 62 (1942).
99) B. Schneider and J. Pliva, *Collection Czechoslov. Chem. Commun. Suppl.*, **19**, 653 (1954).
100) D. W. Mayo, H. E. Opitz and J. S. Peake, *J. Chem. Phys.*, **23**, 1344 (1955).
101) A. H. Sharbaugh, J. K. Bragg, T. C. Madison and V. G. Thomas, *Phys. Rev.*, **76**, 1419 (1949).
102) F. Francois and M. Buisset, *Compt. rend.*, **230**, 1946 (1950).
103) J. Wouters, M. Hemptinne and P. Capron, *Am. Soc. Sci., Bruxelles, Ser. I*, **57**, 25 (1937).
104) K. Yamasaki, A. Kotera, M. Yokoi and M. Iwasaki, *J. Chem. Phys.*, **17**, 1355,(1949).
105) P. W. Allen and L. E. Sutton, *Acta Cryst.*, **3**, 46 (1950).
106) H. J. Emeléus, A. G. Macdiarmid and A. G. Maddock, *J. Inorg. Nuclear Chem.*, **1**, 194 (1955).
107) R. N. Dixon and N. Sheppard, *Trans. Faraday Soc.*, **53**, 282 (1957).
108) H. R. Linton and E. R. Nixon, *Spectrochim. Acta*, **12**, 41 (1958).
109) T. Tanaka, This Bulletin, **33**, 446 (1960).
110) H. N. Rexroad, D. W. Howgate, R. C. Gunton and J. Ollom, *J. Chem. Phys.*, **24**, 625 (1956).
111) B. P. Dailey, J. M. Mays and C. H. Towns, *Phys. Rev.*, **76**, 136 (1949).
112) W. S. Tatlock and E. G. Rochow, *J. Org. Chem.*, **17**, 1560 (1952).
113) H. Murata, K. Kawai and M. Yokoo, *J. Chem. Soc. Japan, Pure Chem. Sec. (Nippon Kagaku Zasshi)*, **77**, 893 (1956).
114) H. Murata and K. Kawai, ibid., **77**, 1542 (1956).
115) M. Hayashi, ibid., **79**, 436 (1958).

TABLE II. DESIGNATION OF NORMAL VIBRATIONS, SYMMETRY CLASS AND SELECTION RULES

Type of molecule	Symmetry class	Designation	Activity		Interpretation
			Raman	Infrared	
SiX_4	A_1	$\nu_a(SiX_4)$	p*1	i*3	Symmetrical stretching
	E	$\delta_e(SiX_4)$	d*2	i	The 1st kind of deformation
	F_2	$\nu_f(SiX_4)$	d	a*4	Asymmetrical stretching
	F_2	$\delta_f(SiX_4)$	d	a	The 2nd kind of deformation
$SiXY_3$	A	$\nu_a(SiX)$	p	a	Stretching vibration
	A	$\nu_a(SiY_3)$	p	a	Symmetrical stretching
	A	$\delta_a(SiY_3)$	p	a	The 2nd kind of deformation
	E	$\nu_e(SiY_3)$	d	a	Asymmetrical stretching
	E	$\delta_e(SiY_3)$	d	a	The 1st kind of deformation
	E	$\delta_e(SiXY_3)$	d	a	Bending of SiX or wagging of SiY_3
SiX_2Y_2	A_1	$\nu_a(SiX_2)$	p	a	Symmetrical stretching
	A_1	$\nu_a(SiY_2)$	p	a	Symmetrical stretching
	A_1	$\delta_a(SiX_2)$	p	a	The 1st kind of deformation
	A_1	$\delta_a(SiY_2)$	p	a	The 1st kind of deformation
	A_2	$\tau(SiX_2Y_2)$	d	i	Twisting
	B_1	$\nu_b(SiX_2)$	d	a	Asymmetrical stretching
	B_1	$\delta_b(SiX_2Y_2)$	d	a	Rocking of SiX_2 or wagging of SiY_2
	B_2	$\nu_b(SiY_2)$	d	a	Asymmetrical stretching
	B_2	$\delta_b(SiY_2X_2)$	d	a	Rocking of SiY_2 or wagging of SiX_2

*1 polarized *2 depolarized *3 inactive *4 active

coordinate treatment for the individual molecule.

$\nu_a(SiX_4)$ in SiX_4, $\nu_a(SiX_3)$ in SiX_3Y, $\nu_a(SiX_2)$ in SiX_2Y_2 and $\nu_a(SiX)$ in $SiXY_3$ are interpreted as symmetrical stretching vibrations of Si–X in which X atoms vibrate in phase back and forth in the direction of the bonds. $\nu_f(SiX_4)$ in SiX_4, $\nu_e(SiX_3)$ in SiX_3Y and $\nu_b(SiX_2)$ in SiX_2Y_2 are interpreted as asymmetrical stretching vibrations of Si–X in which X atoms vibrate out of phase in the direction of the bonds. The deformation vibrations $\delta_e(SiX_4)$ in SiX_4, $\delta_e(SiX_3)$ in SiX_3Y and $\delta_a(SiX_2)$ in SiX_2Y_2 make one group called the first kind of deformation vibrations. This kind produces the change in the angle between the two adjacent bonds. The second kind of deformation vibrations which inculdes $\delta_f(SiX_4)$ in SiX_4 and $\delta_a(SiX_3)$ in SiX_3Y is a symmetrical deformation vibration with respect to the threefold axes. As for $\delta_e(SiXY_3)$, two alternative ways for interpretation are possible. If X is a lighter atom than Y, $\delta_e(SiXY_3)$ should be interpreted as a bending of X, whereas, in the opposite case it should be interpreted as a wagging of Y_3. $\delta_b(SiX_2Y_2)$ may be interpreted either as a wagging vibration in which

$\nu_a(SiX_4)$ $\delta_e(SiX_4)$ $\nu_f(SiX_4)$ $\delta_f(SiX_4)$

Fig. 1. Normal vibrations of SiX_4.

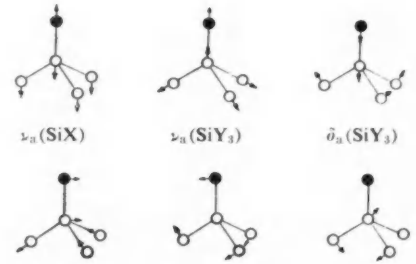

$\nu_a(SiX)$ $\nu_a(SiY_3)$ $\delta_a(SiY_3)$

$\nu_e(SiY_3)$ $\delta_e(SiXY_3)$ $\delta_e(SiY_3)$

Fig. 2. Normal vibrations of $SiXY_3$.

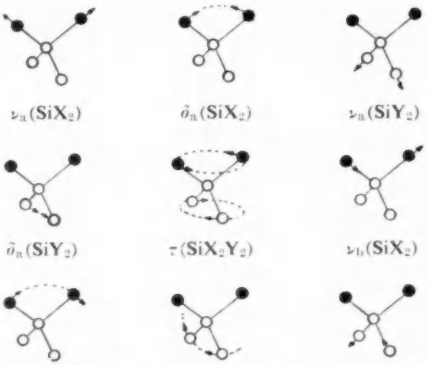

$\nu_a(SiX_2)$ $\delta_a(SiX_2)$ $\nu_a(SiY_2)$

$\delta_a(SiY_2)$ $\tau(SiX_2Y_2)$ $\nu_b(SiX_2)$

$\delta_b(SiX_2Y_2)$ $\delta_b(SiY_2X_2)$ $\nu_b(SiY_2)$

Fig. 3. Normal vibrations of SiX_2Y_2.

two X atoms swing as a unit in SiX_2 plane or as a rocking vibration in which two Y atoms swing back and forth parallel to the same plane. The situation is the same for $\delta_b(SiY_2X_2)$ if X is replaced by Y and vice versa. $\tau(SiX_2Y_2)$ is interpreted as a twisting vibration of SiX_2 in respect to SiY_2. This vibration depends upon the nature of the X atom as well as of the Y atom.

All of the published data are tabulated in Tables III—V in accordance with the above designations. Some values are from Raman spectra of the liquid state and some from infrared spectra of the liquid or gaseous states. In most instances, the differences in the frequencies reported with the different methods or by various investigators were not sufficiently

Table III. Normal frequencies of SiX_4 type molecules

SiX_4	$\nu_a(SiX_4)$	$\delta_e(SiX_4)$	$\nu_f(SiX_4)$	$\delta_f(SiX_4)$
SiH_4	2187	974.6	2190.6	914.2
SiD_4	(1582)[c]	(689)[c]	1597	681
SiF_4	800	268	1031	391
$SiCl_4$	424	150	610	221
$SiBr_4$	249	90	487	137
SiI_4	168	63	405	94
$Si(CH_3)_4$	598	202	696	239
$Si(C_2H_5)_4$	553	160	736	303
$Si(OCH_3)_4$	640	251	844	308
$Si(OC_2H_5)_4$	654	240	792	305

c: Calculated value

Table IV. Normal frequencies of $SiXY_3$ type molecules

$SiXY_3$	$\nu_a(SiX)$	$\nu_a(SiY_3)$	$\delta_a(SiY_3)$	$\nu_e(SiY_3)$	$\delta_e(SiY_3)$	$\delta_e(SiXY_3)$
$SiHD_3$	2182	1573	683	1598	683	851
$SiHF_3$	2314.5	858.6	425.2	998.6	305.5	844.5
$SiHCl_3$	2274	497	250	600	179	810
$SiHBr_3$	2234	360	168	470	113	767
$SiDF_3$	1688	854	421.9	994.4	302.2	628.5
$SiFH_3$	872.0	2206	989.7	2196	943.4	728.1
$SiFD_3$	888	1577	704	1615	(764)[c]	549
$SiClH_3$	551	2201	949	2195	954.4	664.0
$SiClD_3$	538	1581	702	1616	(734)[c]	488
$SiClBr_3$	583	291	173	489	102	159
$SiClI_3$	557	220	114	411	73	134
$SiH(CH_3)_3$	2118	625	219	718	251	908
$SiF(CH_3)_3$	898	620	206	695	259	290
$SiCl(CH_3)_3$	487	640	242	700	188	330
$SiCl(C_2H_5)_3$	464	592	221	739	160	295
$SiCl(OCH_3)_3$	510	717	264	845	—	357?
$SiCl(OC_2H_5)_3$	520	695	290	799	—	—
$SiBrH_3$	430	2200	930	2196	950.4	632.6
$SiIH_3$	362	2192	903	2206	941	592
$SiID_3$	352	1575	664	1607	—	435
$SiBrCl_3$	368	545	191	610	205	135
$SiICl_3$	333	519	169	600	197	123
$SiBr(CH_3)_3$	373	632	238	704	177	214
$SiI(CH_3)_3$	331	627	231	704	164	198
$Si(CH_3)H_3$	700	2167	940	2167	980	540
$Si(CH_3)F_3$	700	900	390	982	332	229
$Si(CH_3)Cl_3$	764	458	229	577	163	229
$Si(CH_3)Br_3$	746	314	153	453	98	186
$Si(C_2H_5)Cl_3$	715	447	187	580	152	224
$Si(OCH_3)Cl_3$	808	450	226	602	170	295
$Si(OC_2H_5)Cl_3$	775	475	215	603	171	249

C: calculated value

great to be of concern relative to the problem of the characteristic frequencies for the molecules. The assignments in the literature were, in large part, without ambiguity for most of the silanes in Tables III—V. Some new assignment are proposed in the light of the correlation rule developed in this work. For $Si(CH_3)_3Cl$, 188 cm^{-1} should be assigned to $\delta_e(SiC_3)$ because the first kind of deformation vibration of Si–C usually appears near 200 cm^{-1}; and $\delta_e(SiC_3)$ should lie at a lower frequency than $\delta_a(SiC_3)$ as in the case of ethyl chlorosilanes. For $Si(CH_3)_2Cl_2$, 241 cm^{-1} should be assigned to $\delta_b(SiC_2Cl_2)$, which belongs to B_1

Table V. Normal frequencies of SiX_2Y_2 type molecules

SiX_2Y_2	$\nu_a(SiX_2)$	$\nu_a(SiY_2)$	$\delta_a(SiX_2)$	$\delta_a(SiY_2)$	$\nu_b(SiX_2)$	$\nu_b(SiY_2)$	$\delta_b(SiX_2Y_2)$	$\delta_b(SiY_2X_2)$	$\tau(SiX_2Y_2)$
SiH_2D_2	2189	1587	944	682.5	2183	1601	743	862	(844)[c]
SiH_2F_2	2245	870	984.8	321.7	2250	(978)[c]	728.2	(905)[c]	(785)[c]
SiH_2Cl_2	2200	531	953	188	2200	592	610	877	710
SiH_2Br_2	2206	393	925	122	2232	456	556	828	688
$SiH_2(CH_3)_2$	2143	954	658	228	2165	732	875	472	703
SiD_2F_2	1614	878.5	708	319	1619	950	579.2	680.2	(563)[c]
$SiCl_2Br_2$	563	326	191	111	605	508	144	182	122
$SiCl_2I_2$	538	276	160	83	589	418	—	149	111
$Si(CH_3)_2F_2$	670	828	213	330	786	952	271	496	213
$Si(CH_3)_2Cl_2$	688	473	232	168	805	553	241	298	177
$Si(C_2H_5)_2Cl_2$	695	458	190	157	746	650 ?	241	299	—
$Si(OCH_3)_2Cl_2$	772	481	250	183	851	590	315	364	—
$Si(OC_2H_5)_2Cl_2$	744	490	240	—	813	598	295	—	—
$Si(CH_3)_2Br_2$	682	355	208	118	797	426	208	208	166

c: Calculated value

Table VI. Characteristic frequencies for silanes

		Number of data
Si–H		
Stretching		
a) symm.	2118~2315 cm^{-1}	16
b) asymm.	2142~2250 cm^{-1}	11
Deformation		
a) 1st kind	925~ 985 cm^{-1}	11
b) 2nd kind	903~ 990 cm^{-1}	6
Si–D		
Stretching		
a) symm.	1573~1688 cm^{-1}	8
b) asymm.	1597~1649 cm^{-1}	7
Deformation		
a) 1st kind	683~ 708 cm^{-1}	6
b) 2nd kind	664~ 704 cm^{-1}	5
Si–C		
Stretching		
a) symm.	553~ 764 cm^{-1}	18
b) asymm.	695~ 805 cm^{-1}	13
Deformation		
a) 1st kind	160~ 232 cm^{-1}	12
b) 2nd kind	221~ 303 cm^{-1}	8
Si–O		
Stretching		
a) symm.	640~ 808 cm^{-1}	8
b) asymm.	782~ 851 cm^{-1}	6
Deformation		
a) 1st kind	240~ 251 cm^{-1}	4
b) 2nd kind	264~ 308 cm^{-1}	4
Si–F		
Stretching		
a) symm.	800~ 900 cm^{-1}	10
b) asymm.	950~1031 cm^{-1}	7
Deformation		
a) 1st kind	268~ 332 cm^{-1}	7
b) 2nd kind	390~ 425 cm^{-1}	4
Si–Cl		
Stretching		
a) symm.	424~ 583 cm^{-1}	23
b) asymm.	577~ 610 cm^{-1}	15
Deformation		
a) 1st kind	150~ 205 cm^{-1}	15
b) 2nd kind	169~ 250 cm^{-1}	8
Si–Br		
Stretching		
a) symm.	249~ 373 cm^{-1}	10
b) asymm.	426~ 507 cm^{-1}	7
Deformation		
a) 1st kind	90~ 118 cm^{-1}	7
b) 2nd kind	137~ 173 cm^{-1}	4
Si–I		
Stretching		
a) symm.	168~ 362 cm^{-1}	7
b) asymm.	405~ 418 cm^{-1}	3
Deformation		
a) 1st kind	63~ 83 cm^{-1}	3
b) 2nd kind	94~ 114 cm^{-1}	2

Table VII. Bond lengths

(a) SiX_4

	SiH_4	SiD_4	SiF_4	$SiCl_4$	$SiBr_4$	SiI_4	$Si(CH_3)_4$
Si–X(Å)	1.48	1.48	1.54	2.02	2.15	2.46	1.90

(b) SiX_3Y

	SiH_3F	SiF_3H	SiD_3F	SiF_3D	SiH_3Br	$SiBr_3H$	$SiHCl_3$	$SiCl_3H$
Si–X	1.48	1.56	1.48	1.56	1.48	2.16	1.48	2.02
Si–Y	1.59	1.48	1.59	1.48	2.21	1.48	2.05	1.48
	$SiCl_3Br$	$SiBr_3Cl$	SiD_3H	$SiF_3(CH_3)$	$SiCl_3I$	SiI_3Cl	$Si(CH_3)_3Cl$	$SiCl_3(CH_3)$
Si–X	2.02	2.15	1.48	1.55	2.02	2.46	1.87	2.02
Si–Y	2.15	2.02	1.48	1.88	2.46	2.02	2.03	1.88

(c) SiX_2Y_2

	SiH_2F_2	SiD_2F_2	SiH_2Br_2	SiH_2Cl_2	$SiCl_2Br_2$	SiH_2D_2	$Si(CH_3)_2Cl_2$
Si–X	1.48	1.48	1.48	1.48	2.02	1.48	1.87
Si–Y	1.59	1.59	2.21	2.05	2.15	1.48	2.03

and 298 cm^{-1} to $\tilde{\omega}_b(SiCl_2C_2)$, which belongs to B_1. This assignment is justified from the result of the normal coordinate treatment in which 245 cm^{-1} and 304 cm^{-1} were calculated[5] for $\tilde{\omega}_b(SiC_2Cl_2)$ and $\tilde{\omega}_b(SiCl_2C_2)$, respectively. For the antisymmetrical stretching vibration of Si–I in $SiCl_2I_2$ two Raman lines 418 cm^{-1} and 346 cm^{-1} are reported by Dewaulle[6]. 418 cm^{-1} should be assigned to $\nu_b(SiI_2)$ but 436 cm^{-1} is preferably assigned as a combination, 276 + 160 = 436 cm^{-1}.

Discussion of Characteristic Frequency Assignments

The survey of the normal frequencies listed in Tables III–V shows that symmetrical stretching vibrations, or $\nu_s(SiX_4)$ in SiX_4, $\nu_s(SiX_3)$ in SiX_3Y, $\nu_s(SiX_2)$ in SiX_2Y_2 and $\nu_s(SiX)$ in $SiXY_3$ appear in a narrow frequency range characteristic for the Si–X. In Table VI the characteristic frequencies ranges and the number of the data from which the ranges have been decided are tabulated. The generalized values of the bond lengths, similarly from this review, are listed in Table VII. More detailed inspection shows the correlation: $\nu_s(SiX_4) < \nu_s(SiX_3) < \nu_s(SiX_2) < \nu_s(SiX)$, where X represents C, O, F, Cl, Br and I. Since the Raman line due to this vibration is generally a sharp, strong, and polarized line, this frequecy may be used as a key frequency for the S–X symmetrical stretching mode.

The asymmetrical stretching vibrations: $\nu_t(SiX_4)$ in SiX_4, $\nu_a(SiX_3)$ in SiX_3Y, and $\nu_b(SiX_2)$ in SiX_2Y_2, also occur in a narrow range, characteristic for Si–X. These occur, without exception, in a higher frequency range than the corresponding symmetrical stretching vibrations. Since the infrared band due to this vibration is very strong, this may be used as a key band for Si–X if it lies in a region available for infrared measurements.

If the term "deformation vibration" defines the type of nomal vibration in which some of the atoms vibrate in the direction perpendicular to bands then all the other types of vibrations are included in this category. Among these, the first and the second kind of deformation vibrations may be expected as characteristic frequencies, since these fall in a rather narrow range as defined by the bonds concerned. These are included in Table VI. For Si–H or Si–D, the ranges for the first kind and the second kind of deformation vibrations overlap each other. For the rest, in most of the cases, the second kind of deformation occurs at a higher frequency range than the first kind.

The other types of vibrations such as $\tilde{\omega}_e(SiXY_3)$, $\tilde{\omega}_b(SiX_2Y_2)$ and $\tau(SiX_2Y_2)$ are generally found as broad frequency ranges so that it is difficult to assign a characteristic frequency. However, if one or more hydrogens are present, the modes: $\tilde{\omega}_e(SiHX_3)$, $\tilde{\omega}_e(SiH_3X)$, $\tilde{\omega}_b(SiH_2X_2)$, $\tilde{\omega}_b(SiX_2H_2)$ and $\tau(SiH_2X_2)$ could be characteristic, each for their own structure since the mass of the hydrogen is so very small, relative to the rest of the system.

Generally, as the mass of the atom attached to the silicon atom increases, there is a corresponding decrease in frequency for both the stretching and deformation vibrations. The effect of electronegativity on the frequency of a particular vibration is, however, striking. Thus, for example, the symmetric stretching vibrations of Si–F occcur in a higher frequency range than those of Si–C even though the atomic weight of fluorine is greater than that of carbon.

Si–H.—The symmetrical stretching vibration

of Si–H appears in the range 2118~2315 cm^{-1}. If the molecule has more than two Si–H bonds, the asymmetrical stretching vibration is also observed in the range 2142~2250 cm^{-1} in addition to the symmetrical vibration. The asymmetrical mode falls, as expected, in a higher range than the symmetrical mode. The general correlation: $\nu_a(SiH_3X) < \nu_a(SiH_2X_2) < \nu_a(SiHX_3)$ is true for all of the halogenated silanes. It is striking that in the series of methyl silanes the Si–H symmetric stretching frequencies decrease appreciably as the number of methyl groups increases.

Relative to the deformation vibration, both the first and the second kinds of deformations appear in an almost identical frequency range, 903~990 cm^{-1}. The separation is rather small and, in most of the cases, the higher frequency is assigned to the first kind of deformation.

Since the mass of the hydrogen atom is very small compared with the others, vibrations such as $\delta_s(SiX_3H)$, $\delta_s(SiH_3X)$, $\delta_b(SiH_2X_2)$, $\delta_b(SiX_2H_2)$ and $\tau(SiH_2X_2)$ may be considered as the hydrogen bending or deformation vibrations. Although examples for these modes are very limited at present, it is apparent that these are to be found in the following ranges:

$\delta_s(SiX_3H)$	767~908 cm^{-1}	(5 examples)
$\delta_s(SiH_3X)$	540~728 cm^{-1}	(5 examples)
$\delta_b(SiH_2X_2)$	469~919 cm^{-1}	(5 examples)
$\delta_b(SiX_2H_2)$	828~919 cm^{-1}	(5 examples)
$\tau(SiH_2X_2)$	688~844 cm^{-1}	(5 examples)

Si–D.—Eight deuterated silanes were used in assigning the frequency range of the Si–D vibration. Although deuterium has twice the atomic weight of hydrogen, the Si–D vibration can still be regarded as that of a very light atom vibrating against an atom of infinite mass. Thus many features of this class resemble the case of Si–H.

The symmetrical stretching vibrations occur in the range of 1573~1688 cm^{-1} while the asymmetrical stretching vibrations occur in the region 1597~1649 cm^{-1}. The higher frequencies are always assigned to the non-symmetrical vibrations. It is striking that the stretching vibration of Si–D in $SiDF_3$ has very high frequency (1688 cm^{-1}) compared with the stretching vibration of Si–D in the other compounds. This is the same as in the case of $SiHF_3$, where $\nu_a(SiH)$ was assigned to 2314.5 cm^{-1}, which seems an extraordinarily high value for the stretching vibration of Si–H.

The Si–D deformation vibrations, both the first kind and the second kind, occur in the frequency range 664~708 cm^{-1}, and higher frequencies are assigned to the second kind of deformation.

Si–C.—The Si–C symmetrical stretching vibrations occur in the frequency range of 553~764 cm^{-1} while the asymmetrical stretching vibrations occur in the range of 695~805 cm^{-1}. The tendency of the frequency shift depending on the number of the carbon atoms attached to the silicon atom is apparent, i.e., $\nu_a(SiC_4) < \nu_a(SiC_3) < \nu_a(SiC_2) < \nu_a(SiC)$. For the asymmetrical stretching vibrations, the relation, $\nu_f(SiC_4) < \nu_e(SiC_3) < \nu_e(SiC_2)$ is also true, if a particular series, such as $Si(CH_3)_4-Si(CH_3)_3Cl-Si(CH_3)_2Cl_2$, is considered. The deformation vibrations occur in the frequency range 160~259 cm^{-1} for the first kind, and 206~303 cm^{-1} for the second kind. The latter appaears, without exception, in a higher frequency range than the former.

Si–O–C.—The Si–O symmetrical stretching vibrations in the linkage of Si–O–C occur in the frequency range of 640~808 cm^{-1}, while the asymmetrical stretching vibrations occur in the range of 792~851 cm^{-1}. The frequencies of the symmetrical stretching vibrations decrease as the number of methoxy or ethoxy groups attached to the silicon atom increases, i.e.: $\nu_a(SiO_4) < \nu_a(SiO_3) < \nu_a(SiO_2) < \nu_a(SiO)$. The asymmetric vibration frequencies are concentrated in a rather narrow range, and the correlation $\nu_f(SiO_4) < \nu_e(SiO_3) < \nu_e(SiO_2)$ is true for any series, such as: $Si(OCH_3)_4-Si(OCH_3)_3Cl-Si(OCH_3)_2Cl_2$.

Owing to the very limited data, the frequency range for the deformation vibrations can not be decided with any certainty. From the available information, it appears that the first and second kinds of deformation vibrations occur in the range 240~308 cm^{-1}.

Si–Halogen.—The Si–halogen stretching modes occur in the range of 168~1031 cm^{-1}. The broad frequency range is due to the large variations in atomic weights for the halogen atoms, i.e.: F = 19.00 to I = 126.9. As the atomic weight of the atom attached to the silicon atom increases, a corresponding decrease in the frequency of the symmetrical and asymmetrical Si–X stretching vibrations is observed. For example, in the SiX_4 series, the Si–X stretching frequency decreases in the order: 800~424–249~168 cm^{-1}, for SiF_4, $SiCl_4$, $SiBr_4$ and SiI_4 respectively. In any series of the type SiX_4–SiX_3Y–SiX_2Y_2–$SiXY_3$, where X is a halogen atom and Y is different or a non-halogen atom, the frequencies of the symmetrical stretching vibration, i.e., $\nu_a(SiX_4)$, $\nu_a(SiX_3)$, $\nu_a(SiX_2)$, $\nu_a(SiX)$, increase as the number of the halogen atoms attached to the silicon atom decreases. By contrast, the frequencies of the asymmetrical stretching vibrations: $\nu_f(SiX_4)$, $\nu_e(SiX_3)$ and $\nu_b(SiX_2)$ do not show this trend. It is apparent that these are limited to narrower ranges than

the symmetrical vibrations. Thus, for Si–Cl, the range of the symmetrical frequencies is 424~583 cm^{-1} whereas the range of the asymmetrical is 577~610 cm^{-1}. It is also seen that the asymmetrical modes always occur in a higher frequency range than the corresponding symmetrical stretching modes. The first kind of deformation vibrations occurs in a definite region for each kind of halogen, e. g.: $\delta_e(SiCl_4)$ in $SiCl_4$, $\delta_e(SiCl_3)$ in $SiCl_3Y$ and $\delta_a(SiCl_2)$ in $SiCl_2Y_2$. All are in the range, 150~205 cm^{-1}. The second kind of deformation vibrations usually occurs in a higher frequency range than the first kind. The other deformation vibrations occur in a range so wide that to list it would be of little significance.

Summary

The status of knowledge relative to the vibrational assignments, molecular structure, and spectral data for a series of about one hundred silanes has been surveyed and is reported in brief tabular form. A scheme of simplified vibrational modes is discussed, and used to develop the assignment of fundamentals for some fifty five silanes. Some new assignments are proposed in the light of a correlation rule which has been developed. Tables of characteristic frequencies, and the best values for bond distances, based on this work, are presented.

The authors wish to thank Fred Behnke for assitance with the compilation of the literature and the summary in Table I. This work was made possible, in part, by a grant from the National Science Foundation, Washington, D. C.

Department of Chemistry
Rensselaer Polytechnic Institute
Troy, New York, U. S. A.

Syntheses and Infrared Absorption Spectra of Deuterated Polyvinyl Alcohols $-(-CD_2-\underset{\displaystyle OH(D)}{\underset{|}{CD}}-)_n-$*1

By Hiroyuki TADOKORO, Hiroshi NAGAI*2, Syûzô SEKI and Isamu NITTA*3

(Received February 20, 1961)

We have previously reported[1] that the 1141 cm^{-1} band in the infrared absorption spectra of polyvinyl alcohol (PVA) increases the intensity sensitively with crystallization (heat-treatments), and the optical density of this band is approximately in linear relationship with the degree of crystallinity determined by the methods of density and of the sorption of water vapor. We have further concluded that the 1141 cm^{-1} band is a so-called "crystallization-sensitive" band. We have also made the deuteration of the OH group of PVA in order to clarify the assignment of this band[2-4], and further we have undertaken the deuteration of the main-chain of this polymer for the same purpose. In addition we have measured the infrared pleochroism of the doubly oriented PVA samples, and have shown that the experimental facts obtained so far can be explained fairly well, when we tentatively assign this band to the skeletal vibration of the planar zig-zag chain in the crystalline region[3,5,6].

On the other hand, Krimm, Liang and Sutherland[7] have reported that this band

*1 Read at the Annual Meeting of the Society of Polymer Science, Osaka, May, 1960.
*2 Present address: Electrical Communication Laboratory, Nippon Telegraph & Telephone Public Corporation, Musashino, Tokyo.
*3 Present address: Kwansei Gakuin University, Uegahara, Nishinomiya-shi.

1) H. Tadokoro, S. Seki and I. Nitta, This Bulletin, **28**, 559 (1955).
2) H. Tadokoro, S. Seki and I. Nitta, *J. Chem. Phys.*, **23**, 1351 (1955).
3) H. Tadokoro, S. Seki and I. Nitta, *J. Polymer Sci.*, **22**, 563 (1956).
4) H. Tadokoro, This Bulletin, **32**, 1252 (1959).
5) H. Tadokoro, S. Seki, I. Nitta and R. Yamadera, *J. Polymer Sci.*, **28**, 244 (1958).
6) H. Tadokoro, This Bulletin, **32**, 1334 (1959).
7) S. Krimm, C. Y. Liang and G. B. B. M. Sutherland, *J. Polymer Sci.*, **22**, 227 (1956).

should not be assigned to the crystalline band, but to the C–O–C stretching mode of the ether linkage produced between the molecular chains by heat-treatment. On the contrary, we have reconfirmed the linear relationship between the band intensity and the density for a number of samples subjected to heat-treatments under various conditions, by using the density-gradient tube method[6,8,9]. And furthermore we have accumulated experimental evidences for assigning this band to the crystalline band, such as comparison with the X-ray diffraction data on the formalized samples, swollen samples, etc.[6,8]

Quite recently Krimm[10] has considered the band to be a crystalline band and suggested that this band may be associated with the ν(CO) mode of a portion of a chain in which an intramolecular hydrogen bond is formed between two neighboring OH groups that are on the same side of the plane of the carbon chain. On the other hand Liang and Pearson[11] have made the factor group analysis of PVA crystal based upon the symmetry of the average crystal structure deduced from X-ray analysis[12]. Then they have assigned the 1141 cm^{-1} band to the symmetric skeletal stretching modes as follows:

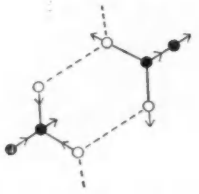

In order to make such detailed assignments, further accumulation of the experimental data as well as the calculation of the normal modes of vibrations*4 would be necessary.

In this paper we wish to report the syntheses

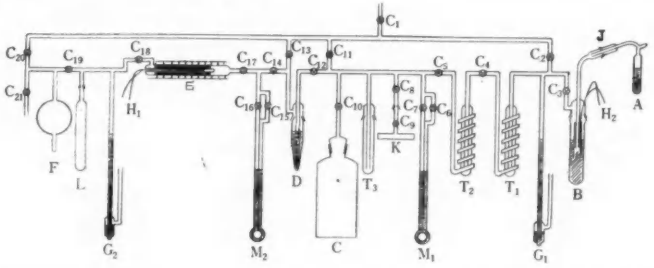

Fig. 1. The apparatus for the synthesis of α, β, β-trideuterovinyl acetate.

A: D_2O. B: CaC_2 (vessel made of Telex). C: Gas vessel for C_2D_2 (20 l.). D: CH_3COOD. E: Reaction tube (made of Telex). F: Gas vessel for adjusting the pressure. G: Safety valve. H_1: Thermocouple (copper-Constantan). H_2: Thermocouple (Chromel-Almel). J: Joint K: Gas cell for infrared measurements. M: Mercury manometer. T_1 and T_2: Trap. T_3: Trap made of Telex. L: Trap for product. C_1–C_{21}: Cock.

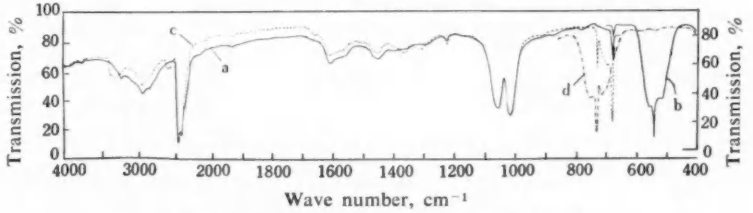

Fig. 2. Infrared spectra of acetylene-d_2 and acetylene.
a: C_2D_2 (degree of deuteration 97% at 200 mmHg)
b: C_2D_2 (degree of deuteration 97% at 70 mmHg)
c: C_2D_2 (degree of deuteration 94% at 200 mmHg)
d: C_2H_2 (at 70 mmHg)

8) H. Tadokoro, K. Kôzai, S. Seki and I. Nitta, ibid., **26**, 379 (1957).
9) H. Tadokoro, K. Kôzai, S. Seki and I. Nitta, *Chem. High Polymers* (*Kôbunshi Kagaku*), **16**, 418 (1959).
10) S. Krimm, *Fortschr. Hochpolym.-Forsch.*, **2**, 51 (1960).
11) C. Y. Liang and F. G. Pearson, *J. Polymer Sci.*, **35**, 303 (1959).
12) C. W. Bunn, *Nature*, **161**, 929 (1948).
*4 The calculation of the normal modes of vibration of PVA is going on at Professor T. Shimanouchi's Laboratory of the University of Tokyo (T. Shimanouchi and M. Tasumi, Annual Meeting of the Society of Polymer Science, May, 1960).

and the infrared spectra of the deuterated PVA's $-(-CD_2-\underset{\underset{OH(D)}{|}}{CD}-)_n-$, and also the spectra of the intermediate products.

Preparation of the Samples

As has already been reported, the OH group of PVA can be easily deuterated by the isotope exchange reaction with deuterium oxide, but the CH group can not be deuterated by such a simple method. Hence we have synthesized deuterated PVA's according to the following scheme:

$$CaC_2 \xrightarrow{D_2O} C_2D_2$$

$$(CH_3COO)_2O \xrightarrow{D_2O} CH_3COOD$$

$$C_2D_2 + CH_3COOD \xrightarrow{(CH_3COO)_2Zn} CD_2{=}CD{-}OCOCH_3$$

$$\xrightarrow{\text{polymerization}} -(-CD_2-\underset{\underset{OCOCH_3}{|}}{CD}-)_n-$$

$$\xrightarrow{\text{saponification}} -(-CD_2-\underset{\underset{OH}{|}}{CD}-)_n-$$

$$\xrightarrow{D_2O} -(-CD_2-\underset{\underset{OD}{|}}{CD}-)_n-$$

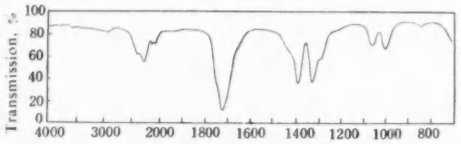

Fig. 3. Infrared spectrum of acetic acid-*d* (degree of deuteration 92%, at liquid state).

Fig. 1 shows the outline of the apparatus used for the synthesis of α, β, β-trideuterovinyl acetate. The system can be highly evacuated by using a mercury diffusion pump and a rotary pump. The vessel B made of Telex*5 holds calcium carbide which was dried at about 580°C for about four hours under high vacuum (10^{-4} mmHg or below). The container of deuterium oxide A may be rotated at the joint J, and acetylene-d_2 is generated by dropping deuterium oxide into B. The generated acetylene-d_2 is transferred to the trap T_1 cooled with liquid nitrogen, and then warmed up to the dry-ice temperature by exchanging the refrigerant. The same procedure was repeated at the trap T_2 and then acetylene-d_2 is transferred to the trap T_3 cooled with liquid nitrogen. In this way impurities and excess deuterium oxide were eliminated from acetylene-d_2. Then acetylene-d_2 is held in the gas vessel C (about 20 l.). The purity of the acetylene-d_2 gas was checked by measuring the infrared spectra. K is the gas cell for this purpose equipped with the windows of AgCl plates.

Acetic acid-*d* was prepared by heating the equal mole mixture of acetic anhydride and deuterium oxide at 110°C for about four hours in a sealed tube. The acetic anhydride used had been purified by distillation, standing for several days with sodium metal and subsequent distillation (b. p.:

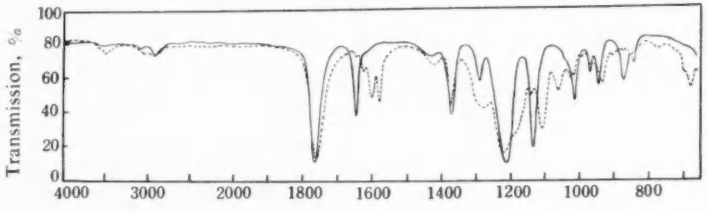

Fig. 4. Infrared spectra of α, β, β-trideuterovinyl acetate (----) and vinyl acetate (——) at liquid state.

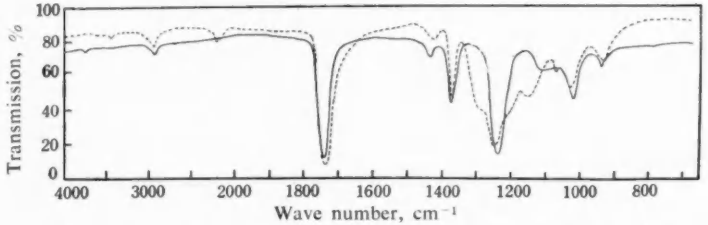

Fig. 5. Infrared spectra of poly-α, β, β-trideuterovinyl acetate (----) and polyvinyl acetate (——).

*5 Boro-silicate glass manufactured by Tôshiba Electric Co., Ltd.

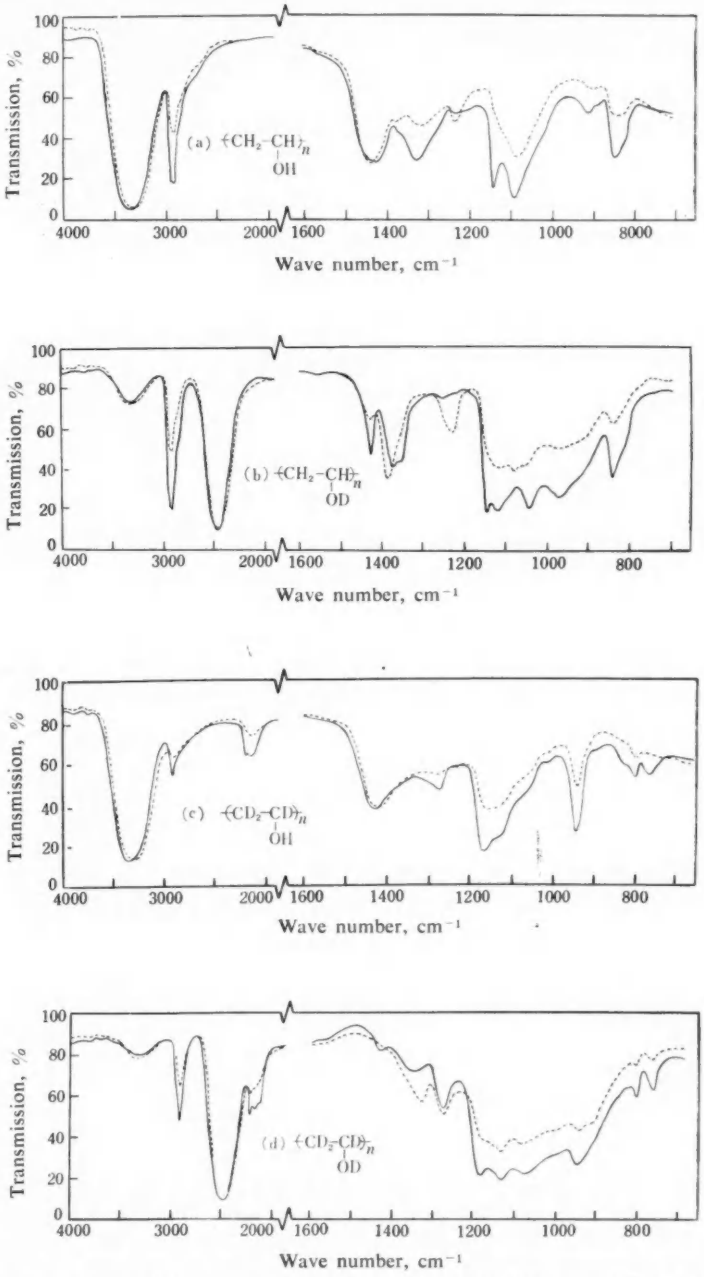

Fig. 6. Infrared dichroism of (a) PVA, (b) PVA-*d*, (c) PV-d_3A and (d) PV-d_3A-*d*.
—— Electric vector perpendicular to elongation.
---- Electric vector parallel to elongation.

TABLE I. INFRARED SPECTRA AND TENTATIVE

PVA			PVA-*d*			PV-d_3A		
Frequency cm^{-1}	Plechroism	Intensity	Frequency cm^{-1}	Dichroism	Intensity	Frequency cm^{-1}	Dichroism	Intensity
3340[a]	—	vs				3340[a]	—	vs
2937	⊥ (⊥)[a]	s	2937	⊥	s			
						(2905)[b]	⊥	m
2908	⊥ (∥)	s	2908	⊥	s			
2840	⊥	sh	2840	⊥	sh			
			2470[a]	—	vs			
						2200	⊥	m
						2145	⊥	m
						2105	⊥	sh
1440[c]	∥	s						
			1428	⊥	m	1425[c]	⊥	m
1420[c]	⊥	m				1420[c]	∥	m
			1383	∥	s			
1376	⊥	w	1376	⊥ ?	m			
			1360	⊥	sh			
1326[d] 1315	⊥	m						
			1256	⊥ ?	sh	1265	⊥	m
1232	∥	w	1230	∥	m			
1141	⊥ (∥)	s	1148	⊥	s	1165	⊥	s
						1125	⊥	sh
			1122	⊥	s			
1093	⊥ (⊥)	s						
1083	∥	m	1083	∥	m			
						1055	⊥	sh
			1094	⊥	s			
			977	⊥	m			
						940	⊥	s
			930	⊥	sh			
913	⊥ (∥)	m						
890	⊥ (∥)	vw						
849	⊥ (∥)	m	842	⊥	m			
835	⊥ (⊥)	sh	825	⊥	sh			
						823	⊥	sh
						797	⊥	w
						760	⊥	w
640[c]	∥	sh						
610	⊥	m						
480	⊥	m						
410	?	w						
360	⊥	w						

a) The ν(OH) band at about 3340 cm^{-1} shows no appreciable dichroism at the absorption peak, but shows a perpendicular and parallel nature at the higher frequency and lower frequency sides, respectively. The ν(OD) band at about 2470 cm^{-1} also shows the same behavior.

b) The wave numbers in parentheses are for the bands associated with the residual hydrogen atoms because of the incompleteness of deuteration.

c) The band at about 1430 cm^{-1} splits into 1440 and 1420 cm^{-1} in the polarized spectra because of the difference of their dichroism.

ASSIGNMENTS OF PVA, PVA-*d*, PV-d_3A AND PV-d_3A-*d*

Frequency cm^{-1}	PV-d_3A-*d* Dichroism	PV-d_3A-*d* Intensity	Tentative assignments[f]
			ν(OH)
			ν_a(CH_2)
(2905)[b]	⊥	m	ν(residual CH)
			ν_s(CH_2)
2470[a]	—	vs	ν(OD)
2200	⊥	m	ν_a(CD_2)
2145	⊥	m	ν_s(CD_2)
2105	⊥	sh	
(1428)[b]	⊥	vw	Superposition of δ(CH_2) and a coupling band (coupling of δ(OH) and 1383 cm^{-1} band of PVA-*d*). 1428 cm^{-1} band of PVA-*d* is δ(CH_2)
			w(CH) or w(CH_2)
			δ(CH) ?
1330	∥	m	
			Coupling of δ(OH) and 1383 cm^{-1} band of PVA-*d*
1272	⊥ ?	m	
			w(CH_2) or w(CH)
1185	⊥	s	Crystalline band (see text)
1135	∥	m	
1130	⊥	s	
			Mainly due to ν(CO)
1085	∥	m	
1080	⊥	s	
			Mainly due to ν(CO)
			δ(OD)
940	⊥	s	
			Skeletal or CH_2
905	—	sh	
			Skeletal or CH_2
			r(CH_2)
797	⊥	w	
757	⊥	w	

d) The band at about 1325 cm^{-1} has its absorption peaks at 1326 and 1315 cm^{-1} in the cases of perpendicular and parallel radiation, respectively.

e) The data in the region lower than 640 cm^{-1} is reproduced from the paper by Krimm et al.[7]

f) ν: stretching, ν_a: antisymmetric stretching, ν_s: symmetric stretching, δ: bending, w: wagging, r: rocking.

g) The notation ⊥ and ∥ in parentheses refer to the polarization with respect to the plane of the zig-zag carbon chain[5,14].

139~140°C). Acetic acid-*d* was put in the vessel D. Acetylene-d_2 gas, after bubbling through vessel D, was introduced into the reaction-vessel E. Then the gas mixture was caught in the vessel L cooled with liquid nitrogen. The catalyst used was zinc acetate carried on active charcoal kindly supplied by Dr. T. Omae of the Nippon Gôsei Kagaku Co., Ltd. The reaction temperature was about 200°C. The obtained vinyl-d_3-acetate was purified by using a concentric distillation column (Taika Kôgyô Co., Ltd., Osaka). The polymerization of vinyl-d_3-acetate was carried out in a sealed glass tube with α,α'-azobisisobutyronitrile catalyst at 60°C for about 24 hr.

Infrared Spectra of the Intermediate Products. —Fig. 2 is the infrared spectra of acetylene-d_2. The degree of deuteration was estimated by using the ν_5 band (CH symmetric deformation, C_2H_2: 729.2 cm^{-1}, C_2HD: 676 cm^{-1}, C_2D_2: 538.7 cm^{-1}) assuming that the absorption coefficients of the above bands are equal in the spectra of C_2H_2, C_2HD and C_2D_2. A spectrum of the sample of lower degree of deuteration (about 94%) was reproduced for reference. The intensity of the 676 cm^{-1} band, which is absent in the spectrum of C_2H_2 (curve d), is very strong in the spectrum of the 94% C_2D_2 (curve c), but weak in the case of the 97% C_2D_2 (curve b). Accordingly the ν_5 mode of C_2HD is considered to be assigned to the 676 cm^{-1} band, although this mode has been so far assigned to the 687 cm^{-1} band by Stitt[13].

Fig. 3 is a spectrum of acetic acid-*d*, the degree of deuteration of which was estimated to be about 92% by using the intensity ratio of the bands of OH and OD stretching.

Fig. 4 shows the spectra of vinyl-d_3-acetate (broken line) and of vinyl acetate (solid line). Fig. 5 shows the spectra of polyvinyl-d_3-acetate (broken line) and of polyvinyl acetate (solid line). It should be noticed that the spectra of the monomer and polymer in the 1300~1100 cm^{-1} region show a change similar to that of deuteration. The 1235 cm^{-1} band of polyvinyl acetate and the 1212 cm^{-1} band of vinyl acetate, which are considered to be assigned to the stretching mode of ester linkage, shift to the higher frequency 1245 and 1220 cm^{-1}, respectively. This behavior is interesting in relation to the shift of the 1141 cm^{-1} band of PVA to higher frequency with deuteration as will be discussed later.

Spectra of PVA and Deuterated PVA's. —In Fig. 6 the polarized infrared spectra of PVA, PVA-*d*, poly-α,β,β-trideuterovinyl alcohol (PV-d_3A) and poly-α,β,β-trideuterovinyl alcohol-*d* (PV-d_3A-*d*) are shown. The solid and broken curves represent the spectra obtained with radiation polarized, respectively, perpendicular and parallel to the direction of elongation. The spectral data and the tentative assignments for PVA and deuterated PVA's are given in Table I. In the column of pleochroism of PVA the notations $\perp$ and $\parallel$ in parenthesis refer to the polarization with respect to the plane of the zig-zag carbon chain[5,14].

The OH stretching band at 3340 cm^{-1} shifts to 2470 cm^{-1} with the deuteration of the OH group, but the CH_2 stretching bands at about 2930 cm^{-1} are not affected by this type of deuteration. By the deuteration of the CH group these bands shift to about 2200 cm^{-1}. Both these bands due to the OH and CH groups shift to lower frequencies, when all the hydrogen atoms are deuterated. The residual 2930 cm^{-1} band is due to the incomplete deuteration of the CH group.

The 1141 cm^{-1} band of PVA and the 1165 cm^{-1} band of PV-d_3A are inferred to be due to the similar origins of absorption mechanism from the following similarities:

1) The distinguished dichroism,
2) The similar intensity,
3) The increase of the intensity with heat-treatment (Fig. 7), and

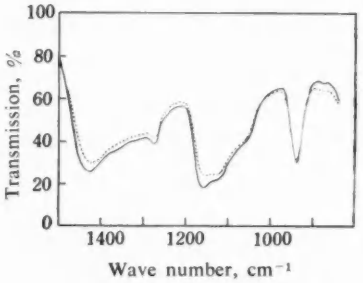

Fig. 7. Spectral change of PV-d_3A by heat-treatment.
---- No-treatment
—— Treated at 160°C for 20 min.

4) The small shift to higher frequencies with deuteration of the OH group. The 1141 cm^{-1} band of PVA shifts to 1148 cm^{-1} and the 1165 cm^{-1} band of PV-d_3A to 1185 cm^{-1} with deuteration of the OH group.

Thus the 1165 cm^{-1} band of $-(-CD_2-\underset{\underset{OH}{|}}{CD}-)_n-$ is considered to be the crystalline band corresponding to the 1141 cm^{-1} band of PVA.

The experimental facts we have found so far about the 1141 cm^{-1} band are summarized as follows:

13) F. Stitt, *J. Chem. Phys.*, **8**, 56 (1940).

14) E. J. Ambrose, A. Elliott and R. B. Temple, *Proc. Roy. Soc.*, **A199**, 183 (1949).

1) The intensity increases with crystallization by heat-treatment, and shows a parallel relationship with the crystallinity determined by the density and the sorption of water vapor[1,8,9].

2) The band behaves in a parallel way with the X-ray diffraction rings due to the crystalline region, when the sample is formalized or swollen in water[6,8].

3) The band exhibits strong perpendicular dichroism in the case of an elongated sample, and distinguished pleochorism in the doubly oriented sample of PVA. The transition moment of this band is parallel to the zig-zag plane, while that of the 1093 cm^{-1} band is perpendicular to the zig-zag plane[3-6]. Furthermore, we have obtained another new experimental fact as follows.

4) The shift of this band with deuteration of the CH or OH group is small. This new experimental fact also supports our tentative assignment of 1141 cm^{-1} band mainly due to the stretching vibration of the extended zig-zag chain in the crystalline region. Here, of course, a considerable coupling of the vibration of the oxygen atom with the skeletal vibrations should be expected.

Next, we proceed to the interpretation of the other bands. Although we can not make any conclusive assignments of these bands merely from the present data, we may discuss here the tentative assignments of the several main bands. We have reported already that the 1430 cm^{-1} band of PVA should be a superposition of $\delta(CH_2)$ and some other band related to the OH group (probably $\delta(OH)$), since the intensity of this band decreases sensitively on deuteration and there remains a sharp band which is certainly attributed to the $\delta(CH_2)$ mode. The 1383 cm^{-1} band was tentatively considered to be $w(CH_2)$ or $w(CH)$, and the 1376 cm^{-1} to be $\delta(CH)$. This inference was confirmed, since these bands disappear in the spectra of PV-d_3A-d.

The bands near 850 cm^{-1} of PVA were considered to be skeletal or of CH_2 vibrations, because there was quite a little effect of deuteration. Especially the 835 cm^{-1} band having the pleochroism perpendicular to the plane of zig-zag chain was assigned to $r(CH_2)$. All these bands disappear by the deuteration of the main chain. The bands near 760 cm^{-1} of PV-d_3A and PV-d_3A-d are supposed to be due to $r(CD_2)$ mode. But further inference about the origin of the bands may be difficult, because of the complexity which is possibly due to the strong coupling among the group vibrations.

At present we are aiming to accumulate results of further experiments such as the infrared measurements of the highly doubly oriented samples of $-(-CD_2-\underset{\displaystyle OH(D)}{\underset{|}{CD}}-)_n-$, the preparation of the more highly deuterated samples, and of the selectively deuterated samples, $-(-CD_2-\underset{\displaystyle OH(D)}{\underset{|}{CH}}-)_n-$, $-(-CH_2-\underset{\displaystyle OH(D)}{\underset{|}{CD}}-)_n-$, etc.

The authors wish to express their sincere thanks to Professor S. Murahashi of this Faculty, Professor T. Shimanouchi of the University of Tokyo and Dr. T. Omae of Nippon Gôsei Kagaku Co., Ltd. for helpful advice and criticism. The authors are also indebted to Mr. A. Nozaki for his cooperation in the construction of the apparatus.

Department of Polymer Science (*H. T.*)
Department of Chemistry
(*H. N., S. S. & I. N.*)
Faculty of Science
Osaka University
Nakanoshima, Osaka

The Study of Adsorption of Detergents at a Solution-Air Interface by Radiotracer Method. IV. The Valency and Concentration Effects of Added Electrolytes on the Adsorption of Alkyl Sulfate Ion

By Ryohei MATUURA, Hideo KIMIZUKA and Akira MATSUBARA

(Received February 18, 1961)

The preceding study on the effect of excess electrolytes on the adsorption of dodecyl sulfate ion using the radiotracer method has confirmed directly the fact that the presence of excess electrolytes increases both the equilibrium amount and the rate of adsorption of the dodecyl sulfate ion[1], the result which was deduced by a number of authors from surface tension measurements of the solution[2]. However, in the presence of a large excess of electrolytes the rate of adsorption was too rapid to be measured accurately and also the adsorption isotherm was nearly independent of the type of added electrolytes.

We may expect to obtain further data concerning the effects of added electrolytes on the rate and the amount of adsorption of the detergent if we explore the region of the more dilute concentrations of the added electrolytes and/or the detergent. The present paper describes the results of such experiments and the discussions about them.

Experimental and Results

The method of preparation and purification of the samples and the procedure used for the experiments have already been described[1,3]. The specific activities of the radioactive sodium dodecyl sulfate (SDS), sodium tetradecyl sulfate (STS) and sodium hexadecyl sulfate (SHS) used were ca. 10 mc. per millimole. The temperatures of the experiments were 29.5 $\pm$1.5°C.

In the study on the valency effect, the concentrations of electrolytes were all 10^{-4} mol./l., and those of SDS ranged from 5×10^{-6} to 5×10^{-5} mol./l. In the study on the effect of the excess salt the concentrations of detergents were 4×10^{-6} mol./l. for SDS and 2×10^{-6} mol./l. for STS and SHS and those of salt were changed from 10^{-3} mol./l. to 1 mol./l.

The rate of adsorption and the adsorption isotherm of dodecyl sulfate ion (DS^-) in the presence of electrolytes are shown in Figs. 1 and 2, respectively. In Fig. 1, K represents the constant in the rate equation

$$\Gamma_t = K\sqrt{t} \qquad (1)$$

where Γ_t denotes the amount of adsorption at time t[4].

As is seen from these figures, both the rate and the equilibrium amount of the adsorption of DS^- increase with the increase in cationic valency of the electrolyte, while they are almost independent of the anionic valency. Table I shows the values of rate constant K_0 of the equation

$$K = K_0 C \qquad (2)$$

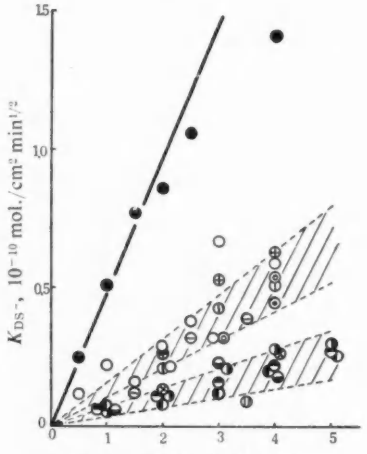

Fig. 1. Effect of added electrolytes on the rate of adsorption of DS^-, 29.5$\pm$1°C. Concentrations of electrolytes are all 10^{-4} mol./l.

I ◑ NaCl, ◐ Na_2SO_4, ◍ Na_2CO_3, ◓ $K_3Fe(CN)_6$, ◒ KCl.
II ○ $MgCl_2$, ⓘ $CoCl_2$, ⊖ $HgCl_2$, ⊕ $MnCl_2$, ⊗ $Zn(CH_3COO)_2$, ◎ $CaCl_2$, ⊙ $Ca(OH)_2$.
III ● $AlCl_3$.

1) R. Matuura, H. Kimizuka and K. Yatsunami, This Bulletin, 32, 646 (1959).
2) N. K. Adam and H. L. Shute, *Trans. Faraday Soc.*, 34, 758 (1938); G. C. Nutting, F. A. Long and W. D. Harkins, *J. Am. Chem. Soc.*, 62, 1496 (1940), etc.
3) R. Matuura, H. Kimizuka, S. Miyamoto and R. Shimozawa, This Bulletin, 31, 532 (1958).
4) R. Matuura, H. Kimizuka, S. Miyamoto, R. Shimozawa and K. Yatsunami, ibid., 32, 404 (1959).

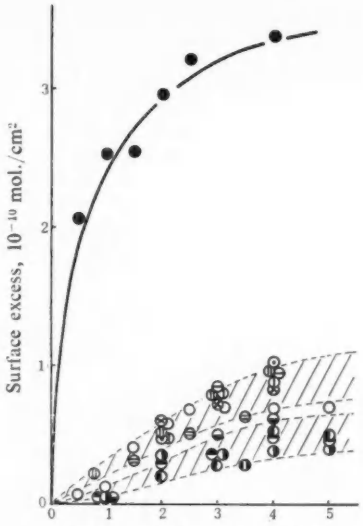

Fig. 2. Effect of added electrolytes on the equilibrium adsorption of DS^-, 29.5±1°C. Concentrations of electrolytes are all 10^{-4} mol./l.

I { NaCl, Na_2SO_4, Na_2CO_3, $K_3Fe(CN)_6$, KCl.
II { $MgCl_2$, $CoCl_2$, $HgCl_2$, $MnCl_2$, $Zn(CH_3COO)_2$, $CaCl_2$, $Ca(OH)_2$.
III $AlCl_3$.

TABLE I. RATE CONSTANT K_0 OF THE ADSORPTION OF DS^- IN THE PRESENCE OR ABSENCE OF ELECTROLYTE. THE CONCENTRATIONS OF SDS, $5\times10^{-6}\sim5\times10^{-5}$ mol./l.; THE CONCENTRATION OF ELECTROLYTE, 10^{-4} mol./l. K_0 IN 10^{-3} cm./min$^{1/2}$. 29.5±1.5°C

	No added salt	Added electrolyte		
		Valency of cation		
		1	2	3
K_0	0.35±0.1	0.52±0.2	1.35±0.3	4.30±0.5

where C is the concentration of SDS[4].

The value of K_0 in the absence of added electrolyte calculated according to the simple diffusion theory[5] is 22.8×10^{-3} cm./min$^{1/2}$. It is seen from Table I that the rate constants increase in the presence of electrolyte, showing a greater increase the higher the cationic valency, but the values are less than the rate constant of the simple diffusion theory.

The effects of electrolyte concentrations on the rate constants and the equilibrium adsorptions of DS^-, tetradecyl sulfate ion (TS^-) and hexadecyl sulfate ion (HS^-) are shown in Figs. 3 and 4, respectively. These figures indicate that the presence of excess sodium chloride remarkably increases the equilibrium adsorption as well as the rate constants of the alkyl sulfate ions. It must be noted here that the rate constant does exceed the value of the simple diffusion theory when the concentration of the salt becomes great as indicated in the cases of TS^- and HS^-. Unfortunately the diffusion coefficients of TS^- and HS^- in the presence of excess salt have not been known, and so we calculated the rate of adsorption by the simple diffusion theory using the diffusion coefficient in the absence of added electrolyte. But the condition described above will be held even when the diffusion coefficient in the presence of added salt is used, because it may generally be considered as less than that in the absence of salt*.

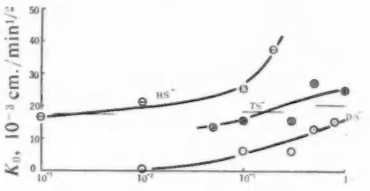

Fig. 3. Effect of salt concentration on the rate constant of adsorption of the alkyl sulfate ion. 29.5±1.5°C. Concentrations of detergents are 4×10^{-6} mol./l. for SDS and 2×10^{-6} mol./l. for STS and SHS. Horizontal lines indicate the values expected from the simple diffusion theory.

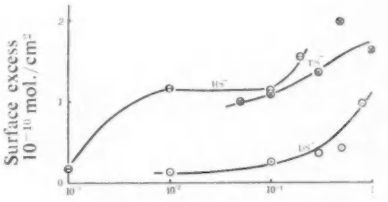

Fig. 4. Effect of salt concentration on the adsorption of the alkyl sulfate ion. 29.5±1.5°C. Concentrations of detergents are 4×10^{-6} mol./l. for SDS and 2×10^{-6} mol./l. for STS and SHS.

5) A. F. H. Ward and L. Tordai, *J. Chem. Phys.*, **14**, 453 (1946).

* We have measured the self-diffusion coefficient of DS^- at the concentration of 4×10^{-4} mol./l. in the presence (0.1 N) and absence of sodium chloride and found the values, at 25°C, to be 5.6×10^{-6} and 6.5×10^{-6} cm²/sec., respectively. We are going to measure the corresponding values of TS^- and HS^-, the result of which will be published in a separate paper after the work has been completed.

Discussion

The simple diffusion theory proposed by Ward and Tordai[5] assumed that the adsorption takes place as a result of the formation of the subsurface of zero concentration, which is taken to be the region of the thickness of a few molecular diameters being situated in the immediate vicinity of the surface. The formation of a subsurface of zero concentration is explained by the fact that the surface active solute finds a position of lower potential energy in the surface than in the bulk. According to this theory, at the initial stage of the formation of the adsorbed layer, the solute molecules will diffuse from the bulk to the subsurface more slowly than they do from the subsurface to the surface, on the assumption that the equilibrium is established instantaneously between the latter two regions.

It has, however, been shown that the simple diffusion theory fails to explain quantitatively our experimental results of the adsorption of alkyl sulfate ions without added inorganic electrolytes[1], and the present result also shows that the simple diffusion theory does not hold for the adsorption of DS^- in the presence of a small concentration of inorganic electrolytes, as is shown in Table I. Also the results of the experiments on the adsorption of non-electrolytes from the solution so far reported by several authors can not be explained by the simple diffusion theory[6]. All these results showed that the rate of adsorption is smaller than the value expected from the simple diffusion theory.

As the factors responsible for the delay in the rate of adsorption Blair[6] proposed an energy barrier for the adsorption of non-electrolytes and Doss[7] an electrical potential barrier for the surface active electrolytes. Some other factors, e.g., the reorientation[8] and the surface pellicle formation[9], have also been considered. Of course, these various factors taken together are responsible for the retardation of the adsorption rate of alkyl sulfate ions at the solution-air interface. It is difficult to cover the whole experimental result by any single theory. For example, let us consider Doss' theory of electrical potential barrier. According to this theory, the electrical double layer at the surface resists the adsorption of surface active ion owing to the electrical repulsion. The rate differs from the value of the diffusion theory, which may be regarded as being essentially identical with the simple diffusion theory, by a factor

$$\exp\left(-\frac{x\varepsilon\zeta'_0}{kT}\right) \tag{3}$$

where x denotes the fraction of surface covered by the adsorbed molecules, ε, the elementary charge, k, the Boltzmann constant and T, the absolute temperature. ζ'_0 is given by

$$\zeta'_0 = \frac{4\pi\rho}{D}\sqrt{\frac{1000\,DkT}{4\pi N\varepsilon^2\sum_i c_i z_i^2}} \tag{4}$$

where ρ is the surface charge density at monolayer adsorption, D, the dielectric constant of medium, N, the Avogadro number and c_i, the concentration of i-th ion having valency z_i. Eqs. 3 and 4 predict that the rate of adsorption at the given amount of adsorption depends upon the ionic strength of the solution. From Fig. 1 and Table I it may be seen that the rate of adsorption does not depend on the anionic valencies in spite of their different ionic strengths of added electrolytes, but depends essentially on the cationic valencies. These facts can not be explained by Doss' theory mentioned above. Cassie and Palmer[10] deduced from their consideration on the structure of the adsorbed film, assuming Gouy-Chapman's diffuse double layer, that the film of long chain anions will be remarkably influenced by the presence of a high valent cation, while it will be independent of the nature of the anion in solution. Our result agrees with this view and also with observation on the surface[2] or interfacial tension[11]. Of course, the electrical double layer formed at the surface will be supposed to resist the adsorption of surface active ion, but the quantitative explanation for it should be given in a somewhat different way.

As the concentration of the added electrolyte becomes larger, the rate of adsorption of alkyl sulfates becomes faster until it reaches the value predicted by the simple diffusion theory in the case of DS^-, while in the cases of TS^- and HS^- the rate constants exceed the simple diffusion values, as shown in Fig. 3. It is not easy to explain by the prevailing theories the reason why the rates of adsorption of TS^- and HS^- exceed the values of simple diffusion theory in the presence of a large excess of electrolyte.

Addison[12] proposed that the difference between the dynamic and the static surface tension is a measure of the driving force for the adsorption, which is introduced in his theory

6) C. M. Blair, Jr., ibid., **16**, 113 (1948).
7) K. S. G. Doss, *Kolloid-Z.*, **86**, 205 (1939).
8) A. E. Alexander, *Trans. Faraday Soc.*, **37**, 15 (1941).
9) J. W. McBain and L. H. Perry, *Ind. Eng. Chem.*, **31**, 35 (1939); M. E. L. McBain and L. H. Perry, *J. Am. Chem. Soc.*, **62**, 989 (1940).
10) A. B. D. Cassie and R. C. Palmer, *Trans. Faraday Soc.*, **37**, 156 (1941).
11) C. Robinson, *Nature*, **139**, 626 (1937).
12) C. C. Addison, *J. Chem. Soc.*, **1944**, 477.

explicitly as the surface activity. At equilibrium there is a concentration gradient near the surface. Since the ordinary diffusion takes place from higher to lower concentrations, the equilibrium state may be supposed to be the state at which the osmotic force due to the concentration gradient is equilibrated with an adsorptive force such as the driving force suggested by Addison.

In general, both the driving force and the activation energy may be considered to be the factors responsible for the rate of adsorption. It may be pointed out here that the difference between the amount of solute in a dynamic surface and that in an equilibrium surface is a measure of the driving force and so the equilibrium adsorption becomes a measure of the driving force at the instant of the formation of the fresh surface. Thus the higher surface active molecule may drift to the surface faster than the lower surface active one providing the activation energy remains in the constant. The change in the rate of adsorption caused by the foreign substance should, therefore, be attributed not only to the change in activation energy, but also to the change in surface activity.

By comparing Figs. 1 and 2 it is seen that the presence of polyvalent cation increases both the rate and the amount of equilibrium adsorption of DS^- at a given concentration of SDS. This means that the higher rate of adsorption should be related to the larger amount of adsorption in addition to the lowering of activation energy. This is also true for the case of Figs. 3 and 4. The fact that the rate constants of TS^- and HS^- exceed the predicted value of the diffusion theory indicates clearly that the surface activity should be taken into account in the theory of the rate of adsorption of detergent at the solution surface.

Summary

The adsorption of dodecyl sulfate ion in the presence of various inorganic electrolytes whose concentrations are all 10^{-4} mol./l. and the adsorption of alkyl sulfate ions in the presence of the excess salt were measured by using S-35 labeled alkyl sulfates.

In the presence of various electrolytes, both the rate of adsorption and the equilibrium adsorption of dodecyl sulfate ion increase with the cationic valency of added electrolyte, while they are almost independent of the anionic valency.

In the presence of the excess salt, both the rate and the equilibrium adsorption of the alkyl sulfate ions increase with the salt concentration. With increasing concentration of salt the rate of adsorption of the dodecyl sulfate ion approaches the rate of the simple diffusion theory, while that of tetradecyl- and hexadecyl sulfate ion exceeds the value predicted by the simple diffusion theory.

It was pointed out that the higher rate of adsorption is attributed to the higher surface activity of solute.

The idea of surface activity was explicitly introduced in the explanation for the adsorption process and the discussions for the theories proposed earlier were given.

Department of Chemistry
Faculty of Science
Kyushu University
Hakozaki, Fukuoka

Determination of Ortho-, Pyro- and Tripolyphosphate by the Use of a Small Column of Ion-exchange Resin

By Shigeru OHASHI* and Shichiro TAKADA

(Received February 27, 1961)

The determination of ortho-, pyro- and tripolyphosphate in their mixture is usually carried out by paper chromatography[1] or ion-exchange chromatography[2]. In paper chromatographic determination satisfactory separation of the chain phosphates can be obtained only in acid chromatographic solvent mixtures. Therefore, care must be taken about partial hydrolysis of the condensed phosphates during a chromatographic separation. When paper chromatographic separation is performed at room temperature (15~30°C), a correction due to the hydrolysis of the condensed phosphates should be applied, depending on the temperature. When the separation is performed at a lower temperature then 5°C, the correction due to the hydrolysis is negligible, but a long time is consumed for the separation. On the other hand in the ion-exchange chromatographic determination the phosphates adsorbed by a column are successively eluted with a buffered solution of potassium chloride of pH 4~9. Therefore in the process of the elution the condensed phosphates are not hydrolyzed practically, but by the use of a column of the usual scale a long time is consumed for the separation.

The purpose of this paper is to present a rapid method for the determination of mixed ortho-, pyro- and tripolyphosphate by the use of a small column of ion-exchange resin. The continuous-gradient elution method by Jameson[2h] was applied and a paper micro-fraction collector was used.

* Present address: Department of Chemistry, Faculty of Science, Kyushu University, Fukuoka.

1) a) J. P. Crowther, *Anal. Chem.*, **26**, 1383 (1954), b) H. Grunze and E. Thilo, *Sitz. ber. deut. Akad. Wiss. Berlin, Kl. Math. allgem. Naturw.*, **1953**, No. 5, 26 pp., c) E. Karl-Kroupa, *Anal. Chem.*, **28**, 1091 (1956), d) H. Hettler, *J. Chromatog.*, **1**, 389 (1958), e) D. N. Bernhart and W. B. Chess, *Anal. Chem.*, **31**, 1026 (1959), and f) M. J. Smith, ibid., **31**, 1023 (1959).

2) a) S. Lindenbaum, T. V. Peters, Jr., and Wm. Rieman III, *Anal. Chim. Acta*, **11**, 530 (1954), b) C. E. Higgins and W. H. Baldwin, *Anal. Chem.*, **27**, 1780 (1955), c) J. A. Grande and J. Beukenkamp, ibid., **28**, 1497 (1956), d) J. P. Ebel and N. Busch, *Compt. rend.*, **242**, 647 (1956), e) M. Matsuhashi, *J. Biochem.*, **44**, 65 (1957), f) W. B. Chess and D. N. Bernhart, *Anal. Chem.*, **31**, 1116 (1959), g) R. H. Kolloff, *ASTM Bull.*, No. **237**, 74 (1959), and h) R. F. Jameson, *J. Chem. Soc.*, **1959**, 752.

Experimental

The assembly of apparatus used in this investigation is shown in Fig. 1.

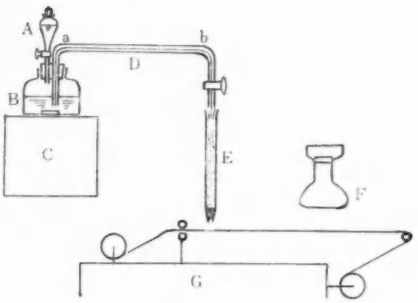

Fig. 1. Apparatus.
A: Stock bottle, B: Mixing bottle,
C: Magnetic stirrer, D: Capillary,
E: Column, F: Infrared lamp,
G: Paper micro-fraction collector.

Ion-exchange Column.—A coarser part of Dowex 1-X 4 (200~400 mesh) of chloride form was filled in a capillary, 2.6 mm. in diameter and 60 mm. in height.

Phosphate Samples.—Disodium hydrogen orthophosphate dodecahydrate, tetrasodium pyrophosphate decahydrate and pentasodium tripolyphosphate hexahydrate were used.

Elution.—Solutions of potassium chloride of various concentrations were buffered with sodium formate and formic acid. The concentrations of sodium formate and formic acid were kept constant (HCOONa 5.1 g./l. and 80% HCOOH 2.5 ml./l.) and the pH of the solution was regulated with aqueous ammonia. The solution of potassium chloride in a stock bottle was continuously added to a mixing bottle which contained 10 ml. of water initially. Then the solution in the mixing bottle was introduced to the ion-exchange column. The flow rate was regulated to be about 30 sec./drop.

Fraction Collector.—By the use of a paper micro-fraction collector[3] manufactured by Mitamura the eluted solution was collected drop by drop on a piece of filter paper and was dried immediately with an infrared lamp.

3) N. Tamiya, T. Soda and Y. Yoshino, This Bulletin, **27**, 393 (1954).

Qualitative Observation on the Separation of Phosphates. — After the separation the filter paper containing phosphates was sprayed with a solution which was made by mixing 5 ml. of 60% perchloric acid, 1 ml. of concentrated hydrochloric acid, and 1 g. of ammonium heptamolybdate tetrahydrate and diluting this to 100 ml. with water. The sprayed paper was dried under the infrared lamp, then placed under an ultraviolet lamp and irradiated until blue spots appeared.

Quantitative Analysis of Phosphate Mixtures. — The paper area containing each phosphate species was cut into small pieces and was burned to ashes in a crucible. The ash was digested with nitric acid and the acid solution was evaporated to dryness. The residue was dissolved in a diluted solution of sulfuric acid and the phosphate was determined colorimetrically according to the method of Karl-Kroupa[10].

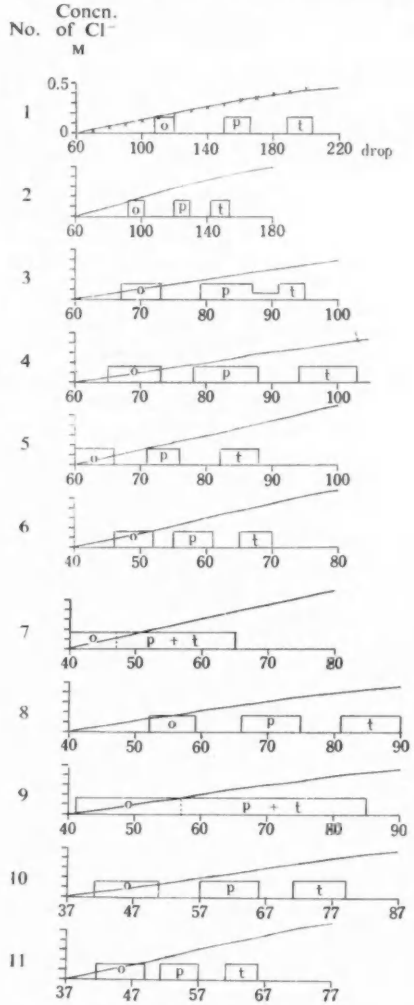

Fig. 2. Separation of phosphate mixtures.
o: Orthophosphate, p: Pyrophosphate,
t: Tripolyphosphate.

Results and Discussion

Experimental results for the dependence of separation of phosphate mixtures on the elution conditions are summarized in Fig. 2 and Table I. The rectangles in Fig. 2 indicate only the positions of phosphate species in the elutions but not their concentrations. The variation of the concentration of chloride ion in the eluant is expressed by the equation,

$$x = a(1 - e^{-ft/v}) \qquad (1)$$

where x (mol./l.) is the concentration of chloride ion in the mixing bottle, a (mol./l.) is the concentration of chloride ion in the stock bottle, f (ml./min.) is the flow rate, v(ml.) is the volume of solution in the mixing bottle and t (min.) is the time from the start of mixing. The curves in Fig. 2 indicate the concentration of chloride ion in the eluant calculated from Eq. 1. The cross marks in Fig. 2-1 indicate the concentration of chloride ion determined experimentally.

Table I. Conditions of experiments shown in Fig. 2

No.	Amount of phosphate γg.		Concn. of KCl in the stock bottle M	pH of KCl soln.
1	Each	20	0.75	5.5
2	〃	20	1	5.5
3	〃	20	2	5.5
4	〃	20	2	4.5
5	〃	20	3	4.5
6	〃	20	3	4.5
7	〃	100	3	4.5
8	〃	100	2	4.5
9	〃	300	2	4.5
10	〃	100	2	4.5
11	Ortho 100) Pyro 10 Tripoly 10)		3	4.5

The capillary between a and b in Fig. 1 was shortened step by step to promote the efficiency of the elution. In the experiments of Fig. 2-1~5, 6~9 and 10~11, the capillaries of the length 41.5, 24.0 and 20.7 cm. were used, respectively.

Jameson[2h] used 0.75 M solution of potassium chloride of pH 5.5 as a stock solution to determine the compositions of strong phosphoric acids. Using a potassium chloride solution of the same concentration and pH as those used by Jameson, the authors tested the separation of the phosphate mixture. The separation of 20 γg. as phosphorus of each phosphate species is complete, but too much eluant is consumed

(Fig. 2-1). The same amounts of the phosphate mixture can be separated by the use of 1 M potassium chloride of pH 5.5 (Fig. 2-2), but in the case of 2 M potassium chloride of pH 5.5 the separation of pyro- and tripolyphosphate is incomplete (Fig. 2-3). The use of 2 or 3 M potassium chloride of pH 4.5 can separate 20 γg. as phosphorus of each phosphate species (Fig. 2-4 and 5, and 6). The separation of 100 γg. as phosphorus of each phosphate species can not be achieved by the use of 3 M potassium chloride of pH 4.5 (Fig. 2-7). On the other hand 2 M potassium chloride of pH 4.5 should be used for that purpose (Fig. 2-8 and 10). However, 2 M potassium chloride of pH 4.5 can not separate 300 γg. as phosphorus of each phosphate species (Fig. 2-9).

As shown in Fig. 2-10, 100 γg. as phosphorus of each phosphate species can be separated by letting only 79 drops of the eluant flow. Similarly 100 γg. of orthophosphate, 10 γg. of pyrophosphate and 10 γg. of tripolyphosphate, as phosphorus in all cases, can be separated satisfactorily by letting only 66 drops of the eluant flow (Fig. 2-11).

TABLE II. RESULTS OF ANALYSES OF PHOSPHATE MIXTURES

Sample	Phosphate species	% P Calcd.	Found, this method	Found, paper chromatography[1c]
Pure phosphate mixture	Ortho-	50.1	50.4	50.8
	Pyro-	49.9	49.6	49.2
Pure phosphate mixture	Ortho-	66.8	67.5	—
	Pyro-	33.2	32.5	—
Commercial sodium tripolyphosphate	Ortho-	—	0.0	0.0
	Pyro-	—	7.6	7.2
	Tripoly-	—	92.4	92.8

The results of the quantitative analyses obtained by the precent procedure are shown in Table II. The first and the second sample are synthetic mixtures of pure alkali orthophosphate and pyrophosphate and the third sample is a commercial sodium tripolyphosphate. For comparison, the paper chromatographic analyses were carried out for the first and the third sample by the method of Karl-Kroupa[1c]. The data obtained by the present method were well coincident with the calculated values and the data obtained by paper chromatography.

Summary

The authors presented the new rapid method for the determination of ortho-, pyro- and tripolyphosphate in the mixture by the use of a small column, 2.6 mm. in diameter and 60 mm. in height, of ion-exchange resin, Dowex 1—X4 (200～400 mesh). The continuous-gradient elution method was applied and the paper micro-fraction collector was used. For example, by the use of 2 M potassium chloride of pH 4.5 as the stock solution, 100 γg. as phosphorus of each phosphate species can be separated by letting only 79 drops of the eluant flow. The quantitative data obtained by the present method were well coincident with the calculated values or the data obtained by the paper chromatography.

Department of Chemistry
Faculty of Science
Kanazawa University
Kanazawa

Forschung über die katalytische Entwässerung des Isoamylalkohols. I.

Von Akira MITSUTOMI

(Eingegangen am 26. September, 1960)

Die Gewinnung der Olefine durch Entwässerung des Isoamylalkohols geschieht entweder nach dem sogenannten „Flüssigkeits oder Gasphase-verfahren". Bei dem erst genannten Flüssigkeitsverfahren liefert Isoamylalkohol in der unter Zusatz von konzentrierter Schwefelsäure unterhalb von 100°C erfolgenden Entwässerung Amylen in 15～18%iger Ausbeute sowie Isoamyläther in ca. 27%iger Ausbeute, wie die Arbeiten von Norris und Reuter[1], und von Cramer und Cambell[2] klar zeigen. Die hier entstehenden Amylene sind zwar nach ihrem Siedepunkt, 32～42°C, als ein Gemisch aus Methyläthyläthylen und Trimethyläthylen

1) J. P. Norris und R. Reuter, *J. Am. Chem. Soc.*, **49**, 2624 (1927).
2) P. I. Cramer und J. M. Campbell, *Ind. Eng. Chem.*, **29**, 234 (1937).

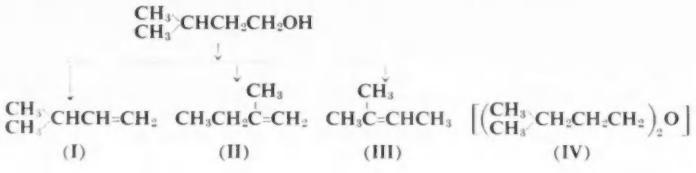

anzunehmen, sie sind aber auf das Mischverhältnis, die chemischen Zusammensetzung noch nicht geprüft.

Abgesehen von der Diskontinuierlichkeit von diesem Verfahren, kann es wenn auch nur für Olefine-Herstellung als geeignet nicht angesprochen werden. Aus dem Standpunkt, für die industrielle Produktion das kontinuierlich arbeitende Gasphase-Verfahren technisch fertigzubringen, hat der Verfasser diese Forschung durchgeführt.

Ipatiew[3] berichtet für das Gasphase-Verfahren, dass man durch Zuführung des Isoamylalkohols durch das bei 540°C vorher erhitzte mit Aluminiumoxyd gefüllte Eisenrohr ein Gemisch des Isopropyläthylens (I) mit kleiner Menge Methyläthyläthylen (II) und Trimethyläthylen (III) erhält, ohne dabei aber Isoamyläther (IV) festzustellen.

Ipatiew[4] hat ferner bei der Prüfung der Isomerisation von Isopropyläthylen erkannt, dass bei Abwesenheit von Katalysatoren diese Isomerisation auch bei Erhitzung bis zu 400, 500 und 540°C immer ausbleibt, während bei Anwesenheit von Aluminiumoxyd als Katalysator bereits im Bereich von 450～535°C das Isopropyläthylen ca. 50～60% zu Trimethyläthylen isomerisiert wird. In der Genenwart von Kieselgur wird es ca. 20%.

Auch Adams, Kamm und Marvel[5] haben berichtet, dass durch Entwässerung des Isoamylalkohols bei 500～540°C unter Anwendung des Aluminiumoxyds und Bimssteins als Katalysator Isopropyläthylen mit 70～80%iger Ausbeute dargestellt werden konnte, ohne aber Trimetyläthylen bilden zu lassen.

Nach Norris und Reuter[6] bildet sich nur Isopropyläthylen, wenn Isoamylalkohol durch Aluminiumoxyd als Katalysator bei 375～400°C entwässert wird, und das wird erst nach Erhitzung bei 375～450°C in der Gegenwart von Aluminiumsulfat als Katalysator nur um 45% zu Trimethyläthylen isomerisiert, während beim Vorhandensein der Phosphorsäure als Katalysator die genannte Isomerisation des Isopropyläthylens bei 450°C absolut ausbleibt und erst bei 500°C nur um 15～29% eintritt.

3) W. I. Ipatiew, *Ber.*, **36**, 2000 (1903).
4) W. I. Ipatiew, ebenda, **36**, 2003 (1903).
5) R. Adams, O. Kamm und C. S. Marvel, *J. Am. Chem. Soc.*, **40**, 1950 (1918).
6) J. F. Norris and R. Reuter, ebenda., **49**, 2627 (1927).

Es ist zwar von Kashima[7] angegeben, dass aus *n*-Amylalkohol bei Anwendung der japanischen Säureerde als Katalysator *n*-Amylen und *n*-Amyläther dargestellt wurden. Aber von der Stellung der Doppelbindung von diesem *n*-Amylen ist keineswegs erwähnt. Fujita[8] hat unter Erhitzung des mit Aktivkohle gefüllten Kupferrohrs bei 320～340°C ein Gemisch aus Isoamylalkohol und Wasser hindurchgezogen, und ausser Isobutylen und Isopropyläthylen noch die Bildung von Isoamyläther, Isobutan, Isovaleraldehyd und Isovalersäure ermittelt.

Es muss von den oben genannten Arbeiten überhaupt gesagt werden, dass sie mit Ausnahme von Fujita die Trennung der Reaktionsprodukte und deren Ermittelung sehr ungründlich behandelten und weiterer eingehender Prüfung bedürfen.

Die Olefine, der Gegenstand der Arbeiten, die durch Entwässerung der niedrigen Alkohole gebildet werden, haben einander sehr naheliegende Siedepunkte, so dass die Trennung der einzelnen Olefinen mit grösseren Schwierigkeiten verbunden sind. Üblicherweise wird das Gemisch unter Benutzung des unterschiedlichen Löslichkeitsgrades gegenüber 60%iger Schwefelsäure getrennt. Mit solch einer Methode können die einzelnen Olefine in ihrem primären Zustande keineswegs alle voneinander getrennt werden. Solche in verhältnismässig geringer Menge vorhandenen Olefine können als reiner Verlust weder erfasst noch rein dargestellt werden.

Ferner kann als für diese Arbeiten überhaupt gemeinsamer Nachteil angeschprochen werden, dass ausgerechnet die Frage immer noch offengelassen ist, nämlich welche Typen Katalysatoren geeignet sind, um gewisse Typen Olefinen durch Entwässerung von Alkohol zu gewinnen.

Dieser Umstand kommt selbstverständlich daher, dass, wie bereits beschrieben, die Bestimmung der chemischen Zusammensetzung und des Mischverhlätnisses von den Reaktionsprodukten äusserst unbeachtet behandelt ist. Der Verfasser hat die unentbehrlichen Bedingungen bestimmt, Trimethyläthylen durch das Gasphase-Verfahren kontinuierlich herzustellen, und den Reaktionsmechanismus geklärt.

7) K. Kashima, Dieses Bulletin, **4**, 177 (1929).
8) Y. Fujita, ebenda, **9**, 11 (1934).

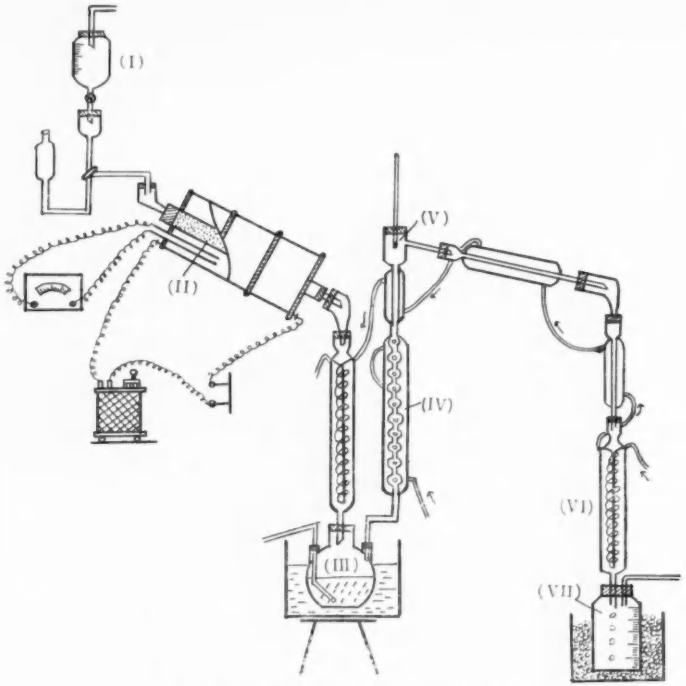

Abb. 1. Experimentelle Vorrichtung.

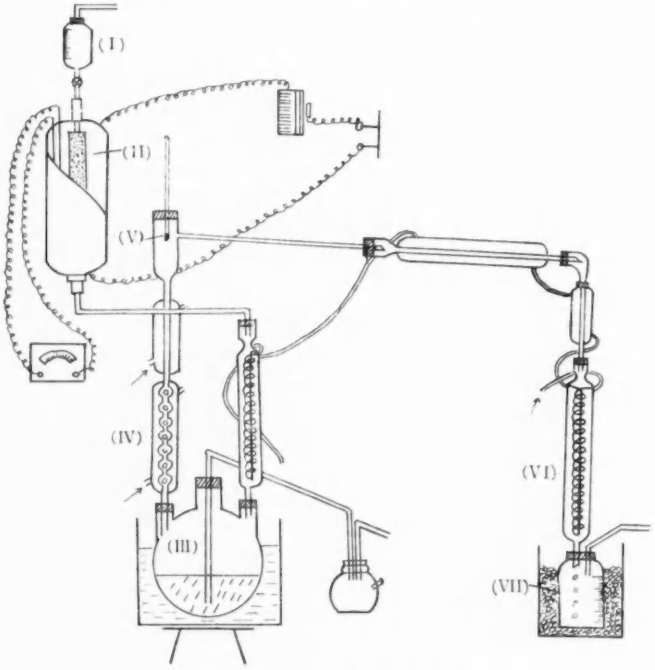

Abb. 2. Experimentelle Vorrichtung.

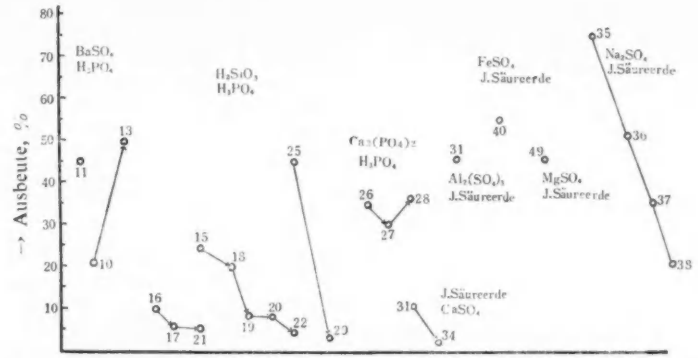

Abb. 3. Verglich der Ausbeute von der vierten Fraktion bei verschiedenen katalystoren.

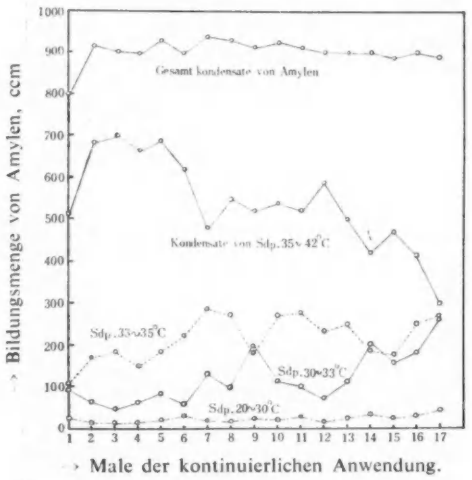

Abb. 4

Aggregateinheit	Nr. 1
Versuchsreihenummer	59~75
Dauer der kontinuierlichen Anwendung	186 Std.

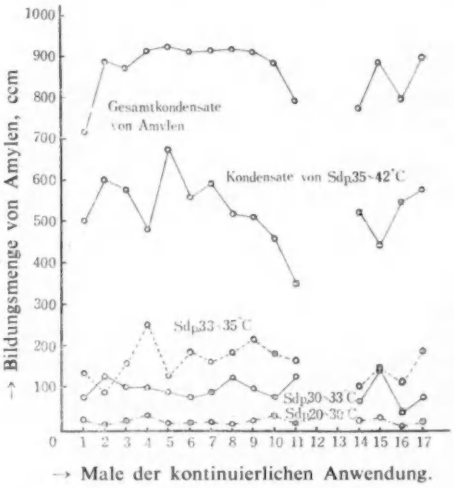

Abb. 5

Aggregateinheit	Nr. 3	Nr. 2
Versuchsreihenummer	80~90	76~79

Zu diesem Zweck wurden die Hochfeindestillation, Fluoreszenz Indikator Adsorptionsanalyse, Infrarot Spektrographie sowie Gas-Chromatographie herangezogen.

Beschreibung der Versuche

Die beiden Vorrichtungen, einmal die horizontale Type, andersmal die vertikale Type, wurden für Entwässerung von Isoamylalkohol nach dem Gasphase-Verfahren verwendet, mit aber annähernd gleichen Ergebnissen. Das Ausgangsmaterial, Isoamylalkohol, tritt tröpfenweise in gewissen Zeitabständen von dem kalibierten Behälter ins Reaktionsrohr aus. In dem Reaktionsrohr sind die in Korngrösse vereinheitlichten Katalysatoren eingepackt und von Aussern her elektrisch geheizt. Die durch Reaktion zu bildenden Olefine und weitere gasförmige Substanzen wandern über den Kühler in den Behälter ein. Dieser Behälter liegt in dem Wasserbad und bleibt unterhalb von 100°C.

Das unverwandelte Isoamylalkohol verbleiben in dem Behälter, während die Olefine mit niedrigem Siedepunkte allein durch den Kühler hinaufsteigen, in den Kühler, wo sie stark abgekühlt werden, und die Vorlage aufgesammelt werden.

Die Kondensate werden nach Feindestillation in 4 Fraktionen eingeteilt: 20~30°C, 30~33°C, 33~35°C, 35~42°C.

Die vierte Fraktion bestehen hauptsächlich aus Trimethyläthylen. Anhand deren prozentualen Ausbeute wurde das katalysatorische Vermögen beurteilt.

Als Katalysatoren wurden 15 folgende Substanzen in verschiedenen Kombinationen eingesetzt: Al_2O_3,

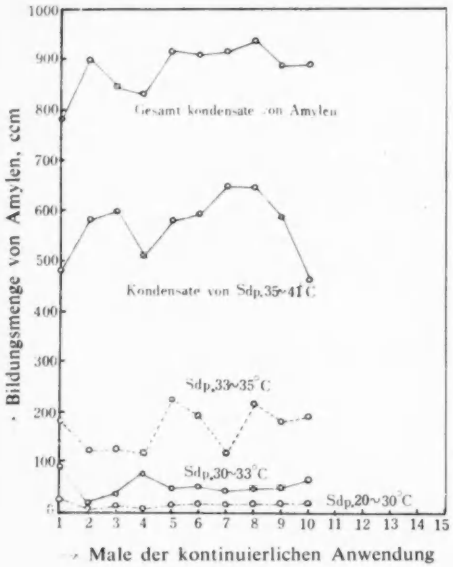

Abb. 6

Aggregateinheit Nr. 4
Versuchsreihenummer 91～100

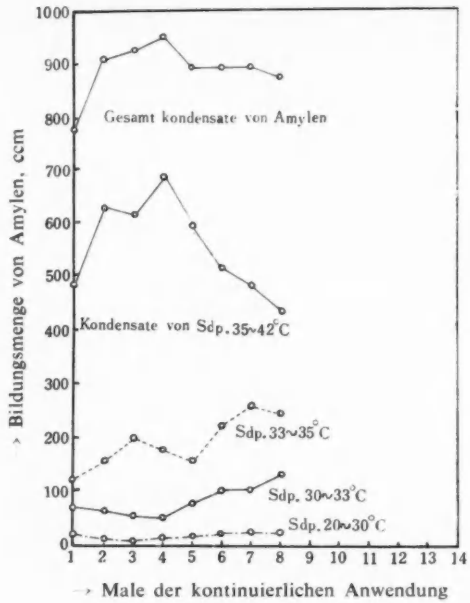

Abb. 7

Aggregateinheit Nr. 5
Versuchsreihenummer 101～108

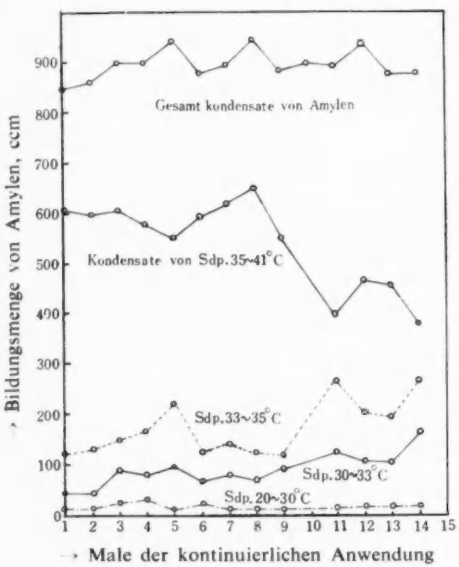

Abb. 8

Aggregateinheit Nr. 6
Versuchsreihenummer 109～122

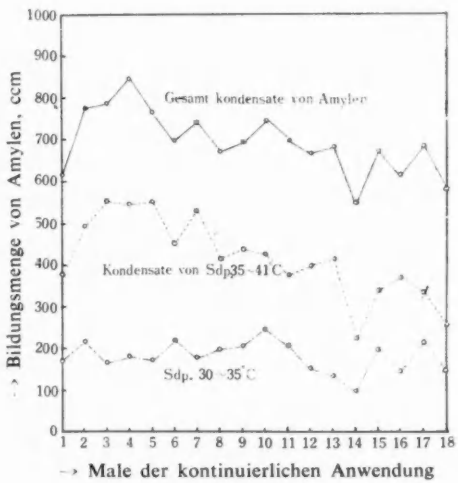

Abb. 9

Aggregateinheit Nr. 7
Versuchsreihenummer 123～140
Dauer der kontinuierlichen Anwendung 220 Std.

$BaSO_4$, H_3PO_4, H_2SiO_3, $ZnSO_4$, $FeSO_4$, $MgSO_4$, $ZnCl_2$, $Ca_3(PO_4)_2$, $Al_2(SO_4)_3$, $CaSO_4$, Na_2SO_4, $KHSO_4$, Stärke, japanische Säureerde.

Der Kakalysator wurde in geeignetem Verhältnis gemischt, mit etwas Wasser zugesetzt, angeteigt, in geeignete Korngrösse verformt, zuerst bei 60°C für 2 Std, dann bei 120°C für 1 Std erhitzt und aufgetrocknet.

Ergebnisse

Die Versuchsergebnisse liessen folgenden Schluss ziehen: Bei dem Aluminiumoxyd als Katalysator zeigte sich die Gesammtmenge von den dritten und vierten Fraktionen nur als 5.5%, ausserdem dieselbe von den Ersten und Zweiten auch als 27%. Unter allen Umständen war Aluminiumoxyd als Katalysator für vorliegenden Versuch unbrauchbar.

Die Resultaten beim Einsatz anderer Katalysatoren sind in Tabelle I aufgezeichnet.

Die Tabelle I umfasst die beiden extremen Ausbeute, nämlich des Maximum und Minimum an der Ausbeute von der vierten Fraktion, die beim gleichen, mehr als zweimal kontinuierlich eingesetzten Mischkatalysator erhalten wurde. Die in der Tabelle I angegebenen Versuchsnummer sind identisch mit denselben in der Tabelle II. In der Tabelle II weisen sie die Beschreibung der verwendeten Reaktionsröhre auf.

Kurz gefasst, ist der Aluminiumoxyd-Katalysator für Fabrikation des Trimethyläthylens ungeeignet. Wenn daher solche Katalysatoren, die über 50%ige Ausbeute des Trimethyläthylens erzielen lassen, aus Tabelle I gesucht werden, können Mischkatalysatoren aus Kieselsäure und Phosphorsäure, aus Natriumsulfat, Eisensulfat oder Magnesiumsulfat mit jeweiligem Zusatz von japanischer Säureerde gefunden werden. Besonders beim Natriumsulfat ist durch Reaktion bei 400°C die Ausbeute von 72% an Trimethyläthylen erzielbar. Die genannte Ausbeute gilt aber nur für das erste Mal. Bei kontinuierlichen Reaktionen vermindert sich diese in einer fortwährenden Abschwächung wie 72.0→53.0→36.5→20.0%.

Auch der Mischkatalysator aus Kieselsäure und Phosphorsäure wies anfangs 55%ige Ausbeute auf, sank aber nach viermaliger kontinuierlicher Anwendung auf 5.5%ige Ausbeute ab. Bei anderen Katalysatoren blieb es fast gleich. Nach 70 bzw. 120 Std kontinuierlicher Anwendung ist das Entwässerungs- und Isomerisations-vermögen fast restlos verlorengegangen, somit sind alle für vorliegenden Versuch vollkommen ungeeignet.

Daher hat der Verfasser zwei Reaktionsröhre in Serie gestellt. In dem ersten Reaktionsrohr soll hauptsächlich die Entwässerung erfolgen, während in dem zweiten die Isomerisation gefördert wird, um die Ausbeute von Trimethyläthylen steigen zu lassen. Mit dieser Absicht wurden die Versuche unter Einsatz verschiedener Katalysatoren angestellt. Die Reaktionstemperatur betrug im ersten Reaktionsrohr 350~450°C und im zweiten 275~320°C. Auch in diesem Fall vermindert sich die Ausbeute an Trimethyläthylen mit Vermehrung der kontinuierlichen Reaktionsmale, um endlich bei dem fünften Mal bis auf 20.0% abzusinken, wie die Tabelle III klar anzeigt.

Die Versuchsergebnisse, die in Tabelle III

Tabelle I. Beziehung zwischen Katalysatorensorten und Ausbeute an Trimethyläthylen

Mischkatalysatoren		Ausbeute an vierten Fraktion			
		min. Werte		max. Werte	
Basis-Substanz	Zusatz	Versuchs Nr.	%	Versuchs Nr.	%
$BaSO_4$	H_3PO_4	12	6.0	13	45.0
H_2SiO_3	H_3PO_4	21	5.5	24	55.5
$Ca_3(PO_4)_2$	H_3PO_4	27	30.0	28	37.5
$CaSO_4$	J. S.[a)]	34	9.5	31	42.0
$Al_2(SO_4)_3$	J. S.	—	—	30	44.5
Na_2SO_4	J. S.	38	20.0	35	72.0
$KHSO_4$	J. S.	—	—	39	30.0
$FeSO_4$	J. S.	—	—	40	56.0
$MgSO_4$	J. S.	—	—	41	50.0

a) J. S.: Japanische Säureerde.

Tabelle II. Beziehung zwischen Grösse der Reaktionsröhre und Versuchsreihe Nummern

Grösse des Reaktionsröhre		Material	Versuchsreihe Nummer
Durchmesser	5 cm	Eisen	13, 24, 30, 34, 35, 38, 39
Länge	54 cm		
Durchmesser	3.4 cm	Silica	12, 21, 27, 28, 31, 40, 41
Länge	62.5 cm		

Tabelle III. Ausbeute an der vierten Fraktion bei Anordnung der zweien Reaktionsröhre in Serie

Inhalt des Mischkatalysators		Ausbeute an der vierten Fraktion			
		min. Werte		max. Werte	
das erste Reaktionsrohr	das zweite Reaktionsrohr	Versuchs Nr.	%	Versuchs Nr.	%
$Ca_3(PO_4)_2+H_3PO_4$	$Al_2(SO_4)_3$	47	20.0	44	67.5
Na_2SO_4	$Al_2(SO_4)_3$	58	20.0	51	72.0
$FeSO_4$	$Al_2(SO_4)_3$	—	—	56	56.0
$MgSO_4$	$Al_2(SO_4)_3$	—	—	57	50.0

Tabelle IV. Beziehung zwischen Malenanzahl der kontinuierlichen Anwendung und der Ausbeute der flüssigen Produkte und des Trimethyläthylens

Reaktionstemp. °C	450	420~450	450	450	450	450	450	450	450	445
Abtröpfelungsmenge von Alkohol, ccm/Std	100	100	90	80	80	100	100	100	100	200
Male der kontinuierlichen Anwendung	1	2	3	4	5	6	7	8	9	10
Gesamtausbeute der Amylen, vol. %	80.0	92.0	92.0	91.0	93.0	91.0	94.0	94.0	93.0	94.0
Ausbeute des Trimethyläthylens, vol. %	52.5	66.0	69.0	65.8	67.5	63.5	48.0	55.0	52.0	53.9
Unverwandelte Alkohol, vol. %	6	3.5	2.5	1.5	2.0	2.0	1.0	2.0	2.5	2.0

Tabelle V. Beziehung zwischen den Einsatzbedingungen und den Grössenordungen der Reaktionsröhre

Nummer des Reaktionsrohrs	Durchmesser cm	Länge cm	Material	Versuchsreihenummer	kontinuirliche Anwendung		Durchschnittsausbeute von Gesamtamylen vol. %	Fraktion von Sdp. 35~41°C vol. %
					Male	Dauer, Std		
1	3.4	62.5	Eisen	1	17	170	90.8	54.9
2	3.4	62.5	〃	2	4	40	82.1	53.1
3	3.4	62.5	〃	3	11	110	86.8	51.2
4	5.0	54.0	〃	4	10	100	88.9	56.3
5	3.4	62.5	〃	5	10	100	88.3	56.5

verzeichnet sind, zeigten, dass die Haltbarkeit des Vermögens arm und somit für kontinuierliche Reaktion ungeeignet ist.

Der Mischkatalysator aus Zinksulfat und japanischer Säureerde zeigte im Unterschied von den anderen in der Ausbeute von Trimethyläthylen bei der ersten Anwendung 52.5%, und die der Zweiten noch eine Höhe von 66%, also deutete auf Möglichkeit einer kontinuierlichen Anwendung an. Daher wurden 64 Male Versuche angestellt, womit endlich festgestellt wurde, dass diesser Katalysator für Entwässerung und Isomerisation des Isoamylalkohols zur hochprozentigen Gewinnung des Trimethyläthylens fabrikatorisch sehr geeignet ist. Der Auszug aus den zahlreichen Versuchsergebnissen wird zum Beispiel in Tabelle IV gegeben.

Wenn also mit dem in Tabelle V bezeichneten Reaktionsrohr Nr. 1 Isoamylalkohol 1000 ccm bei 420~450°C reagiert wird, beträgt die Ausbeute des Trimethyläthylens auch nach 10-maliger kontinuierlicher Anwendung ein- und desselben Katalysators stets über 50%, mit nur geringfügiger Nebenbildung von Isopropyläthylen und Methyläthyläthylen.

Dies liefert den Beweis dafür, dass der Zinksulfat-Katalysator zu dem Zweck des Verfassers befriedigenderweise vorzüglich ist. Dieser Umstand ist auch bei 52 Male, unter Einsatz der Reaktionsröhrenummer 2, 3, 4 und 5 klar feststellbar.

Um diejenigen Ergebnisse handelt es sich bei den Versuchen Nr. 1—5. Tabelle V zeigt eine zum Vergleich derer zusammengefasste Aufstellung.

Es sei noch hinzugefügt, dass die Ausbeute an Trimethyläthylen in solcher Versuche fast die Gleichen wie in Tabelle IV sind und somit hier fortgelassen wurden.

Zusammenfassung

Die Methode, die hauptsächlich aus Trimethyläthylen bestehenden Olefine aus Isoamylalkohol nach dem Gasphase-Verfahren zu gewinnen, wurde ausgearbeitet. Nach der Feststellung, dass der von Ipatiew vorgeschlagene Katalysator, Aluminiumoxyd, zu diesem

Zweck ungeeignet ist, wurden verschiedene Katalysatoren, auf ihr Vermögen, Trimethyläthylen zu liefern, untersucht, mit dem Ergebnis, dass ein Gemisch des Zinksulfat es mit der japanischen Säureerde das beste Vermögen besitzt. Ihre Eignung wurde nach weiterer Forschung unter Modifizierung der Bedingungen ermittelt.

Zum Schluss sei noch davon erwähnt, dass die vorliegende Arbeit der Leitung von Herrn Professor Dr. Eiichi Funakubo an der Technischen Fakultät der Universität zu Osaka verdankt ist.

Chemisches Institut der Technischen Fakultät der Universität zu Osaka
Miyakojima-ku, Osaka

Forschung über die katalytische Entwässerung des Isoamylalkohols. II. Prüfung der Bedingungen für kontinuierliche Dehydratisierung bei Zinksulfat-Katalysator

Von Akira MITSUTOMI

(Eingegangen am 26. September, 1960)

Der Verfasser hat bereits in der I. Mitteilung[1] betont, dass für kontinuierliche Fabrikation der hauptsächlich aus Trimethyläthylen bestehenden Olefinen, ausgehend von Isoamylalkohol, der Zinksulfat-Katalysator das beste Vermögen besitzt.

Um die Entwässerung und Isomerisation beim Einsatz dieses Katalysators genauer zu forschen und unter Anwendung der labormässig grösstmöglichen Apparatur die geeigneten Bedingungen für Olefin-Produktion zu ermitteln, wurden folgende Reihen Versuche gestellt.

Beschreibung der Versuche

Zubereitung der Katalysatoren. — Es wurden kristallines Zinksulfat und japanische Säureerde gut vermischt, mit Zusatze von etwas Wasser genügend angeteigt, in passende Korngrösse verarbeitet, zuerst bei 60°C 2 Std, dann bei 120°C 1 Std erhitzt und abgetrocknet. Die Erhitzungsgewichtsabnahme u. s. w. stehen in Tabelle I.

Es wurden von den Katalysatoren 3 Sorten, nämlich Nr. 1, 2 und 3, wie in Tabelle II angegeben, präpariert und auf katalysatorisches Vermögen, Haltbarkeit u. s. w. geprüft.

Für Reaktionsröhre wurden die Eiserne verwendet. Die einzelnen Grössen, die Versuchsnummern, wobei die Betreffenden eingesetzt wurden, und weitere Angaben sind in Tabelle III verzeichnet.

Versuchsmethode. — Mittelgrosse und grosse Reaktionsröhre, deren Grössenordnung bereits in Tabelle III angegeben ist, wurden in gleicher Weise aufgestellt wie in der I. Mitteilung. Drein wurden unter Variierung der Temperaturen 1000 ccm Isoamylalkohol eingeschickt, wasserabgespaltet, isomerisiert und die Produkte, eingeteilt in 3 folgenden Fraktionen, und die Ausbeute wurde geprüft: bis 30°C, 30~35°C, 35~41°C.

Indem andererseits mit 1000 ccm Isoamylalkohol als einmaliger Einschickung ein und derselbe Katalysator kontinuierlich angewandt wurde, wurde derselbe unter Beobachtung der Änderungen von Ausbeute auf seine Haltbarkeit geprüft.

Ferner wurden unter folgendem Grundsatz Versuche angestellt: (I) Bei Versuchsreihennummer 1 bis 6 wurde unterm Einsatz der mittelgrossen Reaktionsröhre bei Einhaltung der Temperatur zu ca. 398~540°C der Katalysator Nr. 1 auf das Vermögen geprüft. (II) Bei Versuchsreihennummer 7 bis 9 wurde unterm Einsatz der Reaktionsröhr mit etwas grösserem Durchmesser bei ca. 380~451°C Reaktionstemperatur der Katalysator Nr. 1 geprüft. (III) Bei Versuchsreihennummer 10 bis 12 wurde der Katalysator Nr. 1 bei Absenkung der Reaktionstemperatur auf 320~410°C auf das Vermögen geprüft. (IV) Bei Versuchsreihennummer 16~18 wurde der Katalysator Nr. 2 und bei denen 13~15 derselbe Nr. 3 auf das Vermögen geprüft. (V) Unter dem Einsatz des labormässig zulässigen möglichstgrossen Reaktionsrohrs wurde der Katalysator Nr. 1 auf das Vermögen geprüft. Unter variierten Temperaturen wurden 96 Male Versuche angestellt. (VI) Mit gleichgrossem Reaktionsrohr wie oben wurde der Katalysator Nr. 2 geprüft. Es waren die Versuchsreihe Nr. 16~18.

Versuchsergebnisse

Unter Einhaltung der gleichen Bedingungen mit Ausnahme der Reaktionstemperatur wurden unabhängig voneinander 290 Male Experimente durchgeführt, indem ein neuer Katalysator

1) A. Mitsutomi, This Bulletin, 34, 1518 (1961).

TABELLE I. GEWICHTSABNAHME DER KATALYSATOREN NACH ERHITZUNG

	Gewicht g	Kornzahl	Gewicht g	Kornzahl	Gewicht g	Kornzahl
Vor Trocknen	10	37	50	186	100	302
Nach Trocknen	6	37	29.6	186	58	302
Erhitzungsgewichtsabnahme	4	37	20.4	186	42	302
Durchschnittsgewicht eines Korns	0.4		0.592		0.58	
Durchschnittsdurchmesser eines Korns, mm	6.4		6.4		6.4	

TABELLE II. ZUSAMMENSETZUNG DER KATALYSATOREN UND VERSUCHAREIHENNUNMERN

Sorten	Katalysator Zusammensetzung			Reaktionsrohr	
	Zinksulfat	Japanische Säureerde	Zusatz	Mittelgrosses Versuchsnummer	Grosses Versuchsnummer
Nr. 1	30	70	H_2O	1～ 9	10～12
Nr. 2	50	50	H_2O		16～18
Nr. 3	30	70	NH_4OH	13～15	

TABELLE III. REAKTIONSROHRGRÖSSE UND VERSUCHSREIHENUMMERN

Reaktionsrohr		Einfüllungs-volumen cm^3	Katalysatoren		Versuchs-nummer	Reaktions-temperatur °C
Durchmesser cm	Länge cm		Sorten	Einpackungs-menge kg		
5.2	56	1560	Nr. 1	1.156	1～ 6	398～540
2.9	65	1560	Nr. 1	1.156	7～ 9	380～451
2.9	56	1560	Nr. 3	1.170	13～15	380～450
5.1	122	2512	Nr. 1	1.86	10～12	320～410
5.1	122	2512	Nr. 2	1.93	16～18	300～370

TABELLE IV. FABRIKATIONSERGEBNIS VON AMYLEN NACH DEM GASPHASE-VERFAHREN

Versuchs-reihen-nummer	Reaktions-temperatur, °C	Ausbeute, vol. %				unver-wandelter Alkohol, Vol. %
		Gesamte Amylene	Fraktion von			
			bis 30°	30～35°	35～41°	
1	455～511	68.0	0	22.0	66.1	1.8
2	450～540	67.0	0	26.4	62.8	3.5
3	450～499	76.0	0	22.1	70.2	2.2
4	410～450	62.0	0	27.2	57.0	3.0
5	400～450	78.0	0	28.3	63.5	4.0
6	398～451	84.0	0	27.3	63.8	2.5
7	400～445	74.0	0	19.8	69.6	2.1
8	380～449	78.0	0	29.0	57.0	3.5
9	380～450	71.0	0	28.2	57.9	4.2
13	390～430	82.0	3.8	30.3	57.8	16.7
14	380～430	84.0	2.1	30.5	59.5	8.8
15	380～450	84.0	2.4	31.3	59.2	7.5
10	350～410	70.0	6.3	23.5	69.0	9.0
11	320～400	78.0	0.8	21.6	73.0	17.5
16	300～345	78.0	1.9	13.1	73.0	12.5
17	300～350	70.0	1.1	15.2	72.0	12.0
18	300～370	80.0	1.5	16.0	72.5	19.0
12	320～390	81.0	1.1	22.3	74.0	6.4

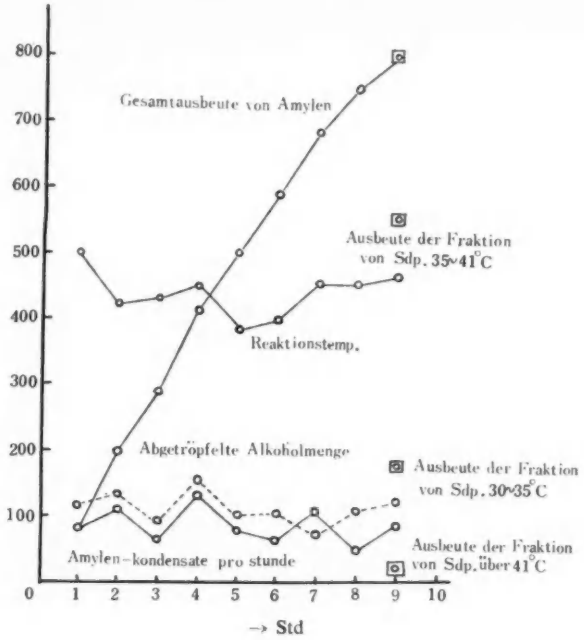

Abb. 1
Versuchsreihennummer 125 Reaktionstemp. 390~455°C

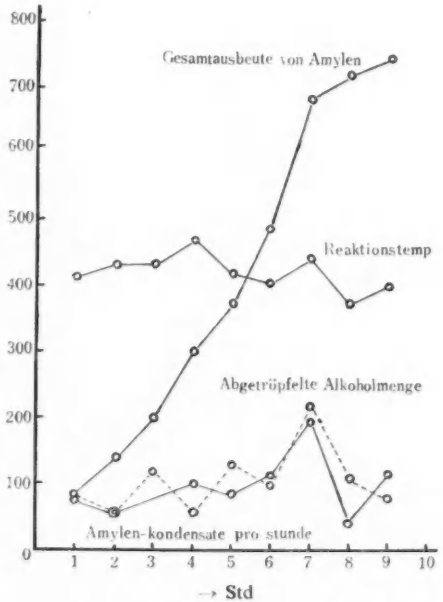

Abb. 2
Versuchsreihennummer 127
Reaktionstemp. 360~450°C

jeweils eingesetzt wurde. Von den Versuchsergebnissen wurden die als typisch Erscheinenden ausgesucht und zum Vergleich auf eine Tabelle IV gebracht.

Wird die Überlegenheit durch die Fraktion von Sdp. 35~41°C, Ausbeute an Amylen und des Wiedergebungsvermögen entschieden, so lässt sich finden, dass die Reaktionstemperatur von gegen 350±30°C herum für den Zweck vorliegender Versuche die optimal Bedingung darstellt, wie die Ergebnisse bei der aus Exp. Nr. 10, 11, 12, 16, 17 und 18 bestehenden Gruppe zeigen.

Bei einer höheren Temperatur erhält man nur in seltenen Fällen gute Ausbeute, wie es bei Exp. Nr. 3 der Fall ist, aber es lässt sich nicht gut wiedergeben. Im Gegensatz hierzu ist das Wiedergebungsvermögen von den Resultaten bei Exp. Nr. 8, 9, 13, 14 und 15 ausgezeichnet gut, aber ausgerechnet die Ausbeute an Trimethyläthylen ist als verhältnismässig schlecht zu bezeichnen. Im Gegenteil davon verbessert sich die Ausbeute der Fraktion von Sdp. 30~35°C. Die dabei herschende Reaktionstemperatur von ca. 400±30°C ist als geeignet für unsere Forschung nicht anzusprechen.

Ferner, die mit dem Fortschreiten der Reaktion ununterbrochen eintretenden Destillatsmengen von Amylen und die drei,

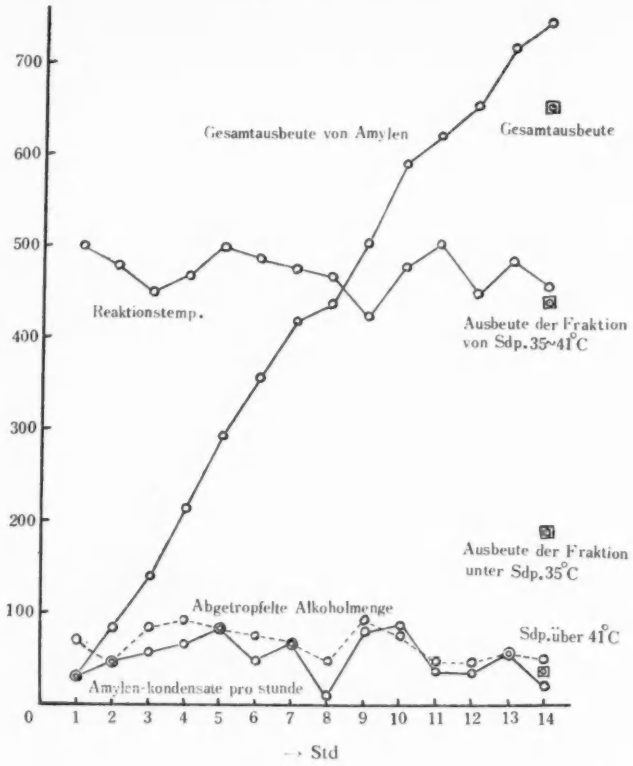

Abb. 3

Versuchsreihennummer 129 Reaktionstemp. 450~499°C

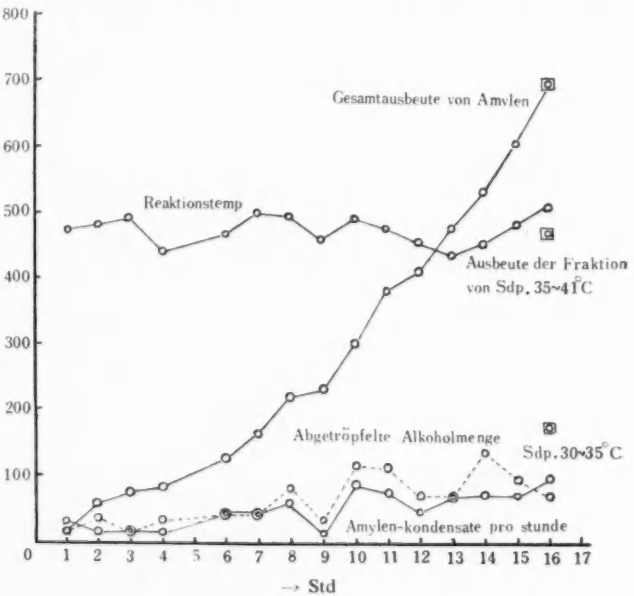

Abb. 4

Versuchsreihennummer 130 Reaktionstemp. 450~510°C

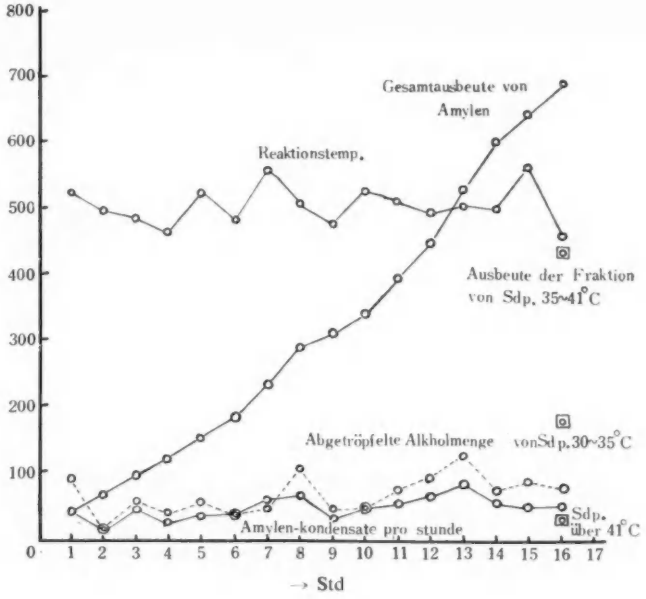

Abb. 5

Versuchsreihennummer 134 Reaktionstemp. 450～540 C

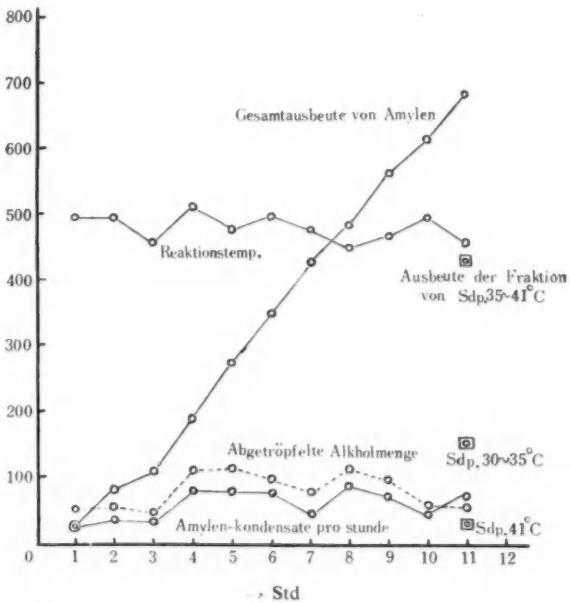

Abb. 6

Versuchsreihennummer 135 Reaktionstemperatur 455～511 C

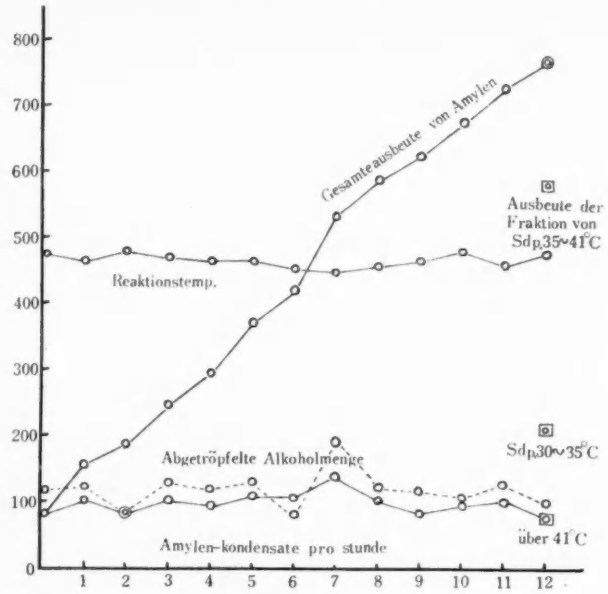

Abb. 7

Versuchsreihennummer 142 Reaktionstemperatur 405~437°C

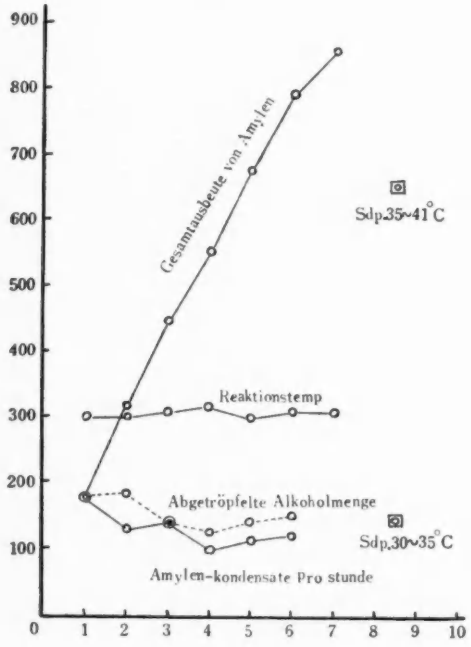

Abb. 8

Versuchsreihennummer 159
Reaktionstemperatur 300~315°C

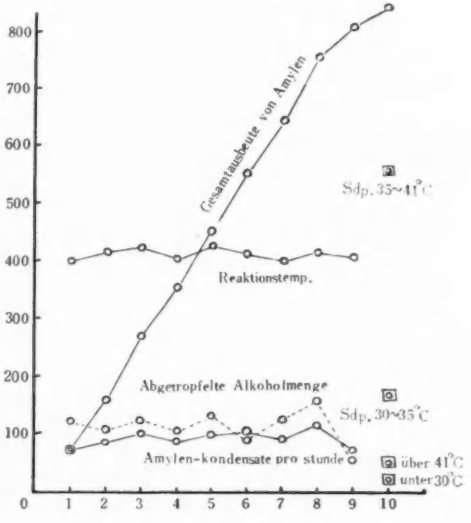

Abb. 9

Versuchsreihennummer 172
Reaktionstemperatur 405~420°C

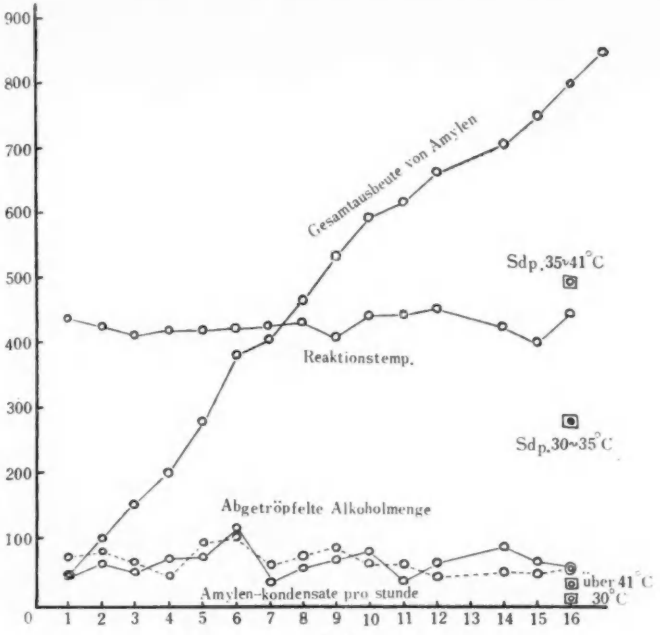

Abb. 10
Versuchsreihennummer 179 Reaktionstemperatur 400~450°C

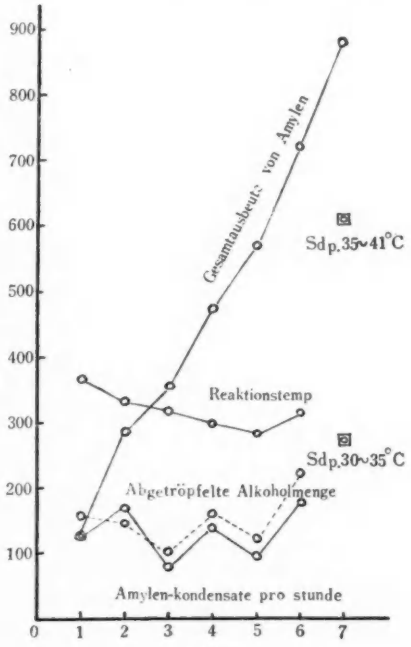

Abb. 11
Versuchsreihennummer 185
Reaktionstemperatur 280~365°C

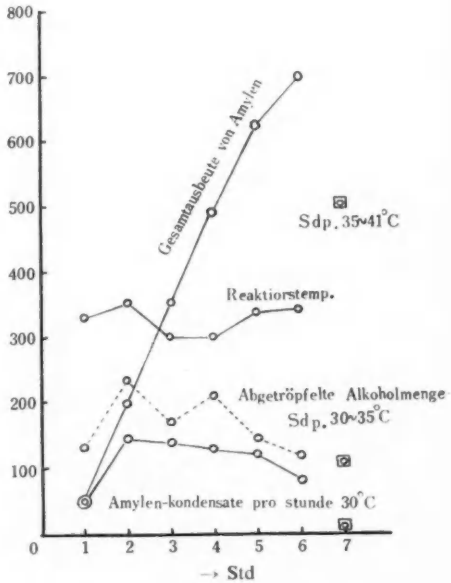

Abb. 12
Versuchsreihennummer 199
Reaktionstemperatur 300~350°C

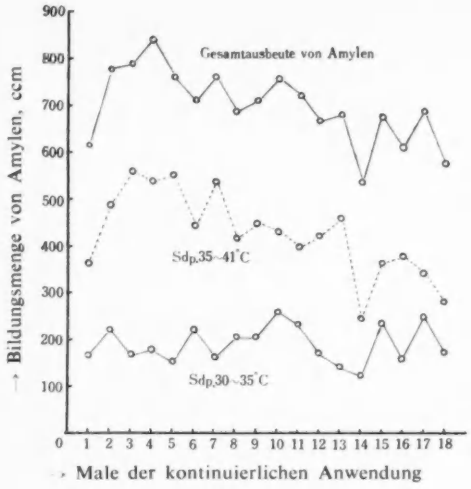

Abb. 13

Versuchsreihennummer	123~140
Dauer der kontinuierlichen Anwendung	220
Male der kontinuierlichen Anwendung	18
Katalysator	Nr. 1

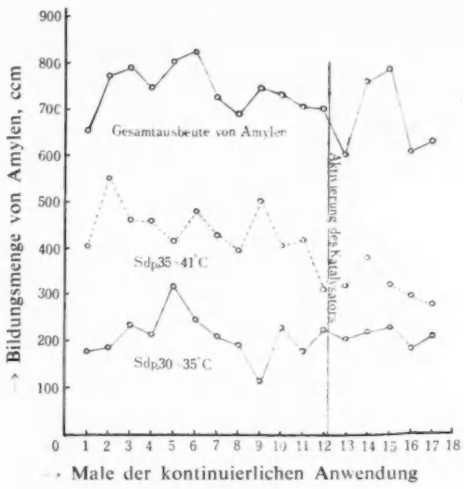

Abb. 14

Versuchsreihennummer	141~157
Dauer der kontinuierlichen Anwendung	234
Male der kontinuierlichen Anwendung	17
Katalysator	Nr. 1

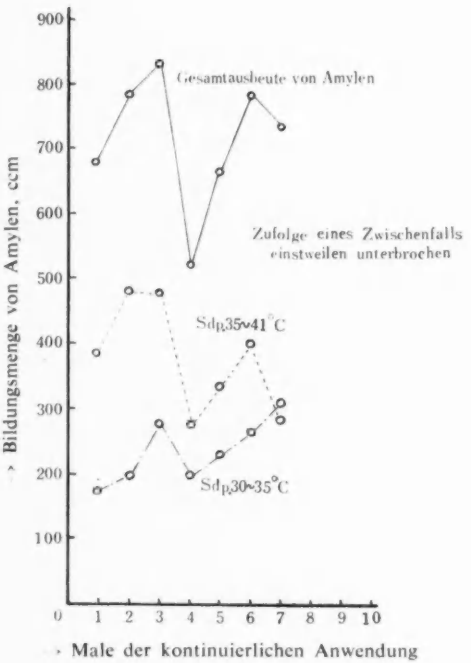

Abb. 15

Versuchsreihennummer	164~170
Dauer der kontinuierlichen Anwendung	86
Male der kontinuierlichen Anwendung	7
Katalysator	Nr. 2

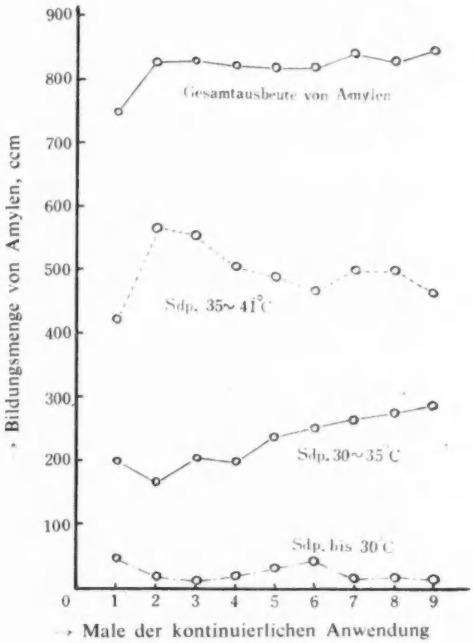

Abb. 16

Versuchsreihennummer	171~179
Dauer der kontinuierlichen Anwendung	99
Katalysator	Nr. 3
Temperatur	28~35°C

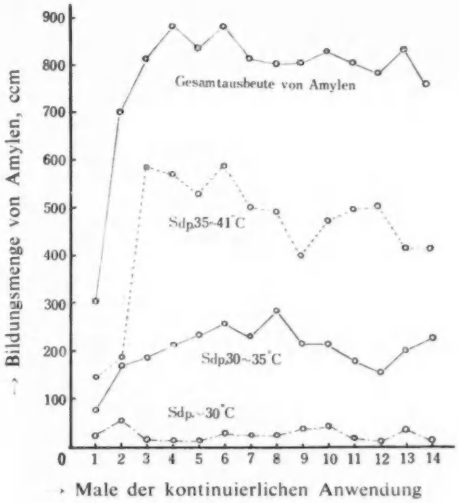

Abb. 17

Versuchsreihennummer	180~193
Dauer der kontinuierlichen Anwendung	87
Male der kontinuierlichen Anwendung	14
Katalysator	Nr. 1
Temperatur	15~23°C
Grosses Reaktionsrohr	(122×5.1)

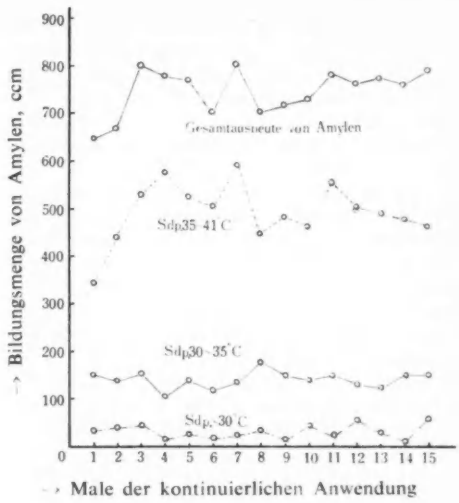

Abb. 18

Versuchsreihennummer	194~208
Dauer der kontinuierlichen Anwendung	100
Male der kontinuierlichen Anwendung	15
Katalysator	Nr. 2
Temperatur	11~19°C
Grosses Reaktionsrohr	

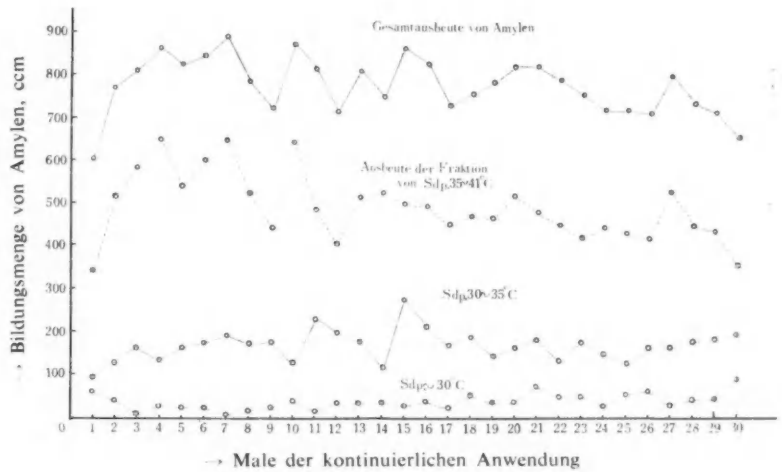

Abb. 19

Versuchsreihennummer	209~238
Dauer der kontinuierlichen Anwendung	174
Male der kontinuierlichen Anwendung	30
Katalysator	Nr. 1
Temperatur	6~13.5°C
Grosses Reaktionsrohr	

unabhängig davon bei der fraktionierten Destillation erhaltenen Sorten von Olefinen wurden auf ein Diagramm gebracht und die mit dem Ablauf der Zeit herlaufende Bildung von Olefinen wurde beobachtet. Dann wurden zwei im Labor anwendbare grösstmögliche Reaktionsröhre wurden für längere Zeit kontinuierlich erfolgende Versuche eingesetzt. Hierbei wurden die Katalysatoren Nr. 1, 2 und 3 (Tabelle V) in Unabhängigkeit voneinander eingesetzt und die Reaktionstemperaturen wurden nur auf drei Bedingungsarten, nämlich 450±30°C, 380 ±30°C und 400±30°C, beschränkt. Und jeweils für 220, 100 und 99 Stunden wurde die Reaktion fortgesetzt. Eine Einsicht in diese Versuchsergebnisse lässt wissen, dass die Bildung von Olefinen beim Einsatz von Katalysator Nr. 3 höchst glatt erfolgt und das Dehydratisierungsvermögen des Katalysators fast nicht nachlässt. Von den gebildeten Amylenen verhält sich die vorwiegend aus Trimethyläthylen bestehende Fraktion bei Sdp. 35～40°C regelmässig und sie ist mengenmässig mehr als die zwei anderen Fraktionen.

TABLE V. DIE ZUSAMMENSETZUNG DER ZINKSULFAT-KATALYSATOREN

Sorten der Katalysatoren	Zinksulfat, %	Japanische Säureerde, %	Zusatz
Nr. 1	30	70	Wasser
Nr. 2	50	50	Wasser
Nr. 3	30	70	Ammoniak

Es lässt sich ausserdem vermuten, dass irgendeines Verhältnis unter diesen Dreien besteht.

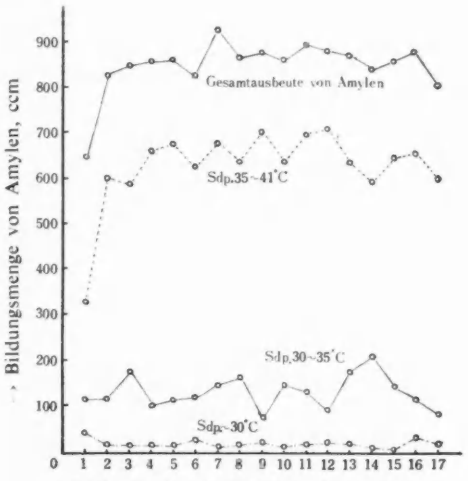

Abb. 20

Versuchsreihennummer	239～255
Dauer der kontinuierlichen Anwendung	104
Male der kontinuierlichen Anwendung	17
Katalysator	Nr. 1
Grosses Reaktionsrohr	
Temperatur	5～14°C

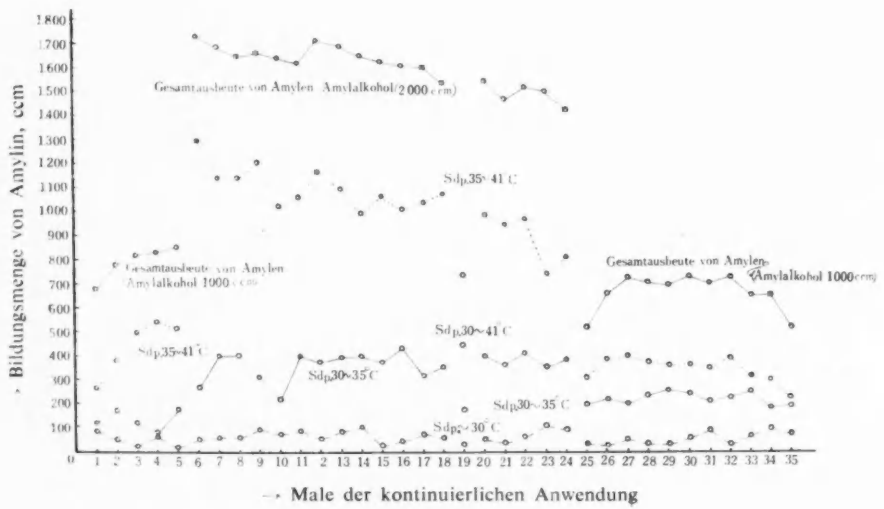

Abb. 21

Versuchsreihenummer	256～290
Dauer der kontinuierlichen Anwendung	246
Male der kontinuierlichen Anwendung	35
Katalysator	Nr. 1
Temperatur	6.5～11.5°C
Grosses Reaktionsrohr	(122×5.1)

Aus der obigen Forschungsarbeit wurden folgende Folgerungen gezogen:

(I) Das Gemisch des Zinksulfates mit der japanischen Säureerde erweist sich für Gewinnung des Trimethyläthylens aus Isoamylalkohol als das beste.

(II) Die Katalysatoren mit drei folgenden Zusammensetzungen wurden in bezug auf Leistungen verglichen. Es wurde gefunden, dass der Katalysator Nr. 3 die besten Ergebnissen aufweist, und dass derselbe Nr. 1 als der nächstbeste in Frage kommt. Der Katalysator Nr. 2 ist als der schlechteste ausgefallen.

Das heisst, bei Zinksulfat ist es unnötig, viel zu verwenden. Mit 30% davon ist es ausreichend. Bei Zusatz geringer verd. Ammoniak werden die besten Ergebnisse erzielt.

(III) Die optimale Reaktionstemperatur liegt bei ca. 400°C. Bei unzweckmässig höherer Temperatur tritt Abbau des Katalysators und weitere unzweckdienliche chemische Änderung mit schlechten Ergebnissen ein.

(IV) Als Katalysator ist solcher in Kugeln mit ca. 8～10 mm Durchmesser angebracht.

(V) Nach Einpackung des Katalysators in Reaktionsrohr ist es nötig, zuerst denselben zur Aktivierung bei ca. 500°C zu erhitzen.

(VI) Die Reaktion soll unter gewöhnlichem Druck erfolgen. Eine Druckerhöhung ist unnötig.

(VII) Als das Reaktionsrohr kann ruhig gewöhnliches Eisen benutzt werden.

(VIII) Der Zinksulfat-Katalysator lässt auch nach einer ununterbrochenen Verwendung keinerlei beachtenswerte Veränderung an der Leistung feststellen. Er hat solche von anderen Katalysatoren nicht erreichbar Haltbarkeit. Es ist somit klar geworden, dass Amylen in der kontinuierlichen Arbeitsweise herstellbar ist.

(IX) Selbst in einem äusserst unglücklichen Fall wird bei dieser Arbeitsweise Isoamylalkohol nur noch um ca. 15% unverändert und immer noch zurückgewonnen. Dies kann nach Trennung von Wasser wiederum ins Reaktionsrohr eingeschickt werden.

Zusammenfassung

Um die höchst geeigneten Bedingungen zu bestimmen, worunter aus Isoamylalkohol die hauptsächlich aus Trimethyläthylen bestehenden Olefine gewonnen werden, wurden labormässig zulässige grösste Vorrichtung herangezogen und das Zinksulfat Gemisch als Katalysatoren auf ihre Leistungen untersucht. Bei dem Mischverhältnis von 30 : 70 erwies sich das Gemisch des Zinksulfates mit der japanischen Säureerde als das Beste. Auch nach 246 stündigem ununterbrochenem Einsatz wurde noch keinerlei grössere Änderung an seiner katalysatorischen Leistung ermittelt.

Hinsichtlich des vorteilhaften Umstandes, dass die Reaktion unterm Einsatz gewöhnlichen Eisenmaterials bei normalem Druck und dem Temperaturbereich von 350±30°C erfolgt, wurde der Zinksulfat-Katalysator als höchst geeignet für Entwässerung und Isomerisation des Isoamylalkohols beurteilt.

Zum Schluss sei noch davon erwähnt, dass die vorliegende Arbeit der Leistung von Herrn Professor Dr. Eiichi Funakubo an der Technischen Fakultät der Universität zu Osaka verdankt ist.

Chem. Institut der Techn. Fakultät der Universität zu Osaka Miyakojima-ku Osaka

SHORT COMMUNICATIONS

On the Influence of Sodium Oxide upon the Crystal Structure of Tricalcium Silicate

By Goro YAMAGUCHI and Hiroshi UCHIKAWA

(Received August 10, 1961)

The crystal structure of pure $3CaO \cdot SiO_2$ and the solid solution of the system $3CaO \cdot SiO_2$-Al_2O_3-MgO, so-called alite, had been determined[1,2]. No results, however, had been reported on the influence of Na_2O upon $3CaO \cdot SiO_2$ and there existed a need for detailed investigation on this system.

In the present paper, the authors describe the results of the investigation on the formation and decomposition of the solid solution of the system $3CaO \cdot SiO_2$-Na_2O and its crystal structure.

Pure $3CaO \cdot SiO_2$ was synthesized by following procedures, that is, the mixtures of alkali free guaranteed reagent of $CaCO_3$ and SiO_2 were heated in platinum crucible at 1500°C, then cooled rapidly, pulverized, reheated several times until no free CaO was found. Then various amount of guaranteed reagent of Na_2CO_3 were added to $3CaO \cdot SiO_2$ and mixed sufficiently, heated at 1450°C for 30 min. and then cooled rapidly to room temperature.

This procedure was necessary to obtain the well-crystallized $3CaO \cdot SiO_2$-Na_2O solid solution. Chemical compositions, refractive indices and specific gravity of the solid solution of this system are shown in Table I.

X-Ray diffraction pattens of the characteristic peaks at 51～52°C in 2θ corresponding to (220) of Jeffery's trigonal cell[1,2] of the $3CaO \cdot SiO_2$-Na_2O solid solution measured by slow scanning and high resolution are shown in Fig. 1.

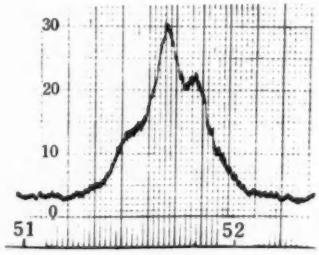

Fig. 1. X-Ray diffraction pattern of the characteristic peak of $3CaO \cdot SiO_2$-Na_2O solid solution (specimen No. 6).

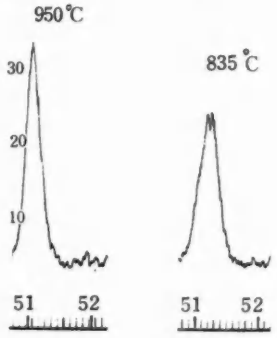

Fig. 2. High temperature X-ray diffraction patterns of the solid solution of the system $3CaO \cdot SiO_2$-Na_2O (specimen No. 6).

These characteristic peaks were triplet until Na_2O content increased to 0.33% and then changed to doublet. Further increase of a Na_2O content made no remarkable change of the X-ray diffraction patterns of the $3CaO \cdot SiO_2$-Na_2O solid solution until 0.71%. More further addition of Na_2CO_3 decomposed it into β-$2CaO \cdot SiO_2$, $Na_2O \cdot CaO \cdot SiO_2$ and free CaO. The triplet ⇄ doublet change seemed corresponding to triclinic ⇄ monoclinic transition.

In differential thermal analysis, the low Na_2O samples showed two endothermic and exothermic peaks at 900～1000°C corresponding to the reversible transitions of triclinic ⇄ monoclinic ⇄ trigonal, but the high Na_2O (0.3～0.7% of Na_2O) samples showed one endothermic and exothermic peak of the monoclinic ⇄ trigonal transition.

In high temperature X-ray diffraction, doublet peaks of the high Na_2O sample changed to singlet at about 900°C as shown in Fig. 2.

From the results of X-ray diffraction and differential thermal analysis, the high Na_2O solid solution was considered to be monoclinic structure. Assuming that this solid solution have Yamaguchi and Miyabe's monoclinic cell[2] corresponding to pseudo-orthorhombic cell

1) J. W. Jeffery, *Acta Cryst.*, 5, 26 (1952).
2) G. Yamaguchi and H. Miyabe, *J. Am. Ceram. Soc.*, 43, 219 (1960).

TABLE I. CHEMICAL COMPOSITION, REFRACTIVE INDICES AND SPECIFIC GRAVITY OF SYNTHESIZED PURE $3CaO \cdot SiO_2$ AND THE SOLID SOLUTION OF THE SYSTEM $3CaO \cdot SiO_2$-Na_2O

	Notation of specimen	SiO_2	CaO	Na_2O	Total	F. CaO	Sp. gr.	Refractive Indices α	Refractive Indices γ
Pure $3CaO \cdot SiO_2$		26.14	73.85	—	99.99	0.00	3.149	1.718±0.002	1.723±0.002
$3CaO \cdot SiO_2$-Na_2O solid solution	No. 1	26.13	73.81	0.05	99.99	0.12	—	—	—
	No. 2	26.10	73.74	0.14	99.98	0.34	—	—	—
	No. 3	26.08	73.67	0.25	100.00	0.73	—	—	—
	No. 4	26.05	73.61	0.33	99.99	0.85	—	1.717±0.002	1.721±0.002
	No. 5	26.02	73.50	0.48	100.00	1.36	—	1.716±0.002	1.720±0.002
	No. 6	25.97	73.34	0.71	100.02	2.92	—	1.715±0.002	1.718±0.002

derived from Jeffery's trigonal cell[1], lattice constants were determined by precise X-ray diffraction as follows:

a=12.262 a. u., b=7.053 a. u., c=25.086 a. u., $\beta = 90°07'$.

Calculated value of interplaner spacing from these lattice constants coinside with those obtained by the precise measurement of the diffraction peaks.

By heating for three hours at 1450°C, the monoclinic high Na_2O solid solution released Na_2O and changed into the triclinic low Na_2O solid solution.

The gradual decomposition of $3CaO \cdot SiO_2$ into $2CaO \cdot SiO_2$ and free CaO occurred at about 1250°C was fairly accelerated in the solid solution, compared with that of pure $3CaO \cdot SiO_2$.

The rate of hydration of the solid solution was larger than that of pure $3CaO \cdot SiO_2$.

This solid solution seems significant because alite in commercial portland cement clinker contains a few amount of Na_2O and effect of Na_2O can not be little.

Department of Applied Chemistry
Faculty of Engineering
The University of Tokyo
Hongo, Tokyo (*G. Y.*)

Central Research Laboratory of
Onoda Cement Company
Toyosu, Tokyo (*H. U.*)

*Zur einfachen Bestimmung im Wasser Milliardestelmenge vorhandenen Kupfers(II) durch Anreicherung mit Mikroschicht der Chelatbildungsharze**

Von Masatoshi FUJIMOTO

(Eingegangen am 2. August, 1961)

In einer vorhergehenden Mitteilung[1] wurde eine spezifische „Harztüpfelmethode[2,3]" zum Nachweise geringer Menge Kupfers(II) mit den Kugeln eines Chelatbildungsharzes, „Dowex A-1 Chelating Resin[4],*1", vorgeschlagen, dessen Haftgruppe, Iminodiacetat-gruppe, durch starke Chelatbildung mit Kupfer(II) am Rande der Kugeln ohne Zusatz spezifischer Reagens eine charakteristische Himmelblaufarbe liefert. Bei der vorliegenden Arbeit wurde es neu gezeigt, daß beim Durchlaufen einer Wasserprobe, die nur Spurenmenge Kupfers(II) enthalten ist, eine dünne Mikroschicht des genannten Chelatbildungsharzes eine deutliche und der Kupfer(II)-menge entsprechende Hellgrün- bzw. Blaufarbe annimmt, welche eine eindeutige und leistungsfähige, halbquantitative Analyse der Milliardestelmenge Kupfers(II) an der Wasserprobe ermöglicht.

* Mikroanalyse mit Hilfe von Ionenaustauscherharzen. XVIII. (Eine vorläufige Mitteilung für eine Reihe der Untersuchungen über Ultramikroanreicherungsverfahren mit Ionenaustauscherschicht).

1) XVII. Mitteilung der Reihe: M. Fujimoto, Dieses Bulletin, **34**, 1342 (1961).

2) M. Fujimoto, ebenda, **30**, 283 (1957).

3) Zusammensetzung der Daten für Harztüpfelmethode bei M. Fujimoto, *Chemist-Analyst*, **49**, 4 (1960).

4) Vgl. „Dowex A-1 Chelating Resin", The Dow Chemical Co., Code No. 164-180 (1959); T. Richard und Wm. Rieman III, *Anal. Chim. Acta*, **24**, 202 (1961).

*1 Die Probe des Dowex A-1 Chelatbildungsharzes wurde von Herren Dr. A. J. Barnard, Jr., sowie Dr. J. R. Skidmore gegeben, wofür der Verfasser zum herzlichsten Dank verpflichtet ist.

TABELLE I. RESULTATE DER GEGENWÄRTIGEN ULTRAMIKROSCHÄTZUNG VON KUPFER(II)-GEHALT BEI DEN VERSCHIEDENEN WASSERPROBEN

Probewasser		Durchlaufgeschwindigkeit (μl/Sek)	(cm/Sek)	V_B[c] (ml)	scheinbare Farbintensität[d] (nach 500 ml	Farbton der Harzschicht Durchlauf)	ausgeschätzter Kupfer(II)-gehalt
Probe-A		70	0.56	$\geqslant$100	−	blaßgelb	$<4\times10^{-9}$
Probe-B		100	0.80	$\simeq$200	++	hell grünlich blau	$\simeq4\times10^{-7}$
Probe-C		140	1.1	$\geqslant$1000	−	blaßgelb	$<4\times10^{-9}$
Probe-D		90	0.72	$\geqslant$1000	−	blaßgelb	$<4\times10^{-9}$
1		70	0.56	$\geqslant$1000	−	blaßgelb	
2		70	0.56	$>$1000	−	blaßgelb	
4	μg Cu(II)[a]	70	0.56	$\simeq$1000	±	blaßgelb ?	
10	pro 1	66	0.52	$\simeq$450	(+)	hell grünlich gelb	
20	Liter	50	0.40	$\simeq$300	+	hell bläulich grün	
40	Probe-	95	0.76	$\simeq$200	++	hell grünlich blau	
100	wassers	100	0.80	$\simeq$75	++	grünlich blau	
200		60	0.48	$\simeq$40	+++	intensiv grünlich blau (himmelblau)	
10[b]		3.2	0.14	$\simeq$80	+	hell grünlich gelb (nach 80 ml Durchlauf)	

Probe-A: durch UNIBED-Austauschersäule entionisiertes Wasser; B: mit einem Messingapparat destilliertes Wasser; C: mit Schliffglasapparat umdestilliertes Wasser; D: Trinkwasser aus Wasserleitung. a Umkristallisiertes Kupfersulfat wurde mit dem entionisierten Wasser versetzt. b Es wurde hier eine Kapillarharzschicht wie Abb. 1-c angewandt, wobei starker Einfluß der Durchlaufgeschwindigkeit auf die Färbung der Harzschicht beobachtet wurde. c Ein Volumen des Wassers, nach dessen Durchlauf erste Grünfarbe an den Harzkugeln in der Schicht sicher erkennbar wird. d −: nicht erkennbar, ±: unsicher, (+): schwach, +: sicher, ++, +++: intensiv.

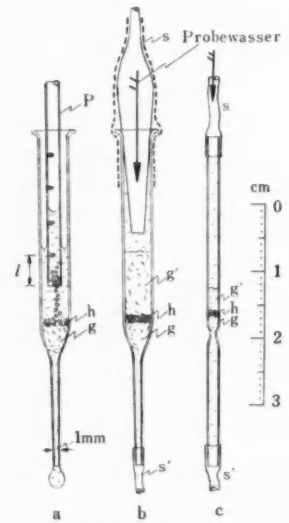

Abb. 1 Mikroharzschicht zur Anreicherung kleinster Menge der Ionen.

Man dreht ein Glasröhrchen 4 mm im Durchmesser und 3 bis 5 cm lang wie Abb. 1 aus[5], und verstöpft dieses etwa 5 mm lang mit einer Watte der feinsten Glaswolle g. Dann läßt man darauf gerade 10 μl der genannten Harzkugeln (50-100 mesh und in der Ammoniumform) mit entionisiertem Wasser zusammen mittels einer vorher je 10 μl eingeteilten Kapillarpipette P*2 absinken.

Man packt locker andere Glaswolle g' um etwa 5-10 mm lang gerade auf diese Harzschicht h wie Abb. 1-b ein. Man steckt einen gereinigten, feinen Polyäthylenschlauch*3 s ins Probewasser ein und läßt dieses mit Hilfe eines Aspirators durch die obenerwähnte Harzschicht h und den Schlauch s' mit mäßiger Geschwindigkeit durchfließen*4. Je 10 bzw. 100 ml Durchlaufen des Probewassers beobachtet man die Färbung an der Harzschicht h unter Vergrößerung mit einer Lupe. Tabelle I zeigt die einigen Beispiele über verschiedene Wasserproben ausgeführter Bestimmungen.

5) Vgl. M. Fujimoto, Dieses Bulletin, **29**, 595 (1956).

*2 Aus der einem Tropfen (etwa 0.04 ml) entionisierten Wassers entsprechenden Länge der Kapillarpipette kann man die gerade 10 μl-Gehalt entsprechende Länge (l) leicht bestimmen.

*3 Einen feinen Polyäthylenschlauch von beliebigem Durchmesser kann man aus einem Schlauche 1 cm im Durchmesser leicht ausdrehen, indem man diesen über einer kleinen Flamme eines Brenners bis zur anscheinenden Durchsichtigkeit gelind erhitzen läßt, und diesen etwas weichenden Schlauch langsam und stark bis zum gewünschten Durchmesser auszieht und im kalten Wasser rasch erstarren läßt.

*4 Anwendung des Wasserdrucks an Stelle des Absaugens zum Durchlaufen des Probewassers ermöglicht noch einfache Anreicherung, worüber der Verfasser zur Zeit noch eingehenden Versuch durchführt.

Die oben mit einem Chelatbildungsharze ausgeführte Ultramikroanreicherungsmethode für außerordentlich verdünnten Bestandteil sei dadurch bis zur noch niedrigen Konzentration wie Billionstel oder weniger ($<10^{-12}$) erfolgreich zu erweitern, daß man, unter genau regulierter Durchlaufgeschwindigkeit der Flüssigkeit, verschiedenartige Adsorptionsmittel, z. B., Kationen- oder Anionenaustauscher sowie anorganische Austauscher, mit empfindlichsten und spezifischen Reagenzien zusammen verwendet. Der Verfasser führt darüber eine Reihe der Untersuchungen aus, die später genau berichtet werden.

Laboratorium für analytische Chemie
Chemisches Institut der wissenschaftlichen Fakultät
Universität Tokyo
Tokyo, Hongo

Experimental Evidence for the Theoretical Condensation Isotherm on Spheres Arranged in the Closest Packing

By Izumi HIGUCHI, Yataro USHIKI and Reiko SUZUKI

(Received August 3, 1961)

One of the contentions of the capillary condensation theory is that the shape of isotherms in the range of high relative pressure is determined by the pore distribution of the sorbent. Hitherto, however, we have not known any process to control precisely the pore distribution of sorbent in its preparation. Therefore the contention seems to have no experimental evidence.

In the former report[1,2] one of us calculated three types of theoretical capillary condensation isotherms which were given by spheres of the sorbent when they were arranged linearly, or two dimensionally, or in the closest packing. A number of experimental isotherms given by corpuscular sorbents, consisting of non-porous particles, exhibited unquestionably the capillary condensation in the range of relative pressure, which was anticipated from the theory and the size of particles, arranged in the two dimensional closest packing. If we can get a corpuscular sorbent of which packing type is previously known, the theoretical condensation isotherms will be confirmed experimentally. Experimental isotherms of benzene and methanol at 0°C on the porous Vycor glass are shown in Figs. 1 and 2. The shape of sorption and desorption isotherms are very similar to what we can theoretically obtain for the corpusclar sorbent if the elementary spheres are arranged in the closest packing. Porous Vycor glass, considering from its preparation process and

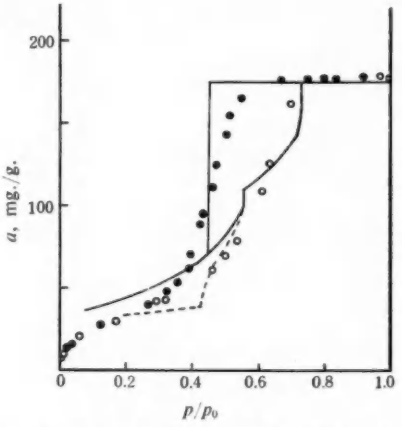

Fig. 1. Sorption isotherm of benzene at 0°C on porous Vycor glass. Circles, sorption data; solid circles, desorption data; the solid line, the theoretical condensation isotherm; the dotted line, the theoretical one, taking into account the vapor pressure correction.

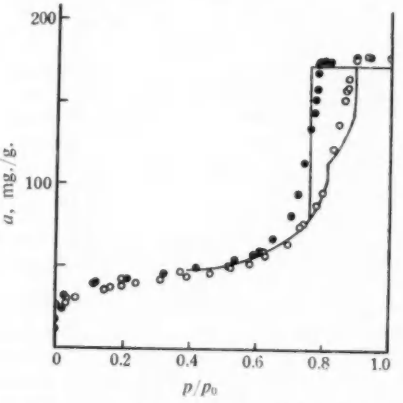

Fig. 2. Sorption isotherm of methanol on porous Vycor glass at 0°C. Circles, sorption data; solid circles, desorption data; the solid line, the theoretical condensation isotherm.

1) I. Higuchi and H. Utsugi, *J. Chem. Phys.*, **20**, 1180 (1952).
2) I. Higuchi and H. Utsugi, *Sci. Repts. Tohoku Univ. Ser. I*, **36**, 27 (1952); *J. Chem. Soc. Japan, Pure Chem. Sec. (Nippon Kagaku Zasshi)*, **73**, 395, 397 (1952).

its hardness, seems to be the most suitable sorbent which is idealized to be consisting of spherical silica particles arranged in the closest packing. The average diameter of elementary particles assumed to be spherical can be calculated from BET area, which is obtained experimentally with benzene isotherm. Then, theoretical condesation isotherms for benzene or methanol can be calculated from the $V(y)$-y relation given in the previous report[2], wherein $V(y)$ denotes the condensed liquid volume per the unit volume of sorbent and y is the radius of curvature of the condensed liquid surface divided by the radius of spherical particles.

The theoretical ones, exhibited by solid lines in the figures, are in good agreement with the experimental values. This is a more satisfactory agreement than expected, because the packing model used in the calculation is quite an idealized one.

From the success mentioned above, we can draw a number of important conclusions for the sorption phenomena: (1) The structure of porous Vycor glass is idealized to be consisting of almost spherical particles arranged in the closest packing. (2) Both sorption and desorption isotherms in the range of high relative pressure are due to the capillary condensation of the sorbate. (3) Kramer-McBain mechanism for the hysteresis[3] in isotherms is confirmed experimentally to be very reasonable.

Both works of Barrer et al[4]. and Kiselev et al.[5] seem to be excellent extensions from the similar standpoint for the capillary condensation theory and hysteresis mechanism. Barrer et al. calculated various theoretical condensation isotherms for a number of single pores different in their shapes and gave a reasonable formula to compute the isotherm for the contact zone between spheres. According to our precise numerical estimations, it is not adequate to calculate the condensed liquid volume between contact spheres by their scheme because the difference in volume between their model and ours is so minor as to be practically negligible. On the other hand, calculations of vapor pressure of the sorbate by our approximation using the usual Thomson equation is rather serious for the linear packing of spheres. Fortunately, however, it is not so serious, as mentioned previously[2] for the closest packing wherein true two dimensional concave meniscus is prevalent between spheres. The correction for this effect is shown by the dotted line in Fig. 1, indicating that our approximation adapted previously may not essentially influence the theory.

The authors gratefully express their appreciation to Dr. Goodman in Corning Glass Corp. and Dr. A. T. Ree for the donation of porous Vycor glass.

College of Arts and Sciences
Tohoku University
Sendai

3) J. W. McBain, *J. Am. Chem. Soc.*, **57**, 691 (1935).
4) R. M. Barrer, N. McKenzie and J. S. S. Reay, *J. Colloid Sci.*, **11**, 479 (1957).
5) A. P. Karnaukhov, and A. V. Kiselev, *Zhur. Fiz. Khim.*, **31**, 3635 (1957); *Chem. Abstr.*, **52**, 5928 (1958).

Synthesis of 4,6-Di-(D-glucopyranosyl)-deoxystreptamine

By Sumio Umezawa and Yukio Ito

(Received August 9, 1961)

Recently, it has been shown that a essential group for antibiotic character of neomycin[1], kanamycin[2] and paromomycin[3] belongs to the glucosides of deoxystreptamine, however, synthesis of the allied glucosides has not been reported as yet*. In continuation of our work[2d] on kanamycin, we have synthesized 4, 6-di-(β-D-glucopyranosyl)deoxystreptamine (IV).

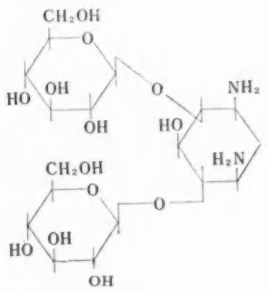

1) F. A. Kuehl, M. N. Bishop and K. Folkers, *J. Am. Chem. Soc.*, **73**, 881 (1951); K. L. Rinehart and P. W. K. Woo, ibid., **83**, 643 (1961).
2) a) H. Umezawa, K. Maeda, M. Murase and H. Mawatari, *J. Antibiotics (Japan), Ser. A*, **11**, 163 (1958). b) M. J. Cron, O. B. Fardig, D. L. Johnson, D. F. Whitehead, I. R. Hooper and R. U. Lemieux, *J. Am. Chem. Soc.*, **80**, 4115 (1958). c) H. Ogawa, T. Ito, S. Kondo and S. Inoue, *J. Antibiotics (Japan), Ser. A*, **11**, 169 (1958); *Bull. Agr. Chem. Soc. Japan*, **23**, 289 (1959). d) S. Umezawa, Y. Ito and S. Fukatsu, *J. Antibiotics (Japan), Ser., A*, **11**, 162 1958); This Bulletin, **32**, 81 (1959).
3) T. S. Haskell, J. C. French and Q. R. Bartz, *J. Am. Chem. Soc.*, **81**, 3483 (1959).
* It should be noted that a related compound, *O*-(β-D-2-amino-2-deoxyglucopyranosyl) derivative of *d, l-trans*-2-aminocyclohexanol was synthesized: T. Suami and S. Umezawa, This Bulletin, to be published.

Addition of excess carbobenzoxychloride in toluene to an aqueous solution of deoxystreptamine made alkaline with sodium hydroxide gave, in 48% yield, *N, N'*-dicarbobenzoxydeoxystreptamine (I), m. p. 233~235°C. Found: C, 62.06; H, 6.23; N, 6.55. Calcd. for $C_{22}H_{26}O_7N_2$: C, 61.38; H, 6.09; N, 6.51%.

N, N'-Dicarbobenzoxydeoxystreptamine (I) failed to react with acetobromoglucose in benzene, chloroform, dioxane or dimethylformamide, however, it has been found that the condensation proceeded in nitromethane. To a suspension of I (1.63 mmol.) in nitromethane was added acetobromoglucose (5.35 mmol.) and powdery mercuric cyanide (5.5 mmol) and the suspension was stirred for twenty-four hours at 27°C. Extraction with chloroform followed by evaporation of the solvent gave a crude product, which was recrystallized from absolute ethanol to afford, in 76% yield, *N, N'*-dicarbobenzoxy-4, 6-di-(tetraacetyl-D-glucosyl)deoxystreptamine (II), m. p. 253~254°C, $[\alpha]_D^{17.5}$ −9.6° (*c* 1.965, chloroform). Found: C, 54.83; H, 5.53; N, 2.85. Calcd. for $C_{50}H_{62}O_{25}N_2$: C, 55.05; H, 5.73; N, 2.57%.

Infrared spectrum: ν_{max}^{Nujol} 3480, 3340 (OH, NH); 1760 (acetyl C=O); 1700 (C=O in $OCOCH_2C_6H_5$); 1520 (CONH); 1220; 1160, 1075 (glucoside); 1035 (alicyclic secondary alcohol); 903 (β-glucoside); 733, 695 (monosubstituted benzene).

Hydrolysis of II (1.0 g.) with methanolic ammonia at room temperature followed by evaporation in vacuo and washing with ethyl acetate gave a crude product, which was recrystallized from water-dioxane-ethanol (5: 1: 10) to afford colorless needles (0.38 g.) of *N, N'*-dicarbobenzoxy-4,6-di-(D-glucosyl) deoxystreptamine (III), m.p. 288~290°C (decomp.), $[\alpha]_D^{17.5}$ −5.67° (*c* 1.43, pyridine). Found: C, 54.16; H, 6.06; N, 3.81. Calcd. for $C_{34}H_{46}N_2O_{17}$: C, 54.11; H, 6.14; N, 3.71%. Infrared spectrum: ν_{max}^{Nujol} 3350, 1700, 1545, 1295, 1230, 1165, 1075, 1035, 890, 735, 695 cm^{-1}.

Hydrogenolysis of III (0.5 g.) with palladium catalyst in water-dioxane (1:1) followed by evaporation in vacuo and washings with dioxane, ether and ethanol gave a crude product, which was recrystallized from water-ethanol to afford colorless crystals of 4, 6-di-(β-D-glucosyl)deoxystreptamine (IV), $[\alpha]_D^{20}$ −4.69° (*c* 1.01, water). The product darkened and decomposed at about 190~230°C. Found: C, 43.91; H, 7.26; N, 5.37. Calcd. for $C_{18}H_{34}O_{13}N_2$: C, 44.43; H, 7.06; N, 5.76%. Infrared spectrum: ν_{max}^{Nujor} 3340, 1600 (NH_2), 1165, 1075, 1035, 890 cm^{-1}.

The positions of attachment of two D-glucoses to deoxystreptamine was substantiated by periodate oxidation of 4, 6-di-(tetraacetyl-D-glucosyl)deoxystreptamine diacetate (V), which was obtained by hydrogenolysis of II with palladium catalyst in dioxane-acetic acid -water. The compound decomposed at about 270°C (darkening at about 180°C). Found: C, 48.62; H, 6.46; N, 3.14. Calcd. for $C_{34}H_{50}N_2O_{21}\cdot 2CH_3\cdot CO_2H$: C, 48.40; H, 6.21; N, 2.97%.

Upon oxidation with sodium periodate in aqueous 50% dioxane for twenty-nine hours, V did not consume the oxidant, while, in parallel experiments, methyl α-D-glucoside and β-pentaacetyl-D-glucose consumed 1.97 and 0.1 mol. of the oxidant respectively. The glucosidic linkages in III or IV are therefore on C-4 and C-6 of deoxystreptamine.

Infrared spectra of the products (III, IV) showed absorption at 890 cm^{-1} which is characteristic of β-glucosidic linkage, Moreover, a rough calculation** of the anomeric contribution (A) of the glucosidic linkages in IV gave a negative value (−13141), the presence of two β-linkages being suggested.

The structure of IV has a close resemblance to that of kanamycin, however, there is a characteristic difference regarding the configuration of anomeric carbon atoms. IV showed no antibiotic activity. The syntheses of allied compounds containing α-linkages of amino sugars are in progress.

The authors are indebted to Mr. S. Nakada for the microanalyses.

Department of Applied Chemistry
Faculty of Engineering
Keio University, Tokyo

** By substitution of 2B (24000) of D-glucose into the equation $[M]_D = 2A + 2B$: $-2281 = 2A + 24000$.

Effect of Impurities on the ^{81}Br Quadrupole Resonance in p-Dibromobenzene

By Juro MARUHA, Jun KOIZUMI, Masahiko SUHARA and Tokuzo TONOMURA

(Received September 6, 1961)

Some investigations have been done concerning the effect of impurities on the nuclear quadrupole resonance absorption of ^{35}Cl in molecular crystals[1,2]. In particular Monfils

1) See for instance: J. Duchesne, "Advances in Chemical Physics", Vol. II, Ed. by I. Prigogine, Interscience Publishers, Inc., New York (1959), p. 190.
2) S. Kojima, S. Ogawa, M. Minematsu and M. Tanaka, *J. Phys. Soc. Japan*, **13**, 446 (1958).

and Grosjean derived an equation for the line height (I) of the absorption curve as follows[3]:

$$I = I_0 \exp(-NC) \qquad (1)$$

where C is the concentration of impurity, and N, a "characteristic number", represents the number of resonant nuclei per impurity molecule whose resonance have been perturbed so they can no longer contribute to the central portion of the line. The main effect of impurity was considered the lattice defect due to the volume difference between the resonant atom and the substituted one[1,2]. For bromine compound, however, only one investigation has been reported. Dreyfus and Dautreppe studied the intensity of the resonance line of ^{79}Br in p-dibromobenzene[4]. The present paper contains the study of the effect of impurities on the resonance line of ^{81}Br in p-dibromobenzene.

The spectrometer used was similar one reported by Kojima[5]. The intensity of resonance line war observed with a video amplifier and an oscilloscope. The frequency of the resonace was about 224 Mc/sec. Samples are carefully purified and mixed, then sealed into glass tubes. The mixed sample in each tube was melted and crystallized slowly by standing overnight. The tube containing the mixed crystal was placed in a r-f coil of the spectrometer. All the measurements were carried out at 4±1°C, hence p-dibromobenzene exists in the α-phase.

The results are shown in Fig. 1, graphically. In each case plots of log (I/I_0) vs. C is not a single straight line but is nearly hyperbolic. If a linear relation is assumed in the small impurity region, the characteristic number is calculated according to Eq. 1, from the slope. These values are listed in Table I. The values

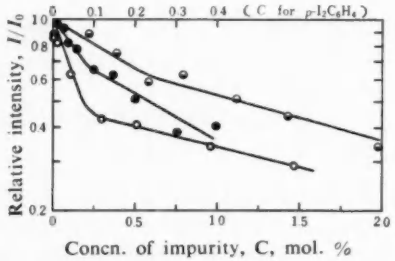

Fig. 1. Variation of relative intensities with concentration of impurities.
◒ p-BrC_6H_4Cl ● p-$I_2C_6H_4$ ○ p-$Cl_2C_6H_4$

obtained for p-dichlorobenzene and p-diiodobenzene are not consistent with the Dreyfus and Dautreppe's values. In their experiment log (I/I_0) decreases linearly with C over wide concentration range for the above two cases, whereas it is hyperbolic for the case of p-bromochlorobenzene, and they considered the latter is an exceptional case. On the contrary Kojima et al. showed in their experiment concerning the ^{35}Cl resonance[2] that the results are always hyperbolic, as we obtained. Thus the results of Dreyfus and Dautreppe are considered to be dubious.

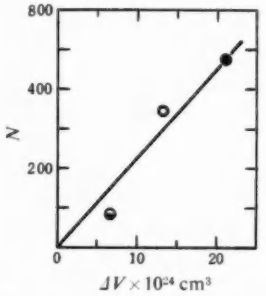

Fig. 2. Relation between characteristic number and volume difference.
● p-$I_2C_6H_4$ ○ p-$Cl_2C_6H_4$ ◒ p-BrC_6H_4Cl

TABLE I. CHARACTERISTIC NUMBER AND VOLUME DIFFERENCE

Impurity molecule	N	ΔV (10^{-24} cm³)	$N^{a)}$
p-BrC_6H_4Cl	82	− 6.63	—
p-$Cl_2C_6H_4$	348	−13.26	32
p-$I_2C_6H_4$	475	+21.14	80

a) Dreyfus and Dautreppe's value.

The relation between the characteristic number (N) and the volume difference (ΔV) is shown in Fig. 2, and can be expressed by

$$N = k\Delta V \qquad (2)$$

where k is 22.5×10^{24} cm^{-3}. Compared with the corresponding results for chlorine compounds[6], it may also be true for the bromine compound that the main effect of impurity is attributed to the volume difference between the Br atom and the substituted one.

Department of Chemistry
Faculty of Science
Kanazawa University
Sengoku-cho, Kanazawa

3) A. Monfils and D. Grosjean, *Physica*, **22**, 541 (1956).
4) B. Dreyfus and D. Dautreppe, *Compt. rend.*, **243**, 1517 (1956).
5) S. Kojima, K. Tsukada, K. Shimauchi and A. Hinaga, *J. Phys. Soc. Japan*, **9**, 795 (1954).
6) R. E. Michel and R. D. Spence, *J. Chem. Phys.*, **26**, 954 (1957).

Syntheses of α-Keto Amides and Acids from Ethyl Alkylidenecyanoacetate

By Minoru IGARASHI and Hiroshi MIDORIKAWA

(Received September 9, 1961)

The present paper deals with a novel preparation of α-keto amides and acids from ethyl alkylidenecyanoacetate as starting material. The synthetic steps are shown in the following scheme.

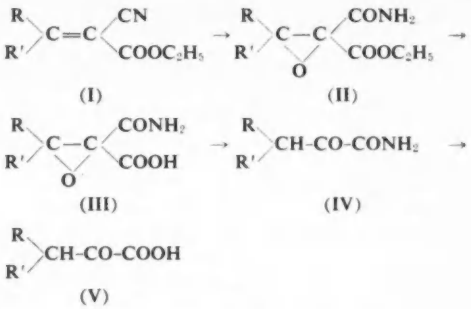

Payne and Williams[1] have shown that α, β-unsaturated acids such as crotonic and maleic

TABLE I. PREPARATION OF EPOXYAMIDE II FROM ETHYL ALKYLIDENECYANOACETATE (I)

$RR'C(O)C(CONH_2)COOEt$

R	R'	M. p., °C	Yield, %	Formula	Calcd. C	Calcd. H	Calcd. N	Found C	Found H	Found N%
Methyl	Methyl	101	61	$C_8H_{13}O_4N$	51.33	7.00	7.48	50.89	6.53	7.45
Methyl	Ethyl	77	80	$C_9H_{15}O_4N$	53.72	7.51	6.96	53.28	7.45	7.01
Methyl	Isobutyl	69	71	$C_{11}H_{19}O_4N$	57.62	8.35	6.11	57.37	8.01	6.15
Methyl	Hexyl	88	64	$C_{13}H_{23}O_4N$	60.98	9.01	5.44	60.62	8.78	5.42
Propyl	Propyl	99	50	$C_{12}H_{21}O_4N$	59.24	8.70	5.76	58.85	8.40	5.84
Methyl	Phenyl	91	70	$C_{13}H_{15}O_4N$	62.64	6.07	5.62	62.40	6.01	5.59
Cyclohexyl		111	65	$C_{11}H_{17}O_4N$	58.13	7.54	6.16	58.23	7.45	6.07
Cyclopentyl		123	75	$C_{10}H_{15}O_4N$	56.32	7.09	6.57	55.99	6.83	6.53

TABLE II. PREPARATION OF α-KETOAMIDE IV FROM III

$RR'CHCOCONH_2$

R	R'	M. p., °C	Yield, %	Formula	Calcd. C	Calcd. H	Calcd. N	Found C	Found H	Found N%
Methyl	Methyl	112	50	$C_5H_9O_2N$	52.16	7.88	12.17	51.89	7.77	11.99
Methyl	Ethyl	71	52	$C_6H_{11}O_2N$	55.79	8.58	10.85	55.81	8.59	10.85
Propyl	Propyl	63	80	$C_9H_{17}O_2N$	63.13	10.00	8.18	62.84	9.49	8.20
Methyl	Phenyl	116	64	$C_{10}H_{11}O_2N$	67.78	6.26	7.91	67.53	6.11	7.84
Cyclohexyl		120	48	$C_8H_{13}O_2N$	61.91	8.44	9.03	62.07	8.18	9.02
Cyclopentyl		144	40	$C_7H_{11}O_2N$	59.55	7.85	9.92	59.37	7.62	9.91

TABLE III. PREPARATION OF α-KETO ACID V FROM III

$RR'CHCOCOOH$

R	R'	M. p., °C (B. p., °C/mmHg)	Yield, %	Oxime M. p., °C	Oxime Formula	Oxime Calcd. N	Oxime Found N%
Methyl	Ethyl	40 (82~84/18)	75	164	$C_6H_{11}O_3N$	9.65	9.51
Methyl	Isobutyl	89 (140~143/7)	80	132 (decomp.)	$C_9H_{13}O_3N$	8.09	8.03
Methyl	Hexyl	(126~129/8)	92	90 (decomp.)	$C_{10}H_{19}O_3N$	6.96	6.81
Propyl	Propyl	(145~148/7)	80	144 (decomp.)	$C_9H_{17}O_3N$	7.48	7.33
Methyl	Phenyl	53	90	120 (decomp.)	$C_{10}H_{11}O_3N$	7.25	7.02
Cyclohexyl		50	98	170	$C_8H_{13}O_3N$	8.18	8.18
Cyclopentyl		54	60	131 (decomp.)	$C_7H_{11}O_3N$	8.91	8.92

1) G. B. Payne and P. H. Williams, *J. Org. Chem.*, **24**, 54 (1959).

acids are efficiently epoxidized with hydrogen peroxide using sodium tungstate as catalyst, and Payne[2] has also established that ethyl isopropylidenecyanoacetate is converted to the corresponding epoxyamide by the use of hydrogen peroxide and sodium hydroxide.

In the present work, ethyl alkylidenecyanoacetate was epoxidized at 70~80°C in ethanol containing 30% hydrogen peroxide and sodium tungstate dihydrate. The resulting epoxyamide II reacted with alcoholic alkali at room temperature to give the compound III. Decarboxylation and rearrangment of III to α-ketoamide IV was readily accomplished by heating with a small amount of water. Further, the treatment of III and IV with dilute hydrochloric acid affored α-keto acid V in a good yield. The compounds IV and V formed the corresponding oximes. The compounds which were prepared by this process are listed in Tables I–III.

The method appears to be generally applicable in the synthesis of α-keto amide and acid.

Details of this study will be published elsewhere.

The authors wish to express their sincere thanks to Dr. Taro Hayashi and Dr. Tatsuo Takeshima for their kind advice.

The Institute of Physical and Chemical Research
Komagome, Bunkyo-ku, Tokyo

2) G. B. Payne, ibid., **26**, 654 (1961).

Rhodium-Platinum Oxide as a Catalyst for the Hydrogenation of Organic Compounds. II[1]. *Catalyst Preparation and Effects of Platinum in Rhodium-Platinum Oxide*

By Shigeo NISHIMURA

(Received September 20, 1961)

It was reported previously[1-3] that rhodium-platinum(3 : 1) oxide prepared exactly in the same way as Adams platinum oxide is easily reduced with hydrogen to the metals at the ordinary temperature and pressure and that the resulting rhodium-platinum black is an excellent catalyst retaining the nature of a pure rhodium catalyst and is substantially superior to Adams platinum and palladium catalysts both in activity and in selectivity in the hydrogenation of various organic compounds.

It has been found that the activity of rhodium-platinum(3 : 1) oxide and also that of rhodium oxide are considerably enhanced by fusing the corresponding chlorides with sodium nitrate for a shorter time at a lower temperature than as directed in the preparation of platinum oxide[4]. The rhodium-platinum(3 : 1) catalyst prepared in this way is not only more active, but also more easily dissolved in aqua regia than reported previously. This fact prompted the author to prepare a catalyst which retains the nature of a rhodium catalyst and can be completely recovered with aqua regia. Rhodium-platinum oxide of various compositions has been prepared by the improved procedure and the activity and selectivity have been studied in the hydrogenation of toluene and acetophenone in acetic acid. The results are summarized in Table I. The catalysts containing 70 to 90% of rhodium are the most active and selective. On the other hand, those containing about 30% or more of platinum dissolve on gently heating in aqua regia without leaving any insoluble residue. Thus the requirements mentioned above are satisfied to a large extent by the catalyst consisting of 70% of rhodium and 30% of platinum, which dissolves in aqua regia practically with no residue, and yet is nearly as active and as selective as rhodium-platinum(3 : 1) oxide.

Though rhodium oxide is not easily reduced with hydrogen as noted previously[2], that prepared by the improved procedure can be reduced to the metal in 3~4 hr. at 30°C or in about 1 hr. at 45~50°C in acetic acid under the atmospheric pressure of hydrogen. The resulting rhodium black, however, is unexpectedly less active than rhodium-platinum (3 : 1) oxide as shown in the hydrogenation of toluene. The proportion of hydrogenolysis in the hydrogenation of acetophenone is somewhat greater with rhodium oxide than with rhodium-platinum(3 : 1) oxide (see Table I). Thus, the platinum in rhodium-platinum oxide promotes the reduction of the oxide to the metals, makes the resulting catalyst more active and selective than the pure rhodium catalyst, and makes it possible to recover the metals with aqua regia.

1) Part I: S. Nishimura, This Bulletin, **34**, 32 (1961).
2) S. Nishimura, ibid., **33**, 566 (1960).
3) S. Nishimura, T. Onoda and A. Nakamura, ibid., **33**, 1356 (1960).
4) R. Adams, V. Voorhees and R. L. Shriner, "Organic Syntheses", Col. Vol. I, 2nd Ed., John Wiley & Sons, Inc., New York (1941), p. 463.

TABLE I. CATALYTIC HYDROGENATION OF TOLUENE AND OF ACETOPHENONE WITH RHODIUM-PLATINUM OXIDE OF VARIOUS COMPOSITIONS[a)]

Catalyst		Time for the reduction of oxide to metal	Hydrogenation of toluene (0.921 g.)		Hydrogenation of acetophenone (0.601 g.)	
Rh(%)	Pt(%)	min.	Initial rate[b)] ml./min.	Time min.	H_2 uptake mol./mol.	Time min.
100	0	210	88	23	4.08	30
90	10	50	110	15	4.03	20
80	20	30	106	16	4.02	22
75	25	24	108	15	4.02	20
70	30	20	103	16	4.02	20
60	40	16	91	16	4.05	24
50	50	11	87	17	4.08	36
25	75	5	49	25	4.15	50
0	100	2	19	83	4.65	75

a) Each hydrogenation was carried out with 50 mg. of oxide in 20 ml. of acetic acid at 30°C under the atmospheric pressure of hydrogen. The substance to be hydrogenated was added after the oxides was reduced to the metal.

b) Initial rate refers to 50 mg. of catalyst metal.

Procedure for the Preparation of Rhodium-Platinum (7 : 3) Oxide. — A mixture of the chlorides corresponding to 0.30 g. of rhodium and 0.13 g. of platinum in the weights of the metals is fused with 20 g. of sodium nitrate in the same way as in the preparation of platinum oxide[5]. After a violent evolution of the oxides of nitrogen has almost subsided, the temperature is raised and kept at 460~480°C for about 10 min. After cooling, the solidified mass is rinsed in distilled water. The solid is collected, washed with 100 ml. of 0.5% aqueous sodium nitrate, and then dried over calcium chloride. The yield is 0.665 g., which is quantitative on the basis of the metal content (65%) of the oxide.

The author wishes to express his sincere gratitude to Professor Yoshiyuki Urushibara for his continued encouragement.

Department of Chemistry
Faculty of Science
The University of Tokyo
Hongo, Tokyo

5) Cf. Ref. 4, p. 463.

Naphthalene as an Isolatable Reaction Intermediate in the Catalytic Vapor-phase Oxidation of Methylnaphthalenes to Phthalic Anhydride

By Charles J. NORTON

(Received August 22, 1961)

Naphthalene has not been reported previously as a reaction intermediate in the heterogeneous vapor-phase oxidation of either monomethylnaphthalenes or dimethylnaphthalenes with air over vanadia catalyst at reactions which yield phthalic anhydride[1-3]. Recently, Morita tried unsuccessfully to detect naphthalene as an intermediate in the oxidation of 2-methylnaphthalene and naphthalene-1- and 2-carboxylic acid. For this reason, he concluded that naphthalene is not a reaction intermediate in the oxidation of methylnaphthalenes to phthalic anhydride[4].

The purpose of this communication is to report the discovery and isolation of naphthalene as an isolatable reaction intermediate under reaction conditions which are well known to effect its further oxidation to phthalic anhydride[1-6].

1) J. K. Dixon and J. E. Longfield, "Catalysis", Ed. by P. H. Emmett, Vol. VII., Reinhold (1960), Chap. 3, pp. 196-222.
2) R. N. Shreve and R. W. Welborn, *Ind. Eng. Chem.*, **35**, 279 (1943).
3) C. R. Kinney and I. Pincus, ibid., **43**, 2880 (1951).
4) S. Morita, This Bulletin, **33**, 511 (1960).
5) N. L. Franklin, P. H. Pinchbeck and F. Popper, *Trans. Inst. Chem. Eng.*, **43**, 280 (1956).
6) A. F. D'Alessandra and A. Farkas, *J. Colloid Sci.*, **11**, 653 (1956).

TABLE I. FLUID-BED OXIDATIONS IN AIR OVER VANADIA CATALYST[1]

Feed	Reaction condition: Temp. °C	Contact time sec.	Air-to-feed ratio l.(air)/g.(feed)	Mol. % coversion to various product: PA[2]	MA[3]	NQ[4]	HC[5]	N[6]	CO_2[7]
A. Oxidations at conditions for good phthalic anhydride pronduction									
Naphthalene	375	0.69	29	50.5	2.2	1.4	25.8[8]	—	20.1
22% 1-Methylnaphthalene, 78% 2-Methylnaphthalene	375	0.66	91	30.9	2.6	3.1	3.8	(0.5)[10]	59.6
22% 1-Methylnaphthalene, 78% 2-Methylnaphthalene	375	0.45	82	37.4	2.3	1.8	19.5	(2.3)[10]	39.1
2-Methylnaphthalene	375	0.49	99	37.8	5.9	3.6	13.4	(1.7)[10]	39.3
1,2-Dimethylnaphthalene	375	0.48	148	19.7	22.7	4.2	13.2	(1.0)[10]	40.2
1,7-Dimethylnaphthalene	375	0.48	165	15.5	3.0	1.1	4.9	(0.0)[10]	75.5
2,3-Dimethylnaphthalene	375	0.41	133	49.0	2.5	2.9		8.8[11]	36.8
B. Oxidations at milder conditions than required for good phthalic anhydride production									
1-Methylnaphthalene	324	0.26	7.34	low[9]	—	—	—	4.02[12]	—
1-Methylnaphthalene	324	0.15	6.78	low[9]	—	—	—	4.34[12]	—
1-Methylnaphthalene	347	0.10	4.71	low[9]	—	—	—	2.18[12]	—

1) Davison powdered vanadia oxidation catalyst, 100～200 mesh, activated in air at 430°C for 2 hr.
2) PA = Phthalic anhydride
3) MA = Maleic anhydride
4) NQ = Naphthoquinone
5) HC = Total recovered hydrocarbons
6) N = Naphthalene
7) CO_2 determined by difference
8) Largely naphthalene
9) Phthalic anhydride produced in low yield, but not determined.
10) Determined by elution chromatography; too little to confirm by auxiliary analyses.
11) Determined by elution chromatography and confirmed by melting point and infrared and ultraviolet spectrometry.
12) Determined by gas-liquid chromatographic analyses.

The experiments related below were carried out in a laboratory fluid-bed catalytic flow reactor equipped with air and liquid feed devices, and a temperature controller. The condensable reaction products were caught in a series of traps and analyzed by a combination of gravimetric, spectrometric, and chromatographic procedures. Experimental conditions a reults are summarized in Table I.

Naphthalene was first isolated in an 8.8 mol. per cent conversion in the reaction product mixture obtained from 2, 3-dimethylnaphthalene under conditions which gave a 49.0 weight per cent conversion to phthalic anhydride. This naphthalene was separated from the product mixture by means of elution chromatography with petroleum ether over alumina. The identity and purity of the reaction product were established by m. p., 80.1～80.7°C, and gas-liquid chromatographic, infrared and ultraviolet spectrometric comparisons with an authentic sample of naphthalene.

Only small amounts of naphthalene were detected by elution chromatograms in the product mixtures obtained from the oxidation of 1-methylnaphthalene under the reaction conditions for good phthalic anhydride yields. However, improved conversions of 2.18 to 4.34 mol. per cent naphthalene were obtained under milder reaction conditions, which gave low yields of phthalic anhydride (see Part B, Table I). These reaction product mixtures were distilled to obtain a 15.2 g. naphthalene cut, b. p. 214～223°C/629 mmHg, which on recrystallization from ethanol gave an infrared spectrum entirely superimposable with one of an authentic naphthalene sample.

These experimental results conclusively demonstrate that naphthalene is an isolatable reaction intermediate in the heterogeneous vapor-phase oxidation of 2, 3-dimethylnaphthalene to phthalic anhydride. Although the naphthalene conversions were too small to be confirmed under conditions favoring good phthalic anhydride production from either 1- or 2-dimethylnaphthalene, larger naphthalene conversions were demonstrated and confirmed in the oxidation of 1-methylnaphthalene at milder reaction conditions, which are less favorable for good phthalic anhydride production. Consequently, any reaction mechanism or kinetic analysis for the heterogeneous vapor-phase

oxidation of methylnaphthalenes over vanadia must consider naphthalene as an isolatable reaction intermediate which is produced in sufficient quantities to be desorbed from the catalyst and detected.

The author wishes to acknowledge the assistance of T. E. Moss in the experimental work.

The Denver Research Center
The Ohio Oil Company
Littleton, Colorado

Sudachitin, a New Flavone Pigment of Sudachi

By Tokunaru HORIE, Mitsuo MASUMURA and F. Shigeo OKUMURA

(Received August 14, 1961)

A new flavone pigment was isolated in a 0.005% yield from the ether extract of the green fruit of *Citrus sudachi Hort ex Shirai*, one of the species of the family Rutaceae, which is produced only in Tokushima prefecture, Shikoku. The name, sudachitin is suggested for this new flavone. A better yield was obtained from the alcohol extract (0.014%) accompanying a second new flavone of m. p. 271～273°C from the mother liquor of sudachitin purifications in 0.004% yield.

Sudachitin crystallized as yellow needles from a mixture of ethyl acetate and methanol (1 : 1), 239.5～240.5°C, and its analytical values agreed with the formula $C_{18}H_{16}O_8$. When treated with metallic magnesium and hydrochloric acid, it gave typical reddish-orange color reaction for flavone pigments. It gave a greenish brown color with ferric chloride, indicating the presence of free hydroxyl groups.

The conversion of sudachitin (I) into a triacetate (II), $C_{24}H_{22}O_{11}$, m. p. 167.5～168.5°C, with acetic anhydride, and into a trimethyl ether (III), $C_{21}H_{22}O_8$, m. p. 135.5～136.5°C, with dimethyl sulfate, or into a triethyl ether (IV) $C_{24}H_{28}O_8$, m. p. 143～144°C, with diethyl sulfate, revealed the presence of three hydroxyl groups. These three derivatives gave the positive flavone color test with metallic magnesium and hydrochloric acid, but did not show a ferric chloride test. Diazomethane converted sudachitin into a dimethyl ether (V), $C_{20}H_{20}O_8$, m. p. 143～144°C, suggesting the existence of a free hydroxyl group at the 5-position of the flavone ring, at this stage, the similarity of the above two derivatives of sudachition to the nobiletin previously isolated by Robinson and coworkers[1], the structure of which has been confirmed as 3′, 4′, 5, 6, 7, 8-hexamethoxy flavone[2,3] (III), was noticed. The ultraviolet spectra of sudachitin trimethyl ether (III) and nobiletin*, and of sudachitin dimethyl ether (V) and 5-hydroxy-3′, 4′, 6, 7, 8-pentamethoxy flavone* were shown to be identical. The mixed melting point of the above two pairs also did not show any depression. From the above evidence, it is clear that the position of six substituents in sudachitin should be at 3′, 4′, 5, 6, 7 and 8

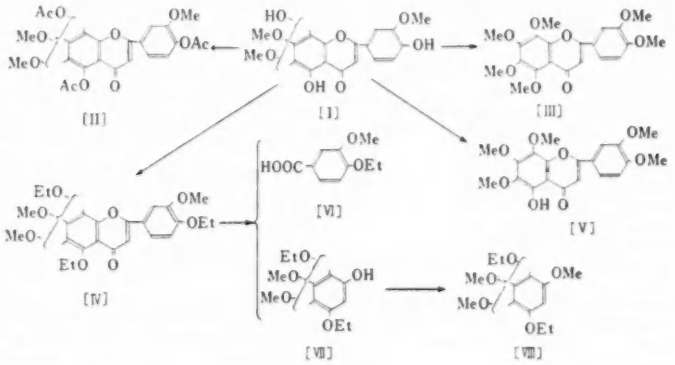

Fig. 1

1) Kwong-Fong Tseng, *J. Chem. Soc.*, **1938**, 1003; R. Robinson, Kwong-Fong Tseng, ibid., **1938**, 1004.
2) Z. Horii, *J. Pharm. Chem. Japan* (*Yukagaku Zasshi*), **60**, 614 (1940).
3) A. Tsukamoto and T. Ohtaki, ibid., **67**, 9 (1947).
* Samples of nobiletin and 5-hydroxy-3′, 4′, 6, 7, 8-pentamethoxy flavone were kindly provided by Dr. Z. Horii, University of Osaka.

positions, and one of the three free hydroxyl groups should be at the 5-position in the flavone ring.

In order to obtain furthur evidence regarding the position of the remaining two free hydroxyl groups, sudachitin triethyl ether (IV) was refluxed for 6 hr. in 10% potassium hydroxide solution. Acidificatin of the mother liquor from the ether extract of the hydrolysis mixture, gave a white precipitate in an 84% yield, which recrystallized from benzene, gave colorless needles, m. p. 193~194°C[4], (Found: C, 60.95; H, 6.23. Calcd. for $C_{10}H_{12}O_4$: C, 61.22; H, 6.16%). The mixed melting point with 4-ethoxy-3-methoxybenzoic acid[4] (VI) synthesized from vanillin was not depressed. From this fact, the position of the second free hydroxyl group was proved to be the 4′-position in the flavone ring. From the ether extract of the above mentioned hydrolysis mixture which had been saturated with carbon dioxide before ether extraction, there was obtained an oily product VII which gave a positive phenol test with ferric chloride. This was converted with dimethyl sulfate into a methyl ether, a diethoxy-trimethoxy benzene (VIII), whose analytical values agreed with the formula $C_{13}H_{20}O_5$ (Found: C, 61.04; H, 7.95. Calcd. for $C_{13}H_{20}O_5$: C, 60.92; H, 7.87%).

In the light of these findings, it was concluded that sudachitin most probably is the trihydroxy-trimethoxy flavone shown as structure I in Fig. 1.

An attempt to establish the relative positions of the hydroxyl- and methoxyl-groups on the benzene ring of VIII by direct comparison with three isomeric diethoxy-trimethoxybenzenes failed, because the amount of diethoxy-trimethoxybenzene from sudachitin was too small to purify.

The synthesis of three isomeric triethoxy-trimethoxy flavone which is only remaining way to confirm the final structure of sudachitin, is now in progress.

Department of Applied Chemistry
Faculty of Engineering
University of Tokushima
Tokushima

4) F. Tiemann, *Ber.*, 8, 1130 (1875).